Naser A. Anjum · Sarvajeet Singh Gill
Narendra Tuteja *Editors*

Enhancing Cleanup of Environmental Pollutants

Volume 2: Non-Biological Approaches

Springer

Enhancing Cleanup of Environmental Pollutants

Naser A. Anjum • Sarvajeet Singh Gill
Narendra Tuteja
Editors

Enhancing Cleanup of Environmental Pollutants

Volume 2: Non-Biological Approaches

Springer

Editors
Naser A. Anjum
CESAM-Centre for Environmental and Marine Studies, Department of Chemistry
University of Aveiro
Aveiro, Portugal

Sarvajeet Singh Gill
Stress Physiology and Molecular Biology Laboratory
Centre for Biotechnology
Maharshi Dayanand University
Rohtak, Haryana, India

Narendra Tuteja
Amity Institute of Microbial Technology
Amity University
Noida, India

ISBN 978-3-319-55422-8 ISBN 978-3-319-55423-5 (eBook)
DOI 10.1007/978-3-319-55423-5

Library of Congress Control Number: 2017937331

Printed on acid-free paper

This Springer imprint is published by Springer Nature
The registered company is Springer International Publishing AG
The registered company address is: Gewerbestrasse 11, 6330 Cham, Switzerland

Preface

Environmental and organismal (flora, fauna, and human) health can be impacted by varied chemical pollutants, continuously increasing in major environmental compartments. Notably, the bioavailability, stabilization, and degradation of pollutants are the major drivers that control the pollutant's exclusion, remediation/accumulation, and/or metabolism, performed by innovative technology involving biological (plants and associated microbes, etc.) and/or non-biological/(electro) chemical strategies.

This two-volume work is an effort to gather information on and get insights into biological and non-biological (chemical) approaches extensively studied and adopted for the speedy cleanup of pollutants from environmental compartments. In *Volume 1*, (a) important concepts such as biological remediation strategies to enhance soil quality at contaminated sites were overviewed; (b) synergistic influences of tolerant plants and rhizospheric microbial strains on the remediation of pesticide-contaminated soil were highlighted; and (c) the role of plant types such as hyperaccumulator plants in the cleanup of polluted soils was discussed. Overall, the literature available on the major mechanisms and underlying natural inherent traits of various plants and microbes for tolerating, excluding, remediating, accumulating, or metabolizing a variety of pollutants were critically appraised and elaborated in *Volume 1*. Non-biological (chemical) approaches for enhancing the cleanup of contaminated soils have been dealt in *Volume 2*. In brief, *Volume 2* (a) highlighted important concepts such as the role of metallic iron in the decontamination of hexavalent chromium polluted waters; (b) discussed nanoscale materials and electrochemical approaches used in water and soil remediation; and (c) elaborated in detail the synthesis and characterization of cation composite exchange material and its application in removing toxic metals.

A good equilibrium between theory and practice without compromising the basic conceptual framework of the concerned topic has been ensured in this treatise.

This work can be a useful asset to students, researchers, and policy makers specializing in the areas of soils/sediments and aquatic pollution, environmental chemistry/microbiology/plant physiology/molecular biology, sustainable development, ecology, soil biology, and related disciplines.

Aveiro, Portugal — Naser A. Anjum
Rohtak, India — Sarvajeet Singh Gill
Noida, India — Narendra Tuteja

Acknowledgements

We are thankful to the contributors for their interest, significant contributions, and cooperation that eventually made this book possible. Thanks are also due to all the teachers, seniors and research students. We would especially like to thank our family members as without their unending support, motivation and encouragement, this gruelling task would have never been accomplished.

We would like to offer our sincere thanks to Dr. Sherestha Saini (editor, *Environmental Sciences*, New York, USA) for her kind consideration of this volume. The exceptional kind support provided by Dr. Saini and Mr. Silembarasanh Panneerselvam (Simbu) (book project coordinator, *Springer Nature*) and their team at Springer deserves praises, which made our efforts successful.

The financial support to our research from the Foundation for Science and Technology (FCT), Portugal; the Aveiro University Research Institute/Centre for Environmental and Marine Studies (CESAM); the Department of Biotechnology (DBT); the University Grants Commission (UGC); and the Department of Science and Technology (DST), New Delhi, India, are gratefully acknowledged.

Aveiro, Portugal — Naser A. Anjum
Rohtak, India — Sarvajeet Singh Gill
Noida, India — Narendra Tuteja

Contents

Contributors

Tauqeer Abbas Department of Civil and Environmental Engineering, North Dakota State University, Fargo, ND, USA

Rehan Ahmad Department of Environmental Sciences and Engineering, Government College University, Faisalabad, Pakistan

Shafaqat Ali Department of Environmental Sciences and Engineering, Government College University, Faisalabad, Pakistan

R.B. Amal Raj Centre for Biopolymer Science and Technology, A Unit of CIPET, Cochin, India

Naser A. Anjum CESAM-Centre for Environmental and Marine Studies and Department of Chemistry, University of Aveiro, Aveiro, Portugal

V. Asensio Department of Plant Biology and Soil Science, Faculty of Biology, University of Vigo, Vigo, Pontevedra, Spain

Department of Plant Nutrition, University of São Paulo – Center of Nuclear Energy in Agriculture (USP-CENA), Piracicaba, SP, Brazil

Hafiz Faiq Bakhat Department of Environmental Sciences, COMSATS Institute of Information Technology, Vehari, Pakistan

K. Balasubramanian Department of Materials Engineering, Defence Institute of Advanced Technology (DU), Ministry of Defence, Pune, India

Irshad Bibi Institute of Soil and Environmental Sciences, University of Agriculture Faisalabad, Faisalabad, Pakistan

Southern Cross GeoScience, Southern Cross University, Lismore, NSW, Australia

Rani Bushra Department of Applied Physics, Aligarh Muslim University, Aligarh, UP, India

E.F. Covelo Department of Plant Biology and Soil Science, Faculty of Biology, University of Vigo, Vigo, Pontevedra, Spain

Camille Dumat Centre d'Etude et de Recherche Travail Organisation Pouvoir (CERTOP), UMR5044, Université J. Jaurès - Toulouse II, Toulouse, France

Pietro P. Falciglia Department of Civil Engineering and Architecture, University of Catania, Catania, Italy

Fabián Fernández-Luqueño Sustainability of Natural Resources and Energy Program, Cinvestav-Saltillo, Ramos Arizpe, Coahuila, CP, Mexico

R. Forján Department of Plant Biology and Soil Science, Faculty of Biology, University of Vigo, Vigo, Pontevedra, Spain

Selvia García-Mayagoitia Sustainability of Natural Resources and Energy Program, Cinvestav-Saltillo, Ramos Arizpe, Coahuila, CP, Mexico

Marius Gheju Faculty of Industrial Chemistry and Environmental Engineering, Politehnica University Timisoara, Timisoara, Romania

Sarvajeet Singh Gill Stress Physiology and Molecular Biology Laboratory, Centre for Biotechnology, Maharshi Dayanand University, Rohtak, Haryana, India

Renuka R. Gonte Department of Materials Engineering, Defence Institute of Advanced Technology (DU), Ministry of Defence, Pune, India

R.S. Guedes Institute of Agricultural Sciences, Federal Rural University of Amazonia, Belém, Brazil

Sundaram Gunasekaran Department of Biological Systems Engineering, University of Wisconsin-Madison, Madison, WI, USA

Muhammad Imran Department of Environmental Sciences, COMSATS Institute of Information Technology, Vehari, Pakistan

Iqbal I.M. Ismail Centre for Excellence in Environmental Studies, King Abdul Aziz University, Jeddah, Kingdom of Saudi Arabia

Sana Khalid Department of Environmental Sciences, COMSATS Institute of Information Technology, Vehari, Pakistan

Mohammad Zain Khan Environmental Research Laboratory, Department of Chemistry, Aligarh Muslim University, Aligarh, UP, India

Fernando López-Valdez Instituto Politécnico Nacional-CIBA, Tlaxcala, CP, Mexico

P. Marcet Department of Plant Biology and Soil Science, Faculty of Biology, University of Vigo, Vigo, Pontevedra, Spain

Nabeel Khan Niazi Institute of Soil and Environmental Sciences, University of Agriculture Faisalabad, Faisalabad, Pakistan

Southern Cross GeoScience, Southern Cross University, Lismore, NSW, Australia

Mohammad Oves Centre for Excellence in Environmental Studies, King Abdul Aziz University, Jeddah, Kingdom of Saudi Arabia

Carolina Pérez-Morales Instituto Politécnico Nacional-CIBA, Tepetitla de Lardizábal, Tlaxcala, CP, Mexico

Sergio R. Pérez-Ríos ICAP—Instituto de Ciencias Agropecuarias, Universidad Autónoma del Estado de Hidalgo, Tulancingo, Hidalgo, CP, Mexico

Huda A. Qari Centre for Excellence in Environmental Studies, King Abdul Aziz University, Jeddah, Kingdom of Saudi Arabia

Marina Rafiq Department of Environmental Sciences, COMSATS Institute of Information Technology, Vehari, Pakistan

A. Rodríguez-Vila Department of Plant Biology and Soil Science, Faculty of Biology, University of Vigo, Vigo, Pontevedra, Spain

Hina Rizvi Department of Environmental Sciences and Engineering, Government College University, Faisalabad, Pakistan

Muhammad Rizwan Department of Environmental Sciences and Engineering, Government College University, Faisalabad, Pakistan

Cesar R. Sarabia-Castillo Sustainability of Natural Resources and Energy Program, Cinvestav-Saltillo, Ramos Arizpe, Coahuila, CP, Mexico

Mohammad Shahadat Department of Biochemical Engineering and Biotechnology, Indian Institute of Technology IIT Delhi, New Delhi, India

Muhammad Shahid Department of Environmental Sciences, COMSATS Institute of Information Technology, Vehari, Pakistan

Munazzam Jawad Shahid Department of Environmental Sciences and Engineering, Government College University, Faisalabad, Pakistan

Zia Ahmad Shaikh Department of Biochemical Engineering and Biotechnology, Indian Institute of Technology IIT Delhi, New Delhi, India

Khadija Siddique Department of Environmental Sciences and Engineering, Government College University, Faisalabad, Pakistan

Narendra Tuteja Amity Institute of Microbial Technology (AIMT), Noida, UP, India

Mohammad Kashif Uddin Basic Engineering Sciences, College of Engineering, Majmaah University, Al-Majmaah, Kingdom of Saudi Arabia

Federico G.A. Vagliasindi Department of Civil Engineering and Architecture, University of Catania, Catania, Italy

Nael G. Yasri Department of Chemical and Petroleum Engineering, University of Calgary, Calgary, AB, Canada

Non-biological Approaches for Enhancing the Cleanup of Environmental Pollutants: An Introduction

Naser A. Anjum, Sarvajeet Singh Gill, and Narendra Tuteja

Abstract This chapter introduces the book *Enhancing Cleanup of Environmental Pollutants: Non-biological Approaches*. Discussion in significant chapters set out in this book focuses on major approaches for the enhanced pollutants clean-up based mainly on the use of techniques involving principles of chemistry and associated areas. Chapter overviews presented herein can benefit potential readers of this book.

Keywords Environmental pollution • Pollutants • Remediation • Non-biological approach • Soil amendments

Introduction

Environmental compartments including soil and water have always been vital to humans and fundamental to human health. A myriad of harmful chemicals are being continuously added to soil and water and making these environmental compartments unhealthy for life. Physical, chemical and phytoremediation techniques have been suggested as major strategies for the minimization of the loads of pollutants in environmental compartments. However, in these techniques, particularly in phytoremediation approach, the natural inherent traits of various plants and associated microbes for excluding, remediating/accumulating or metabolizing a variety of pollutants are lagging behind due to low or negligible bioavailability,

N.A. Anjum (✉)
CESAM-Centre for Environmental and Marine Studies and Department of Chemistry, University of Aveiro, 3810-193 Aveiro, Portugal
e-mail: anjum@ua.pt

S.S. Gill (✉)
Stress Physiology and Molecular Biology Laboratory, Centre for Biotechnology, Maharshi Dayanand University, Rohtak 124001, Haryana, India
e-mail: ssgil14@gmail.com

N. Tuteja
Amity Institute of Microbial Technology (AIMT), E3 Block, Sector 125, Noida 201303, UP, India

N.A. Anjum et al. (eds.), *Enhancing Cleanup of Environmental Pollutants*,
DOI 10.1007/978-3-319-55423-5_1

stabilization and degradation of major pollutants in contaminated environmental compartments. Hence, in the present volume, selected chapters contributed by eminent scientists, researchers and environmental/chemical engineers from over the globe aim to enlighten major non-biological approaches for making the availability of pollutants to plants and associated microbes easy and their subsequent degradation, absorption, adsorption, extraction/remediation/stabilization and minimization of their environmental load speedy.

Chapter Overviews

Electrochemical techniques are in use for the pollutants remediation and have provided elegant solutions for speeding the remediation of pollutant types. A thorough description on the electrochemical methods for remediation of a variety of dilute pollutants, organic contaminants, organic complexes with metals and recovery of heavy metals is provided by Yasri and Gunasekaran (Chap. 2). The authors advocated the versatility, energy efficiency, environmental compatibility and cost-effectiveness of electrochemical methods for pollutants remediation. Hydrocarbon compounds, including fuel and petrochemical products, have contaminated soils and water. Chemical, physical or biological approaches cannot always be feasible for remediating hydrocarbon-polluted soils because of their ineffectiveness and expensiveness or too lengthy nature. Microwave heating-mediated remediation of hydrocarbon-polluted soils can be a major approach alternative to the aforesaid strategy. In addition to its simplicity, safety, flexibility and cost-effectiveness, microwave heating can offer the potential to significantly reduce treatment times, risk of contamination and costs due to the direct interaction of microwaves with the soil and its ability to overcome heat and mass transfer limitations. To this end, Falciglia and Vagliasindi (Chap. 3) report the theoretical background of microwave heating process and the related techno-economic features for ex situ full-scale applications in remediation activities of hydrocarbon contaminants. Considering its classification as the class A human carcinogen and its increasing levels in environmental compartments, arsenic has gained a substantial attention in recent years. In an effort by Khalid and co-workers (Chap. 4), a link between arsenic speciation and its biogeochemical behaviour was established in complex soil-plant systems. Additionally, the authors also overviewed different biogeochemical processes potentially governing environmental behaviour of arsenic in the soil-plant system and highlighted the role of the chemical speciation of arsenic affects in the biogeochemical behaviour (adsorption/desorption, mobility, bioavailability/phytoavailability) in the soil-plant system. A discussion is also presented on the relationship of soil physicochemical properties (pH, clay contents, biological and microbial conditions, presence of organic and inorganic ligands and competing anions/cations) with chemical speciation of arsenic as well as its biogeochemical behaviour in the soil-plant system. Aquatic environment including water bodies is being significantly contaminated with toxic heavy metal ions and

pathogenic bacteria. Hence, the scarcity of fresh and pure water is considered as a biggest threat to human and animal life on the Earth. Nanotechnology-based water purification/treatment systems for efficient and effective decontamination of water bodies have gained attention recently. Focused at nanoscale composite materials, Khan et al. (Chap. 5) provide insights into processes and mechanisms underlying the role of nanocomposite materials in the removal of pollutants from polluted water bodies. Being the largest water-consuming industry in the world, the textile industry is responsible for the occurrence of many pollutants such as dyes, degradable organics, detergents, stabilizing agents, desizers, inorganic salts and heavy metals in its wastewater. Notably, the percolation of the said pollutants into the groundwater is posing a serious threat to the health and socioeconomic life of the people. Siddique et al. (Chap. 6) present a critical review on the textile wastewater treatment options and also describe major advantages and limitation of the textile wastewater treatment strategies. Among the existence of mainly two of its most stable oxidation states, (+III) and (+VI) of chromium, Cr(VI) exhibits its high mobility in the environment, significantly contribute to pollution of air, soil and waters, and is the most hazardous for all living matters. Metallic iron (Fe^0) is used for the abatement of Cr(VI) pollution in aquatic system. Despite the substantial research work on the removal of Cr(VI), done during last 25 years, there is no consensus at this time in what regards the mechanism underlying the metallic iron (Fe^0)-mediated clean-up of Cr(VI) pollution. In an effort, Gheju (Chap. 7) attempts to provide an overview of chromium occurrence, chemistry and toxicity. The author also does a critical review of existing knowledge on this subject. It was argued that the mechanism of Cr(VI) removal with Fe^0 is more complex than the simple reductive precipitation.

A range of physical or chemical processes such as adsorption, electrochemical methods, chemical precipitation, ultrafiltration and coagulation floatation is known to affect the abstraction of metals-metalloids from contaminated media. Extensively used methods based on the precipitation or oxidation-reduction may lead to a secondary pollution. Notably, adsorption is accepted as one of the most adequate and fiscal methods for the abstraction of metal ions at low ion concentrations. However, in order to describe the adsorption mechanism for the interaction of metal ions/dyes on the adsorbent surface, for the design of an adsorption process and to determine the efficiency of adsorption, it is required to have information about adsorption isotherms. To this end, Amal Raj et al. (Chap. 8) provide insights into the toxic metals adsorption by functional styrene-maleic acid copolymer beads. The authors also made their effort to develop well-organized styrene-maleic acid copolymer beads and composites for adsorption of toxic chemicals. It was also advocated to use hydrogen as a highly innovative and eco-friendly method for large-scale clean-up of polluted water. In recent years, some new processes such as bio-sorption, neutralization, precipitation, ion exchange, adsorption, etc., have been developed and extensively used for the removal of toxic metals-metalloids from wastewater. In particular, ion exchange was reported to be the most helpful method in adsorption of metal ions because ion exchangers have high capacity and specificity for the metal ions, even if found in low concentrations. Also, many

hybrid ion exchangers with conjugated properties of polymer and intrinsic properties of inorganic exchanger have been introduced. To this end, in addition to overviewing major toxic metal-metalloid and their biotoxicity, Kashifuddin and Bushra (Chap. 9) synthesize, characterize and discuss the role and underlying mechanism of composite cation exchange materials in the remediation of toxic metal ions.

The use of amendments (organic and mineral) has also been considered as an important tool for enhancing the remediation and bioremediation of contaminated compartments such as soils. However, scientific and technological bases are required for properly adding these amendments in the polluted soils and also for reaching high-pollutants degradation rates. Forján and co-workers (Chap. 10) and Fernández-Luqueño and co-workers (Chap. 11) discuss ins and outs of amendments (organic and mineral)-mediated enhancements in the decontamination of soils polluted with inorganic and polycyclic aromatic hydrocarbons. Parallel to the trace element contamination, the massive generation of organic waste by human activities has also contaminated environmental compartments. Proposal of several alternatives to avoid landfilling and promote recycling has also been made. In this context, organic amendments were reported to precipitate complex, adsorb and absorb pollutants thereby reducing the bioavailability of the pollutants, as well as to improve soil structure and fertility. Forján and co-workers provide examples in support of organic amendments-assisted remediation of soils polluted with inorganic contaminants. The addition of organic amendments in polluted soils is considered one of the most promising recovery techniques at present, because it makes use of waste which would in most cases unutilized for any activities and cause other damage to the environment. Organic amendments such as biochar, technosols, sewage sludge and compost were argued to convert waste into environmental benefits at low cost. Generated primarily during the incomplete combustion of organic materials (e.g., coal, oil, petrol and wood), polycyclic aromatic hydrocarbons have become ubiquitous environmental pollutants and need attention. This is because a range of negative effect of polycyclic aromatic hydrocarbons has been reported on the human and environmental health and on the agricultural soils as a route of contaminants entering the food chain. Fernández-Luqueño and co-workers analyse the relevant state of the art on the role of organic and mineral amendments for remediation of polycyclic aromatic hydrocarbons and also discuss the main advantages and disadvantages of this approach. Additionally, some experiences on remediation and bioremediation of polycyclic aromatic hydrocarbon-polluted soils are also shared by these authors.

Electrochemical Technologies for Environmental Remediation

Nael G. Yasri and Sundaram Gunasekaran

Abstract Contamination of environmental compartments with a myriad of chemical pollutants is inevitable. Many physical, biological, photolytic, chemical, and electrochemical techniques are in use for the pollutant remediation. Notably, elegant solutions to remediating environmental pollutants have been provided by electrochemical methods. Literature supports the versatility, energy efficiency, environmental compatibility, and cost-effectiveness of electrochemical methods for pollutant remediation. This chapter aims to describe electrochemical methods for remediation of a variety of dilute pollutants, organic contaminants, organic complexes with metals, and recovery of heavy metals. Additionally, effort has also been made to discuss major bioelectrochemical methods for the generation of energy from waste stream as power source.

Keywords Environmental pollution • Remediation • Electrochemistry • Electrochemical technologies • Bioelectrochemistry

Introduction

Advances in technology and increased consumer demand for goods and services have resulted in increased amounts of pollutants present in the environment. The pollutants are usually categorized under different subtypes, and various regulatory bodies often refer to those that are most dangerous to the environment as belonging to a "Black List," which includes persistent organic pollutants (POPs) such as organohalogen, organophosphorus, some metals, and their organometallic complexes. Many POPs

N.G. Yasri (✉)
Department of Chemical and Petroleum Engineering, University of Calgary, 2500 University Drive, T2N 1N4 Calgary, AB, Canada
e-mail: nael.yasri@ucalgary.ca

S. Gunasekaran (✉)
Department of Biological Systems Engineering, University of Wisconsin-Madison, 460 Henry Mall, Madison, WI 53706, USA
e-mail: guna@wisc.edu

N.A. Anjum et al. (eds.), *Enhancing Cleanup of Environmental Pollutants*,
DOI 10.1007/978-3-319-55423-5_2

are toxic and resistant to conventional biological and chemical wastewater treatments and bioaccumulate in the environment (Calow 2009).

Many problems associated with hazardous wastes, however, can be avoided if proper actions are taken in the early stages by either waste reduction (cutting down the amount of waste at the origin) or waste elimination (replacing hazardous materials with "green" chemicals or using treatment processes which reduce the amount of waste requiring ultimate disposal). This would necessitate ensuring that waste is recovered as much as possible and when necessary disposed off using methods that are benign to the health of humans and the environment. However, it is said that municipal wastewater may contain as much as 9.3 times the amount of energy required for its treatment (Fan et al. 2012). Waste streams, therefore, can be considered as a preliminary source of energy and technologies, which can generate energy from waste, and are considered as "green" or environmentally friendly (Harnisch et al. 2015; Liu et al. 2005). Consequently, it is important to consider the following hierarchy of priorities while dealing with wastes: prevention, reduction, reuse, recycle, and appropriate utilization of waste as a source of energy (Wang et al. 2010c).

The many techniques used in the remediation of wastes fall under the major categories of physical, biological, photolytic, chemical, and electrochemical. Of these, electrochemical methods often provide elegant solutions to remediating environmental pollutants (Janssen and Koene 2002; Ota et al. 2014); they offer several advantages over other methods such as versatility, energy efficiency, amenability to automation, environmental compatibility, and cost-effectiveness.

Generally, electrochemistry is considered a physicochemical discipline with wide-ranging applications that are directly or indirectly useful in our daily life. These include chemical conversion for energy generation, energy storage (battery charging/discharging), metal coating, surface technology, biological systems (nervous, cardiology, and cells), corrosion, electroanalysis, sensor, electrosynthesis, pollution control, recycling, treatment, remediation, and disinfection (Ota et al. 2014). Electrochemical techniques have been used since the early 1960s for the treatment of wastewater containing metallic, organic, and inorganic compounds (Chen and Hung 2007; Comninellis 2010; Rajkumar and Palanivelu 2004). The technique is known for its broad adaptability. For example, in an electrochemical cell various types of reactions such as oxidation, reduction, phase separation, dilution, concentration, and biological and photolytic reactions can be monitored directly or indirectly. Separation of the reaction products is feasible by implementing various established designs or controlling reactors and/or reaction conditions. Pollutants of different types or phases, i.e., solids, liquids, or gases, could be dealt with. Also, electrochemical reactors are scalable for treating solution volumes ranging from milliliters to barrels or more. Electrochemical treatment is usually performed at temperatures lower than non-electrochemical approaches, which leads to increased energy efficiency. Varying the applied potential, design of electrochemical cells, and choice of electrodes could help minimize power losses, voltage drops, and unwanted side reactions. Additionally, data collected in terms of current and voltage facilitate process automation and control. External control of the

electron transfer across the interfaces causes the electrons to obtain a specific energy, thus making electrons the main reagent for the interface reaction; this "clean reagent" promotes environmentally benign technology (Chen and Hung 2007; Comninellis 2010). For example, a prudent choice of electrode type (interface surface) enhances the selectivity of the electrode and hence prevents the production of unwanted side reactions. Overall, electrochemical processes are generally simple and, if properly designed, cost-effective.

Commonly, pollutant species which are targeted for electrochemical treatment are rather dilute, seldom exceeding in concentrations a few hundred or thousand parts per million (ppm). Therefore, electrochemical pollutant remediation falls under the electrochemistry of dilute solutions, which is completely different from that of treating concentrated media. For example, electrochemical properties of effluents contaminated with toxic heavy metals are different from those of electroplating or electrowinning media, which are very dilute. Accordingly, the design considerations of electrochemical cells for treating dilute streams are different than those for concentrated solutions.

The applications of electrochemical technologies for industrial recycling and effluent treatment include the removal, recovery, and separation of dissolved metals, destruction of dissolved organic materials, and treatment of waste gases. More recently, electrochemical technology is used to generate electric power or hydrogen from waste products in the so-called microbial fuel cells (MFCs) (Logan 2008) or microbial electrolysis cells (MECs) (Logan et al. 2008), respectively. Considering other applications, electrochemistry can be used to control electrode potentials for detoxification of specific biological inhibitor compounds, such as phenolic and furfural produced during various chemical and biological platform treatments (Lee et al. 2015).

Given the above, this chapter aimed to describe electrochemical methods for remediation of a variety of dilute pollutants, organic contaminants, organic complexes with metals, and recovery of heavy metals. In addition, electrochemical methods to generate energy from waste stream as power source are also included.

Electrochemistry: The Basics

Electrochemistry is the science that deals with the consequences of transferring electric charges from one phase to another; in particular, it deals with the electric properties at interfaces. For example, when two phases (a metal electrode and an electrolyte solution containing ions) are brought into contact, some ions in one phase tend to transfer to the other, carrying their electric charge. This creates a potential difference across the region between the two phases. This region is called an interface (or electrode interface), and the potential is called the interface potential (or electrode potential). Thereby, in an electrochemical cell, at one electrode-electrolyte interface, electrons leave the electrode (electron source, cathode), and the particles (cations) of the solution are reduced. At the other interface,

the electrode (electron sink, anode) takes electrons from the particles, and oxidation takes place. External control of electron transfer rates across the interface causes the electrons to obtain specific energy.

The definitions and sign conventions of anode and cathode used are conventional, with anode always being the site of oxidation and cathode, the site of reduction. The conventional signs of currents and potentials measured at the both sites (anode/cathode) depend on the type of electrochemical cell. For example, in a galvanic cell (e.g., batteries), where reactions are spontaneous, the cathode is assigned positive (electron sink, where reduction takes place). However, in the electrolysis cell where current or potential is applied to drive a chemical reaction, the anode is assigned positive. The control of the sign and the rate of electrons exchange at the interfaces in the electrochemical cell are additional advantages to possibly control the chemical reactions through an applied potential, which can help promote process automation.

Electrolysis can be used for wastewater treatment exploiting the oxidation/reduction reactions at the electrodes (Chen 2010). Reduction takes place at the cathode by the action of diffused cations toward the surface (e.g., deposition of metal ions on cathode) generating cathodic currents; while at the same time, anions diffuse toward the anode for oxidation to take place at the surface generating anodic currents.

General Aspect of Electrochemistry

Before describing the main electrochemical treatment technique and the mechanisms involved, it is helpful to review the basics of electrochemistry, which is necessary to understand the performance of various remediation processes. Efficiency calculation of the electrochemical remediation process are summarized in [Box 1].

Box 1 Calculation of Efficiency Parameters

Current Efficiency and Energetic Parameters

Electrochemical remediation of pollutants is usually monitored on the basis of change in the pollutant concentration in the treated solution or by using collective parameters such as chemical oxygen demand (COD, in mg O_2 L^{-1}) and/or total organic carbon (TOC, in mg carbon L^{-1}). The effectiveness of the electrolysis process (α) to remediate substances is monitored by the percentage removal (%) calculated as:

$$\alpha\,(\%) = \frac{\text{actual decreace in concentration}}{\text{initial material concentration}} \times 100 \qquad (1)$$

(continued)

Box 1 (continued)

The data of concentration variation also allow calculating efficiency parameters for determining the efficiency of electrochemical processes in terms of electrical charge consumed. To calculate the instantaneous current efficiency (ICE), which is defined as the ratio of current effectively used in the remediation process (I_{ef}) at a given time (t) to the applied current (I_{appl}),.

$$\mathrm{ICE}(\%) = I_{ef}/I_{appl} \tag{2}$$

For example, the ICE for COD removal during electrolysis in a batch operation at a constant current is calculated as (Brillas et al. 2009):

$$\mathrm{ICE}\ (\%) = \frac{(\mathrm{COD}_t - \mathrm{COD}_{t+\Delta t})FV_S}{8I_{appl}\Delta t} \times 100 \tag{3}$$

where, COD_t and $\mathrm{COD}_{t+\Delta t}$ are the COD values at times t and $t + \Delta t$ (s), F is the Faraday constant (96,485 C mol^{-1}), V_S is the solution volume (L), the constant 8 is the oxygen equivalent mass (g eq^{-1}), and I_{appl} is the applied current (A).

Similarly, the current efficiency is the ratio of theoretical to actual energy required for given electrochemical reaction. The theoretical energy requirement is usually calculated from the expected reaction product from Faraday's laws if there were no side reactions, and the actual energy required is calculated from the input energy to the system. For example, applying 2 Faradays (2 × 96,485 C) of electrical charge to Cu electroplating cell should theoretically deposit mole equivalent of copper metal on the cathode (where 2 is the number of electrons charge on the cathode to deposit one Cu atom). On the other hand, considering COD decay (mg $\mathrm{O_2\ L}^{-1}$) for electrochemical organic remediation process, average current efficiency (ACE) at time t is given by Eq. 4.

$$\mathrm{ACE}\ (\%) = \frac{\Delta\mathrm{COD}_t\, FV_S}{8It} \times 100 \tag{4}$$

Other practical parameter is electrochemical energy consumption (EEC), defined as the energy (kWh) required to treat unit volume (m^3) of effluent or unit COD (mg COD^{-1}) or unit TOC (mg TOC^{-1}) (Brillas et al. 2009). EEC is considered an important parameter in comparing the efficiency of different electrochemical remediation methods in regard to energy-related calculations. The EEC (kWh) during operational time (t in h) at constant current (I in A) and voltage (E in V) can be estimated per unit volume (Vs in m^3), unit COD mass, or per unit TOC mass according to Eqs. 5, 6, and 7, respectively (Brillas et al. 2009).

(continued)

Box 1 (continued)

$$\mathrm{EEC}\left(\mathrm{kWh\ m^{-3}}\right) = \frac{E_{\mathrm{cell}} I t}{V_{\mathrm{s}}} \tag{5}$$

$$\mathrm{EEC}\left(\mathrm{kWh\ (g\ COD)^{-1}}\right) = \frac{E_{\mathrm{cell}} I t}{(\Delta \mathrm{COD})_t\, V_{\mathrm{s}}} \tag{6}$$

$$\mathrm{EEC}\left(\mathrm{kWh\ (g\ TOC)^{-1}}\right) = \frac{E_{\mathrm{cell}} I t}{(\Delta \mathrm{TOC})_t\, V_{\mathrm{s}}} \tag{7}$$

Usually electrochemical treatment like any other treatment can proceed in either batch or continuous operation. In a batch operation, the volume of effluent treated is constant during the treatment period (the solution can be stirred, circulated, or statically stable). In a continuous operation, wastewater is continuously allowed to flow through and treated. In the continuous system, an important parameter is hydraulic retention time (HRT), or the hydraulic residence time, defined as the average duration; the effluent remains in the reactor and calculated by dividing the volume of reactor by effluent flow rate (Eq. 8).

$$\mathrm{HRT\ (min)} = \frac{\mathrm{Volume\ of\ reactor\ (mL)}}{\mathrm{Flow\ rate\ (mL/min)}} \tag{8}$$

Parameters, such as α, ICE, ACE, and EEC, can all be calculated for continuous operation to be compared with various electrochemical treatment approaches.

Faraday's Law

Faraday's law is the basic law that governs the theory of electrochemistry. It states that (a) amount of chemical change produced by an electric current is directly proportional to the quantity of electricity that passes during a certain time and (b) amounts of different substances liberated by a given quantity of electricity are proportional to their chemical equivalent weights. Faraday's law is expressed in terms of the weight (w in g) of metal deposited at the electrode as:

$$w = \frac{I\, t\, A}{z\, F} \tag{9}$$

where: I is applied current (A), t is duration (s), A is atomic weight of metal deposited (g), z is metal valence, and F is Faraday constant (96,487 C/mol).

The Faraday constant is the quantity of electricity required to deposit the equivalent weight in grams of a metal (atomic weight = equivalent

weight × valence). This means that (a) by measuring the quantity of electricity that passes, one has a measure of the chemical change that will be produced and (b) by knowing the chemical equivalent weight of a substance, one can predict the amount of substance that will be reacted by a given quantity of electricity.

Current Density and Limiting Current Density

The current density (J), defined as the current per unit area of electrode, is very important in electrochemical operations. The character of the reactants, the distribution, and the efficiency of the process all depend on J. Limiting current density (J_L) is defined as the current density at which ions deplete as rapidly as they can diffuse (reach and react) to the electrode surface. The J_L of any electrolyte increases with the concentration of ions. In this way the current efficiencies obtainable also increase. J_L is related to the thickness of the diffusion layer (region at the electrolyte-electrode interface where concentration gradient occurs compared to the bulk solution) by the following expression:

$$J_L = \frac{k}{d} \tag{10}$$

where d is thickness of the diffusion layer

$$k = \frac{D\, n\, F\, C}{1 - N} \tag{11}$$

where D is diffusion coefficient, n is ion valence, N is transport number, C is concentration of ionic species, and F is the Faraday constant.

Note that when C is low (low ion concentration), N is normally zero; thus:

$$k = \frac{D\, n\, F\, C}{d} \tag{12}$$

If d is constant, a decrease in ionic concentration will produce a proportional decrease in J_L. Similarly, by decreasing d it is possible to increase J_L and thereby increase reaction rates.

Overvoltage

The reaction potential for reversible and irreversible reactions at the electrode surface is known, by convention, as electrode potential. In some cases, high kinetic barrier has to be overcome for the interface reaction to occur, which is achieved by

applying an extra potential (extra energy) called overvoltage (η) (or over potential). The value of η is directly related to both voltage of the electrochemical cell and efficiency of the process. There are a number of types of η, whose source and how it influences the course of the electrochemical reactions are described below.

(i) Concentration overvoltage: When current is passed through a cell, the activity of ions (concentration) near the electrode changes. Taking the deposition of metal ions on the cathode surface as an example, the replenishment of these ions from the bulk solution is not as fast as the deposition process. This delay in replenishment causes a difference in concentration, which lowers the equilibrium potential. This difference in the equilibrium potential is termed as concentration overvoltage (η_c).

(ii) Activation overvoltage: The energy lost due to the slowness of electrochemical reactions and the dissociation of molecules at the electrode interface for an electrochemical reaction to take place is called activation overvoltage (η_{act}). This can simply be explained by the fact that most metal ions are hydrated in solution, and the coordination sphere of the ions must be distorted and the water molecules freed from their association with the metal ion for the process of deposition to take place. This portion of energy form an energy barrier consists of two components: the activation energy of the charge transfer reaction toward the electrode surface and the electric energy associated with the interaction between ions and the electrode. For most metals depositing on a cathode η_{act} is fairly small and can usually be neglected, unless i is very large. However, certain metals and all gases show evidence of considerable η_{act}.

The relation between current and η_{act} is a logarithmic function given by the Tafel equation (Eq. 13) (Zoski 2006).

$$\eta_{act} = a + b\log J \tag{13}$$

where a and b are constants dependent on the reaction mechanism and J is current density.

(iii) Resistance overvoltage: The most common form of resistance overvoltage (η_r) arises from the passage of electric current through an electrolyte solution surrounding the electrode. Such a solution shows resistance to current flow resulting to an ohmic (IR_{ex}) drop in potential between the electrodes. A less common form of η_r is caused by the formation of a surface-adherent film that itself possesses substantial resistance. In some cases, one or both electrodes are covered with a film of resistance different from that of the origin.

The evolution of hydrogen and oxygen at the electrode surfaces during the electrolysis of dilute aqueous solutions of acid or bases is well known and considered a prominent phenomenon in the electrolysis of dilute effluents. Hydrogen overvoltage (η_H) is of great importance in the electrolysis solutions containing metal ions. In fact, if there was no η_H, many metals could not be deposited from aqueous solution. η_H depends strictly on the cathode (material and surface).

Some cathodes cause a large η_H value, which will allow some metal ions to deposit on the surface without the evolution of hydrogen gas or allow metal deposition and hydrogen evolution to take place at the same time. η_H is higher on smooth surfaces than on rough ones and has a value that varies from negligible on platinum surface and quite low on graphite to perhaps as much as 1 volt on mercury.

Mechanism of Electrolysis and the Transport of Ions

The ability of a solvent, especially water, to ionize substances dissolved in it makes electrolysis possible. However, the demand for electric charge at the interface cannot be met by ions, which remain stationary in the solution, or just move about at random. Different ions move at different rates from the bulk solution to the interface between solution and electrode, and electron transfer processes at the interfaces accompany this. An example is the case of using metal salt as an electrolyte in normal electroplating solutions. As metal is deposited at cathode, the solution in its immediate vicinity is depleted of metal ions. If plating is to continue, these ions must be replenished. There are three possible ways in which ions reach the electrode surface, which may also occur simultaneously. These mass transfer methods are (Zoski 2006) (1) diffusion, (2) convection, and (3) and migration and are detailed below:

1. Diffusion occurs as a result of concentration gradient being set up at the electrode interface with electrolyte. A difference in concentration can arise when electrochemical reaction occurs at the electrode surface, converting ions, and consuming out of a solution by electron transfer, so reducing the concentration of ions near the electrode compared with the concentration a few thousand angstroms further into the liquid. This gives rise to the movement of species from higher to lower concentration. Hence, diffusion occurs for ionic or uncharged species through the solution as a result of concentration gradient.
2. Convection occurs as a result of hydrodynamic flow and can be characterized as either forced or natural. Forced convection occurs when the solution is stirred, and natural convection occurs when the solution is stirred or not. When differences in pressure, density, or temperature exist in various parts of the electrolyte, then the liquid begins to move as a whole or in parts. For example, when metal ions are deposited on the electrode, the density of the solution at the electrode-solution interface is reduced. This density change causes an influx of ions from the surrounding solution to move toward the electrode, independently of that caused by diffusion. Lower-density solution at the vicinity of the electrode surface flows upward, while the higher density solution flows down into the bulk solution creating a convection current. The difference between diffusion and convection, therefore, is that diffusion occurs because of change in concentration of ions and convection because of density variation.

3. Migration involves movement of cations and anions through a solution under the influence of an applied potential between electrodes placed in the solution. The movement is initiated due to the attraction of opposing charges, i.e., the potential gradient will act upon the ions to push the positive ions toward the negative electrode and the negative ions toward the positive electrode. If the moving species are neutralized (uncharged) or the concentration of ions reacting at the electrode is small compared to the concentration of other ions in the solution, the effect of ionic migration is negligible compared to that of diffusion.

Treating Methods for Metals and Inorganic and Organic Metal Complexes

Several methods are used for the removal and recovery of metal ions from industrial effluents including chemical precipitation (Özverdi and Erdem 2006; Pérez et al. 2010), adsorption (Babel and Kurniawan 2003; Guo et al. 2010; Li et al. 2003), biosorption (Sulaymon et al. 2014), solvent extraction (Kocaoba and Akcin 2005), cementation (Konsowa 2010), membrane filtration (Borbély and Nagy 2009; Landaburu-Aguirre et al. 2010), ion exchange (Alyüz and Veli 2009), coagulation (Charerntanyarak 1999), flocculation (Beltrán Heredia and Sánchez Martín 2009), flotation (Kurniawan et al. 2006), reverse osmosis (Dialynas and Diamadopoulos 2009), electrodialysis (Abou-Shady et al. 2012; Chaudhary et al. 2000), and electrochemical treatment (Tao et al. 2014). However, there are practical limitations to most of these methods arising mostly from the presence of organic, complexing, or chelating regents present in streams.

Similarly, for effluents containing organic materials, there are many possible ways to remediate them. However, the efficiency of many of these methods is reduced in the presence of heavy metal ions, and this is particularly true if the organic species form strong complexes with the metal ions in solution (Quivet et al. 2006). The presence of organic and inorganic species with metal ions changes the chemical, physical, and toxicological properties of the metal ions (Bradl 2005). For example, the presence of ethylenediaminetetraacetic acid (EDTA) as a complexing agent in a metal-containing solution will result in the formation of anion charged complex (Eq. 14).

$$M^{2+} + H_2Y^{2-} \rightarrow MY^{2-} + 2H^{+} \tag{14}$$

where EDTA is assigned the formula H_4Y; disodium salt (Na_2H_2Y) supplies the complex-forming ion H_2Y^{2-} in aqueous solution. The ligand is normally hexadentate and reacts with heavy metals (M^{n+}) in 1:1 ratio. Thus divalent metal ions (M^{2+}), for example, react with disodium salt as shown in equation (Chaudhary et al. 2000).

These metals anions are stable and soluble at moderately high pH (>8), which prevent the process of metal hydroxide precipitation when attempt is made to remove heavy metals by precipitation at high pH. Additionally, the presence of metal ions can retard the destruction of organic contaminants with the efficiency of recovery of the metal being reduced by the complexing species (Carrier et al. 2006). The treatment approaches for these complexes include ion exchange (Nabi et al. 2006), reverse osmosis (Ujang et al. 2010), and nanofiltration (Gao et al. 2014). These methods generate concentrated solutions from which the metal must be removed/recovered prior to liquid disposal. The alternative treatment method includes breaking the metal-organic complex into free metal and free chelating agent, followed by separation of the metal in an insoluble form with the organic agent discharged for subsequent treatment. Breaking the metal-reagent bonds requires chemical or other form of energy input into the system. For example, catalytic decomposition applying catalytic advance oxidation (CAO) such as photolytic treatment is applied to degrade organics incorporated with metals using photoactive species such as titanium dioxide (TiO_2) or hydrogen peroxide (H_2O_2) at a certain pH (Soderquist et al. 2012). The combination of two techniques such as catalytic decomposition by applying advance oxidation, say by ultraviolet (UV) irradiation, followed by electrochemical removal of freed heavy metals ions (Chaudhary et al. 2009) is a promising method to remove heavy metals over relatively long decomposition periods.

Processes other than CAO require the use of chemicals as oxidants which is disadvantageous due to the addition of more chemicals to the waste streams that may complicate the treatment process (Prairie et al. 1993). For example, Katoh (1986) patented a process to treat liquid wastes containing chelated heavy metal compounds, which involves pH adjustment, iron polysulfate addition to form an iron chelate compound, then removal of the formed product via flocculation, and precipitation of the flocs at high pH. Other researchers applied similar approaches but attempted to reduce the use of aggressive and hazardous chemicals such as acids and bases. Al-Zoubi et al. (2015) proposed a method to treat industrial effluents containing heavy metals employing the coagulation/flocculation principles. They used various types of polymers to reduce the use of iron (Fe) or aluminum (Al) ions as flocculants to remove heavy metals and can be discharged into designated receptacles for further treatment.

Considering both their value and adverse impact on the environment, heavy metals should be reclaimed from industrial effluents. Generally, the coagulation/flocculation system creates sludge, which will contain the removed pollutants that require further treatment or disposal (discussed in detail later. This is also true for electrocoagulation or electroflocculation systems, where sacrificial Fe or Al electrodes are employed to generate coagulants. Kaspar et al. (Morkovsky et al. 1999) patented a process and apparatus for electrocoagulation treatment of industrial wastewater employing sacrificial electrodes conjugated with foaming system to flocculate pollutants. Some advance research has been performed to improve the performance of electrochemical coagulation/flocculation system by adding steps such as disinfection/oxidation with ozone, UV, and ultrasonic treatment, as well as

recirculation in the electromagnetic field to reduce or to treat the sludge (Visnja et al. 2013).

Overall, the aforementioned treatment methods simultaneously remove, to a certain extent, mixed heavy metals from solution. However, considering the value of heavy metals, for the treatment process to be effective, their separation and recovery from waste streams have to be taken into account.

Electrochemical Approaches for Separation, Removal, and Recovery of Metals

Electrochemical methods to remove heavy metals involve the deposition of metal ions from effluents on cathode surface and have the advantages of recovery as well as removal. The electrodeposition (ED) process can be performed by imposing either fixed current or fixed potential. Essentially, in an electrochemical cell containing mixed metal ions, the deposition reaction at the cathode, which requires the least negative potential, will initially take place, especially if the deposition potential of any alternative process is much more negative and almost exclusively if the alternative potential is only slightly more negative. If the potential is made sufficiently negative to produce a second reaction, that reaction may occur simultaneously, and if potential is made enough for the electrolysis of water to occur, hydrogen will start to produce at cathode surface. There are exceptions for some metals that cannot be deposited from aqueous solutions such as titanium (Ti) and Fe, which are very active metals and cannot be electroplated on electrode. The metal ions with associate ligands (water or complex anion) attach themselves at certain preferred sites (irregular surfaces); at the same time, metal ions bound to the electrode surface and partially neutralize their charge, and the associated ligands dissociate to diffuse back into the solution. Monoatomic growth layers are produced until several neighboring lattices meet to form a coating on the electrode. The nucleation energy, energy required for the formation of nuclei on the cathode surface, can be calculated from Eq. 15.

$$\Delta G = -N^* z_i e_0 \, |\eta| + \varphi(N) \tag{15}$$

where N^* is number of atoms per nucleus growth (cluster), z_i is charge of the metal ion, e_0 is elementary charge of the electron, $|\eta|$ is absolute value of the applied overvoltage, and $\varphi(N)$ represents the increased surface tension caused by the addition of new atoms.

Applying the same principle at the anode side, the reaction, which requires the least positive potential, occurs at the anode, unless the potential becomes so positive that a second reaction is possible. In aqueous electrolyte solution, if applied potential is sufficient to produce oxygen, the electrolysis of water will take place. Under some electrochemical conditions, metals may react at the anode surface to form metal oxides. This phenomenon is well established going back to the early

nineteenth century, when electrochemists used galvanic cells as power source to produce metal oxide-coated anode (Schlesinger and Paunovic 2014). The formation of metal oxide on anode depends on the metal ion present and pH of the electrolyte. For example, during the electrolysis of lead ions, deposition of lead on the cathode and lead oxide on the anode will occur simultaneously over a wide pH range. However, with most transition metals a film of metallic hydroxide may form on the anode in alkaline media (according to Eqs. 16 and 17), which is converted subsequently as a result of applied potential to metal oxide. The electrochemical formation of metal oxide film on anode is widely utilized in the modern development of solar cells. However, in some cases the presence of such films reduces the current flowing through the electrochemical cell, and hence the film acts as an insulator.

$$M^{n+}_{(aq)} + OH^{-}_{(aq)} \rightarrow M(OH)_{n(ads)} \tag{16}$$

$$M(OH)_{n(ads)} \rightarrow M_2O_{n(s)} + 2nH^{+}_{(aq)} + ne^{-} \tag{17}$$

In developing potential methods for recovering metal ions from secondary sources, often the solution to be treated will contain more than one metal ion in dilute concentrations, for example, in effluents originating from metal-coating baths, dissolution of spent solder, wire scrap in mining, and hydrometallurgical leaching solutions. In these cases, we need to reclaim individual metals separately for the process to be efficient and economical. Generally, a multistep chemical process is employed including acid/alkali leaching, followed by extraction, cementation, precipitation, or electrowinning (Clancy et al. 2013; Crundwell et al. 2011). Applying electrochemical separation is also possible. Hence, a selective ED of individual metal can be achieved theoretically by careful control of electrode potential and solution media (Grimshaw et al. 2011). There have been several attempts on separate ED from mixed metal ion solutions, e.g., Cu/Cd, Zn/Cu, and Pb/Cu (Doulakas et al. 2000). In many cases, especially those involving Cu, the difference in standard electrode potential ensures that selective ED is effective. A selective ED process can be performed by stabilizing the cathode voltage at the metal potential (referenced to a standard calomel electrode), which allows the selected metal at the selected potential to deposit on the cathode surface. However, the selectivity can be disturbed if impurities or complexing agents of inorganic/organic species are presented. For example, from standard reduction potentials of Sn, Pb, and In (−0.1364, −0.1263, and −0.338 V, respectively), we presume that selective separation of Sn/In and Pb/In is possible. However, in an acidic leaching solution, Pb was electrodeposited on cathode and removed from solution but not indium (Yasri 2001), thus separate ED of In, Sn, and Pb would require careful control of the acidity of the solution and in the presence of complexing agent (Grimes et al. 2017).

Electrochemical methods employing membrane technology (i.e., electrodialysis) are effective for scale-up and metal ion separation. The process of metal separation can be performed by adding chemicals that selectively complex (mask) one group of elements and prevent transportation across the cation exchange membrane (CEM)

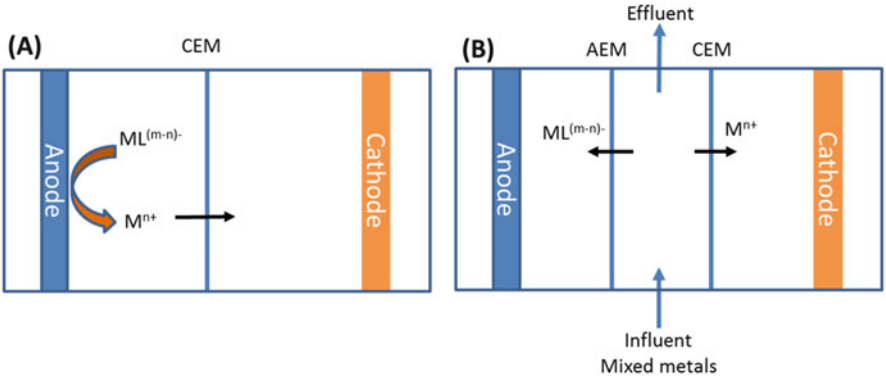

Fig. 1 Two-compartment (**a**) and three-compartment (**b**) electrodialysis cell (Adapted from Chaudhary et al. (2000) and Yasri (2001))

while allowing transportation of unmasked hydrated cations (Allen and Chen 1993; Da browski et al. 2004; Pedersen et al. 2005; Sadrzadeh et al. 2008). The basic concept of the separation process using electrodialysis with enhanced cation and anion exchange is demonstrated in Fig. 1 (Chaudhary et al. 2000; Yasri 2001). Briefly, in a three-compartment electrodialysis cell (Fig. 1b), the separation is achieved by exploiting the greater stability of the complexing agent such as EDTA with one of the metal mixtures. For example, in a three-compartment electrodialysis cell, Ni-$(EDTA)^{2-}$ complex and hydrated Co^{2+} ions are separated by electro-transferring from the feed solution to the electrodialysis anolyte and catholyte chambers, respectively (Chaudhary et al. 2000; Yasri 2001). Applying the same principle, various metal ions are separated, e.g., Cu and Pd from Co (Yasri 2001).

In an electrodialysis system, problems may arise when using a system with a two-compartment cell, i.e., anolyte and catholyte chambers without a middle chamber (see Fig. 1a). The masked metal-EDTA complex will be in immediate contact with the anode surface, which may oxidize due to the anodic oxidation process that causes dissociation of the metal complex, freeing the associated metal and permitting the movement of metal toward the catholyte chamber, which reduces efficiency of the separation process. Here, it is important to use a three-compartment electrodialysis cell (Fig. 1b), in which the metal-EDTA is transferred to the anolyte chamber. Although this complex can be destroyed at the anode surface to release the hydrated metal ions, due to the natural properties of the anion exchange membrane (AEM), these ions cannot cross the membrane to return to the feed or catholyte compartments. Moreover, during the separation process, in the catholyte chamber the hydrated metal ions will either remain in solution or deposit on the cathode depending on the electrolysis condition (e.g., pH, cathode material, type of hydrated metal ions, and concentration).

Electrolysis of Dilute Metal Solutions

Generally, as consequences of industrial processing, toxic metal species, which are to be treated, are found in dilute concentrations, rarely in excess of a few hundred or thousand ppm. During electrolysis, however, the transport of ions in dilute solutions (<1000 ppm) is completely different from that in concentrated solutions. This presents problems for ED and removal of the metals from dilute solutions. Electrolyzing solution containing dilute metal ions, the concentration of these ions will form a gradient from the bulk of the electrolyte to the surface of the electrode where the value at the electrode is zero (that metal ions deposit in metallic structure) at limiting current density creating a diffusion layer (or boundary layer) of thickness ~ 0.5 mm (in unstirred solution). Figure 2 illustrates the boundary layer established between the electrode surface and the bulk of the electrolyte. It can be distinguished that in addition to the concentration gradient, ions are forced to move by convection and migration. But, due to the low concentration of ions in dilute solutions, the most effective way to transport the ion across the boundary layer up to the electrodes is by diffusion. For metal ions to be deposited on the electrode and removed from dilute solutions, the ions must cross the diffusion layer, and for this to occur, the effective thickness of this layer must be small. If the boundary layer thickness is not reduced and the current density is increased beyond that which brings the ion concentration to zero at the electrode surface, then other competing reactions such as the evolution of hydrogen will take place and lower the efficiency of the metal deposition process.

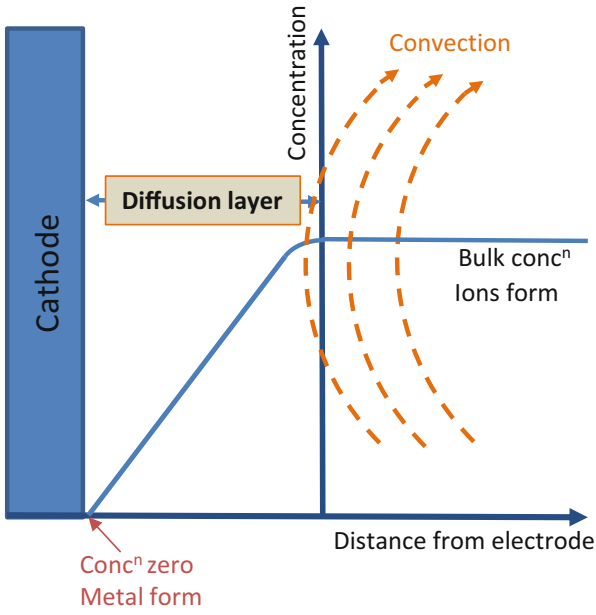

Fig. 2 Diffusion layer is established between a cathode surface and the solution. The concentration gradient of metal ions varies from zero at the cathode surface to the bulk concentration

Fick's laws (Zoski 2006) govern the diffusion of ions in the electrolysis processes. In Fick's first law, the steady-state diffusion flux is theoretically shown to be proportional to the gradient of concentration. Fick's second law is the basis for the treatment of most time-dependent diffusion problems in electrochemistry. In Fick's first law (Eq. 18), the rate of diffusion is directly proportional to the concentration of the dissolved substances, and the rate of diffusion in any given direction is directly proportional to the rate at which the concentration diminishes in that direction.

$$\frac{\mathrm{d}Q}{\mathrm{d}t} = -D(C_\mathrm{b} - C_\mathrm{e})/\mathrm{d}x \tag{18}$$

where $\mathrm{d}Q/\mathrm{d}t$ = flux of the material per second per unit area, D = diffusion coefficient, C_b = concentration of ion studied in the bulk, C_e = concentration of ion studied at the electrode, $\mathrm{d}x$ = distance over which the concentration change occurs, and $(C_\mathrm{b} - C_\mathrm{e})/\mathrm{d}x$ = concentration gradient.

When the ionic concentration is reduced, the forces diffusing the ions to the electrode become progressively less effective, and the diffusion layer becomes more and more depleted of ions. Therefore, the maximum rate at which deposition can occur progressively decreases along with the upper limit of current density, which can be used.

Electrochemical Removal and Recovery of Metals

Electrochemical technologies widely used for toxic metal removal are electrocoagulation (EC), electroflotation (EF), and electrodeposition (ED) (Fu and Wang 2011). Electrochemical treatment is preferred if valuable metals are to be recovered and returned to the production cycle. However, due to the low metal concentration and the presence of various complexing materials in industrial wastes, the task is not as easy as theoretically predicted.

EC and EF are utilized to remediate effluents containing both organic pollutants and heavy metals; thus the principles of both methods are discussed in detail later in sections below. Basically, EC involves the generation of coagulants in situ by electrochemically dissociating Fe or Al anodes into electrolyte solution to coagulate with pollutants at appropriate conditions. EF is a solid/liquid separation process that floats pollutants to the surface by bubbles of hydrogen and oxygen gases generated from water electrolysis. Both techniques can help remove a number of toxic heavy metals from effluents, e.g., Zn (II), Cu (II), Co (II), Ni (II), Ag (I), Cr (III), and Cr (VI). Although heavy metals are removed, huge volumes of sludge generated during the process require further chemical or physicochemical treatments if metals are to be reclaimed. Valuable heavy metals, therefore, are potentially lost in the process. Thus processes such as ED in which metals are reclaimed on the electrode surface are more advantageous.

ED is a clean and effective method usually applied to recover metals from wastewater. It can be appropriately engineered and designed to suit different end-of-industrial operations. Metals can be recovered on the cathode and directly reused or returned to the commercial cycle by melting or dissolving as an anode in electroplating (Issabayeva et al. 2006). Nevertheless, ED of metals from a dilute stream (<1000 ppm), as mentioned previously, poses several major problems due to low mass transfer. To improve the efficiency of ED of metals from low concentration solutions, the required condition is $J < J_L$. Depleting all metal ions in the bulk solution is a time-consuming process. The alternative approach is to increase J_L by reducing the thickness of diffusion layer. This can be achieved by increasing the mass transfer of ions either by increasing the movement of the metal ions through agitation of the solution or by concentrating the ions in the vicinity of the electrode surface. A number of electrolytic cell designs have been proposed to enhance mass transfer within the cell, which involve agitation in combination with a moderately high electrode surface area per unit electrode volume (Kammel 1984). The agitation methods have involved rotating electrodes, mechanical stirring of solution, air agitation, turbulence promoters, slurry, or fluidized bed agitation (Grimm et al. 1998; Houghton and Kuhn 1974; Janssen and Koene 2002; Kammel 1984; Kim et al. 1998; Thilakavathi et al. 2012).

An extended surface electrolysis cell was developed by *Robertson*, with helix sandwich electrode configuration named "Swiss roll" cell (Robertson and Ibl 1977; Fig. 3a). Though good removal of heavy metals ions is achieved from dilute solutions using this cell, claiming the recovered metals was a problem, which required periodic stripping either by leaching the deposited metal in a proper acidic solution or anode dissolution in electrochemical cell.

Agitation of electrolyte between the cathode surface and the solution was employed in various cell designs, e.g., circulating the electrolyte using pumps or by air injection, ultrasound, electrode rotation, or hydraulic agitation of nonconductive particles in the space between the electrodes (Ota et al. 2014; Zoski 2006). Promising metal recovery of various types was achieved by using *Chemilec* cell, which is a fluidized bed cell with inert beads as the fluidizing medium. In *Chemilec* cell (Fig. 3b), the concentration of metal ions increases in the vicinity of the high surface area electrode due to the motion of the fluidized beads and hence increases the recovery rate (Segundo et al. 2012). While some of these cells can be effective in solutions of metal ion concentrations of ~50–150 mg/L (Ferreira 2008; Robertson and Ibl 1977), the performance is limited at the low end and thus does not meet the discharge level, which is typically less than 5.0 ppm and often below 1.0 ppm (Segundo et al. 2012).

The use of concentrator material is a useful in dealing with dilute solutions, which has been described in our recent patent disclosure (Gunasekaran and Yasri 2016). Concentrator electrochemical technique (CET) is used to improve deposition by concentrating metal ions in the electrolyte in an area close to cathode surface. This can be performed by housing a concentrator medium in close vicinity of the cathode surface. Concentrator material (CM) should have a good affinity to metal ions which effectively collects them from the bulk solution at active sites and

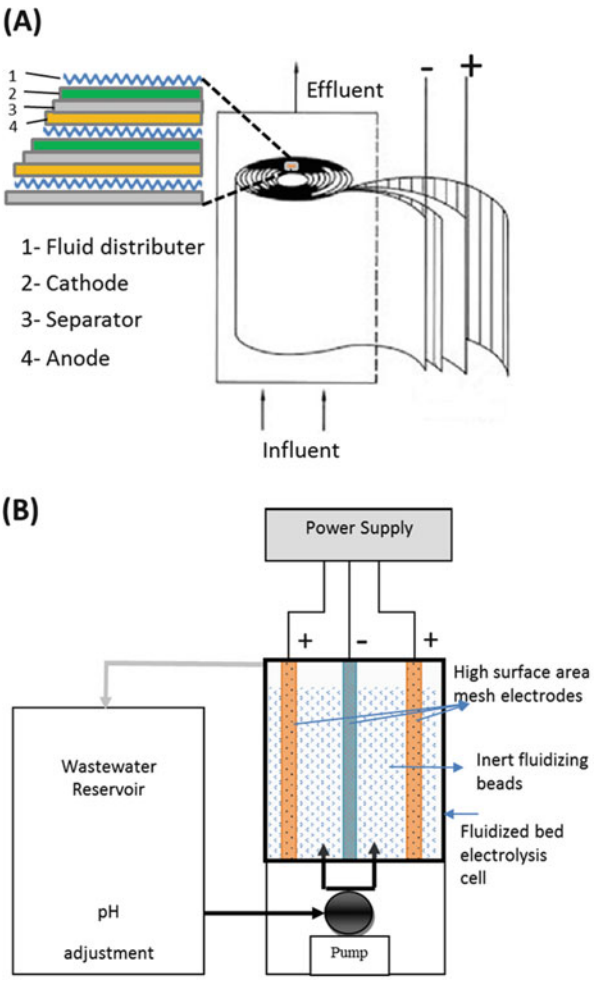

Fig. 3 (**a**) Swiss roll cell (Adapted from Robertson and Ibl 1977), (**b**) *Chemilec cell* consisting of an electrolysis chamber containing inert beads "fluidized" by fluid pressure (Adapted from Yasri 2001)

then releases these ions near the cathode surface improving the condition of ion transfer and ultimately increasing the deposition rate (Gunasekaran and Yasri 2016).

Figure 4a illustrates that the presence of CM reduces the effective distance of ion transfer from "a" to "b," creating a new cell with metal ions concentrated near the electrode surface to increase the metal deposition efficiency (Gunasekaran and Yasri 2016). Very rapid removal of toxic metals (i.e., Cd^{2+}, Cu^{2+}, and Pb^{2+}) from dilute solutions has been achieved using CM compared to that obtained without CM (Yasri 2001).

CET can improve the process of removal and recovery of metals that can be electrochemically deposited on cathode. However, there are exceptions. Some metals such as Ti and Fe, which are very active metals, cannot be electroplated on cathode from aqueous solutions. Smara et al. (Smara et al. 2007) described a

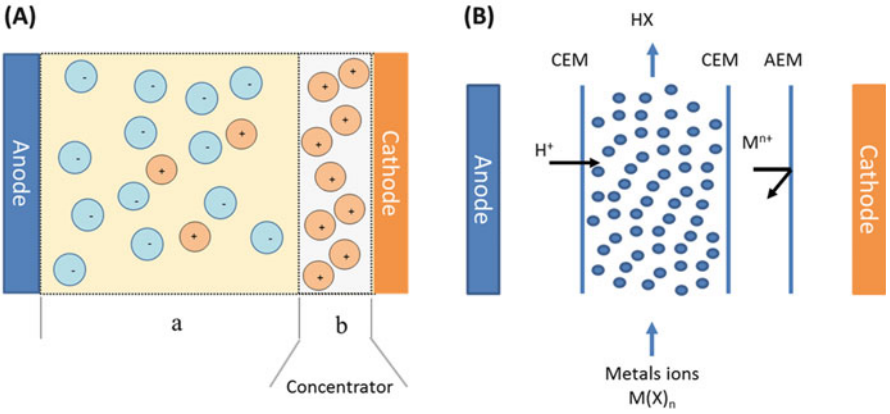

Fig. 4 (**a**) Concentrator material placed near a cathode in an electrochemical cell acts as a concentrating cathode and reduces the effective distance of ion transport from "a" to "b." (**b**) Schematic of a hybrid ion-exchange/electrodialysis cell (Adapted from Smara et al. 2007)

different CET, in which heavy metals are removed from dilute mixtures by a hybrid ion-exchange/electrodialysis process. Toxic heavy metals such as Pb^{2+}, Cu^{2+}, Zn^{2+}, and Cd^{2+} were removed from dilute solutions to meet the discharge limit by continuous electro-permutation combining ion-exchange resins and membranes. Various types of CM such as activated carbon granules, activated carbon cloth, modified graphite, or functionalized copolymers surface can be used, where the choice depends mainly on the affinity of heavy metals to be treated toward the CM and the presence of various organic complexes in the effluent (Yasri 2001). The presence of organic species or complexes with metal ions may result in the alteration of metal ion charge and formation of complexes or chelate, which have low or no affinity to react or adsorb on the CM. Thus the presence of organic species may retard the removal rate of metallic ions.

The most important advantage of using CET is that the process of metal removal accompanies in situ regeneration of the CM within the system. Thus, during electrolysis, reduction of metal ions and water occurs on the cathode surface along with the oxidation of water and other anions at the anode. The electrolysis of water releases H^+ ions and hydronium ions (H_3O^+) on the anode, which move toward the cathode and bring about in situ regeneration of the CM. Thus the in situ regeneration allows prolonged use of CM without the need for external chemical or physical regeneration.

Electrochemical Approaches for Remediation of Organics

Biological treatment is the most popular and highly economical option for treating effluents containing dissolved organics. However, bioremediation is mainly effective for organic molecules, which are biodigestible or biodegradable. When organic

compounds are resistant to biological treatment, however, they will persist in the environment, and in some cases the pollutants adversely affect the traditional biological treatment by inhibiting the biological species. In such cases, effective pretreatment should be considered prior to discharging off to the biological treatment plant. For example, traditional biological inhibitors such as aromatic phenolic compounds or basic heterocyclic aldehyde compounds (e.g., furfural, hydroxymethylfurfural, etc.) are produced during natural hydrolysis of a wide variety of plant materials containing polysaccharide or from industries, which could find their way into the biological treatment plant. Although these compounds are considered toxic to bacteria, they are very soluble and can form highly stable soluble complexes with toxic heavy metals that make the solubilization and hence mobilization of the metal pollutants possible. Evidence shows that underestimating the aggregation of such materials in aqueous systems can adversely affect the health of humans and the environment (Suanon et al. 2016).

A possible strategy to treat such pollutants is by detoxifying the unwanted inhibitor products via a pretreatment, e.g., reduction with chemicals, photolytic treatment, electrochemical treatment, etc. This will render the effluent bioavailable for the subsequent traditional biological treatments. However, selectively remediating one compound in a mixture is not an easy task, and other unwanted by-products could be produced. Thus, a careful thought, analysis, and optimization of the detoxification process coupled with subsequent biological treatment is necessary to eliminate the adverse effects of by-products or to entirely remediate the inhibitors.

Electrochemical treatment is often thought of as an elegant solution to remediation problems due to the ability to control the level of electron transfer of both oxidation and reduction processes. Accordingly, various cell designs have been used to remediate many toxic, biologically resistant, and inhibitor materials (Lee et al. 2015). Thus electrochemistry could be considered in some cases as complete treatment step and in others as a complement to other remediation processes (e.g., biological). For example, selective detoxification of organic compounds that act as bio-inhibitors could be achieved in situ with biological treatment by either oxidation or reduction in electrochemical cell (Cha and Choi 2015). During oxidation, either the generated oxygen at the electrode interface or the electrode itself will accept electrons from organic pollutants using electric energy, break gradually of organic bonding, and form intermediates which differ in molecular shape from the original (that are not recognizable by microorganism as the original inhibitor) (Panizza and Cerisola 2009). During reduction, molecules, for example, microbiological inhibitor “furfural” or “hydroxymethylfurfural,” gain electrons from the electrode surface and reduce to the corresponding alcohol or other reduced molecules that are not inhibitors. The process of electrochemical remediation is highly dependent on the effluent conditions, concentration, and the presence of other pollutants and the fate of end-of-pipe effluent for posttreatment. The electrochemical treatments suitable for organic remediation are (a) electrocoagulation, (b) electro-oxidation, (c) electro-Fenton’s oxidation, (d) electroadsorption, and (e) electro-biological oxidation.

Electrocoagulation

Electrocoagulation (EC) is a technique rapidly growing area of wastewater treatment that uses both principles of electrochemistry and coagulation. Coagulation or flocculation is the process by which particles aggregate and precipitate from colloidal suspension. These aggregation processes are alternative to chemical precipitation for the removal of dissolved and suspended pollutants such as organics or metals from aqueous solutions. Coagulation involves the reduction of electrostatic repulsive forces between the colloidal particles in the solution. It is different from flocculation, which depends on the presence of bridging compounds to form chemical bonding links between the colloidal particles and enmesh the particles in relatively large masses called floc networks (Sahu et al. 2014).

In EC although both agglomeration processes of coagulation and flocculation occur simultaneously, the process is named after coagulation. Generally, the process of coagulation is enhanced by adding certain ions to solution to reduce the electrostatic repulsion between particles to aggregate. Similarly, in EC the electric current helps to reduce electrostatic repulsion, agglomerate organic constituents, and other suspended solids in water. The agglomerated organics have the ability to adsorb certain ionic constituents, making it possible to separate and remove flocculent with a majority of suspended organics and some ionic constituents. A broader approach of electrocoagulation refers to an applied sufficient voltage to sacrificial anodes, such as Fe or Al, allowing the oxidation of anode materials and forming Fe or Al hydroxide flocculent (gelatinous metal hydroxides) within the electrolyte, which can help settle colloidal particles or unwanted pollutant species from the electrolyte (Khandegar and Saroha 2013; Mollah et al. 2001).

Principle

The hydrated metal ions at the anode, particularly those with a charge of +3 or more, tend to act as Brönsted acids (lose H^+ ions from the water molecules bound to them in aqueous solution, Eqs. 19 and 20). The acidity of a metal ion increases with charge and decreases with increasing radius.

$$Fe(H_2O)_6^{3+} \rightarrow Fe(H_2O)_5OH^{2+} + H^+ \rightarrow Fe(H_2O)_4(OH)_2^+ + H^+ \quad (19)$$

$$Fe(H_2O)_6^{3+} + 3HCO_3^- \rightarrow Fe(OH)_{3(S)} + 3CO_2 + 6H_2O \quad (20)$$

The tendency of hydrated metal ions to behave as acids may have a profound effect on the coagulation chemistry. Hydroxide, OH^-, bonded to a metal ion, may function as a bridging group to join two or more metal hydroxides together allowing a dehydration-dimerization process (Eq. 21).

$$2\left[Fe(H_2O)_5OH\right]^{2+} \rightarrow \left[Fe_2(H_2O)_8(OH)_2\right]^{4+} + 2H_2O \quad (21)$$

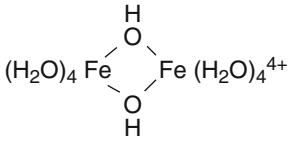

Additional hydrogen ions may detach from water molecules in the dimers, providing OH^- anion for further bonding and leading to the formation of polymeric hydrolytic species. These types of polymers will continue to grow, forming colloidal hydroxyl polymers that eventually precipitate due to gravity, which collectively remove pollutants along within their pores. At the same time, during electrolysis, water is also electrolyzed, producing small bubbles of oxygen at the anode and hydrogen at the cathode. These bubbles attach to flocculated particles and make them lighter and float them to the surface. Besides the coagulation and flocculation processes, synthetic polyelectrolytes such as starch and cellulose derivatives, proteinaceous materials, and gums composed of polysaccharides may be added to stimulate coagulant aggregation. More recently, selected synthetic polymers, including neutral polymers and anionic and cationic polyelectrolytes, that enhance agglomeration have come into use (Sahu et al. 2014).

In the EC cell, as in any electrochemical cell, other reactions occur simultaneously with the aforementioned coagulation reactions, including cathodic reduction of reducible particles, anodic oxidation, and mass transfer of ions in solution, which complicate the process and prevent the prediction of final products. These make EC a complex synergistic process with several reactions and mechanisms occurring simultaneously to remove pollutants.

Metals other than Fe and Al have a similar tendency to form polymeric species with OH^- as a bridging group. These are Be(II), Bi(III), Ce(IV), Co(III), Cu(II), Ga (III), Mo(V), Pb(II), Sc(II), Sn(IV), and U(VI). In commercial and practical EC processes, however, anode materials preferably used are Fe and Al; this is due to the wider pH range (~4 to 11) useful with these ions, reduced cost, and avoidance of introducing environmentally unfriendly metal species into the end of the treatment residues.

Apparatus

The basic EC apparatus consists of electrolysis chamber containing one or more pairs of anode and cathode connected to an external power source (Fig. 5). The design of the electrolysis chamber should expose the contaminated water to electrolysis in batch or continuous system. The electrodes can be designed as plates, perforated plates, or tubes to maximize the efficiency. The electrodes as mentioned earlier could be composed of different materials; however, the most often used are

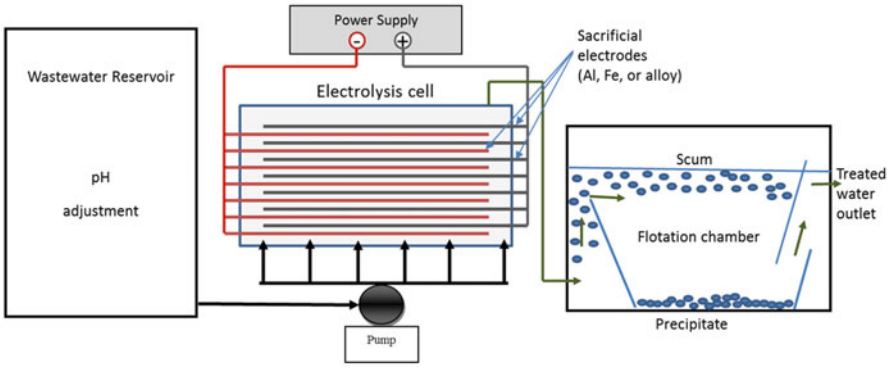

Fig. 5 Schematic presentation of the electrocoagulation reactor. Gravity and floatation are the driving forces for dewatering of the treated effluent

Al, Fe, or stainless steel. A series of electrolysis reaction chambers can be used each with different electrode materials. The electric system, composed of control power supply with typical direct current, is required, although using alternating current technology may prevent the formation of an oxide layer on the anode. The effluent then has to pass to a system to dewater the precipitated/coagulated solids. The principle of dewatering system is to stimulate precipitation of floc/coagulant similar to the settling tank used in conventional treatment plants.

The process optimization of the EC treatment typically includes the type of sacrificial electrode material, distance between the electrodes, electrolyte pH, applied current density, retention time (or reaction time) of the electrolyte, and possible additives to stimulate coagulation or flocculation of particles.

The EC devices are engineered and marketed in various designs that range from electrochemical cells containing simple set of anodes and cathodes to very complex electrochemical assemblies. EC can be attached to an acquisition system to control both the electrode potential and the process of anode scarification. Additionally, EC can also be put in situ with decantation units for precipitate accumulation and integrated with other utilities such as ultrasonic probe, ultraviolet light, or ozone generator, thus achieving in situ so-called advance oxidation.

The EC technique has been extended using bipolar packed beds with metal rings (Öğütveren and Koparal 1992), beads (Jeong et al. 2012), or flat surface (Hu et al. 2008) as bipolar electrodes isolated from each other by electrolyte. The metal bipolar electrodes have to be made of sacrificial metals applying the same principle of the EC, e.g., steel, Fe, or Al can be used. A bipolar packed bed reactor is particularly convenient in achieving high mass transfer because of the large electrode surface area. This arrangement will greatly increase the rate of sacrificial bipolar material to produce coagulant.

Applicability

The EC technology may be effective in the near-neutral water, where coprecipitation with Fe (or Al) hydroxide could remediate relatively clean water. Potential applications of EC system may include pretreatment, or final stage for effluent containing mainly colloidal particles, dissolved organic, suspended solids, and heavy metals, e.g., a high-density sludge in domestic water treatment plant, neutral tailing water in mining industries, and wastewater from food processing, petroleum, oil-sands, and pulp and paper mill industries. However, posttreatment is still required in some cases to final remediation and removal of coagulants formed.

Advantages and Limitations

The main advantage of using EC is its low capital cost, low energy consumption, and minimum requirement of added chemicals, which lower the contamination of the aggregate residues (except for coagulant materials used). The removed pollutants, total dissolved solids, and suspended solids aggregate after treatment (or concentrated) within the coagulants with no major alteration of their chemical structure (except the partial oxidation of some organics due to reaction at the anode surface). Thus, making the recovery of chemicals added from the precipitate after treatment is possible. This is especially important when dealing with high-value chemicals and critical metals or even to reuse the treated effluent.

One of the major limitations of EC, however, is that it can be barely selective for removing a group of pollutants, e.g., heavy metal mixture could be removed simultaneously with organic presences in solution. Other limitations include the need for regularly replacing sacrificial anodes when used, limited efficiency of the process for certain pollutants, and the need for additional control steps to enhance conductivity and pH adjustment (Do and Chen 1994). For example, when the Fe/Al anode of the EC system is oxidized in acidic conditions, no flocculent is formed because Fe and Al are soluble below pH 3. Additionally, the main drawback of EC system is the volume of accumulated precipitates that requires additional treatment units to isolate and dewater the residues.

Electro-Fenton's Oxidation

The Fenton's process, originated by Henry John Horstman Fenton in the late nineteenth century, indicates that highly reactive hydroxyl radicals are formed during the reaction of hydrogen peroxide (H_2O_2) and ferrous (II) ions. Since this finding, reagents involving both H_2O_2 and Fe^{2+} are named Fenton's reagent; however, the application of this as an oxidizing reagent was only realized in the

late 1960s (Huang et al. 1993). During the process H_2O_2 is dissociated and consumed, whereas organic-enriched electrons are oxidized and ferrous ions catalyze the process.

Principle of Fenton's Reaction

The main principles of the Fenton's reaction are the dissociation of the reagent H_2O_2 during the oxidation of Fe^{2+} to Fe^{3+}, the formation of hydroxide anion (OH^-), and the highly reactive hydroxyl radical ($OH^\bullet$) (reaction 22), which attacks and destroys organic pollutants.

$$Fe^{2+} + H_2O_2 \rightarrow Fe^{3+} + OH^- + OH^\bullet \tag{22}$$

The ferrous ions (Fe^{2+}) in Fenton's reagent act as catalyst to initiate the decomposition of H_2O_2 in chain reactions to generate hydroxyl radicals.

Similar to the coagulation process, Fenton's reagent can be generated chemically or electrochemically. Chemically, H_2O_2 is spiked into a solution containing ferrous ions, whereas, electrochemically, the hydroxide radicals are generated in situ within the electrochemical cell. A simplified overall Fenton reaction (Eq. 23) suggests that H^+ (acid environment) is needed for the decomposition of H_2O_2 and to produce the maximum amount of hydroxyl radicals (Walling 1975).

$$2Fe^{2+} + H_2O_2 + 2H^+ \rightarrow 2Fe^{3+} + H_2O \tag{23}$$

Fenton reaction is categorized as one of the advanced oxidation processes (AOPs) (Oturan et al. 2011). The main function of AOPs is the generation of highly reactive free radicals to break the backbone structure of organic pollutants. In Fenton reaction, Fe^{2+} act as redox catalyst for $OH^\bullet$ to break carbon-hydrogen bond in organic molecules and initiate radical chain reactions. Although hydroxyl radicals ($HO^\bullet$) are unstable electrophiles that are effective in destroying organic bonding, the process is very slow in the absence of Fe^{2+}; whereas, the reagent reacts rapidly and non-selectively with nearly all electron-rich organic compounds in the present of Fe^{2+} as catalyst (Wang and Xu 2011). Metal ions other than Fe, for example, cobalt, manganese, and copper, have been used as catalyst to improve the efficiency in Fenton reaction (Pimentel et al. 2008); however Fe^{2+} is the most effective when used at an optimal concentration of 0.1 M soluble $FeSO_4$.

The process of generating radicals in Fenton reaction involves a complex sequence of chain reactions in an aqueous solution. Investigation performed by Barb et al. (1951) on the reactions of ferrous and ferric ions with H_2O_2 suggested that the free radical formation consists of the following chain reactions steps:

$$Fe^{2+} + H_2O_2 \rightarrow Fe^{3+} + OH^- + OH^\bullet \tag{24}$$

$$HO^{\bullet} + H_2O_2 \rightarrow HOO^{\bullet} + H_2O \quad (25)$$

$$Fe^{3+} + HOO^{\bullet} \rightarrow Fe^{2+} + H^{+} + O_2 \quad (26)$$

$$Fe^{2+} + HOO^{\bullet} \rightarrow Fe^{3+} + HOO^{-} \quad (27)$$

$$Fe^{2+} + OH^{\bullet} \rightarrow Fe^{3+} + OH^{-} \quad (28)$$

Equation 24 serves as a chain initiation step and Eqs. 27 and 28 as termination steps, and the cycle in Eqs. 24, 25, and 26 forms the oxidation and regeneration of reagents steps (Neyens and Baeyens 2003). Although many evidences suggest the involvement of hydroxyl radicals in the oxidation of various organic compounds (Walling 1975), others claimed that the reaction between H_2O_2 and Fe(II) produces ferryl ion (FeO^{2+}; an oxidizing Fe(IV) species) as an active intermediate species in the Fenton chemistry (see Eqs. 29 and 30 (Deguillaume et al. 2005)). The presence of ferryl ions suggests a non-radical oxidation reaction pathway of organic substances.

$$Fe^{2+} + H_2O_2 \rightarrow FeO^{2+} + H_2O \quad (29)$$

$$FeO^{2+} + H_2O_2 \rightarrow Fe^{2+} + H_2O + O_2 \quad (30)$$

However, two reaction pathways for the first step in Fenton chemistry are a radical pathway, which considers the production of $OH^{\bullet}$ as a main radical and a non-radical pathway to produce ferryl ions (Deguillaume et al. 2005).

Moreover, Fe (II) acts as catalyst, which means regeneration of ions should take place during the process. Studies have shown that the reaction of H_2O_2 with Fe^{2+} primarily leads to oxidation of Fe^{2+} to ferric ions (Fe^{3+}), which immediately forms an Fe (III)-hydroperoxy complex formulated as $Fe^{III}(HO_2)^{2+}$ (Neyens and Baeyens 2003). A spectrophotometric study has confirmed that the formation of these complexes is very fast that equilibria are attained within a few seconds after mixing of Fe(III) and H_2O_2 solutions (De Laat and Gallard 1999). Once formed, the Fe(III)-hydroperoxy complexes are assumed to decompose to yield Fe^{2+} and $HOO^{\bullet}$:

$$Fe^{3+} + H_2O_2 \rightarrow Fe^{III}(HOO)^{2+} + H^{+} \quad (31)$$

$$Fe^{III}(HOO)^{2+} \rightarrow Fe^{2+} + HOO^{\bullet} \quad (32)$$

The presence of both $HOO^{\bullet}$ and Fe^{2+} in solution leads to a series of chain reactions involving various highly oxidizing free radicals and ions as noted in reactions below:

$$Fe^{2+} + HOO^{\bullet} \rightarrow Fe^{3+} + HOO^{-} \quad (33)$$

$$Fe^{3+} + HOO^{\bullet} \rightarrow Fe^{2+} + O_2 + H^{+} \quad (34)$$

$$OH^{\bullet} + H_2O_2 \rightarrow H_2O + HOO^{\bullet} \quad (35)$$

Oxidation of organic molecules (RH) coexist in solution with Fenton reagent will be initiated by attacking both $OH^{\bullet}$ radicals and Fe ions to produce active organic radicals ($R^{\bullet}$), charged organic species, and dimer species, those react to cause further chemical decomposition of the organic compounds (Neyens and Baeyens 2003).

$$OH^{\bullet} + RH \rightarrow H_2O + R^{\bullet} \tag{36}$$

$$R^{\bullet} + Fe^{3+}(\text{Oxidising}) \rightarrow R^{+} + Fe^{2+} \tag{37}$$

$$R^{\bullet} + Fe^{2+}(\text{Reducing}) \rightarrow R^{-} + Fe^{3+} \tag{38}$$

$$2R^{\bullet}(\text{Rimeriztion}) \rightarrow R - R \tag{39}$$

Organic radicals ($R^{\bullet}$) are very reactive species that simultaneously react in chain reactions to produce spectra of various radical products that may be of higher oxygen content of alkoxyl ($RO^{\bullet}$), alkylperoxyl ($ROO^{\bullet}$), or higher oxidation state. The formed radicals react further causing chemical decomposition of organic contaminant.

$$R^{\bullet} + H_2O_2 \rightarrow ROH + OH^{\bullet} \tag{40}$$

$$R^{\bullet} + O_2 \rightarrow ROO^{\bullet} \tag{41}$$

A mixture of original organic contaminant, free radicals, and ions will continue to react in chain reactions. However, if the pH of the solution reaches a value from 3 to 7, Fe(III) ions generated in the above redox reactions react with hydroxide ions in a similar manner to those found in coagulation process, to form ferric-hydroxo complexes according to Eq. 42.

$$2\left[Fe(H_2O)_sOH\right]^{2+} \rightarrow \left[Fe_2(H_2O)_8(OH)_2\right]^{4+} + 2H_2O \tag{42}$$

These complexes can be observed as small flocs during the Fenton oxidation step that takes relatively a long time to complete (overnight). This observation may account as a termination step and also for the coagulation capability of Fenton's reagent. Thus organic molecules may be captured within the flocs and account for some chemical oxygen demand (COD) removal during the process.

Principle of Electro-Fenton Oxidation

The application of electrochemical field to Fenton process is more efficient than that of Fenton's reagent operated at the same conditions (Zhang et al. 2006). This was attributed to the efficient cathodic regeneration of Fe^{2+} (Brillas et al. 2009). Figure 6 depicts the typical interface reactions occurring at the electrode surfaces during electro-Fenton oxidation (EFO). In EFO, however, highly reactive $OH^{\bullet}$ are generated in situ within the electrochemical cell, which helps the process

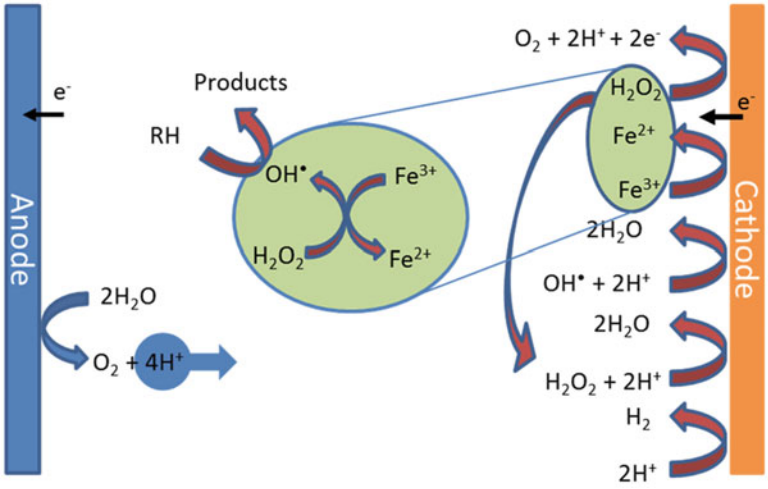

Fig. 6 Schematic illustration of the major reactions occurring during the electro-Fenton process. RH represents the organic pollutants, which undergo oxidation

in many ways, e.g., avoiding the transportation of H_2O_2 reagent, controlling the process of $OH^{\bullet}$ production, and avoiding the storage of H_2O_2 that leads to partial loss of reagent activity. Moreover, in the EFO, Fe sulfate is added as a source of Fe^{2+} catalyst; however, to maintain the catalyst property of Fe^{2+}, the oxidized form (Fe^{3+}) will be reduced at the cathode surface at relatively low reduction potential (E = 0.77 V vs. standard hydrogen electrode, SHE) (Brillas et al. 2009). Thus, the electrode surface will serve to add an extra step to accelerate the production of $OH^{\bullet}$ by increasing the speed of Fe^{2+} production (see Eq. 24).

Categories of electro-Fenton process can be divided based on the process operation and method of introducing the reagent into the reactor; i.e., reagent Fe^{2+} and H_2O_2 are either added externally or generated in the electrochemical reactor (Zhang et al. 2006). In the first case, Fe^{2+} (or Fe^{3+}) are externally added whereas H_2O_2 is internally generated at the electrodes (see electrochemical production of H_2O_2 in the next section). In the second case both H_2O_2 and Fe^{2+} are generated within the cell using a sacrificial Fe or steel anode. The third case involves external simultaneous addition of both reagents (Fe ions either Fe^{2+} or Fe^{3+} and H_2O_2) and is known as Fere-Fenton method (Chou et al. 1999).

The kinetics of electro-Fenton oxidation process is presented in Eq. 43, and the kinetics of organic decomposition is determined using Eq. 44:

$$\mathrm{RH} + \mathrm{OH}^{\bullet} \rightarrow \text{Oxidation products} \tag{43}$$

$$\frac{\mathrm{d}[\mathrm{RH}]}{\mathrm{d}t} = K_{\mathrm{abs}}\,[\mathrm{RH}][\mathrm{OH}^{\bullet}] \tag{44}$$

where K_{abs} is the absolute rate constant of the reaction and [RH] and [$OH^{\bullet}$] the concentration of organic and hydroxyl radicals, respectively.

Considering, however, $OH^{\bullet}$ are reactive species and their concentration never accumulates in solution, they could be considered constant, and the kinetic rate of reaction, therefore, is considered first order.

Electrochemical Production of H_2O_2

As mentioned previously, H_2O_2 could be produced as a result of electrolysis at certain conditions in aqueous media. We present a brief description of the possible mechanism of H_2O_2 production to give an overview of the electro-Fenton process. For more details on the conditions required to produce stable H_2O_2 with higher yield, readers are referred to various articles in the literature (Brillas et al. 2009). Basically, H_2O_2 could be electrogenerated using parallel plates in an electrochemical cell to reduce dissolved oxygen (DO) or sparged O_2 (or air) in acidic solutions containing dilute supporting electrolyte (Qiang et al. 2002). DO is reduced in acidic medium at the cathode surface to H_2O_2 according to Eq. 45.

$$O_2 + 2H^+ + 2e \rightarrow H_2O_2 \tag{45}$$

In electro-Fenton, the in situ production of H_2O_2 is a value-added process that reduces the hazardous transportation of the material itself and avoids dissociation of H_2O_2 during storage. Electrochemical production of H_2O_2 occurs at low potential ($E^o = 0.44$ V vs. SCE), in homogeneous environment, with divided or undivided cells. In undivided electrochemical cell, the main competing reaction is the decomposition of H_2O_2 itself at the cathode surface to produce water molecules (Eq. 46). Thus, the cathode material has a significant impact on the decomposition of H_2O_2, which is attributed to the hydrogen overpotential of the cathode material. Reports show that the decomposition rate of H_2O_2 on graphite cathode in alkaline solutions is less than on metal cathodes such as copper, stainless steel, lead, and nickel (Sudoh et al. 1985). Graphite exhibits a high overpotential for H_2 evolution and low catalytic activity for H_2O_2 decomposition, along with relatively good stability, conductivity, and chemical resistance.

$$H_2O_2 + 2H^+ + 2e \rightarrow H_2O \tag{46}$$

Though, the use of flow-type electrochemical cell system helps to avoid accumulation of H_2O_2 at the cathode surface (Eloy Isarain-Chávez et al. 2013). Thus H_2O_2 production from DO in flow-type system will serve the purpose for Fenton process and can be carried out selectively in acidic medium.

Advantages and Limitations of the Electro-Fenton Process

Unlike the Fenton, the electro-Fenton process is less expensive and less risky in handling chemicals, especially for H_2O_2 production, which could be generated in situ. Additionally, the main advantage is the extra control parameter of the electrode potential that allows controlling anode scarification, overall process degradation, and continuous regeneration of ferrous (II) catalyst at the cathode, which advance the degradation rate of organic pollutants and minimize sludge production (Nidheesh and Gandhimathi 2012). As compared with the Fenton process, the electro-Fenton is highly efficient, with less sludge production; however, sludge is still produced and dewatering of the end product precipitate is one of the drawbacks.

Parameters limiting the operation of electro-Fenton process include the pH of the effluent treated, rate of DO (or O_2 sparging), applied current, Fe^{2+} concentration, H_2O_2 concentration, electrode type, and cell design. Most of these parameters are optimizable for the best efficiency and least cost.

The pH of the electrolyte solution is considered the most important factor for the electro-Fenton process. Many interference reactions may occur due to variations in the pH. For example, Fe species begin to precipitate as $Fe(OH)_3$ at pH $>$ 3 that reduce the electro-Fenton and enhance removing pollutants via electrostatic attraction and coagulation (Mollah et al. 2001). However, researchers have reported that at lower pH values, Fe ions form stable complex species with H_2O_2, which also participates and inhibits the Fenton process (Wang et al. 2010c). However, pH 3 is considered optimal for the Fenton (and electro-Fenton) process, which helps the stability of oxonium ions ($H_3O_2^+$) according to Eq. 47; at this low pH decomposition reaction may also take place according to Eq. 48.

$$H_2O_2 + H^+ \rightarrow 2H_3O_2^+ \tag{47}$$

$$H_2O_2 + 2H^+ + 2e^- \rightarrow 2H_2O \tag{48}$$

At higher pH (7.0<), however, H_2O_2 rapidly decomposes to oxygen and water (Wang and Lemley 2001). Though, according to many reports pH ~3.0 is the most efficient for the electro-Fenton process (Brillas et al. 2009). But, considering the fact that pH of treated wastewater is usually higher than 3.0, adjusting the optimal pH to 3.0 is problematic and disadvantageous to the electro-Fenton process because of the additional step of pH adjustment as well as the chemicals needed.

In contrast, during the in situ production of H_2O_2, oxygen is sparged into the system (see electrochemical production of H_2O_2). Meaning that increasing the oxygen sparging rate can increase the DO concentration and the mass transfer rate of DO, hence increasing the production of H_2O_2 (Wang et al. 2010c). Therefore, the rate of DO or external O_2 supply to the system will have a profound effect on the process (considering that there is no other external H_2O_2 source to the system). One of the important factors affecting the DO rate is temperature, i.e., the DO rate decreases with increasing temperature. Although some reports showed

that increasing the temperature of operation will increase the generation rate of oxidizing species (such as $HO^{\bullet}$ or high-valence Fe species) (Sun et al. 2007), higher temperature will also increase self-decomposition of H_2O_2 (Özcan et al. 2008), and the optimum operating temperature is about 30 °C (Umar et al. 2010).

Moreover, the applied current can limit the electro-Fenton process, which even provokes reverse reactions or competitive reactions such as hydrogen production at the cathode and oxygen discharge at the anode. Accordingly, some studies have indicated that the upper limit of current density in the electro-Fenton process is about 6.4 A/m^2 and not exceeding 10 A/m^2 (Jiang and Zhang 2007).

Similarly, increasing the concentration of Fe^{2+} in the electro-Fenton process will enhance the consumption of $HO^{\bullet}$ radicals according to termination reaction (Eq. 28). Thus, increasing the Fe^{2+} concentration may adversely affect the process. Hence, the effects of both components of Fenton's reagent (Fe^{2+} and H_2O_2) are closely linked, and the optimization experiments are usually performed on the basis of their ratio ($[Fe^{2+}]/[H_2O_2]$) (Brillas et al. 2009; Ting et al. 2009). Depending on the persistence of the effluent to be treated, however, the level of $[Fe^{2+}]$ in the electro-Fenton process can range from 0.2 mM (Liu et al. 2007a) up to 2.0 mM (Wang et al. 2010c) and not exceeding 15 mM (Wang et al. 2008). Whereas for H_2O_2 the initial concentration should range from 25 mM (Ting et al. 2009) up to about 60 mM (Anotai et al. 2010).

Additionally, the feeding mode of H_2O_2 has a profound effect on the treatment process (Ting et al. 2009). H_2O_2 could be fed to electro-Fenton cell in single addition and in a timed sequence or, as discussed previously, produced in situ electrochemically. When H_2O_2 is added in one step or fed in quick sequence, its initial concentration will be the highest during the reaction, which will unfavorably affect the lifetime and the level of the produced hydroxyl radicals in the medium that to be scavenged by the H_2O_2 itself according to Eq. 50 (Zhang et al. 2007).

$$Fe^{2+} + HO^{\bullet} \rightarrow Fe^{3+} + OH^{-} \tag{49}$$

$$HO^{\bullet} + H_2O_2 \rightarrow HOO^{\bullet} + H_2O \tag{50}$$

Considering the weaker oxidizing power of hydroperoxyl radical ($HOO^{\bullet}$) and to avoid the scavenging effect, sequential addition of H_2O_2 or in situ production is preferred.

Apparatus

The essential part of electro-Fenton reactors and the design of the apparatus are mostly depending on the design of the electrolytic chamber and the type of the electrodes housed in it. Several types of reactors have been utilized with various designs to optimize the efficiency of the process and to assist the method of

introducing the reagents into the reactor. Typical electrolytic reactors and electrodes used for the process and found in the literature have been reviewed and summarized by Brillas et al. (2009) and Nidheesh and Gandhimathi (2012). Briefly, reactors used for electro-Fenton's process are oxygen or air bubbling reactor (Brillas and Casado 2002; Rosales et al. 2012; Rosales et al. 2009), divided electrolytic chambers, or undivided electrolytic cell. On laboratory scale, air bubbling reactor with moderate volume (not exceeding 1.0 L) has been successfully used to decolor dye and textile wastewater (Rosales et al. 2012; Rosales et al. 2009). The reactor is usually designed to produce H_2O_2 electrochemically via oxygen reduction on the cathode. Therefore, continuous saturation of air at atmospheric pressure is made by bubbling air near the cathode to insure a constant O_2 level in the chamber. Similarly, diaphragm-divided or undivided electrolytic cells could be utilized as an electro-Fenton reactor with in situ H_2O_2 electrogenerated at the cathode (or fed from external sources to catholyte chamber). Divided apparatus usually consist of two half-cells (a cathodic compartment and an anodic compartment), which are connected by a salt bridge or brought together with diaphragm or membrane separator. The effluent is treated in the cathodic chamber in batches or as continues flow. Electrolysis occurs under constant current conditions using a direct current power supply between the cathode and the anode. Since the cathode material highly influences process efficiency, it should be chosen to have low interface oxygen overpotential to facilitate rapid production of hydroxyl radicals simultaneously with the reduction of Fe (III) ions. Reaction at the cathode surface is the key to the process that cathode is denoted, in some cases, as the working electrode whereas the anode is denoted as a counter electrode. Various materials or chemically modified surface of graphite, carbon, activated carbon, carbon cloth, boron-doped diamond (BDD), Pt, or stainless steel are used as cathodes for wastewater treatment (Nidheesh and Gandhimathi 2012). The use of different composite cathode materials or surface-modified nanoparticles is emerging as cathode materials for lower interface overpotential and enhances more uniform current distribution at the electrode surface. These include chitosan (Li et al. 2009), carbon nanotubes decorated nanoparticles (Ai et al. 2008), and graphene-based nanocomposite (Le et al. 2015). On the other side, anodes are placed at an appropriate distance away from the cathode, considering that the higher distance between the electrodes leads to an increase in ohmic drop through the electrolyte and then an equivalent increase in cell voltage and energy consumption. Additionally, selection of unstable anode will cause deterioration of electrode in electrolytic cells. Therefore, dissolution-resistant anode that is highly stable and unable to electrolyze into solution is ideal for the process. The most stable anode for electro-Fenton conditions is Pt; however, due to its high cost, materials such as BDD, titanium coated with TiO_2, IrO_2/RuO_2, $IrO_2/SnO_2/Sb_2O_5$, etc. are used.

Electro-Oxidation

Electrochemical oxidation or "anodic oxidation" was introduced in the early 1970s to destroy organic molecules and has been applied widely for the treatment of wastewater from the textile and related industries. The technique is very effective in color removal by breaking the conjugated bonds in dye molecules; during the process colorless compounds are formed upon rupturing the dye molecule. It means that the conjugated chromophore systems which give color to dye molecules in some cases are easy to rupture, which points to the fact that the molecule is only partially decomposed to colorless compounds. This was satisfactory to the textile industries to meet with the public demands to reduce dye and color leached into the wastewater system. Although this satisfies the requirement of decolorization, it is unlikely that the method will lead to complete mineralization without going through a series of organic intermediates. The degradation of dye molecules can result in the formation of noncolored dye fragments and can result in the formation of environmentally unfriendly degradation products such as aromatic amines and chloro-organic compounds (Donaldson et al. 2002).

For anodic oxidation, an electrochemical cell requires a two-electrode system of cathode and anode (mesh or plate). Multiple electrodes could be used; however, the types of anode material and electrolyte have a great impact on the oxidation mechanism, on the end products and the efficiency of the oxidation process. High oxygen evolution, stable, non-sacrificial anodes are required for prolonged operation and to avoid electrode dissolution during electrolysis. On the other side of the cell, depending on the application, cathode consisting of mild steel, titanium, or graphite is widely used.

Generally, electrochemical oxidation takes place in an electrolyte that facilitates transfer of ions between two electrodes. When conductivity of the effluent is low, electrolyte should be added to increase the conductivity and to help generate free radicals for the oxidation process to take place. In this process organic compounds are oxidized effectively with little consumption of chemicals and with little or no sludge production. Previous investigations have shown that salt (NaCl) is an effective electrolyte for the electro-oxidation (EO) of organics from wastewater.

In EO, two mechanisms can be distinguished for remediation of organic pollutants: (1) direct anodic oxidation that occurs at the electrode-solution interface and (2) indirect anodic oxidation that occurs via surface active specious generated continuously at the electrode surface and reacts within the electrolyte to convert the carbon backbone structures of pollutant molecules to smaller fractions or theoretically to carbon dioxide and water. Spontaneous direct and indirect mechanisms could also occur during remediation.

Direct Anodic Oxidation

In direct electrolysis, generally, at a specific electrode potential, the pollutants are oxidized after adsorption at the electrode surface. The mechanism generally involves the formation and adsorption of hydroxyl radicals at the anode surface (M) (Eq. 51) (Guven et al. 2008), which enhances the participation of organic pollutants (R) in direct electron transfer at the electrode surface and hence the process of oxidation (Eq. 52).

$$H_2O + M \rightarrow M[OH^{\bullet}] + H^+ + e^- \quad (51)$$

$$R + M[OH^{\bullet}] \rightarrow M + RO + H^+ + e^- \quad (52)$$

The process is known as catalytic electrode oxidation, and a specific potential is required to allow oxidation to occur that is called "catalytic oxidation potential". Depending on the anode surface material and its electrocatalytic activity, oxidation is theoretically possible at a potential lower than the oxygen overpotential (no oxygen evolution). Oxygen is transferred from water to the organic pollutant with the aid of electric energy at the anode surface interface. In this reaction, water is the source of oxygen atoms for the oxidation of organic molecules to form ideally an oxidized form of the molecules at the anode.

Traditionally, noble metals such as Pt and palladium, as well as metal oxide-coated anodes, e.g., iridium dioxide, ruthenium-titanium dioxide, iridium-titanium dioxide, and lead dioxide, possess high oxygen overpotential and are good catalysts to use as anode for direct anodic oxidation. Recently, metal nanoparticles (MNP) and their derivatives have emerged as promising electrode materials for direct electrochemical oxidation at fixed anodic potential due to their large surface-to-volume ratio, biocompatibility, and low price. Popular MNP candidates for electrode modification are cobalt (Co) (Yin et al. 2009), nickel (Ni) (Chauke et al. 2010), iron (Fe(II,III)) (Yin et al. 2011), zinc (Zn) (Najafi et al. 2014), ruthenium (Ru) (Li et al. 2010), and tungsten (W) (Peng et al. 2014). However, the main problem of EO using MNP-modified electrodes is the inherent structure of these materials and oxidation susceptibility of pollutant, leading to deactivation of MNP and their derivatives, commonly called electrode poisoning effect, due to the high affinity of MNP to adsorb pollutants forming of a polymer layer on the anode surface (Jiao et al. 2014). Thus deactivation is less pronounced with weaker adsorption properties or inert surface such as BDD (Panizza and Cerisola 2009).

A promising new generation of electrodes modified with nanoparticles of non-metallic, carbon-based backbone structure is under investigation for various electrocatalytic oxidation purposes. Materials such as carbon nanotubes (Ruoff and Lorents 1995), graphene (Geim and Novoselov 2007), graphene oxide (Dreyer et al. 2010), and modified structure of these materials are widely investigated. Typically, chemical reactions performed on organic molecules and surfaces have been used as starting points for chemical functionalization of these carbon-based nanomaterial structures. Specifically, changing the doping level with foreign atoms

is an effective method to intrinsically modify the properties of pristine host materials (Lim et al. 2010). Among them, nitrogen doping plays a critical role in regulating the electronic (Wang et al. 2010e) and the catalytic properties of the modified electrode (Yasri et al. 2014, Yasri et al. 2015a). The heteroatoms present in the graphitic framework make these catalysts nonelectron neutral, favor the molecular adsorption and consequently enhance specific redox reactions at the electrode interface (Liang et al. 2012). Doped carbon-based backbone structures find wide applications as metal-free, cost-effective electrodes for highly efficient electrochemical catalytic oxidation.

Indirect Electro-Oxidation

Indirect EO involves attacking the pollutant molecules within the bulk solution by several oxidizing species formed under the electrolysis conditions at sufficient applied potential (Israilides et al. 1997; Kim et al. 2002b). It can be performed at overpotential exceeding the value of oxygen evolution, so that water discharges at the electrode, forming free radicals during the process of oxygen evolution that ideally oxidizes organic pollutants to release CO_2 at the anode and discharge protons. However, when no electrolyte is present, current efficiency is reduced due to oxygen evolution at the electrode surface. On the other hand, the idea of indirect EO is to oxidize pollutants in a sustainable manner; thus avoiding high overpotential is preferred to prevent electrode fouling. Attempt is usually made to facilitate indirect electron transfer between anode surface and pollutants by electrochemically generating redox reagents at low potential; these materials act as electron shuttle or mediator between the electrode and the organic pollutants.

Generally, electrolytes act as mediators or redox catalyst in the reaction media enhancing the destruction efficiency of pollutants (Panizza and Cerisola 2009). In this case, if electrolyte is present, various species and radicals may be formed to attack organics spontaneously. Hence the type of oxidation products and intermediates would highly depend on the type of electrolyte present. For example, oxidizing species could be formed upon anodic reaction, e.g., active chlorine, ozone, and persulfates, or at cathodic reaction, e.g., hydrogen peroxide. If chlorine is in the solution, species such as Cl_2, $Cl^{\bullet}$, ClO^-, ClO_2, $Cl_2^{\bullet -}$, O_3, $OH^{\bullet}$, $O^{\bullet}$, H_2O_2, O_2, H_2, and CO_2 can be formed in the electrolyte (Donaldson et al. 2002; Israilides et al. 1997; Park et al. 2009). In these cases, highly tolerant electrode should be used, to prevent fouling of the electrode or polymer formation at the electrode surface. Though, active radicals and ions present within the medium may integrate into the system to react with organic pollutants. For instance, considering a basic scenario when electrolyzing solution containing chloride ions (Cl^-), this will result in the formation of Cl_2 as well as hydronium ions (H_3O^+) at the anode surface, and at the same time water molecules are hydrolyzed at the cathode surface to form hydroxyl ions (OH^-). Chlorine will participate indirectly in anodic oxidation by

forming hypochlorite ions (ClO^-) in alkaline medium (Eq. 53) and chlorite (ClO_2^-) and chlorate (ClO_3^-) ions (Eqs. 54 and 55) in stronger alkaline medium (Fernandes et al. 2004).

$$Cl_2 + 2OH^- \rightarrow ClO^- + H_2O + Cl^- \tag{53}$$

$$ClO^- + 2OH- \rightarrow ClO_2^- + H_2O + 2e^- \tag{54}$$

$$ClO_2^- + 2OH^- \rightarrow ClO_3^- + H_2O + 2e^- \tag{55}$$

Ions and radicals formed at the electrode surfaces are free to move within the electrolyte and react with organics to produce intermediates during the process. The potentials of various species to react with pollutants and to form intermediates are strongly dependent on the pH, the initial electrolyte concentration, the pollutant, the electrode type and the solution medium (Al-Haq and Gómez-López 2012; Panizza and Cerisola 2009).

Numerous researchers have studied the mechanism of anodic oxidation and the possible intermediate products. For instance, dyes such as blue 2 K decolorized during anodic oxidation due to the breakdown of diazo conjugated bonding according to Eq. 56 (Naumczyk et al. 1996).

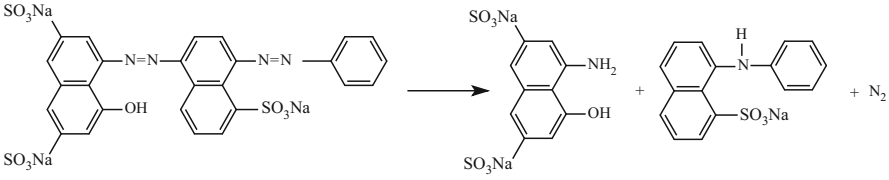

(56)

It has been also reported that in the presence of salt NaCl as electrolyte, there is evidence for the formation of chlorinated organic products (Naumczyk et al. 1996). For example, dyes such as light orange 6 and methylene blue are oxidized in the presence of hypochlorite or in electrochemical reactor to form various fragments containing chlorine in their structure (see Eq. 57 (Naumczyk et al. 1996) and scheme in Fig. 7 (Donaldson et al. 2002; Yasri 2001)):

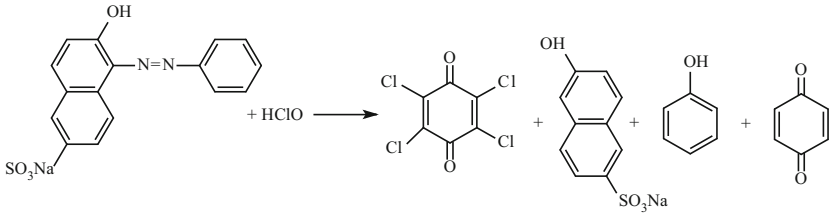

(57)

Since these intermediates, and particularly the chlorinated compounds, may be more harmful to the aqueous environment than the organic molecules from which

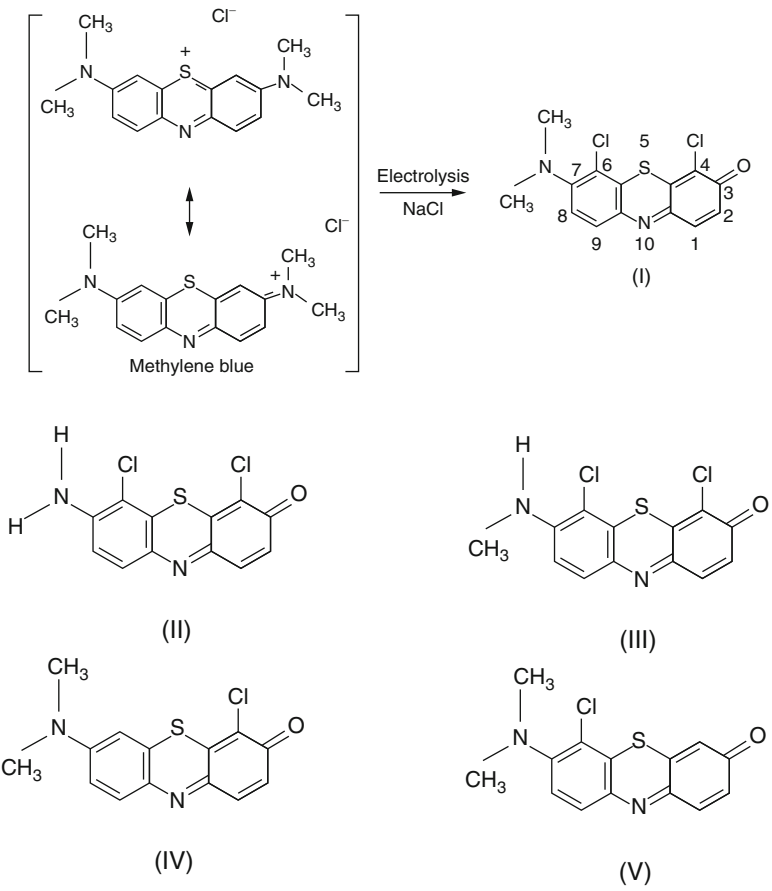

Fig. 7 Intermediate (I–V) formed during the electrochemical oxidation of methylene blue in chlorinated medium (From Donaldson et al. (2002) and Yasri (2001))

they are formed, it is necessary to set additional process to eliminate the discharge of hazardous products to waste stream. In this aspect we and others have shown such chlorinated intermediates can be effectively eliminated (Cong and Wu 2007; Yasri 2001) if subjected to further activated carbon polishing (Rajkumar and Palanivelu 2004) or electroadsorption treatment (Yasri et al. 2015b).

Electrochemical System for Electro-Oxidation

Due to the wide range and diverse features of industrial wastes and conditions that usually contain a mixture of organic and inorganic compounds, no common EO reactor is in use. Process optimization is achieved by the nature and structure of the

electrode material, experimental conditions, and electrolyte composition. Hence, no single end-of-pipe reactor design is suitable for all EO applications. The most important part in EO apparatus are the electrodes that serve as catalyst for the oxidation reaction. To high destruction efficiency, many different electrodes (especially anodes) have been investigated for their direct and/or indirect EO ability. In practice, however, most anodes are capable of both direct and indirect EO, i.e., by applying high overvoltage; both reactions could occur simultaneously to participate in organic oxidation and oxygen evolution reactions.

There are numerous electrode types for remediating various pollutants (Martinez-Huitle and Ferro 2006; Panizza and Cerisola 2009; Wu et al. 2014). Among these Pt is considered as ideal anode for EO of various pollutants, e.g., phenol, chlorophenols, glucose, benzene, hydroxybenzoic acid, methanol and formic acid, synthetic dyes, herbicides, and naphthalene-sulfonic acids (Panizza and Cerisola 2009). Pt electrodes are commonly known as dimensionally stable anodes (DSA) as they are highly stable under relatively high applied voltage, inert to many chemical reactions, and have low hydrogen and oxygen overpotentials, i.e., hydrogen is oxidized and protons are reduced readily at the Pt surface in aqueous solution. In practice, however, since the cost of Pt electrodes is high, industries prefer to replace it with other type of DSAs.

Electrodes of pristine metal (M) coated with metal oxide (MO) such as ruthenium oxide (RuO_2), iridium oxide (IrO_2), tin oxide (SnO_2), antimony pentoxide (Sb_2O_5), lead dioxide (PbO_2), or mixed metal oxides (that contain more than one metal oxide) find their application as DSAs with practical oxidation efficiency. The pristine electrodes usually are of nontoxic, rigid, easy to fabricate metals such as titanium (Ti) or tin (Sn) and Ti being the most popular due to its physical properties, e.g., low density, easy machinability, high anticorrosion, and relatively low cost. Pristine Pb electrode coated with PbO_2 (Pb/PbO_2) has been tested for EO of organics and considered as a stable anode material, relatively inexpensive and effective in oxidizing pollutants. However, the high toxicity of Pb, its propensity for electrochemical corrosion, and the need to avoid Pb contamination due to the release of Pb^{2+} prevent the use of Pb/PbO_2 as a stable anode (Martinez-Huitle and Ferro 2006).

Generally, metal oxides represent one of the most important categories of solid catalysts due to their acid-base and redox properties, which are widely used as active phases in either chemical or electrochemical reactions (Wu et al. 2014). The use of metal oxide (or mixed metal oxide)-coated electrode (M/MO) enhances the oxygen evolution reaction, allows the use of anode at fairly high potential, and due to their surface properties increases the catalytic oxidation of organics (Wu et al. 2014). Moreover, mixed metal oxides may exhibit, in some cases, a significant improvement in catalytic activity than their respective single-component metal oxides, perhaps due to the increase in active acidic or basic sites or change in the chemical states of the metal ions (Alaya and Rabah 2013). Electrodes coated with metal oxides may be prepared by electrodeposition at the anode surface (anodization) by applying electric potential to solution containing the desired metal ions after adjusting pH suitably. Other appropriate surface-spreading methods,

e.g., sol-gel, spin coating, chemical vapor deposition, or thermochemical decomposition (Wu et al. 2014), are also used to prepare such electrodes.

The important fact in M/MO anode is that during the synthesis, metal oxides are formed at the anode surface at applied potential by oxidizing the metal species present in solution, so that increasing the applied potential to value exceeding the synthesis potential will stabilize the MO on anode. This explains the stability (un-deterioration) of metal oxide-coated anode when operating at high cell voltage and can be categorized as DSA.

Titanium base metal coated with RuO_2 is usually a good catalyst when dealing with solution containing chlorine and hence is utilized for chloralkali processing (Panizza and Cerisola 2009). On the other hand, IrO_2-coated Ti is a good electrode for oxygen evolution and used for water electrolysis and metal electrowinning (Kulandaisamy et al. 1997). Considering other types of coating, SnO_2 doped with Sb or other entities such as Ar, B, Bi, F, Cl, P, etc. finds wide applications in electrochemical oxidation. Chemically, SnO_2 is a semiconductor (n-type) with low conductivity (Donaldson 2007); however, when SnO_2 is doped with an electron donor or acceptor, the conductivity is highly improved. For example, electrode coated with Sb-doped SnO_2 exhibits a good conductivity with oxygen overpotential (1.9 V vs. SHE) that is slightly higher than that of Pt electrode (i.e., 1.6 V vs. SHE in 0.5 M H_2SO_4). This property makes Sb-doped SnO_2 attractive for anodic oxidation of organics. Indeed, SnO_2-Sb_2O_5-coated Ti electrode advanced Pt anode with nearly fivefold higher in efficiency and completes remediation of a wide range of organic compounds from wastewater (Ding et al. 2007; Stucki et al. 1991). Although laboratory research documents the high advantage of Ti/SnO_2-Sb_2O_5 electrode, commercially it is unavailable due to the short service life (maximum of 15 h) (Ding et al. 2007).

There is a growing interest in BDD as a new electrode material that has high conductivity, which is commercially feasible at fairly reasonable cost (Panizza and Cerisola 2009). The electrode is usually prepared from pristine conductive or nonconductive materials such as Si, Ta, Nb, W, Mo, and glassy carbon (Martinez-Huitle and Ferro 2006; Panizza and Cerisola 2009). The pristine material is coated with diamond by energy-assisted (plasma or hot filament) chemical vapor deposition; it is made conductive by doping with various levels of boron atoms (Scarsbrook et al. 2007). These types of electrodes possess (Fuchigami et al. 2014) a wide potential window (~ 3.0 V between oxygen and hydrogen evolution), stability in very aggressive media, and inert surface with low adsorption properties of organic pollutants. Thus, BDD are widely used for near-complete remediation of a wide range of organic pollutants in wastewater, e.g., textile dyes (Faouzi et al. 2007), bisphenol (Murugananthan et al. 2008), phenolic compounds (Iniesta et al. 2001; Morão et al. 2004), endocrine disruptor compounds (Yoshihara and Murugananthan 2009), carboxylic acids (Gandini et al. 2000), benzoic acid (Montilla et al. 2002), organic acids (Chailapakul et al. 2000), pharmaceutical waste (Brillas et al. 2005; Murugananthan et al. 2010), surfactants (Panizza et al. 2005), and real wastewater (Zhu et al. 2009).

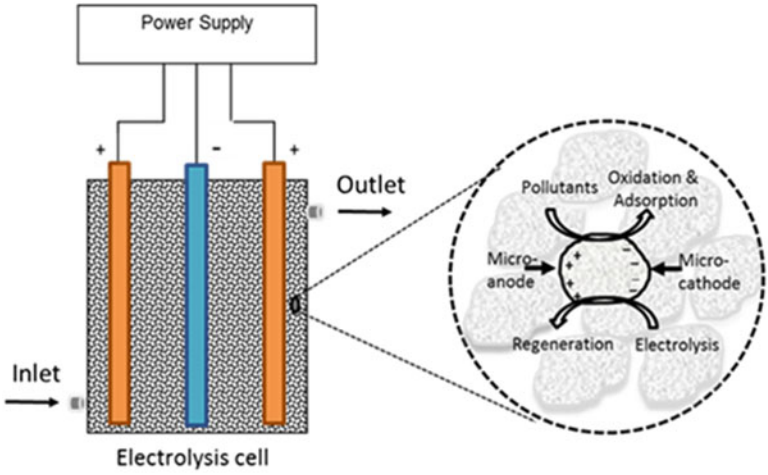

Fig. 8 Schematic representation of electroadsorption (EA) unit. Under the applied electric field, micro-anodes and micro-cathodes are established on adsorbent particles. The formation of numerous microelectrolytic cells enhances simultaneous oxidation, adsorption, and regeneration processes

Other anode materials widely employed for EO are carbon-based and graphite electrodes, such as graphite rod, graphite felt, carbon cloth, carbon paper, granules, and brushes. For graphite electrodes (sheets or rod), the current efficiency of anodic oxidation is low (Martinez-Huitle and Ferro 2006). Increasing the applied potential is accompanied by surface deterioration due to exfoliation of the surface particles (to form partially oxidized graphene nanoparticles (Yasri et al. 2014)), which reduces the lifetime and limits their application for anodic oxidation (Martinez-Huitle and Ferro 2006). However, the use of these types of electrodes is preferred as they are very cheap and possible to be fabricated with high porosity and large surface area and can combine adsorption and electrochemical degradation of pollutants. Indeed, the possible use of graphite material, especially of granule activated carbon as adsorbents and at the same time in applied field as electrode oxidizers has widened the scope of their applications in the so-called three-dimensional (3-D) electrode systems (Yasri et al. 2015b). In 3-D electrode system, the graphite particles are filled in the electrochemical system as in packed bed (see Fig. 8) or as fluidized bed to act as electroadsorption (EA) cell.

Adsorption is commonly used to remove dilute toxicants from effluents. This is done in an EA cell by means of adsorbent particles of activated carbon under an applied electric filed. This system is not only helpful in enhancing the adsorption property of the adsorbent but also in increasing oxidation via a mechanism that involves creation of bipolar field on the adsorbent particles. Thus, the adsorbent particles placed within the electric field form micro-anodes and micro-cathodes at their two extremities. This essentially leads to the formation of a large number of microelectrolytic cells. For example, when using activated carbon granules as adsorbents, the graphite particles become such microelectrodes. The effective

number of cells created will enhance the adsorption properties and at the same time destroy pollutants (Zhang et al. 2013; Ding et al. 1987).

The use of such an EA system has been very effective in remediating organic pollutants such as dyes (Yasri 2001). However, if the adsorption capacity of pollutants on the activated carbon is already low because of the nature or the lack of active sites on both of adsorbents and the adsorbed materials, the presence of electric filed will not enhance greatly the capacity of adsorption. Thus treatment of effluents using EA unit alone is likely not suitable for effective remediation. Therefore, it is important to look for methods that can create active sites (Yasri et al. 2015).

Bioelectrochemical Approaches for Organic Remediation

Energy generation from waste is one of the key sustainable technologies. Municipal wastewaters may contain as much as tenfold the energy required for its treatment (Fan et al. 2012). Energy from waste can be generated in various forms during primary treatment, e.g., electricity, heat, or production of fuel. In biological treatment, biotic entities digest soluble organic or inorganic entities from waste streams to produce metabolism products such as alcohol, methane, or hydrogen. Electrochemical applications have utilized some of the natural bacterial processes for energy conservation at electrodes in either or both anode and cathode compartments for electron donors and acceptors, respectively (Rittmann 2008). Thus, these devices transform chemical energy into electric energy via electrochemical reactions involving microbes or enzymes. For example, dissimilatory Fe-reducing bacteria (DMRB) (e.g., *Shewanella* and *Geobacter*) oxidize organics and transfer electrons to anodes. The energy in the electrons can be utilized for electricity generation in a microbial fuel cell (MFC) (Kato et al. 2012; Kim et al. 2002a) or for hydrogen gas production in a microbial electrolysis cell (MEC) (Cheng and Logan 2011). These systems contain an anode, a cathode, an electrolyte, and an electric circuit; microbial growth at one or both electrodes is either separated into two chambers or located in one (Fig. 9). The main difference between MFC and MEC is a stand for adding a small amount of voltage (>0.2 V) in MEC to that produced by bacteria at the anode to allow for the production of H_2 at cathode surface. Also, the operational conditions at the cathode are different for MFC and MEC. MFC is usually operated with an excess of dissolved O_2, whereas for MEC the condition should be optimized for cathode system to allow the promotion of H_2 production. Both systems hold the same anodic principles, i.e., the microbes grow at the anode surface, degrade organic and/or inorganic substrates via their metabolisms, to produce electric power in MFCs (Fig. 9a) or as electron source to produce hydrogen in MECs (Fig. 9b).

Hydrogen is widely considered as imperative in building a sustainable energy future as it does not release any greenhouse gases upon combustion (Edwards et al. 2007). Thus, MEC is considered a new sustainable development for hydrogen

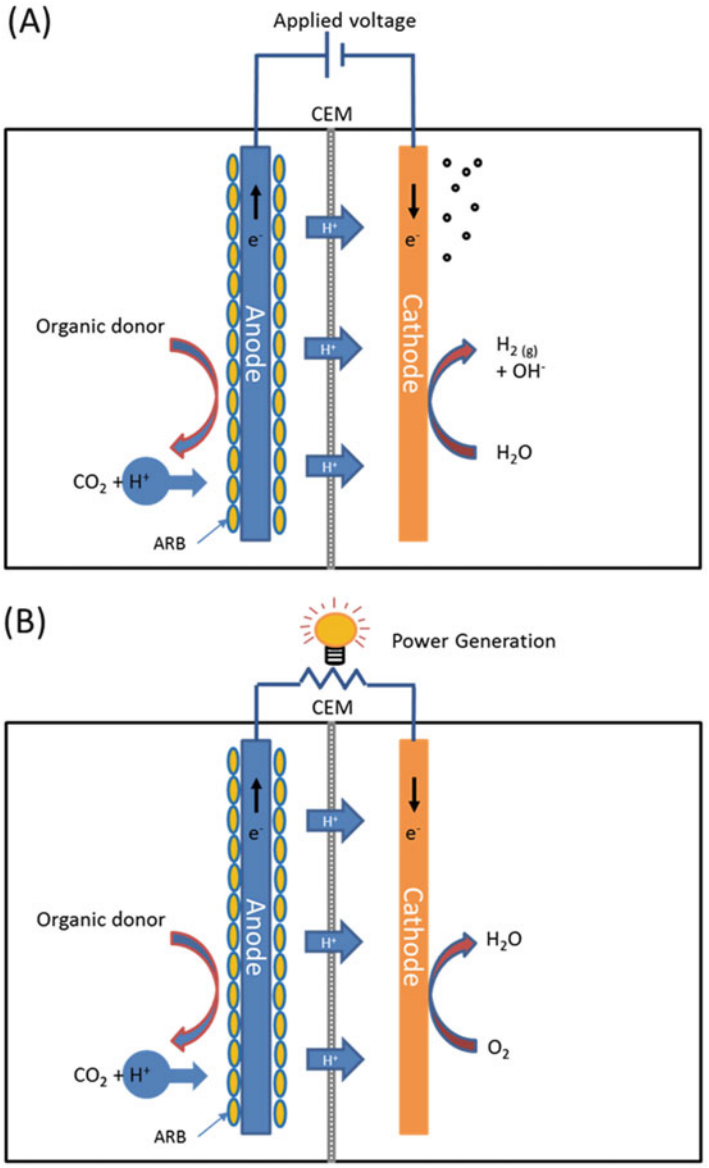

Fig. 9 Schematic diagrams of (**a**) MEC and (**b**) MFC systems consisting of two-compartment cells of anolyte and catholyte separated by cation exchange membrane (CEM). MEC produces H_2 by combining substrate utilization reaction at the anode by anodic respiring bacteria under small applied potential, and MFC produces electric current by combining two half-cell reactions of substrate utilization on the anode and oxygen reduction at the cathode

production (Cheng and Logan 2007a) that utilizes waste as a source of feed to various types of biomass (Wang and Ren 2013). The growth of anodic respiring bacteria (ARB) forming an exoelectrogen biofilm on anode as the main part of MEC to remediate organic waste releases protons to the anolyte medium and donates electrons to anode (Fig. 9a). The electrons flow toward the cathode, combine with protons, and release H_2 if only enough energy is provided to overcome the endothermic energy barrier of hydrogen overvoltage.

Theoretically, the maximum yield for complete oxidation of 1 mole glucose is 12 moles of H_2 (Eq. 58). For comparison, in the fermentation process, however, a 1 mole of glucose will produce maximum 4 moles H_2 if acetate is formed (Eq. 59) or 2 moles H_2 if butyrate is formed (Eq. 60). Moreover, the oxidation of glucose and its fermentation products of acetate and butyrate (Eqs. 58, 61, and 62) are not directly converted to H_2 without an external energy input (note that the free energy values of reactions are not spontaneous under standard conditions). Therefore, the use of MEC to oxidize these chemicals will theoretically provide the extra energy to remediate waste and produce additional H_2.

$$C_6H_{12}O_6 + 12H_2O \rightarrow 6HCO_3^- + 6H^+ + 12H_2 \quad \Delta G^\circ = +3.2 \quad \text{kJ/mol} \tag{58}$$

$$C_6H_{12}O_6 + 4H_2O \rightarrow 2CH_3COO^- + 2HCO_3^- + 4H^+ + 4H_2 \quad \Delta G^\circ = -206.3\text{kJ/mol} \tag{59}$$

$$C_6H_{12}O_6 + 2H_2O \rightarrow 2CH_3CH_2CH_2COO^- + 2HCO_3^- + 3H^+ + 2H_2 \quad \Delta G^\circ = -256.8\text{kJ/mol} \tag{60}$$

$$CH_3COO^- + 4H_2O \rightarrow 2HCO_3^- + H^+ + 4H_2 \quad \Delta G^\circ = +104.6\text{kJ/mol} \tag{61}$$

$$CH_3CH_2CH_2COO^- + 10H_2O \rightarrow 4HCO_3^- + 3H^+ + 10H_2 \quad \Delta G^\circ = +257.3\text{kJ/mol} \tag{62}$$

In MECs, although bacteria are the cornerstone entities to metabolize substrates and provide energy, the system design, electrolyte properties, and anode and cathode materials also influence the performance of the reactor. Thus, it is necessary to optimize the MEC design and operating conditions to maximize H_2 production and minimize cost. Various parameters affecting H_2 production rate and bacteria enrichment for the better biofilm performance are briefly discussed herein. Methods of various parameters calculation are also presented in [Box 2].

Box 2 Calculation of Yield and Efficiency of MEC System

For simplicity, the following calculations are based on acetate as substrate (not complex) in the MEC system. A typical batch MEC system is shown in Fig. 9a. The electrodes are powered at a specified voltage (not exceeding 1.0 V) using a direct current power supply, connecting in series through a known resistor (R_Ω) with a data acquisition system to record the voltage drop

(continued)

Box 2 (continued)

across the resistor. The outcome current is calculated applying Ohm's law ($I = V/R_{\Omega}$), where V is the measured voltage drop across the resistor. The generated biogases from MECs are usually collected using the water displacement method, measuring the volume and determining the composition by using a proper gas chromatograph analysis for hydrogen, methane, and nitrogen (Yang et al. 2015). The H_2 yield is calculated based on molar ratio of the actual hydrogen production to substrate utilized,

$$Y_{H_2} = \frac{n_{H_2\ \mathrm{mol}}\,(\text{hydrogen produced})}{n_{S\ \mathrm{mol}}(\text{substrate consumed})} \tag{63}$$

The moles of H_2 produced are given from the volume (mL) of actual hydrogen production by applying ideal gas law;

$$n_{H_2} = \frac{V_{H_2} P}{R\,T} \tag{64}$$

where p (atm), T (K), and R the ideal gas constant (0.08206 L atm/K mol).

The number of moles of the substrate utilized (n_S) is usually calculated based on the soluble chemical oxygen demand (SCOD) consumed during the cycle; e.g., in the following oxidation reaction of acetate substrate:

$$C_2H_4O_2 + 2O_2 \rightarrow 2H_2O + 2CO_2 \tag{65}$$

$$n_S(\mathrm{mol}) = \frac{\Delta\mathrm{SCOD}\ (\mathrm{mg})}{2 \times 32\ (O_2)} \times \frac{\mathrm{g}}{1000} \tag{66}$$

where ΔSCOD (mg) is SCOD consumed during the cycle; 32 is the molecular weight of oxygen.

Considering that the theoretical maximal production of H_2 from acetate is 4 moles,

$$CH_3COOH + 2H_2O = 4H_2 + 2CO_2 \tag{67}$$

The overall H_2 recovery ($R_{H_2}, \%$) is calculated as a ratio of actual amount of hydrogen produced to the theoretical amount of hydrogen that should be produced by the same amount of substrate:

$$R_{H_2}(\%) = \frac{n_{H_2}\ (\mathrm{mol})}{n_{th}(\mathrm{mol})} \tag{68}$$

(continued)

Box 2 (continued)

$$n_{\text{th}} = 4n_{\text{s}} = \frac{2\Delta\text{SCOD (mg)}}{32\ (\text{O}_2)} \times \frac{\text{g}}{1000} \tag{69}$$

On the other hand, ideally the fraction of electrons recovered as current is released at the cathode surface as hydrogen. Thus, identifying the coulombic efficiency (CE) would represent fraction of electrons, which is recovered as current versus that in the starting organic matter. Accordingly, CE is calculated from the theoretical maximal production of H_2 (n_{th}) and the current recovery over time using Eqs. 70 and 71.

$$CE = \frac{n_{CE}}{n_{\text{th}}} \tag{70}$$

$$n_{CE} = \frac{\int_{t=0}^{t} I_{90}\text{d}t}{2F} \tag{71}$$

where n_{CE} (mol) is the number of moles of hydrogen that could be recovered based on measured current and found by calculating the area under the curve of current density versus time throughout the reaction period, n_{th} (mol) is the number of moles of hydrogen theoretically produced from ΔSCOD consumed, dt is time interval (s), 2 in the Eq. 71 is the number of electrons used to convert hydrogen charge ($2H^+ = 2e^- \rightarrow H_2$), and I_{90} is the average current (A) recorded over time (t) and converted to cover the 90% of the charge accumulation. The use of I_{90} is more accurate when analyzing MEC performance in a batch process because it eliminates small current densities at the end of the cycle and focuses on the most useful part of the current generation cycle (Ivanov et al. 2013).

The cathodic hydrogen recovery (r_{cat}) is indicative of the number of moles of hydrogen recovered at the cathode compared to the moles that theoretically could have been produced from the current and is calculated using Eq. 72.

$$r_{\text{cat}} = \frac{n_{\text{H}_2}}{n_{\text{CE}}} \tag{72}$$

Volumetric hydrogen production rate (HPR) (m^3 $H_2/m^3/d$) should be normalized to the cathode liquid volume.

Calculation of Energy Recovery

The energy content of the amount of hydrogen recovered is compared with energy input. The source of energy input to the system is based on (i) the external electric energy input (η_{E}), (ii) energy input from the substrate (η_{S}), and (iii) energy input in both electricity and substrate ($\eta\text{E} + \text{S}$).

(continued)

Box 2 (continued)

The energy recovery based on external electric energy input is calculated from Eq. 73:

$$\eta_{\mathrm{E}} = \frac{-W_{\mathrm{H_2}}}{W_{\mathrm{in}}} \tag{73}$$

where $W_{\mathrm{H_2}}$ (J) is the energy content of the hydrogen and W_{in} (J) is the energy input to the system. Whereas, the energy content of hydrogen is calculated from heat of enthalpy ($\Delta H_{\mathrm{H_2}}$) (Eq. 74):

$$W_{\mathrm{H_2}} = n_{\mathrm{H_2}}.\Delta H_{\mathrm{H_2}} \tag{74}$$

where $n_{\mathrm{H_2}}$ (mol) is the number of moles of H_2 produced and $\Delta H_{\mathrm{H_2}} = -285$ kJ/mol is heat of enthalpy of H_2.

The energy input to the system (W_{in}, J) is equal to the total energy input (W_{ps}, J) subtracted from the energy loss on the external resistor (W_{R}, J) (see Eqs. 75 and 76).

$$W_{\mathrm{in}} = W_{\mathrm{ps}} - W_{\mathrm{R}} \tag{75}$$

$$\mathrm{W_{in}} = \int_{t=0}^{t} \left(IE_{\mathrm{PS}} - I^2 R_{\mathrm{ex}}\right) \mathrm{d}t \tag{76}$$

where R_{ex} the external resistor (Ω), I (A) the current based on voltage drop measured across the external resistor, E_{PS} (V) the applied voltage of the power source, and dt (s) the time interval.

Energy recovery based on both the energy input and the energy in the substrate is calculated from Eq. 77.

$$\eta_{\mathrm{E+S}} = \frac{-W_{\mathrm{H_2}}}{W_{\mathrm{in}} - W_{\mathrm{S}}} \tag{77}$$

where W_{S} (J) is the amount of energy added by substrate, and given in Eq. 78;

$$W_{\mathrm{S}} = n_{\mathrm{S}} \Delta H_{\mathrm{S}} \tag{78}$$

where n_{S} (mol) is the number of moles of substrate consumed during a batch cycle and ΔH_{S} the heat of enthalpy of the substrate ($\Delta H_{\mathrm{Acetate}} = -874.3$ kJ/mol).

(continued)

Box 2 (continued)

Biomass Distribution Analysis

To estimate the COD distribution in MEC systems, we assume that the only COD sinks are the production of gases and biomass (suspended, attached, and produced). Thus, the following overall mass balance equation should be established:

$$\mathrm{COD_{initial}} = \mathrm{COD_{H2}} + \mathrm{COD_{biomass,sus}} + \mathrm{COD_{biomass,att}} + \mathrm{COD_{final}} \quad (79)$$

where $\mathrm{COD_{initial}}$ is the initial COD in the anode chamber, $\mathrm{COD_{H2}}$ is the COD equivalent of hydrogen gas production during the studied cycle, $\mathrm{COD_{biomass,sus}}$ is the COD for suspended biomass net accumulation over the incubation time in the anode chamber, $\mathrm{COD_{biomass,att}}$ is the COD for attached biomass accumulated on the anode material over the cycle period, and $\mathrm{COD_{final}}$ is the SCOD in the anode chamber at the end of the studied cycle.

According to the mass balance (Eq. 79), the only unknown COD sink is the attached biomass ($\mathrm{COD_{biomass,att}}$), whereas $\mathrm{COD_{biomass,sus}}$ can be determined according to Eq. 80, and the $\mathrm{COD_{H2}}$ is calculated via Eq. 81 (Lee et al. 2008), i.e., each 1 mL of H_2 produced is equivalent to 0.654 mg COD (at 25 °C), and considering the fact that gas produced out of the cathode chamber is almost pure H_2 without any methane,

$$\mathrm{COD_{biomass,sus}} = (\mathrm{TCOD} - \mathrm{SCOD})_{\mathrm{final}} - (\mathrm{TCOD} - \mathrm{SCOD})_{\mathrm{initial}} \quad (80)$$

$$1\ \mathrm{mL\ H_2} = \frac{1\ \mathrm{mmol\ H_2}}{22.4\ \mathrm{mL}} \frac{273.15\mathrm{K}}{298.15\mathrm{K}} \frac{2\mathrm{meq\ e^-}}{\mathrm{mmol\ H_2}} \frac{8\ \mathrm{mg\ COD}}{\mathrm{meq\ e^-}} = 0.654\ \mathrm{mg\ COD} \quad (81)$$

Exoelectrogenic Microorganisms

Microorganisms that can directly transfer electrons outside the cell to the electron acceptor (anode) without the need for exogenous mediators are known as exoelectrogens. These microorganisms are usually grown in anaerobic condition on anode surface as electron acceptor and utilize organics present in the effluent as electron donor. Electrochemical gradients are the backbone of basic cellular functions, including chemosmotic transport and ATP synthesis (Amit Kumar et al. 2012). The mechanisms of extracellular electron transfer have been proposed in three pathways: (i) through direct electron transfer through microbial outer membrane cytochromes; (ii) by electron shuttle molecules, mediated by the grown biofilm; and (iii) via a solid conductive protein produced by bacteria and shaped like nanowires or pili (Amit Kumar et al. 2012; Logan 2009a; Lovley 2008; Torres et al. 2010). Extracellular electron transfer mechanisms are not mutually exclusive within a species nor in one pathway. For example, *Shewanella oneidensis* can

transfer electrons via methods producing riboflavins that can function as electron shuttle. *Geobacter sulfurreducens* also has an outer membrane cytochrome and can produce nanowires that can conduct electrons through a 50-μm thick anodic biofilm (Nevin et al. 2008) but does not produce flavins or other mediators (i.e., pyocyanin, melanin, or quinones).

The analyte chamber in MEC operates in anoxic environment, which promotes the growth of anaerobic bacteria; however, the type of dominant entities enriched from activated sludge from wastewater treatment plant contains mixed culture inocula, which are strongly affected by the feeding substrate present in the electrolyte solution (effluent type). For example, *Pelobacter propionicus* and *Geobacter* are dominant in MECs fed with phosphate buffer solution and acetate as the substrate (Chae et al. 2008). *Shewanella* and *Pseudomonas* were the dominant bacteria in the two-chamber MEC with acetate as the substrate and carbonate buffer and sewage sludge as the inoculum (Liu et al. 2007b). *Pelobacter* is the dominant bacteria in the suspension and anodic fractions of an ethanol-fed MEC inoculated with sludge (Parameswaran et al. 2010).

Anode System

Continuous development of anodes for beneficial microbial attachment and substrate utilization in MEC system is critical for better performance of MECs (Baudler et al. 2015; Wagner et al. 2012). Important factors affecting the immobilization of biological entities in MECs are the type of anode materials and their configuration (He et al. 2015). Immobilization in biological system is generally defined as the physical confinement or localization of viable cells including enzymes, cellular organelles, animal and plant cells to a certain supporting region for biocatalytic purposes. Immobilization is performed to limit free transportation of biota while retaining their catalytic activities, which differ from those of the surrounding environment.

Generally, microbial cell immobilization (MCI) on supporting region is categorized as (i) passive, using the natural tendency of microorganisms to attach and grow on natural or synthetic surfaces, and (ii) active, with the help of flocculating agents, chemical attachment, and gel encapsulation. In both the selection of the support material is crucial. For wastewater treatment, support materials should meet the criteria of insolubility, nonbiodegradability, nontoxicity, simplicity of immobilization procedure with high retention to specific organisms, and preferably low cost. Other physical characteristics such as material high porosity, non-swelling, and compressible are also of concern.

Conductive carbonaceous materials are favored for anodic MCI (Logan 2010; Logan et al. 2008), and the choice of these materials for cultivating ARB is always related to their conductivity, chemical stability, adsorptive capacity, porosity, and high surface area (Logan 2010; Logan et al. 2008). Carbonaceous fabric anodes that

are usually utilized in MEC are carbon cloth, carbon fiber, carbon felt, carbon mesh, carbon paper, and granular carbon (Logan 2009b).

Increasing the surface area enhances the performance of the reactor by increasing the volume of the biofilm and hence the ARB reactive sites. For example, Yasri and Nakhla (2017) found that filling the anode chamber with granular activated carbon increases the efficiency and the corresponding H_2 conversion rate. However, this improvement is still limited considering the faster H_2 production rate achieved in some biological system, i.e., dark fermentation (Lee et al. 2010). Thus, effort was made to favor adhesion of microorganisms to positively charged anode by treating anode surface with ammonia at a high temperature (700 °C, 5% ammonia gas for 1 h), which results in faster startup of H_2 production (Cheng and Logan 2007b). Several similar methodologies such as surface pretreatment of carbon cloth anode (or carbon mesh as a cheaper alternative) with aqueous ammonia, phosphate buffer, metal doping (Yasri & Nakhla 2017), or nitric acid have been investigated (Zhang et al. 2014b). Moderate to slight increase in anode performance was attributed to the enhancement of electron transfer and better MCI on the anode surface (Zhang et al. 2014b). Factors affecting the MCI conditions at the anode, such as applied voltage, electrolyte conductivity, electrode arrangement, pH, substrate types, and electrode porosity, have been extensively studied (Wang et al. 2010b).

The effect of applied voltage on the MEC system performance was inconclusive. Commault et al. (2013) noted an influence of different anode potentials on the type of *Geobacter* strains grown in MECs (Commault et al. 2013), i.e., different strains will grow from mixed culture inoculum at different potentials. However, Logan et al. (Zhu et al. 2014) suggested that the same exoelectrogenic communities self-regulate their exocellular electron transfer pathways to adapt to different anode potentials. To understand the effect of potential, the voltammograms obtained from grown biofilm have to be analyzed to answer the question, how different sets of potentials affect the performance of the bioelectrochemical system?

The porosity of the anode surface represents also an impotent factor to improve the mass and charge transport limitations of the electrolyte, which highly influence the performance of bioelectrochemical systems (Dhand et al. 2014; Sleutels et al. 2009, 2011). Increasing the porosity will increase the surface area of the biofilm on the interface and hence increase the active reaction sites (Dhand et al. 2014). Reports indicate that increasing porosity as well as conductivity of the electrode can be achieved by modifying the anode surface with various nanoparticles such as Fe (Xu et al. 2012) or conductive polymer such as poly (3,4-ethylenedioxythiophene) (PEDOT) (Liu et al. 2015). The role of varying the porosity or conductivity of anodes using Fe nanoparticles or sulfur-containing chemical (such as PEDOT) is not clearly understood. For example, it has been reported that the conductivity of the electrolyte in the anolyte chamber has a significant effect on the performance of ARB (Lacroix et al. 2014; Rousseau et al. 2013) and that the H_2 increased from 0.13 to 0.82 m^3 H_2/m^3 per day when the electrolyte conductivity increased from 7.5 to 15 mS/cm (Verea et al. 2014). This phenomenon was related to an increase in electron-shuttling effect between the biofilm and the electrode surface, which reduces the inner resistance

(Lacroix et al. 2014; Rousseau et al. 2013; Verea et al. 2014). However, the conductive material may be a natural favorite to attract bacteria, and the enhancement of ARB performance may be not due to their conductive properties. For example, metal sulfides, especially those containing Fe, Ca, K, or Mg, play a major role in microbial growth under anoxic and oxic conditions and are found at the active centers of a wide variety of redox and catalytic species (Bertini et al. 1994; Lapinsonnière et al. 2012; Picot et al. 2011). These species include simple soluble electron transfer mediators (e.g., Fe(II)/Fe(III), sulfate/sulfide redox couple (Schroder 2007), Ca^{2+} ions (Fitzgerald et al. 2013), membrane-bound components of electron transfer chains, and some complex metalloenzymes (Amend et al. 2004; Bertini et al. 1994; Ghasemi et al. 2013; Lapinsonnière et al. 2012; Lovley and Phillips 1986; Schippers 2004; Weber et al. 2006). Despite the neutral attraction of ARB to these materials, research emphasizes the importance of increasing conductivity of anode surface modification with suitable conductive chemicals to induce cultivation of ARB, stimulate catabolism, conduct electrons, and consequently improve current density (Baudler et al. 2015; Gnana Kumar et al. 2014; Kang et al. 2015; Kato et al. 2012; Li et al. 2011; Luckarift et al. 2012; Tang et al. 2015; Zhao et al. 2010). For example, Kang et al. (2015) observed superior biocatalytic enhancement when PEDOT was coated on carbon felt anode and inoculated in an effluent originating from palm oil mill waste to catalyze acetate oxidation. Although PEDOT, which was used for anode modification, contain element sulfur that may stimulate bacterial growth, the enhancement was attributed to the better conductivity of the modifying material. The unanswered question is whether the improvement in the performance of MEC system is due to surface conductivity or due to the attraction of bacteria to attach to trace element present in the electrode.

On the other hand, the anode arrangement can be considered as an effective parameter to reduce the inner resistance (Li et al. 2014). For example, Liang et al. (2011) separately placed two anodes, either on one side or both sides of cathode in parallel within a membraneless MEC. They found that the MEC with anodes on both sides of cathode improved current and H_2 production rate by 72% and 118%, reaching 621.3 ± 20.6 A/m^3 and 5.56 m^3 H_2/m^3 per day, respectively.

The limitation of pH inside the anolyte compartment is an important factor affecting current, bacterial growth, and electron transfer which is also tied to proton transfer within the biofilm (Babauta et al. 2012b). Babauta et al. (2012b) confirmed this effect and concluded that (a) pH can vary within the biofilm at different growth phases, (b) pH is not always a limiting factor in a biofilm, and (c) biofilms respire in a unique internal environment that variation of pH and redox potential are associated only with the biofilm.

Substrates are considered as the feed sources for ARB, existing in the effluent, and are converted or oxidized within the MEC system. Kadier et al. (2014) have reviewed the substrates used in MECs (ranging from simple to complex effluent resulted from real wastewater, fermentable and non-fermentable organic materials), their performance, and future potential usage for sustainable system. The substrates discussed include from complex to simple sources such as molasses industrial (methanol rich), food processing, winery, potato processing, dairy manure, refinery,

swine, and domestic wastewater. Of these, the complex substrates help in establishing a diverse and electrochemically active microbial community, while simple substrates degrade easily and improve H_2 production rate.

Thus, although the microbe/electrode interactions stem from the abilities of bacteria to extracellular electron transfer to solid metals as terminal electron acceptors, electron transfer to electrodes does not necessarily share identical cellular components (Babauta et al. 2012a). Thus microbe/electrode interactions remain enigmatic with both ecological and evolutionary origins. Further research is needed to shed more light on these bioelectrochemical processes.

Cathode System

Hydrogen production in MEC occurs at the cathode surface, located in the catholyte chamber and operated in air-saturated electrolyte. The hydrogen evolution reaction (HER) on plain carbon electrodes is very slow and requires a high overvoltage (−0.42 V) to drive H_2 production (Logan et al. 2008). To reduce the overvoltage barrier, Pt is usually used as a catalyst. Pt-catalyzed electrodes are commercially available and also are easily prepared by mixing commercially available Pt/carbon powder with a chemical binder (Cheng et al. 2006). This forms a paste in which the Pt loading can be varied by changing the mass of Pt in the paste.

Major disadvantages of using Pt are high cost and the possibility of being poisoned by chemicals such as sulfide, which is a common constituent of wastewater. Various other metals, alloys, modified electrode surfaces, or reducing biofilms are used as alternative for Pt as cathode (Rozendal et al. 2008). Kundu et al. (2013) reviewed the type of cathode material, catalysts, and modifications that are suitable for H generation in microbial electrolysis cell. Among the materials used, stainless steel, Ni alloys, Pd nanoparticles, and decorated cathode are very good for H_2 evolution. Nevertheless, cost-effective catalysts are the key to successful industrial application of MEC.

Unlike plain carbon materials, carbonaceous cathode doped with nanoparticles containing, e.g., MoS_2, has been reported effective and even competes with Pt cathode (Hou et al. 2014; Tenca et al. 2013). Nevertheless, due to the toxicity of most metal ions and for the purpose of keeping the MECs as environmentally friendly technology, replacement with nonmetallic composition becomes advantageous. Many successful applications have been reported using nanocomposites of carbonaceous materials doped with nitrogen (Zhang et al. 2014a), phosphate (Munoz et al. 2010), sulfur, or their mixtures (Ghasemi et al. 2013, Zheng et al. 2014).

Membrane

The use of membrane in MEC system is to separate anaerobic microbial condition at the anode from aerobic condition at the cathode, to minimize H_2 losses, and to

prevent mixing with CO_2 in the anode chamber. However, the presence of membrane disadvantages the system by increasing potential losses and reducing energy recovery associated with the resistance accompanied by its existence (Logan et al. 2008). Although membraneless system can be employed, research shows the production of methane in combination with H_2 due to the growth of cathodic reducing bacteria (methanogenic bacteria) that reduce of CO_2 according to Eq. 82 (Bajracharya et al. 2015).

$$8H^+ + CO_2 + 4e^- \rightarrow CH_4 + 2H_2O \tag{82}$$

Membranes used in MEC can be either CEMs or AEMs (Logan 2008). The use of CEMs allows transportation of H^+ and other cations present in solution, such as Na^+, K^+, $NH_4{}^+$, Ca^{2+}, and Mg^{2+}, toward the catholyte chamber. However, typical pH of wastewater and the inoculating medium of MECs is about neutral (pH ~7.0), and the proton concentration is about 10^{-4} mM (Rozendal et al. 2007), which is far less than the concentration of cation species other than protons in wastewater (typically 4–5 orders of magnitude higher). As a result, electrodialysis of cation mainly occurs in the MECs provided with CEM by the transport of cation species other than protons through the membrane. The cation transportation to catholyte chamber other than protons will therefore alter the anolyte medium surrounding the bacteria, as well as create a pH difference (gradient) between the catholyte and the anolyte chambers which will negatively affect the MEC performance by creating an extra potential loss and competing reactions other than hydrogen evolution at the cathode surface (Rozendal et al. 2007).

The utilization of AEM instead of CEM is useful in a sense that electrodialysis of anion toward the anode from the cathode rather than the transport of cations from the anode to the cathode will prevent the transportation of the other cation to the catholyte chamber (Rozendal et al. 2007). The transport of hydroxide (OH^-) anion toward the analyte chamber will leave behind hydronium (H_3O^+) ions that react at the cathode surface to evolve hydrogen. The electrolysis of water (Eq. 83) at the cathode will provide, in this case, the extra hydroxide ions that diffuse through membrane via the effective ion transportation mechanism toward the anode that equilibrates the exchange of charges and electrons in the system.

$$2H_2O + 2\,e^- \rightarrow 2OH^- + H_2 \tag{83}$$

Concept of MEC System

Understanding the principles and behavior of electrochemical interface reactions between biotic entities in biofilm, substrate utilization, and abiotic surface phase of electrode is important to continue advancements in MEC systems. Electrochemical studies for MECs include voltammogram analysis of the interface reactions, performance of the biofilm in both cathode and anode (Yoho et al. 2015), and determination of the kinetic parameters of biofilm growth on electrodes.

The correlation between current generation, ARB, and the electrode has been well established, indicating that the electron generation is a consequence of biocatalytic substrate utilization to transfer via various extracellular electron transfer (EET) to the final electrode port (Lovley 2008; Reguera et al. 2005; Richter et al. 2009). However, information about the interfacial anodic voltammogram at the electrode-biofilm is limited. Generally, the kinetic response of electron shuttles at the electrode interface (i.e., current density-voltage, J-V response) is defined by mass-transport processes according to Butler-Volmer equation (Torres et al. 2008). However, in the case of biofilm interface, the production of conductive matrices (wiring within the biofilm), which is directly attached to the anode, will be considered as an extension of the anode material, and thus the biofilm containing a solid conductive matrix can be called a "biofilm anode" (Torres et al. 2008). The bacterial kinetics and the J-V response model in this case will differ from Butler-Volmer equation and that variance directly affected by the bacteria should be considered.

Electrochemists commonly use Nernst model to describe redox potential as a function of electron concentration at the electrode interface. Biologists, on the other hand, use Monod kinetics to describe the dependence of biological growth on the concentration of electron donor and acceptor (substrate) (Wang et al. 2010d). Marcus et al. (Kato Marcus et al. 2007) combined the above two models and proposed the Nernst-Monod model (Eq. 84) to describe the bacterial kinetics under the influence of the anode potential E (V), where the reduction potential of interface electron controls the bacterial donation activity, i.e., current exchange at the interface.

The ideal electrode J-V representation for ARB influences electron shuttling through self-produced mediators and is a sigmoidal-shape voltammogram presented in Fig. 10a (Kato Marcus et al. 2007; Torres et al. 2008). An experimental current response of the biofilm anode to potential at slow scan rate (1.0 mV s^{-1}) is presented in Fig. 10b. Usually when applying a slow scan rate, the voltammogram shows an ideal "steady state"; that is, the catalytic current does not depend on the scan direction (Marsili et al. 2008) to allow ARB to reach a steady metabolic condition at all potentials, i.e., reach a steady state. In bioelectrochemistry, the low-scan cyclic voltammetry (LSCV) is a powerful technique, as it measures the steady-state response of ARB as a function of the anode potential (Torres et al. 2010).

The main assumption for the use of the Nernst-Monod model is that microbial kinetics controls the rate of current generation. This is usually performed by evaluating the anode potential losses APL (η_{anode}) in an ARB biofilm anode. The APL (η_{anode}) is defined as an electrocatalytic potential of active site as close as possible to the redox potential of the substrate being oxidized. Characterizing these potential losses is an important factor in the development of MFCs and MECs. The main postulation of this hypothesis is that, lower APL will translate to a higher catalytic current, higher energy output, and hence higher efficiency of the process. Thus, the twofold task in optimizing MEC system is to produce a high current density using minimum anode materials at a low anode potential (being as close as

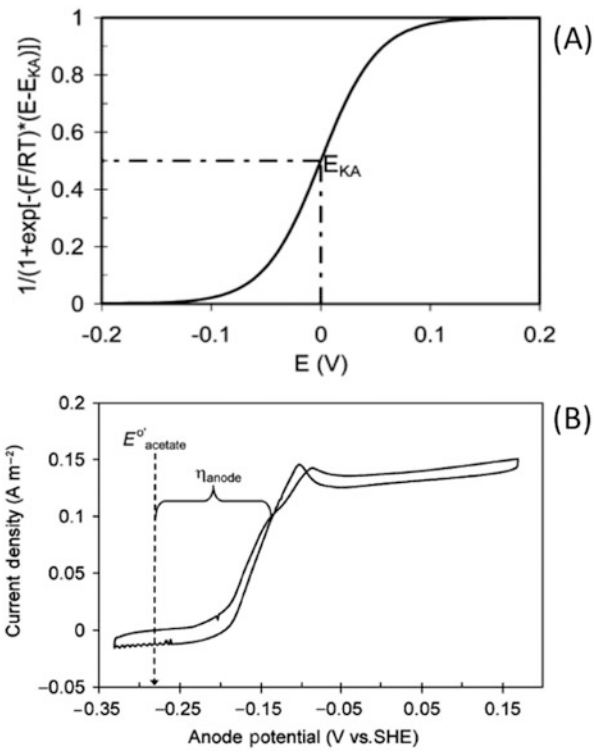

Fig. 10 Ideal plot of the Nernst-Monod model for $E_{KA} = 0$ V and T = 30 °C (Torres et al. 2008) (**a**) and low-scan cycle voltammetry of ARB biofilm for acetate as substrate (**b**) (Adapted from Torres et al. 2010)

possible to the redox potential of the substrate being oxidized). Thus, the practical goal in MECs is to find an ARB community (or system) that can achieve both aims by producing a high current density at a low anode potential (Torres et al. 2010).

$$J = J_{\max}\left(\frac{1}{1+\exp-\frac{F}{RT}(E-E_{KA})}\right) \tag{84}$$

where J = current density (A m^{-2}); J_{max} = maximum current density (A m^{-2}); R = ideal gas constant (8.3145 J mol^{-1} K^{-1}); F = Faraday constant (96,485 coulomb per $mol^{-1}e^{-1}$); T = temperature (303.15 K); and E_{KA} = potential at which $J = ½\, J_{max}$.

Figure 10b depicts an example LSCV curve produced with freshly formed ARB biofilm producing maximum current density of about 0.15 $A.m^{-2}$ (Torres et al. 2008). The voltage is scanned back and forth between −0.33 and +0.15 V vs. the standard hydrogen electrode (SHE) at 1 mVs^{-1}. The forward and backward curves are similar to each other, indicating steady-state conditions that are not affected by the scanning direction. η_{anode} can be measured from this curve by calculating E_{donor} (for acetate as electron donor in this case, $E^{\circ}_{acetate} = -0.285$ vs. SHE). At $E_{anode} = E_{donor}$, ARB cannot gain any energy-transferring electrons to the anode;

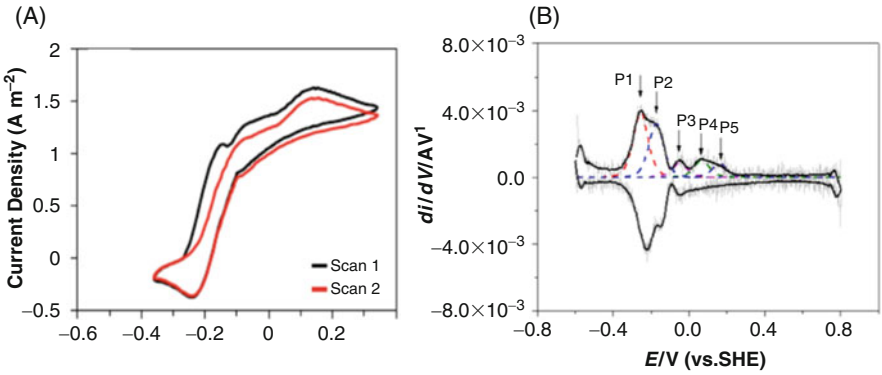

Fig. 11 Two consecutive cyclic voltammograms of *Geoalkalibacter subterraneus* inoculated in Fe(III)-containing cultures, recorded at 1 mV s^{-1} after day 7 of biofilm growth (**a**) (Adapted from Badalamenti et al. 2013). Derivative CVs suggest multiple electron transport pathways pointed out by *arrows*, and *dashed lines* represent Nernst-Monod fit (**b**) (Adapted from Yasri and Nakhla 2016)

therefore, $J = 0$. As E_{anode} becomes more positive, the ARB metabolic rate increases (indicated by the increase in J) until saturation.

The Nernst-Monod equation is proved to be a good model to describe the kinetics of bioelectric current that generates from pure bacterium culture and electron-shuttling pathways. However, in the real experimental situation when mixed culture is inoculated (instead of pure culture) and when the pristine material of electrode is made of mixed composition (not pure material), the J-V voltammogram may show in some cases sigmoidal shape, but the interpretation of kinetic data becomes complicated. In these cases, the CV curves will not fit the Nernst-Monod model, even with the selection of an appropriate $J_{\max}$ and E_{KA}. This is largely due to the occurrence of several EET pathways. For example, results from Badalamenti et al. (2013) show sigmoidal-shape CVs with various convex shapes indicating multiple EET pathways (Fig. 11a). The CV curve will emphasize significant deviations from Nernst-Monod model (Yasri and Nakhla 2016; Yoho et al. 2015, 2014).

In these cases, however, derivative cycle voltammetry (DCV) can be used to distinguish multiple EET pathways (red curve in Fig. 11b), which are reflected by the multiple convexes appearing on the DCV (Yoho et al. 2015). The results from Yasri and Nakhla (2016) indicate possible fitting of the forward DCV scan portions using multiple derivatives of Nernst-Monod equations (Fig. 11b). The derivative of the Nernst-Monod equation is best described by convex shape of dJ/dV (mA V^{-1}) versus anode potential (V) (Yasri and Nakhla 2016; Yoho et al. 2015). Fitting first derivative of Nernst-Monod equation to the DCVs can provide an important tool to differentiate EET pathways under multiple EET conditions (Yasri and Nakhla 2016; Yoho et al. 2014, 2015). The forward and the backward DCV scans reveal that there are multiple visible convex and concave shapes, respectively, that may be associated with different electron transport pathways (Yasri and Nakhla 2016).

The use of the derivative of the forward CV scan for fitting with multi-Nernst-Monod equations is to provide the overall response of the oxidation part of the scan (Yasri and Nakhla 2016). These forward curves can be fit using various derivatives of Nernst-Monod equation ($n = 1$) at the midpoint potential of each convex shape by adjusting the current values. Each Nernst-Monod fit represents one electron transfer pathway. Thus, from the DCV shapes and from the multi-Nernst-Monod fits, we could presume the existence of multiple EET pathways associated with various potentials using different types of electrode. The variations in the potential of EET pathways for different electrodes can be an indication of the various types of ARB growing on the electrode (Yasri and Nakhla 2016; Yoho et al. 2015).

It is interesting at this point to discuss the driving force for the interface reactions. For example, the DCV in Fig. 11b shows four main pathways corresponding to four values of E_{KA} in Nernst-Monod model. The lower E_{KA} value (pathway 1) corresponds to lower bioelectrocatalytic potential. Comparing the overall bioelectrocatalytic potential (E_{KA}) of different biological communities on different electrodes will provide idea about the corresponding potentials of pathways and hence the anode potential losses (APL, η_{anode}). Thus, the lower APL (lower E_{KA}) will translate to a higher current density and hence higher energy output and efficiency (Torres et al. 2010). In a similar approach, Zhu et al. (2014) studied the effect of different anode potentials on the CVs of non-turnover (starving biofilm conditions) to assess microbial community variations. They similarly observed that the faster electrocatalytic processes were accompanied by a shift of the anodic peaks toward the negative direction (Zhu et al. 2014). Further research is needed to optimize electrode materials or growth of biofilms to reduce energy required to catalyze the substrates being oxidized.

Conclusions and Perspectives

Interfacial electron transfer between electrodes and aqueous phases containing pollutants can be successfully exploited in electrochemical systems for remediation of environmental pollutants. Proper design of reactors, careful choice of materials, and systematic control of parameters can lead to effective pollutant remediation, material recovery, and even energy generation from waste streams. The concentrator technique can be used to recover valuable heavy metals from dilute waste streams and return the metals back to the industrial cycle. In case of waste streams containing multiple metallic constituents, each can be simultaneously recovered and separated by selective electrochemical deposition or in electrodialysis system. Exploiting the stability of metal complexes with suitable masking ligands readily performs these.

Electrochemical remediation of organic constituents can be achieved by implementing various electrochemical designs and principles. Among these, the techniques for remediating waste and simultaneously generating energy are the most promising. The utilization of the basic chemical principles of coagulation,

flotation, Fenton oxidation, chemical oxidation, and adsorption in electrochemical cell provides enhancement in the performance of different electrochemical techniques such as electrocoagulation, electroflotation, electro-Fenton oxidation, electro-oxidation, and electroadsorption. Each process exhibits certain technical advantages and disadvantages. The cost of electrochemical remediation is generally lower than their chemical remediation counterparts. However, future developments in electrochemical remediation technologies should be dictated not only by the cost but also by the need to meet the public expectations and the regulatory guidelines. An advantageous direction for new research is to explore the use of organic wastes as resources for cost-effective energy generation. In this regard microbial electrochemical techniques show promise. However, there are challenges to overcome such as the low current density, slow rate of remediation, limited scale-up, poor portability, etc. Generally, the investment in electrochemical remediation processes would be more promising if research focuses on integrating the electrochemical technique to assist other remediation process as sources of electron donor and acceptor at the electrode interface.

List of Notations/Abbreviations and Symbols

Notations/abbreviations

3-D: three dimensional	EEC: electrochemical energy consumption
ACE: average current efficiency	EET: extracellular electron transfer
AEM: anion exchange membrane	EF: electrochemical flotation
APL: anode potential losses (η_{anode})	EFO: electro-Fenton oxidation
ARB: anodic respiring bacteria	EO: electro-oxidation
ATP: adenosine triphosphate	HPR: hydrogen production rate (m^3 $H_2/m^3/d$)
BDD: boron-doped diamond	HRT: hydraulic retention time
CAO: catalytic advance oxidation	ICE: instantaneous current efficiency
CE: coulombic efficiency	LSCV: low-scan cyclic voltammetry
CEM: cation exchange membrane	M/MO: metal/metal oxide
CET: concentrator electrochemical technique	MCI: microbial cell immobilization
CM: concentrator material	MEC: microbial electrolysis cell
COD: chemical oxygen demand	MFC: microbial fuel cell
CV: cycle voltammetry	MNP: metal nanoparticles
DC: direct current	MO: metal oxide
DCV: derivative cycle voltammetry	PEDOT: poly(3,4-ethylenedioxythiophene
DMRB: dissimilatory Fe-reducing bacteria	POPs: persistent organic pollutants
DO: dissolved oxygen	RH: organic molecules (pollutants)
DSA: dimensionally stable anodes	SCE: saturated calomel electrode
EA: electroadsorption	SCOD: soluble chemical oxygen demand
EC: electrochemical coagulation or electrocoagulation	SHE: saturated hydrogen electrode
	TCOD: total chemical oxygen demand
ED: electrodeposition	TOC: total organic carbon
EDTA: ethylenediaminetetraacetic acid	UV: ultraviolet

Symbols

η_{act}: activation overvoltage	N^*: *number of atoms per nucleus growth*
η_H: hydrogen overvoltage	n: ion valence,
η_r: resistance overvoltage	η: overvoltage
R_{H_2}: overall H_2 recovery (%)	N: transport number
W_{H_2}: energy content of the hydrogen (J)	η_c: concentration overvoltage
Y_{H_2}: hydrogen yield	η_E: energy recovery based on external electric energy input
n_{CE}: H_2 production from current (mol)	η_{E+S}: energy recovery based on external electric energy input and substrate input
n_{th}: theoretical maximal production of H_2 (mol)	n_{H2}: number of moles of the hydrogen (mol)
ΔH: enthalpy (kJ/mol)	η_S: energy recovery based on substrate input
ΔG: nucleation energy (J)	n_S: number of moles of the substrate utilized (mol)
A: atomic weight of metal (g)	p: pressure (atm)
C: concentration	Q: electric charge (coulomb)
D: diffusion coefficient	R: ideal gas constant)
d: thickness of the diffusion layer	r_{cat}: cathodic hydrogen recovery (%)
E: voltage (volt)	R_{ex}: ohmic external resistance (ohm)
E_{KA}: potential when $J = ½ J_{max}$	t: duration time (s)
E_{PS}: the applied voltage (Volt)	T: temperature (303.15 K)
e_0: *elementary charge of the electron*	V_S: solution volume (L)
F: Faraday constant (96,485 coulomb per $mol^{-1}e^{-1}$)	W_{in}: energy input to the system (J)
I_{90}: current (A) for 90% of the charge accumulation	W_R: energy loss on the external resistor (J)
I_{appl}: applied current (Amp)	W_S: energy added by substrate (J)
I_{ef}: effective current (Amp)	z: metal valence
J: current density (Amp m^{-2})	α: percentage removal or efficiency (%)
J_{max}: maximum current density (A m^{-2})	$\varphi(N)$: *variation in surface tension*
K_{abs}: *the kinetic rate constant of reaction*	

References

Abou-Shady A, Peng C, Almeria OJ, Xu H (2012) Effect of pH on separation of Pb (II) and NO_3^- from aqueous solutions using electrodialysis. Desalination 285:46–53

Ai Z, Xiao H, Mei T, Liu J, Zhang L, Deng K, Qiu J (2008) Electro-Fenton degradation of rhodamine B based on a composite cathode of Cu_2O nanocubes and carbon nanotubes. Phys Chem C 112:11929–11935

Alaya MN, Rabah MA (2013) Surface acidity and catalytic activity of aged /SnO_2 catalyst supported with WO_3. J Alloys Compd 575:285–291

Al-Haq MI, Gómez-López VM (2012) Electrolyzed oxidizing water, decontamination of fresh and minimally processed produce. Wiley-Blackwell, New York, pp 135–164

Allen HE, Chen PH (1993) Remediation of metal contaminated soil by EDTA incorporating electrochemical recovery of metal and EDTA. Environ Prog 12:284–293

Alyüz B, Veli S (2009) Kinetics and equilibrium studies for the removal of nickel and zinc from aqueous solutions by ion exchange resins. J Hazard Mater 167:482–488

Al-Zoubi H, Ibrahim KA, Abu-Sbeih KA (2015) Removal of heavy metals from wastewater by economical polymeric collectors using dissolved air flotation process. J Water Process Eng 8:19–27

Amend JP, Rogers KL, Meyer-Dombard DAR (2004) Microbially mediated sulfur-redox: energetics in marine hydrothermal vent systems. Geol Soc Am Spec Pap 379:17–34

Amit Kumar KK, Lens P, Leech D (2012) Does bioelectrochemical cell configuration and anode potential affect biofilm response? Biochem Soc Trans 40:1308–1314

Anotai J, Su C-C, Tsai Y-C, Lu M-C (2010) Effect of hydrogen peroxide on aniline oxidation by electro-Fenton and fluidized-bed Fenton processes. J Hazard Mater 183:888–893

Babauta J, Renslow R, Lewandowski Z, Beyenal H (2012a) Electrochemically active biofilms: facts and fiction. A review. Biofouling 28:789–812

Babauta JT, Nguyen HD, Harrington TD, Renslow R, Beyenal H (2012b) pH, redox potential and local biofilm potential microenvironments within Geobacter sulfurreducens biofilms and their roles in electron transfer. Biotechnol Bioeng 109:2651–2662

Babel S, Kurniawan TA (2003) Low-cost adsorbents for heavy metals uptake from contaminated water: a review. J Hazard Mater 97:219–243

Badalamenti JP, Krajmalnik-Brown R, Torres CI (2013) Generation of high current densities by pure cultures of anode-respiring *Geoalkalibacter* spp. under alkaline and saline conditions in microbial electrochemical cells. MBio 4(3):e00144–e00113. doi:10.1128/mBio.00144-13

Bajracharya S, ter Heijne A, Dominguez Benetton X, Vanbroekhoven K, Buisman CJN, Strik DPBTB, Pant D (2015) Carbon dioxide reduction by mixed and pure cultures in microbial electrosynthesis using an assembly of graphite felt and stainless steel as a cathode. Bioresour Technol 195:14–24

Barb WG, Baxendale JH, George P, Hargrave KR (1951) Reactions of ferrous and ferric ions with hydrogen peroxide. Part I.-the ferrous ion reaction. Trans Faraday Soc 47:462–500

Baudler A, Schmidt I, Langner M, Greiner A, Schroder U (2015) Does it have to be carbon? Metal anodes in microbial fuel cells and related bioelectrochemical systems. Energy Environ Sci 8:2048–2055

Beltrán Heredia J, Sánchez Martín J (2009) Removing heavy metals from polluted surface water with a tannin-based flocculant agent. J Hazard Mater 165:1215–1218

Bertini I, Gray HB, Lippard SJ, Valentine JS (1994) Bioinorganic chemistry. University Science Books, Mill Valley

Borbély G, Nagy E (2009) Removal of zinc and nickel ions by complexation–membrane filtration process from industrial wastewater. Desalination 240:218–226

Bradl H (2005) Heavy metals in the environment: origin interaction and remediation. Academic Press, New York

Brillas E, Casado J (2002) Aniline degradation by electro-Fenton® and peroxi-coagulation processes using a flow reactor for wastewater treatment. Chemosphere 47:241–248

Brillas E, Sirés I, Arias C, Cabot PL, Centellas F, Rodríguez RM, Garrido JA (2005) Mineralization of paracetamol in aqueous medium by anodic oxidation with a boron-doped diamond electrode. Chemosphere 58:399–406

Brillas E, Sirés I, Oturan MA (2009) Electro-Fenton process and related electrochemical technologies based on Fenton's reaction chemistry. Chem Rev 109:6570–6631

Calow PP (2009) Handbook of Ecotoxicology Technology & Engineering. Wiley, New York, p 900

Carrier M, Perol N, Herrmann J-M, Bordes C, Horikoshi S, Paisse JO, Baudot R, Guillard C (2006) Kinetics and reactional pathway of Imazapyr photocatalytic degradation influence of pH and metallic ions. Appl Catal B Environ 65:11–20

Cha HG, Choi K-S (2015) Combined biomass valorization and hydrogen production in a photoelectrochemical cell. Nat Chem 7:328–333

Chae K-J, Choi M-J, Lee J, Ajayi FF, Kim IS (2008) Biohydrogen production via biocatalyzed electrolysis in acetate-fed bioelectrochemical cells and microbial community analysis. Int J Hydrog Energy 33:5184–5192

Chailapakul O, Popa E, Tai H, Sarada BV, Tryk DA, Fujishima A (2000) The electrooxidation of organic acids at boron-doped diamond electrodes. Electrochem Commun 2:422–426

Charerntanyarak L (1999) Heavy metals removal by chemical coagulation and precipitation. Water Sci Technol 39:135–138

Chaudhary AJ, Donaldson JD, Grimes SM, Yasri NG (2000) Separation of nickel from cobalt using electrodialysis in the presence of EDTA. J Appl Electrochem 30:439–445

Chaudhary AJ, M-u H, Grimes SM (2009) Simultaneous recovery of metals and degradation of organic species: copper and 2,4,5-trichlorophenoxyacetic acid (2,4,5-T). J Hazard Mater 165:825–831

Chauke V, Matemadombo F, Nyokong T (2010) Remarkable sensitivity for detection of bisphenol a on a gold electrode modified with nickel tetraamino phthalocyanine containing Ni–O–Ni bridges. J Hazard Mater 178:180–186

Chen CCG (2010) Electrochemistry for the environment. Springer Science, New York

Chen G, Hung YT (2007) Electrochemical wastewater treatment processes. In: Wang LK, Hung Y-T, Shammas NK (eds) Advanced physicochemical treatment technologies. Handbook of environmental engineering. Humana Press Inc., Totowa

Cheng S, Logan BE (2007a) Sustainable and efficient biohydrogen production via electrohydrogenesis. Proc Natl Acad Sci U S A 104:18871–18873

Cheng S, Logan BE (2007b) Ammonia treatment of carbon cloth anodes to enhance power generation of microbial fuel cells. Electrochem Commun 9:492–496

Cheng S, Logan BE (2011) High hydrogen production rate of microbial electrolysis cell (MEC) with reduced electrode spacing. Bioresour Technol 102:3571–3574

Cheng S, Liu H, Logan BE (2006) Power densities using different cathode catalysts (Pt and CoTMPP) and polymer binders (Nafion and PTFE) in single chamber microbial fuel cells. Environ Sci Technol 40:364–369

Chou S, Huang Y-H, Lee S-N, Huang G-H, Huang C (1999) Treatment of high strength hexamine-containing wastewater by electro-Fenton method. Water Res 33:751–759

Clancy M, Bettles CJ, Stuart A, Birbilis N (2013) The influence of alloying elements on the electrochemistry of lead anodes for electrowinning of metals: a review. Hydrometallurgy 131–132:144–157

Commault AS, Lear G, Packer MA, Weld RJ (2013) Influence of anode potentials on selection of Geobacter strains in microbial electrolysis cells. Bioresour Technol 139:226–234

Comninellis CC (2010) Electrochemistry for the environment. Springer, New York, pp 1–563

Cong YQ, Wu ZC (2007) Self-regeneration of activated carbon modified with palladium catalyst for electrochemical dechlorination. Chin Chem Lett 18:1013–1016

Crundwell F, Moats M, Ramachandran V, Robinson T, Davenport WG (2011) Extractive metallurgy of nickel cobalt and platinum group metals. Elsevier Ltd, Amsterdam

Dąbrowski A, Hubicki Z, Podkościelny P, Robens E (2004) Selective removal of the heavy metal ions from waters and industrial wastewaters by ion-exchange method. Chemosphere 56:91–106

De Laat J, Gallard H (1999) Catalytic decomposition of hydrogen peroxide by Fe(III) in homogeneous aqueous solution: mechanism and kinetic modeling. Environ Sci Technol 33:2726–2732

Deguillaume L, Leriche M, Chaumerliac N (2005) Impact of radical versus non-radical pathway in the Fenton chemistry on the iron redox cycle in clouds. Chemosphere 60:718–724

Dhand V, Rao MV, Prasad JS, Mittal G, Rhee KY, Kim HJ, Jung DH (2014) Carbon nanospheres synthesized via solution combustion method: their application as an anode material and catalyst for hydrogen production. Carbohydr Lett 15:198–202

Dialynas E, Diamadopoulos E (2009) Integration of a membrane bioreactor coupled with reverse osmosis for advanced treatment of municipal wastewater. Desalination 238:302–311

Ding Z, Min CW, Hui WQ (1987) A study on the use of bipolar-particles-electrodes in decolorization of dyeing effluents and its principle. Water Sci Technol 19(3-4):391–400

Ding H-Y, Feng Y-J, Liu J-F (2007) Preparation and properties of $Ti/SnO_2–Sb_2O_5$ electrodes by electrodeposition. Mater Lett 61:4920–4923

Do JS, Chen ML (1994) Decolourization of dye-containing solutions by electrocoagulation. J Appl Electrochem 24:785–790

Donaldson JD (2007) The chemistry of bivalent tin, progress in inorganic chemistry. Wiley, New York, pp 287–356
Donaldson JD, Grimes SM, Yasri NG, Wheals B, Parrick J, Errington WE (2002) Anodic oxidation of the dye materials methylene blue, acid blue 25, reactive blue 2 and reactive blue 15 and the characterisation of novel intermediate compounds in the anodic oxidation of methylene blue. J Chem Technol Biotechnol 77:756–760
Doulakas L, Novy K, Stucki S, Comninellis C (2000) Recovery of Cu, Pb, Cd and Zn from synthetic mixture by selective electrodeposition in chloride solution. Electrochim Acta 46:349–356
Dreyer DR, Park S, Bielawski CW, Ruoff RS (2010) The chemistry of graphene oxide. Chem Soc Rev 39:228–240
Edwards PP, Kuznetsov VL, David WIF (2007) Hydrogen energy. Philos Trans Royal Soc London A Math Phy Eng Sci 365:1043–1056
Eloy Isarain-Chávez CR, Martínez-Huitle CA, Peralta-Hernández JM (2013) On-site hydrogen peroxide production at pilot flow plant: application to electro-Fenton process. Int J Electrochem Sci 8:3084–3094
Fan Y, Han S-K, Liu H (2012) Improved performance of CEA microbial fuel cells with increased reactor size. Energy Environ Sci 5:8273–8280
Faouzi AM, Nasr B, Abdellatif G (2007) Electrochemical degradation of anthraquinone dye alizarin red S by anodic oxidation on boron-doped diamond. Dyes Pigments 73:86–89
Fernandes A, Morao A, Magrinho M, Lopes A, Goncalves I (2004) Electrochemical degradation of C. I. Acid Orange 7. Dyes Pigments 61:287–296
Ferreira BK (2008) Three dimensional electrodes for the removal of metals from dilute solutions: a review. Miner Process Extr Metall Rev 29:330–371
Fitzgerald LA, Petersen ER, Leary D, Biffinger JC (2013) Shewanella frigidimarina microbial fuel cells and the influence of divalent cations on current output. Biosens Bioelectron 40:102–109
Fu F, Wang Q (2011) Removal of heavy metal ions from wastewaters: a review. J Environ Manag 92:407–418
Fuchigami T, Atobe M, Inagi S (2014) Fundamentals and applications of organic electrochemistry: synthesis, materials, devices. Wiley, Chichester, p 240
Gandini D, Mahé E, Michaud PA, Haenni W, Perret A, Comninellis C (2000) Oxidation of carboxylic acids at boron-doped diamond electrodes for wastewater treatment. J Appl Electrochem 30:1345–1350
Gao J, Sun S-P, Zhu W-P, Chung T-S (2014) Chelating polymer modified P84 nanofiltration (NF) hollow fiber membranes for high efficient heavy metal removal. Water Res 63:252–261
Geim AK, Novoselov KS (2007) The rise of graphene. Nat Mater 6:183–191
Ghasemi M, Daud WRW, Hassan SHA, Oh S-E, Ismail M, Rahimnejad M, Jahim JM (2013) Nano-structured carbon as electrode material in microbial fuel cells: a comprehensive review. J Alloys Compd 580:245–255
Gnana kumar G, Kirubaharan CJ, Udhayakumar S, Karthikeyan C, Nahm KS (2014) Conductive polymer/graphene supported platinum nanoparticles as anode catalysts for the extended power generation of microbial fuel cells. Ind Eng Chem Res 53:16883–16893
Grimes SM, Yasri NG, Chaudhary AJ (2017) Recovery of critical metals from dilute leach solutions – Separation of indium from tin and lead. Inorg Chim Acta 461:161–166
Grimm J, Bessarabov D, Sanderson R (1998) Review of electro-assisted methods for water purification. Desalination 115:285–294
Grimshaw P, Calo JM, Hradil G (2011) Cyclic electrowinning/precipitation (CEP) system for the removal of heavy metal mixtures from aqueous solutions. Chem Eng J 175:103–109
Gunasekaran SM, Yasri N (2016) Method to remediate effluents containing metals complexed with organic and/or inorganic species. Wisconsin Alumni Research Foundation, Madison
Guo M, Qiu G, Song W (2010) Poultry litter-based activated carbon for removing heavy metal ions in water. Waste Manag 30:308–315

Guven G, Perendeci A, Tanyolac A (2008) Electrochemical treatment of deproteinated whey wastewater and optimization of treatment conditions with response surface methodology. J Hazard Mater 157:69–78

Harnisch F, Rosa LFM, Kracke F, Virdis B, Krömer JO (2015) Electrifying white biotechnology: engineering and economic potential of electricity-driven bio-production. Chem Sus Chem 8:758–766

He Y, Liu Z, X-h X, Li B, Zhang Y, Shen R, Zhu Z, Duan N (2015) Carbon nanotubes simultaneously as the anode and microbial carrier for up-flow fixed-bed microbial fuel cell. Biochem Eng J 94:39–44

Hou Y, Zhang B, Wen Z, Cui S, Guo X, He Z, Chen J (2014) A 3D hybrid of layered MoS_2/nitrogen-doped graphene nanosheet aerogels: an effective catalyst for hydrogen evolution in microbial electrolysis cells. J Mater Chem A 2:13795–13800

Houghton RW, Kuhn AT (1974) Mass-transport problems and some design concepts of electrochemical reactors. J Appl Electrochem 4:173–190

Hu C-Y, Lo S-L, Kuan W-H, Lee Y-D (2008) Treatment of high fluoride-content wastewater by continuous electrocoagulation–flotation system with bipolar aluminum electrodes. Sep Purif Technol 60:1–5

Huang CP, Dong C, Tang Z (1993) Advanced chemical oxidation: its present role and potential future in hazardous waste treatment. Waste Manag 13:361–377

Iniesta J, Michaud PA, Panizza M, Cerisola G, Aldaz A, Comninellis C (2001) Electrochemical oxidation of phenol at boron-doped diamond electrode. Electrochim Acta 46:3573–3578

Israilides CJ, Vlyssides AG, Mourafeti VN, Karvouni G (1997) Olive oil wastewater treatment with the use of an electrolysis system. Bioresour Technol 61:163–170

Issabayeva G, Aroua MK, Sulaiman NM (2006) Electrodeposition of copper and lead on palm shell activated carbon in a flow-through electrolytic cell. Desalination 194:192–201

Ivanov I, Ren L, Siegert M, Logan BE (2013) A quantitative method to evaluate microbial electrolysis cell effectiveness for energy recovery and wastewater treatment. Int J Hydrog Energy 38:13135–13142

Janssen LJJ, Koene L (2002) The role of electrochemistry and electrochemical technology in environmental protection. Chem Eng J 85:137–146

Jeong J-Y, Kim H-K, Kim J-H, Park J-Y (2012) Electrochemical removal of nitrate using ZVI packed bed bipolar electrolytic cell. Chemosphere 89:172–178

Jiang C-C, Zhang J-F (2007) Progress and prospect in electro-Fenton process for wastewater treatment. J Zhejiang Univ Sci A 8:1118–1125

Jiao S, Jin J, Wang L (2014) Tannic acid functionalized N-doped graphene modified glassy carbon electrode for the determination of bisphenol a in food package. Talanta 122:140–144

Kadier A, Simayi Y, Kalil MS, Abdeshahian P, Hamid AA (2014) A review of the substrates used in microbial electrolysis cells (MECs) for producing sustainable and clean hydrogen gas. Renew Energy 71:466–472

Kammel R (1984) Metal recovery from dilute aqueous solutions by various electrochemical reactors. In: Bautista R (ed) Hydrometallurgical process fundamentals, NATO conference series. Springer, New York, pp 617–646

Kang YL, Ibrahim S, Pichiah S (2015) Synergetic effect of conductive polymer poly (3,4-ethylenedioxythiophene) with different structural configuration of anode for microbial fuel cell application. Bioresour Technol 189:364–369

Kato Marcus A, Torres CI, Rittmann BE (2007) Conduction-based modeling of the biofilm anode of a microbial fuel cell. Biotechnol Bioeng 98:1171–1182

Kato S, Hashimoto K, Watanabe K (2012) Microbial interspecies electron transfer via electric currents through conductive minerals. Proc Natl Acad Sci U S A 109:10042–10046

Katoh S (1986) Method of treating liquid wastes containing heavy metal chelate compounds. Google Patents

Khandegar V, Saroha AK (2013) Electrocoagulation for the treatment of textile industry effluent – a review. J Environ Manag 128:949–963

Kim S, Jeung S, Moon H (1998) Removal and recovery of heavy metal ions in fixed and semi-fluidized beds. Korean J Chem Eng 15:637–643

Kim HJ, Park HS, Hyun MS, Chang IS, Kim M, Kim BH (2002a) A mediator-less microbial fuel cell using a metal reducing bacterium, *Shewanella putrefaciens*. Enzym Microb Technol 30:145–152

Kim TH, Park C, Lee J, Shin EB, Kim S (2002b) Pilot scale treatment of textile wastewater by combined process (fluidized biofilm process-chemical coagulation-electrochemical oxidation). Water Res 36:3979–3988

Kocaoba S, Akcin G (2005) Removal of chromium (III) and cadmium (II) from aqueous solutions. Desalination 180:151–156

Konsowa AH (2010) Intensification of the rate of heavy metal removal from wastewater by cementation in a jet reactor. Desalination 254:29–34

Kulandaisamy S, Rethinaraj JP, Chockalingam SC, Visvanathan S, Venkateswaran KV, Ramachandran P, Nandakumar V (1997) Performance of catalytically activated anodes in the electrowinning of metals. J Appl Electrochem 27:579–583

Kundu A, Sahu JN, Redzwan G, Hashim MA (2013) An overview of cathode material and catalysts suitable for generating hydrogen in microbial electrolysis cell. Int J Hydrog Energy 38:1745–1757

Kurniawan TA, Chan GYS, Lo W-H, Babel S (2006) Physico–chemical treatment techniques for wastewater laden with heavy metals. Chem Eng J 118:83–98

Lacroix R, Silva SD, Gaig MV, Rousseau R, Delia M-L, Bergel A (2014) Modelling potential/current distribution in microbial electrochemical systems shows how the optimal bioanode architecture depends on electrolyte conductivity. Phys Chem Chem Phys 16:22892–22902

Landaburu-Aguirre J, Pongrácz E, Perämäki P, Keiski RL (2010) Micellar-enhanced ultrafiltration for the removal of cadmium and zinc: use of response surface methodology to improve understanding of process performance and optimisation. J Hazard Mater 180:524–534

Lapinsonnière L, Picot M, Barrière F (2012) Enzymatic versus microbial bio-catalyzed electrodes in bio-electrochemical systems. Chem Sus Chem 5:995–1005

Le TXH, Bechelany M, Champavert J, Cretin M (2015) A highly active based graphene cathode for the electro-Fenton reaction. RSC Adv 5:42536–42539

Lee H-S, Parameswaran P, Kato-Marcus A, Torres CI, Rittmann BE (2008) Evaluation of energy-conversion efficiencies in microbial fuel cells (MFCs) utilizing fermentable and non-fermentable substrates. Water Res 42:1501–1510

Lee H-S, Vermaas WFJ, Rittmann BE (2010) Biological hydrogen production: prospects and challenges. Trends Biotechnol 28:262–271

Lee KM, Min K, Choi O, Kim K-Y, Woo HM, Kim Y, Han SO, Um Y (2015) Electrochemical detoxification of phenolic compounds in lignocellulosic hydrolysate for *Clostridium* fermentation. Bioresour Technol 187:228–234

Li Y-H, Ding J, Luan Z, Di Z, Zhu Y, Xu C, Wu D, Wei B (2003) Competitive adsorption of Pb^{2+}, Cu^{2+} and Cd^{2+} ions from aqueous solutions by multiwalled carbon nanotubes. Carbon 41:2787–2792

Li J, Ai Z, Zhang L (2009) Design of a neutral electro-Fenton system with Fe@Fe_2O_3/ACF composite cathode for wastewater treatment. J Hazard Mater 164:18–25

Li Q, Li H, Du G-F, Xu Z-H (2010) Electrochemical detection of bisphenol a mediated by $[Ru(bpy)_3]^{2+}$ on an ITO electrode. J Hazard Mater 180:703–709

Li C, Zhang L, Ding L, Ren H, Cui H (2011) Effect of conductive polymers coated anode on the performance of microbial fuel cells (MFCs) and its biodiversity analysis. Biosens Bioelectron 26:4169–4176

Li X-H, Liang D-W, Bai Y-X, Fan Y-T, Hou H-W (2014) Enhanced H_2 production from corn stalk by integrating dark fermentation and single chamber microbial electrolysis cells with double anode arrangement. Int J Hydrog Energy 39:8977–8982

Liang D-W, Peng S-K, Lu S-F, Liu Y-Y, Lan F, Xiang Y (2011) Enhancement of hydrogen production in a single chamber microbial electrolysis cell through anode arrangement optimization. Bioresour Technol 102:10881–10885

Liang J, Jiao Y, Jaroniec M, Qiao SZ (2012) Sulfur and nitrogen dual-doped mesoporous graphene electrocatalyst for oxygen reduction with synergistically enhanced performance. Angew Chem Int Ed 51:11496–11500

Lim H, Lee JS, Shin H-J, Shin HS, Choi HC (2010) Spatially resolved spontaneous reactivity of diazonium salt on edge and basal plane of graphene without surfactant and its doping effect. Langmuir 26:12278–12284

Liu H, Grot S, Logan BE (2005) Electrochemically assisted microbial production of hydrogen from acetate. Environ Sci Technol 39:4317–4320

Liu H, Li XZ, Leng YJ, Wang C (2007a) Kinetic modeling of electro-Fenton reaction in aqueous solution. Water Res 41:1161–1167

Liu W-Z, Wang A-J, Ren N-Q, Zhao X-Y, Liu L-H, Yu Z-G, Lee D-J (2007b) Electrochemically assisted biohydrogen production from acetate. Energy Fuel 22:159–163

Liu X, Wu W, Gu Z (2015) Poly (3,4-ethylenedioxythiophene) promotes direct electron transfer at the interface between *Shewanella loihica* and the anode in a microbial fuel cell. J Power Sources 277:110–115

Logan BE (2008) Microbial fuel cells. Wiley, Hoboken

Logan BE (2009a) Exoelectrogenic bacteria that power microbial fuel cells. Nat Rev Microbiol 7:375–381

Logan BE (2009b) Scaling up microbial fuel cells and other bioelectrochemical systems. Appl Microbiol Biotechnol 85:1665–1671

Logan B (2010) Scaling up microbial fuel cells and other bioelectrochemical systems. Appl Microbiol Biotechnol 85:1665–1671

Logan BE, Call D, Cheng S, Hamelers HVM, Sleutels THJA, Jeremiasse AW, Rozendal RA (2008) Microbial electrolysis cells for high yield hydrogen gas production from organic matter. Environ Sci Technol 42:8630–8640

Lovley DR (2008) The microbe electric: conversion of organic matter to electricity. Curr Opin Biotechnol 19:564–571

Lovley DR, Phillips EJP (1986) Organic matter mineralization with reduction of ferric iron in anaerobic sediments. Appl Environ Microbiol 51:683–689

Luckarift HR, Sizemore SR, Farrington KE, Roy J, Lau C, Atanassov PB, Johnson GR (2012) Facile fabrication of scalable, hierarchically structured polymer/carbon architectures for bioelectrodes. ACS Appl Mater Interfaces 4:2082–2087

Marsili E, Rollefson JB, Baron DB, Hozalski RM, Bond DR (2008) Microbial biofilm voltammetry: direct electrochemical characterization of catalytic electrode-attached biofilms. Appl Environ Microbiol 74:7329–7337

Martinez-Huitle CA, Ferro S (2006) Electrochemical oxidation of organic pollutants for the wastewater treatment: direct and indirect processes. Chem Soc Rev 35:1324–1340

Mollah MYA, Schennach R, Parga JR, Cocke DL (2001) Electrocoagulation (EC)- science and applications. J Hazard Mater 84:29–41

Montilla F, Michaud PA, Morallón E, Vázquez JL, Comninellis C (2002) Electrochemical oxidation of benzoic acid at boron-doped diamond electrodes. Electrochim Acta 47:3509–3513

Morão A, Lopes A, Pessoa de Amorim MT, Gonçalves IC (2004) Degradation of mixtures of phenols using boron doped diamond electrodes for wastewater treatment. Electrochim Acta 49:1587–1595

Morkovsky PE, Kaspar DD, Petru JM (1999) Process and apparatus for electrocoagulative treatment of industrial waste water. US Patents

Munoz LD, Erable B, Etcheverry L, Riess J, Basséguy R, Bergel A (2010) Combining phosphate species and stainless steel cathode to enhance hydrogen evolution in microbial electrolysis cell (MEC). Electrochem Commun 12:183–186

Murugananthan M, Yoshihara S, Rakuma T, Shirakashi T (2008) Mineralization of bisphenol a (BPA) by anodic oxidation with boron-doped diamond (BDD) electrode. J Hazard Mater 154:213–220

Murugananthan M, Latha SS, Bhaskar Raju G, Yoshihara S (2010) Anodic oxidation of ketoprofen - an anti-inflammatory drug using boron doped diamond and platinum electrodes. J Hazard Mater 180:753–758

Nabi SA, Naushad M, Khan AM (2006) Sorption studies of metal ions on napthol blue–black modified Amberlite IR-400 anion exchange resin: separation and determination of metal ion contents of pharmaceutical preparation. Colloids Surfaces A Physicochem Eng Aspects 280:66–70

Najafi M, Khalilzadeh MA, Karimi-Maleh H (2014) A new strategy for determination of bisphenol a in the presence of Sudan I using a ZnO/CNTs/ionic liquid paste electrode in food samples. Food Chem 158:125–131

Naumczyk J, Szpyrkowicz L, Zilio-Grandi F (1996) Electrochemical treatment of textile wastewater. Water Sci Technol 34:17–24

Nevin KP, Richter H, Covalla SF, Johnson JP, Woodard TL, Orloff AL, Jia H, Zhang M, Lovley DR (2008) Power output and columbic efficiencies from biofilms of Geobacter sulfurreducens comparable to mixed community microbial fuel cells. Environ Microbiol 10:2505–2514

Neyens E, Baeyens J (2003) A review of classic Fenton's peroxidation as an advanced oxidation technique. J Hazard Mater 98:33–50

Nidheesh PV, Gandhimathi R (2012) Trends in electro-Fenton process for water and wastewater treatment: an overview. Desalination 299:1–15

Öğütveren ÜB, Koparal S (1992) Electrochemical treatment of water containing dye-stuffs: anodic oxidation of Congo red and xiron blau 2RHD. Int J Environ Stud 42:41–52

Ota K-I, Kreysa G, Savinell RF (2014) Encyclopedia of applied electrochemistry. Springer, New York

Oturan MA, Oturan N, Edelahi MC, Podvorica FI, Kacemi KE (2011) Oxidative degradation of herbicide diuron in aqueous medium by Fenton's reaction based advanced oxidation processes. Chem Eng J 171:127–135

Özcan A, Şahin Y, Savaş Koparal A, Oturan MA (2008) Carbon sponge as a new cathode material for the electro-Fenton process: comparison with carbon felt cathode and application to degradation of synthetic dye basic blue 3 in aqueous medium. J Electroanal Chem 616:71–78

Özverdi A, Erdem M (2006) Cu^{2+}, Cd^{2+} and Pb^{2+} adsorption from aqueous solutions by pyrite and synthetic iron sulphide. J Hazard Mater 137:626–632

Panizza M, Cerisola G (2009) Direct and mediated anodic oxidation of organic pollutants. Chem Rev 109:6541–6569

Panizza M, Delucchi M, Cerisola G (2005) Electrochemical degradation of anionic surfactants. J Appl Electrochem 35:357–361

Parameswaran P, Zhang H, Torres CI, Rittmann BE, Krajmalnik-Brown R (2010) Microbial community structure in a biofilm anode fed with a fermentable substrate: the significance of hydrogen scavengers. Biotechnol Bioeng 105:69–78

Park H, Vecitis CD, Hoffmann MR (2009) Electrochemical water splitting coupled with organic compound oxidation: the role of active chlorine species. J Phys Chem C 113:7935–7945

Pedersen AJ, Ottosen LM, Villumsen A (2005) Electrodialytic removal of heavy metals from municipal solid waste incineration fly ash using ammonium citrate as assisting agent. J Hazard Mater 122:103–109

Peng L, Dong S, Xie H, Gu G, He Z, Lu J, Huang T (2014) Sensitive simultaneous determination of diethylstilbestrol and bisphenol a based on Bi_2WO_6 nanoplates modified carbon paste electrode. J Electroanal Chem 726:15–20

Pérez RM, Cabrera G, Gómez JM, Ábalos A, Cantero D (2010) Combined strategy for the precipitation of heavy metals and biodegradation of petroleum in industrial wastewaters. J Hazard Mater 182:896–902

Picot M, Lapinsonnière L, Rothballer M, Barrière F (2011) Graphite anode surface modification with controlled reduction of specific aryl diazonium salts for improved microbial fuel cells power output. Biosens Bioelectron 28:181–188

Pimentel M, Oturan N, Dezotti M, Oturan MA (2008) Phenol degradation by advanced electrochemical oxidation process electro-Fenton using a carbon felt cathode. Appl Catal B Environ 83:140–149

Prairie MR, Evans LR, Stange BM, Martinez SL (1993) An investigation of titanium dioxide photocatalysis for the treatment of water contaminated with metals and organic chemicals. Environ Sci Technol 27:1776–1782

Qiang Z, Chang J-H, Huang C-P (2002) Electrochemical generation of hydrogen peroxide from dissolved oxygen in acidic solutions. Water Res 36:85–94

Quivet E, Faure R, Georges J, Paisse JO, Herbreteau B, Lanteri P (2006) Photochemical degradation of imazamox in aqueous solution: influence of metal ions and anionic species on the ultraviolet photolysis. J Agric Food Chem 54:3641–3645

Rajkumar D, Palanivelu K (2004) Electrochemical treatment of industrial wastewater. J Hazard Mater 113:123–129

Reguera G, McCarthy KD, Mehta T, Nicoll JS, Tuominen MT, Lovley DR (2005) Extracellular electron transfer via microbial nanowires. Nature 435:1098–1101

Richter H, Nevin KP, Jia H, Lowy DA, Lovley DR, Tender LM (2009) Cyclic voltammetry of biofilms of wild type and mutant Geobacter sulfurreducens on fuel cell anodes indicates possible roles of OmcB, OmcZ, type IV pili, and protons in extracellular electron transfer. Energy Environ Sci 2:506–516

Rittmann BE (2008) Opportunities for renewable bioenergy using microorganisms. Biotechnol Bioeng 100:203–212

Robertson PM, Ibl N (1977) Electrolytic recovery of metals from waste waters with the 'Swiss-roll' cell. J Appl Electrochem 7:323–330

Rosales E, Pazos M, Longo MA, Sanromán MA (2009) Electro-Fenton decoloration of dyes in a continuous reactor: a promising technology in colored wastewater treatment. Chem Eng J 155:62–67

Rosales E, Iglesias O, Pazos M, Sanromán MA (2012) Decolourisation of dyes under electro-Fenton process using Fe alginate gel beads. J Hazard Mater 213–214:369–377

Rousseau R, Dominguez-Benetton X, Délia M-L, Bergel A (2013) Microbial bioanodes with high salinity tolerance for microbial fuel cells and microbial electrolysis cells. Electrochem Commun 33:1–4

Rozendal RA, Hamelers HVM, Molenkamp RJ, Buisman CJN (2007) Performance of single chamber biocatalyzed electrolysis with different types of ion exchange membranes. Water Res 41:1984–1994

Rozendal RA, Jeremiasse AW, Hamelers HVM, Buisman CJN (2008) Hydrogen production with a microbial biocathode. Environ Sci Technol 42:629–634

Ruoff RS, Lorents DC (1995) Mechanical and thermal properties of carbon nanotubes. Carbon 33:925–930

Sadrzadeh M, Mohammadi T, Ivakpour J, Kasiri N (2008) Separation of lead ions from wastewater using electrodialysis: comparing mathematical and neural network modeling. Chem Eng J 144:431–441

Sahu O, Mazumdar B, Chaudhari PK (2014) Treatment of wastewater by electrocoagulation: a review. Environ Sci Pollut Res 21:2397–2413

Scarsbrook GA, Martineau PM, Twitchen DJ, Whitehead AJ, Cooper MA, Dorn BSC (2007) Boron doped diamond, US7160617 B2. Google Patents

Schippers A (2004) Biogeochemistry of metal sulfide oxidation in mining environments, sediments, and soils. Geol Soc Am Spec Pap 379:49–62

Schlesinger M, Paunovic M (2014) Modern electroplating. Wiley, Hoboken

Schroder U (2007) Anodic electron transfer mechanisms in microbial fuel cells and their energy efficiency. Phys Chem Chem Phys 9:2619–2629

Segundo JEDV, Salazar-Banda GR, Feitoza ACO, Vilar EO, Cavalcanti EB (2012) Cadmium and lead removal from aqueous synthetic wastes utilizing Chemelec electrochemical reactor: study of the operating conditions. Sep Purif Technol 88:107–115

Sleutels THJA, Lodder R, Hamelers HVM, Buisman CJN (2009) Improved performance of porous bio-anodes in microbial electrolysis cells by enhancing mass and charge transport. Int J Hydrog Energy 34:9655–9661

Sleutels THJA, Hamelers HVM, Buisman CJN (2011) Effect of mass and charge transport speed and direction in porous anodes on microbial electrolysis cell performance. Bioresour Technol 102:399–403

Smara A, Delimi R, Chainet E, Sandeaux J (2007) Removal of heavy metals from diluted mixtures by a hybrid ion-exchange/electrodialysis process. Sep Purif Technol 57:103–110

Soderquist TJ, Chesniak OM, Witt MR, Paramo A, Keeling VA, Keleher JJ (2012) Evaluation of the catalytic decomposition of H_2O_2 through use of organo-metallic complexes--a potential link to the luminol presumptive blood test. Forensic Sci Int 219:101–105

Stucki S, Kötz R, Carcer B, Suter W (1991) Electrochemical waste water treatment using high overvoltage anodes part II: anode performance and applications. J Appl Electrochem 21:99–104

Suanon F, Sun Q, Dimon B, Mama D, Yu C-P (2016) Heavy metal removal from sludge with organic chelators: comparative study of N, N-bis(carboxymethyl) glutamic acid and citric acid. J Environ Manag 166:341–347

Sudoh M, Kitaguchi H, Koide K (1985) Electrochemical production of hydrogen peroxide by reduction of oxygen. J Chem Eng Japan 18:409–414

Sulaymon AH, Yousif SA, Al-Faize MM (2014) Competitive biosorption of lead mercury chromium and arsenic ions onto activated sludge in fixed bed adsorber. J Taiwan Inst Chem Eng 45(2):325–337

Sun J-H, Sun S-P, Wang G-L, Qiao L-P (2007) Degradation of azo dye Amido black 10B in aqueous solution by Fenton oxidation process. Dyes Pigments 74:647–652

Tang X, Li H, Du Z, Wang W, Ng HY (2015) Conductive polypyrrole hydrogels and carbon nanotubes composite as an anode for microbial fuel cells. RSC Adv 5:50968–50974

Tao H-C, Lei T, Shi G, Sun X-N, Wei X-Y, Zhang L-J, Wu W-M (2014) Removal of heavy metals from fly ash leachate using combined bioelectrochemical systems and electrolysis. J Hazard Mater 264:1–7

Tenca A, Cusick RD, Schievano A, Oberti R, Logan BE (2013) Evaluation of low cost cathode materials for treatment of industrial and food processing wastewater using microbial electrolysis cells. Int J Hydrog Energy 38:1859–1865

Thilakavathi R, Balasubramanian N, Srinivasakannan C, Shoaibi AA (2012) Modeling particulate bed electrode for metal recovery. Int J Electrochem Sci 7:1371–1385

Ting W-P, Lu M-C, Huang Y-H (2009) Kinetics of 2,6-dimethylaniline degradation by electro-Fenton process. J Hazard Mater 161:1484–1490

Torres CI, Marcus AK, Parameswaran P, Rittmann BE (2008) Kinetic experiments for evaluating the Nernst−Monod model for anode-respiring bacteria (ARB) in a biofilm anode. Environ Sci Technol 42:6593–6597

Torres CI, Marcus AK, Lee H-S, Parameswaran P, Krajmalnik-Brown R, Rittmann BE (2010) A kinetic perspective on extracellular electron transfer by anode-respiring bacteria. FEMS Microbiol Rev 34:3–17

Ujang Z, Hamdzah M, Ozaki H (2010) A method for treating wastewater containing heavy metals. Google Patents

Umar M, Aziz HA, Yusoff MS (2010) Trends in the use of Fenton, electro-Fenton and photo-Fenton for the treatment of landfill leachate. Waste Manag 30:2113–2121

Verea L, Savadogo O, Verde A, Campos J, Ginez F, Sebastian PJ (2014) Performance of a microbial electrolysis cell (MEC) for hydrogen production with a new process for the biofilm formation. Int J Hydrog Energy 39:8938–8946

Visnja O, Nenad M, Denis P (2013) Process and device for electrochemical treatment of industrial wastewater and drinking water. Google Patents
Wagner RC, Porter-Gill S, Logan BE (2012) Immobilization of anode-attached microbes in a microbial fuel cell. AMB Express 2(1):1
Walling C (1975) Fenton's reagent revisited. Acc Chem Res 8:125–131
Wang Q, Lemley AT (2001) Kinetic model and optimization of 2,4-D degradation by anodic Fenton treatment. Environ Sci Technol 35:4509–4514
Wang H, Ren ZJ (2013) A comprehensive review of microbial electrochemical systems as a platform technology. Biotechnol Adv 31:1796–1807
Wang JL, Xu LJ (2011) Advanced oxidation processes for wastewater treatment: formation of hydroxyl radical and application. Crit Rev Environ Sci Technol 42:251–325
Wang C-T, Hu J-L, Chou W-L, Kuo Y-M (2008) Removal of color from real dyeing wastewater by electro-Fenton technology using a three-dimensional graphite cathode. J Hazard Mater 152:601–606
Wang A, Liu W, Ren N, Cheng H, Lee D-J (2010a) Reduced internal resistance of microbial electrolysis cell (MEC) as factors of configuration and stuffing with granular activated carbon. Int J Hydrog Energy 35:13488–13492
Wang LK, Ivanov V, Tay J-H, Hung Y-T (2010b) Environmental biotechnology, 10. Springer Science & Business Media, New York
Wang A, Liu W, Ren N, Zhou J, Cheng S (2010c) Key factors affecting microbial anode potential in a microbial electrolysis cell for H_2 production. Int J Hydrog Energy 35:13481–13487
Wang Y, Shao Y, Matson DW, Li J, Lin Y (2010d) Nitrogen-doped graphene and its application in electrochemical biosensing. ACS Nano 4:1790–1798
Wang C-T, Chou W-L, Chung M-H, Kuo Y-M (2010e) COD removal from real dyeing wastewater by electro-Fenton technology using an activated carbon fiber cathode. Desalination 253:129–134
Weber KA, Achenbach LA, Coates JD (2006) Microorganisms pumping iron: anaerobic microbial iron oxidation and reduction. Nat Rev Microbiol 4:752–764
Wu W, Huang Z-H, Lim T-T (2014) Recent development of mixed metal oxide anodes for electrochemical oxidation of organic pollutants in water. Appl Catal A General 480:58–78
Xu ST, Liu H, Fan YZ, Schaller R, Jiao J, Chaplen F (2012) Enhanced performance and mechanism study of microbial electrolysis cells using Fe nanoparticle-decorated anodes. Appl Microbiol Biotechnol 93:871–880
Yang N, Hafez H, Nakhla G (2015) Impact of volatile fatty acids on microbial electrolysis cell performance. Bioresour Technol 193:449–455
Yasri NG (2001) Developments of electrochemistry in Environmental Technology. Brunel University, p 304
Yasri NG, Nakhla G (2016) Electrochemical behavior of anode-respiring bacteria on doped carbon electrodes. ACS Appl Mater Interfaces 8:35150–35162. doi:10.1021/acsami.6b09907
Yasri NG, Nakhla G (2017) The performance of 3-D graphite doped anodes in microbial electrolysis cells. J Power Sources 342:579–588
Yasri NG, Sundramoorthy AK, Chang W-J, Gunasekaran S (2014) Highly selective mercury detection at partially oxidized graphene/poly(3,4-ethylenedioxythiophene):poly(styrenesulfonate) nanocomposite film modified electrode. Front Math 1:33
Yasri NG, Sundramoorthy AK, Gunasekaran S (2015a) Azo dye functionalized graphene nanoplatelets for selective detection of bisphenol a and hydrogen peroxide. RSC Adv 5:87295–87305
Yasri NG, Yaghmour A, Gunasekaran S (2015b) Effective removal of organics from corn wet milling steepwater effluent by electrochemical oxidation and adsorption on 3-D granulated graphite electrode. J Environ Chem Eng 3:930–937
Yin H-S, Zhou Y-L, Ai S-Y (2009) Preparation and characteristic of cobalt phthalocyanine modified carbon paste electrode for bisphenol a detection. J Electroanal Chem 626:80–88

Yin H, Cui L, Chen Q, Shi W, Ai S, Zhu L, Lu L (2011) Amperometric determination of bisphenol a in milk using PAMAM–Fe_3O_4 modified glassy carbon electrode. Food Chem 125:1097–1103

Yoho RA, Popat SC, Torres CI (2014) Dynamic potential-dependent electron transport pathway shifts in anode biofilms of *Geobacter sulfurreducens*. Chem Sustain Chem 7:3413–3419

Yoho RA, Popat SC, Rago L, Guisasola A, Torres CI (2015) Anode biofilms of *Geoalkalibacter ferrihydriticus* exhibit electrochemical signatures of multiple electron transport pathways. Langmuir 31:12552–12559

Yoshihara S, Murugananthan M (2009) Decomposition of various endocrine-disrupting chemicals at boron-doped diamond electrode. Electrochim Acta 54:2031–2038

Zhang H, Zhang D, Zhou J (2006) Removal of COD from landfill leachate by electro-Fenton method. J Hazard Mater 135:106–111

Zhang H, Fei C, Zhang D, Tang F (2007) Degradation of 4-nitrophenol in aqueous medium by electro-Fenton method. J Hazard Mater 145:227–232

Zhang C, Jiang Y, Li Y, Hu Z, Zhou L, Zhou M (2013) Three-dimensional electrochemical process for wastewater treatment: a general review. Chem Eng J 228:455–467

Zhang B, Wen Z, Ci S, Chen J, He Z (2014a) Nitrogen-doped activated carbon as a metal free catalyst for hydrogen production in microbial electrolysis cells. RSC Adv 4:49161–49164

Zhang J, Li J, Ye D, Zhu X, Liao Q, Zhang B (2014b) Enhanced performances of microbial fuel cells using surface-modified carbon cloth anodes: a comparative study. Int J Hydrog Energy 39:19148–19155

Zhao Y, Watanabe K, Nakamura R, Mori S, Liu H, Ishii K, Hashimoto K (2010) Three-dimensional conductive nanowire networks for maximizing anode performance in microbial fuel cells. Chem Eur J 16:4982–4985

Zheng Y, Jiao Y, Li LH, Xing T, Chen Y, Jaroniec M, Qiao SZ (2014) Toward design of synergistically active carbon-based catalysts for electrocatalytic hydrogen evolution. ACS Nano 8:5290–5296

Zhu X, Ni J, Lai P (2009) Advanced treatment of biologically pretreated coking wastewater by electrochemical oxidation using boron-doped diamond electrodes. Water Res 43:4347–4355

Zhu X, Yates MD, Hatzell MC, Ananda Rao H, Saikaly PE, Logan BE (2014) Microbial community composition is unaffected by anode potential. Environ Sci Technol 48:1352–1358

Zoski C (2006) Handbook of electrochemistry. Elsevier, Boston

Microwave Heating-Mediated Remediation of Hydrocarbon-Polluted Soils: Theoretical Background and Techno-Economic Considerations

Pietro P. Falciglia and Federico G.A. Vagliasindi

Abstract Massive amounts of soil and water have been contaminated with hydrocarbon compounds, including fuel and petrochemical products, because of economic and industrial activities. Several chemical-physical or biologic treatments have been studied to remediate hydrocarbon-polluted soils; however, these alternatives may be ineffective, expensive or too lengthy. Otherwise, ex situ conventional thermal desorption was successfully applied to remove organic contaminants, presenting excellent removal values in a very short time but requiring high energy and costs. Microwaves (MW) are a part of the electromagnetic spectrum occurring in the frequency range of 300 MHz–300 GHz, and recently, their application has been identified as a potential tool for hydrocarbon-polluted soil remediation. Compared to other remediation methods, MW heating has advantages including simplicity, safety, flexibility and cost-effectiveness since it offers the potential to significantly reduce treatment times, risk of contamination and costs due to the direct interaction of microwaves with the soil and its ability to overcome heat and mass transfer limitations. In conventional heating systems, the energy is transferred through conduction, convection and radiation, while in MW heating, energy is supplied directly to soil by molecular interaction with the electromagnetic field generated. Therefore, the components of the soil are heated individually and instantaneously, overcoming limits imposed by material heat transfer properties. Literature studies have shown that MW remediation has the potential to remove polar and semipolar organic pollutants from soil. The key factor of the remediation process is represented by the mechanism due to a partial dissipation of the electromagnetic field energy and its conversion into heat, avoiding the limitations of conductive heating phenomena of conventional thermal desorption treatment. This chapter discusses the theoretical background including MW heating process and the related techno-economic features for ex situ full-scale applications in remediation activities of hydrocarbon contaminants.

P.P. Falciglia (✉) • F.G.A. Vagliasindi
Department of Civil Engineering and Architecture, University of Catania,
Viale A. Doria, 6, 95125 Catania, Italy
e-mail: ppfalci@dica.unict.it

N.A. Anjum et al. (eds.), *Enhancing Cleanup of Environmental Pollutants*,
DOI 10.1007/978-3-319-55423-5_3

Keywords Hydrocarbon pollution • Remediation • Soils • Microwave heating

Introduction

Massive amounts of soil and groundwater have been contaminated with total petroleum hydrocarbons (TPHs) because of economic and industrial activities (Tatáno et al. 2013; Islam et al. 2015). In recent years, a number of chemical-physical or biologic treatments have been investigated to remediate hydrocarbon-polluted soils (Silva-Castro et al. 2013; Jagtap et al. 2014; Liu et al. 2014). However, these alternatives may be ineffective, expensive or too lengthy (Liu et al. 2014), whereas, reports have demonstrated that thermal treatments could be successfully used to remedy hydrocarbon-polluted soils or rocks due to their versatility, removal efficiency and required time (Chen et al. 2010; Falciglia et al. 2011a; Qi et al. 2014; Switzer et al. 2014; Yang et al. 2014). On the other hand, conventional thermal techniques may be expensive especially due to fuel costs, making innovative low-cost thermal treatments an option strongly desired. Recently, microwave (MW) heating remediation has attracted great attention in the environmental field representing a potential remedial alternative for contaminated matrices or wastes (Barba et al. 2012; Tyagi and Lo 2013; Al-harahsheh et al. 2014; Pereira et al. 2014; Falciglia et al. 2015). MW heating offers the potential to significantly reduce treatment times and costs due to the direct interaction of electromagnetic waves with the soil and their ability to overcome heat transfer limitations. In fact, heating time is three orders of magnitude lower than with conventional heating as reported (Robinson et al. 2009). Other merits that should make MW application desirable are (a) homogeneous heating of the contaminated materials, (b) low energy consumption linked to short remediation times, (c) high flexibility with possibility of instantaneously controlling the power-temperature response and (d) selective heating (in the presence of polar contaminants) (Tyagi and Lo 2013).

Principles of Microwave Heating and Organic Contaminant Removal

MWs are a part of the electromagnetic spectrum occurring in the frequency range of 300 MHz–300 GHz, and their ability to heat rapidly and selectively the contaminated matrices leads to the possibility of significant energy savings and the need of much smaller process equipment by which strictly control the automatic implementation of heating processes (Benedetto and Calvi 2013; Robinson et al. 2014). Notably, the key factor of the remediation process is represented by the mechanism of partial dissipation of the electromagnetic field energy and its conversion into heat necessary for the thermal desorption of the organic contaminants. In fact, in a conventional thermal desorption treatment, the soil temperature increasing depends

mainly on conduction process, whereas in the case of microwave radiation, the penetration of the generated alternating electric field into the contaminated soil induces the rotation of the dipoles of polar or semipolar substances present in the soil such as water and hydrocarbon contaminants, respectively. The intermolecular friction results in the generation of heat. Moreover, MWs are highly absorbed by materials with a high dielectric loss factor (absorbing) while passing through the low loss (transparent) material, resulting in a selective, uniform and rapid heating. Therefore, heating times can be significantly reduced compared with those required when using conventional heating methods (Robinson et al. 2009).

The internal electric field (E) magnitude generated by MW irradiation decreases with the distance from the irradiating source (d) due to the energy conversion into heat, and its dependence on d (m) can be evaluated by Eq. 1 assuming that the microwaves are partially absorbed by the medium according to the law of Lambert and Beer (Barba et al. 2012; Falciglia and Vagliasindi 2014):

$$E_{\mathrm{d}} = E_0 \cdot e^{-\frac{d}{D_{\mathrm{p}}}} \tag{1}$$

where E_0 is the incident electric field (V m^{-1}) and D_{p} is the penetration depth (m) that represents the ability of the electromagnetic waves to penetrate into the medium. In particular, D_{p} is defined as the distance from the emission point at which E drops to 0.37 from its value at the emission point. For low loss dielectric materials (i.e. soil) ($\varepsilon''/\varepsilon' << 1$), D_{p} is given by the simplified form expressed in the Eq. 2:

$$D_p = \frac{\lambda_0}{2\pi} \cdot \frac{\sqrt{\varepsilon'}}{\varepsilon''} \tag{2}$$

where λ_0 is the wavelength of the irradiation (m), whereas ε' (−) and ε'' (−) are the real parts (dielectric constant) and the imaginary parts (dielectric loss factor) of the complex permittivity, respectively. The electric power $\dot{Q}$ dissipated into heat per unit of volume during the MW irradiation depends on the frequency of the applied electromagnetic field and the dielectric and thermal properties of the medium. The dissipation is quantified by Eq. 3, which is derived from Maxwell's equations (Metaxas and Meredith 1993):

$$\dot{Q} = \frac{1}{2}\omega\epsilon_0\varepsilon''\left|E^2_{\max}\right| = \omega\epsilon_0\varepsilon''\left|E^2\right| \tag{3}$$

where ω is the angular frequency ($\omega = 2\pi f$), ε_0 is the permittivity of free space ($8.85{\cdot}10^{-12}$ F m^{-1}), $E_{\max}$ is the electromagnetic field peak value (V m^{-1}) and E is the electromagnetic field effective value (V m^{-1}). Consequently, the increase of temperature (T) with time (t) (°C min^{-1}) can be quantified by the following equation (Falciglia et al. 2016a):

$$\frac{\Delta T}{\Delta t} = \frac{P}{c_{\mathrm{p}} \cdot \rho} = \frac{\omega \cdot \varepsilon_0 \cdot \varepsilon'' |E|^2}{c_{\mathrm{p}} \cdot \rho} \tag{4}$$

where c_{p} is the heat capacity of the medium (KJ kg^{-1} °C^{-1}) and ρ is its density (kg m^{-3}).

The dielectric constant ε' denotes the electric energy storage capacity of the medium, while the dielectric loss factor ε'' can be considered as the ability of the medium to convert electromagnetic energy into heat due to the dielectric polarisation of the particles in an alternating electric field. Substances, which exhibit a large value of loss factor, are good microwave absorbers, whereas substances whose loss factor is close to zero can be considered to be microwave transparent (Metaxas and Meredith 1993). For most hydrocarbon contaminants, for example, diesel fuel, which are classified as semipolar compounds having dielectric properties similar to those of soils, the key factor of the remediation process is not represented by a selective heating/desorption of the contaminant alone but by the final temperature of the contaminated soil. In addition, as the amount of water in soil (as soil moisture) increases, so does MW removal efficiency due to water high dielectric properties and, consequently, high MW-absorbing features (Falciglia et al. 2013). However, during the MW irradiation the increase of the soil temperature (T) depends also on the conduction phenomena. The energy equation taking into account heat transferring by conduction is expressed in the form (Falciglia et al. 2015)

$$\rho c_{\mathrm{p}} \frac{\partial T}{\partial t} = -k \nabla^2 T + \dot{Q} \tag{5}$$

where k is the thermal conductivity (W m^{-1} $^{\circ}\mathrm{C}^{-1}$).

Overall, organic contaminant removal could be due to four different processes: (a) vaporisation due to the surpassing of the heat of vaporisation threshold, (b) molecular bond breaking and consequently transformation of contaminant molecules into derivatives or other smaller molecules, (c) selective vaporisation due to the contaminant localised temperature achievable thanks to contaminant dielectric properties (polarity) significantly higher than the soil ones and (d) contaminant stripping due to steam distillation processes. The first process is generally observed in conventional thermal desorption treatment (Falciglia et al. 2011b) or in MW remediation of soils contaminated with low polar compounds where treatment temperature is higher than the contaminant boiling point. The second process is frequently observed, for example, in irradiating process of PAHs (Librando et al. 2014) or PAH derivatives (Rafael and Morel 2013). Selective vaporisation occurs when a significant hydrocarbon removal takes place even if the global soil temperature is significantly lower than the contaminant boiling point. Finally, in the presence of water as soil moisture, the soil temperature increase induces the physical process of evaporation-contaminant stripping phenomena.

Parameters Influencing the Contaminant Removal Efficiency

Contaminants and High Dielectric Materials

In the last few years, several studies on contaminated soil remediation by MW have been performed in order to understand the fundamentals of the treatment of hydrocarbon-contaminated soils or to investigate the effects of process parameters on the contaminant removal efficiency. Dauerman et al. (1992) and George et al. (1995) showed the first experimental results that proposed the MW remediation technique as a promising treatment of hazardous wastes. Several authors performed removal of PCBs from contaminated soil. Liu et al. (2008) investigated the effect of a 10-min MW remediation at 750 W on a 20 g PCB-polluted soil sample to which a microwave absorber had been added. They showed an increase in contaminant removal, with increasing soil moisture, to maximum values close to 100% at moisture content of 20% (dry basis). Huang et al. (2011) demonstrated that the maximum removal efficiency, for a soil polluted by PCBs at 5 mg kg^{-1} and treated at 800 W for a period of 45 min, is about 95%. The removal efficiency of crude oil contaminant of 95% (initial contaminant concentration in soil = 7.8%) was observed for a 15 min at 800 W treatment enhanced by different microwave absorbers such as activated carbon powder or graphite fibres (Li et al. 2009). Yuan et al. (2006) investigated the remediation of soil contaminated with hexachlorobenzene (HCB) using a domestic microwave oven and powdered MnO_2 as a microwave absorber. Their results showed that a complete removal of HCB was obtained with 10-min microwave treatment. Kawala and Atamanczuk (1998) also obtained similar results in terms of removal efficiency in a pilot-scale study for the remediation of a TCE-polluted soil, where a microwave power of 600 W was supplied intermittently for 75 h. After the treatment the contaminant concentration decreased from 5000–22,300 to 8–29 mg kg^{-1}, confirming the possibility of the use of microwave heating as a remediation technique of volatile and semi-volatile compound-polluted sandy soils and that the use of low-power generators for the supply of microwave energy may help to reduce the costs of the full-scale remediation interventions. In the case of diesel-contaminated soils, Falciglia et al. (2013) reported a maximum soil temperature achievable of 260 °C corresponding to contaminant removal of 95% for soil samples treated at 1000 W for 60 min. Microwave treatment was also shown to be efficient in a short time for the remediation of soil polluted with PAHs (Falciglia et al. 2016b; Robinson et al. 2009), PCPs (Di and Chang 2001) and antibiotics (Lin et al. 2010).

The above-mentioned works suggest that treatment power, time, soil dielectric characteristics and microwave absorbents used are key factors in remedial processes and that MW remediation is very effective for a large number of polar and non-polar volatile and semi-volatile hydrocarbons, but in the case of non-polar compounds, their dielectric properties could limit the treatment removal efficiency. In addition, their results revealed that an improvement of contaminant removal was

obtained with the addition of energy absorbents such as Cu_2O, MnO_2, NaOH, iron powder, graphite or granular activated carbons. However, for non-polar organic compounds such as diesel or kerosene, defined as transparent (low dielectric loss material), it was showed that they could also be efficiently removed using water as the MW-absorbing phase (Kawala and Atamanczuk 1998).

Water Content as Soil Moisture

In MW remediation of hydrocarbon-contaminated soils, the energy supplied as irradiation jointly with the moisture content in soil has been shown to have a significant effect on the final temperature reachable during MW heating and consequently on contaminant removal efficiency (Falciglia et al. 2013). The same authors reported that a significant soil temperature increase was achievable for the moisturised sandy soils (8 and 12%) with respect to dry soil (contaminated soil without water content). For instance, a difference in soil temperature up to 40 °C was observed between soils with 0 and 12% water content, considering a 1000 W MW treatment. This specific behaviour strictly depends on the dielectric properties of the moisturised soils, which are characterised by higher loss factor (ε'') values than for dry soils, denoting a higher ability of the soil to convert electromagnetic energy into heat due to the dielectric polarisation of the particles in an alternating electric field. Specifically, in the case of dry soils, hydrocarbon removal decreases from 95 to 90% for MW treatment at 1000 W for 60 min. For time shorter than 18 min, it was shown to be lower than 77% (i.e. 77, 74 and 63% for 12, 8 and 0% water content, respectively). Studies clearly show that final soil temperature influences contaminant removals; however, in the presence of water, decontamination efficiency can be heavily improved by evaporation and contaminant stripping phenomena. In addition, the presence of a vapour stream leads to an increase of vapour pressure resulting in a reduction of the temperature needed for the contaminant desorption and consequently in an increase in removal efficiency. This presents a major influence on the lighter (volatile) hydrocarbon fractions. Progressively, the evaporation of the lightest fractions produces a solubilisation and consequently an extraction of the heaviest fractions that are removed; this also being due to the physical phenomena of water vapour stripping. Hence, in the presence of stripping processes, lighter hydrocarbon fractions act as solvents for those that are heavier.

Soil Texture

Similarly to the role of soil moisture in the effectiveness of MW remediation process, also soil texture has been shown to have a significant effect on TPH removal by applying conventional (Falciglia et al. 2011b) or MW (Falciglia and

Table 1 Dielectric and thermodynamic properties of several soil textures (Falciglia and Vagliasindi 2015)

	Medium sand	Fine sand	Silt	Clay
Parameter	*MS* (200–350 μm)	*FS* (75–200 μm)	*S* (10–75 μm)	*C* (<4.0 μm)
Soil mineral	Silica sand	Silica sand	Silica flower	Kaolin
Specific heat capacity (KJ kg^{-1} °C^{-1})	932	957	1083	1105
Dielectric constant (ε')	7.21	7.08	4.06	3.22
Loss factor (ε'')	0.78	0.72	0.67	0.60

Vagliasindi 2015) thermal desorption treatment. However, in the case of contaminant desorption by MW heating, soil textures play a major role under two major points: maximum soil temperature achievable and contaminant adsorption/desorption phenomena occurring during irradiation.

Based on Eqs. 1 and 4, MW penetration into the soil and contaminated soil temperature strictly depend on the dielectric and thermodynamic properties of the irradiated soils that, in turn, significantly change depending on the texture of the soil. Specifically, ε' and ε'' values increased with increasing the soil texture (Table 1), having a significant effect on the temperature variation. Change in soil texture alters the MW penetration and the permittivity of the sample, and hence the strength of the electric fields in the soil and the power dissipated in it, resulting in a high temperature difference between the irradiated matrices. On the other hand, residual contaminant concentration strictly depends also on different contaminant adsorption processes influenced by the specific surface area, lowest for sandy soil and highest for clayey soil. Moreover, for clayey soil, the presence of intercrystalline layers able to trap contaminants that penetrate into the layers and high porosity values, which increased the contaminant diffusion phenomena, represents limiting factors in desorption processes.

Difference in dielectric and thermodynamic properties results in a significant variation of final temperature (T) that was shown to follow the order: $T_{MS} > T_{FS} \gg T_S > T_C$ (MS, medium sand; FS, fine sand; S, silt; C, clay) (Falciglia and Vagliasindi 2015). Specifically, a marked difference of temperature was observed between sandy (MS, FS) and fine texture (S, C) soils, with the maximum difference observed between MS and C soils in a wide range (24–65 °C) depending on the power applied. The variation of T with time (t) showed a final soil temperature (60-min MW irradiation) of about 125 °C for medium sand and lower than 100 °C for clayey soil. After a 1000 W heating, T increased up to about 265 and 200 °C, respectively. It is important to highlight how soil texture influences in a different way MW and conventional thermal heating processes. It was in fact shown that when different soils were heated using conventional ex situ thermal heating (T oven = 100–300 °C), where conduction and convection are the main heat transfer processes, the highest soil temperature was reached in clayey soil at

every temperature of treatment (Falciglia et al. 2011b). Additionally, both maximum temperature achievable at the end of the irradiation by different soil textures and the different adsorption/desorption processes result in a total hydrocarbon removal for medium sandy soils and in a removal lower than 90% for clayey soil ($P = 1000$ W) (Falciglia and Vagliasindi 2015).

Techno-Economic Analysis for Ex Situ Applications

A schematic ex situ MW treatment plant generally includes that polluted soil is loaded into a hopper and by means of a screw belt passes through the cavity of the plant where it is cleaned by MW irradiation (Falciglia and Vagliasindi 2014; Buttress et al. 2016) (Fig. 1). The volatile organic compounds (VOCs) produced are treated in a dedicated off-gas treatment line. The treating capability of such MW system depends on the maximum thickness (D) of the soil layer, and it can be evaluated expressing the electric field (E) variation as a function of the soil thickness. Data reported in Fig. 2 allows the identification of D as a function of the specific operating power P and soil moisture. It is evident the influence of the soil moisture on the E penetration into the soil, and this clearly remarks that, especially at the lowest powers, MW penetration is limited in the case of dry or low water content soils. In this case, the absence or low content of water results in a drastic drop of electric field with values close to 0 for minimal values of soil thickness of about 30 cm. On the other hand, a significant difference of soil moisture does not influence the remedial processes if a P higher than 30 kW kg^{-1} is employed. Overall, for an effective remediation, soil layer values in the range 30–70 cm should be considered for the plant design activities (Falciglia and Vagliasindi 2016).

The effectiveness of the treatment, and in particular times required to reach a specific remediation target, is strictly influenced by the contaminant removal kinetics achievable during the MW irradiation. It was experimentally shown that,

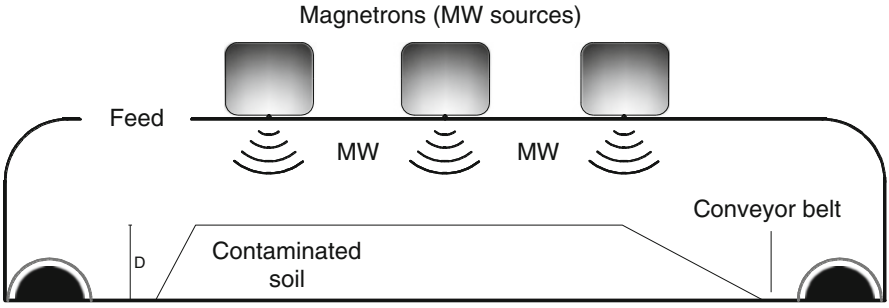

Fig. 1 Schematic presentation of an ex situ microwave plant for polluted soil remediation

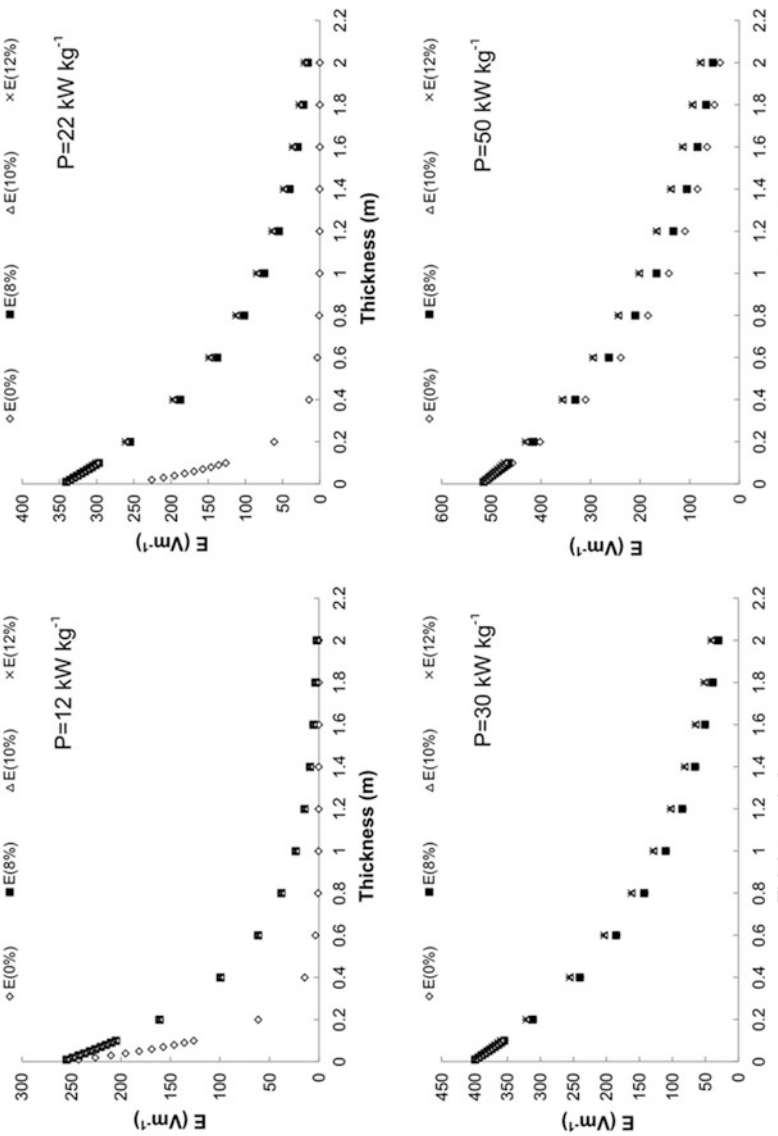

Fig. 2 Changing of internal electric field in the soil (E) generated by microwave application as a function of the soil thickness for all the soil moistures investigated (0, 8, 10 and 12%) at different specific powers (P)

Table 2 k and n of kinetic model at different powers (P) for several soil moistures

Moisture (%)	0		8		10		12	
P (kW kg^{-1})	k (min^{-1})	n	k (min^{-1})	n	k (min^{-1})	n	k (min^{-1})	n
12.5	0.053	0.623	0.145	0.430	0.246	0.361	0.250	0.371
22.0	0.074	0.715	0.207	0.533	0.269	0.490	0.277	0.499
30.0	0.092	0.762	0.277	0.517	0.337	0.494	0.341	0.497
50.0	0.128	0.710	0.369	0.458	0.428	0.477	0.429	0.481

similar to conventional thermal desorption process, MW heating is characterised by an exponential decay kinetic:

$$C = C_0 e^{-kt^n} \tag{6}$$

where t (min) is the heating time, k (min^{-1}) is the decay rate and n is the shape term. For the remediation of hydrocarbon-polluted soils, k and n values as a function of the operating condition applied and soil moisture are reported in Table 2 (Falciglia and Vagliasindi 2015). For any initial contaminant concentration (C_0) given, the knowledge of k and n parameters allows the calculation of the residual concentration values (C) as a function of operating power (P) and treatment time (t) by means of the Eq. 6, and, consequently, it is fundamental in assessing the change in energy efficiency and cost of a MW thermal remedial process.

The knowledge of the kinetic parameters permits the calculation of the minimum treatment time (t) required to reach a specific remediation target. Figure 3 shows t as a function of the initial contamination level (C_0) when the remedial target is set to 500 mg kg^{-1} (TPHs) (Falciglia and Vagliasindi 2016). Time values as a function of initial contamination level (C_0) follow a linear trend for all the soil moistures, with the exception of dry soils following an exponential trend. Specifically, focusing on P values equal or higher than 22 kW kg^{-1}, which guarantee a good penetration action of MWs into the soil, it was shown that remediation times not higher than 100 min are needed, for moisturised soils, in order to remediate hydrocarbon contamination up to 5000 mg kg^{-1}. For each condition, the knowledge of time (t)-power (P) values allows also the calculation of the specific energy (E) required and related cost (C_E) (Fig. 4). E is reported in a wide range (5–35 kWh kg^{-1}) for C_0 values from 1500 to 5000 mg kg^{-1}. The same behaviour is reflected in C_E, for which values in the range 20–160 € ton^{-1} were found for $C_0 > 1500$ mg kg^{-1} (sandy soil). The presence of humidity in the soil determines a C_E reduction up to about 70 € ton^{-1}, highlighting again being a critical key factor for the optimisation of a full-scale MW treatment.

The treating capability and the effectiveness of MW remedial system were also affected by soil texture type. Electric field (E) variation for different soil textures (medium sand, *MS*; fine sand, *FS*; silt, *S*; and clay, *C*) is reported in Fig. 5 (Falciglia and Vagliasindi 2016). For P lower than 22 kW kg^{-1}, E penetration drops significantly for thickness values lower than 1 m. Data highlights that also soil texture

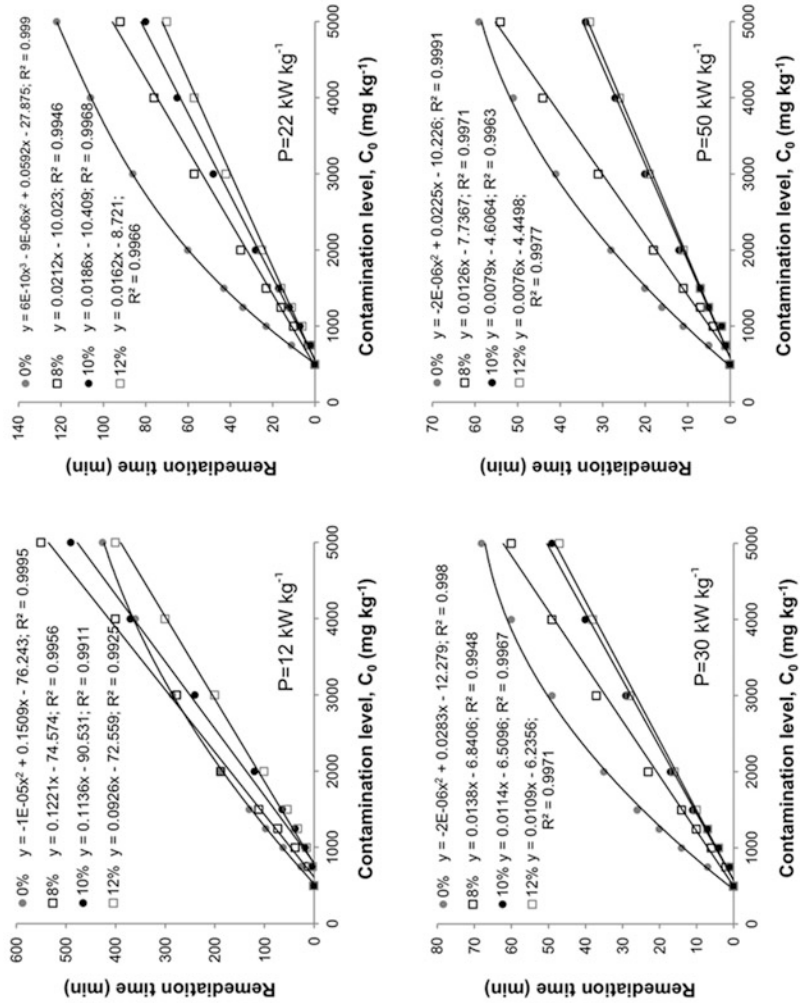

Fig. 3 Remediation times required to reach the remediation target (500 mg kg^{-1} – TPHs) as a function of the initial contamination level (C_0) for all the soil moistures investigated (0, 8, 10 and 12%) at different specific powers (P)

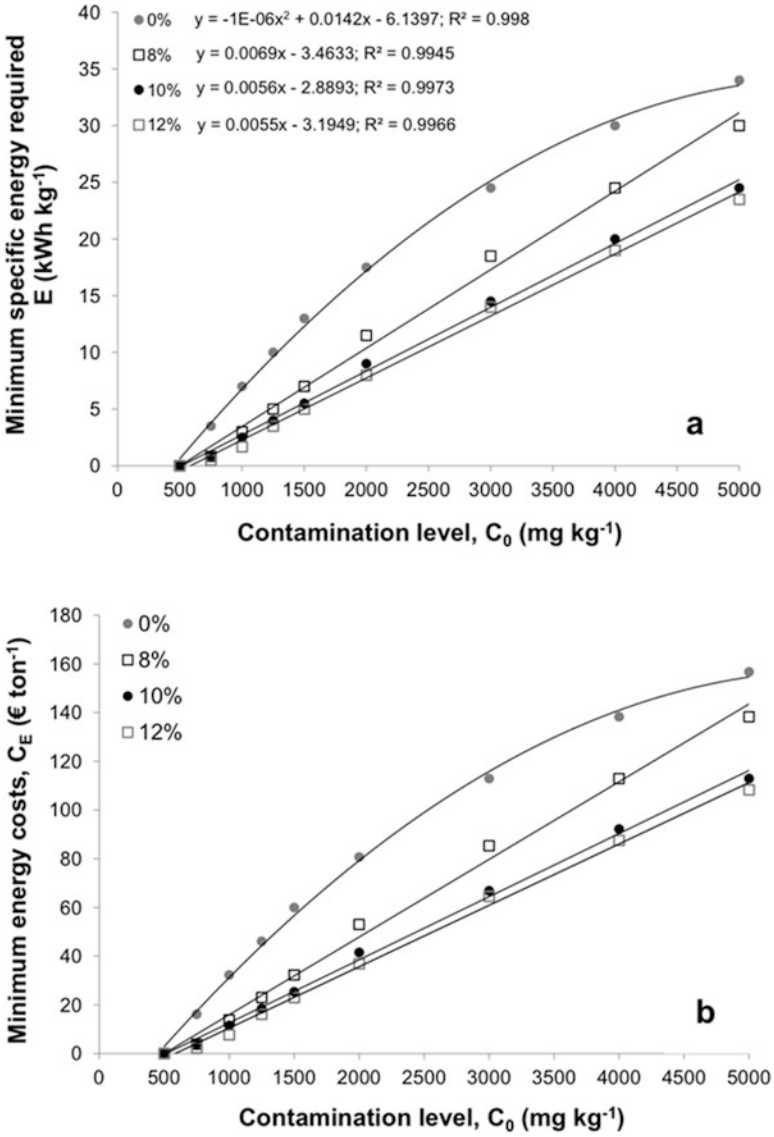

Fig. 4 Minimum specific energy required (E) (**a**) and related specific energy cost (C_E) (**b**) to reach the remediation target (500 mg kg^{-1} – TPHs) as a function of the initial contamination level (C_0) for all the soil moistures investigated (0, 8, 10 and 12%)

significantly influences the electric field penetration irrespective of the power applied and confirms that soil layer values lower than about 70 cm should be considered for design activities. Even for different textures, kinetic model better expressing the variation of residual TPH concentration as a function of the

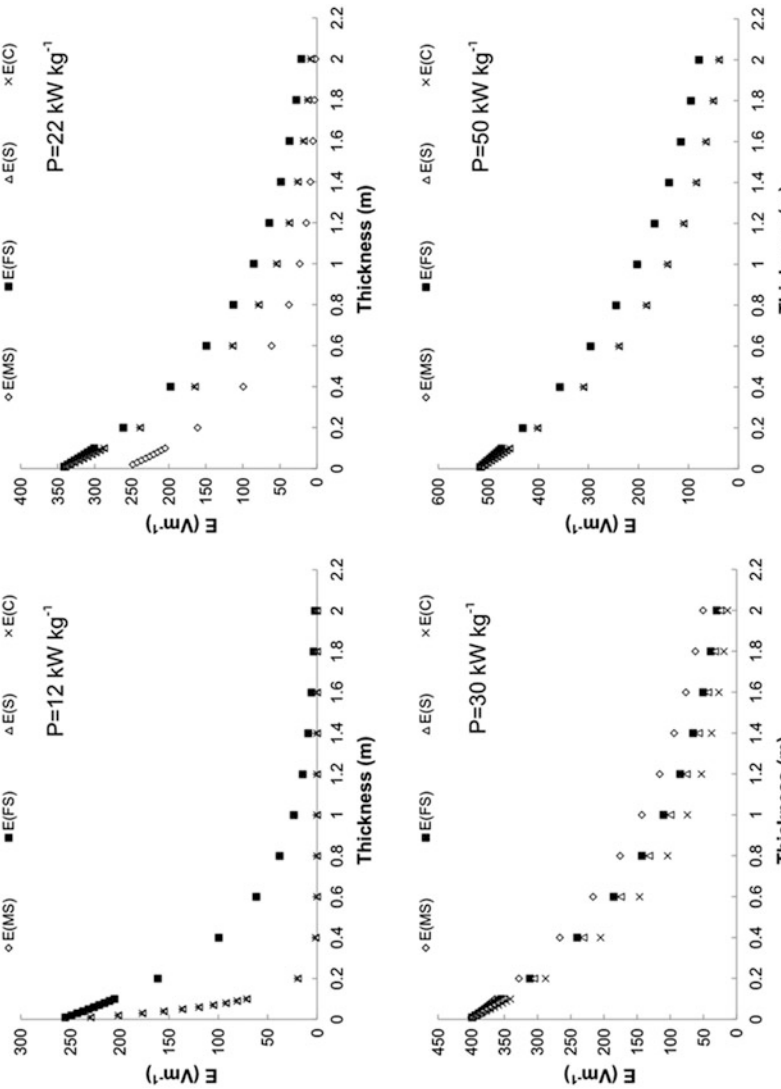

Fig. 5 Changing of internal electric field in the soil (E) generated by microwave application as a function of the soil thickness for MS, FS, S and C soil textures at different specific powers (P)

Table 3 k and n of kinetic model at different powers (P) for several soil textures

Texture	Medium sand (MS)		Fine sand (FS)		Silt (S)		Clay (C)	
P (kW kg^{-1})	k (min^{-1})	n	k (min^{-1})	n	k (min^{-1})	n	k (min^{-1})	N
12.5	0.269	0.388	0.246	0.361	0.177	0.409	0.122	0.485
22.0	0.268	0.523	0.269	0.49	0.223	0.48	0.167	0.556
30.0	0.334	0.528	0.337	0.494	0.307	0.433	0.206	0.631
50.0	0.450	0.516	0.428	0.477	0.343	0.531	0.265	0.549

treatment time is again that was expressed in the Eq. 6 (Falciglia and Vagliasindi 2015). Related k and n parameters experimentally assessed for sandy, silty and clayey soils and the minimum treatment time (t) (target: $C = 500$ mg kg^{-1} – TPHs) as a function of C_0 are reported in Table 3 and Fig. 6, respectively (Falciglia and Vagliasindi 2016). The variation of t with C_0 for different soil textures clearly shows that the nature of the soil heavily influences the effectiveness of the remedial treatment especially if low P values are applied. Specifically, highest electric field values previously reported for sandy soils resulted in the shortest remediation times for the same group of soils. Consequently, soil textures influence energy consumptions that were reported in the range 17–35 kWh kg^{-1} for the maximum C_0 considered (Fig. 7a). The possibility of using low remediation times for sandy soils results in a most economical treatment (Fig. 7b), whereas, double costs are required for the treatment of clayey soils (maximum cost of 160 € ton^{-1}) with respect to a medium sandy soil. Therefore, the remediation of fine texture soils, such as silt or clay, could be unsuitable.

It is clear that soil features and contaminant, as well as the specific operating conditions applied, heavily influenced the overall treatment costs. However, very limited information on MW cost are available in scientific and technical literature. In a recent study where different MW irradiation conditions have been investigated, Buttress et al. (2016), evaluating a continuous microwave processing system for hydrocarbon removal from contaminated soils (energy dose of 150kWh t^{-1}), report an average operating cost of about 20 € ton^{-1} to reach a maximum contaminant removal of 75%.

Comparison to Other Hydrocarbon Removal Treatments

Contaminant removal values observed jointly with remediation times are hardly achievable by other treatments, especially if bioremediation or bioagumentation treatments are involved. In this case, a hydrocarbon removal not higher than about 80% and remediation times up to 300 days were generally observed. Lee et al. (2007) reported a maximum biodegradation ratio of hydrocarbon of 59.4% for a remediation time of 12 days by applying a bench-scale enhanced bioremediation decontamination treatment of a low permeability soil artificially contaminated with

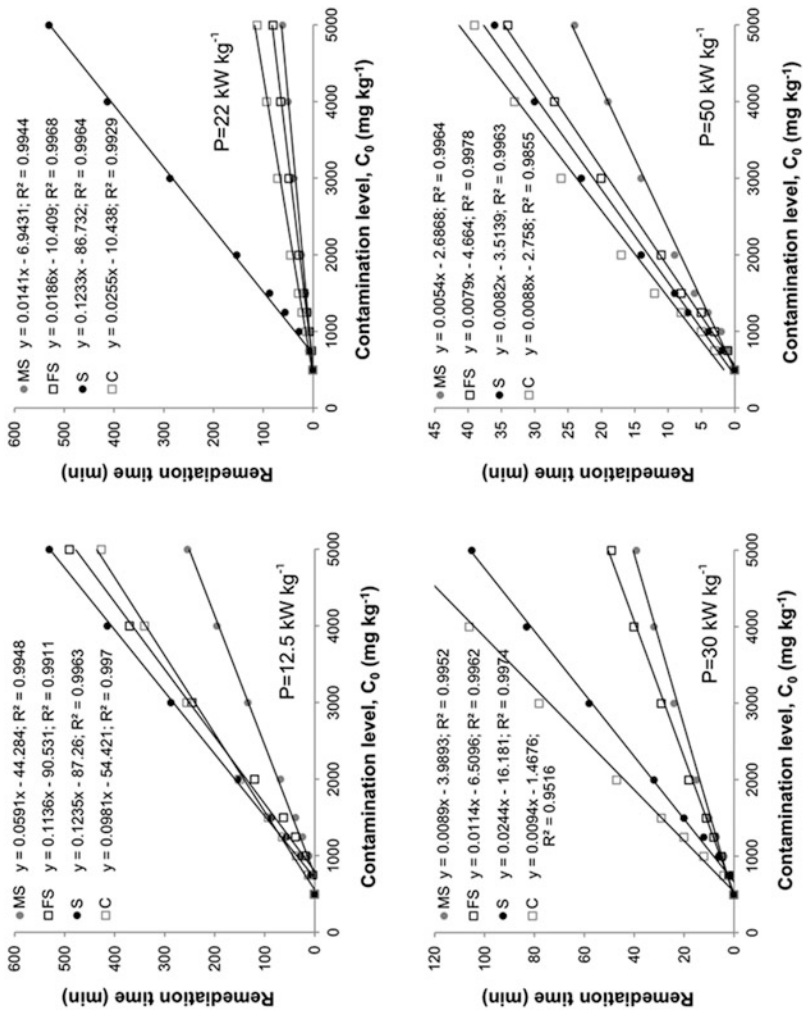

Fig. 6 Remediation times required reaching the remediation target (500 mg kg^{-1} – TPHs) as a function of the initial contamination level (C_0) for MS, FS, S and C soil textures at different specific powers (P)

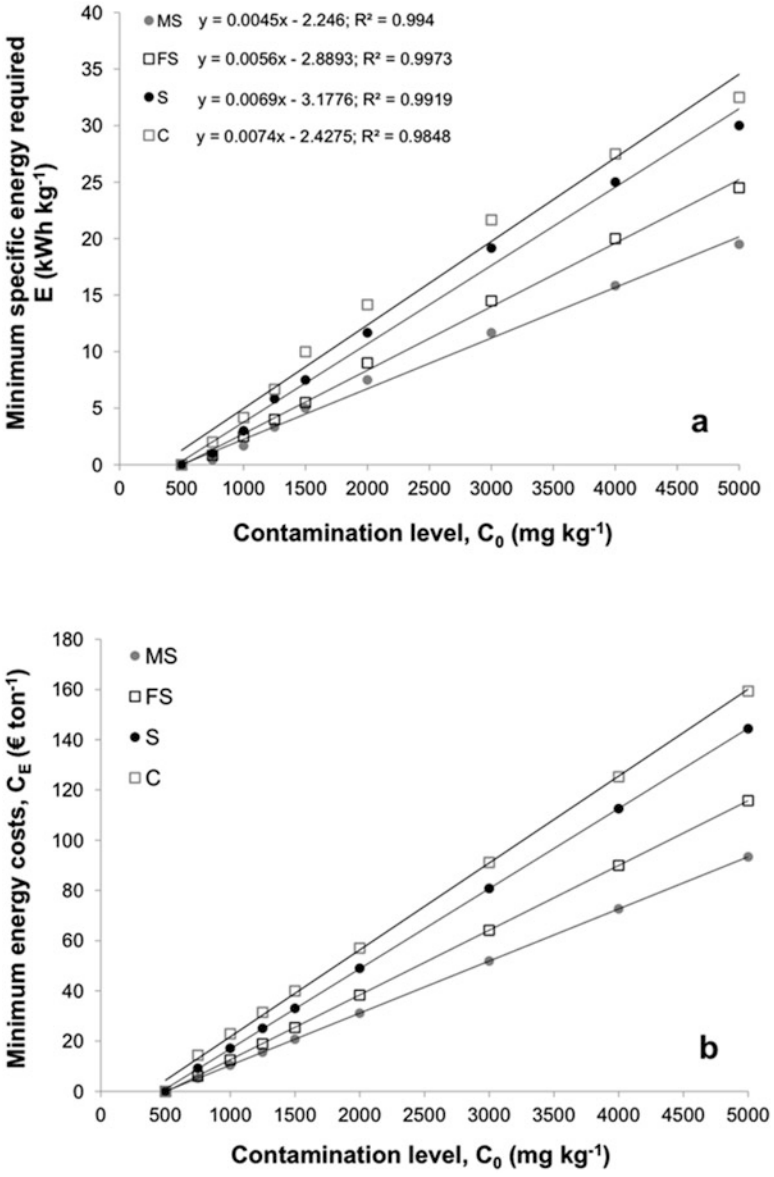

Fig. 7 Minimum specific energy required (E) (**a**) and related specific energy cost (C_E) (**b**) to reach the remediation target (500 mg kg^{-1} – TPHs) as a function of the initial contamination level (C_0) for MS, FS, S and C soil textures

diesel (2500 mg kg^{-1}). Li et al. (2007) showed that, for a sandy soil artificially contaminated with diesel fuel at different rates (from 500 to 50,000 mg kg^{-1}), the natural biodegradation reached a maximum value in the range of 70–73% for a total incubation period of 110 days. Łebkowska et al. (2011) found an 80% removal for a

sandy soil polluted by TPHs at 5300 mg kg^{-1} treated by ex situ biopile remediation for a period of about 2 months. Lower TPH removal in the range of 37–50% was obtained by Fernández et al. (2011). Liu et al. (2013) showed results from a lab-scale bioagumentation of diesel-contaminated soils artificially contaminated with diesel oil ranging from 4000 to 12,000 mg kg^{-1}. Authors have observed a contaminant degradation efficiency ranging between 59 and 73% after about 300 days of treatment. Recently, Mena et al. (2015) reported data on the application of coupled electrokinetic soil flushing (EKSF) and bioremediation through innovative biological permeable reactive barriers (Bio-PRBs) for the removal of TPH from spiked clay soils. Authors showed a contaminant removal rate of 30% in a period as short as 2 weeks. Da Rosa et al. (2015) showed results from an experimental study aimed at removing petroleum (5% w/w) and diesel oil (5% w/w) from soil using microfoams of biological and chemical surfactants. Their findings reported that the use of microfoams produced with rhamnolipid for the cleaning of petroleum-contaminated soil resulted in a removal efficiency of about 45%. However, also the application of chemical treatments could likewise lead to not high hydrocarbon removals. Do et al. (2009) showed that a chemical oxidation treatment of a diesel-polluted soil at 5000 mg kg^{-1}, using peroxymonosulphate/cobalt, was characterised by a maximum degradation of 47% and that a sequential injection treatment using a large quantity of chemicals was needed to reach a contaminant degradation of 88%.

High performances of MW treatment can be reached by using conventional thermal desorption remediation or a limited number of chemical-physical treatments which are generally quite costly. Falciglia et al. (2011b) found that applying a conventional ex situ thermal desorption (TD) technique, a soil temperature in the range of 175–250 °C was sufficient to completely decontaminate a TPH-polluted fine sandy soil with costs up to 560 US$ ton^{-1}. The USEPA (2004) reported an average cost of fuel consumption ranging from 200 to 400 € ton^{-1} for hydrocarbon-polluted soil remediation by conventional ex situ thermal desorption with a rotary kiln system. Islam et al. (2012, 2014) found that the application of 2 h of subcritical water extraction (SCWE) treatment produced a 99% of the hydrocarbon removal from a sandy soil at 250 °C and that its costs are in the range of US$ ton^{-1} 250–US$ ton^{-1} 733. Khalladi et al. (2009) reported for a diesel extraction treatment for soils using an ionic surfactant sodium dodecyl sulphate column process that an elimination rate of 97% was achieved after a soil washing with a rate of 3.2 mL/min. In terms of cost, the Federal Remediation Technologies Roundtable (FRTR) (1997) reports a minimal cost of US$ 361 per m^3 for a typical ex situ chemical extraction process. Other researchers have shown electrokinetic (EK) decontamination to be somewhat ineffective for diesel removal from soils thereby suggesting that only enhanced processes should be used in order to reach contaminant removal higher than 95% (Tsai et al. 2010; Pazos et al. 2012). In conclusion, based on the range of costs reported for the most effective remedial treatment, it is clear that energy costs calculated for MW heating jointly with short remediation times make MW technique a suitable alternative to conventional thermal or physical-chemical treatments for the remediation of hydrocarbon-polluted soils, especially if sandy soils are considered.

Remarks and Future Prospects

Based on the above considerations, it is clear that parameters such as soil texture and water content or operating conditions are strictly linked to the effectiveness of the remedial treatment. Specifically, the mass and the thickness of the soil bed are directly related making their jointly selection fundamental in order to reach a cost-effective treatment. When the bed is too high, specifically greater than the penetration depth of the electric field, the microwaves do not reach the bottom of the bed with an adequate intensity. Thus, until the penetration depth is reached, the larger the bed height (and hence the mass), the greater the total amount of energy absorbed by the material. Overall, results showed that MW technology may become economically viable with an optimised process and that there is significant potential for reducing the environmental impact of hydrocarbon-polluted soils. Specifically, in order to achieve a cost-effective remedial intervention, the treatment of soils with low moisture or a fine-grain size should be avoided. Overall, energy costs lower than 160 € ton^{-1} (110 ton^{-1} for sandy soils) and, in some cases also of about 20 € ton^{-1}, with short remediation times make MW heating a suitable alternative to conventional thermal or physical-chemical treatments for the remediation of hydrocarbon-polluted soils. All data reported here (residence time, applied power and specific energy costs) can be used as the foundation for process scale-up and the preliminary design of a continuous MW heating unit. The possibility to significantly improve the removal performance of ex situ system by means of using high dielectric materials of considering an in situ application represents at the moment the main challenges of research activities on MW heating remediation.

References

Al-harahsheh M, Kingman S, Al-Makhadmah L, Hamilton IE (2014) Microwave treatment of electric arc furnace dust with PVC: Dielectric characterization and pyrolysis-leaching. J Hazard Mater 274:87–97

Barba AA, Acierno D, d'Amore M (2012) Use of microwaves for in-situ removal of pollutant compounds from solid matrices. J Hazard Mater 207–208:128–135

Benedetto A, Calvi A (2013) A pilot study on microwave heating for production and recycling of road pavement materials. Construct Build Mater 44:351–359

Buttress AJ, Binner E, Yi C, Palade P, Robinson JP, Kingman SW (2016) Development and evaluation of a continuous microwave processing system for hydrocarbon removal from solids. Chem Eng J 283:215–222

Chen F, Liu X, Falta RW, Murdoch LC (2010) Experimental demonstration of contaminant removal from fractured rock by boiling. Environ Sci Technol 44:6437–6442

Dauerman L, Windgasse G, He Y, Lu Y (1992) Microwave treatment of hazardous wastes: feasibility studies, The Hazardous Management Research Center. New Jersey Institute of Technology Newark, Newark

Di P, Chang DPY (2001) Investigation of polychlorinated biphenyl removal from contaminated soil using microwave-generated steam. J Air Waste Manage Assoc 51:482–488

Do SH, Jo JH, Jo YH, Lee HK, Kong SH (2009) Application of peroxymonosulfate/cobalt (PMS/Co(II)) system to treat diesel contaminated soil. Chemosphere 77:1127–1131

Falciglia PP, Vagliasindi FGA (2014) Remediation of hydrocarbon-contaminated soils by ex situ microwave treatment: technical, energy and economic considerations. Environ Technol 35–18:2280–2288

Falciglia PP, Vagliasindi FGA (2015) Remediation of hydrocarbon polluted soils using 2.45 GHz frequency-heating: Influence of operating power and soil texture on soil temperature profiles and contaminant removal kinetics. J Geochem Explor 151:66–73

Falciglia PP, Vagliasindi FGA (2016) Techno-economic analysis of hydrocarbon-polluted soil treatment by using ex situ microwave heating: influence of soil texture and soil moisture on electric field penetration, operating conditions and energy costs. J Soil Sediment 16:1330–1344

Falciglia PP, Giustra MG, Vagliasindi FGA (2011a) Influence of soil texture on contaminant adsorption capacity and removal efficiency in ex-situ remediation of diesel polluted soil by thermal desorption. Chem Ecol 27(1):119–130

Falciglia PP, Giustra MG, Vagliasindi FGA (2011b) Low-temperature thermal desorption of diesel polluted soil: Influence of temperature and soil texture on contaminant removal kinetics. J Hazard Mater 185:392–400

Falciglia PP, Urso G, Vagliasindi FGA (2013) Microwave heating remediation of soils contaminated with diesel fuel. J Soil Sediment 13(8):1396–1407

Falciglia PP, Mancuso G, Scandura P, Vagliasindi FGA (2015) Effective decontamination of low dielectric hydrocarbon-polluted soils using microwave heating: Experimental investigation and modelling for in situ treatment. Sep Purif Technol 156:480–488

Falciglia PP, Maddalena R, Mancuso G, Messina V, Vagliasindi FGA (2016a) Lab-scale investigation on remediation of diesel-contaminated aquifer using microwave energy. J Environ Manage doi 167:196–205

Falciglia PP, De Guidi G, Catalfo A, Vagliasindi FGA (2016b) Remediation of soils contaminated with PAHs and nitro-PAHs using microwave irradiation. Chem Eng J 296:162–172

Federal Remediation Technologies Roundtable (1997) Remediation Technologies Screening Matrix and Reference Guide, Version 3.0. Chemical Extraction (Ex Situ Soil Remediation Technology)

Fernández MD, Pro J, Alonso C, Aragonese P, Tarazona JV (2011) Terrestrial microcosms in a feasibility study on the remediation of diesel-contaminated soils. Ecotoxicol Environ Saf 74:2133–2140

George CE, Azwell DE, Adams PA, Rao GVN (1995) Evaluation of steam as a sweep gas in low temperature thermal desorption processes used for contaminated soil clean up. Waste Manag 15:407–416

Huang G, Zhao L, Dong Y, Zhang Q (2011) Remediation of soils contaminated with polychlorinated biphenyls by microwave-irradiated manganese dioxide. J Hazard Mater 186:128–132

Islam MN, Jo YT, Park JH (2012) Remediation of PAHs contaminated soil by extraction using subcritical water. J Indus Eng Chem 18:1689–1693

Islam MN, Jo YT, Park JH (2014) Subcritical water remediation of petroleum and aromatic hydrocarbon-contaminated soil: a semi-pilot scale study. Water Air Soil Pollut 225:2037

Islam MN, Park HS, Park JH (2015) Extraction of diesel from contaminated soil using subcritical water. Environ Earth Sci 74:3059–3066

Jagtap SS, Woo SM, Kim TS, Dhiman SS, Kim D, Lee JK (2014) Phytoremediation of diesel-contaminated soil and saccharification of the resulting biomass. Fuel 116:292–298

Kawala Z, Atamaczuk T (1998) Microwave-enhanced thermal decontamination of soil. Environ Sci Technol 32:2602–2607

Khalladi R, Benhabiles O, Bentahar F, Moulai-Mostefa N (2009) Surfactant remediation of diesel polluted soil. J Hazard Mater 164:1179–1184

Łebkowska M, Zborowska E, Karwowska E, Miaskiewicz-Peska E, Muszynski A, Tabernacka A, Naumczyk J, Jeczalik M (2011) Bioremediation of soil polluted with fuels by sequential

multiple injection of native microorganisms: Field-scale processes in Poland. Ecol Eng 37:1895–1900
Lee GT, Ro HM, Lee SM (2007) Effects of triethyl phosphate and nitrate on electrokinetically enhanced biodegradation of diesel in low permeability soils. Environ Technol 28–8:853–860
Li H, Zhang Y, Kravchenko I, Xu H, Zhang CG (2007) Dynamic changes in microbial activity and community structure during biodegradation of petroleum compounds: a laboratory experiment. J Environ Sci 19:1003–1013
Li D, Zhang Y, Quan X, Zhao Y (2009) Microwave thermal remediation of crude oil contaminated soil enhanced by carbon fiber. J Environ Sci 21:1290–1295
Librando V, Bracchitta G, De Guidi G, Minniti Z, Perrini G, Catalfo A (2014) Photodegradation of anthracene and benzo[a]anthracene in polar and apolar media: new pathways of photodegradation. Polycycl Aromat Compd 34:264–279
Lin L, Yuan S, Chen J, Wang L, Wan J, Lu X (2010) Treatment of chloramphenicol-contaminated soil by microwave radiation. Chemosphere 78:66–71
Liu X, Zhang Q, Zhang G, Wang R (2008) Application of microwave irradiation in the removal of polychlorinated biphenyls from soil contaminated by capacitor oil. Chemosphere 72:1655–1658
Liu PWG, Chang TC, Chih-Hung C, Wang MZ, Hsu HW (2013) Effects of soil organic matter and bacterial community shift on bioremediation of diesel-contaminated soil. Int Biodeter Biodegr 85:661–670
Liu PWG, Chang TC, Chen CH, Wang MZ, Hsu HW (2014) Bioaugmentation efficiency investigation on soil organic matters and microbial community shift of diesel-contaminated soils. Int Biodeter Biodegr 95:276–284
Mena E, Ruiz C, Villaseñor J, Rodrigo MA, Cañizares P (2015) Biological permeable reactive barriers coupled with electrokinetic soil flushing for the treatment of diesel-polluted clay soil. J Hazard Mater 283:131–139
Metaxas AC, Meredith RJ (1993) Industrial microwave heating, IEE power engineering series 4. Peter Pregren LTD, London
Pazos M, Plaza A, Martín M, Lobo MC (2012) The impact of electrokinetic treatment on a loamy-sand soil properties. Chem Eng J 183:231–237
Pereira MS, de Ávila Panisset CM, Martins AL, de Sá CHM, de Souza Barrozo MA, Ataíde CH (2014) Microwave treatment of drilled cuttings contaminated by synthetic drilling fluid. Sep Purif Technol 124:68–73
Qi Z, Chen T, Bai S, Yan M, Lu S, Buekens A, Yan J et al (2014) Effect of temperature and particle size on the thermal desorption of PCBs from contaminated soil. Environ Sci Pollut Res 21:4697–4704
Rafael A, Morel M (2013) Phototransformations of dinitropyrene isomers on models of the atmospheric particulate matter. Atmos Environ 75:171–178
Robinson JP, Kingman SW, Snape CE, Shang H, Barranco R, Saeid A (2009) Separation of polyaromatic hydrocarbons from contaminated soils using microwaves heating. Sep. Purif Technol 69:249–254
Robinson J, Binner E, Saeid A, Al-Harahsheh M, Kingman S (2014) Microwave processing of oil sands and contribution of clay minerals. Fuel 135:153–161
da Rosa CFC, Freire DMG, Ferraz HC (2015) Biosurfactant microfoam: application in the removal of pollutants from soil. J Environ Chem Eng 3:89–94
Silva-Castro GA, Rodelas B, Perucha C, Laguna J, González-López J, Calvo C (2013) Bioremediation of diesel-polluted soil using biostimulation as post-treatment after oxidation with Fenton-like reagents: Assays in a pilot plant. Sci Total Environ 445–446:347–355
Switzer C, Pironi P, Gerhard JI, Rein G, Torero JL (2014) Volumetric scale-up of smouldering remediation of contaminated materials. J Hazard Mater 268:51–60
Tatàno F, Felici F, Mangani F (2013) Lab-scale treatability tests for the thermal desorption of hydrocarbon-contaminated soils. Soil Sed Contam 22:433–456

Tsai TT, Sah J, Kao CM (2010) Application of iron electrode corrosion enhanced electrokinetic-Fenton oxidation to remediate diesel contaminated soils: A laboratory feasibility study. J Hydrol 380:4–13

Tyagi VK, Lo SL (2013) Microwave irradiation: A sustainable way for sludge treatment and resource recovery. Renew Sustain Energy Rev 18:288–305

US-EPA (2004) Remediation technology cost compendium – year 2000, Solid Waste and Emergency Response, EPA-542-R-01-009

Yang B, Xue N, Ding Q, Vogt RD, Zhou L, Li F, Wu G et al (2014) Polychlorinated biphenyls removal from contaminated soils using a transportable indirect thermal dryer unit: Implications for emissions. Chemosphere 114:84–92

Yuan S, Tian M, Lu X (2006) Microwave remediation of soil contaminated with hexachlorobenzene. J Hazard Mater B137:878–885

Arsenic Behaviour in Soil-Plant System: Biogeochemical Reactions and Chemical Speciation Influences

Sana Khalid, Muhammad Shahid, Nabeel Khan Niazi, Marina Rafiq, Hafiz Faiq Bakhat, Muhammad Imran, Tauqeer Abbas, Irshad Bibi, and Camille Dumat

Abstract Arsenic (As) is classified as a Class A human carcinogen and has gained a substantial attention in recent years owing to its high levels currently observed in the environment and adverse impacts on human health. Several studies have delineated the biogeochemical behaviour of As in soil-plant system in relation to its chemical speciation and bioavailability. This chapter establishes a link between As speciation and biogeochemical behaviour of As in complex soil-plant systems. It gives an overview of different biogeochemical processes that govern environmental behaviour of As in soil-plant system; highlights how the chemical speciation of As affects its biogeochemical behaviour (adsorption/desorption, mobility, bioavailability/phytoavailability) in soil-plant system; and discusses relationship of soil physico-chemical properties (pH, clay contents, biological and microbial conditions, presence of organic and inorganic ligands and competing anions/cations) with chemical speciation of As as well as its biogeochemical behaviour in soil-plant system.

Keywords Arsenic • Biogeochemical behaviour • Soil physico-chemical properties • Soil-plant transfer

S. Khalid • M. Shahid (✉) • M. Rafiq • H.F. Bakhat • M. Imran
Department of Environmental Sciences, COMSATS Institute of Information Technology, Vehari 61100, Pakistan
e-mail: muhammadshahid@ciitvehari.edu.pk

N.K. Niazi • I. Bibi
Institute of Soil and Environmental Sciences, University of Agriculture Faisalabad, Faisalabad 38040, Pakistan

Southern Cross GeoScience, Southern Cross University, Lismore 2480, NSW, Australia

T. Abbas
Department of Civil and Environmental Engineering, North Dakota State University, Fargo, ND 58108-6050, USA

C. Dumat
Centre d'Etude et de Recherche Travail Organisation Pouvoir (CERTOP), UMR5044, Université J. Jaurès—Toulouse II, 5 allée Antonio Machado, 31058 Toulouse, France

N.A. Anjum et al. (eds.), *Enhancing Cleanup of Environmental Pollutants*,
DOI 10.1007/978-3-319-55423-5_4

Introduction

Environmental contamination by heavy metal(loid)s is a widespread dilemma nowadays (Pourrut et al. 2013; Shahid et al. 2015a; Bibi et al. 2016). Many of these heavy metal(loid)s are highly toxic and can induce a significant health risks (Xiong et al. 2016a; Mombo et al. 2015). In particular, arsenic (As) has long been a prevalent civic concern (Rafiq et al. 2017). Arsenic is a highly toxic and carcinogenic metalloid. The European Union has classified the compounds of As as toxic for the environment under directive 67/548/EEC. Arsenic and its compounds are recognized as Group 1 carcinogens by the International Agency for Research on Cancer (IARC) of the World Health Organization (WHO) and the US Environmental Protection Agency (EPA), (Rosas-Castor et al. 2014). Arsenic has been ranked No. 1 among the top 20 priority hazardous substances by the Agency for Toxic Substances and Disease Registry (ATSDR 2013). Moreover, As is currently observed in soils and waters at the global scale. Nevertheless, the biogeochemical behaviour of As species within the soil and its plant accumulation are studied inadequately because of its diverse phase transitions in the soil-plant system depending on physico-chemical process of soil formation (Liang et al. 2011). Some of the As compounds are soluble, but its migration intensity in soils is very low, because of its sorption by organic compounds, iron hydroxides and because of some clayey minerals (Kabata-Pendias and Pendias 1989). Therefore, it is highly necessary to study and understand the biogeochemical behaviour of this metalloid in soil-plant system.

Environmental contamination of soil-plant systems with As poses a severe risk for human and environmental health, thereby affecting thousands of people globally with As toxicosis (Foucault et al. 2013; Niazi et al. 2011; Abdul et al. 2015). Soil-plant transfer and consumption of food contaminated with As is considered to be the major pathway (>90%) of human exposure to toxic metals (Foucault et al. 2013). Exposure to moderate or high levels of As can cause numerous physiological, morphological and biochemical disorders in almost all forms of living organisms (Rahman et al. 2014; Abdul et al. 2015). Acute and chronic As exposures result in arsenicosis, which is a general expression used for As-associated adverse health issues, such as integumentary, gastrointestinal, respiratory diseases, haematopoietic, non-pitting oedema, reproductive disorders, diseases of the blood vessels, high blood pressure, diabetes, cardiovascular and liver problems and cancer of the kidney, liver, skin, bladder and lung (Foucault et al. 2013; Rahman et al. 2014; Abdul et al. 2015; Shakoor et al. 2015a). The adverse health issues of arsenicosis depend strongly on the applied level, extent of exposure and the dietary status of the exposed organism (Rosas-Castor et al. 2014). Arsenic contamination problem has been mainly associated with flood-plain/alluvial soils and sediments; for example, in India, Bangladesh and Pakistan along the river sediments originating from the mountains of Himalaya, Cambodia, Vietnam, Myanmar, Nepal and China (Anup and Kalu 2015; Niazi et al. 2015).

The presence of As in soil-plant systems may have hazardous environmental and health consequences. It is well known that the biogeochemical behaviour of As in soil relies on its mobility, solubility and bioavailability, which in turns varies with its chemical speciation (Xu et al. 2016). It is found predominantly in the inorganic form (multiple oxidation states; +5, +3, 0 and −3) but can be found as the organic mono- and dimethyl arsenates/aresenites. Arsenate (As(V)) and arsenite (As(III)) are the most dominant inorganic species of As in contaminated soil and sediment environments. The dissociation constant (pK) values for As(III) range between 9.22 and 13.40, while for As(V) pK values range from 2.20 to 11.53 (Shakoor et al. 2015a). The existence of As in different chemical forms (organic or inorganic) in the plant-soil system is highly dynamic and interconverts rapidly through redox cycling and/or methylation of inorganic form to the organic form (Abbas and Meharg 2008).

Several dynamic mechanisms/processes occurring in soil can alter chemical speciation of As in soil and thus participate in determining bioavailability and phyto-uptake of As in soil-plant system (Kumpiene et al. 2007). These processes/mechanisms can be physical, chemical and biological in nature, which include precipitation/dissolution, sorption-desorption, oxidation-reduction, redox conditions, As-ligand complex formation, biological transformations, volatilization, uptake by plants and leaching to groundwater (Vaxevanidou et al. 2012).

The comparative significance of these processes depends on soil physico-chemical properties (pH, organic matter, clay contents, biological and microbial conditions, metal burdens, presence of organic and inorganic ligands and oxides of Fe, Al and Mn) (Rojas et al. 2013). These factors/processes individually or combinedly can alter biogeochemical behaviour of As and the degree of soil As contamination. Any change in these soil physico-chemical and/or biological properties or the processes/mechanisms occurring in soil causes an alteration in the speciation and the mobility of As.

Thus, data regarding As chemical speciation in soil-plant system in relation to soil physico-chemical properties can be a useful contribution to risk assessment and (phyto)remediation studies. Several previous studies evaluated, compared and reported the biogeochemical behaviour of As in soil-plant system under different exposed conditions. However, the mechanisms controlling As biogeochemical behaviour in soil-plant system are not well understood. In the present book chapter, we summarized the relationship that exists between As mobility, bioavailability and speciation in soil under various soil factors and conditions. Actually a high knowledge of As fate in the environment will increase the efficiency of its risk management.

Arsenic Sources in Soil

Arsenic is a naturally occurring toxic semimetal and was first reported by Albertus Magnus in 1250. Arsenic ranks the 20th most abundant element in the Earth's crust (0.0001%), 14th in seawater and 12th in the human body (Kalia and Joshi 2009).

Table 1 Concentration of arsenic in soil reported in different countries worldwide

Sr. #	As level (mg kg^{-1})	Country	References
1	23	Sweden	Uddh-Söderberg et al. (2015)
2	131.5	Korea	Ko et al. (2015)
3	12.2	China	Liu et al. (2015)
4	16.08	China	Cai et al. (2015)
5	10.367	China	Jiang et al. (2015)
6	64	Bolivia	Acosta et al. (2015)
7	354	China	Wei et al. (2015)
8	41	Chile	Bustos et al. (2015)
9	13.6	China	Liang et al. (2014)
10	1.1	Iran	Bagherifam et al. (2014a, b)
11	7490	Spain	Beesley et al. (2014)
12	18.8	China	Tong et al. (2014)
13	4357	Itlay	Marabottini et al. (2013)
14	27.9	Australia	Tighe et al. (2013)
15	7	Europe	Tarvainen et al. (2013)
16	9.8	China	Wang at al. (2013)
17	40.9	Uganda	Nabulo et al. (2012)
18	0.01-4230	South Korea	Kwon et al. (2012)
19	7.1	Tanzania	Marwa et al. (2012)
20	9.62	India	Tiwari et al. (2011)
21	16.7	Nepal	Dahal et al. (2008)
22	36	Itlay	Ungaro et al. (2008)
23	3.21	Ethiopia	Fitamo et al. (2007)
24	0.5 to 2.5	USA	Kabata-Pendias and Mukherjee (2007)
25	6.8	Finland	Mäkelä-Kurtto et al. (2007)

Arsenic occurs naturally and commonly in the Earth's crust, as a component of several minerals/compounds (Shakoor et al. 2015b). Arsenic concentration in uncontaminated soil is mainly related to the composition of the parent material. Depending on the nature of anthropogenic and geogenic sources, As level in soil may vary from <1 to 250,000 mg k^{-1} (Mahimairaja et al. 2005). However, As level in soil fluctuates greatly among countries due to differences in soil parent material (Table 1) as well as anthropogenic activities.

Various natural and anthropogenic sources can release As from the Earth's crust to the environment (water, atmosphere and soil). The most widespread sources of As in soil and water are natural sources, such as volcanic activities, weathering and erosion of minerals and rocks and geothermal waters (Rahman et al. 2014). Every year, significant amount of As is thus redistributed from the contaminated aquifer to different compartments of environment, i.e. water and soil (Ali and Tarafdar 2003).

Owing to its useful properties, As is used in several industrial processes, which has transferred naturally occurring As in the Earth's crust into water–soil–plant system (Beesley and Marmiroli 2011). Arsenic is commonly used for strengthening

alloys of lead and copper (e.g. car batteries). Anthropogenic activities, including mining, industrial processes, As-containing herbicides, fungicides and insecticides in agriculture, As-contaminated groundwater and CCA (copper, chromate and arsenate) wood preservative, have contributed significantly in increasing As levels in different compartments of environment (Niazi et al. 2012; Rahman et al. 2014). Arsenic concentration in soil may reach up to 1000 mg/kg as a result of human activities (Smith et al. 1998). Approximately 50,000 tons of As is released every year by human activities (Bolan et al. 2014). Burning of coal is estimated to discharge about 45,000 tons of As annually and thus contribute significantly towards environmental contamination of As (Bolan et al. 2014). In 1992, about 23,900 metric tons of As was used, out of which 67% was used for wood preservative CCA production (Fayiga et al. 2007). Soil irrigation with As-contaminated groundwater has increased soil As level in excess of 83 mg/kg in Bangladesh (Abedin et al. 2002). Soil As levels up to 1000 mg As/kg have been reported in many mining and agricultural areas of Australia and the United States (Smith et al. 1998; Niazi et al. 2015). Roychowdhury (2010) reported that in the two studied districts of Nadia and Murshidabad, almost 11.2 and 50.7 kg of As per year are withdrawn, respectively, from 18 to 23 shallow tube wells.

Pesticides have been reported to be the major source of As in agricultural soils (Cai et al. 2015). Widespread use of As-containing pesticides to increase crop production resulted in an increased concentration of As in agricultural areas. In France, these As-containing pesticides are nowadays forbidden; however, their past uses induced soil pollution due to As persistence in the environment. Actually, several As-containing pesticides such as magnesium arsenate ($MgAsO_4$), calcium arsenate ($CaAsO_4$), lead arsenate ($PbAsO_4$), Paris green [$Cu(CH_3COO)_2$*3Cu $(AsO_2)_2$] and zinc arsenate ($ZnAsO_4$) had been used extensively as pesticides in agriculture during 1880–1950 (Merry et al. 1983), which resulted in As contamination of agricultural soils. The use of As-containing pesticides on large areas of sugarcane farming in Hawaii resulted in total soil As level ranging from 40 to 900 mg kg^{-1} (Cutler et al. 2013).

Arsenic Contamination in Soil

According to Kabata-Pendias and Mukherjee (2007), background concentrations of As in soil vary between 0.5 mg kg^{-1} and 80 mg kg^{-1} (average 10 mg kg^{-1}). It is reported that the total As content in uncontaminated natural soils is generally less than 10 mg/kg (Adriano 2001). In the United States, As concentration of uncontaminated natural soil varies from 0.1 to 40 mg/kg with an average of 5 to 6 mg/kg (Girouard and Zagury 2009) and rarely exceed 15 mg/kg (Smith et al. 1998). Arsenic concentration in sediments ranges from 3 to 10 mg kg^{-1}, depending on the texture and nature of minerals (Adriano 2001). However, local concentrations of As may vary depending on geological history and parent materials of soil.

Arsenic is rarely found as a pure metalloid but as a component of sulphur-containing minerals. Arsenic has been identified as the structural component (both in organic and/or inorganic forms) of approximately 200 different naturally occurring minerals (Bissen and Frimmel 2003). The dissolution and desorption of naturally occurring As rocks and minerals are the main sources of As contamination of groundwater and soil (Polizzotto et al. 2006; Roychowdhury 2010). Commonly found As-containing minerals include arsenopyrite, enargite, tennantite, galena, iron pyrite, chalcopyrite, realgar, orpiment and sphalerite (Shakoor et al. 2015b). In ores, As is generally found in sulphide form associated to arsenopyrite, pyrite or pyrrhotite (Nriagu et al. 2007). Arsenic contents of igneous rocks vary greatly up to 100 mg/kg with an average value of 2–3 mg/kg. Sedimentary rocks differ widely in their As contents; limestone and sandstone contains very small amount of As (usually less than 20 mg/kg), whereas manganese ores contain up to 15,000 mg/kg of As (Bolan et al. 2014). Similarly, sulphide ores are reported to contain As contents up to 8000 mg/kg (Chilvers and Peterson 1987). Therefore, As contents differ greatly in soil and greatly depends on the composition of parent material (rocks and ores) from which the soil was developed.

High level of As in groundwater and soil (exceeding the threshold levels of 10 μg L^{-1} and 20 mg kg^{-1}, respectively, set by the USEPA) has been detected in over 105 countries worldwide (Naujokas et al. 2013) (Table 1). It has been estimated that over 200 million people in the world are at the health risk of As poisoning due to ingestion of As-rich water, including Minnesota, Spain, North Mexico, Canada, Japan, Poland, Pakistan, Argentina, India, Saudi Arabia, New Zealand, Bangladesh, Argentina, Nepal, Australia, Chile, Hungary, China, Peru, Mexico, Taiwan, Thailand and the United States (Shakoor et al. 2015b). The highest As level and worst As-induced poisoning have been reported in Bangladesh and several states in India (Shakoor et al. 2015a). According to a report, 59 out of 64 districts in Bangladesh have As contents above the WHO safe limit (Chakraborti et al. 2010). Arsenic levels of 3700 μg L^{-1} and 4730 μg L^{-1} have been investigated in South Parganas (India) and Noakhali (Bangladesh), respectively (Brammer and Ravenscroft 2009; Chakraborti et al. 2010). It is estimated that almost 43 million people in (West Bengal) India and 80 million people in Bangladesh have been exposed to health risk from As-contaminated drinking water (Sharma et al. 2014).

Bioavailability of Arsenic in Soil

Bioavailability of an element relies primarily on the solid-phase speciation, concentration and the type of binding to soil particles (Niazi et al. 2011; Shahid et al. 2015a). Bioavailability of a metalloid is a complex and dynamic process and is governed by biological, chemical and physical processes and their interactions (Shahid et al. 2013a, b). Extractable fraction of the As may provide better indication of its mobility and bioavailability in soils (Adriano 2001). Normally, the percent of the plant-available As to the total As in soil is small, and the amount of As could be

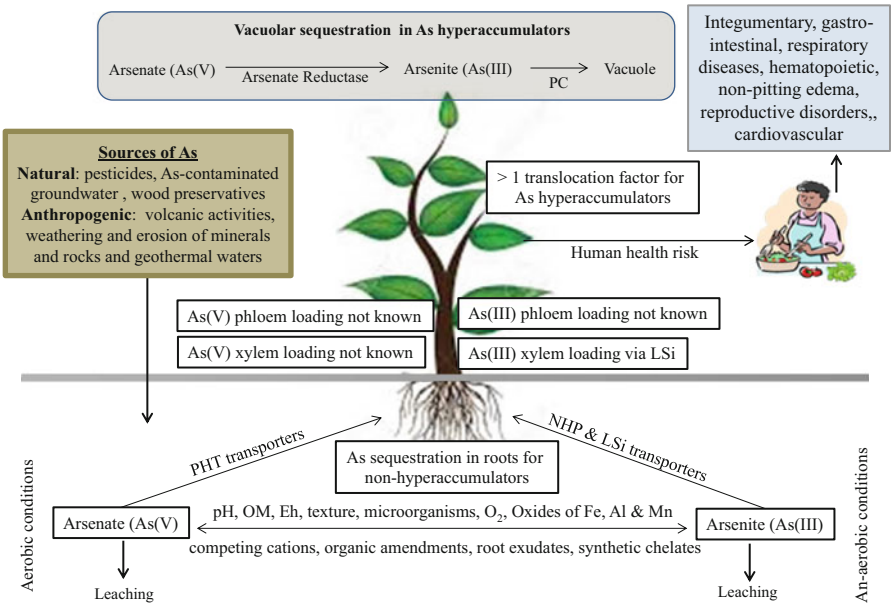

Fig. 1 Biogeochemical behaviour of arsenic in soil-plant system. In soil, As mainly exists as inorganic (arsenate and arsenite) species, which are highly dynamic, and interconvert rapidly through variation in soil physico-chemical properties (pH, Eh, SOM, etc.). From soil, As(V) enters the plants via PHT transporters (LeBlanc et al. 2013), while As(III) is taken up through NHP and LSi transporters (Mitani-Ueno et al. 2011). LSi is involved in As(III) xylem loading; however, As (III) phloem loading and As(V) xylem and phloem loading are not yet well known. For non-hyperaccumulators, As mainly sequesters in plant roots, while hyperaccumulating plants (*Pteris vittata*) transfer major portion of As to aerial parts. Inside plants, arsenate reductase generally reduces arsenate to arsenite using glutathione as a reductant. The arsenite is then chelated by phytochelatins and is transferred to vacuoles of root cells (*Abbreviations*: *As(III)* arsenite, *As(V)* arsenate, *OM* organic matter, *Fe* iron, *Al* aluminium, *Mn* manganese, *PC* phytochelatin)

absorbed by the plant even as the hyperaccumulator is limited (Huang and Matzner 2006). These factors include oxidation-reduction, pH, soil texture, soil organic contents, microbial and biological conditions, metal level, the presence of organic and inorganic ligands and competing cations (Niazi et al. 2011; Shahid et al. 2012a; Xiong et al. 2016b) (Fig. 1). These parameters either separately or in combination make the simulation of metal availability to plants by altering metal speciation and behaviour in soil-plant system. They also determine whether As is adsorbed, precipitated, chelated or leached through the soil profile or absorbed by plants. Besides, these factors affect the maximum acceptable limit of As in soils above which As phyto-uptake may become a risk to human and environmental health (Jiang et al. 2013).

Chemical Speciation of As in Soil

The term 'metal speciation' was first introduced in mid-nineteenth century by Goldberg (1954) to better understand the biogeochemical cycling of trace metals in seawater. Chemical speciation is the existence of an element in different chemical forms and possible oxidation states which together make up its total concentration in a system (Shahid et al. 2011; Nearing et al. 2014; Pierart et al. 2015). According to Shuman and Luxmoore (1991), a metal may exist in soil in different forms including (i) free ionic form, (ii) exchangeable, (iii) adsorbed on soil inorganic or organic constituents, (iv) precipitated as solids and (v) presenting as structural component of primary and secondary minerals.

Nowadays, it is well known that the biological availability or potential toxicity of metalloids depends on their chemical speciation rather than their total concentrations (Nearing et al. 2014; Shahid et al. 2014a, b, 2015b). Total concentration of As in soil system does not fully represent its biogeochemical behaviour in natural environment (Belogolova et al. 2015). For example, the part of As that exists as integral component of stable minerals is usually not accessible for biological activity (Newman and Jagoe 1994). On the other hand, the part of As adsorbed on different soil constituents is easily extractable and available for biological reactions/processes (Bergqvist et al. 2014; Li et al. 2015).

Speciation of As in natural media has attained significant importance. It is because of the fact that biological availability, physiological effects and potential toxicity of As primarily rely on the type of individual As species (Lenoble et al. 2013). In general, the portion of metal that is dissolved in soil solution in the form of free ions is considered to correlate better with physiological effects and potential toxicity (Shahid et al. 2017a). In order to fully understand the biogeochemical behaviour of As in soil-plant system, it is of great importance to evaluate the chemical speciation of As in addition to its total concentration even if the portion of free As in soil solution strongly correlates ($R = 0.99$) with total As contents in soils (Huang and Matzner 2006).

Arsenic occurs commonly and naturally in different chemical forms and oxidation states in natural environment. The oxidation state of As determines its biogeochemical behaviour (relative mobility, bioavailability and toxicity) in soil-plant system. In nature, As mainly exists in these oxidation states: As(III) and As(V) (Joseph et al. 2015). The existence of As in different oxidation states is greatly affected by conditions of ambient environment. The other major forms of As present in natural media include monomethylarsonite [MMA(III)], dimethylarsenite [DMA(III)], monomethylarsonate [MMA(V)], dimethylarsinate [DMA(V)], arsenosugars, arsenocholine, arsenobetaine, tetramethylarsonium ion and trimethylarsine oxide (Joseph et al. 2015). The inorganic forms of As (arsenate and arsenite) also exist in different chemical forms with the same oxidation states (arsenite III and arsenate V) such as fully protonated As acids and arsenous, as well as a number of different oxoanions (Sadiq 1994). Depending on pH and redox potential (Eh) of soil, the thermodynamically stable and predominant forms of As in soils and waters are H_2AsO_4, $HAsO_2^{4-}$ and H_3AsO_3. Among these, H_2AsO_4 is the most predominant

species in aerobic soils (Warren and Alloway 2003). Arsenate is highly stable and is readily adsorbed to soil components such as oxides and hydroxides of metals, organic matter and clays. Arsenite predominates under reduced soil conditions, and it is 60 times more mobile, soluble and toxic than As(V).

Traditionally, speciation of metals/metalloids such as As in soils has been evaluated by indirect methods such as selective electrodes, high-performance liquid chromatography AA, colorimetric procedures, sequential extraction, polarography and gas chromatography AA (Nearing et al. 2014; Xu et al. 2016). However, these techniques have some limitations in natural environment due to the low concentration of metals generally observed. These approaches are very time consuming and complex. The use of speciation computer programs/models provides a rapid and alternative approach to estimate metal speciation (Shahid et al. 2011, 2017b). These programs use formation constants of metal complexes and estimate the chemical speciation and oxidation state of a metal in soil solution of known composition. These computer models require input data such as the pH, redox potential and pCO_2 and concentration of the metal, inorganic and organic ligands and major cations. Output data of these programs include an estimation of the concentration of free and complexed metals at equilibrium under specified conditions.

Influence of pH on Biogeochemical Behaviour of As

In As-contaminated soils, pH is the master variable governing chemical speciation and biogeochemical behaviour (mobility, bioavailability and partitioning between the soil solid and solution phase) in soil-plant system. Depending on the soil texture, redox conditions and the nature of the mineral constituents, the specificity of As adsorption on the surface of certain soil components is greatly influenced by soil pH. The mobility and bioavailability of As increases in soil as the soils become more acidic, mainly at pH values below 5 (Carbonell-Barrachina et al. 2000) or 5.5 (Signes-Pastor et al. 2007). Generally, the low pH values in soil results in the increase of the soluble As fraction, which increases its phytoavailability. Variation in soil pH also affects As speciation in soil and consequently its behaviour in soil-plant system. In soil environment, the relative distribution of As(V) and As(III) changes with the change in soil pH (Adra et al. 2015).

The effect of pH on As speciation, mobility, bioavailability and sorption/desorption on the surface of soil constituents changes with soil type (Li et al. 2011). Fu et al. (2011) considered that instead of direct action, soil pH influences As behaviour in soil-plant system by governing the interaction between As and bearing phases of soil constituents. Increasing soil pH results in As adsorption and precipitation to different metal-binding sites of soils constituents and reduces its dilution and concentration in soil solution (Sauvé et al. 2000). It is reported that As co-precipitates with calcium or sulphate at higher soil pH (Moreno-Jiménez et al. 2013). Pongratz (1998) reported that As is mainly sorbed on Fe and Al oxides under acidic conditions, whereas this species is sorbed onto calcium under alkaline soil

conditions. Simultaneously, soil carbonate contents also play key role towards As adsorption under alkaline conditions over a wide range of redox conditions (Ryu et al. 2010). Griffin and Shimp (1978) reported increased sorption of As(III) by montmorillonite and kaolinite over a pH range of 3–9. At a lower pH value, the adsorption of As(V) on calcium oxides is weaker than on oxides of Fe and Al (Woolson et al. 1971). Bhattacharya et al. (2010) reported a negative correlation between As level and soil pH in rice but was contradicted by Ahmed et al. (2011) who reported a positive correlation between As phytoavailability and soil pH. Akins and Lewis (1976) used sequential fractionation procedure to evaluate the effect of pH (from 4 to 8) on As adsorption by soil constituents and found that Fe-As is the predominant species followed by Al-As at low pH (pH 4), whereas Ca-As is the most abundant species at high pH (pH 6–8). This behaviour of As in relation to soil pH resembles with that of phosphate. Adriano (2001) showed that Ca-P is the most abundant species under alkaline and calcareous soils, whereas Al-P and Fe-P dominate under acid soils. Most of the soil amendments (natural or synthetic like biochar) affect As biogeochemical behaviour in soil indirectly by altering soil pH.

We evaluated the effect of pH on chemical speciation of As(III) and As(V) in nutrient solution using Visual MINTEQ (ver. 3.0) (Fig. 2). The composition of

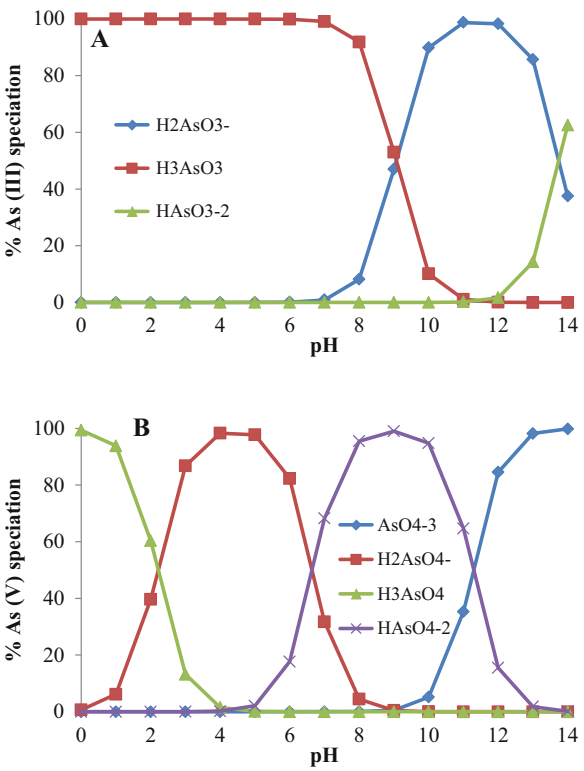

Fig. 2 Effect of solution pH on (**a**) As(III) and (**b**) As (V) speciation in nutrient solution. The speciation calculations are made by Visual MINTEQ (ver. 3.0)

nutrient solution used for calculating chemical speciation of metalloids in this study includes 5 mM KNO_3, 5 mM $Ca(NO_3)_2$, 2 mM KH_2PO_4, 1.5 mM $MgSO_4$, 9.11 μM $MnSO_4$, 1.53 μM $ZnSO_4$, 0.235 μM $CuSO_4$, 24.05 μM H_3BO_3, 0.1 μM Na_2MoO_4 and 268.6 μM Fe. This modified nutrient solution is used in several previous heavy metal risk assessment and remediation studies (Shahid et al. 2014c, d). Results showed that As(III) is mainly present in three forms including $H_2AsO_3^-$, H_3AsO_3 and $HAsO_3^{2-}$. H_3AsO_3 was the most available form of As present in higher % at pH 0–9, whereas the other two forms of As, $H_2AsO_3^-$ and $HAsO_3^{-2}$, dominated in the nutrient solution at higher pH. H_3AsO_3 was present 53–100% at pH <9.0. In case of As(V), AsO_4^{-3}, $H_2AsO_4^-$, $H_2AsO_4^-$ and $HAsO_4^{-2}$ are the different chemical forms predicted in nutrient solution at pH 0–14 (Fig. 2). However, these forms of As(V), AsO_4^{-3}, $H_2AsO_4^-$, $H_3AsO_4^-$ and $HAsO_4^{-2}$ dominated the nutrient solution, respectively, at pH ranges 12–14, 3–6, 1–2 and 7–11. Similar results were reported by Wilson et al. (2010) and Acosta et al. (2015), where $HAsO_2^{-4}$ and H_2AsO_4 dominated in pH range of 4.0 and 9.0. Similarly, Beesley et al. (2014) reported predominance of $H_2AsO_4^-$ (96%) under low pH (3.0–4.0) and high percentage of $HAsO_4^{2-}$ (73%) at pH 6.0–7.0.

Influence of Redox Potential on Biogeochemical Behaviour of As

Arsenic is a highly redox sensitive metalloid, and its biogeochemical behaviour is mainly governed by redox reactions (Gorny et al. 2015). A pronounced effect of redox conditions is expected because of variation in the solubility of As(V) and As (III). Soil redox condition varies with seasonal variations, mainly with changes in groundwater levels. It is well known that the solubility and mobility of As in soil system strongly rely on redox potential variations. This is because of the fact that the concentration of dominant inorganic species of As (As(III) and As(V) having different mobility and solubility) alters with variation in redox conditions, which in turn influences As bioavailability. In general, decrease in soil redox potential increases the solubility of As in soil. Under oxidizing conditions (high Eh values, 100 to + 200 mV), inorganic As(V) is the predominant species of As. At high Eh value, As(V) is highly adsorbed and/or co-precipitated with different minerals, especially iron and manganese oxides. Moderately reducing conditions (0 to +100 mV) cause partial dissolution of As(V) in pore waters. At low Eh values (0 to −200 mV), As(V) is reduced into As(III), and As(III) is the predominant inorganic As species. Thus, As(V) is reduced to As(III) when the conditions changed from oxic (100 to + 200 mV) to reduced form (0 to −200 mV). This can have a profound effect on mobility and bioavailability of As in soil-plant system.

It is noteworthy that both arsenate and arsenite can coexist in natural environment under oxidizing conditions (Wang and Zhao 2009). Arsenic speciation in soil-

plant system is dynamic with interconversion of arsenate and arsenite through redox cycling (Abbas and Meharg 2008). For example, when the soil conditions vary from reduced (0 to −200 mV) to oxic condition (100 to + 200 mV), arsenite get oxidized to arsenate. Under oxic conditions, Ona-Nguema et al. (2010) reported the oxidation of arsenite into arsenate by ferrihydrite or magnetite in the presence of Fe. Goethite and Fe(II) induced oxidation of arsenite into arsenate under anoxic conditions has been demonstrated by Amstaetter et al. (2010). Lake Pavin in France illustrates a real effect of redox conditions on As speciation (Seyler and Martin 1989), where As(V) dominates (>85%) in well-oxidized surface waters. On the other hand, As(III) dominates (51–90%) at depth below the redoxcline. The main redox couples likely involved in the redox speciation of As are Mn(IV)/Mn(II), O_2/H_2O, NO_3^-/NO_2^- Fe(III)/Fe(II), NO_3^-/N_2, CO_2/CH_4 and SO_4^{2-}/HS^-.

Influence of Organic Matter on Biogeochemical Behaviour of As

Organic matter is a crucial soil component that plays a key role in determining mobility, sorption/desorption and bioavailability of As in soil (Anwar et al. 2013). Soil organic matter is highly variable with respect to its structural and chemical composition and functionalities (Shahid et al. 2012b). Soil organic matter consists of dissolved and suspended particles. Dissolved organic matter (DOM) is composed of humic (20%) and non-humic compounds (80%) (Rosas-Castor et al. 2014). Non-humic compounds are generally less hydrophobic and include amino acids, carbohydrates, hydrophilic acids and proteins, whereas humic substances are highly hydrophobic and consist of humin, humic acids (HAs) and fulvic acids (FAs) (Fakour and Lin 2014). The portion of SOM that is found in soluble form plays key role in determining the sorption/desorption of As in soil. Humic acids influence the concentrations of labile and free metals and their consequent mobility and bioavailability in soil by forming metal-HS complexes (Sánchez-Marín et al. 2010). Soil organic matter exists in soluble (dissolved) and solid form (suspended) depending on environmental conditions (Shahid et al. 2012b). When present in dissolved form, HAs form complexes with As and other metals. In solid phase, HAs adsorb metalloids from the aqueous system via different functional groups. However, there is a lack of harmony regarding the effect of organic matter on As solubility, mobility and bioavailability. Some studies have reported HS-induced decrease in As bioavailability (Janoš et al. 2010), whereas other reported an increase in As bioavailability (McCauley et al. 2009). An increase in As mobility and leaching in soil amended with organic amendment has been reported (Hartley et al. 2009). The SOM-induced increase in As mobility is most likely due to competition between As and dissolved organic carbon for sorption sites in soil (Redman et al. 2002). Negatively charged HSs outcompete As from binding sites in soil (Grafe et al. 2002) due to higher binding energies than As leading to enhanced

As solubility, mobility and bioavailability (Lin et al. 2008). Therefore, SOM may play a key role in determining biogeochemical behaviour of As in soil-plant system (Grafe et al. 2001).

The formation of As-HA complexes is via two different ways. First, organic matter can adsorb As using Fe, Al and Mn cations by forming cationic bridges between the negatively charged surface of organic matter and the anionic As (Buzek et al. 2013). Secondly, organic matter forms As-HA complexes by different functional groups such as quinone, phenolic, COOH, alcoholic and enolic OH, lactone and hydroxyquinone (Fakour and Lin 2014). Bennett et al. (2012) used 3-mercaptopropyl-functionalized silica gel to develop a selective diffusive gradient in thin film for arsenite based on the attraction between SH group of HSs and As (III). Using X-ray absorption spectroscopy (XAS), Langner et al. (2011) showed that SOM can completely complex As by forming covalent bonds with arsenite. Different functional groups present on SOM have different binding capacities (Shahid et al. 2012b); therefore HS may form complexes with As having diverse binding energies (Fakour and Lin 2014). Generally, a strong bond is formed between As and N functional groups of HSs (<10% of total binding sites). However, a weak As-HA complex is formed between As and phenolic or carboxylic groups of HAs (>90% of total binding sites) (Fakour and Lin 2014).

Soil organic matter also influences As solubility, mobility, bioavailability and chemical speciation in soil by altering As chemical speciation through modification in soil conditions. For example, organic matter can result in arsenite oxidation to arsenate as well as arsenate reduction to arsenite (Redman et al. 2002). Soils with high organic matter produce reducing conditions (Ryu et al. 2010), which cause change in soil redox potential via proliferation of microorganisms. The reduction of arsenate into arsenite due to high-soil organic matter has also been reported (Redman et al. 2002). There is extensive literature supporting SOM-induced variation in As behaviour due to variation in soil properties (Rowland et al. 2006). Organic matter can alter the formation of soluble complexes soil redox potential and the available adsorption sites (Wang and Mulligan 2006). Soil organic matter can also influence biogeochemical behaviour of As in soil indirectly by affecting several soil processes such as oxidation/reduction, sorption/desorption and precipitation/solubilization. These soil mechanisms govern soil soluble-adsorbed As contents. Moreover, these processes also affect solubility and mobility of As in soil by modifying soil bio-physico-chemical properties such as mycorrhization, CEC, pH, redox status, competing ion concentration as well as chemical form of organic and inorganic ligands.

Influence of Biochar on Biogeochemical Behaviour of As

In recent years, biochars are particularly studied as a novel carbon rich material to adsorb As and heavy metals in contaminated water and soil (Bolan et al. 2014; Niazi et al. 2016). Biochar is a porous carbonaceous charcoal prepared by the

pyrolysis of organic compounds such as municipal waste, crop residues, animal wastes, wood and different industrial wastes (Jones et al. 2011). Recent reports showed that biochar has a number of agronomic benefits such as increase in carbon content (Lehmann and Joseph 2009), soil water holding capacity (Thies and Rillig 2009), enhanced soil productivity (Atkinson et al. 2010) and reduction in leaching of soluble macronutrients due to rise in soil pH (Laird et al. 2010). Biochar is capable to sequester high levels of metalloids owing to its high nanoporosity, surface area and other physio-chemical properties (Lehmann and Joseph 2009). Biochar-induced increased adsorption/sorption of As strongly influences the behaviour and fate of As in soil-plant environment (Beesley et al. 2010). It contains several functional groups (carboxylic, alcoholic and hydroxyl groups, etc.) and forms complexes with As. For instance, Zhang et al. (2013) showed that the Langmuir maximum capacity of biochar to As(V) is around 17,410 mg/kg, which is not only higher than that of Al_2O_3 adsorbent but also comparable to those of activated Al_2O_3. Beesley et al. (2013) reported that addition of biochar increased the mobility and bioavailability of As in soil. Biochar-mediated increase in extractable contents of As in soil has also been reported (Gregory et al. 2014), which agrees with several other studies (Beesley et al. 2013).

Previous studies report contradictory effects regarding the fate and behaviour of As in biochar-amended soils. However, there is harmony that application of biochar significantly affects the biogeochemical behaviour of As in soil (Gregory et al. 2014). The mechanisms underlying biochar-induced remediation of contaminated sites are generally governed by several heterogeneous processes including adsorption, electrostatic bindings and precipitation (Tang et al. 2013). Application of biochar increases negative charges on soil surface due to the increased CEC and reduced zeta potential (Tang et al. 2013). Therefore, there will be increased electrostatic binding between negatively charged soil surfaces and As having positive charge. Biochar-induced change in As behaviour in soil is attributed to variation in cation exchange, pH and redox status of the soil (Lehmann et al. 2011). Unlike metals, As mobility and solubility in soil increases following an increase in soil pH (Moreno-Jimenez et al. 2013). It is widely reported that the addition of biochar to soils resulted in pH increase (Jones et al. 2012). The liming effect of biochar raises soil pH and consequently enhances the mobility and solubility of As in soil (Joseph et al. 2010). Therefore, biochar application can enhance the bioavailability of As in soil and thus decreases remediation times for contaminated soil. However, some counterevidences suggest the potential risk of As leaching when biochars are applied to soils with high levels of As concentrations (Beesley and Marmiroli 2011).

Biochar-induced increase in As mobility and bioavailability can be due to a combination of increased soil alkalinity and competition between As and P for binding sites. In addition to As, biochars also enhance the mobility and bioavailability of P in soil (Beesley et al. 2013). Recently, Beesley et al. (2014) reported that application of biochar resulted in two times enhanced water-extractable PO_4-P concentration. Since, As and phosphate are chemically analogous to each other; thus increase in P availability results in the dissolution of As from soil particles into

solution (Neupane and Donahoe 2013). Moreover, the physical structure of biochar also affects the biogeochemical behaviour of As in soil. The presence of macro-, micro- and nanopores in the structure of biochar matrix results in Fe and Mn reduction (Joseph et al. 2010), both indicating a negative redox potential. Under such scenario, As adsorption to soil is reduced resulting in increased mobility and bioavailability of As in soil (Moreno-Jimenez et al. 2013).

There are some studies which reported no or non-significant effect of biochar on As solubility in soil. For example, Lucchini et al. (2014) reported that wood-derived biochar does not affect the solubility of As and heavy metals (copper (Cu), zinc (Zn), cadmium (Cd), nickel (Ni)) in soil, even after repeated applications. Similarly, Hartley et al. (2009) and Namgay et al. (2010) observed no significant increase in As bioavailability after biochar application. Any effect of biochar on As solubility in soil is probably due to increase in soil pH. The studies which reported no effect of biochar on As mobility and solubility are mainly due to no effect of biochar on soil pH. It is reported that the middle- to long-term application of wood-derived biochar does not enhance As mobility in unpolluted soils, since the rise in soil pH was only temporary (Namgay et al. 2010). Wingate (2008) reported that application of biochar (1% w/w) enhanced soil pH to just below 5 and did not affect mobilization of As. Even some studies reported decrease in As bioavailability in contaminated soils (Hossain et al. 2010). The reduction in exchangeable As after biochar addition was likely due to a reduction in CEC and the formation of insoluble As-biochar complexes. Some studies reported temporary decrease in the water-extractable As level (Gregory et al. 2014). Biochar-induced decrease in As solubilization can be due to its precipitation with metal cations, such as Ca^{2+}. These As salts release As again to the water-extractable phase after redissolution (Beesley and Marmiroli 2011). On the other hand, the liming effect of biochar may become more obvious, thus enhancing solubilization of As due to the associated pH increase.

Influence of Plant Root Exudates on Biogeochemical Behaviour of As

Plants are also known to affect the mobility and bioavailability of As in the rhizosphere soil by exudating low molecular weight organic acids (LMWOAs) (Shahid et al. 2012c; Austruy et al. 2014; Bergqvist et al. 2014). LMWOAs, which include tartaric, acetic, fumaric, oxalic and citric acids, generally originate by microbial metabolites or decay of soil organic matter (Quartacci et al. 2009; Abbas et al. 2016). These organic acids affect mobility and bioavailability of As by chelating/complexing *via* functional groups (Bergqvist et al. 2014). For example, the carboxylic functional groups, which are structural component of most LMWOAs, have been reported as potential extracting reagents for metalloids (Elliot and Shastri 1999). However, the influence of different LMWOAs towards As mobility and speciation differs with the type of LMWOAs and soil (Hinsinger

and Courchesne 2008). Gonzaga et al. (2012) extracted As from soil using different root exudate acids and demonstrated a strong correlation between the As levels in plant and soil. Organic acids released by roots of As hyperaccumulators ferns *Pteris vittata* and *Pteris biaurita* significantly enhanced plant-available and plant-extractable As in the soil (Gonzaga et al. 2009). Tu et al. (2004) reported that organic acids such as phytic acid and oxalic acid increased As transport and phytoavailability. Arsenic hyperaccumulators (*Pteris vittata* and *Pteris biaurita*) are capable to solubilize 'non-labile As' by exudating oxalic or phytic acids from their roots (Gonzaga et al. 2008).

LMWOAs affect the behaviour and fate of As in soil by directly affecting chelation, acidification, redox reactions and precipitation or indirectly, through their influence on physical and chemical properties of the rhizosphere and microbial activity (Quartacci et al. 2009). Yan et al. (2012) reported that oxalate, citrate and single superphosphate can increase the $NaHCO_3$-extractable As without any proper trend. Moreno-Jiménez et al. (2013) reported that the extractable As concentration in rhizosphere soil was two times higher than the bulk soil. This shows that plant root exudates influence As solubility most likely by affecting the As present on ion exchange sites. Plant root exudates are also reported to modify As sorption/desorption in soil by changing rhizosphere chemistry and processes taking place (Mucha et al. 2010). LMWOAs can mediate As desorption from soil particles especially As associated with oxides and hydroxides of Al, Fe and Mn.

The release and composition of root exudates vary with plant type and applied As level. Under normal conditions, root exudates flow through the lipid bilayer very slowly in response to the electrochemical gradient. However, under metalloid stress conditions, increased amount of root exudates is released due to activation of H^+-ATPases (Quartacci et al. 2009) or expression of anion channels embedded in the plasma membrane (Rengel 2002). Therefore, some studies suggested that LMWOAs play more important role than soil pH, owing to their role and release in accordance to plant need and environmental conditions (Qin et al. 2004). However, there is still confusion whether different plant species exudate organic acids of the same quality and at the same rate.

The As hyperaccumulator plants have potential to solubilize and uptake unavailable As in soils perhaps by exudating organic acids (Tu et al. 2004). Gonzaga et al. (2006) found that *Pteris vittata* (As hyperaccumulator) caused 9% increase in soil organic contents in the rhizosphere than *Nephrolepis exaltata* (non-As hyperaccumulator). In a hydroponic study, Tu et al. (2004) reported that As hyperaccumulator *Pteris vittata* secreted 300–500% more oxalic acid and 40–106% more phytic acid compared to non-As hyperaccumulator *Nephrolepis exaltata* under As stress. This showed that plant root exudates can solubilize As in soil by replacing it from with Fe/Al complexes. Plant root exudates can also enhance As phytoavailability by forming complexes with cations on soil mineral surfaces or decreasing As absorption on soil constituents. Bergqvist et al. (2014) reported that the extractable As concentration in the rhizosphere soil of carrot, lettuce and spinach was almost double compared with the bulk soil. Similar results

of higher extractable As in the rhizosphere soil as compared to bulk soil was reported by Kuppardt et al. (2010) in *Zea mays*.

Influence of Clay Contents on Biogeochemical Behaviour of As

Soil clay contents also affect mobility and solubility of As in soil. The adsorption capacity and affinity of soil for As(V) depend on soil texture and mineralogical composition. It is reported that soil clay contents are more effective than any other soil parameter for the retention of As and heavy metals in soil (Malandrino et al. 2011). In general, As is retained and adsorbed at higher levels in soil with a higher clay contents (Doušová et al. 2011). The mobility and bioavailability of As is lower in clay and clay loam soils (fine grained soils) compared to loam and sand soil (coarse grained soils) (Kirkham 2006). Sorption of As on clay varies in decreasing order of kaolinite > vermiculite > montmorillonite (Dickens and Hiltbold 1967).

The adsorption of As on clay depends on the type and quantity of clay (Corwin et al. 1999). Owojori et al. (2010) reported that clayey soils contain large amounts of binding sites which can retain high level of As. The adsorption of As on clay usually takes place by the formation of inner-sphere complexes or ion exchange reactions (Abollino et al. 2003). Usman et al. (2004) reported that the exchangeable and water-extractable metal contents decreased after soil amendment with clay minerals. Long ageing time results in increased dehydration of adsorbed As on clay minerals leading to less desorption of As due to stronger bonding (Lin and Puls 2000).

Influence of Metal Oxides in Soil on Biogeochemical Behaviour of As

The Fe/Mn oxides are ubiquitous in nearly all types of soils. The oxides and hydroxides of Fe and Mn are present in soil at varying levels (between 10 and 1000 mg kg^{-1}) and play an important role in determining chemical speciation and behaviour of As in soil (Sparks 2003). These oxides have high surface area and sorption affinity for As due to their small particle size (Sposito 2008). Nowadays, it is well eminent that the adsorption/desorption of As in natural solids greatly varies with the level of oxides and/or hydroxides of Fe, Al and Mn (Doušová et al. 2009). Generally, high levels of As are found in soils with high concentrations of Fe and Mn oxide or hydroxide (Bagherifam et al. 2014a). Some studies reported a moderate positive correlation ($r \geq 0.64$) between Fe and Mn content (oxides and hydroxides) in soil and the total As concentration (Neidhardt et al. 2012). The analysis of soil polluted by metalloids near mining sites showed that soil As was primarily

found in association with oxides and/or hydroxides of Fe, Al and Mn (Bagherifam et al. 2014a). Qi and Donahoe (2008) used a seven-step metal extraction procedure and showed that >80% of the extractable As (HNO_3 digestible) in soil was found associated with Fe and Mn oxides and oxyhydroxides.

The oxides and/or hydroxides of Al, Fe and Mn present are considered as key scavengers of As in natural soil environments, thus decreasing greatly their solubility, mobility, bioavailability and bioaccessibility (Bagherifam et al. 2014b). Soil amendments containing Fe and Mn oxides and oxyhydroxides have been widely studied for the treatment of As-contaminated sites due to the high binding affinity of Fe and Mn oxides for As (Garau et al. 2014). For example, Cutler et al. (2014) reported that application of two Fe sources (ferric chloride and ferrous sulphate) greatly reduced As bioavailability causing 30–41% reduction of in vitro bioaccessible As over a period of 2 years. The presence of Mn and Fe in soil is reported to form Fe or Mn plaques on the plant root surface, thus decreasing As absorption (Mallick et al. 2011). Neidhardt et al. (2012) observed that the presence of 6% Fe_2O_3 concentration in soil resulted in reduced phytoavailability and uptake by *Zea mays*.

The adsorption of different As species on mineral surface of Mn and Fe can be via two processes: (i) chemical (specific) and physical (nonspecific). The chemical adsorption is via the formation of inner-sphere complexes between As and Mn and Fe oxides. On the other hand, the physical adsorption is via outer-sphere complexation. The chemical adsorption (inner-sphere complexation) of As on oxides and/or hydroxides of Fe, Al and Mn is much stable and stronger compared to physical adsorption (outer-sphere complexation). The chemical adsorption is the result of coordinate-covalent bonding between As and metal oxides, whereas physical adsorption is due to electrostatic bonding. There is widespread literature reporting the formation of inner-sphere surface complexes between As and Fe and Mn oxides using extended X-ray adsorption fine structure (XAFS) spectroscopy (Goldberg and Johnston 2001).

The absorption of As on oxides and/or hydroxides of Al, Fe and Mn is highly dynamic and varies with the change in soil physico-chemical properties and the presence of organic and inorganic ligands (Dousova et al. 2012). Soil pH greatly affects As adsorption on oxides and/or hydroxides of Fe, Al and Mn by modifying net charge on functional groups of mineral surfaces. The adsorption of As on oxides and/or hydroxides of Fe and Mn occurs via surface complexation between negatively or positively charged functional groups such as OH and As ions. The mineral surfaces containing Fe and Mn may contain positive or negative charge depending on soil pH values (McBride 1994). Low soil pH causes double protonation of hydroxyl groups present at the surface of the iron oxide resulting in positive charge of iron oxide. At a certain pH (point of zero charge, usually pH between 5.5 and 9), the surface charge of iron oxide becomes neutral due to protonation of hydroxyl group with only one proton. At high-soil pH values, the hydroxyl group is fully deprotonated resulting in a negative charge on iron oxide surface. LMWOAs (oxalate, citrate, malate and tartrate) block As sorption onto oxides and/or hydroxides of Fe, Al and Mn (Dousova et al. 2012).

Influence of Phosphate on Biogeochemical Behaviour of As

Soil phosphate (P) contents are reported to play a key role in mobilization/immobilization processes of As in soils (Rahman et al. 2014). Several previous studies reported that As and phosphate are analogous to each other owing to their similar physical and chemical properties. Arsenate and phosphate compete for the same adsorption sites present on the surface of soil constituents (Rahman et al. 2014). Competitive binding of As(V) and P to soil particles is well known on mineral surfaces such as goethite (Sharma and Sohn 2009; Feng et al. 2013) and ferrihydrite (Sharma and Sohn 2009). Biswas et al. (2014) evaluated the effect of different competing ions on arsenite and arsenate adsorption onto Fe oxyhydroxide and reported that the competition ability of competing ions decreases in the order of phosphate > Fe(II) > H_4SiO_4 > HCO_3. Several previous studies supported P-induced As mobilization and solubilization in soil (Cao et al. 2003). Therefore, phosphate is considered to be a good marker of As mobilization and solubilization in soil (Huang and and Matzner 2006). The desorption of As by P from the surfaces of soil particles is via ion exchange reactions (Kaplan and Knox 2004). Removal of As from contaminated soil particles with phosphate solutions has been studied and reported extensively (Tokunaga and Hakuta 2002). For example, phosphoric acid is reported to be highly effective in rapid removal of As from contaminated soil by dissolving As present on oxides and hydroxides in soil (Tokunaga and Hakuta 2002). Recently Cutler et al. (2014) reported that the addition of P caused a significant increase in in vitro bioaccessible As. Some studies have also reported co-precipitation of P minerals and As (Henke 2009). These studies reported that As forms solid solutions of chlorapatites and fluorapatites by substituting P (Grisafe and Hummel 1970). Using this technique, some authors removed As from solution via precipitation of Ca-P-As(V) minerals at pH 8–10. The adsorption and desorption of As and P on iron oxides are very similar with regard to pH dependence.

The effect of P on As phytoavailability in soil and uptake by plant is generally attributed to competition between As and of P for adsorption on soil constituents and uptake by plant roots (Bolan et al. 2014). The effect of phosphorus on As bioavailability is via two processes. Firstly, phosphate has more binding affinity for soil particles compared to As(V) and hence assists As desorption and solubilization in soil (Ravenscroft et al. 2001). Secondly, As does not have any specific uptake transporter in plants and is usually taken up by phosphate transporters (Meharg and MacNair 1992). However, the overall influence of P on As bioavailability in soils varies with the degree of P-induced As solubilization in soils and competition for As uptake by plant roots. Abbas and Meharg (2008) reported that treatment of PO_4^{3-} in hydroponic experiments significantly decreased the influxes of As by 50% using different maize varieties. Similarly, the presence of As in soil affects phosphorus uptake by plants. Mallick et al. (2011) reported that addition of As under hydroponic conditions reduced phosphate ion content in the root and leaves of the maize plant.

Influence of Calcium on Biogeochemical Behaviour of As

Different inorganic compounds, especially cations, also play an important role in biogeochemical behaviour of As. The effects of these cations are either by precipitating properties or by competing like calcium, which is reported to compete with As in soil-plant system. The presence of Ca along with As in soil system causes precipitation of these cations in different mineral form. Owing to binding and precipitation capacity of Ca-bearing compounds, Ca is used for the immobilization of As in remediation studies. However, the formation and precipitation of these Ca-As-bearing minerals depends on soil physico-chemical properties (Hassan et al. 2014). Juillot et al. (1999) reported that application of Ca in the form of gypsum forms resulted in a reaction between dissolved calcium with As(V) followed by formation and precipitation of 1:1 calcium arsenate pharmacolite ($CaHAsO_4.2H_2O$), haidingerite ($CaHAsO_4.H_2O$) and weilite ($CaHAsO_4$). Similarly, Rodriguez et al. (2008) reported that the reaction of gypsum with arsenate started at pH 9 and 25 C° temperature followed by surface precipitation of sainfeldite [$Ca_5(HAsO_4)_2(AsO_4)_2$•$4H_2O$] and guerinite [$Ca_5(HAsO_4)_2(AsO_4)_2$•$9H_2O$]. Recently, Chen et al. (2014) reported that there is high As removal efficiency of calcium sulphate anhydrous whiskers (CSAW), and byproduct gypsum, when present in lower concentration range (below 40 mg L^{-1}). However, the removal efficiency of CSAW was less than 60% for As(III). Thus, the interaction mechanism between arsenate and CSAW material could be a combination of adsorption and surface dissolution-precipitation (Chen et al. 2014). Moreover, the interaction mechanism of As with Ca varies with its chemical form (As(III) or As(V)).

Lime is also used to immobilize As in soil via adsorption and surface dissolution-precipitation processes. Lime-reducing soil As availability is possibly attributed to formation of As-Ca complexes (Moon et al. 2004). CaO_2 dissolves in H_2O to form H_2O_2 and $Ca(OH)_2$ via reaction $CaO_2 + 2H_2O \longrightarrow H_2O_2 + Ca(OH)_2$ (Northup and Cassidy 2008). It has been evident that calcium hydroxide ($Ca(OH)_2$) has a high efficiency for the capture of As in comparison to other minerals such as kaolinite, alumina and silica (Ghosh-Dastidar et al. 1996). This high capturing efficiency of ($Ca(OH)_2$) is due to the formation of low solubility Ca-As precipitates such as $Ca_4(OH)_2(AsO_4)_2 4H_2O$ and $Ca_5(AsO_4)_3(OH)$ (Bothe and Brown 1999). The As(III) stabilization can be increased by CaO_2 into the soil by following reaction $AsO^{-2} + H_2O_2 + 2OH\text{-} \longrightarrow AsO_4^{-3} + 2H_2O$ (Fuessle and Taylor 2004). Therefore, CaO_2 is considered a potential amendment for As immobilization in soil (Chuan-ping et al. 2012). Moreover, a combined application of Ca with P (Ca-P) is considered to be the best treatment for As immobilization in contaminated soil (Neupane and Donahoe 2012). Owing to high capturing efficiency, Ca-bearing minerals are also used as additives to coal for in situ capturing of As and Se vapours and in turn reduce their emission into ambient (Zhang et al. 2015).

Calcium is also reported to interfere and compete with As plant uptake and affects its transportation from soil to root and root to shoots. Recently, Liu et al. (2014) reported that soil application of CaO_2 significantly reduced As accumulation in celery shoots, which was attributed to decrease in bioavailable (labile) portion of As in the soil and the formation of stable and immobile crystalline Fe and Al oxide-bound As.

Influence of Silicon on Biogeochemical Behaviour of As

Silicon (Si) is the second most abundant element in the Earth's crust, and its concentration in soil solution ranges from 0.1 to 0.6 mM. Since Si is ubiquitous in soil-plant system and is inevitable for the plants, so all plants grown in the soil medium contain considerable concentrations of Si in their tissues ranging from 0.1 to 10% on dry weight basis (Epstein 2009). However, Si does not have any necessary role for the growth of higher plants, but the beneficial effects of Si have been reported in plants under biotic and abiotic stresses. It has been reported that exogenous application of Si improves plant growth under water stress and metalloid toxicity (Liang et al. 2007). As reported earlier, As(V) is taken up by the plant roots through high-affinity phosphate transporters (Meharg and MacNair 1992), while As(III) enters plant roots through Si transporters. Various mechanisms have been reported about the beneficial effects of Si under As stress, i.e. improved photosynthetic activity (Sanglard et al. 2014), reduced oxidative stress by detoxification of reactive oxygen species (Tripathi et al. 2013), reduced As uptake and improved selectivity of Si over arsenite (Sanglard et al. 2014).

From the reported studies, it is evident that plants have the strategy to avoid extra-exposure to As. Among these strategies, As(III) exclusion through Si influx transporter LSi_1 is an important one, but this only contributes 15–20% of the total As(III) exclusion (Zhao et al. 2010). The other possibility is the active exclusion of the arsenite through H^+ gradient-driven antiporter, as identified in the yeast (Wysocki et al. 1997). Unfortunately, the excluded form, arsenite, is more mobile and may readily be taken up by the plant roots. In this context, arsenite oxidation can be an important way to reduce the arsenite transport from the soil solution to the roots (Jia et al. 2014). This is achieved through inclusion of Si in the root medium, which enhances the oxidation power of the plant roots (Fleck et al. 2011). In addition, Si may reduce the arsenite transport within the plants from roots to shoots through Si deposition in the endodermis of roots that reduces the apoplastic bypass flow and creates a barrier in the apoplastic movement of toxic ions (Saqib et al. 2008). Moreover, apoplastic Si deposition changes the binding properties of the cell wall, thus increasing the adsorption capacity of the cell wall reducing the toxic mineral ions (Saqib et al. 2008). The other possible strategy by which Si added to root medium reduces the toxic effect of As may be due to activation of the plant antioxidant systems such as superoxide dismutase, catalase and glutathione reductase that results in reduced lipid peroxidation of the plasma membrane (Tripathi et al. 2013) and may help in maintaining the plasma membrane and tonoplast H^+-ATPase activities as described in case of salinity toxicity (Liang et al. 2006). These processes may improve the compartmentation and sequestration of the As into the vacuoles and reduce the overall impact in the living systems.

Influence of Synthetic Organic Ligands on Biogeochemical Behaviour of As

The role of organic ligands on biogeochemical behaviour of metalloids in soil-plant system has been mainly studied due to high affinity of organic ligands for metals (Shahid et al. 2012d, 2014e). Different synthetic chelating agents are used for soil amendments of metalloids, which act differently towards metal mobilization/immobilization in soil. The most commonly used synthetic chelating agents include nitrilotriacetic acid (NTA), ethylenediaminetetraacetic acid (EDTA), glycol ether diamine tetraacetic acid (EDGA), diethylenetriaminepentaacetic acid (DTPA) and ethylenediamine disuccinate (Shahid et al. 2012d, 2014f; Saifullah et al. 2015). These compounds are highly effective in mobilizing the metalloids, thereby increasing their subsequent absorption by plant roots. However, the effectiveness of these chelates in mobilizing soil metalloids varies with different factors, including As species, As chelate ratio, the presence of competing cations, soil pH and the extent of metalloid retention onto soil constituents. Synthetic organic ligands are capable to extract As on exchange sites of both organic and inorganic complexes (Leleyter et al. 2012).

Synthetic organic ligands form soluble complexes with As and increase the exchangeable fraction of As in soil (Mühlbachová 2011). The total amount of extractable As(III) increases after the addition of EDTA (Aydin and Coskun 2013). Owing to high affinity for metals, synthetic organic ligands release As from various soil constituents, especially metals associated with organic matters and oxides of Fe and Mn (Udovic and Lestan 2009). Moreover, synthetic organic ligands can extract As bound with sulphide and organic soil components, which are usually not easily phytoavailable (Ramos-Miras et al. 2011). However, the effect of different synthetic organic ligands on As behaviour in soil-plant system is different.

It is reported that organic ligands affect the pH of soil, which in turn affects As availability in soil. Ligand-induced increase in As solubility can be due to the change (decrease) in soil pH, i.e. associated with the application of organic ligands (Signes-Pastor et al. 2007). For example, Abbas and Abdelhafez (2013) showed that EDTA has an acidic physiological effect and significantly decreased soil pH values after 8 weeks of incubation. Several reported studies have shown that the soil pH decreased significantly followed by EDTA application (Mühlbachová 2009). Some authors also reported the direct effect of organic ligands application on As behaviour in soil. Aydin and Coskun (2013) reported that application of EDTA 15 days prior to harvest resulted in more solubilization of arsenite and increased the amount of arsenite accumulated into watercress. Chiu et al. (2005) evaluated the extraction efficiency of nine chelating agents and found the following order of extraction efficiency of chelating agents: NTA > HEIDA > HEDTA > citric acid > EDTA > EGTA >CDTA > DTPA > malic acid. This showed that application of NTA can significantly enhance As mobilization in soil, but the applied rate of NTA should be > 10 mmole kg^{-1}.

The presence of synthetic organic ligands also affects As uptake and partitioning inside the plants. Abbas and Abdelhafez (2013) reported that application of EDTA combined with As(III) resulted in increased absorption of As by maize plants. They also showed that EDTA enhanced the rate of As translocation towards aerial parts. Arsenic uptake and translocation increases with increasing rate of EDTA application. Similar results were reported by Rahman et al. (2011) who showed that the presence of EDTA in growth medium remarkably increased As uptake in the shoots of rice plants. Chiu et al. (2005) reported that the application of NTA in As-amended soil increased threefold of As in shoots of *Vetiveria zizanioides* and *Zea mays*. Yang et al. (2012) observed that the shoot concentrations of As, Cd and Pb in *Arundo donax* were increased significantly by the addition of EDTA. Rahman et al. (2008) showed that EDTA enhanced As uptake in tissues of *S. polyrhiza* due to EDTA-induced mobilization of As adsorbed on iron plaque of plant surface. Previously, it was shown that addition of iron in the soil solution enhanced As adsorption on Fe plaque on the rice seedling roots (Azizur Rahman et al. 2011). Moreover, De Gregori et al. (2004) reported high correlation coefficient values between EDTA extractable As fraction and the As content in alfalfa plants. Still, there is confliction regarding the application of different synthetic organic ligands to As-contaminated soil and resulting As mobilization in soil and accumulation by plants.

Influence of Microorganisms on Biogeochemical Behaviour of As

Soil microbial activity influences As behaviour in soil especially in the rhizosphere soil (Yamamura and Amachi 2014; Gorny et al. 2015). Soil microorganisms are found abundantly in rhizosphere soil where they are reported to cause As solubilization in soil, thereby affecting As mobility and bioavailability in soil system (Rahman et al. 2014). Soil microbes solubilize As-bearing minerals via different processes and increase As availability (Sheng and Xia 2006). Bai et al. (2008) reported that inoculation of arbuscular mycorrhizal fungal strain for 10 weeks increased As phytoavailability to maize plant. Similarly, Rahman et al. (2014) showed increased As uptake to maize roots by microbial interactions. The use of Glomus mosseae and Acaulospora morrowiae as arbuscular mycorrhizal affected the root As efflux and reduced As bioavailability to corn plant (Hua et al. 2014).

Microorganisms play a major role in redox transforming of As by reducing As (V) to As(III) and vice versa (Gorny et al. 2015). A number of As(III)-oxidizing and As(V)-reducing prokaryotes have been identified and isolated from As-contaminated environments (Ghosh et al. 2015), which are capable of mediating As transformations in agricultural and forest soils (Corsini et al. 2010) as well as groundwater sediments and aquifer (Kulp et al. 2007). Microbial-induced As (V) reduction in uncontaminated natural soils is well known (Xu et al. 2016) and is the main source of high level of As in naturally contaminated waters (Lockwood

et al. 2014). Microbial-induced As(V) reduction occurs via dissimilatory reduction (Zobrist et al. 2000) or intracellular mechanism of detoxification (Ghosh et al. 2015). Arsenate-reducing microorganisms such as *Crysiogenes arsenates*, *Geospirillum barnesi*, *Geospirillum arsenophilus*, *Bacillus arsenicoselenatis* and *Desulfutomaculum auripigmentum* use As(V) as a terminal electron acceptor in their respiratory process (Vaxevanidou et al. 2012). Microbial sulphate reduction results in sulphate and As(V) reduction to sulphide and As(III), respectively, which precipitates as As_2S_3. Since As(III) is more soluble and mobile compared to As(V), therefore As(III) reduction may result in subsequent leaching (Bolan et al. 2014). Thus, one of the mechanism causing As mobilization in soil is the reduction of As (V) to mobile As(III) in the aqueous medium. On the contrary, microbes may cause As(III) oxidation to As(V) which is then precipitated via Fe ions (Chandraprabha and Natarajan 2011). Bacterial species, such as *Agrobacterium tumefaciens*, *Alcaligenes faecalis*, *Bacillus* and *Geobacillus*, are capable to cause enzymatic oxidation of arsenite into arsenate by synthesizing arsenite oxidases (Yamamura and Amachi 2014). During As(V) oxidation to As(III), bacteria obtain an electron required for their metabolism. This mechanism of transferring As(V) into less toxic As(III) is generally regarded as a process of detoxification (Ghosh et al. 2015). Bahar et al. (2012) isolated a new As(III)-oxidizing bacterium *Stenotrophomonas* sp. from a low As-containing soil.

Soil microorganisms may also cause indirect release of As in soil solution by reductive dissolution of soil iron oxides. Numerous reports highlighted the ability of certain bacteria to release As by catalytic reduction of ferric oxides (Bolan et al. 2014). Iron plaque is formed on plant roots by iron oxidizing bacteria or abiotic oxidation (Weiss et al. 2003), which serves as ideal substrates for iron-reducing bacteria due to crystalline or amorphous structure (Hansel et al. 2001). However, some authors reported that the Fe(III) reduction may result in a secondary Fe phases which can sorb As (Kocar et al. 2006; Tufano et al. 2008). Soil microbes can also affect As bioavailability indirectly by affecting soil P status. Bai et al. (2008) reported that arbuscular mycorrhizal fungal inoculation enhanced As bioavailability compared to non-inoculated maize plants. Similarly, Yu et al. (2009) showed decreased As bioavailability in soil after arbuscular mycorrhizal inoculation.

The transfer of toxic inorganic As to less toxic organo-arsenical species is termed as methylation that occurs via soil microbial activity. The methylation of inorganic As to organic As is considered to be a tolerance/detoxification mechanism adopted by some microorganisms (Zhang et al. 2015). During this process, CH_3 groups replace one or more OH groups resulting in the formation of monomethylarsonic and di- and tri-methylarsines (O'Neill 1995). During methylation, As(V) is converted to As(III) followed by several step process to form organic As compounds, such as MMA(V), DMA(V), TMA and finally trimethylarsine (Rahman et al. 2014). Methylation may take place under aerobic or anaerobic environmental conditions by a variety of microorganisms. Under anaerobic conditions, some yeasts, fungi and bacteria can volatilize (AsH_3), the methylated As (Suess and Planer-Friedrich 2012). During methylation, a significant amount of As may be lost from soil by volatilization. However, this As loss via methylation never exceeds 0.01% of the total As emissions from natural sources (Woolson 1983).

Soil-Plant Transfer of As

Generally, As is considered non-essential for living plants and other organisms; however, As is naturally found in plants. Some studies even reported the beneficial effect of As to plants at very low concentrations (Gulz et al. 2005). Arsenic concentration in plants seldom exceeds 1.0 mg kg^{-1} (Adriano 2001). Austruy et al. (2013) reported that the As content was less than 0.1% of dry matter in *Agrostis capillaris*, *Solanum nigrum* and *Vicia faba* when grown on As-contaminated soil. Arsenic uptake by plants is mainly through roots (Neidhardt et al. 2015), which can be via active (requires energy) or passive pathways (does not require energy). Arsenic uptake by plants relies on its speciation and concentration in soil and correlate to bioavailable/extractable As level in soil (Martínez-Sánchez et al. 2011). Arsenic mainly enters the plant in inorganic form (Neidhardt et al. 2015) via transporter proteins, which is likely governed by the concentration gradient of As between plant cells and growth media. Till date, no As-specific transporters for uptake by plants have been reported (Ghosh et al. 2015). It is reported that As(V) enters the plants through P cell channels (Ghosh et al. 2015). Lei et al. (2012) used synchrotron X-ray microprobe and revealed that P and As (V) were cotransported via P channels. The cotransportation of P and As(V) inside plants can be increased by P deficiency or As(V) exposure but restrained by energy release inhibition caused by sodium orthovanadate or 2,4-dinitrophenol.

The P channels responsible for As(V) entrance to plants are formed by proteins called P transporter proteins (PHT) (Smith et al. 2003; Nussaume et al. 2011). In *Arabidopsis thaliana*, nine PHT1–9 have been identified. It is hypothesized that PHT4 and PHT1 may be involved in As(V) uptake, but the relative combinations of PHTs are still not well known (LeBlanc et al. 2013). Conversely, the uptake of As (III) is governed by nodulin-26-like intrinsic proteins (NIPs). In contrast to PHT proteins, NIP transporter channels are bidirectional. Therefore, As(III) may move in both directions depending on the concentration gradient between the growth medium and the cells. Arsenite and organic arsenic species are also reported to pass through the Si influx (LSi_1) and Si efflux transporters (LSi_2) to be taken up and transported from soil solution to the xylem stream (Li et al. 2009; Mitani-Ueno et al. 2011). Among these transporters, LSi_1 allows the bidirectional movement of Si and arsenite, through which Si/arsenite enters from soil solution to the root cells and some of the arsenite is excluded from the cytosol to the external medium, while LSi_2 is an efflux transporter present in the endodermis of the root cells and facilitates the exclusion of Si/arsenite into the stele and xylem cells. However, As hyperaccumulator ferns, such as *Pteris vittata and Pityrogramma calomelanos*, are reported to uptake As(III) via a different set of proteins (Niazi et al. 2012). Therefore, further study is needed in this regard. Recently, Xu et al. (2015) reported that under arsenite stress conditions, Arabidopsis NIP3;1 plays a key role towards As uptake by plants and its translocation to aerial parts. The Arabidopsis NIP3;1 mutants resulted in reduced As accumulation in plant shoots and enhanced arsenite tolerance compared to wild-type plants. Similarly, NIP3;1 NIP1;1 double mutant exhibited enhanced root and shoot growth and strong arsenite tolerance under high arsenite level.

The ability of a plant to uptake metalloids is generally represented by soil-to-plant transfer factors (Xiong et al. 2014), which depend on soil type, As speciation and concentration, type of plant species, plant age and the presence of chelating agents/transporters in the roots. Soil-to-plant transfer factors for As normally range from 0.01 to 0.1 for non-hyperaccumulating plants and greater than 1 for hyperaccumulator plants. It is reported that the As soil-plant transfer decreased with increasing As concentration in the hydroponic media (Mallick et al. 2011). Similarly, As sequestration on thiol ligands and Fe oxide plaques in plant roots also results in reduced As uptake by plants (Pan et al. 2014; Neidhardt et al. 2015; Matsumoto et al. 2015). Moreover, the presence of arbuscular mycorrhizal fungi on plant roots also restricts As plant uptake (Yang et al. 2009). Similarly, some authors reported variation in As soil-plant translocation efficiency caused by the type and properties of soil (Gulz et al. 2005) higher As soil-plant transfer on sandy loam soil (4.7%) than silty loam soil (0.4%).

In majority of the plant species (mostly non-hyperaccumulators), plant roots commonly accumulate major portion of As, and a small part is translocated from root to shoot (Austruy et al. 2013). Arsenic sequestration in plant root tissues can be 200 times higher than in the shoot (Smith et al. 2008), suggesting that roots are responsible for accumulating most of the As in the plants (Madejón and Lepp 2007). The increased uptake of As in plant root tissues has been reported in *Zea mays*, *Helianthus annuus* (Neidhardt et al. 2015), *Oryza sativa* (Rahman et al. 2011), *Phaseolus vulgaris* (Ye et al. 2010), *Hydrilla verticillata* (Xue and Yan 2011), *Triticum* (Shi et al. 2015) and *Solanum lycopersicum* (Cobb et al. 2000). The percent accumulation of As in plant roots varies with rhizosphere As concentration, As speciation and plant type (Rahman et al. 2014). The reason behind increased sequestration of As in plant roots and decreased translocation to other parts of the plant is not well explained in the literature. However, it is reported that root to shoot transfer of As is greatly influenced by phosphate nutritional status, which hinders As transfer from the roots towards other aerial parts of the plants. It is reported that low- and high-affinity plasma membrane carrier proteins have a more attraction for phosphate than As(V) (Meharg and Macnair 1990). The presence of phosphate greatly affects root to shoot translocation of As(III) compared to As(V) (Abedin et al. 2002). The root to shoot translocation of As varies with plant species. Arsenite mainly accumulated in xylem sap of *Pteris vittata*, *Oryza sativa*, *Cucumis sativus* and *Solanum lycopersicum*, while As(V) predominated in xylem sap of *Holcus lanatus*, *Brassica juncea*, *Triticum aestivum* and *Ricinus communis* exposed to either As(V/III) (Ye et al. 2010). Hyperaccumulator plant species accumulate a major portion of absorbed As in the aerial parts of plants (Francesconi 2002).

Arsenic translocation from root to shoot and percent accumulation in different plant tissues greatly relies on As speciation. Raab et al. (2007) reported that DMA (V) translocation from root to shoot was 3 and 10 times higher than As(V) and MMA (V), respectively, for 46 corn species grown under hydroponic conditions. Abedin et al. (2002) reported that the translocation of As(III) or As(V) was significantly higher than that of MMA and DMA. Smith et al. (2008) reported that arsenite was the dominant species (57–78%) of the total As concentration, while As(V) comprised

between 16 and 27% in rice roots. Rice grains can accumulate up to 89% of DMA (Williams et al. 2005; Ackerman et al. 2005). Quaghebeur and Rengal (2004) reported that As(III) comprised between 67 and 90% of the total As in the roots of *Arabidopsis thaliana*. Xue and Yan (2011) showed that As(V) was the dominant form in roots, and As(III) was the dominant form in leaves of *Hydrilla verticillata*.

Arsenic Hyperaccumulators

Remediation of As-contaminated soil is indispensable to save the environment from their hazardous effects (Niazi et al. 2011, 2012; Ullah et al. 2015a, b). Elimination of metalloids from contaminated soil is a challenging task owing to practical/technical complexity and cost involved (Barceló and Poschenrieder 2003). During the last two to three decades, several bio-physico-chemical techniques have been developed to extract metalloids from contaminated sites. Among these, phytoremediation is reported to be the most effective because of its eco-friendly, natural, economical/feasible, sustainable and practical nature (Arshad et al. 2008; Ullah et al. 2015a, b; Sabir et al. 2015). Phytoremediation is based on the mechanism that certain plant species have the potential to detoxify and remediate polluted sites by eliminating the pollutants from soils (Smith et al. 2008). Meharg and Hartley-Whitaker (2002) summarized in detail As hyperaccumulators. They reported that As hyperaccumulators grow well on As-contaminated soil because these plants possess an efficient defensive/tolerance mechanism for As uptake, conversion, detoxification and removal. These plants can accumulate 100 times As than the tolerant or normal non-accumulating plants (Wei and Chen 2006; Khalid et al. 2017). Moreover, hyperaccumulating plants have high (> 1.0) translocation factor from roots to shoot (Wei and Chen 2006).

A number of plant species have been reported to sequester excessive amounts of As without incurring damage to basic biochemical processes (*Cytisus striatus*, *Holcus lanatus*, *Pteris vittata*, *Pteris cretica*, *Pityrogramma calomelanos*) (Niazi et al. 2012). Among these, *Pteris vittata* is reported to be the most effective and can accumulate up to 22,630 mg/kg As in the fronds (Wang et al. 2002). Niazi et al. (2011) showed that *P. calomelanos* var. *austroamericana* (gold dust fern) accumulated up to 1600 mg As kg^{-1} dry weight after 10 months of growth at a historic cattle dip site in NSW, Australia. However, the use of ferns in field conditions is not highly practical due to slow growth rates and low light-intensity requirement to flourish. Singh et al. (2010) compared the accumulation and tolerance potential of 12 Indian ferns and reported that *Pteris cretica*, *Pteris vittata*, *Nephrolepis exaltata* and *Adiantum capillus-veneris* can be considered as As accumulator based on the As uptake in different plant parts.

Arsenic hyperaccumulators can operate well even under high-soil As situations. In fact, metal hyperaccumulators have evolved or naturally contain a very complex defence mechanism to avoid metal-induced tissue dysfunctioning and cell injury (Shahid et al. 2014g). In As hyperaccumulating plants, after As uptake several

defence mechanisms become active by which they tolerate metal toxicity (Tang et al. 2010). These processes help plants to keep the level of As(V) or As(III) in different plant tissues (especially sensitive tissues like leaves) that do not harm the plants. These defensive mechanisms include active and increased excretion, As binding to the cell wall, restricted As distribution to sensitive tissues, As chelation by organic molecules and sequestration in vacuoles. The compartmentalization of As in above ground plant cell vacuoles plays key role in the arsenic hyperaccumulation in *Pteris vittata* (Shen et al. 2014). However, the mechanism (s) of As transfer to above ground plant cell vacuoles are not well known. In addition to vacuolar compartmentation, most of the defence mechanisms in *Pteris vittata* against As toxicity rely on enzymatic antioxidant systems (catalase, dismutases, peroxidase, dehydroascorbate reductase, monodehydroascorbate reductase and glutathione reductase) and metabolic compounds (glutathione, phytochelatins, tocopherols and carotenoids).

Hyperaccumulating plants are capable to detoxify metal-induced ROS production via increased levels of these antioxidant enzymes and metabolic compounds (Shahid et al. 2014g). In contrast to other metal hyperaccumulating plants, As hyperaccumulators transport the As towards aerial parts and store it in the leaf vacuoles. Arsenic transfer towards aerial plant parts and subsequent sequestration in leaf vacuoles are achieved with the help of different peptides and proteins. In As hyperaccumulator plants, AR enzyme reduces As (V) to As (III), which is then complexed with free thiol groups followed by storage of the arsenite-thiolate complex in vacuole (Shen et al. 2014).

Threshold Levels of As in Soil, Water and Food

Humans can be exposed to As via several pathways, crops–soil–water being the major pathways (Khan et al. 2009). Groundwater contaminated with high levels of As has been reported worldwide, Bangladesh and West Bengal, India, facing the most serious groundwater As problem in the world (Bundschuh et al. 2012). Keeping in view the toxicity of As, the World Health Organization, Food and Drug Administration and USEPA set the As standard for drinking water at 10 μg L^{-1}. It has been reported that when drinking water levels of As are at the WHO's 10 μg/L limit, 0.05 mg/kg As in rice contributes to 60% of the dietary As exposure (Williams et al. 2009). However, the Department of Environmental Protection for New Jersey (NJDEP 2006) has set a drinking water limit of As at 5 μg L^{-1}. In some countries like India, Bangladesh, Pakistan, China, Taiwan and Vietnam, the threshold level of As is still 50 μg L^{-1} (Nriagu et al. 2007). The WHO has reported the median lethal dose of 1–5 mg As/kg in humans. It is reported that exposure to 70–80 mg of As_2O_3 by ingestion can be hazardous for human beings (Vallee et al. 1960).

Although not standardized, the general threshold limit of As in soil is 24 mg kg^{-1} regarding human health safety that needs a toxicological risk assessment and 50 mg/kg for agricultural soils (MAFF 1993). According to Karczewska et al.

(2013), the threshold level of As in Polish soils used for recreation, forestry and agriculture is set at 20 mg kg^{-1}. Inorganic As has an oral LD50 between 11–150 mg As kg^{-1} and 15–293 mg As kg^{-1} bodyweight in laboratory animals and rats, respectively (Ng 2005). In countries, such as Australia, Argentina, Chile, Hungary, China, Peru, Mexico, Thailand, Taiwan and the United States (O'Reilly et al. 2010), the total As concentrations in groundwater and soil exceeding the limit established by the USEPA (10 μg L^{-1} and 20 mg kg^{-1}, respectively) have been found (USEPA 2015).

Arsenic threshold level in most food crops is not yet finalized by many regulatory authorities and organizations. For example, Llorente-Mirandes et al. (2014) reported that no limits exist in the European Union on As, either inorganic or total, in foods (European Union Regulation 1881/2006) (Llorente-Mirandes et al. 2014). On the other hand, China has a maximum allowable concentration of total As in mushrooms of 0.5 and 1.0 mg As kg^{-1}, for fresh and dry mushrooms, respectively (MHC 2005). Recently, the European Food Safety Authority (EFSA) and the FAO/WHO Joint Expert Committee on Food Additives (JECFA) (FAO/WHO) evaluated dietary exposure to As and reported the urgent need for further data on As species in food commodities, in order to improve the background data for future risk assessment analysis. Several proficiency tests on As in different foodstuffs have been organized (de la Calle et al. 2012).

Conclusions and Remarks

In this review, we have comprehensively compiled, compared and evaluated the literature concerning biogeochemical behaviour of As (chemical speciation and bioavailability in soil and uptake by plants) under different soil conditions. This information is useful for understanding the biogeochemical behaviour of As in soil-plant system. Arsenic contamination of soil and water occurs via anthropogenic and natural sources. Anthropogenic activities include mining, industrial activities and the use of pesticides in agriculture and wood preservative. Natural As sources contribute major parts towards As soil and water contamination and include weathering and erosion of rocks and minerals and biological processes. Threshold levels of As in soil, plant and water as well as their assessment methods are not well established so far, in many countries worldwide. Arsenic occurs naturally in various chemical species in soil which varies greatly regarding their biogeochemical behaviour. Total soil As concentration is a poor proxy for predicting biogeochemical behaviour of As in soil. The chemical species and distribution of As in soil are governed by a number of reactions that involve adsorption/desorption, precipitation/dissolution and As-ligand complex formation. These highly dynamic soil processes vary with the variations in soil physico-chemical properties (pH; soil texture; organic matter; P, Fe, Mn and Al oxides; biological and microbial conditions; metal burdens; and the presence of organic and inorganic ligands). Plants uptake As *via* roots by phosphate and silicon transporters. No As-specific

transporter has been identified so far for As phyto-uptake. As is sequestered mainly in plant root with very low translocation in above ground plant parts. As hyperaccumulators store As in vacuoles as a detoxification mechanism. Knowledge of As speciation in soil-plant system is ideal in the context of soil remediation and risk assessment studies.

References

Abbas MHH, Abdelhafez AA (2013) Role of EDTA in arsenic mobilization and its uptake by maize grown on an As-polluted soil. Chemosphere 90(2):588–594

Abbas MHH, Meharg AA (2008) Arsenate, arsenite and dimethyl arsinic acid (DMA) uptake and tolerance in maize (*Zea mays L.*). Plant and Soil 304(1–2):277–289

Abbas G, Saqib M, Akhtar J, Murtaza G, Shahid M, Hussain A (2016) Relationship between rhizosphere acidification and phytoremediation in two acacia species. J Soil Sediment 16 (4):1392–1399

Abdul MKS, Jayasinghe SS, Chandana EPS, Jayasumana C, De Silva PMCS (2015) Arsenic and human health effects: a review. Environ Toxicol Pharmacol 40(3):828–846

Abedin MJ, Cotter-Howells J, Meharg AA (2002) Arsenic uptake and accumulation in rice (*Oryza sativa* L.) irrigated with contaminated water. Plant and Soil 240(2):311–319

Abollino O, Aceto M, Malandrino M, Sarzanini C, Mentasti E (2003) Adsorption of heavy metals on Na-montmorillonite. Effect of pH and organic substances. Water Res 37(7):1619–1627

Ackerman AH, Pa C, Parks AN, Fricke MW, Ca S, Creed JT, Heitkemper DT, Vela NP (2005) Comparison of a chemical and enzymatic extraction of arsenic from rice and an assessment of the arsenic absorption from contaminated water by cooked rice. Environ Sci Technol 39:5241–5246

Acosta JA, Arocena JM, Faz A (2015) Speciation of arsenic in bulk and rhizosphere soils from artisanal cooperative mines in Bolivia. Chemosphere. doi:10.1016/j.chemosphere.2014.12.050

Adra A, Morin G, Ona-Nguema G, Brest J (2015) Arsenate and arsenite adsorption onto Al-containing ferrihydrites. Implications for arsenic immobilization after neutralization of acid mine drainage. Appl Geochem 9:1–8

Adriano DC (2001) Trace elements in terrestrial environments. Biogeochemistry, bioavailability and risks of metals. Springer, New York, vol 32, p 374

Ahmed ZU, Panaullah GM, Gauch H, McCouch SR, Tyagi W, Kabir MS, Duxbury JM (2011) Genotype and environment effects on rice (*Oryza sativa L.*) grain arsenic concentration in Bangladesh. Plant and Soil 338:367–382

Akins MB, Lewis RJ (1976) Chemical distribution and gaseous evolution of arsenic-74 added to soils as DSMA-74As1. Soil Sci Soc Am 40(5):655–658

Ali M, Tarafdar SA (2003) Arsenic in drinking water and in scalp hair by EDXRF: a major recent health hazard in Bangladesh. J Radioanal Nucl Chem 256:297–305

Amstaetter K, Borch T, Larese-Casanova P, Kappler A (2010) Redox transformation of arsenic by Fe(II)-activated goethite (α-FeOOH). Environ Sci Technol 44(1):102–108

Anup KC, Kalu S (2015) Soil pollution status and its remediation in Nepal. In: Hakeem K, Sabir M, Ozturk M, Murmet A (eds), Soil remediation and plants: prospects and challenges, Boston, Elsevier, ISBN:978–0–12-799,937-1, pp. 313–329

Anwar T, Ahmad I, Tahir S (2013) reporting pesticide residues in soil of Lodhran district, Punjab, Pakistan. Intl J Biol Res 1(2):143–147

Arshad M, Silvestre J, Pinelli E, Kallerhoff J, Kaemmerer M, Tarigo A, Shahid M, Guiresse M, Pradere P, Dumat C (2008) A field study of lead phytoextraction by various scented *Pelargonium* cultivars. Chemosphere 71:2187–2192

Atkinson CJ, Fitzgerald JD, Na H (2010) Potential mechanisms for achieving agricultural benefits from biochar application to temperate soils: a review. Plant and Soil 337(1):1–18

ATSDR: Agency for Toxic Substances and Disease Registry (2013) http://www.atsdr.cdc.gov/substances/toxsubstance.asp?toxid=3

Austruy A, Wanat N, Moussard C, Vernay P, Joussein E, Ledoigt G, Hitmi A (2013) Physiological impacts of soil pollution and arsenic uptake in three plant species: *Agrostis capillaris*, *Solanum nigrum* and *Vicia faba*. Ecotoxicol Environ Saf 90:28–34

Austruy A, Shahid M, Xiong T, Castrec M, Payre V, Niazi NK, Sabir M, Dumat C (2014) Mechanisms of metal-phosphates formation in the rhizosphere soils of pea and tomato: environmental and sanitary consequences. J Soil Sediment 14:666–678

Aydin D, Coskun OF (2013) Comparison of EDTA-enhanced phytoextraction strategies with *Nasturtium officinale* (Watercress) on an artificially arsenic contaminated water. Pak J Bot 45(4):1423–1429

Bagherifam S, Komarneni S, Lakzian A, Fotovat A, Khorasani R, Huang W, Ma J, Wang Y (2014a) Evaluation of Zn-Al-SO_4 layered double hydroxide for the removal of arsenite and arsenate from a simulated soil solution: isotherms and kinetics. Appl Clay Sci 95:119–125

Bagherifam S, Lakzian A, Fotovat A, Khorasani R, Komarneni S (2014b) *In situ* stabilization of As and Sb with naturally occurring Mn, Al and Fe oxides in a calcareous soil: bioaccessibility, bioavailability and speciation studies. J Hazard Mater 273:247–252

Bahar MM, Megharaj M, Naidu R (2012) Arsenic bioremediation potential of a new arsenite-oxidizing bacterium *Stenotrophomonas* sp. MM-7 isolated from soil. Biodegradation 23 (6):803–812

Bai J, Lin X, Yin R, Zhang H, Junhua W, Xueming C, Yongming L (2008) The influence of arbuscular mycorrhizal fungi on As and P uptake by maize (*Zea mays L.*) from As-contaminated soils. Appl Soil Ecol 38:137–145

Barceló J, Poschenrieder C (2003) Phytoremediation : principles and perspectives. Contrib to Sci Inst d'Estudis Catalans, Barcelona 2(3):333–344

Beesley L, Marmiroli M (2011) The immobilisation and retention of soluble arsenic, cadmium and zinc by biochar. Environ Pollut 159(2):474–480

Beesley L, Moreno-Jiménez E, Gomez-Eyles JL, Moreno-Jimenez E (2010) Effects of biochar and greenwaste compost amendments on mobility, bioavailability and toxicity of inorganic and organic contaminants in a multi-element polluted soil. Environ Pollut 158(6):2282–2287

Beesley L, Marmiroli M, Pagano L, Pigoni V, Fellet G, Fresno T, Vamerali T, Bandiera M, Marmiroli N (2013) Biochar addition to an arsenic contaminated soil increases arsenic concentrations in the pore water but reduces uptake to tomato plants (*Solanum lycopersicum* L.) Sci Total Environ 454–455:598–603

Beesley L, Inneh OS, Norton GJ, Moreno-Jimenez E, Pardo T, Clemente R, Dawson JJC (2014) Assessing the influence of compost and biochar amendments on the mobility and toxicity of metals and arsenic in a naturally contaminated mine soil. Environ Pollut 186:195–202

Belogolova GA, Sokolova MG, Gordeeva ON, Vaishlya OB (2015) Speciation of arsenic and its accumulation by plants from rhizosphere soils under the influence of *Azotobacter* and *Bacillus* bacteria. J Geochem Explor 149:52–58

Bennett WW, Teasdale PR, Welsh DT, Panther JG, Stewart RR, Price HL, Jolley DF (2012) Inorganic arsenic and iron(II) distributions in sediment porewaters investigated by a combined DGTcolourimetric DET technique. Environ Chem 9(1):31–40

Bergqvist C, Herbert R, Persson I, Greger M (2014) Plants influence on arsenic availability and speciation in the rhizosphere, roots and shoots of three different vegetables. Environ Pollut 184:540–546

Bhattacharya P, Samal C, Majumdar J, Santra SC (2010) Arsenic contamination in rice, wheat, pulses, and vegetables: a study in an arsenic affected area of West Bengal, India. Water Air Soil Pollut 213:3–13

Bibi I, Icenhower J, Niazi NK, Naz T, Shahid M, Bashir S (2016) Clay minerals: structure, chemistry and significance in contaminated environments and geological CO_2 sequestration.

In: Prasad MNV, Shih K (eds) Environmental materials and waste: resource recovery and pollution prevention. Elsevier Inc., Boston, pp 543–567

Bissen M, Frimmel FH (2003) Arsenic – a review. Part I: occurrence, toxicity, speciation, mobility. Acta Hydrochim Hydrobiol 31(1):9–18

Biswas A, Gustafsson JP, Neidhardt H, Halder D, Kundu AK, Chatterjee D, Berner Z, Bhattacharya P (2014) Role of competing ions in the mobilization ofarsenic in groundwater of Bengal Basin: insight from surface complexation modeling. Water Res 55:30–39

Bolan N, Kunhikrishnan A, Thangarajan R, Kumpiene J, Park J, Makino T, Kirkham MB, Scheckel K (2014) Remediation of heavy metal(loid)s contaminated soils – to mobilize or to immobilize? J Hazard Mater 266:141–166

Bothe JV, Brown PW (1999) Arsenic immobilization by calcium arsenate formation. Environ Sci Technol 33(21):3806–3811

Brammer H, Ravenscroft P (2009) Arsenic in groundwater: a threat to sustainable agriculture in South and South-east Asia. Environ Int 35(3):647–654

Bundschuh J, Litterd MI, Parvezg F, Román-Rossh G, Nicollii HB, Jeanc JS, Liuj CW, Lópezk D, Armiental MA, Guilhermem LRG, Cuevasn AG, Cornejoo L, Cumbalq L, Toujaguez R (2012) One century of arsenic exposure in Latin America: a review of history and occurrence from 14 countries. Sci Total Environ 429:2–35

Bustos V, Mondaca P, Verdejo J, Sauvé S, Gaete H, Celis-Diez JL, Neaman A (2015) Thresholds of arsenic toxicity to Eisenia fetida in field-collected agricultural soils exposed to copper mining activities in Chile. Ecotoxicol Environ Saf 122:448–454

Buzek F, Cejkova B, Dousova B, Jackova I, Kadlecova R, Lnenickova F (2013) Mobilization of arsenic from acid deposition – the Elbe River catchment, Czech Republic. Appl Geochem 33:281–293

Cai L, Xu Z, Bao P, He M, Dou L, Chen L et al (2015) Multivariate and geostatistical analyses of the spatial distribution and source of arsenic and heavy metals in the agricultural soils in Shunde, Southeast China. J Geochem Explor 148:189–195

Cao X, Ma LQ, Shiralipour A (2003) Effects of compost and phosphate amendments on arsenic mobility in soils and arsenic uptake by the hyperaccumulator, *Pteris vittata L*. Environ Pollut 126(2):157–167

Carbonell-Barrachina AA, Jugsujinda A, Burlo F, Delaune RD, Patrick WH (2000) Arsenic chemistry in municipal sewage sludge as affected by redox potential and pH. Water Res 34 (1):216–224

Chakraborti D, Rahman MMM, Das B, Murrill M, Dey S, Chandra Mukherjee S et al (2010) Status of groundwater arsenic contamination in Bangladesh: a 14-year study report. Water Res 44 (19):5789–5802

Chandraprabha MN, Natarajan KA (2011) Mechanism of arsenic tolerance and bioremoval of arsenic by *Acidithiobacilus ferrooxidans*. J Biochem Technol 3(2):257–265

Chen ML, Ma LY, Chen XW (2014) New procedures for arsenic speciation: a review. Talanta 125:78–86

Chilvers DC, Peterson PJ (1987) Lead, mercury, cadmium and arsenic in the environment. Global Cycling Arsenic 1:279–301

Chiu KK, Ye ZH, Wong MH (2005) Enhanced uptake of As, Zn, and Cu by *Vetiveria zizanioides* and *Zea mays* using chelating agents. Chemosphere 60:1365–1375

Chuan-ping L, Chun-ling L, Xiang-hua X, Chuang-an W, Fang-Bai L, Gan Z (2012) Effects of calcium peroxide on arsenic uptake by celery (*Apium graveolens* L.) grown in arsenic contaminated soil. Chemosphere 86:1106–1111

Cobb GP, Sands K, Waters M, Wixson BG, Dorward-King E (2000) Accumulation of heavy metals by vegetables grown in mine wastes. Environ Toxicol Chem 19(3):600–607

Corsini A, Cavalca L, Crippa L, Zaccheo P, Andreoni V (2010) Impact of glucose on microbial community of a soil containing pyrite cinders: role of bacteria in arsenic mobilization under submerged condition. Soil Biol Biochem 42(5):699–707

Corwin DL, David A, Goldberg S (1999) Mobility of arsenic in soil from the Rocky mountain arsenal area. J Contam Hydrol 39(1–2):35–58

Cutler WG, Brewer RC, El-Kadi A, Hue NV, Niemeyer PG, Peard J, Ray C (2013) Bioaccessible arsenic in soils of former sugar cane plantations, Island of Hawaii. Sci Total Environ 442:177–188

Cutler WG, El-Kadi A, Hue NV, Peard J, Scheckel K, Ray C (2014) Iron amendments to reduce bioaccessible arsenic. J Hazard Mater 279:554–561

Dahal BM, Fuerhacker M, Mentler A, Karki KB, Shrestha RR, Blum WEH (2008) Arsenic contamination of soils and agricultural plants through irrigation water in Nepal. Environ Pollut 155(1):157–163

De Gregori I, Fuentes E, Olivares D, Pinochet H (2004) Extractable copper, arsenic and antimony by EDTA solution from agricultural Chilean soils and its transfer to alfalfa plants (*Medicago sativa L.*) J Environ Monit 6(1):38–47

De La Calle MB, Baer I, Robouch P, Cordeiro F, Emteborg H, Baxter MJ, Brereton N, Raber G, Velez D, Devesa V, Rubio R, Llorente-Mirandes T, Raab A, Feldmann J, Sloth JJ, Rasmussen RR, D'Amato M, Cubadda F (2012) Is it possible to agree on a value for inorganic arsenic in food? The outcome of IMEP-112. Anal Bioanal Chem 404(8):2475–2488

Dickens R, Hiltbold AE (1967) Movement and persistence of methanearsonates in soil. Weeds 5:299–304

Doušová B, Fuitová L, Grygar T, Machovic V, Kolousek D, Herzogová L, Lhotka M (2009) Modified aluminosilicates as low-cost sorbents of As(III) from anoxic groundwater. J Hazard Mater 165:134–140

Doušová B, Lhotka M, Grygar T, Machovic V, Herzogová L (2011) *In situ* co-adsorption of arsenic and iron/manganese ions on raw clays. Appl Clay Sci 54(2):166–171

Dousova B, Buzek F, Rothwell J, Krejcova S, Lhotka M (2012) Adsorption behavior of arsenic relating to different natural solids: soils, stream sediments and peats. Sci Total Environ 433:456–461

Elliott HA, Shastri NL (1999) Extractive decontamination of metal-polluted soils using oxalate. Water Air Soil Pollut 110(3–4):335–346

Epstein RA (2009) Simple rules for a complex world. Harvard University Press, Massachusetts, United States

Fakour H, Lin TF (2014) Experimental determination and modeling of arsenic complexation with humic and fulvic acids. J Hazard Mater 279:569–578

Fayiga AO, Ma LQ, Zhou Q (2007) Effects of plant arsenic uptake and heavy metals on arsenic distribution in an arsenic-contaminated soil. Environ Pollut 147(3):737–742

Feng Q, Zhang Z, Chen Y, Liu L, Zhang Z, Chen C (2013) Adsorption and desorption characteristics of arsenic on soils: kinetics, equilibrium, and effect of $Fe(OH)_3$ colloid, H_2SiO_3 colloid and phosphate. Procedia Environ Sci 18(86):26–36

Fitamo D, Itana F, Olsson M (2007) Total contents and sequential extraction of heavy metals in soils irrigated with wastewater, Akaki, Ethiopia. Environ Manag 39(2):178–193

Fleck AT, Nye T, Repenning C, Stahl F, Zahn M, Schenk MK (2011) Silicon enhances suberization and lignification in roots of rice (*Oryza sativa*). J Exp Bot 62:2001–2011

Foucault Y, Lévêque T, Xiong T, Schreck E, Austruy A, Shahid M, Dumat C (2013) Green manure plants for remediation of soils polluted by metals and metalloids: ecotoxicity and human bioavailability assessment. Chemosphere 93(7):1430–1435

Francesconi KA (2002) Applications of liquid chromatography-electrospray ionization-single quadrupole mass spectrometry for determining arsenic compounds in biological samples. Appl Organomet Chem 16(8):437–445

Fu Y, Chen M, Bi X, He Y, Ren L, Xiang W, Qiao S, Yan S, Li Z, Ma Z (2011) Occurrence of arsenic in brown rice and its relationship to soil properties from Hainan Island, China. Environ Pollut 159:1757–1762

Fuessle RW, Taylor MA (2004) Stabilization of arsenite wastes with prior oxidation. J Environ Engg 130(9):1063–1066

Garau G, Silvetti M, Castaldi P, Mele E, Deiana P, Deiana S (2014) Stabilising metal(loid)s in soil with iron and aluminium-based products: microbial, biochemical and plant growth impact. J Environ Manage 139:146–153

Ghosh P, Rathinasabapathi B, Teplitski M, Ma LQ (2015) Bacterial ability in AsIII oxidation and AsV reduction: relation to arsenic tolerance, P uptake, and siderophore production. Chemosphere. doi:10.1016/j.chemosphere.2014.12.046

Ghosh-Dastidar A, Mahuli SK, Agnihotri R, Fan L (1996) Investigation of high-reactivity calcium carbonate sorbent for enhanced SO_2 capture. Indus Engg Chem Res 35:598–606

Girouard E, Zagury GJ (2009) Arsenic bioaccessibility in CCA-contaminated soils: influence of soil properties, arsenic fractionation, and particle-size fraction. Sci Total Environ 407 (8):2576–2585

Goldberg ED (1954) Marine geochemistry. Chemical scavengers of the sea. J Geol 62:249–265

Goldberg S, Johnston CT (2001) Mechanisms of arsenic adsorption on amorphous oxides evaluated using macroscopic measurements, vibrational spectroscopy, and surface complexation modeling. J Colloid Interface Sci 234:204–216

Gonzaga MIS, Santos JAG, Ma LQ (2006) Arsenic chemistry in the rhizosphere of *Pteris vittata* L. and *Nephrolepis exaltata* L. Environ Pollut 143:254–260

Gonzaga MIS, Santos JAG, Ma LQ (2008) Phytoextraction by arsenic hyperaccumulator *Pteris vittata* L. from six arsenic-contaminated soils: repeated harvests and arsenic redistribution. Environ Pollut 154(2):212–218

Gonzaga MIS, Ma LQ, Santos JAG, MIS M (2009) Rhizosphere characteristics of two arsenic hyperaccumulating *Pteris* ferns. Sci Total Environ 407(16):4711–4716

Gonzaga MIS, Ma LQ, Pacheco EP, dos Santos WM (2012) Predicting arsenic bioavailability to hyperaccumulator *Pteris vittata* in arsenic-contaminated soils. Int J Phytoremediation 14 (10):939–949

Gorny J, Billon G, Lesven L, Dumoulin D, Madé B, Noiriel C (2015) Arsenic behavior in river sediments under redox gradient: a review. Sci Total Environ 505:423–434

Grafe M, Eick MJ, Grossl PR (2001) Adsorption of arsenate (V) and arsenite (III) on goethite in the presence and absence of dissolved organic carbon. Soil Sci Soc Am J 65(6):1680

Grafe M, Eick MJ, Grossl PR, Saunders AM (2002) Adsorption of arsenate and arsenite on ferrihydrite in the presence and absence of dissolved organic carbon. J Environ Qual 31:1115–1123

Gregory SJ, Anderson CWN, Camps Arbestain M, McManus MT (2014) Response of plant and soil microbes to biochar amendment of an arsenic-contaminated soil. Agric Ecosyst Environ 191:133–141

Griffin RA, Shimp NF (1978) Attenuation of pollutants in municipal landfill leachate by clay minerals: US Environmental Protection Agency, Cincinnati, Ohio. EPA-600/2–78-1570H

Grisafe DA, Hummel FA (1970) Pentavalent ion substitutions in the apatite structure part B. Color J Solid State Chem 2:167–175

Gulz PA, Gupta SK, Schulin R (2005) Arsenic accumulation of common plants from contaminated soils. Plant and Soil 272(1–2):337–347

Hansel CM, Fendorf S, Sutton S, Newville M (2001) Characterization of Fe plaque and associated metals on the roots of mine-waste impacted aquatic plants. Environ Sci Technol 35 (19):3863–3868

Hartley W, Dickinson NM, Riby P, Lepp NW (2009) Arsenic mobility in brownfield soils amended with green waste compost or biochar and planted with *Miscanthus*. Environ Pollut 157(10):2654–2662

Hassan F, Abdel-Mohsen M, Elhadidy H (2014) Adsorption of arsenic by activated carbon, calcium alginate and their composite beads. Int J Biol Macromol 68:125–130

Henke KR (2009) Arsenic: environmental chemistry, health threats and waste treatment. Hoboken, Wiley, pp. 1–569

Hinsinger P, Courchesne F (2008) Biogeochemistry of metals and metalloids at the soil-root interface. Wiley-IUPAC Ser Biophys Process Environ Syst 267–311

Hossain MA, Cho JI, Han M, Ahn CH, Jeon JS, An G, Park PB (2010) The ABRE-binding bZIP transcription factor OsABF2 is a positive regulator of abiotic stress and ABA signaling in rice. J Plant Physiol 167:1512–1520

Hua J, Jiang Q, Bai J, Ding F, Lin X, Yin Y (2014) Interactions between arbuscular mycorrhizal fungi and fungivorous nematodes on the growth and arsenic uptake of tobacco in arsenic-contaminated soils. Appl Soil Ecol 84:176–184

Huang JH, Matzner E (2006) Dynamics of organic and inorganic arsenic in the solution phase of an acidic fen in Germany. Geochim Cosmochim Acta 70(8):2023–2033

Janoš P, Vavrova J, Herzogova L, Pilarova V, Jano P, Vávrová J, Harzogová L (2010) Effects of inorganic and organic amendments on the mobility (Leachability) of heavy metals in contaminated soil: a sequential extraction study. Geoderma 159(3–4):335–341

Jia Y, Guo H, Jiang Y, Wu Y, Zhou Y (2014) Hydrogeochemical zonation and its implication for arsenic mobilization in deep groundwaters near alluvial fans in the Hetao Basin, Inner Mongolia. J Hydrol 518:410–420

Jiang JP, Yuan XB, Ye LL, Liao SC, Zhang XH (2013) Characteristics of straw biochar and its influence on the forms of arsenic in heavy metal polluted soil. Appl Mech Mater 409:133–138

Jiang Y, Zeng X, Fan X, Chao S, Zhu M, Cao H (2015) Levels of arsenic pollution in daily foodstuffs and soils and its associated human health risk in a town in Jiangsu Province, China. Ecotoxicol Environ Saf 122:198–204

Jones DL, Murphy DV, Khalid M, Ahmad W, Edwards-Jones G, DeLuca TH (2011) Short-term biochar-induced increase in soil CO_2 release is both biotically and abiotically mediated. Soil Biol Biochem 43(8):1723–1731

Jones DL, Rousk J, Edwards-Jones G, DeLuca TH, Murphy DV (2012) Biochar-mediated changes in soil quality and plant growth in a three year field trial. Soil Biol Biochem 45:113–124

Joseph SD, Camps-Arbestain M, Lin Y, Munroe P, Chia CH, Hook J, Van Zwieten L, Kimber S, Cowie A, Singh BP, Lehmann J, Foidl N, Smernik RJ, Amonette JE (2010) An investigation into the reactions of biochar in soil. Aust J Soil Res 48(6–7):501–515

Joseph T, Dubey B, Ea MB (2015) A critical review of arsenic exposures for Bangladeshi adults. Sci Total Environ 527–528:540–551

Juillot F, Ildefonse P, Morin G, Calas G, Kersabiec aMDe, Benedetti M (1999) Remobilization of arsenic from buried wastes at an industrial site: mineralogical and geochemical control. Appl Geochem 14:1031–1048

Kabata-Pendias A, Mukherjee AB (2007) Trace elements from soil to human. Springer Science & Business Media

Kabata-Pendias A, Pendias K (1989) Mikroelementy v pochvakh i rasteniyakh (Microelements in Soils and Plants). Mir, Moscow, Netherlands, pp 183–184

Kalia K, Joshi DN (2009) Detoxification of arsenic. Handbook of toxicology of chemical warfare agents. Elsevier, Amsterdam, Netherlands, pp 1083–1100

Kaplan DI, Knox AS (2004) Enhanced contaminant desorption induced by phosphate mineral additions to sediment. Environ Sci Technol 38(11):3153–3160

Karczewska A, Lewinska K, Galka B (2013) Arsenic extractability and uptake by velvetgrass *Holcus lanatus* and ryegrass *Lolium perenne* in variously treated soils polluted by tailing spills. J Hazard Mater 262:1014–1021

Khalid S, Shahid M, Niazi NK, Murtaza B, Bibi I, Dumat C (2017) A comparison of technologies for remediation of heavy metal contaminated soils. J Geochem Explor. doi:10.1016/j.gexplo.2016.11.021

Khan MA, Islam MR, Panaullah GM, Duxbury JM, Jahiruddin M, Loeppert RH (2009) Fate of irrigation-water arsenic in rice soils of Bangladesh. Plant and Soil 322(1):263–277

Kirkham MB (2006) Cadmium in plants on polluted soils: effects of soil factors, hyperaccumulation, and amendments. Geoderma 137(1–2):19–32

Ko MS, Kim JY, Park HS, Kim KW (2015) Field assessment of arsenic immobilization in soil amended with iron rich acid mine drainage sludge. J Clean Prod 108:1073–1080

Kocar BD, Herbel MJ, Tufano KJ, Fendorf S (2006) Contrasting effects of dissimilatory iron (III) and arsenic (V) reduction on arsenic retention and transport. Environ Sci Technol 40 (21):6715–6721

Kulp TR, Han S, Saltikov CW, Lanoil BD, Zargar K, Oremland RS (2007) Effects of imposed salinity gradients on dissimilatory arsenate reduction, sulfate reduction, and other microbial processes in sediments from two California soda lakes. Appl Environ Microbiol 73 (16):5130–5137

Kumpiene J, Castillo Montesinos I, Lagerkvist A, Maurice C (2007) Evaluation of the critical factors controlling stability of chromium, copper, arsenic and zinc in iron-treated soil. Chemosphere 67(2):410–417

Kuppardt A, Vetterlein D, Harms H, Chatzinotas A (2010) Visualisation of gradients in arsenic concentrations around individual roots of *Zea mays L.* using agar-immobilized bioreporter bacteria. Plant and Soil 329(1):295–306

Kwon JC, Lee JS, Jung MC (2012) Arsenic contamination in agricultural soils surrounding mining sites in relation to geology and mineralization types. Appl Geochem 27(5):1020–1026

Laird DA, Fleming P, Davis DD, Horton R, Wang B, Karlen DL (2010) Impact of biochar amendments on the quality of a typical Midwestern agricultural soil. Geoderma 158 (3–4):443–449

Langner P, Mikutta C, Kretzschmar R (2011) Arsenic sequestration by organic sulphur in peat. Nat Geosci 5(1):66–73

LeBlanc MS, McKinney EC, Meagher RB, Smith AP (2013) Hijacking membrane transporters for arsenic phytoextraction. J Biotechnol 163(1):1–9

Lehmann J, Joseph S (2009) Biochar systems. Biochar for Environmental Management, Science and Technology, pp 147–181

Lehmann J, Rillig MC, Thies J, Masiello CA, Hockaday WC, Crowley D (2011) Biochar effects on soil biota – a review. Soil Biol Biochem 43(9):1812–1836

Lei M, Wan XM, Huang ZC, Chen TB, Li XW, Liu YR (2012) First evidence on different transportation modes of arsenic and phosphorus in arsenic hyperaccumulator *Pteris vittata*. Environ Pollut 161:1–7

Leleyter L, Rousseau C, Biree L, Baraud F (2012) Comparison of EDTA, HCl and sequential extraction procedures, for selected metals (Cu, Mn, Pb, Zn), in soils, riverine and marine sediments. J Geochem Explor 116–117(3):51–59

Lenoble V, Omanović D, Garnier C, Mounier S, Donlagić N, Le Poupon C, Pižeta I (2013) Distribution and chemical speciation of arsenic and heavy metals in highly contaminated waters used for health care purposes (Srebrenica, Bosnia and Herzegovina). Sci Total Environ 443:420–428

Li X, Cai W, An J, Kim S, Nah J, Yang D, Piner R, Velamakanni A, Jung I, Tutuc E, Banerjee SK, Colombo L, Ruoff RS (2009) Large-area synthesis of high-quality and uniform graphene films on copper foils. Sci Total Environ 324(5932):1312–1314

Li Y, Liu Z, Li Q, Zhao Z, Liu Z, Zeng L, Li L (2011) Removal of arsenic from arsenate complex contained in secondary zinc oxide. Hydrometallurgy 109(3–4):237–244

Li H-B, Li J, Zhu Y-G, Juhasz AL, Ma LQ (2015) Comparison of arsenic bioaccessibility in house dust and contaminated soils based on four in vitro assays. Sci Total Environ 532:803–811

Liang Y, Zhang W, Chen Q, Liu Y, Ding R (2006) Effect of exogenous silicon (Si) on H^+ -ATPase activity, phospholipids and fluidity of plasma membrane in leaves of salt-stressed barley (*Hordeum vulgare L.*) Environ Exp Bot 57:212–219

Liang Y, Sun W, Zhu YG, Christie P (2007) Mechanisms of silicon-mediated alleviation of abiotic stresses in higher plants: a review. Environ Pollut 147(2):422–428

Liang Y, Van Nostrand JD, Deng Y, He Z, Wu L, Zhang X, Li G, Zhou J (2011) Functional gene diversity of soil microbial communities from five oil-contaminated fields in China. ISME J 5 (3):403–413

Liang S, Luo J, Ma LQ (2014) Arsenic enhanced plant growth and altered rhizosphere characteristics of hyperaccumulator *Pteris vittata*. Environ Pollut 194:105–111

Lin Z, Puls RW (2000) Adsorption, desorption and oxidation of arsenic affected by clay minerals and aging process. Environ Geol 39(7):753–759
Lin HT, Wang MC, Seshaiah K (2008) Mobility of adsorbed arsenic in two calcareous soils as influenced by water extract of compost. Chemosphere 71:742–749
Liu R, Yang C, Li S, Sun P, Shen S, Li Z, Liu K (2014) Arsenic mobility in the arsenic-contaminated Yangzonghai Lake in China. Ecotoxicol Environ Saf 107:321–327
Liu X, Zhang W, Hu Y, Hu E, Xie X, Wang L, Cheng H (2015) Arsenic pollution of agricultural soils by concentrated animal feeding operations (CAFOs). Chemosphere 119:273–281
Llorente-Mirandes T, Barbero M, Rubio R, Lopez-Sanchez JF (2014) Occurrence of inorganic arsenic in edible Shiitake (*Lentinula edodes*) products. Food Chem 158:207–215
Lockwood CL, Mortimer RJG, Stewart DI, Mayes WM, Peacock CL, Polya DA, Lythgoe PR, Lehoux AP, Gruiz K, Burke IT (2014) Mobilisation of arsenic from bauxite residue (red mud) affected soils: effect of pH and redox conditions. Appl Geochem 51:268–277
Lucchini P, Quilliam RS, DeLuca TH, Vamerali T, Jones DL (2014) Does biochar application alter heavy metal dynamics in agricultural soil? Agric Ecosyst Environ 184:149–157
Madejón P, Lepp NW (2007) Arsenic in soils and plants of woodland regenerated on an arsenic-contaminated substrate: a sustainable natural remediation? Sci Total Environ 379 (2–3):256–262
MAFF (1993) Code of good practice for the protection of soil. Ministry of Agriculture, Fisheries and Food, London
Mahimairaja S, Bolan NS, Adriano DC, Robinson B (2005) Arsenic contamination and its risk management in complex environmental settings. Adv Agron 86:1–82
Mäkelä-Kurtto R, Eurola M, Justén A, Backman B, Luoma S, Karttunen V, Ruskeeniemi T (2007) Arsenic and other elements in agro-ecosystems in Finland and particularly in the Pirkanmaa region, pp 1–121
Malandrino M, Abollino O, Buoso S, Giacomino A, La Gioia C, Mentasti E (2011) Accumulation of heavy metals from contaminated soil to plants and evaluation of soil remediation by vermiculite. Chemosphere 82(2):169–178
Mallick S, Sinam G, Sinha S (2011) Study on arsenate tolerant and sensitive cultivars of *Zea mays* L.: differential detoxification mechanism and effect on nutrients status. Ecotoxicol Environ Saf 74(5):1316–1324
Marabottini R, Stazi SR, Papp R, Grego S, Moscatelli MC (2013) Mobility and distribution of arsenic in contaminated mine soils and its effects on the microbial pool. Ecotoxicol Environ Saf 96:147–153
Martínez-Sánchez MJ, Martínez-López S, García-Lorenzo ML, Martínez-Martínez LB, Pérez-Sirvent C (2011) Evaluation of arsenic in soils and plant uptake using various chemical extraction methods in soils affected by old mining activities. Geoderma 160(3–4):535–541
Marwa EMM, Meharg AA, Rice CM (2012) Risk assessment of potentially toxic elements in agricultural soils and maize tissues from selected districts in Tanzania. Sci Total Environ 416:180–186
Matsumoto S, Kasuga J, Taiki N, Makino T, Arao T (2015) Inhibition of arsenic accumulation in Japanese rice by the application of iron and silicate materials. Catena 135:328–335
McBride MB (1994) Environmental chemistry of soils. Oxford University Press, Oxford, UK
McCauley A, Jones C, Jacobsen J (2009) Soil pH and organic matter. Nutrient Management Module 8. Montana State University. Available from http://landresources.montana.edu/NM/Modules/Module8.pdf
Meharg AA, Hartley-Whitaker J (2002) Arsenic uptake and metabolism in arsenic resistant and nonresistant plant species. New Phytol 154(1):29–43
Meharg AA, Macnair MR (1990) An altered phosphate uptake system in arsenate-tolerant *Holcus lanatus* L. New Phytol 116(1):29–35
Meharg AA, MacNair MR (1992) Genetic correlation between arsenate tolerance and the rate of influx of arsenate and phosphate in *Holcus lanatus*. Heredity 69(4):336–341

Merry RH, Tiller KG, Alston AM (1983) Accumulation of copper, lead and arsenic in some Australian orchard soils. Soil Res 21(4):549–561

MHC (2005) Maximum levels of contaminants in foods, GB 2762–2005. Ministry of Health of China, Beijing

Mitani-Ueno N, Yamaji N, Zhao FJ, Ma JF (2011) The aromatic/arginine selectivity filter of NIP aquaporins plays a critical role in substrate selectivity for silicon, boron, and arsenic. J Exp Bot 62(12):4391–4398

Mombo S, Foucault Y, Deola F, Gaillard I, Goix S, Shahid M, Schreck E, Pierart A, Dumat C (2015) Management of human health risk in the context of kitchen gardens polluted by lead and cadmium near a lead recycling company. J Soil Sediment. doi:10.1007/s11368–015–1069-7

Moon DH, Dermatas D, Menounou N (2004) Arsenic immobilization by calcium-arsenic precipitates in lime treated soils. Sci Total Environ 330(1–3):171–185

Moreno-Jiménez E, Clemente R, Mestrot A, Meharg A (2013) Arsenic and selenium mobilisation from organic matter treated mine spoil with and without inorganic fertilisation. Environ Pollut 173:238–244

Mucha AP, Almeida CMR, Aa B, Vasconcelos MTSD (2010) LMWOA (low molecular weight organic acid) exudation by salt marsh plants: natural variation and response to Cu contamination. Estuar Coast Shelf Sci 88(1):63–70

Mühlbachová G (2009) Microbial biomass dynamics after addition of EDTA into heavy metal contaminated soils. Plant Soil Environ 55(12):544–550

Mühlbachová G (2011) Soil microbial activities and heavy metal mobility in long-term contaminated soils after addition of EDTA and EDDS. Ecol Eng 37(7):1064–1071

Nabulo G, Black CR, Craigon J, Young SD (2012) Does consumption of leafy vegetables grown in peri-urban agriculture pose a risk to human health? Environ Pollut 162:389–398

Namgay T, Singh B, Singh BP (2010) Influence of biochar application to soil on the availability of As, Cd, Cu, Pb, and Zn to maize (*Zea mays L.*) Soil Res 48(7):638–647

Naujokas MF, Anderson B, Ahsan H, Vasken Aposhian H, Graziano JH, Thompson C, Suk WA (2013) The broad scope of health effects from chronic arsenic exposure: update on a worldwide public health problem. Environ Health Perspect 121(3):295–302

Nearing MM, Koch I, Reimer KJ (2014) Complementary arsenic speciation methods: a review. Spectrochim Acta – Part B At Spectrosc 99:150–162

Neidhardt H, Norra S, Tang X, Guo H, Stüben D (2012) Impact of irrigation with high arsenic burdened groundwater on the soil-plant system: results from a case study in the Inner Mongolia, China. Environ Pollut 163:8–13

Neidhardt H, Kramar U, Tang X, Guo H, Norra S (2015) Arsenic accumulation in the roots of *Helianthus annuus* and *Zea mays* by irrigation with arsenic-rich groundwater: insights from synchrotron X-ray fluorescence imaging. Chemie der Erde-Geochemistry

Neupane G, Donahoe RJ (2012) Attenuation of trace elements in coal fly ash leachates by surfactant-modified zeolite. J Hazard Mater 229–230:201–208

Neupane G, Donahoe RJ (2013) Calcium-phosphate treatment of contaminated soil for arsenic immobilization. Appl Geochem 28:145–154

Newman MC, Jagoe CH (1994) Ligands and the bioavailability of metals in aquatic environments. In: Hamelink JL, Landrum PF, Bergman HL, Benson WH (eds) Bioavailability: physical, chemical, and biological interactions. CRC Press, Boca Raton, pp 39–62

Ng JC (2005) Environmental contamination of arsenic and its toxicological impact on humans. Environ Chem 2(3):146–160

Niazi NK, Singh B, Van Zwieten L, Kachenko AG (2011) Phytoremediation potential of *Pityrogramma calomelanos var. austroamericana* and *Pteris vittata* L. grown at a highly variable arsenic contaminated site. Int J Phytoremediation 13(9):912–932

Niazi NK, Singh B, Van Zwieten L, Kachenko AG (2012) Phytoremediation of an arsenic-contaminated site using *Pteris vittata* L. and *Pityrogramma calomelanos var. austroamericana*: a long-term study. Environ Sci Pollut Res 19(8):3506–3515

Niazi NK, Singh B, Minasny B (2015) Mid-infrared spectroscopy and partial least-squares regression to estimate soil arsenic at a highly variable arsenic-contaminated site. Intl J Environ Sci Tech 12(6):1965–1974

Niazi NK, Murtaza B, Bibi I, Shahid M, White JC, Nawaz MK, Bashir S, Murtaza G (2016) Removal and recovery of metals by biosorbents and biochars derived from biowastes. In: MNV P, Shih K (eds) Environmental materials and waste: resource recovery and pollution prevention. Elsevier, San Diego. doi:10.1016/B978–0–12-803,837-6.00007-X

NJDEP (2006) New Jersey Department of Environmental Protection. http://www.nj.gov/health/epht/arsenic.shtml

Northup A, Cassidy D (2008) Calcium peroxide (CaO2) for use in modified Fenton chemistry. J Hazard Mater 152(3):1164–1170

Nriagu JO, Bhattacharya P, Mukherjee AB, Bundschuh J, Zevenhoven R, Loeppert RH (2007) Arsenic in soil and groundwater: an overview. Trace Metals Contam Environ 9:3–60

Nussaume L, Kanno S, Javot H, Marin E, Pochon N, Ayadi A, Nakanishi TM, Thibaud MC (2011) Phosphate import in plants: focus on the PHT1 transporters. Front Plant Sci 2:83. doi:10.3389/fpls.2011.00083

O'Neill P (1995) Arsenic. In: Alloway BJ (ed) Heavy metals in soils, Blackie, NewYork, vol 2. pp 105–121

O'Reilly J, Watts MJ, Shaw RA, Marcilla AL, Ward NI (2010) Arsenic contamination of natural waters in San Juan and La Pampa, Argentina. Environ Geochem Health 32(6):491–515

Ona-Nguema G, Morin G, Wang Y, Foster AL, Juillot F, Calas G, Brown GE Jr (2010) XANES evidence for rapid arsenic (III) oxidation at magnetite and ferrihydrite surfaces by dissolved O_2 via Fe^{2+}-mediated reactions. Environ Sci Tech 44(14):5416–5422

Owojori OJ, Reinecke AJ, Rozanov AB (2010) Influence of clay content on bioavailability of copper in the earthworm *Eisenia fetida*. Ecotoxicol Environ Saf 73(3):407–414

Pan W, Wu C, Xue S, Hartley W (2014) Arsenic dynamics in the rhizosphere and its sequestration on rice roots as affected by root oxidation. J Environ Sci (China) 26(4):892–899

Pierart A, Shahid M, Séjalon-Delmas N, Dumat C (2015) Antimony bioavailability: knowledge and research perspectives for sustainable agricultures. J Hazard Mater 289:219–234

Polizzotto ML, Harvey CF, Li G, Badruzzman B, Ali A, Newville M, Sutton S, Fendorf S (2006) Solid-phases and desorption processes of arsenic within Bangladesh sediments. Chem Geol 228:97–111

Pongratz R (1998) Arsenic speciation in environmental samples of contaminated soil. Sci Total Environ 224:133–141

Pourrut B, Shahid M, Douay F, Dumat C, Pinelli E (2013) Molecular mechanisms involved in lead uptake, toxicity and detoxification in higher plants. In: Heavy metal stress in plants. Springer, Heidelberg, pp 121–147

Qi Y, Donahoe RJ (2008) The environmental fate of arsenic in surface soil contaminated by historical herbicide application. Sci Total Environ 405:246–254

Qin F, Shan XQ, Wei B (2004) Effects of low-molecular-weight organic acids and residence time on desorption of Cu, Cd, and Pb from soils. Chemosphere 57:253–263

Quaghebeur M, Rengel Z (2004) Arsenic uptake, translocation and speciation in pho1 and pho2 mutants of *Arabidopsis thaliana*. Physiol Plant 120(2):280–286

Quartacci MF, Irtelli B, Gonnelli C, Gabbrielli R, Navari-Izzo F (2009) Naturally-assisted metal phytoextraction by *Brassica carinata*: role of root exudates. Environ Pollut 157 (10):2697–2703

Raab A, Williams PN, Meharg A, Feldmann J (2007) Uptake and translocation of inorganic and methylated arsenic species by plants. Environ Chem 4(3):197–203

Rafiq M, Shahid M, Abbas G, Shamshad S, Khalid S, Niazi NK, Dumat C (2017) Comparative effect of calcium and EDTA on arsenic uptake and physiological attributes of *Pisum sativum*. Int J Phytorem. doi:10.1080/15226514.2016.1278426

Rahman MA, Mamunur Rahman M, Kadohashi K, Maki T, Hasegawa H (2011) Effect of external iron and arsenic species on chelant-enhanced iron bioavailability and arsenic uptake in rice (*Oryza sativa L.*) Chemosphere 84(4):439–445

Rahman MA, Hasegawa H, Ueda K, Maki T, Rahman MM (2008) Influence of EDTA and chemical species on arsenic accumulation in *Spirodela polyrhiza L.* (duckweed). Ecotoxicol Environ Saf 70(2):311–318

Rahman MA, Hogan B, Duncan E, Doyle C, Krassoi R, Rahman MM, Naidu R, Lim RP, Maher W, Hassler C (2014) Toxicity of arsenic species to three freshwater organisms and biotransformation of inorganic arsenic by freshwater phytoplankton (*Chlorella sp*. CE-35). Ecotoxicol Environ Saf 106:126–135

Ramos-Miras JJ, Roca-Perez L, Guzmán-Palomino M, Boluda R, Gil C (2011) Background levels and baseline values of available heavy metals in Mediterranean greenhouse soils (Spain). J Geochem Explor 110(2):186–192

Ravenscroft P, McArthur JMM, Hoque BA (2001) Geochemical and palaeohydrological controls on pollution of groundwater by arsenic. Arsenic Exposure and Health Effects IV, In, pp 53–78

Redman AD, Macalady DL, Ahmann D (2002) Natural organic matter affects Arsenic speciation and sorption onto hematite. Environ Sci Technol 36(13):2889–2896

Rengel Z (2002) Genetic control of root exudation. Plant and Soil 245(1):59–70

Rodríguez JD, Jiménez A, Prieto M, Torre L, García-Granda S (2008) Interaction of gypsum with As (V)-bearing aqueous solutions: surface precipitation of guerinite, sainfeldite, and Ca_2 NaH $(AsO_4)_2$ •$6H_2O$, a synthetic arsenate. Am Mineral 93:928–939

Rojas R, Morillo J, Usero J, Delgado-Moreno L, Gan J (2013) Enhancing soil sorption capacity of an agricultural soil by addition of three different organic wastes. Sci Total Environ 458–460:614–623

Rosas-Castor JM, Guzmán-Mar JL, Hernández-Ramírez A, Garza-González MT, Hinojosa-Reyes L (2014) Arsenic accumulation in maize crop (*Zea mays*): a review. Sci Total Environ 488–489:176–187

Rowland HAL, Polya DA, Lloyd JR, Pancost RD (2006) Characterisation of organic matter in a shallow, reducing, arsenic-rich aquifer, West Bengal. Org Geochem 37(9):1101–1114

Roychowdhury T (2010) Groundwater arsenic contamination in one of the 107 arsenic-affected blocks in West Bengal, India: status, distribution, health effects and factors responsible for arsenic poisoning. Int J Hyg Environ Health 213(6):414–427

Ryu J-H, Gao S, Tanji KK (2010) Speciation and behavior of arsenic in evaporation basins, California, USA. Environ Earth Sci 61:1599–1612

Sabir M, Waraich EA, Hakeem KR, Öztürk M, Ahmad HR, Shahid M (2015) Phytoremediation. In: Hakeem K, Sabir M, Ozturk M, Murmet A (eds) Soil remediation and plants: prospects and challenges, contaminated soil is indispensable. Elsevier, Boston, pp 85–105 ISBN:978–0–12-799,937-1

Sadiq M (1994) Arsenic chemistry in soils: an overview of thermodynamic predictions and field observations. Water Air Soil Pollut 93:117–136

Saifullah SM, Zia-Ur-Rehman M, Sabir M, Ahmad HR (2015) Phytoremediation of Pb-contaminated soils using synthetic chelates. In: Hakeem K et al (eds) Soil remediation and plants. Elsevier, San Diego, pp 397–414

Sánchez-Marín P, Santos-Echeandía J, Nieto-Cid M, Álvarez-Salgado XA, Beiras R (2010) Effect of dissolved organic matter (DOM) of contrasting origins on Cu and Pb speciation and toxicity to *Paracentrotus lividus* larvae. Aquat Toxicol 96:90–102

Sanglard LMVP, Martins SCV, Detmann KC, Silva PEM, Lavinsky AO, Silva MM, Detmann E, Araújo WL, Damatta FM (2014) Silicon nutrition alleviates the negative impacts of arsenic on the photosynthetic apparatus of rice leaves: an analysis of the key limitations of photosynthesis. Physiol Plant:355–366

Saqib M, Zörb C, Schubert S (2008) Silicon-mediated improvement in the salt resistance of wheat (*Triticum aestivum*) results from increased sodium exclusion and resistance to oxidative stress. Funct Plant Biol 35(7):633–639

Sauvé S, Hendershot WH, Allen HE (2000) Solid-solution partitioning of metals in contaminated Soils: dependence on pH, total metal burden, and organic matter. Environ Sci Technol 34 (7):1125–1131

Seyler P, Martin J (1989) Biogeochemical processes affecting arsenic species distribution in a permanently stratified Lake. Environ Sci Technol 23:1258–1263

Shahid M, Pinelli E, Pourrut B, Silvestre J, Dumat C (2011) Lead-induced genotoxicity to *Vicia faba* L. roots in relation with metal cell uptake and initial speciation. Ecotoxicol Environ Saf 74:78–84

Shahid M, Dumat C, Aslam M, Pinelli E (2012a) Assessment of lead speciation by organic ligands using speciation models. Chem Spec Bioavailab 24:248–252

Shahid M, Dumat C, Silvestre J, Pinelli E (2012b) Effect of fulvic acids on lead-induced oxidative stress to metal sensitive *Vicia faba* L. plant. Biol Fertil Soils 48:689–697

Shahid M, Arshad M, Kaemmerer M, Pinelli E (2012c) Long-term field metal extraction by pelargonium: phytoextraction efficiency in relation to plant maturity. Int J Phytoremediation 14:493–505

Shahid M, Pinelli E, Dumat C (2012d) Review of Pb availability and toxicity to plants in relation with metal speciation; role of synthetic and natural organic ligands. J Hazard Mater 219–220:1–12

Shahid M, Ferrand E, Schreck E, Dumat C (2013a) Behavior and impact of zirconium in the soil–plant system: plant uptake and phytotoxicity. Rev. Environ Contam Toxicol 221:107–127

Shahid M, Xiong T, Castrec-Rouelle M, Leveque T, Dumat C (2013b) Water extraction kinetics of metals, arsenic and dissolved organic carbon from industrial contaminated poplar leaves. J Environ Sci 25:2451–2459

Shahid M, Dumat C, Pourrut B, Silvestre J, Laplanche C, Pinelli E (2014a) Influence of EDTA and citric acid on lead-induced oxidative stress to *Vicia faba* roots. J Soil Sediment 14:835–843

Shahid M, Xiong T, Masood N, Leveque T, Quenea K, Austruy A, Foucault Y, Dumat C (2014b) Influence of plant species and phosphorus amendments on metal speciation and bioavailability in a smelter impacted soil: a case study of food-chain contamination. J Soil Sediment 14:655–665

Shahid M, Dumat C, Pourrut B, Sabir M, Pinelli E (2014c) Assessing the effect of metal speciation on lead toxicity to *Vicia faba* pigment contents. J Geochem Explor 144:290–297

Shahid M, Pinelli E, Pourrut B, Dumat C (2014d) Effect of organic ligands on lead-induced oxidative damage and enhanced antioxidant defense in the leaves of *Vicia faba* plants. J Geochem Explor 144:282–289

Shahid M, Sabir M, Ali MA, Ghafoor A (2014e) Effect of organic amendments on phytoavailability of nickel and growth of berseem (*Trifolium alexandrinum*) under nickel contaminated soil conditions. Chem Spec Bioavailab 26:37–42

Shahid M, Austruy A, Echevarria G, Arshad M, Sanaullah M, Aslam M, Nadeem M, Nasim W, Dumat C (2014f) EDTA-enhanced phytoremediation of heavy metals: a review. Soil Sediment Contam An Intl J 23:389–416

Shahid M, Pourrut B, Dumat C, Nadeem M, Aslam M, Pinelli E (2014g) Heavy-metal-induced reactive oxygen species: phytotoxicity and physicochemical changes in plants. Rev Environ Contam Toxicol 232:1–44

Shahid M, Khalid S, Abbas G, Shahid N, Nadeem M, Sabir M, Aslam M, Dumat C (2015a) Heavy metal stress and crop productivity. In: Hakeem KR (ed) Crop production and global environmental issues. Springer, Cham. doi:10.1007/978–3–319-23,162-4_1

Shahid M, Dumat C, Pourrut B, Abbas G, Shahid N, Pinelli E (2015b) Role of metal speciation in lead-induced oxidative stress to *Vicia faba* roots. Russ J Plant Physiol 62:448–454

Shahid M, Dumat C, Khalid S, Schreck E, Xiong T, Niazi NK (2017a) Foliar heavy metal uptake, toxicity and detoxification in plants: A comparison of foliar and root metal uptake. J Hazard Mater 325:36–58

Shahid M, Dumat C, Khalid S, Niazi NK, Antunes PMC (2017b) Cadmium bioavailability, uptake, toxicity and detoxification in soil-plant system. Rev Environ Contam Toxicol 241:73–137

Shakoor MB, Niazi NK, Bibi I, Murtaza G, Kunhikrishnan A, Seshadri B, Ali F (2015a) Remediation of arsenic-contaminated water using agricultural wastes as biosorbents. Crit Rev Environ Sci Technol. doi:10.1080/10643389.2015.1109910

Shakoor MB, Niazi NK, Bibi I, Rahman MM, Naidu R, Dong Z, Arshad M (2015b) Unraveling health risk and speciation of arsenic from groundwater in rural areas of Punjab, Pakistan. Int J Environ Res Public Health 12:12,371–12,390

Sharma VK, Sohn M (2009) Aquatic arsenic: toxicity, speciation, transformations, and remediation. Environ Int 35(4):743–759

Sharma AK, Tjell JC, Sloth JJ, Holm PE (2014) Review of arsenic contamination, exposure through water and food and low cost mitigation options for rural areas. Appl Geochem 41:11–33

Shen H, He Z, Yan H, Xing Z, Chen Y, Xu W, Ma M (2014) The fronds tonoplast quantitative proteomic analysis in arsenic hyperaccumulator *Pteris vittata L.* J Proteomics:1–12

Sheng XF, Xia JJ (2006) Improvement of rape (*Brassica napus*) plant growth and cadmium uptake by cadmium-resistant bacteria. Chemosphere 64(6):1036–1042

Shi GL, Zhu S, Bai SN, Xia Y, Lou LQ, Cai QS (2015) The transportation and accumulation of arsenic, cadmium, and phosphorus in 12 wheat cultivars and their relationships with each other. J Hazard Mater 299:94–102

Shuman LM, Luxmoore RJ (1991) Chemical forms of micronutrients in soils. In: Luxmoore R (ed) Micronutrients in agriculture, 2nd edn. SSSA, Madison, pp 113–144

Signes-Pastor A, Burló F, Mitra K, Carbonell-Barrachina AA (2007) Arsenic biogeochemistry as affected by phosphorus fertilizer addition, redox potential and pH in a west Bengal (India) soil. Geoderma 137(3–4):504–510

Singh N, Raj A, Khare PB, Tripathi RD, Jamil S (2010) Arsenic accumulation pattern in 12 Indian ferns and assessing the potential of *Adiantum capillus-veneris*, in comparison to *Pteris vittata*, as arsenic hyperaccumulator. Bioresour Technol 101(23):8960–8968

Smith E, Naidu R, Alston AM (1998) Arsenic in the soil environment. A review. Adv Agron 64:149–195

Smith FW, Mudge SR, Rae AL, Glassop D (2003) Phosphate transport in plants. Plant and Soil 248 (1–2):71–83

Smith E, Juhasz AL, Weber J, Naidu R (2008) Arsenic uptake and speciation in rice plants grown under greenhouse conditions with arsenic contaminated irrigation water. Sci Total Environ 392 (2–3):277–283.

Sparks DL (2003) Environmental soil chemistry. Academic Press, San Diego

Sposito G (2008) The chemistry of soils. Oxford University Press, New York

Suess E, Planer-Friedrich B (2012) Thioarsenate formation upon dissolution of orpiment and arsenopyrite. Chemosphere 89(11):1390–1398

Tang Y, Wang J, Gao N (2010) Characteristics and model studies for fluoride and arsenic adsorption on goethite. J Environ Sci 22(11):1689–1694

Tang J, Zhu W, Kookana R, Katayama A (2013) Characteristics of biochar and its application in remediation of contaminated soil. J Biosci Bioeng 116(6):653–659

Tarvainen T, Albanese S, Birke M, Poňavič M, Reimann C (2013) Arsenic in agricultural and grazing land soils of Europe. Appl Geochem 28:2–10

Thies JE, Rilling MC (2009) Characteristics of biochar: biological properties. In: Biochar for environmental management: science and technology. Earthscan, London, pp 85–105

Tighe M, Lockwood PV, Ashley PM, Murison RD, Wilson SC (2013) The availability and mobility of arsenic and antimony in an acid sulfate soil pasture system. Sci Total Environ 463–464:151–160

Tiwari KK, Singh NK, Patel MP, Tiwari MR, Rai UN (2011) Metal contamination of soil and translocation in vegetables growing under industrial wastewater irrigated agricultural field of Vadodara, Gujarat, India. Ecotoxicol Environ Saf 74(6):1670–1677

Tokunaga S, Hakuta T (2002) Acid washing and stabilization of an artificial arsenic-contaminated soil. Chemosphere 46(1):31–38

Tong J, Guo H, Wei C (2014) Arsenic contamination of the soil–wheat system irrigated with high arsenic groundwater in the Hetao Basin, Inner Mongolia, China. Sci Total Environ 496:479–487

Tripathi P, Tripathi RD, Singh RP, Dwivedi S, Goutam D, Shri M, Trivedi PK, Chakrabarty D (2013) Silicon mediates arsenic tolerance in rice (*Oryza sativa L.*) through lowering of arsenic uptake and improved antioxidant defence system. Ecol Eng 52:96–103

Tu S, Ma L, Luongo T (2004) Root exudates and arsenic accumulation in arsenic hyperaccumulating *Pteris vittata* and non-hyperaccumulating *Nephrolepis exaltata*. Plant and Soil 258(1–2):9–19

Tufano KJ, Reyes C, Saltikov CW, Fendorf S (2008) Reductive processes controlling arsenic retention: revealing the relative importance of iron and arsenic reduction. Environ Sci Technol 42(22):8283–8289

Uddh-Söderberg TE, SGunnarsson SG, Hogmalm KJ, Lindegård MIBG, Augustsson ALM (2015) An assessment of health risks associated with arsenic exposure via consumption of homegrown vegetables near contaminated glassworks sites. Sci Total Environ 536:189–197

Udovic M, Lestan D (2009) Pb, Zn and Cd mobility, availability and fractionation in aged soil remediated by EDTA leaching. Chemosphere 74(10):1367–1373

Ullah S, Shahid M, Zia-Ur-Rehman M, Sabir M, Ahmad HR (2015a) Phytoremediation of Pb-Contaminated soils using synthetic chelates. In: Hakeem K, Sabir M, Ozturk M, Murmet A (eds) Soil remediation and plants. Elsevier, Boston, pp 397–414

Ullah A, Heng S, Munis MFH, Fahad S, Yang X (2015b) Phytoremediation of heavy metals assisted by plant growth promoting (PGP) bacteria: a review. Environ Exp Bot 117:28–40

Ungaro F, Ragazzi F, Cappellin R, Giandon P (2008) Arsenic concentration in the soils of the Brenta Plain (Northern Italy): mapping the probability of exceeding contamination thresholds. J Geochem Explor 96(2):117–131

USEPA (United States Environmental Protection Agency) (2015) http://water.epa.gov/lawsregs/rulesregs/sdwa/arsenic/index.cfm.

Usman ARA, Kuzyakov Y, Stahr K (2004) Effect of clay minerals on extractability of heavy metals and sewage sludge mineralization in soil. Chem Ecol 20(2):123–135

Vallee BL, Ulmer DD, Wacker WEC (1960) Arsenic toxicology and biochemistry. J Occup Environ Med 2(7):358

Vaxevanidou K, Giannikou S, Papassiopi N (2012) Microbial arsenic reduction in polluted and unpolluted soils from Attica, Greece. J Hazard Mater 241–242:307–315

Wang S, Mulligan CN (2006) Occurrence of arsenic contamination in Canada: sources, behavior and distribution. Sci Total Environ 366(2–3):701–721

Wang S, Zhao X (2009) On the potential of biological treatment for arsenic contaminated soils and groundwater. J Environ Manage 90(8):2367–2376

Wang J, Zhao F-J, Meharg AA, Raab A, Feldmann J, McGrath SP (2002) Mechanisms of arsenic hyperaccumulation in *Pteris vittata*. Uptake kinetics, interactions with phosphate, and arsenic speciation. Plant Physiol 130:1552–1561

Wang Z, Bush RT, Liu J (2013) Arsenic(III) and iron(II) co-oxidation by oxygen and hydrogen peroxide: divergent reactions in the presence of organic ligands. Chemosphere 93 (9):1936–1941

Warren GP, Alloway BJ (2003) Reduction of arsenic uptake by lettuce with ferrous sulfate applied to contaminated soil. J Environ Qual 32:767–772

Wei CY, Chen TB (2006) Arsenic accumulation by two brake ferns growing on an arsenic mine and their potential in phytoremediation. Chemosphere 63(6):1048–1053

Wei B, Yu J, Li H, Yang L, Xia Y, Wu K, Cui N (2015) Arsenic metabolites and methylation capacity among individuals living in a rural area with endemic Arseniasis in Inner Mongolia, China. Biol Trace Elem Res 170(2):300–308

Weiss JV, Emerson D, Backer SM, Megonigal JP (2003) Enumeration of Fe (II)-oxidizing and Fe (III)-reducing bacteria in the root zone of wetland plants: implications for a rhizosphere iron cycle. Biogeochem 64(1):77–96

Williams PN, Price AH, Raab A, Hossain SA, Feldmann J, Meharg AA (2005) Variation in arsenic speciation and concentration in paddy rice related to dietary exposure. Environ Sci Technol 39 (15):5531–5540

Williams G, West JM, Koch I, Reimer KJ, Snow ET (2009) Arsenic speciation in the freshwater crayfish, Cherax destructor Clark. Sci Total Environ 407(8):2650–2658

Wilson SC, Lockwood PV, Ashley PM, Tighe M (2010) The chemistry and behaviour of antimony in the soil environment with comparisons to arsenic: a critical review. Environ Pollut 158 (5):1169–1181

Wingate JR (2008) Development of novel charcoals for the sorption and transformation of heavy metals in contaminated land. Doctoral dissertation, University of Surrey

Woolson EA (1983) Emissions, cycling and effects of arsenic in soil ecosystems. In: Topics in environmental health. Elsevier, Amsterdam, Netherlands, pp 51–139

Woolson EA, Axley JH, Kearney PC (1971) The chemistry and phytotoxicity of arsenic in soils: I Contaminated field soils. Soil Sci Soc Am J 35(6):938–943

Wysocki R, Bobrowicz P, Ułaszewski S (1997) The *Saccharomyces cerevisiae* ACR_3 gene encodes a putative membrane protein involved in arsenite transport. J Biol Chem 272 (48):30,061–30,066

Xiong T, Leveque T, Shahid M, Foucault Y, Mombo S, Dumat C (2014) Lead and cadmium phytoavailability and human bioaccessibility for vegetables exposed to soil or atmospheric pollution by process ultrafine particles. J Environ Qual 43:1593–1600

Xiong T, Dumat C, Pierart A, Shahid M, Kang Y, Li N, Bertoni G, Laplanche C (2016a) Measurement of metal bioaccessibility in vegetables to improve human exposure assessments: field study of soil–plant–atmosphere transfers in urban areas. South China Environ Geochem Health. doi:10.1007/s10653–016–9796-2

Xiong T, Austruy A, Pierart A, Shahid M (2016b) Kinetic study of phytotoxicity induced by foliar lead uptake for vegetables exposed to fine particles and implications for sustainable urban agriculture. J Environ Sci. doi:10.1016/j.jes.2015.08.029

Xu W, Dai W, Yan H, Li S, Shen H, Chen Y et al (2015) Arabidopsis NIP3;1 plays an important role in arsenic uptake and root-to-shoot translocation under arsenite stress conditions. Mol Plant 8(5):722–733

Xu J-Y, Han Y-H, Chen Y, Zhu L-J, Ma LQ (2016) Arsenic transformation and plant growth promotion characteristics of As-resistant endophytic bacteria from As-hyperaccumulator *Pteris vittata*. Chemosphere 144:1233–1240

Xue PY, Yan CZ (2011) Arsenic accumulation and translocation in the submerged macrophyte *Hydrilla verticillata (L.f.)* Royle. Chemosphere 85(7):1176–1181

Yamamura S, Amachi S (2014) Microbiology of inorganic arsenic: from metabolism to bioremediation. J Biosci Bioeng 118(1):1–9

Yan X, Zhang M, Liao X, Tu S (2012) Influence of amendments on soil arsenic fractionation and phytoavailability by *Pteris vittata L*. Chemosphere 88(2):240–244

Yang Y, Shuzhen Z, Honglin H, Lei L, Bei W (2009) Arsenic accumulation and speciation in maize as affected by inoculation with arbuscular mycorrhizal fungus *Glomus mosseae*. J Agric Food Chem 57:3695–3701

Yang M, Xiao XY, Miao XF, Guo ZH, Wang FY (2012) Effect of amendments on growth and metal uptake of giant reed (*Arundo donax L.*) grown on soil contaminated by arsenic, cadmium and lead. Trans Nonferrous Met Soc Chin 22:1462–1469

Ye WL, Wood BA, Stroud JL, Andralojc PJ, Raab A, McGrath SP, Feldmann J, Zhao FJ (2010) Arsenic speciation in phloem and xylem exudates of castor bean. Plant Physiol 154 (3):1505–1513

Yu Y, Zhang S, Huang H, Luo L, Wen B (2009) Arsenic accumulation and speciation in maize as affected by inoculation with arbuscular mycorrhizal fungus *Glomus mosseae*. J Agric Food Chem 57:3695–3701

Zhang G, Ren Z, Zhang X, Chen J (2013) Nanostructured iron(III)-copper(II) binary oxide: a novel adsorbent for enhanced arsenic removal from aqueous solutions. Water Res 47(12):4022–4031

Zhang M, Zhao M, Zhang G, Nowak P, Coen A, Tao M (2015) Calcium-free geopolymer as a stabilizer for sulfate-rich soils. Appl Clay Sci 108:199–207

Zhao FJ, McGrath SP, Meharg AA (2010) Arsenic as a food chain contaminant: mechanisms of plant uptake and metabolism and mitigation strategies. Annu Rev Plant Biol 61:535–559

Zobrist J, Dowdle PR, Davis JA, Oremland RS (2000) Mobilization of arsenite by dissimilatory reduction of adsorbed arsenate. Environ Sci Technol 34(22):4747–4753

Pollutant Decontamination from Water: Role of Nanocomposite Materials

Mohammad Zain Khan, Mohammad Shahadat, Huda A. Qari, Iqbal I. M. Ismail, Zia Ahmad Shaikh, and Mohammad Oves

Abstract Rapid industrialization, urbanization, population growth, and climate change are responsible for contamination and depletion of water resources. Scarcity of fresh and pure water is considered as a biggest threat to human and animal life. For the last two decades, water purification technologies are gaining more and more attention of the public and governmental bodies. Researchers around the globe are focusing on nanotechnology-based water purification/treatment systems for efficient and effective decontamination of water bodies. Nanoscale composite materials have a huge potential to decontaminate water in several ways, due to their high surface area, excellent mechanical strength, high chemical reactivity, and cost-effectiveness. Nanoscale materials are able to remove bacteria, viruses, and inorganic and organic materials from wastewater due to specific binding action (chelation, absorption, ion exchange). A number of nanocomposite materials are playing active role in water purification, for example, metal nanoparticles, bioactive nanoparticles, nanosorbents, nanocatalysts, nanomembranes, carbon nanotubes, many other nanoforms, etc. This chapter discusses the application of different nanocomposite materials in the treatment of wastewater along with their mechanistic approach.

Keywords Nanomaterials • Water purification • Photocatalysis • Heavy metals • Sorption • Ion exchange

M.Z. Khan
Environmental Research Laboratory, Department of Chemistry, Aligarh Muslim University, Aligarh 202002, UP, India

M. Shahadat • Z.A. Shaikh
Department of Biochemical Engineering and Biotechnology, Indian Institute of Technology IIT Delhi, Hauz Khas, New Delhi 110016, India

H.A. Qari • I.I.M. Ismail • M. Oves (✉)
Centre for Excellence in Environmental Studies, King Abdul Aziz University, Jeddah 21589, Saudi Arabia
e-mail: owais.micro@gmail.com; mmateenuddinn@kau.edu.sa

N.A. Anjum et al. (eds.), *Enhancing Cleanup of Environmental Pollutants*,
DOI 10.1007/978-3-319-55423-5_5

Introduction

Toxic heavy metal ion and pathogenic bacterial contamination in water bodies is a serious issue of water pollution, worldwide. With the rapid extension of urbanization and industrializations, these sewage and heavy metals are regularly discharged into the natural water resources and damage the aquatic environment and pollute the water (Rawat et al. 2009; Pereira et al. 2010; Wade et al. 2015). Unlike organic pollutants, heavy metal ions are not biodegradable and have a capability to accumulate in living beings which are extremely harmful to human health (Fu and Wang 2011). Directly or indirectly, when these heavy metal ions are being inhaled or consumed through food or water, they cause severe damage to the body parts. However, these metal ions play important role in cellular function of living beings within a specific concentration range. The metal ions can be considered safe less than the toxicity range. The increment in metal ion concentration beyond the permissible limits causes various cytological and physiological effects. Different types of metal ions and their permissible limits laid down by the WHO together with their physiological effects are shown in Table 1. The main sources of heavy metal ion in water bodies come from industrial by-products, cosmetics, automobiles, and effluents released from electroplating industries and organic toxic pollutants such as pesticides, herbicides, chlorophenol, dyes, and industrial and pharmaceutical by-products discharged.

In addition to heavy metals, several toxic organic compounds (chlorophenols, dyes, etc.) enter the environment through various anthropogenic and industrial operations (USEPA 2002; Khan et al. 2011a; Sitea 2001). Chlorophenols are mainly used in herbicides, insecticides, fungicides, and wood preservative preparation. Chlorophenol compounds and derivatives are highly toxic and persistent in the environment and cause gastrointestinal problems, carcinogenicity, and many other severe effects on organisms (Khan et al. 2011b). Colored wastewater containing toxic and complex dyes is another big problem to be dealt with effectively. Dyes, whether acidic or basic, cause adverse effects to human beings and animals such as asthma, dermatitis, tearing, eye irritation, convulsions, gastritis, tremors, renal failure, vertigo, and coma in humans (Chen et al. 2009). The contamination of these dyes in the water bodies causes serious environmental threat to human health (Asad et al. 2007). All above pollutants are released in to our environment without proper treatment, which lead to contamination of soil and water bodies and create serious environmental problem.

Previously, a number of methods including chemical precipitation, flotation, coagulation-flocculation, ion exchange, and membrane filtration have been used for the treatment of metal ions and organic pollutants from water (Kurniawan et al. 2006). However, the ion-exchange material has gained popularity for being more selective and less expensive as compared to other methods. For the separation of metal ions, a large number of organic and inorganic ion-exchange materials have been synthesized; however, they are associated with certain limitations (Nabi et al. 2011). Application of nanoparticles as a photocatalyst for degrading these

Table 1 Maximum permissible limits of metal ions in water limits and their major effects

Metal ions	WHO limits (mg/L)	Major effects	References
Arsenic (As)	0.05	Gastrointestinal effects and the disorder in central and peripheral nervous system	Hughes et al. (2011), Patel et al. (2012)
Lead (Pb)	0.05	Kidney malfunctioning, anemia, hematological as well as brain damage	Adrrienne and Anne (2010), Liu et al. (2008)
Cadmium (Cd)	0.01	Lung effects in the form of bronchial and pulmonary irritation	Ercal et al. (2001a)
Cadmium (Cd)	0.01	Lung effects in the form of bronchial and pulmonary irritation	Hu and Long (2016), Gorguner and Akgun (2010)
Chromium (Cr)	0.1	Asthma, nasal itching, soreness, carcinogen, shortness of breath, coughing, wheezing, bronchitis, and pneumonia	Dayan and Paine (2001), Dey and Roy (2009)
Copper (Cu)	3.0	Arthritis, fatigue, adrenal burnout, insomnia, scoliosis, osteoporosis, heart disease, cancer, migraine headaches, seizures, tooth decay, skin and hair problems	Selvaraj et al. (2011)
Aluminum (Al)	0.2	Alzheimer's disease as well as other neurotoxic effects	Galindo et al. (2015)
Manganese (Mn)	0.1	Effects on the CNS, including slowed visual reaction time, hand steadiness, and eye-hand coordination	Fryzek et al. (2005)
Nickel (Ni)	0.2	Nickel dermatitis; itching of the fingers, hands, and forearms; lung and nasal cancers	He et al. (2014)
Mercury (Hg)	0.002	Effects on the CNS including erethism, irritability, excessive shyness, tremors, blurred vision, malaise, speech difficulties	Kobal et al. (2004)
Iron (Fe)	0.3	Hemorrhagic gastritis and enteritis with loss of blood, induce oxidative stress, and DNA damage	Puliyel et al. (2015)
Zinc (Zn)	3.0	Papular-pustular skin eruptions in the axilla, inner thigh, inner arm, scrotum, and pubic areas	Hashemi et al. (2007)

pollutants is also an attracting increasing interest. Since nanomaterials have a large surface to volume ratio (greater number of free valences) and porosity, they can be used as an excellent photocatalyst in removing toxic pollutants from natural water streams. In some cases, a polymer backbone has also been incorporated within the nanocomposite for getting special properties like lightweight, increased electric/heat conductivity, enhanced mechanical properties and magnetic properties (Guo et al. 2008), and even improved shape replicability (Huang et al. 2006).

Recent developments in the synthesis and application of nanomaterials have greater impact on research and development due to revealing innovative properties of nanoscale materials. One of the significant advancement in material synthesis is the capability of fabricating materials with well-defined size and shape in

nano-range with specific compositions. Nanocomposite is also included in nano-dimensional phases with distinct structure and chemistry, thereby offering different mechanical, electrical, optical, electrochemical, catalytic, and structural properties from those of their components. Nanocomposite powders have been prepared directly by the mechanical mixing of powders known as mechanosynthesis (Matteazzi and Le-Caer 1992; Nawa et al. 1994) and chemical methods involving the reduction in hydrogen of suitable oxide precursor's hydrothermal methods (Sultana et al. 2015a, b). There are several other routes to prepare materials from oxide precursors. Intimate oxide mixtures have been obtained by the sol-gel route (de-Resende et al. 2009; Oves et al. 2015). The nanostructure materials thus obtained offer a promising platform for high-performance catalysis, photocatalysis, and electrocatalysis systems (Dai et al. 2008; Xie et al. 2009; Liu et al. 2009). During the last decade, it has been employed in medical sciences in several ways like imaging (Waren and Nie 1998), sensing (Vaseashta and Dimova-Malinovska 2005), targeted drug delivery and gene delivery systems, and artificial implants (Farokhzad et al. 2006). The new-age drugs are based on nanoparticles of polymers, metals, or ceramics, which can fight conditions like cancer and infectious disease (Azam et al. 2012). For more than one century, peoples know the benefits of silver. Due to this reason, silver-based materials and compounds have been used to control bacterial infection (Nomiya et al. 2004; Oves et al. 2013; Jain and Pradeep 2005). The present chapter also includes the synthesis, characterization of polyaniline ion-exchange materials, and their application for the removal and recovery of metal ions from wastewater.

Nanocomposite Material for Inorganic Metal Ion Remediation from Wastewater

For more than a decade, nanocomposite materials have been used to extract and pre-concentrate a wide range of trace elements. These nanocomposites exhibit different binding affinities toward trace elements owing to the presence of various functional groups. A number of nanomaterials have been used to study the trace elements in environmental samples, including river water (Tuzen and Soylak 2007), lake water (Wang et al. 2013), tap water (Guo et al. 2011), mineral water, underground water (Wang et al. 2012), rainwater, wastewater (Yang et al. 2012), and drinking water (Sadeghi and Garmroodi 2013). Among these materials, polyaniline-based nanocomposite (ion-exchange) materials have been successfully employed owing to their use in diverse fields including wastewater treatment. Poly-o-toluidine-based nanocomposite and poly-o-toluidine Ce(IV) phosphate ion-exchange materials were synthesized for the analysis and removal of metal ions. It has been used as an indicator electrode for the detection of Cd(II) in electrometric titrations (Khan et al. 2011a, b; Khan and Shaheen 2013). The maximum adsorption of metal ion on the nanocomposite material was confirmed by the physicochemical properties (effect of eluent concentration, elution behavior,

and pH titration studies). An advanced PANI-zirconium titanium phosphate (PZTP) nanocomposite cation exchanger was fabricated from the sol-gel method by the mixing of polyaniline inorganic precipitate with zirconium titanium phosphate (Khan et al. 2010; Khan and Paquiza 2011; Shahdat et al. 2015). These nanocomposite materials have surprisingly high ion-exchange capacity with better chemical and thermal stability. The excellent ion-exchange capacity of this material makes it useful for the removal and recovery of Hg^{2+} and Pb^{2+} ions from environmental waste samples and detection range for Hg^{2+} ions with a wide dynamic range from 10^{-10} to 10^{-1} mol m^{-3} (Khan et al. 2011a, b). Similarly, poly-o-anisidine Sn (IV) tungstate nanocomposite cation exchanger was also reported for the removal of Hg^{2+} ions from wastewater sample (Khan et al. 2012; Khan and Shaheen 2013). A novel PANI/Ti(IV) tungstate composite material was prepared by sol-gel route at pH 1.0 (Nabi et al. 2011). Amorphous morphology of nanocomposite was revealed on the basis of XRD and SEM analyses. Alkali and alkaline earth metals were employed for the determination of ion uptake capacity of the composite material. The material demonstrated improvement in ion-exchange capacity as well as thermal and chemical stability. It can withstand up to 300 °C with 98% retaining of the initial ion-exchange capacity. The distribution coefficients (K_d) of metal ions were observed in nonionic, cationic, and anionic surfactant systems with various concentrations. On the basis of K_d values, the material was found to be selective for Pb^{2+}, Hg^{2+}, Bi^{3+}, and Zr^{4+} ions. The detection and quantification limits for Pb^{2+} ion were 0.85 and 2.85 μg/L, respectively. The nanocomposite material has been explored by achieving some selective separations of metal ions from industrial effluents and natural water. PVC-supported membranes of a PANI-TiP cation exchange nanocomposite were prepared via the solution casting technique in different mixing ratios of PVC and PANI-TiP (Khan et al. 2012). The membrane with a 1:1 ratio of PVC and PANI-TiP was reported best for electrical conductivity, water content, porosity, thickness, and swelling capacity. The K_d values of metal ions were also determined using the PANI-TiP nanocomposite in various concentrations of DMW, HNO_3, H_2SO_4, and CH_3COOH solvents. On the basis of higher K_d values, the PANI-TiP nanocomposite was found to be selective for Pb^{2+} ions. To utilize this material as a potentiometric sensor, an ion selective electrode was developed for the detection of lead ions in solution. The membrane was found to be mechanically stable, with a fast response time that covered a wide dynamic range, and could be used for at least 5 months. Similarly, Shahadat et al. (2012) have also synthesized titanium-based semicrystalline PANI-Ti(IV)As nanocomposite ion-exchange material by sol-gel route. It was a thermally stable ion-exchange material and with ion uptake capacity of 1.37 meq g^{-1} for the Na^+ ion and ability to measure electrical conductivity and photochemical degradation of an organic pollutant. The photochemical activity of PANI-Ti(IV)As nanocomposite can be used for the photochemical degradation of AB-29 and as a conducting material. In spite of cation exchange material, PANI-Ti(IV) nanocomposite can also be employed diversely (a conducting material and a photocatalyst). In another study, Pérez et al. (2015) have prepared nano-hydrotalcite (nano-HT) particles with silica

for the retention of chromium(VI) through anion-exchange mechanism. It exhibits excellent adsorption capacity up to 4 mg/L of Cr(VI) from solutions. Further, the adsorption behavior of nanocomposite was determined by Freundlich isotherm, suggesting a nonuniform surface. The nano-HT can be effectively applied for the separation of Cr(VI) in industrial wastewater. Similarly, amorphous PANI-Ti(IV) arsenophosphate (PANI-Ti(IV)As(IV)P) nanocomposite was synthesized by simple chemical route (Bushra et al. 2014). On the basis of the high K_d values, some heavy toxic metal ion separations were achieved from synthetic mixtures and natural water samples. Further the nanocomposite material was also examined for its conducting behavior and antimicrobial activity as well as photocatalytic degradation of industry dye.

Recently, Zeng et al. (2015) synthesized chitosan/rectorie (CTS/REC)-based nano-hybrid microsphere by mixing varying proportions of 2:1, 3:1, and 4:1 of CTS and REC. The nano-hybrid composite microsphere prepared from a 2:1 ratio has good sorption capacity toward heavy metal ions Cd(II), Cu(II), and Ni(II). The adsorption behavior of the microsphere was examined for metal ion in single and binary mixture of metal systems. Another silica-based mesoporous nanocomposite adsorbent 4-dodecyl-6-(4-hexyloxy phenyl diazenyl) benzene-1,3-diol (DPDB) was prepared for the separation of Ce(III) ions from the industrial effluent. Novel fourth-generation polyamidoamine (PAMAM) dendrimers with ethylenediamine cores (G4-OH) were prepared via the sol-gel chemical route (Barakat et al. 2013). The remediation of heavy metal ions from a synthetic mixture of Cu^{2+}, Cr^{3+}, and Ni^{2+} ions was done by novel PAMAM-TiO_2 composite material. Significant parameters including the pH of the solution, the retention time, the concentration of metal ions, and the material dosage were explored in the proficient removal of metal ions. The batch remediation experiment was conducted to establish the performance of PAMAM/G4-OH nanocomposite toward Cu^{2+}, Cr^{3+}, and Ni^{2+} ions due to the formation of metal chelates. It was also observed that the maximum metal ion recovery was achieved upon equilibration after 1 h at pH 7 for Cu^{2+} and Cr^{3+} ions and at pH 9.0 for the Ni(II) ion. The successful removal of Cu^{2+}, Ni^{2+}, and Cr^{3+} ions suggested that the nanocomposite of PAMAM/G4-OH can be used for the treatment of metal ions from industrial wastewaters. In another study, organic ligand embedded nano-conjugate adsorbent N,N(octane-1,8-diylidene)di (2-hydroxyl-3,5-dimethylaniline) (NCA) was synthesized and anchored onto inorganic mesoporous materials by direct immobilization of Co(II) ions (Awual et al. 2015). Its maximum sorption capacity was up to 165.83 mg/g Co(II) ions. The presence of other coexisting metal ions did not decrease the Co(II) sorption capacity, and the NCA adsorbent had almost no sorption capacity to these coexisting metal ions, which suggested the high sorption selectivity of NCA to Co(II) ions at optimum conditions. The obtained data also clarified the efficient and eco-friendly nature of NCA adsorbent for the treatment of Co(II) ions. Therefore, the proposed adsorbent can be considered as a potential candidate for the removal of Co(II) ions from wastewater.

Nanocomposite Materials for Organic Pollutant Treatment

Syntheses of new nanocomposite materials with excellent adsorption and regenerative capacities are getting more attention in recent environment-related research. In this regard, polypyrrole (PPy) is considered as one of the most commonly used conducting polymer owing to its simple synthesis, nontoxicity, and environmental stability. The existence of positive charges on the nitrogen atoms in PPy facilitates the good adsorption capacity through ion exchange. PPy has capability to undergo protonation or deprotonation during treatment with acid or base. Therefore, the combination of PPy with TiO_2 demonstrates excellent abilities of adsorption and regeneration. Organic pollutant adsorption/deposition on novel TiO_2-coated polypyrrole (PPy/P25 or PPy/TiO_2) composites was performed to remove industrial dye (Feng et al. 2015). The adsorption studies showed that the nanocomposites of PPy/TiO_2 have higher adsorption capacities of methylene blue dye at a high pH. Further, thermodynamic and kinetic parameters were also determined, and pseudo-second-order adsorption behavior was well described by the model and Langmuir isotherm model. However, adsorption capacity of PPy/TiO_2 was 3.6 and 5.5 times higher than either PPy/P25 or pure PPy in initial 30 min, respectively. The thermodynamic studies specified the spontaneous and endothermic nature of the adsorption. The regeneration experiments demonstrated that PPy/TiO_2 can be reused at least seven times without the loss of its original adsorption capacity. Thus, the PPy/TiO_2 nanocomposite can be considered to be a stable adsorbent for the removal of dye. Desorption studies showed that CH_3COOH (1.0 M) was an appropriate desorption agent and, after being activated with NaOH (0.1 M), the PPy/TiO_2 composite could be reused six times without an appreciable loss of its original capacity. The material was also compared with activated carbon and showed significant results in terms of adsorption equilibrium time and adsorption and regeneration capacities relative to activated carbon. Thus, the nanocomposite of PPy/TiO_2 can be effectively used for the analysis of industrial dye from wastewater.

Xiong et al. (2004) improved the photocatalytic efficiency of TiO_2 with PANI and develop PANI/TiO_2 microtubes in the form of microchannels, by using a two-step template method: (i) an anodic aluminum oxide membrane for template and (ii) sol-gel method. The PANI/TiO_2 nanocomposite showed high photodegradation that simultaneously increased with decreasing ratios of PANI/TiO_2. The photocatalytic degradation of the nanocomposite was also confirmed by the accompanying decrease in peak intensity in the FTIR spectra at 1235 cm^{-1}, which was attributed to the C-N stretching mode for the benzenoid unit and the depigmentation of the powders due to the visible light scattering caused by growing cavities. The elemental and XPS analyses of the composite showed that the bulk and surface concentrations of N decreased with irradiation. On the basis of its efficient photolytic degradation, the PANI/TiO_2 nanocomposite is potentially viable and can be used as a photodegradable agent (Bushra et al. 2014).

The fabrication of a Bi_2S_3-TiO_2 heterojunction/polymer fiber composite and its activity toward the degradation of MB via Xe lamp irradiation have been reported earlier by Ma et al. (2012). The polysulfone (PSU)/styrene-maleic anhydride (SMA) copolymer fibers were prepared by electrospinning. Bismuth ions were introduced onto the surface of the polymer followed by the incorporation of sulfide ions under hydrothermal conditions. Finally, TiO_2 was deposited onto the surface of the Bi_2S_3 polymer by the reaction of titanium ions in the presence of urea under hydrothermal conditions. The composite material was tested for the degradation of MB under Xe lamp irradiation, and it showed a superior degradation rate compared to Degussa P25 or Bi_2S_3-TiO_2. The rate of degradation indicated that the Bi_2S_3-TiO_2 heterojunction/polymer fiber composites have good photocatalytic activity, recyclability, and stability under simulated solar irradiation. On the basis of significant finding, Bi_2S_3-TiO_2 heterojunction/polymer nanocomposite can be used for the photochemical degradation of organic pollutant.

Novel poly(vinyl alcohol)-titanium dioxide (PVA-TiO_2) mixed matrix membranes were prepared by incorporating nano-sized TiO_2 and PANI into PVA and cross-linking by adding glutaraldehyde (Ma et al. 2007; Toyao et al. 2013). The membranes were examined for their water uptake capacities and characterized to identify intermolecular interactions, the degree of cross-linking between the PVA matrix and glutaraldehyde, and the morphological and thermal differences between the filled and unfilled membranes. The dehydration of isopropanol by pervaporation was achieved using the membranes. To evaluate the extent of interaction and the degree of membrane swelling, sorption studies were performed in pure liquids as well as feed mixtures of water and isopropanol. It was also observed that with the addition of small amounts of TiO_2 into the cross-linked PVA membrane matrix, its selectivity increased to infinity. Four mixed matrix membranes were prepared, and their PV performances were compared with the unfilled, cross-linked PVA membrane. It was observed that among all the membranes, the un-cross-linked mixed matrix PVA-TiO_2-PANI-0.5 membrane showed the highest swelling characteristics. These novel, thermally stable membranes have enormous prospective uses in future applications for dehydrating isopropanol by pervaporation (Lu et al. 2005).

The photocatalytic degradation of methylene blue and rhodamine-B under visible radiation by the modification of TiO_2 with PANI (using the facile chemisorption approach) was reported (Zhang et al. 2008). The degradation rate was compared with P-25 TiO_2, and it was concluded that PANI/TiO_2 showed two times higher photocatalytic activity than TiO_2. The enhanced degradation was due to the synergic effect and rapid charge, which supported the transport potential of the photogenerated carrier on the PANI/TiO_2 interface. On the basis of its higher photocatalytic efficiency, the PANI/TiO_2 composite can be used for the purification of environmental samples. In the same way, other polyaniline-modified TiO_2 nanocomposites were synthesized for the photolytic degradation of organic pollutants (Amao and Komori 2003). The PANI/TiO_2 nanocomposite showed higher photocatalytic properties and stability than either pure TiO_2 or PANI in the liquid-phase degradation of MO under UV-vis radiation. The nanocomposite also indicated the degradation of 4-chlorophenol and MO in a longer wavelength range ($500\ nm < \lambda < 800\ nm$). As a consequence of good synergic effects between

polyaniline and TiO_2, the nanocomposite played an important role for the photocatalytic degradation and can be applied to the treatment of industrial organic pollutants (Lu et al. 2005).

A palladium/polymeric pyrrole-sodium film containing sodium dodecyl sulfonated titanium (Pd/PPy-SLS/Ti) was synthesized for use in electrodes via the electrochemically reductive dechlorination of 2,4-dichlorophenol (2,4-DCP) in an aqueous solution containing palladium and polymeric pyrrole (Wei et al. 2012). The effects of the dechlorination current and the initial pH of the solution were studied for the removal of chlorine and current efficiency. It was observed that effective removal of 2,4-DCP was achieved with 100% efficiency, while the current efficiency was 33.9% in the presence of 100 mg/L 2,4-DCP under an initial pH of 2.36, a dechlorination current of 5.0 mA, and a dechlorination time of 70 min. The intermediate products were 2-chlorophenol (2-CP) and 4-chlorophenol (4-CP), while the final product was mainly phenol. The stability of the electrode was found to be good, as 100% dechlorination efficiency was maintained after eight reuses. With its high effectiveness, this low cost, stable electrode demonstrated promise for prospective applications in dechlorination processes. Thus, it can be used for the treatment of industrial effluents. The details of some important nanocomposite ion-exchange materials in terms of synthesis, characterization, and their applications for the treatment of pollutants are shown in Tables 2 and 3.

Mechanistic Approach: How Nanoparticles Remediate Pollutants from Water

Photocatalytic Activity

The photocatalytic degradation depends upon the light-harvesting efficiency, the effectiveness of the reaction of the photogenerated electron/hole, and the reaction of photogenerated electron/holes with substrate molecules. The actual reaction occurs when nanocrystals are illuminated with light (light energy more than the band gap energy) and then produce electron/hole pairs. Further holes present in the valence band and electrons in the conduction band. A fraction of these charge carriers reach the crystal surface and react with water and oxygen to generate hydroxyl ($^{\bullet}OH$) and hydroperoxyl radicals ($^{\bullet}OOH$) which then initiate the degradation of the substrate (Bandekar et al. 2014). The photocatalytic degradation involves the generation of electrons (in conduction band) and holes (in valence bands) upon irradiation with UV or solar light (Ahmed et al. 2012). These photogenerated electrons and holes react with water and oxygen to generate hydroxyl ($^{\bullet}OH$) and hydroperoxyl ($^{\bullet}OOH$) radicals which are very reactive and can easily oxidize the substrate. A fraction of these radicals react with the adsorbed molecules resulting in to photocatalysis (Fernandez et al. 2010). The photocatalytic degradation (or oxidation) is rapid, easy, and a very effective method of substrate degradation (Firooz et al. 2011).

Table 2 Advanced techniques for the synthesis and characterization of nanocomposite ion-exchange materials and their applications for the treatment of pollutants

Name of nanocomposite	Synthesis route	Analyses	Applications	References
Poly-o-toluidine Ce(IV)	Sol-gel	UV-vis spectrophotometry, FTIR, SEM/EDX, TGA-DTA, TEM	Ion-selective membrane electrode for Cd^{2+} ions	Khan et al. (2011a, b)
Poly-*o*-toluidine Sn (IV) tungstate	Sol-gel	TEM	Separation of Hg^{2+}	Khan and Shaheen (2013)
PZTP	Sol-gel	AAS, XRD, SEM, TEM, FTIR, TG-DTA	Separation of Hg^{2+} and Pb^{2+}	Khan et al. (2011a, b)
			Ion-selective membrane electrode for Hg^{2+} ions	Khan et al. (2011a, b)
Poly-o-anisidine Sn(IV)	Sol-gel	FTIR, TGA, XRD, SEM, TEM,	Separation of Hg^{2}	Khan and Shaheen (2013)
		TEM	Ion-selective membrane electrode for Hg^{2+} ions	Khan et al. (2012)
PANI-TiW	Sol-gel	FTIR, XRD, SEM, TGA, CHNO, FAAS	Removal of Pb^{2+}, Hg^{2+}, Bi^{3+}, and Zr^{4+} ions	Nabi et al. (2011)
PANI-TiP	Sol-gel	FTIR, SEM, TGA-DTA	Ion-selective membrane electrode for Pb^{2+} ions	Khan et al. (2011a, b)
PANI-Ti(IV)As	Sol-gel	XRD, SEM, TEM	Separation of metal ions and photo-chemical degradation of organic dyes	Shahadat et al. (2012)
Nano-HT	Sol-gel	XRD, TEM	Separation of Cr^{6+}	Pérez et al. (2015)
CTS/REC nano-hybrid	Immobilization method	XRD, FTIR, SEM, TEM	Separation of Cd^{2+}, Cu^{2+}, and Ni^{2+}	Zeng et al. (2015)
DPDB	Sol-gel	SEM	Separation of Ce^{3+} ions	Awual et al. (2015)
PAMAM/G4-OH	Sol-gel	FTIR, XRD, SEM, TEM	Treatment of Cu^{2+}, Ni^{2+}, and Cr^{3+} ions from industrial wastewaters	Barakat et al. (2013)
PANI-Ti(IV)As(IV)P	Sol-gel	FTIR, XRD, SEM, TEM	Treatment of organic, inorganic pollut-ants as antimicrobial agents	Bushra et al. (2014)
NCA	Immobilization method	SEM	Treatment of Co^{2+} ions	Awual et al. (2015)
PPy/P25 or PPy/TiO_2	Sol-gel	XPS, TG, XRD	Removal of MB from the wastewater	Li et al. (2013)

NCA	Sol-gel	SEM, TEM	Co^{2+}	He et al. (2016)
NI/OS	Sol-gel	FTIR, SEM	As^{3+}	Alsohaimi et al. (2015)
HPNC	Sol-gel	SEM	Pb(II)	Nabi et al. (2011)
poly-o-toluidine stannic molybdate	Sol-gel	FTIR, TGA, DTA, XRD, SEM, TEM	Pb(II)	Cui et al. (2014)
SrHAp/Fe_3O_4	Sol-gel	FTIR, SEM, TEM	Pb(II)	Bushra et al. (2015)
PANI-Sn(IV) tungstomolybdate	Sol-gel	SEM, TEM, XRD	Pb(II)	Bushra et al. (2014)
M^{+2}/M^{+6}-LDH	Sol-gel	XPS, XRD, FTIR, SEM	Ion-selective membrane for Pb^{2+}	Mostafa et al. (2016)
SDS-AZS	Sol-gel	FTIR, XRD,TDA, SEM, TEM	Removal of Pb^{2+}	Naushad (2014)
Poly-o-toluidine zirconium (IV) iodosulphosalicylate	Sol-gel	FTIR, XRD, SEM, TEM, TGA	Removal of Cr^{3+}	Lutfullah et al. (2014)
Poly-o-toluidine zirconium (IV)tungstate	Sol-gel	FTIR, SEM, TEM, TGA, XRD	Ba^{2+}, Hg^{2+}, and Pb^{2+}	Bushra et al. (2012)
PZS	Sol-gel	FTIR, XRD, SEM, AFM	Pb^{2+}, Hg^{2+}, and Zr^{6+} ions	Shahadat et al. (2011)
Microtubes of PANI-TiO_2	Sol-gel	SEM, EDS, TEM, UV-vis	Photocatalytic activity	Xiong et al. (2004)
PANI-TiO_2	In situ oxidation	FTIR, UV-vis, XPS	Photocatalytic degradation	Zhang et al. (2006)
R_F-$(MES)_n$-$_F$/PANI/TiO_2, R_F-$(MES)_n$-R_F/An-TiO_2	In situ oxidation	FESEM, UV-vis	Photochromic activity	Sawada et al. (2011)
(PSU)/(SMA)-Bi_2S_3-TiO_2	Hydrothermal method	SEM, HRTEM, XRD, XPS	Photochemical degradation of MB	Ma et al. (2012)
PVA-TiO_2	Hydrothermal method	FTIR, XRD, DSC	Dehydration of isopropanol by pervaporation	Ma et al. (2007)
PANI-TiO_2	Chemisorption method	TEM, FTIR, TGA, UV-vis-diff. HRTEM, Raman	Photocatalytic degradation MB and Rh B	Zhang et al. (2008)
PANI-TiO_2	Hydrothermal method	XRD, TGA, FTIR, UV-vis.	Photocatalytic degradation industrial dyes	Amao and Komori (2003)
Pd/PPy-SLS/Ti	Electrode deposition method	FTIR, XRD, SEM, UV-vis, CV, GCD	Treatment of industrial effluents	Wei et al. (2012)
PAM/ZVP	Sol-gel	TEM, SEM, XRD, FTIR	Congo red dye	Sharma et al. (2016)

Table 3 Representative studies on the nano-materials-mediated removal of metals from water

Nanomaterials	Heavy metals	Absorbing capacity (mg/g)	Functional pH range	References
Aluminosilicate with Fe(II)	As(v)	10	5.5	Doušová et al. (2006)
Biochar-AlOOH	As(v)	17.41	7.5	Zhang and Gao (2013)
α-Fe_2O_3	As(III)	2.41	5.6	Mayo et al. (2007)
ZnO_2	As(III)	9.2	7.0	Cui et al. (2013)
CeO_2-ZrO_2	As(III)	40.7	–	Mayo et al. (2007)
CuI	Cd(II)	136	–	Gao et al. (2012)
AgNPs	Cd(II)	4.67	7	Zuo et al. (2015)
Nitrogen-doped magnetic carbon	Cr(III)	–	8	Shin et al. (2011)
$MnFe_2O_4$	Cr(IV)	31.5	2	Hu and Chen (2005)
Magnetic chitosan	Co(II)	27.5	–	Deng et al. (2003)
Multi-walled carbon nanotubes	As(III), Cd(II), Cu (II), Co(II), Cr(VI), Pb(II), Ni(II), Hg(II)	10–90	5	Di et al. (2006) Li et al. (2002) Tofighy and Mohammadi (2011) Atieh (2011)
Carbon nanotubes	Phenol Acid red Triton X series	–	2–12	Wiśniewski et al. (2012) Szlachta and Wojtowicz (2013) Jadhav et al. (2015)
TiO_2	Red azo die	87	–	Belessi et al. (2009)
ZrO_2	Methylene blue	0.5	7–9	Sandoval et al. (2011)
Fe_3O_4	Orange G Neutral red Cresol red Methyl blue	1883 2 6–35 6	6–8	Chang and Chen (2005) Zhang and Kong (2011)

The photocatalytic reaction has been studied since the photolysis of water by TiO_2 photocatalyst in 1972, and the photogenerated holes or OH radicals can be powerfully oxidized species to decompose and mineralize a large variety of organic compounds (Fonzo et al. 2009; Shang et al. 2010). In this view, nanocomposites have attracted extensive research attentions for many years (Guo et al. 2009). Numerous studies have concentrated on the degradation of toxic organic compounds present in wastewater via photocatalytic activity of various nanomaterials (Kim et al. 2004). The photocatalytic process is based on the generation of electron/hole pairs by means of bandgap radiation; the coupling of different semiconductor oxides seems useful to achieve a more efficient electron/hole pair separation under irradiation and, consequently, a higher photocatalytic activity (Wang et al. 2005). Among the photocatalysts, TiO_2, ZnO, and ferrite have been most widely investigated due to their acceptable photocatalytic activity and chemical stability,

non-environmental effect, and low cost. However, if the materials are prepared in nano-range (1.0–100 nm), their photocatalytic activity is enhanced because of the large enhancement of surface area. On the other hand, CuO, an important p-type narrow bandgap semiconductor, can be used to improve the photocatalytic efficiency of other nanomaterials. Recently, Sultana et al. (2015a, b) reported that SnO_2-SrO nanocomposites synthesized using hydrothermally method show superior photocatalytic activity because of their smaller size. The photocatalytic activity was improved due to the reduction in particle size of the materials which increases the surface to volume ratio. The photodegradation follows the pseudo-first-order kinetics. This improvement in photocatalytic activity was further explained by the fact that photogenerated holes in SnO_2 might get trapped within the SrO nanoparticles increasing charge separation and in turn suppressing the recombination of electron and holes thereby increasing the photocatalytic activity (Firooz et al. 2011). Nilchi et al. (2010) prepared TiO_2-SiO_2 in a 1:1 ratio for good photocatalytic activity as well as thermal stability. TiO_2 photocatalysts have been widely studied in the context of several applications, such as the purification of toxic compounds in polluted water and air, dye-sensitized solar cells, hydrogen production through photocatalytic water splitting, and self-cleaning and antifogging materials (Al-Ekabi and Serpone 1988; Asahi et al. 2001; Anpo and Takeuchi 2003; Jie et al. 2012; Kitano et al. 2012). Li and Wang (2010) worked on ZnO-CuO system for photodegradation of rhodamine B. Ag-TiO_2 nanostructure shows good electrochemical active behavior and fast electron transfer to electrode and hence can be employed for enhanced photodegradation and antibacterial activities (Crespilhoa et al. 2009). Tian et al. (2009) synthesized TiO_2/ZnO nanocomposite film via sol-gel process from directly mixing TiO_2/ZnO sol followed by heat treatment at 500 °C for 2 h in air and proposed that a heat treatment of 5 h is necessary for improving photocatalytic activity of the film for degrading methyl orange dye.

The photocatalytic activity of the nanomaterials can also be employed to explore their fuel cell potential since certain nanomaterials can use sunlight or UV in order to produce fuels such as H_2 and electricity from abundant, nontoxic resources and to decompose environmental pollutants with benign catalysts that would revolutionize our civilization (Wang et al. 2009; Lianos 2011). A recent and quite similar concept has been developed through an alternative nonbiological system in which energy is harvested through oxidation (degradation) of an organic species and termed as photoelectrochemical fuel cell (Lianos 2011; Liu et al. 2011; Kaneko et al. 2012). Kaneko et al. (2006) developed a system that generates electricity via the photoelectrochemically decomposition of various biomass derivatives by employing UV light irradiation of a nano-porous TiO_2 thin-film photoanode and oxygen reduction to form H_2O at a Pt cathode. Raman and Lan (2012) have used even the photomicrobial fuel cell for electricity generation from organic compounds. Sambandam et al. (2009) have used platinum-carbon black-titanium dioxide for fuel cell applications. The following are the series of reactions involved in a photocatalytic fuel cell formed by the combination of a photoreactor and an electrochemical cell (Canterino et al. 2009; Cairns et al. 2011). This is achieved

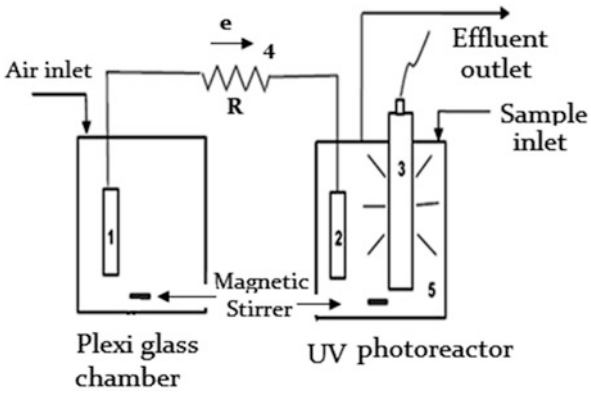

Fig. 1 Schematic of the photocatalytic fuel cell for the proposed work. (*1*, *2*) Electrodes. (*3*) UV lamp. (*4*) Resistance. (*5*) Suspension of nanoparticles containing toxic substrate (Adapted from Canterino et al. 2009)

by combining a photoreactor (based on UV or solar radiation) with an electrochemical half-cell as shown in Fig. 1 (Canterino et al. 2009). It provides many solutions to problems facing industries in the pharmaceutical, biotechnological, oil, energy, and food and drink sectors.

$$\mathrm{TiO_2} \xrightarrow{h\gamma} h\gamma^{\oplus} + e^{-}$$
$$\mathrm{ORG} + h\gamma^{\oplus} \rightarrow \mathrm{ORG}^{+}$$
$$M^{(n+1)+} \rightarrow M^{n+}$$

The above reaction sequence can be utilized for contaminant degradation and electricity generation since the two half-cells would give energy unless and until the concentration of species becomes equal on both sides. When such condition occurs, more substrate can be given to reinitiate the whole process. Canterino et al. (2009) used Cu-TiO_2 for organic removal and electricity generation.

Sorption Behavior

Nanomaterials have a potential for wastewater remediation due to their high treatment efficiency, low cost, and flexibility of applications (both in situ and ex situ). In case of nanomaterials, sorption basically refers to adsorption since they are widely used as effective adsorbents for wastewater decontamination (Farghali et al. 2010). The phenomenon of adsorption is the physical adherence of liquid or gas on the surface of a solid due to the force of attraction of molecules present at the surface, thereby creating a thin film on the solid surface (Yang and Xing 2010). In case of absorption, the fluid permeates into the bulk of the solid. Due to the large number of free valences, nanomaterials show superior adsorption properties which render their use in the field of water purification (Sultana et al. 2012). Moreover, it finds use in

tertiary wastewater treatment as a polishing step before final discharge into natural water bodies. The adsorption is however a very complicated phenomenon involving many different properties such as grain-size distribution, specific surface area, and ion-exchange capacity (Delle Site 2001). The heat of adsorption is an important parameter controlling the adsorbate-adsorbent bond strength as well as the thermodynamic stability of the complex (Hörtz et al. 2015). In general, theory states that adsorption depends upon two aspects – adsorption capacity and affinity. The former is defined as the potential space available for adsorption of the solute (adsorbate), while the latter depends upon the strength of attractive forces between the two (Yang and Xing 2010). Similarly, zeolites are the porous aluminosilicates, an ideal material for sequestering metal ions from contaminated water (Larsen 2007). Granular activated carbon (GAC) is also considered to be the best adsorbent for removing organics present in wastewater (Nishijima et al. 1997). However, its adsorption properties decrease once all the sites are occupied, and therefore, biological granular activated carbon (BGAC) can remove contaminant effectively (Aktas and Cecen 2007; Xing et al. 2008). Nabi et al. (2011) designed a novel and highly selective polyaniline-zirconium(IV)sulfosalicylate cation exchanger for selective recovery of heavy metals such as Pb(II), Hg(II), Zr(IV), etc. Many researchers have reported sorption of the radionuclides Eu(III) using metal hydroxide and clay materials as adsorbent to a function of ionic strength, temperature, and solution concentration. However, the main challenge with these types of adsorbents is the low sorption capacity. There must be a stringent demand for development of low-cost and effective adsorbent with high sorption capacity. Likewise, graphene oxides, due to its high surface to volume ratio along with large amount of oxygen-containing functional groups, can be used as an excellent adsorbent. Several other carbon nanoparticles (e.g., fullerenes, single and multi-walled carbon nanotubes) with excellent sorption properties can be employed in water treatment and solid-phase extraction (Kaur and Gupta 2009; Huck and Bonn 2000). They can be used for enhanced removal of polycyclic aromatic hydrocarbons (PAHs) as well as, e.g., naphthalene, phenanthrene, pyrene, etc. (Yang et al. 2006). Sultana et al. (2012) reported that the rate of adsorption of PANI increases by doping copper ferrite nanocomposites due to their high surface area. They further reported that rate of adsorption depends upon the amount of adsorbent, pH of the medium, temperature, surface area of the adsorbent, etc. Sometimes adsorption is coupled with air oxidation for complete destruction and removal of contaminants (Delmas et al. 2002). In recent years, various groups have investigated the application of metal nanoparticles for carbon dioxide sequestration or clean energy storage (Kang et al. 2015). Many nanomaterials based on metal-organic framework with mesoporous structures are an excellent base material for carbon dioxide adsorption (Furukawa et al. 2013; Kang et al. 2015). They offer high degree of porosity, large surface area, and uniform pore size which render their application in gas storage, chemical separation, sensing, and drug delivery (Li et al. 2009; Chen et al. 2010). Single-crystal adsorption calorimetry (SCAC) is a recently developed technique for comprehensive study of the cover-dependent molar heat of adsorption which in turn provides information about the thermodynamics of adsorption (Schießer et al. 2010; Fischer-Wolfarth et al. 2011; Hörtz et al. 2015).

Chelation

The synthesis of chelate-based nanomaterials has been attracting considerable interest for the removal and recovery of trace elements from environmental wastewaters (Fontanals et al. 2010; Matsuoka and Yoshimura 2010). Flame atomic absorption spectrophotometry coupled with preconcentration procedures is considered as an advantageous technique owing to its simple detection system based on flame atomization instead of flameless techniques, which require more expensive equipment and are found usually much more sensitive to interferences from the matrix (DeMartino et al. 2010; Gregusova and Docekal 2011). The selective removal of toxic metal ions and the recovery of precious metal ions in terms of environmental protection and economic consideration are of great significance (Pyrzynska 2005; Qian et al. 2010). Chelating materials suited to perform this task should possess significant selectivity, enhanced hydrophilicity (Islam et al. 2010a, b, c; Pyrzynska and Trojanowicz 1990), better metal loading capacity, and recyclability. The selectivity of chelating agents depends on the nature of immobilized multidentate ligands, degree of cross-linking the pH of the solution, as well as the type of metal ions (Tobiasz et al. 2009; Islam et al. 2010a, b, c; Panahi et al. 2009). The hydrophobicity of chelating material may rise above by introducing hydrophilic functional groups and increasing their surface area metal ions which facilitates efficient adsorption (Prabhakaran and Subramanian 2003a, b). The ion uptake efficiency of chelating materials can be enhanced by increasing the number of chelating sites as well as the accessibility of metal ions to these sites.

Amberlite XAD adsorbents have potential to form chelating agents with metal ions. These agents are porous spherical polymers based on highly cross-linked, macroreticular polystyrene, aliphatic, phenol-formaldehyde condensate polymers. On the basis of polymeric matrix, it may be divided into two main groups: (i) polystyrene-divinylbenzene-based resins including XAD-1, XAD-2, XAD-4, XAD-16, XAD-1180, XAD-2000, and XAD-2010 and (ii) polyacrylic acid ester-based resins including XAD-7, XAD-8, and XAD-11 (Kara et al. 2005, 2006). Some important physical characteristics in terms of surface area (m^2/g), particle size (mesh), and pore size (Å) of these adsorbents are shown in Table 4. These ion-exchange resins can be modified to chelating agents by using a number of the following methods:

Surface Modification

It is one of the simplest ways to fictionalize the surface of Amberlite XAD-2 using various chelating agents. The analysis of Cu(II) and Ni(II) ions was carried out loading calmagite reagent with Amberlite XAD-2 loaded with (Ferreira et al. 2000a, b) 2-(2-benzothiazolylazo)-2-p-cresol (Ferreira et al. 2001), and a detection limit (3 σ) of 0.15 mg/L and 1.1 μg/L was observed, respectively. Poor distribution coefficients (K_d value) were found for La(III) and Nd(III) ions by using Amberlite

Table 4 XAD adsorbent physical characteristics in terms of surface area, particle size, and pore size

Amberlite	Matrix	Surface area (m^2/g)	Particle size (mesh)	Pore size (Å)
XAD-2	Styrene-divinylbenzene	300	20–60	90
XAD-4	Styrene-divinylbenzene	750	20–60	100
XAD-7	Aliphatic ester	500	20–60	450
XAD-8	Acrylic ester	140	40–60	250
XAD-16	Styrene-divinylbenzene	800	20–60	200
XAD-1180	Styrene-divinylbenzene	500	20–60	400
XAD-2000	Styrene-divinylbenzene	600	20–60	45
XAD-2010	Styrene-divinylbenzene	660	20–60	280

XAD-2 resin impregnated with Cyanex272 {bis (2,4,4-trimethylpentyl) phosphinic acid} and Cyanex302 {bis (2,4,4-trimethylpentyl) monothiophosphinic acid}; however, U(VI) was quantitatively sorbed from 1×10^{-3} mol/L HNO_3 followed by its recovery with 1.0 mol/L HCl from the solid phase (Karve and Rajgor 2008). The proposed method was found simple, selective, and reproducible for the detection of U(VI) with a relative standard deviation of 0.4%. The Later, prepared A batch method was employed to form chelating resin impregnated, Amberlite-XAD-2 with Cyanex272, for the analysis of U(VI) in aqueous solution (Karve and Pandey 2012). The maximum sorption capacity for U(VI) was achieved at 0.168 mmol/g. In addition, sorption equilibrium data for the treatment of U(VI) was well fitted with Langmuir and Freundlich isotherm models.

Chemical Modification

The extensive applications for the treatment of environmental samples were also performed by the chemical modification of Amberlite. In this method, the resin is bonded covalently with different functional groups. The preconcentration of Cd, Hg, Ag, Ni, Co, Cu, and Zn ions was demonstrated by the covalent bonding of Amberlite XAD-2 with 2-(methylthio)aniline and 2-aminoacetylthiophenol through a -NN-NH- group (Guo et al. 2004a, b). A number of physicochemical parameters were also determined, namely, the distribution coefficient and sorption capacity, effect of pH and flow rates of uptake and stripping, as well as effect of effluent concentration and volume of eluent. In terms of practical applicability, the modified resin was effectively used for the treatment of tap water and river water samples. A new azo coupling (-NN-) resin (Amberlite XAD-2-2-aminothiophenol) was used for the determination of Cd(II) and Cu(II) ions (Lemos and Baliza 2005). The enrichment factors for Cd(II) and Cu(II) were found to be 28 and 14, respectively, at the preconcentration time of 60 s while 74 and 35 for preconcentration time of 180 s. The method was applied for the analysis of Cd(II) and Cu(II), in

natural, drinking, and tap water samples. Other functionalized resins (Amberlite XAD-2-Nitroso-R salt (Lemos et al. 2003a), Amberlite XAD-2-3,4-dihydroxybenzoic acid (Lemos et al. 2003b), and Amberlite XAD-2-4,5-dihydroxy- 1,3-benzenedisulfonic acid (Lemos et al. 2005, 2006) have been modified for the determination of Co(II), Cu(II), and Ni(II) ions. The accuracy of the methods was evaluated by the analysis of metal ions in food samples and natural water samples. Tewari and Singh have modified Amberlite XAD-2 with pyrocatechol and thiosalicylic acid for the treatment of Cd(II), Co(II), Cu(II), Fe(III), Ni(II), Zn(II), and Pb(II) using FAAS (Tewari and Singh 2001, 2002). A novel azocalix[4] pyrrole Amberlite XAD-2 polymeric chelating resin was modified for extraction, preconcentration, and sequential separation of Cu(II), Zn(II), and Cd(II) ions using column chromatography prior to their determination by UV-vis spectrophotometry (Jain et al. 2009). The proposed method was effectively used for the analysis of Cu (II), Zn(II), and Cd(II) ions in real water samples. Amberlite XAD-2 functionalized palmitoyl-8-hydroxyquinoline using a modified procedure through chloromethylation (Doğutan et al. 2003). Column method was applied for the preconcentration of Mn(II) from synthetic and seawater samples. The preconcentration factor was 60 with the modified resin together with detection limits (LOD) of spectrophotometry and FAAS for Mn ions (i.e., 17 and 12 μg/L, respectively) which were significantly reduced. However, this method was not adversely affected from high ionic strength media for preconcentration of Mn(II), and the method was found suitable for detection of Mn(II) ions in seawater. Preconcentration and separation of vanadium species in synthetic and seawater were determined using Amberlite XAD-2 copolymer resin with palmitoyl quinolin-8-ol (Filik et al. 2004). Both V(IV) and V(V) ions were adsorbed and preconcentrated onto modified resin and quantitatively eluted from the column using HCl as stripping agent which was analyzed using both spectrophotometer and FAAS. Another chelating Amberlite XAD-2 resin was modified with iminodiacetic acid for the analysis of Cd(II) ions followed by FAAS (Badrinezhad et al. 2012). The material demonstrated 90% recovery of metal ions at pH 7.5, and the proposed method achieved significant accuracy, enrichment factor, preconcentration factor, and simplicity. Batch and column methods were applied for the exclusion of Cd(II), Cr(III), and Pb(II) ions by using modified Amberlite XAD-2 with purpurin from cement-based material and deionized water (Wongkaew et al. 2008). The proposed method gave 86.5% and 89.9% recovery for Cd(II) and Pb(II) ions and RSD less than 2.3% ($n = 14$). The modification of Amberlite XAD-2 was carried out using calcein blue dye for the analysis of Cu (II) ions (Moniri et al. 2011). The sorption capacity of modified resin was 27 mg/g with ten regeneration cycles without any significant loss in capacity. Sorption capacities of some important modified resins are shown in Table 5. Besides the surface and chemical modifications of XAD-2 with different reagents, the modifications of other resins (XAD-4, XAD-16, XAD-1180, XAD-2000, and XAD-2010) are shown in Tables 6, 7, and 8.

Table 5 Sorption capacities of modified resin (XAD-2) using different chelating agents

Reagent	Analyses	Metal ions	Sorption capacity (mgg^{-1})	References
Tiron	FAAS	Cu^{2+}, Cd^{2+}, Co^{2+}, Ni^{2+}, Pb^{2+}, Zn^{2+}, Mn^{2+}, Fe^{3+}, UO^{2}_{2+}	14.0, 9.5, 6.5, 12.6, 12.6, 11.1, 10.0, 5.6, 7.7	Kumar et al. (2000a, b)
Thiosalicylic acid	FAAS	Cd^{2+}, Co^{2+}, Cu^{2+}, Fe^{3+}, Ni^{2+}, Zn^{2+}	22.2, 6.3, 13.9, 3.7, 18.2, 3.1	Tewari and Singh (2000a, b)
Pyrogallol	FAAS	Cu^{2+}, Cd^{2+}, Co^{2+}, Ni^{2+}, Pb^{2+}, Zn^{2+}, Mn^{2+}, Fe^{3+}, U^{4+}	4.53, 5.22, 4.10, 4.09, 6.71, 4.54, 4.51, 4.62, 4.49	Kumar et al. (2001)
Calmagite	FAAS	Cu^{2+}	0.1009	Ferreira et al. (2000a, b)
o-Aminophenol	FAAS	Cu^{2+}, Cd^{2+}, Co^{2+}, Ni^{2+}, Zn^{2+}, Pb^{2+}	3.37, 3.42, 3.29, 3.24, 2.94, 3.32	Kumar et al. (2000a, b)
2-(Methylthio)aniline	FAAS	Cd^{2+}, Hg^{2+}, Ni^{2+}, Co^{2+}, Cu^{2+}, Zn^{2+}	23.67, 37.87, 14.07, 10.35, 8.83, 8.46	Guo et al. (2004a)
2-Aminoacetylthiophenol	ICP-AES	Cd^{2+}, Hg^{2+}, Ag^{2+}, Ni^{2+}, Co^{2+},C^{2+}, Zn^{2+}	21.40, 48.70, 37.29, 17.60, 19.19, 24.07, 19.59	Guo et al. (2004b)
2-Aminothiophenol	FAAS	Cd^{2+}, Cu^{2+}	382.16, 292.10	Lemos and Baliza (2005)
Nitroso R salt	FAAS	Co^{2+}	0.0	Lemos et al. (2003a, b)
Azocalix[4]pyrrole A	FAAS	Cu^{2+}, Zn^{2+}, Cd^{2+}	20.20, 11.42, 18.86,	Jain et al. (2009)
Azocalix[4]pyrrole B	FAAS	Cu^{2+}, Zn^{2+}, Cd^{2+}	27.25, 14.40, 19.63	Jain et al. (2009)
Pyrocatechol	FAAS	Cd^{2+}, Co^{2+}, Cu^{2+}, Fe^{3+}, Ni^{2+}, Zn^{2+}	4.59, 1.35, 5.87, 4.10, 3.11, 1.85	Tewari and Singh (2001)
Chromotropic acid	FAAS	Pb^{2+}	38.60	Tewari and Singh (2002)

(continued)

Table 5 (continued)

Reagent	Analyses	Metal ions	Sorption capacity (mgg^{-1})	References
Pyrocatechol	FAAS	Pb^{2+}	21.69	Tewari and Singh (2001)
Thiosalicylic acid	FAAS	Pb^{2+}	18.50	Tewari and Singh (2001)
Xylenol orange	FAAS	Pb^{2+}	3.50	Tewari and Singh (2001)
Palmitoyl quinolin-8-ol	Spectrophotometric	Mn^{2+}	1.64	Doğutan et al. (2003)
Cyanex272	Spectrophotometric	U^{6+}	39.98	Karve and Pandey (2012)
Purpurin	FAAS	Cd^{2+}, Cr^{3+}, Pb^{2+}	8.43, 3.54, 17.13	Wongkaew et al. (2008)
Calcein blue	FAAS	Cu^{2+}	27.0	Moniri et al. (2011)
Pyrocatechol	FAAS	Cd^{2+}, Co^{2+}, Cu^{2+}, Ni^{2+}	4.01, 1.65, 1.99, 1.43	Lemos et al. (2006)

Binding of Modified Amberlite XAD with Metal Ions

The modified resins with chelating reagents contain a number of donor ligands (-N, -P, -O, -S) that have capability in sorption of heavy metal ions. These ligands including hydroxyl, carboxylic, sulfonic, phosphonic, azo, and amine play a key role to donate the electron pair toward metal ions. The chemical or physical properties of a complex have been recognized by the interaction of electronic and steric properties of the resin; however, the prediction remains very difficult owing to the considerable diversity encountered within different metal centers toward the same ligand, or different ligands can completely modify the chemistry of a metal. This interaction provides significant characteristics of metal complexes toward the sorption of metal ions. The sorption behavior of chelating resin depends on the nature of adsorbent adsorbate, size, charge, surface, pH and temperature, as well as solution conditions (Yang and Xing 2010; Kumar and Ahmad 2011). Various types of interaction (e.g., hydrogen bonding, electrostatic interaction, surface complexation and van der Waal forces, ion exchange) are also responsible for the sorption of metal ions onto the chelating resin. In addition, the carboxylic and phenolic are considered as the major groups for the sorption of metal ions (by the proton exchange) (Kumar et al. 2014; Liu et al. 2013). A schematic diagram of modified resin with metal ions is shown in Fig. 2.

Table 6 Sorption capacities of modified resin (XAD-3) using different chelating agents

Reagent/Organisms	Analyses	Metal ions	Sorption capacity (mg/g)	References
8-Hydroxyquinoline (Oxine)	Spectrophotometry	UO_2^{2+}	0.0	Singh and Maiti (2006)
o-Aminobenzoic acid	FAAS	Pb^{2+}, Cd^{2+}, Co^{2+}, Ni^{2+}, Zn^{2+}	12.22, 8.99, 5.36, 7.10, 7.58	Çekiç et al. (2004)
2,3-Dihydroxy-naphthalene	ICP-AES	Cu^{2+}, Ni^{2+}, Co^{2+}, Cd^{2+}		Hemasundaram et al. (2009)
Ammonium pyrrolidine-dithiocarbamate	ICP-AES	Cd^{2+}, Cu^{2+}, Mn^{2+}, Ni^{2+}, Pb^{2+}, Zn^{2+}	9.47, 11.08, 8.62, 7.21, 10.25, 10.62	Ramesh et al. (2002)
Piperidine dithiocarbamate (pipDTC)	ICP-AES	Cd^{2+}, Cu^{2+}, Mn^{2+}, Ni^{2+}, Pb^{2+}, Zn^{2+}	9.18, 10.76, 8.17, 7.46, 9.86, 10.28	Ramesh et al. (2002)
2-Acetylmercapto-phenyldiazoaminoazobenzene	FAAS	Cd^{2+}, Co^{2+}, Cu^{2+}, Ni^{2+}, Zn^{2+}	20.23, 5.89, 6.03, 9.97, 3.92	Liu et al. (2005)
2,6-Dihydroxyphenyl-diazoaminoazobenzene	FAAS	Cd^{2+}, Co^{2+}, Cu^{2+}, Zn^{2+}	20.23, 9.42, 12.38, 10.46	Liu et al. (2007a, b)
Diethyldithiocarbamates	FAAS	Cu^{2+}, Fe^{2+}, Pb^{2+}, Ni^{2+}, Cd^{2+}, Bi^{2+}		Uzun et al. (2001)
1-Hydrazinophthalazine	AAS	Cu^{2+}, Ni^{2+}, Co^{2+}, Zn^{2+}, Cd^{2+}, Pb^{2+}, Fe^{3+}, Cr^{3+}	78.74, 48.12, 50.09, 48.38, 107.90, 178.10, 73.70, 32.23	Lemos et al. (2008a, b)

(continued)

Table 6 (continued)

Reagent/Organisms	Analyses	Metal ions	Sorption capacity (mg/g)	References
1-(2-Pyridylazo)-2-naphthol	FI-FAAS	Cu^{2+}		Yebra et al. (2001)
1-(2-Pyridylazo)-2-naphthol	AAS	Cd^{2+}, Cu^{2+}, Ni^{2+}, Pb^{2+}, Cr^{3+}, Mn^{2+}		Tuzen et al. (2005)
Salen	AAS	Cu^{2+}, Pb^{2+}, Bi^{2+}	17.3, 26.9, 39.5	Kim et al. (2005)
Succinic acid	Spectrophotometry	U^{6+}	12.3	Metilda et al. (2005)
Schiff bases	FI-FAAS	Cd^{2+}, Co^{2+}, Cu^{2+}, Ni^{2+}, Pb^{2+}		Kara et al. (2009)
O,O-diethyl dithiophosphate	FI-FAAS	Cd^{2+}		dos-Santos et al. (2005)
m-Phenylenediamine	ICP-AES	Rh^{3+}	26.34	Panahi et al. (2009)
2,3-Diaminonaphtalene		Se^{6+}	3.4	Depecker et al. (2009)
2-Aminothiophenol	FAAS	Cd^{2+}, Ni^{2+}	3.20, 1.39	Lemos et al. (2008a, b)
Maleic acid	AAS	Cr^{3+}	3.90	Yalçin and Apak (2004)
Bacillus subtilis	FAAS	Cu^{2+}, Cd^{2+}	1.88, 3.93	Dogru et al. (2007), Kirstein and Turgay (2005)
Diphenylcarbazide complex	UV-vis spectrophotometer	Cr^{3+}	0.85	Rajesh et al. (2008)
Aliquat-336	UV-vis spectrophotometer	La^{3+}, Gd^{3+}	4.73, 4.44	El-Sofany (2008)
Salicylic acid	FAAS	Pb^{2+}, Cu^{2+}, Ni^{2+}, Co^{2+}, Zn^{2+}	78.12, 74.04, 72.99, 73.20, 74.07	Khazaeli et al. (2013)
Catechol	ICP-AES	Cd^{2+}, Cu^{2+}, Ni^{2+}, Pb^{2+}	2.89, 5.69, 2.87, 6.25	Bernard et al. (2008)

(continued)

Table 6 (continued)

Reagent/Organisms	Analyses	Metal ions	Sorption capacity (mg/g)	References
Monoaza dibenzo 18-crown-6-ether	ICP-AES	La^{3+}, Nd^{3+}, Sm^{3+}	9.17, 9.05, 8.08	Dave et al. (2010)
A. tumefaciens	FAAS	Mn^{2+}, Co^{2+}	1.20, 1.70	Baytak and Türker (2005)
Allylphenol	FAAS	Cu^{2+}	106.38	Nezhati et al. (2010)
N,N-bis(salicylidene) cyclohexanediamine	FAAS	Cu^{2+}, Pb^{2+}, Ni^{2+}	22.74, 28.77, 11.93	Topuz and Macit (2011)
1-(2-Thiazolylazo)-2-naphthol	NAA	Cu^{2+}	8.0	Goodwin et al. (2013)
Geobacillus thermoleovorans subsp. stromboliensis	FAAS	Cd^{2+}, Ni^{2+}	4.19, 3.26	Özdemir et al. (2010a, b)
Bacillus sp.	UV-vis spectrophotometry	Th^{4+}	17.24	Özdemir et al. (2010a, b)

Composite Materials as Pollutant Sensors

Nanocomposite materials are also widely used for the detection of toxic gases and vapors and for the identification of several other compounds. A sensor is a device that provides specific quantitative and analytical information in connection to a change in measureable property with respect to change in the surrounding environment (Teles and Fonseca 2008). Sharma et al. (2002) synthesized copper/polyaniline for sensing chloroform vapor at ppm level. Graphene oxide (GO) can be used for potential applications in nanoelectronic, nanosensing, and nanoelectrochemical devices (Berger et al. 2004; Xu et al. 2010, Khan et al. 2016). Carbon nanotubes can be used as electrochemical sensors with high sensitivity, accuracy, and detection limit (Iijima 1991). However, PANI-based nanocomposites showing different colors for different oxidation states can also be used as versatile sensors (Bredas and Street 1985). PANI-coated fluorine-doped tin oxide can be used to detect the optochemical response (Mello and Mulato 2015). Even biodegradable natural polymers such as protein, chitin, and chitosan-doped nanocomposites can be used for the fabrication of electrical, electronic, and chemical sensors (Shukla 2002). PANI/PMMA-based composite fibers show high sensitivity for ammonia gas sensors (Zhang et al. 2014). Wang et al. (2010) developed organic-inorganic nanocomposites comprising ZrO_2-chitosan-Au for amperometric

Table 7 Sorption capacities of modified resin (XAD-16) using different chelating agents

Reagent	Analyses	Metal ions	Sorption capacity (mg/g)	References
1,6-Bis(2-carboxy aldehyde phenoxy)butane	FAAS	Cu^{2+}, Cd^{2+}	5.38, 4.43	Oral et al. (2011)
2,6-Dichlorophenyl-3,3-bis (indolyl)methane	FAAS	Cu^{2+}, Zn^{2+}, Mn^{2+}	70.6, 64.3, 60.1	Ghaedi et al. (2010)
Gallic acid	FAAS	Cr^{3+}, Mn^{2+}, Fe^{3+}, Co^{2+}, Ni^{2+}, Cu^{2+}	11.22, 9.88, 22.50, 16.55, 14.67, 21.84	Sharma and Pant (2009)
4-{[(2-Hydroxyphenyl) imino] methyl}-1,2-benzenediol	FAAS	Zn^{2+}, Mn^{2+}, Ni^{2+}, Pb^{2+}, Cd^{2+}, Cu^{2+}, Fe^{3+}, Co^{2+}	10.98, 6.09, 13.20, 21.75, 6.29, 26.35, 18.98, 14.49	Venkatesh and Singh (2007)
Acetylacetone	AAS	Cr^{3+}, Cr^{6+}	779.84, 977.41	Memon et al. (2009), Singh et al. (2008)
3,4-Dihydroxy benzoyl methyl phosphonic acid	FAAS	U^{6+}, Th^{4+}	395.11, 350.36	Maheswari and Subramanian (2005)
Phthalic acid	AAS	Pb^{2+}	40.0	Memon et al. (2005)
N,N-dibutyl-N-benzoylthiourea		U^{6+}	214.21	Merdivan et al. (2001)
(Bis-2,3,4-trihydroxybenzyl) ethylenediamine		U^{6+}, Th^{4+}, Pb^{2+}, Cd^{2+}	340.36, 276.11, 209.27, 87.67	Prabhakaran and Subramanian (2003a, b, 2005)
Thiocyanate	FAAS	Ag^{2+}	4.66	Tunçeli and Türker (2000a, b)
1,5-Diphenylcarbazone	FAAS	Cr^{6+}	0.40	Tokalıoğlu and Livkebabc (2009)
Nitrosonaphthol	AAS	Ni^{2+}, Cu^{2+}	605.79, 352.14	Memon et al. (2007)
Iodide complex	FAAS	Pd^{2+}	35.6	Tunçeli and Türker (2000a, b), Sabermahani and Taher (2010)
(Salicylaldehyde calix[4] resorcinarenes)	AAS	Cu^{2+}, Co^{2+}, Ni^{2+}, Cd^{2+}	68.5, 61.9, 61.9, 62.5	Ghaedi et al. (2009)

(continued)

Table 7 (continued)

Reagent	Analyses	Metal ions	Sorption capacity (mg/g)	References
2-{[1-(3,4-Dihydroxyphenyl) methylidene] amino}benzoic acid	FAAS	Zn^{2+}, Mn^{2+}, Ni^{2+}, Pb^{2+}, Cd^{2+}, Cu^{2+}, Fe^{2+}, Co^{2+}	12.94, 9.77, 15.78, 26.52, 10.90, 29.71, 28.75, 13.02	Venkatesh and Singh (2005)
Pleurotus eryngii	ICP-OES	Cd^{2+}, Co^{2+}	11.3, 9.8	Özdemir and Kilinc (2012)
N,N-dibutyl-N1-benzoylthiourea	AAS	Ag^{+}	12.40	Ayata et al. (2009)
3-Hydroxyphosphinoyl-2-oxo-propyl)phosphonic acid dibenzyl ester	Spectrophotometer and fluorescence spectrophotometer	U^{6+}, Th^{4+}, La^{3+}	328.46, 308.59, 104.25	Prabhakaran and Subramanian (2004)
Glyoxal-bis (2-hydroxyanil)	FAAS	Al^{3+}	24.28	Islam et al. (2013a, b)
2-(2-Hydroxyphenyl) benzoxazole	FAAS	Al^{3+}	21.58	Islam et al. (2014)

sensing of H_2O_2. Prabhakar et al. (2011) prepared polyurethane-based PANI/Ag nanocomposites to be used as electrochemical sensors. The materials were biocompatible and can be used in biomedical applications. Ansari and Mohammad (2011) developed p-toluenesulfonic acid-based polyaniline-TiO_2 nanocomposite with outstanding electrical conductivity, superior thermal stability, and exceptional ammonia-sensing ability. PANI/Cu nanocomposites can be used for chloroform sensing application (Sharma et al. 2002), while polyacrylate-nanoclay composites offer high gas selectivity (Bhole et al. 2007). Modified resins have been successfully used in the treatment of industrial wastewaters. The successful applications of resins require the fundamental relationship among the structural modifications as well as its physicochemical properties. In this regard, Mohan and Srivastava (1997) highlighted the study of various epoxy resins and curing agents. Further, the modification of epoxy resins and curing agents is well documented in various literatures, which also demonstrated flame resistance, adhesive property, thermal property, and chemical stability of epoxy resins (Mohan 2013). The important roles of chelating agents in various industries confirm its significance and commercial value which led to its presence in various streams that need to be treated up to standards for drinking and industrial discharge water according to the WHO and various regulatory organizations that set similar standards worldwide. Moreover, polymer nanofibers based on PANI, polypyrrole (Ppy), etc. can be used as

Table 8 Modification of other Amberlite XAD with chelating agents

Reagent	Analyses	Metal ions	Sorption capacity (mg/g)	References
XAD-7 Toluidine blue o	Spectrophotometry	Cr^{6+}	20.62	Hosseini-Bandegharaei et al. (2010)
Diamino-4-(4-nitro-phenylazo)-1H-pyrazole	FAAS	Ni^{2+}	7.2	Ciftci et al. (2010)
Brilliant green	Spectrophotometry	Cr^{6+}	5.45	Hosseini et al. (2009)
XAD-1180 1-(2-Thiazolylazo)-2-naphthol	FAAS	Cu^{2+}, Ni^{2+}, Cd^{2+}, Mn^{2+}	0.77, 0.41, 0.57, 0.30	Tokalıoğlu et al. (2009)
Di(2-ethylhexyl)phospho-ric acid	UV-visible spectrophotometer	Bi^{3+}	490.7	Belkhouche and Didi (2010)
Pyrocatechol violet	GFAAS	Al^{3+}	0.59	Narin et al. (2004)
XAD-2000 Diethyldithiocarbamate	FAAS	Cu^{2+}, Fe^{3+}, Zn^{2+}, Mn^{2+}, Cd^{2+}, Pb^{2+}, Ni^{2+}, Co^{2+}	5.63, 5.40, 4.80, 4.76, 4.41, 6.42, 3.80, 6.08	Bulut et al. (2007a, b)
o-Phenylene dioxydiacetic acid	UV-vis Spectrophotometer	U^{6+}, Th^{4+}	28.80, 26.21	Seyhan et al. (2008)
Ammonium pyrrolidinedithiocarbamate	FAAS	Co^{2+}, Cu^{2+}, Cd^{2+}, Ni^{2+}	6.1, 6.4, 6.2, and 6.3	Duran et al. (2009)
α-Benzoin oxime	Spectrophotometry	U^{6+}, Th^{4+}, Zr^{4+}	3.6, 3.3, 2.6	Ghasemi and Zolfonoun (2010)
XAD-2010 Sodium diethyldithiocarbamate	FAAS	Cr^{6+}	4.40	Bulut et al. (2007a, b)
Sodium diethyldithiocarbamate	FAAS	Mn^{2+}, Co^{2+}, Ni^{2+}, Cu^{2+}, Cd^{2+}, Pb^{2+}	5.9, 6.0, 6.1, 6.3, 6.0, 5.7	Duran et al. (2007a, b)

ammonia, NO, and pH sensors (Long et al. 2011). Lu et al. (2009) prepared single and multiple poly(3,4-ethylenedioxythiophene) nanowires. Zhang et al. (2007) prepared poly(methyl vinyl-ether-alt-maleic acid)-doped PANI nanotubes for oligonucleotide sensors. Conducting nanoparticle sensors based on polymer matrix is employed to detect food-borne pathogens (Arshak et al. 2007; Liu et al. 2007a, b). Mills and Hazafy (2009) prepared nanocrystalline SnO_2 and reported its use as a photosensitizer in a colorimetric detection of oxygen gas. Thus, a large group of nanomaterials and polymer-based nanocomposites have been developed for sensing various gases/chemicals. The area can be explored further for proper development and commercialization of electrical, electronic, and chemical sensors.

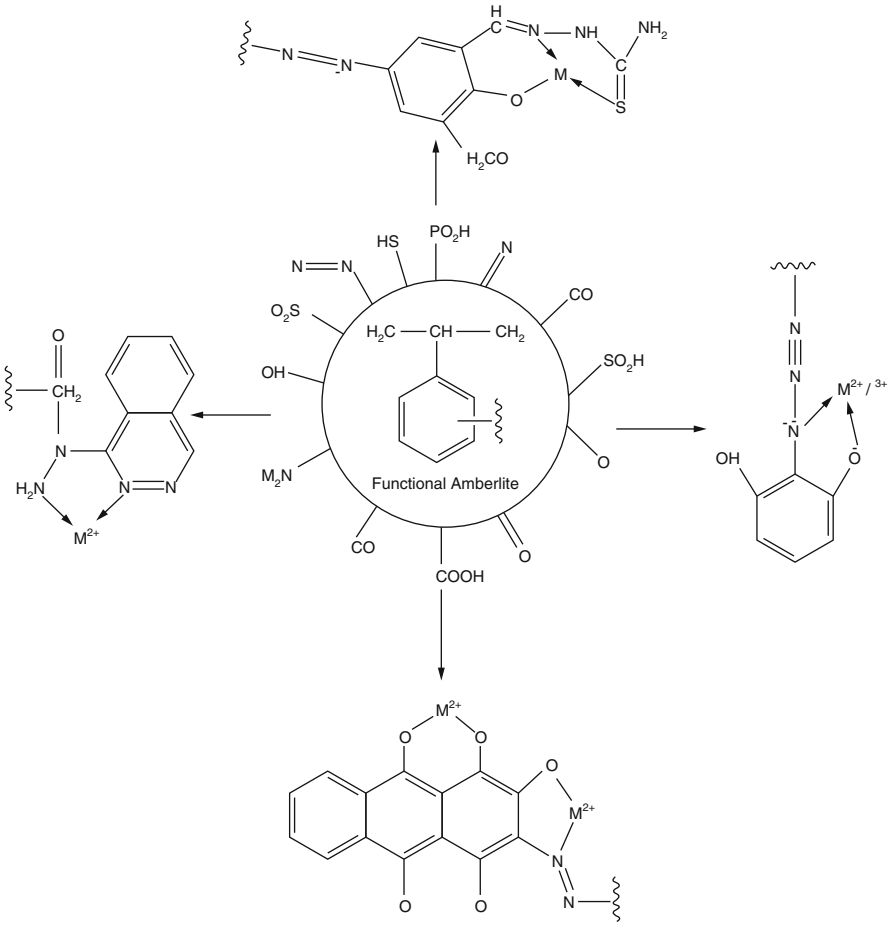

Fig. 2 Coordination of metal ions with chelating resins

Conclusions and Perspectives

A number of chemical routes were used for the synthesis of nanocomposite materials. Among different methods of synthesis, the sol-gel technique is considered as one of the best route because of its low cost and facile synthesis of the desired compound with high purity at a comparatively low temperature. It can also conclude that the incorporation of inorganic precipitate into the matrix of organic polymer not only improved the ion-exchange efficiency but also enhanced its thermal and chemical stability. The increment in ion-exchange capacity was observed due to the development of exchangeable functional groups on the surfaces of the nanocomposites. These nanomaterials have potential to treat organic and inorganic pollutants in industrial wastewaters. Therefore, nanocomposite

ion-exchange materials are unquestionably considered as forthcoming novel materials for remediation of pollutants from industrial effluents. There will also be a growing demand for the synthesis of nanocomposite material, specifically for the environmental applications. Moreover, so far, the work on the application of nanocomposites in treatment of wastewater is still in the research phase and thus needs more attention. These nanocomposite materials showed improved ion-exchange capacity compared to other inorganic ion-exchanger and organic resins. Subsequently, these ion-exchange materials might soon become one of the most influential nanomaterials to create a pollution-free aquatic environment.

Acknowledgments The authors are thankful to all researchers working in the area of nanotechnology and its application to environment protection. Authors also gratefully acknowledged the Centre of Excellence in Environmental Studies (CEES), King Abdulaziz University, Jeddah, and Ministry of Higher Education of the Kingdom of Saudi Arabia.

References

Adrrienne SE, Anne GW (2010) Guidelines for the identification and management of lead exposure in pregnant and lactating women. U.S. Department of Health and Human Services, Atlanta

Ahmed AS, Shafeeq MM, Singla ML, Chaman M, Tabassum S (2012) Temperature dependent structural and optical properties of tin oxide nanoparticles. J Phys Chem Solid 73:943–947

Aktas O, Cecen F (2007) Bioregeneration of activated carbon: a review. Intl J Biodeteriorat Biodegrad 59:257–272

Al-Ekabi H, Serpone N (1988) Kinetics studies in heterogeneous photocatalysis. I. Photocatalytic degradation of chlorinated phenols in aerated aqueous solutions over titania supported on a glass matrix. J Phys Chem 92:5726

Alsohaimi IH, Saikh Wabaidur M, Kumar M, Khan MA, Alothman ZA, Abdalla MA (2015) Synthesis, characterization of PMDA/TMSPEDA hybrid nano-composite and its applications as an adsorbent for the removal of bivalent heavy metals ions. Chem Eng J 270:9–21

Amao Y, Komori T (2003) Dye-sensitized solar cell using a TiO_2 nanocrystalline film electrode modified by an aluminum phthalocyanine and Myristic acid coadsorption layer. Langmuir 19:8872–8875

Anpo M, Takeuchi M (2003) The design and development of highly reactive titanium oxide photocatalyst operating under visible light irradiation. J Catal 216:505

Ansari MO, Mohammad F (2011) Thermal stability, electrical conductivity and ammonia sensing studies on p-toluenesulfonic acid doped polyaniline: titanium dioxide (pTSA/Pani: TiO_2) nanocomposites. Sens Actuators B 157(1):122–129

Arshak K, Adley C, Moore E, Cunniffe C, Campion M, Harris J (2007) Characterisation of polymer nanocomposite sensors for quantification of bacterial cultures. Sens Actuators B 126:226–231

Asad S, Amoozegar MA, Pourbabaee AA, Sarbolouki MN, Dastgheib SMM (2007) Decolorization of textile azo dyes by newly isolated halophilic and halotolerant bacteria. Bioresour Technol 98:2082–2088

Asahi R, Morikawa T, Ohwaki T, Aoki K, Taga Y (2001) Visible-light photocatalysis in nitrogen-doped titanium oxides. Science 293:269

Atieh MA (2011) Removal of chromium (VI) from polluted water using carbon nanotubes supported with activated carbon. Prog Environ Sci 4:281–293

Awual MR, Hasan MM, Shahat A, Naushad M, Shiwaku H, Yaita T (2015) Investigation of ligand immobilized nano-composite adsorbent for efficient cerium(III) detection and recovery. Chem Eng J 265:210–218

Ayata S, Kaynak I, Merdivan M (2009) Solid phase extractive preconcentration of silver from aqueous samples. Environ Monit Assess 153:333–338

Azam A, Ahmed AS, Oves M, Khan MS, Habib SS, Memic A (2012) Antimicrobial activity of metal oxide nanoparticles against gram-positive and gram-negative bacteria: a comparative study. Int J Nanomedicine 7(7):6003–6009

Badrinezhad E, Panahi HA, Manoochehri M (2012) Modification of Amberlite XAD-2 resin with iminodiacetic acid for preconcentration and determination of cadmium in sea water samples. Oceanography 2(8):1–5

Bandekar G, Rajurkar NS, Mulla IS, Mulik UP, Amalnerkar DP, Adhyapak PV (2014) Synthesis, characterization and photocatalytic activity of PVP stabilized ZnO and modified ZnO nanostructures. Appl Nanosci 4:199–208

Barakat MA, Ramadan MH, Alghamdhi MA, Algarny SS, Woodcock HL, Kuhn JN (2013) Remediation of Cu(II), Ni(II) and Cr(III) ions from simulated wastewater by dendrimer titania composites. J Environ Manage 117:50–57

Baytak S, Türker AR (2005) The use of agrobacterium tumefacients immobilized on Amberlite XAD-4 as a new biosorbent for the column preconcentration of iron(III), cobalt(II), manganese (II) and chromium(III). Talanta 65(4):938–945

Belessi V, Romanos G, Boukos N, Lambropoulou D, Trapalis C (2009) Removal of reactive red 195 from aqueous solutions by adsorption on the surface of TiO_2 nanoparticles. J Hazard Mater 170:836–844

Belkhouche NE, Didi MA (2010) Extraction of Bi(III) from nitrate medium by D2EHPA impregnated onto Amberlite XAD-1180. Hydrometallurgy 103:60–67

Berger C, Song ZM, Li TB et al (2004) Ultrathin epitaxial graphite: 2D electron gas properties and a route toward graphene-based nanoelectronics. J Phys Chem B 108:19912

Bernard J, Branger C, Nguyen TLA, Denoyel R, Margaillan A (2008) Synthesis and characterization of a polystyrenic resin functionalized by catechol: application to retention of metal ions. React Funct Polym 68:1362–1370

Bhole YS, Wanjale SD, Kharul UK, Jog JP (2007) Assessing feasibility of polyacrylate–clay nanocomposites towards improvement of gas selectivity. J Membr Sci 306:277–286

Bredas JL, Street GB (1985) Polarons, bipolarons, and solitons in conducting polymers. Acc Chem Res 18:309–315

Bulut VN, Duran C, Tufekci M, Soylak EM (2007a) Speciation of Cr(III) and Cr(VI) after column solid phase extraction on Amberlite XAD-2010. J Hazard Mater 143:112–117

Bulut VN, Gundogdu A, Duran C, Senturk HB, Soylak M, Elci L (2007b) A multi-element solid-phase extraction method for trace metals determination in environmental samples on Amberlite XAD-2000. J Hazard Mater 146:155–163

Bushra R, Shahadat M, Raeisssi AS, Nabi SA (2012) Development of nano-composite adsorbent for removal of heavy metals from industrial effluent and synthetic mixtures; its conducting behavior. Desalination 289:1–11

Bushra R, Shahadat M, Ahmad A, Nabi SA, Umar K, Oves M, Raeissi AS (2014) Synthesis, characterization, antimicrobial activity and applications of polyaniline Ti(IV) arsenophosphate adsorbent for the analysis of organic and inorganic pollutants. J Hazard Mater 264:481–489

Bushra R, Naushad M, Adnan R, Shahadat M, Ansari M, Ahmed A (2015) Electrical and optical properties of synthesized composite material polyaniline-Ti (IV) arsenophosphate. Asian J Chem 27:1121

Cairns WRL, De Boni A, Cozzi G, Asti M, Borla EM, Parussa F, Moretto E, Cescon P, Boutron C, Gabrieli J, Barbante C (2011) The use of cation exchange matrix separation coupled with ICP-MS to directly determine platinum group element (PGE) and other trace element emissions from passenger cars equipped with diesel particulate filters. Anal Bioanal Chem 399:2731–2740

Canterino M, Di-Somma I, Marotta R, Andreozzi R, Caprio V (2009) Energy recovery in wastewater decontamination: simultaneous photocatalytic oxidation of an organic substrate and electricity generation. Water Res 43:2710–2716

Çekiç SD, Filik H, Apak R (2004) Use of an o-aminobenzoic acid-functionalized XAD-4 copolymer resin for the separation and preconcentration of heavy metal(II) ions. Anal Chim Acta 505:15–24

Chang Y, Chen CDH (2005) Adsorption kinetics and thermodynamics of acid dyes on a carboxymethylated chitosan-conjugated magnetic nano-adsorbent. Macromol Biosci 5:254–261

Chen YH, Liu YY, Lin RH, Yen FS (2009) Photocatalytic degradation of p-phenylenediamine with TiO_2-coated magnetic PMMA microspheres in an aqueous solution. J Hazard Mater 163:973–981

Chen B, Xiang S, Qian G (2010) Metal-organic frameworks with functional pores for recognition of small molecules. Acc Chem Res 43:1115–1124

Ciftci H, Yalcin H, Eren E, Olcucu A, Sekerci M (2010) Enrichment and determination of Ni^{2+} ions in water samples with a diamino-4-(4-nitro-phenylazo)-1H-pyrazole (PDANP) by using FAAS. Desalination 256:48–53

Crespilhoa FN, Iost RM, Travain SA, Oliveira ON Jr, Zucolotto V (2009) Enzyme immobilization on Ag nanoparticles/polyaniline nanocomposites. Biotechnol Bioeng 24:3073–3077

Cui H, Su Y, Li Q, Gao S, Shang JK (2013) Exceptional arsenic (III,V) removal performance of highly porous, nanostructured ZrO2 spheres for fixed bed reactors and the full-scale system modeling. Water Res 47:6258–6268

Cui L, Xu W, Guo X, Zhang Y, Wei Q, Du B (2014) Synthesis of strontium hydroxyapatite embedding ferroferric oxide nano-composite and its application in Pb^{2+} adsorption. J Mol Liq 197:40–47

Dai K, Peng TY, Chen H, Zhang RX, Zhang YX (2008) Photocatalytic degradation and mineralization of commercial methamidophos in aqueous titania suspension. Environ Sci Technol 42:1505–1510

Dave SR, Kaur H, Menon SK (2010) Selective solid-phase extraction of rare earth elements by the chemically modified Amberlite XAD-4 resin with azacrown ether. React Funct Polym 70:692–698

Dayan AD, Paine AP (2001) Human & experimental toxicology mechanisms of chromium toxicity, carcinogenicity and allergenicity: review of the literature from 1985 to 2000. Hum Exp Toxicol 20:439–451

Delle Site A (2001) Factors affecting sorption of organic compounds in natural sorbent/water systems and sorption coefficients for selected pollutants. A review. J Phy Chem Ref Data 30:187–439

Delmas H, Wilhelm AM, Polaert I, Fabregat A, Stüber F, Font J (2002) Sequential process of adsorption and catalytic oxidation on activated carbon for (pre)treatment of water polluted by non-biodegradable organic products. Fr. Patent FRXXBL FR. A1 20021227

DeMartino MG, Macarovscha GT, Cadore S (2010) The use of Zincon for preconcentration and determination of zinc by flame atomic absorption spectrometry. Anal Methods 2:1258–1262

Deng S, Bai J, Chen P (2003) Aminated polyacrylonitrile fibers for lead and copper removal. Langmuir 19:5058–5064

Depecker G, Branger C, Margaillan A, Pigot T, Blanc S, Robert-Peillard F (2009) Synthesis and applications of XAD-4-DAN chelate resin for the separation and determination of Se(IV). React Funct Polym 69:877–883

Dey SK, Roy S (2009) Effects of chromium on certain aspects of cellular toxicity. Iran J Toxicol 2:260–267

Di ZC, Ding J, Peng XJ, Li YH, Luan ZK, Liang J (2006) Chromium adsorption by aligned carbon nanotubes supported ceria nanoparticles. Chemosphere 62:861–865

Dogru M, Gul-Guven R, Erdogan S (2007) The use of Bacillus Subtilis immobilized on Amberlite XAD-4 as a new biosorbent in trace metal determination. J Hazard Mater 149:166–173

Doğutan M, Filik H, Apak R (2003) Preconcentration of manganese(II) from natural and sea water on a palmitoyl quinolin-8-ol functionalized XAD copolymer resin and spectrophotometric determination with the formaldoxime reagent. Anal Chim Acta 485:205–212

Doušová B, Grygar T, Martaus A, Fuitová L, Koloušek D, Machovič V (2006) Sorption of AsV on aluminosilicates treated with FeII nanoparticles. J Colloid Interface Sci 302(2):424–431

Duran C, Gundogdu A, Bulut VN, Soylak M, Elci L, Sentürk HB (2007a) Solid-phase extraction of Mn(II), Co(II), Ni(II), Cu(II), Cd(II) and Pb(II) ions from environmental samples by flame atomic absorption spectrometry (FAAS). J Hazard Mater 146:347–355

Duran C, Senturk HB, Gundogdu A, Bulut VN, Elci L, Soylak M (2007b) Determination of some trace metals in environmental samples by flame AAS following solid phase extraction with Amberlite XAD-2000 resin after complexing with 8-hydroxyquinoline. Chin J Chem 25:196–202

Duran A, Tuzen M, Soylak M (2009) Preconcentration of some trace elements via using multiwalled carbon nanotubes as solid phase extraction adsorbent. J Hazard Mater 169:466–471

El-Sofany EA (2008) Removal of lanthanum and gadolinium from nitrate medium using Aliquat-336 impregnated onto Amberlite XAD-4. J Hazard Mater 153:948–954

Ercal N, Hande GO, Nukhet AB (2001a) Toxic metals and oxidative stress. Part I: mechanisms involved in metal induced oxidative damage. Curr Top Med Chem 1:529–539

Farghali AA, Moussa M, Khedr MH (2010) Synthesis and characterization of novel conductive and magnetic nano-composites. J Alloys Compd 499:98–103

Farokhzad OC, Cheng J, Teply BA, Sherifi I, Jon S, Kantoff PW, Richie JP, Langer R (2006) Targeted nanoparticle-aptamer bioconjugates for cancer chemotherapy *in vivo*. Proc Natl Acad Sci U S A 103:6315

Fernandez C, Larrechi MS, Callao PM (2010) An analytical overview of processes for removing organic dyes from wastewater effluents. Trends Anal Chem 29:1202–1211

Ferreira SLC, Ferreira JR, Dantas AF, Lemos VA, Araújo NML, Costa ACS (2000a) Copper determination in natural water samples by using FAAS after preconcentration onto Amberlite XAD-2 loaded with calmagite. Talanta 50:1253–1259

Ferreira SLC, Lemos VA, Moreira BC, Costa ACS, Santelli RE (2000b) An on-line continuous flow system for copper enrichment and determination by flame atomic absorption spectroscopy. Anal Chim Acta 403:259–264

Ferreira SLC, dos Santos WNL, Lemos VA (2001) On-line preconcentration system for nickel determination in food samples by flame atomic absorption spectrometry. Anal Chim Acta 445:145–151

Filik H, Berker KI, Balkis N, Apak R (2004) Simultaneous preconcentration of vanadium(V/IV) species with palmitoyl quinolin-8-ol bonded to Amberlite XAD2 and their separate spectrophotometric determination with 4-(2-pyridylazo)-resorcinol using CDTA as masking agent. Anal. Chim Acta 518:173–179

Firooz AA, Mahjoub AR, Khodadadi AA (2011) Hydrothermal synthesis of ZnO/SnO_2 nanoparticles with high photocatalytic activity. World Acad Sci Eng Technol 52:138–140

Fischer-Wolfarth JH, Hartmann J, Farmer JA, Flores-Camacho JM, Campbell CT, Schauermann S, Freund HJ (2011) An improved single crystal adsorption calorimeter for determining gas adsorption and reaction energies on complex model catalysts. Rev Sci Instrum 82:024102

Fontanals N, Cormack PAG, Marce RM, Borrull F (2010) Mixed-mode ion-exchange polymeric sorbents: dual-phase materials that improve selectivity and capacity. Trends Anal Chem 29:765–799

Fonzo FD, Casari CS, Russo V, Brunella MF, Bassi AL, Bottani CE (2009) Hierarchally organized nanostructured TiO_2 for photocatalytic application. Nanotechnology 20(2):015604

Fryzek JP, Hansen J, Cohen S, Bonde JP, Llambias MT, Kolstad HA, Skytthe A, Lipworth L, Blot WJ, Olsen JH (2005) A cohort study of Parkinson's disease and other neurodegenerative disorders in Danish welders. J occup environ med 47:466–472

Fu F, Wang Q (2011) Removal of heavy metal ions from wastewaters: a review. J Environ Manage 92:407–418

Furukawa H, Cordova KE, O'Keeffe M, Yaghi OM (2013) The chemistry and applications of metal-organic frameworks. Science 341:1230444

Galindo R, López-Delgado A, Padilla I, Yates M (2015) Synthesis and characterisation of hydrotalcites produced by an aluminium hazardous waste: a comparison between the use of ammonia and the use of triethanolamine. Appl Clay Sci 115:115–123

Gao S, Yang J, Li Z, Jia X, Chen Y (2012) Bioinspired synthesis of hierarchically micro/nano-structured CuI tetrahedron and its potential application as adsorbent for Cd(II) with high removal capacity. J Hazard Mater 211–212:55–61

Ghaedi M, Karami B, Ehsani S, Marahel F, Soylak M (2009) Preconcentration–separation of Co^{2+}, Ni^{2+}, Cu^{2+} and Cd^{2+} in real samples by solid phase extraction of a calix [4] resorcinarene modified Amberlite XAD-16 resin. J Hazard Mater 172:802–808

Ghaedi M, Niknam K, Taheri K, Hossainian H, Soylak M (2010) Flame atomic absorption spectrometric determination of copper, zinc and manganese after solid-phase extraction using 2,6-dichlorophenyl-3,3-bis(indolyl)methane loaded on Amberlite XAD-16. Food Chem Toxicol 48:891–897

Ghasemi JB, Zolfonoun E (2010) Simultaneous spectrophotometric determination of trace amounts of uranium, thorium, and zirconium using the partial least squares method after their preconcentration by α-benzoin oxime modified Amberlite XAD-2000 resin. Talanta 80:1191–1197

Goodwin WE, Rao RR, Chatt A (2013) Reversed-phase extraction chromatography–neutron activation analysis (RPEC–NAA) for copper in natural waters using Amberlite XAD-4 resin coated with 1-(2-thiazolylazo)-2-naphthol. J Radioanal Nucl Chem 296:489–494

Gorguner M, Akgun M (2010) Acute Inhalation Injury. The Eurasian Journal of Medicine 42: 28–35

Gregusova M, Docekal B (2011) New resin gel for uranium determination by diffusive gradient in thin films technique. Anal Chim Acta 684:142–146

Guo Y, Din BJ, Liu YW, Chang XJ, Meng SM, Liu JH (2004a) Preconcentration and determination of trace elements with 2-aminoacetylthiophenol functionalized Amberlite XAD-2 by inductively coupled plasma-atomic emission spectrometry. Talanta 62:207–213

Guo Y, Din BJ, Liu YW, Chang XJ, Meng SM, Tian MZ (2004b) Preconcentration of trace metals with 2-(methylthio)aniline-functionalized XAD-2 and their determination by flame atomic absorption spectrometry. Anal Chim Acta 504:319–324

Guo Z, Hahn HT, Lin H, Karki AB, Young DP (2008) Magnetic and magnetoresistance behaviors of particulate iron/vinyl ester resin nanocomposites. J Appl Phys 104:014314

Guo QZ, Mei B, Zhou SX, Shi ZG, Feng YQ, Wu JY, Yan GP, Li L (2009) Synthesis, characterization and application of magnetic-zirconia nanocomposites. J Non-Cryst Solids 355:922–925

Guo Y, Wang Z, Qu W, Shao H, Jiang X (2011) Colorimetric detection of mercury, lead and copper ions simultaneously using protein-functionalized gold nanoparticles. Biosens Bioelectron 26:4064–4069

Hashemi M, Ghavami S, Eshraghi M, Booy EP, Los M (2007) Cytotoxic effects of intra and extracellular zinc chelation on human breast cancer cells. Eur J Pharmacol 557:9–19

He E, Qiu H, Van Gestel CAM (2014) Modelling uptake and toxicity of nickel in solution to enchytraeus crypticus with biotic ligand model theory. Environ Pollut 188:17–26

He X, Fan J, Wooley KL (2015) Stimuli-Triggered Sol-Gel Transitions of Polypeptides Derived from α-Amino Acid N-Carboxyanhydride (NCA) Polymerizations. Chem Asian J 11:437–47

Hemasundaram A, Krishnaiah N, Naidu NVS, Sreedhar B (2009) Synthesis of 2,3-dihydroxynaphthalene-functionalized Amberlite XAD-4 resin: applications for the separation and preconcentration of tracemetal ions prior to their determination by inductively coupled plasma atomic emission spectrometry. Toxicol Environ Chem 91:1429–1441

Hörtz P, Ruff P, Schäfer R (2015) A temperature dependent investigation of the adsorption of CO on Pt(111) using low-temperature single crystal adsorption calorimetry. Surf Sci 639:66–69

Hosseini MS, Hosseini-Bandegharaei A, Raissi H, Belador F (2009) Sorption of Cr(VI) by Amberlite XAD-7 resin impregnated with brilliant green and its determination by quercetin as a selective spectrophotometric reagent. J Hazard Mater 169:52–57

Hosseini-Bandegharaei A, Hosseini MS, Sarw-Ghadi M, Zowghi S, Hosseini E, Hosseini-Bandegharaei H (2010) Kinetics, equilibrium and thermodynamic study of Cr(VI) sorption into toluidine blue o-impregnated XAD-7 resin beads and its application for the treatment of wastewaters containing Cr(VI). Chem Eng J 160:190–198

Hu J, Chen LG (2005) Fast removal and recovery of Cr(VI) using surface-modified jacobsite ($MnFe_2O_4$) nanoparticles. Langmuir 21:11173–11179

Hu P, Long M (2016) Cobalt-catalyzed sulfate radical-based advanced xidation: a review on heterogeneous catalysts and applications. Appl Catal Environ 181:103–117

Huang MT, Choi O, Ju YS, Hahn HT (2006) Heat conduction in graphite-nanoplatelet-reinforced polymer nanocomposites. Appl Phys Lett 89:23117/023111–023117/023113

Huck CW, Bonn GK (2000) Recent developments in polymer-based sorbents for solid-phase extraction. J Chromatogr A 885:51–72

Hughes MF, Beck BD, Chen Y, Lewis AS, Thomas DJ (2011) Arsenic exposure and toxicology: a historical perspective. Toxicol Sci 123:305–332

Iijima S (1991) Helical microtubules of graphitic carbon. Nature 354:56–58

Islam A, Laskar MA, Ahmad A (2010a) Characterization and application of 1-(2-pyridylazo)-2-naphthol functionalized Amberlite XAD-4 for preconcentration of trace metal ions in real matrices. J Chem Eng Data 55:5553–5561

Islam A, Laskar MA, Ahmad A (2010b) Characterization of a novel chelating resin of enhanced hydrophilicity and its analytical utility for preconcentration of trace metal ions. Talanta 81:1772–1780

Islam A, Laskar MA, Ahmad A (2010c) The efficiency of Amberlite XAD-4 resin loaded with 1-(2-pyridylazo)-2-naphthol in preconcentration and separation of some toxic metal ions by flame atomic absorption spectrometry. Environ Monit Assess 175:201–212

Islam A, Ahmad H, Zaidi N, Yadav S (2013a) Selective separation of aluminum from biological and environmental samples using glyoxal-bis(2-hydroxyanil) functionalized amber XAD-16 resin: kinetics and equilibrium studies. Ind Eng Chem Res 52:5213–5220

Islam A, Laskar MA, Ahmad A (2013b) Preconcentration of metal ions through chelation on a synthesized resin containing O, O donor atoms for quantitative analysis of environmental and biological samples. Environ Monit Assess 185:2691–2704

Islam A, Zaidi N, Ahmad H, Yadav S (2014) Synthesis, characterization, and systematic studies of a novel aluminium selective chelating resin. Environ Monit Assess 186:5843–5853

Jadhav AH, Mai XT, Ofori FA, Kim H (2015) Preparation, characterization, and kinetic study of end opened carbon nanotubes incorporated polyacrylonitrile electrospun nanofibers for the adsorption of pyrene from aqueous solution. Chem Eng J 259:348–356

Jain P, Pradeep T (2005) Potential of silver nanoparticle-coated polyurethane foam as an antibacterial water filter. Biotechnol Bioeng 90:59–63

Jain VK, Mandalia HC, Gupte HS, Vyas DJ (2009) Azocalix[4]pyrrole Amberlite XAD-2: new polymeric chelating resins for the extraction, preconcentration and sequential separation of Cu (II), Zn(II) and Cd(II) in natural water samples. Talanta 79:1331–1340

Jie HS, Lee HB, Chae KH, Huh MY, Matsuoka M, Cho SH, Park JK (2012) Nitrogen-doped TiO2 nanopowders prepared by chemical vapor synthesis: band structure and photocatalytic activity under visible light. Res Chem Intermed 38:1171

Kaneko M, Nemoto J, Ueno H, Gokan N, Ohnuki K, Horikawa M, Saito R, Shibata T (2006) Photoelectrochemical reaction of biomass and bio-related compounds with nanoporous TiO_2 film photoanode and O_2-reducing cathode. Electrochem Commun 8:336

Kaneko M, Ueno H, Nemoto J (2012) Direct biomass fuel cell (BMFC) with anode/catalyst comprising a nanocomposite of a mesoporous n-semiconductor film and a metal thin layer: a new concept of catalyst design. Catal Lett 142:469–479

Kang Z, Xue M, Zhang D, Fan L, Pan Y, Qiu S (2015) Hybrid metal-organic framework nanomaterials with enhanced carbon dioxide and methane adsorption enthalpy by incorporation of carbon nanotubes. Inorg Chem Commun 58:79–83

Kara D, Fisher A, Hill SJ (2005) Preconcentration and determination of trace elements with 2,6-diacetylpyridine functionalized Amberlite XAD-4 by flow injection and atomic spectroscopy. Analyst 130:1518–1523

Kara D, Fisher A, Hill SJ (2006) Comparison of some newly synthesized chemically modified Amberlite XAD-4 resins for the preconcentration and determination of trace elements by flow injection inductively coupled plasma-mass spectrometry (ICP-MS). Analyst 131:1232–1240

Kara D, Fisher A, Hill SJ (2009) Determination of trace heavy metals in soil and sediments by atomic spectrometry following preconcentration with Schiff bases on Amberlite XAD-4. J Hazard Mater 165:1165–1169

Karve M, Pandey K (2012) Sorption studies of U(VI) on Amberlite XAD-2 resin impregnated with Cyanex272. J Radioanal Nucl Chem 293:783–787

Karve M, Rajgor RV (2008) Amberlite XAD-2 impregnated organophosphinic acid extractant for separation of uranium(VI) from rare earth elements. Desalination 232:191–197

Kaur A, Gupta UJ (2009) A review on applications of nanoparticles for the preconcentration of environmental pollutants. Mater Chem 19:8279

Khan AA, Paquiza L (2011) Characterization and ion-exchange behavior of thermally stable nanocomposite polyaniline zirconium titanium phosphate: its analytical application in separation of toxic metals. Desalination 265:242–254

Khan AA, Shaheen S (2013) Ion-exchange studies of 'organic–inorganic'nano-composite cation-exchanger: Polyo-anisidine Sn (IV) tungstate and its analytical application for the separations of toxic metals. Composites Part B Eng 44:692–697

Khan AA, Paquiza L, Khan A (2010) An advanced nano-composite cation-exchanger polypyrrole zirconium titanium phosphate as a Th(IV)-selective potentiometric sensor: preparation, characterization and its analytical application. J Mater Sci 45(13):3610–3625

Khan MZ, Mondal PK, Sabir S (2011a) Bioremediation of 2-chlorophenol containing wastewater by aerobic granules-kinetics and toxicity. J Hazard Mater 190:222–228

Khan MZ, Mondal PK, Sabir S, Tare V (2011b) Degradation pathway, toxicity and kinetics of 2,4,6-Trichlorophenol with different co-substrates by aerobic granules in SBR. Bioresour Technol 102:7016–7021

Khan AA, Shaheen S, Habiba U (2012) Synthesis and characterization of poly-o-anisidine Sn (IV) tungstate: a new and novel 'organic–inorganic'nano-composite material and its electroanalytical applications as Hg (II) ionselective membrane electrode. J Adv Res 3:269–278

Khan APP, Khan A, Rahman MM, Asiri AM, Oves M (2016) Lead sensors development and antimicrobial activities based on graphene oxide/carbon nanotube/poly (O-toluidine) nanocomposite. Int J Biol Macromol 89:198–205

Khazaeli S, Nezamabadi N, Rabani M, Panahi HA (2013) A new functionalized resin and its application in flame atomic absorption spectrophotometric determination of trace amounts of heavy metal ions after solid phase extraction in water samples. Microchem J 106:147–153

Kim HG, Hwang DW, Lee JS (2004) An undoped single phase oxide photocatalyst working under visible light. J Am Chem Soc 126:8912–8913

Kim YS, In G, Han CW, Choi JM (2005) Studies on synthesis and application of XAD-4-salen chelate resin for separation and determination of trace elements by solid phase extraction. Microchem J 80:151–157

Kirstein J, Turgay K (2005) A new tyrosine phosphorylation mechanism involved in signal transduction in *Bacillus subtilis*. J Mol Microbiol Biotechnol 9:182

Kitano M, Iyatani K, Afsin E, Horiuchi Y, Takeuchi M, Cho SH, Matsuoka M, Anpo MM (2012) Photocatalytic oxidation of 2-propanol under visible light irradiation on TiO_2 thin films prepared by an RF magnetron sputtering deposition method. Res Chem Intermed 38:1249

Kobal AB, Horvat M, Preze M, Se A, Krsnik M, Dizdarevi T (2004) The impact of long-term past exposure to elemental mercury on antioxidative capacity and lipid peroxidation in mercury miners. J Trace Elem Med Biol 17:261–274

Kumar R, Ahmad R (2011) Biosorption of hazardous crystal violet dye from aqueous solution onto treated ginger waste (TGW). Desalination 265:112–118

Kumar M, Rathore DPS, Singh AK (2000a) Amberlite XAD-2 functionalized with o-aminophenol: synthesis and applications as extractant for copper(II), cobalt(II), cadmium (II), nickel(II), zinc(II) and lead(II). Talanta 51:1187–1196

Kumar M, Rathore DPS, Singh AK (2000b) Metal ion enrichment with Amberlite XAD-2 functionalized with Tiron: analytical applications. Analyst 125:1221–1226

Kumar M, Rathore DPS, Singh AK (2001) Pyrogallol immobilized Amberlite XAD-2: a newly designed collector for enrichment of metal ions prior to their determination by flame atomic absorption spectrometry. Microchim Acta 137:127–134

Kumar R, Khan MA, Haq N (2014) Application of carbon nanotubes in heavy metals remediation. Crit Rev Environ Sci Technol 44(9):1000–1035

Kurniawan TA, Chan GYS, Lo WH, Babel S (2006) Physico-chemical treatment techniques for wastewater laden with heavy metals. Chem Eng J 118:83–98

Larsen SC (2007) Nanocrystalline zeolites and zeolite structures: synthesis, characterization, and applications. J Phys Chem C 111:18464–18474

Lemos VA, Baliza PX (2005) Amberlite XAD-2 functionalized with 2-aminothiophenol as a new sorbent for on-line preconcentration of cadmium and copper. Talanta 67:564–570

Lemos VA, Santos JS, Nunes LS, de Carvalho MB, Baliza PX, Yamaki RT (2003a) Amberlite AD-2 functionalized with Nitroso R salt: synthesis and application in an online system for preconcentration of cobalt. Anal Chim Acta 494:87–95

Lemos VA, Baliza PX, Yamaki RT, Rocha ME, Alves APO (2003b) Synthesis and application of a functionalized resin in on-line system for copper preconcentration and determination in foods by flame atomic absorption spectrometry. Talanta 61(5):675–682

Lemos VA, Baliza PX, Santos JS, Nunes LS, de Jesus AA, Rocha ME (2005) A new functionalized resin and its application in preconcentration system with multivariate optimization for nickel determination in food samples. Talanta 66:174–180

Lemos VA, da Silva DG, de Carvalho AL, de Andrade SD, dos Santos NG, dos Passos AS (2006) Synthesis of Amberlite XAD-2-PC resin for preconcentration and determination of trace elements in food samples by flame atomic absorption spectrometry. Microchem J 84:14–21

Lemos VA, Bezerra MA, Amorim FAC (2008a) On-line preconcentration using a resin functionalized with 3,4-dihydroxybenzoic acid for the determination of trace elements in biological samples by thermospray flame furnace atomic absorption spectrometry. J Hazard Mater 157:613–619

Lemos VA, Novaes CG, Lima AS, Vieira DR (2008b) Flow injection preconcentration system using a new functionalized resin for determination of cadmium and nickel in tobacco samples. J Hazard Mater 155:128–134

Li B, Wang Y (2010) Facile synthesis and photocatalytic activity of ZnO–CuO nanocomposite superlattices and microstructures. Superlattice Microst 47:615–623

Li YH, Wang S, Wei J, Zhang X, Xu C, Luan Z, Wu D, Wei B (2002) Lead adsorption on carbon nanotubes. Chem Phys Lett 357:263–266

Li J, Zhang Q, Feng J, Yan W (2013) Synthesis of PPy-modified TiO2 composite in H2SO4 solution and its novel adsorption characteristics for organic dyes. The Chemical Engineering Journal 225:766–775

Li JR, Kuppler RJ, Zhou HC (2009) Selective gas adsorption and separation in metalorganic frameworks. Chem Soc Rev 38:1477–1504

Lianos P (2011) Production of electricity and hydrogen by photocatalytic degradation of organic wastes in a photoelectrochemical cell: the concept of the photofuelcell: a review of a re-emerging research field. J Hazard Mater 185:575–590

Liu YW, Guo Y, Chang XJ, Meng SM, Yang D, Din BJ (2005) Column solid-phase extraction with 2-Acetylmercaptophenyldiazoaminoazobenzene (AMPDAA) impregnated Amberlite XAD-4 and determination of trace heavy metals in natural waters by flame atomic absorption spectrometry. Microchim Acta 149:95–101

Liu Y, Chakrabartty S, Alocilja E (2007a) Fundamental building blocks for molecular biowire based forward error-correcting biosensors. Nanotechnology 18:1–6

Liu YW, Guo Y, Meng SM, Chang XJ (2007b) Online separation and preconcentration of trace heavy metals with2,6-dihydroxyphenyl-diazoaminoazobenzene impregnated Amberlite XAD-4. Microchim Acta 158:239–245

Liu C, Bai R, Ly QS (2008) Selective removal of copper and lead ions by diethylenetriamine-functionalized adsorbent: behaviours and mechanisms. Water Res 42:1511–1522

Liu W, Chen SF, Zhao W, Zhang SJ (2009) Titanium dioxide mediated photocatalytic degradation of methamidophos in aqueous phase. J Hazard Mater 164:154–160

Liu Y, Li J, Zhou B, Li X, Chen H, Chen Q, Wang Z, Li L, Wang J, Cai W (2011) Efficient electricity production and simultaneously wastewater treatment via a high-performance photocatalytic fuel cell. Water Res 45:3991–3998

Liu XT, Wang MS, Zhang SJ, Pan BC (2013) Application potential of carbon nanotubes in water treatment: a review. J Environ Sci 25:1263–1280

Long YZ, Li MM, Gub C, Wan M, Duvaild JL, Liu Z, Fan Z (2011) Recent advances in synthesis, physical properties and applications of conducting polymer nanotubes and nanofibers. Prog Polym Sci 36:1415–1442

Lu ZX, Zhang ZL, Zhang MX, Xie HY, Tian ZQ, Chen P, Huang H, Pang DW (2005) Core/shell quantum-dot-photosensitized nano-TiO_2 films: fabrication and application to the damage of cells and DNA. J Phys Chem B 109:22663–22666

Lu HH, Lin CY, Hsiao TC, Fang YY, Ho KC, Yang DF, Lee CK, Hsu SM, Lin CW (2009) Electrical properties of single and multiple poly(3,4-ethylenedioxythiophene) nanowires for sensing nitric oxide gas. Anal Chim Acta 640:68–74

Lutfullah, Rashid M, Haseen U, Rahman N (2014) An advanced Cr(III) selective nano-composite cation exchanger: synthesis, characterization and sorption characteristics. J Indus Eng Chem 20:809–817

Ma A, Wei Y, Zhou Z, Xu W, Ren F, Ma H, Wang J (2012) Preparation Bi2S3eTiO2 heterojunction/polymer fiber composites and its photocatalytic degradation of methylene blue under Xe lamp irradiation, polym degrad. Stadtehygiene 97:125–131

Ma X, Su Y, Sun Q, Wang Y, Jiang Z (2007) Enhancing the antifouling property of polyethersulfone ultrafiltration membranes through surface adsorption-crosslinking of poly (vinyl alcohol). Journal of Membrane Science 300:71–78

Maheswari MA, Subramanian MS (2005) AXAD-16-3,4-dihydroxy benzoylmethyl phosphonic acid: a selective preconcentrator for U and Th from acidic waste streams and environmental samples. React Funct Polym 62:105–114

Matsuoka S, Yoshimura K (2010) Recent trends in solid phase spectrometry: 2003–2009. A review. Anal Chim Acta 664:1–18

Matteazzi P, Le-Caer G (1992) Synthesis of nanocrystalline alumina-metal composites by room temperature ball milling of metal oxide and alumina. J Am Ceram Soc 75:2749

Mayo JT, Yavuz C, Yean S, Cong L, Shipley H, Yu W, Falkner J, Kan A, Tomson M, Colvin VL (2007) The effect of nanocrystalline magnetite size on arsenic removal. Sci Technol Adv Mater 8:71–75

Mello HJNPD, Mulato M (2015) Optochemical sensors using electrodeposited polyaniline films: electrical bias enhancement of reflectance response. Sens Actuators B 213:195–201

Memon SQ, Hasany SM, Bhanger MI, Khuhawar MY (2005) Enrichment of Pb(II) ions using phthalic acid functionalized XAD-16 resin as a sorbent. J Colloid Interface Sci 291:84–91

Memon SQ, Bhanger MI, Hasany SM, Khuhawar MY (2007) The efficacy of nitrosonaphthol functionalized XAD-16 resin for the preconcentration/sorption of Ni(II) and Cu(II) ions. Talanta 72:1738

Memon JR, Memon SQ, Bhanger MI, Khuhawar MY (2009) Use of modified sorbent for the separation and preconcentration of chromium species from industrial wastewater. J Hazard Mater 163:511–516

Merdivan M, Düz MZ, Hamamci C (2001) Sorption behaviour of uranium(VI) with N, N-dibutyl-N-benzoylthiourea impregnated in Amberlite XAD-16. Talanta 55:639–645

Metilda P, Sanghamitra K, Gladis JM, Naidu GRK, Rao TP (2005) Amberlite XAD-4 functionalized with succinic acid for the solid phase extractive preconcentration and separation of uranium(VI). Talanta 65:192–200

Mills A, Hazafy D (2009) Nanocrystalline SnO_2-based, UVB-activated, colourimetric oxygen indicator. Sens Actuators B 136:344–349

Mohan P (2013) A critical review: the modification, properties, and applications of epoxy resins. Polym-Plast Technol Eng 52:107–125

Mohan P, Srivastava AK (1997) Synthesis reaction and properties of modified epoxy resins. Polym Rev C37(4):687–716

Moniri E, Panahi HA, Karimi M, Rajabi NA, Faridi M, Manoochehri M (2011) Modification and characterization of Amberlite XAD-2 with calcein blue for preconcentration and determination of copper(II) from environmental samples by atomic absorption spectroscopy. Korean J Chem Eng 28:1523–1531

Mostafa SM, Bakr AA, El Naggar AMA, Sultan E-SA (2016) Water decontamination via the removal of Pb (II) using a new generation of highly energetic surface nano-material: $Co^{2+}Mo^{6+}$ LDH. J Colloid Interface Sci 461:261–272

Nabi SA, Shahadat Md, Bushra R, Oves M, Ahmed F (2011) Synthesis and characterization of polyanilineZr(IV)sulphosalicylate composite and its applications (1) electrical conductivity, and (2) antimicrobial activity studies. Chem Eng J 173(3):706–714

Narin I, Tuzen M, Soylak M (2004) Aluminium determination in environmental samples by graphite furnace atomic absorption spectrometry after solid phase extraction on Amberlite XAD-1180/pyrocatechol violet chelating resin. Talanta 63:411–418

Naushad M (2014) Surfactant assisted nano-composite cation exchanger: development, characterization and applications for the removal of toxic Pb^{2+} from aqueous medium. Chem Eng J 235:100–108

Nawa M, Sekino T, Niihara K (1994) Fabrication and mechanical behaviour of Al_2O_3/Mo nanocomposites. J Mater Sci 29:3185

Nezhati MN, Panahi HA, Moniri E, Kelahrodi SR, Assadian F, Karimi M (2010) Synthesis, characterization and application of allyl phenolmodified Amberlite XAD-4 resin for preconcentration and determination of copper in water samples. Korean J Chem Eng 27:1269–1274

Nilchi A, Janitabar-Darzi S, Mahjoub AR, Rasouli-Garmarodi S (2010) New TiO_2/SiO_2 nanocomposites – phase transformations and photocatalytic studies. Colloids Surf A Physicochem Eng Asp 361:25–30

Nishijima W, Akama T, Shoto E, Okada M (1997) Effect of adsorbed substances on bioactivity of attached bacteria on granular activated carbon. Water Sci Technol 35:203–208

Nomiya K, Yoshizawa A, Tsukagoshi K, Kasuga NC, Hirakawa S, Watanabe J (2004) Synthesis and structural characterization of silver(I), aluminium(III) and cobalt(II) complexes with 4-isopropyltropolone (hinokitiol) showing noteworthy biological activities. Action of silver (I)-oxygen bonding complexes on the antimicrobial activities. J Inorg Biochem 98:46

Oral EV, Dolak I, Temel H, Ziyadanogullari B (2011) Preconcentration and determination of copper and cadmium ions with 1,6-bis(2-carboxy aldehyde phenoxy)butane functionalized amber XAD-16 by flame atomic absorption spectrometry. J Hazard Mater 186:724–730

Oves M, Khan MS, Zaidi A, Ahmed AS, Ahmed F, Ahmad E, Sherwani A et al (2013) Antibacterial and cytotoxic efficacy of extracellular silver nanoparticles biofabricated from chromium reducing novel OS4 strain of Stenotrophomonas maltophilia. PLoS One 8(3): e59140

Oves M, Arshad M, Khan MS, Ahmed AS, Azam A, Ismail IMI (2015) Anti-microbial activity of cobalt doped zinc oxide nanoparticles: targeting water borne bacteria. J Saudi Chem Soc 19(5):581–588

Özdemir S, Kilinc E (2012) Geobacillus thermoleovorans immobilized on Amberlite XAD-4 resin as a biosorbent for solid phase extraction of uranium (VI) prior to its spectrophotometric determination. Microchim Acta 178:389–397

Özdemir S, Gul-Guven R, Kilinc E, Dogru M, Erdogan S (2010a) Preconcentration of cadmium and nickel using the bioadsorbent *Geobacillus thermoleovorans* subsp. Stromboliensis immobilized on Amberlite XAD-4. Microchim Acta 169:79–85

Özdemir S, Erdogan S, Kilinc E (2010b) *Bacillus* sp. immobilized on Amberlite XAD-4 resin as a biosorbent for solid phase extraction of thorium prior to UV–Vis spectrometry determination. Microchim Acta 171:275–281

Panahi HA, Kalal HS, Moniri E, Nezhati MN, Menderjani MT, Kelahrodi SR, Mahmoudi F (2009) Amberlite XAD-4 functionalized with m-phenylenediamine: synthesis, characterization and applications as extractant for preconcentration and determination of rhodium (III) in water samples by inductive couple plasma atomic emission spectroscopy (ICP-AES). Microchem J 93:49–54

Patel MJ, Parmar P, Dave B, Subramanian RB (2012) Antioxidative and physiological studies on Colocasia esculentum in response to arsenic stress. Afr J Biotechnol 11:16241–16246

Pereira FV, Gurgel LVA, Gil LF (2010) Removal of $Zn_2þ$ from aqueous single metal solutions and electroplating wastewater with wood sawdust and sugarcane Bagasse modified with EDTA di-Anhydride (EDTAD). J Hazard Mater 176:856–863

Pérez E, Ayele L, Getschew G, Fetter G, Bosh P, Mayoral A, Diaz I (2015) Removal of chromium (VI) using nanohydrotalcite/SiO2composite. J Environ Chem Eng 3:1555–1561

Prabhakar PK, Raj S, Anuradha PR, Sawant SN, Doble M (2011) Biocompatibility studies on polyaniline and polyaniline–silver nanoparticle coated polyurethane composite. Colloids Surf B Biointerfaces 86:146–153

Prabhakaran D, Subramanian MS (2003a) Enhanced metal extractive behavior using dual mechanism bifunctional polymer: an effective metal chelatogen. Talanta 61:431–437

Prabhakaran D, Subramanian MS (2003b) Selective extraction and sequential separation of actinide and transition ions using AXAD-16-BTBED polymeric sorbent. React Funct Polym 57:147–155

Prabhakaran D, Subramanian MS (2004) Extraction of U(VI), Th(IV), and La(III) from acidic streams and geological samples using AXAD-16-POPDE polymer. Anal Bioanal Chem 380:578–585

Prabhakaran D, Subramanian MS (2005) Selective extraction of U(VI) over Th(IV) from acidic streams using di-bis(2-ethylhexyl) malonamide anchored chloromethylated polymeric matrix. Talanta 65:179–184

Puliyel M, Mainous AG, Berdoukas V, Coates TD (2015) Iron toxicity and its possible association with treatment of cancer: lessons from hemoglobinopathies and rare, transfusion-dependent anemias. Free Radic Biol Med 79:343–351

Pyrzynska K (2005) Recent developments in the determination of gold by atomic spectrometry techniques. Spectrochim Acta Part B 60:1316–1322

Pyrzynska K, Trojanowicz M (1990) Functionalized cellulose sorbents for preconcentration of trace metals in environmental analysis. Crit Rev Anal Chem 29:313–321

Qian S, Huang Z, Fu J, Kuang J, Hu C (2010) Preconcentration of ultra-trace arsenic with nanometre-sized TiO_2 colloid and determination by AFS with slurry sampling. Anal Methods 2:1140–1143

Rajesh N, Jalan RK, Hotwany P (2008) Solid phase extraction of chromium(VI) from aqueous solutions by adsorption of its diphenylcarbazide complex on an Amberlite XAD-4 resin column. J Hazard Mater 150:723–727

Raman K, Lan JCW (2012) Performance and kinetic study of photo microbial fuel cells (PMFCs) with different electrode distances. Appl Energy 100:100–105

Ramesh A, Mohan KR, Seshaiah K (2002) Preconcentration of trace metals on Amberlite XAD-4 resin coated with dithiocarbamates and determination by inductively coupled plasma-atomic emission spectrometry in saline matrices. Talanta 57:243–252

Rawat M, Ramanathan AL, Subramanian V (2009) Quantification and distribution of heavy metals from small-scale industrial areas of Kanpur City, India. J Hazard Mater 172:1145–1149

de-Resende VG, Garcia FL, Peigney A, DeGrave E, Laurent CH (2009) Synthesis of Fe-ZrO_2 nanocomposite powders by reduction in H_2 of a nanocrystalline (Zr, Fe)O_2 solid solution. J Alloys Compd 471:204–210

Sabermahani F, Taher MA (2010) Flame atomic absorption determination of palladium after separation and preconcentration using polyethyleneimine water-soluble polymer/alumina as a new sorbent. J Anal At Spectrom 25:1102–1106

Sadeghi S, Garmroodi A (2013) A highly sensitive and selective electrochemical sensor for determination of Cr(VI) in the presence of Cr(III) using modified multi-walled carbon nanotubes/quercetin screen-printed electrode. Mater Sci Eng C 33:4972–4977

Sambandam S, Valluri V, Chanmanee W, deTacconi NR, Wampler WA, Lin WY et al (2009) Platinum-carbon black-titanium dioxide nanocomposite electrocatalysts for fuel cell applications. Chem Sci 121:655–664

Sandoval R, Cooper AM, Aymar K, Jain A, Hristovski K (2011) Removal of arsenic and methylene blue from water by granular activated carbon media impregnated with zirconium dioxide nanoparticles. J Hazard Mater 193:296–303

dos-Santos EJ, Herrmann AB, Ribeiro AS, Curtius AJ (2005) Determination of Cd in biological samples by flame AAS following on-line preconcentration by complexation with O, O-diethyldithiophosphate and solid phase extraction with Amberlite XAD-4. Talanta 65(2):593–597

Sawada H, Tsuzuki-ishi T, Kijima T, Kawakami J, Lizuka M, Yoshida M (2011) Controlling photochromism between fluoroalkyl end-capped oligomer/polyaniline and N,N'-diphenyl-1,4-phenylenediamine nanocomposites induced by UV-light-re sponsive titanium oxide nanoparticles. J Colloid Interface Sci 359:461–466

Schießer A, Hörtz P, Schäfer R (2010) Thermodynamics and kinetics of CO and benzene adsorption on Pt(111) studied with pulsed molecular beams and microcalorimetry. Surf Sci 604:2098

Selvaraj S, Krishnaswamy S, Devashya V, Sethuraman S, Krishnan UM (2011) Investigations on membrane perturbation by chrysin and its copper complex using self-assembled lipid bilayers. Langmuir 27:13374–13382

Seyhan S, Merdivan M, Demirel N (2008) Use of o-phenylene dioxydiacetic acid impregnated in Amberlite XAD resin for separation and preconcentration of uranium(VI) and thorium (vi). J Hazard Mater 152:79–84

Shahadat M, Bushra R, Shalla AH, Azam A (2011) Synthesis and characterization of nanocomposite ion-exchanger; its adsorption behavior. Colloids Surf B Biointerfaces 87:122–128

Shahadat M, Nabi SA, Bushra R, Raeissi AS, Umar K, Ansari MO (2012) Synthesis, characterization, photolytic degradation, electrical conductivity and applications of a nanocomposite adsorbent for the treatment of pollutants. RSC Adv 2:7207–7220

Shahdat M, Tenq TT, Rafatullah M, Arshad M (2015) Titanium-based nanocomposite materials: a review of recent advances and perspectives. Colloids Surf B Biointerfaces 126:121–137

Shang L, Li B, Donga W, Chen B, Li C, Tang W, Wang G, Wu J, Ying Y (2010) Heteronanostructure of Ag particle on titanate nanowire membrane with enhanced photocatalytic properties and bactericidal activities. J Hazard Mater 178:1109–1114

Sharma RK, Pant P (2009) Preconcentration and determination of trace metal ions from aqueous samples by newly developed gallic acid modified Amberlite XAD-16 chelating resin. J Hazard Mater 163:295–301

Sharma S, Nirkhe C, Pethkar S, Athwal AA (2002) Chloroform vapour sensor based on copper/polyaniline nanocomposite. Sens Actuators B 85:131–136

Sharma G, Kumar A, Naushad M, Pathania D, Sillanpää M (2016) Polyacrylamide@ Zr (IV) vanadophosphate nanocomposite: ion exchange properties, antibacterial activity, and photocatalytic behavior. J Indust Eng Chem 33:201–208

Shin KY, Hong JY, Jang J (2011) Heavy metal ion adsorption behavior in nitrogen-doped magnetic carbon nanoparticles: isotherms and kinetic study. J Hazard Mater 190:36–44

Shukla SK (2002) Synthesis of polyaniline grafter cellulose suitable for humidity sensing. Indus J Engg Mater Sci 19:417–420

Singh BN, Maiti B (2006) Separation and preconcentration of U(VI) on XAD-4 modified with 8-hydroxy quinoline. Talanta 69:393–396

Singh M, Singh S, Prasad S, Gambhir IS (2008) Nanotechnology in medicine and antibacterial effect of Ag nanoparticles. Dig J Nanomater Biostruct 3:115–122

Sitea AD (2001) Factors affecting sorption of organic compounds in natural sorbent/water systems and sorption coefficients for selected pollutants. A review Phys Chem 30:187

Sultana S, Mohammad R, Khan MZ, Umar K (2012) Synthesis and characterization of copper ferrite nanoparticles doped polyaniline. J Alloys Compd 535:44–49

Sultana S, Khan MD, Sabir S, Gani KM, Oves M, Khan MZ (2015a) Bio-electro degradation of azo-dye in a combined anaerobic–aerobic process along with energy recovery. New J Chem 39(12):9461–9470

Sultana S, Mohammad R, Khan MZ, Umar K, Ahmed AS, Shahadat M (2015b) SnO_2–SrO based nanocomposites and their photocatalytic activity for the treatment of organic pollutants. J Mol Struct 1098:393–399

Szlachta M, Wojtowicz P (2013) Adsorption of methylene blue and Congo red from aqueous solution by activated carbon and carbon nanotubes. Water Sci Technol 68:2240–2248

Teles FRR, Fonseca LP (2008) Applications of polymers for biomolecule immobilization in electrochemical biosensors. Mater Sci Eng C 28:1530–1543

Tewari PK, Singh AK (2000a) Amberlite XAD-7 impregnated with xylenol orange: a chelating collector for preconcentration of Cd(II), Co(II), Cu(II), Ni(II), Zn(II) and Fe(III) ions prior to their determination by flame AAS. Fresenius J Anal Chem 367:562–567

Tewari PK, Singh AK (2000b) Thiosalicylic acid-immobilized Amberlite XAD-2: metal sorption behaviour and applications in estimation of metal ions by flame atomic absorption spectrometry. Analyst 125:2350–2355

Tewari PK, Singh AK (2001) Synthesis, characterization and applications of pyrocatecholmodifiedAmberliteXAD-2resin for preconcentration and determination of metal ions in water samples by flame atomic absorption spectrometry (FAAS). Talanta 53:823–833

Tewari PK, Singh AK (2002) Preconcentration of lead with Amberlite XAD-2 and Amberlite XAD-7 based chelating resins for its determination by flame atomic absorption spectrometry. Talanta 56:735–744

Tian J, Chen L, Yin Y, Wang X, Dai J, Zhu Z, Liu X, Wu P (2009) Photocatalyst of TiO2/ZnO nano composite film: preparation, characterization, and photodegradation activity of methyl orange. Surf Coat Technol 204:205–214

Tobiasz A, Walas S, Trzewik B, Grzybek P, Zaitz MM, Gawin M, Mrowiec H (2009) Cu(II)-imprinted styrene–divinylbenzene beads as a new sorbent for flow injection-flame atomic absorption determination of copper. Microchem J 93:87–92

Tofighy MA, Mohammadi T (2011) Adsorption of divalent heavy metal ions from water using carbon nanotube sheets. J Hazard Mater 185:140–147

Tokalıoğlu S, Livkebabc A (2009) A new solid-phase extraction method for the determination of Cu(II) and Fe(III) in various samples by flame atomic absorption spectrometry using N-benzoyl-N-phenylhydroxylamine. Microchim Acta 164:471–477

Tokalıoğlu S, Yılmaz V, Kartal S (2009) Solid phase extraction of Cu(II), Ni(II), Pb(II), Cd(II) and Mn(II) ions with 1-(2-thiazolylazo)-2-naphthol loaded Amberlite XAD-1180. Environ Monit Assess 152:369–377

Topuz B, Macit M (2011) Solid phase extraction and preconcentration of Cu(II), Pb(II), and Ni(II) in environmental samples on chemically modified Amberlite XAD-4 with a proper Schiff base. Environ Monit Assess 173:709–722

Toyao T, Iyatani K, Horiuchi Y (2013) Enhanced photoelectrochemical properties of visible light-responsive TiO2photoanode for separate-type Pt-free photofuel cells by Rh3+ addition. Res Chem Intermed 39:1603–1611

Tunçeli A, Türker AR (2000a) Determination of palladium in alloy by flame atomic absorption spectrometry after preconcentration of its iodide complex on Amberlite XAD-16. Anal Sci 16:81–85

Tunçeli A, Türker AR (2000b) Flame atomic absorption spectrometric determination of silver after preconcentration on Amberlite XAD-16 resin from thiocyanate solution. Talanta 51:889–894

Tuzen M, Soylak M (2007) Multiwalled carbon nanotubes for speciation of chromium in environmental samples. J Hazard Mater 147:219–225

Tuzen M, Narin I, Soylak M, Elci L (2005) XAD-4/PAN solid phase extraction system for atomic absorption spectrometric determinations of some trace metals in environmental samples. Anal Lett 37:473–489

USEPA, United States Environment Protection Agency (2002) EPA Report EPA-822-R-02-047

Uzun A, Soylak M, Elçi L (2001) Preconcentration and separation with Amberlite XAD-4 resin; determination of Cu, Fe, Pb, Ni, Cd and Bi at trace levels in waste water samples by flame atomic absorption spectrometry. Talanta 54:197–202

Vaseashta A, Dimova-Malinovska D (2005) Nanostructured and nanoscale devices, sensors and detectors. Sci Technol Adv Mater 6:312

Venkatesh G, Singh AK (2005) 2-{[1-(3,4-dihydroxyphenyl)methylidene]amino}benzoic acid immobilized Amberlite XAD-16 as metal extractant. Talanta 67:187–194

Venkatesh G, Singh AK (2007) 4-{[(2- Hydroxyphenyl)imino]methyl}-1,2-benzenediol (HIMB) anchored Amberlite XAD-16: preparation and applications as metal extractants. Talanta 71:282–287

Wade C, Otero E, Poon-Kwong B, Rozier R, Bachoon D (2015) Detection of human-derived fecal contamination in Puerto Rico using carbamazepine, HF183 Bacteroides, and fecal indicator bacteria. Mar Pollut Bull. doi:10.1016/j.marpolbul.2015.11.016

Wang C, Xu BQ, Wang XM, Zhao JC (2005) Preparation and photocatalytic activity of $ZnO/TiO_2/SnO_2$ mixture. J Solid State Chem 178:3500

Wang X, Feng Y, Wang H, Qu Y, Yu Y, Ren N, Li N, Wang E, Lee H, Logan BE (2009) Bioaugmentation for electricity generation from corn Stover biomass using microbial fuel cells. Environ Sci Technol 43:6088–6093

Wang J, Yuan R, Chai Y, Li W, Fu P, Min L (2010) Using flowerlike polymer-copper nanostructure composite and novel organic-inorganic hybrid material to construct an amperometric biosensor for hydrogen peroxide. Colloids Surf B Biointerfaces 75:425–431

Wang Y, Xie J, Wu Y, Hu X, Yang C, Xu Q (2013) Determination of trace amounts of Se(IV) by hydride generation atomic fluorescence spectrometry after solid-phase extraction using magnetic multi-walled carbon nanotubes. Talanta 112:123–128

Waren CW, Nie S (1998) Quantum dot bioconjugates for ultrasensitive nonisotopic. Detection Sci 281:2016

Wei Y, Yang R, Chen X, Wang L, Liu JH, Huang XJ (2012) A cation trap for anodic stripping voltammetry: NH3-plasma treated carbon nanotubes for adsorption and detection of metal ions. Anal Chim Acta 755:54–61

Wiśniewski M, Terzyk AP, Gauden PA, Kaneko K, Hattori Y (2012) Removal of internal caps during hydrothermal treatment of bamboo-like carbon nanotubes and application of tubes in phenol adsorption. J Colloid Interface Sci 381:36–42

Wongkaew M, Imyim A, Eamchan P (2008) Extraction of heavy metal ions from leachate of cement-based stabilized waste using purpurin functionalized resin. J Hazard Mater 154:739–747

Xie Y, Huang C, Zhou L, Liu Y, Huang H (2009) Supercapacitor application of nickel oxide–titania nanocomposites. Compos Sci Technol 69:2108–2114

Xing W, Ngo HH, Kim SH, Guo WS, Hagare P (2008) Adsorption and bioadsorption of granular activated carbon (GAC) for dissolved organic carbon (DOC) removal in wastewater. Bioresour Technol 99:8674–8678

Xiong S, Wang Q, Xia H (2004) Template synthesis of polyaniline/TiO_2 bilayer microtubes. Synth Met 146:37–42

Xu Y, Zhou J, Dong J (2010) Infrared absorption spectra of few-layer graphenes studied by first principles calculations. J Phys Lett A 374:796–800

Yalçin S, Apak R (2004) Chromium(III, VI) speciation analysis with preconcentration on a maleic acid-functionalized XAD sorbent. Anal Chim Acta 505:25–35

Yang K, Xing BS (2010) Adsorption of organic compounds by carbon nanomaterials in aqueous phase: Polanyi theory and its application. Chem Rev 110:5989–6008

Yang K, Zhu L, Xing B (2006) Adsorption of polycyclic aromatic hydrocarbons by carbon nanomaterials. Environ Sci Technol 40:1855–1861

Yang W, Yang R, Chen X, Wang L, Liu JH, Huang XJ (2012) A cation trap for anodic stripping voltammetry: NH3-plasma treated carbon nanotubes for adsorption and detection of metal ions. Anal Chim Acta 755:54–61

Yebra MC, Carro N, Enríquez MF, Moreno-Cid A, García A (2001) Field sample preconcentration of copper in sea water using chelating minicolumns subsequently incorporated on a flow-injection-flame atomic absorption spectrometry system. Analyst 126:933–937

Zeng L, Chen Y, Zhang Q, Guo X, Peng Y, Xiao H, Chen X, Luo (2015) Adsorption of Cd(II), Cu(II) and Ni(II) ions by cross-linking chitosan/rectorite nano-hybrid compositemicrospheres. Carbohydr Polym 130:333–343

Zhang MB, Gao S (2013) Removal of arsenic, methylene blue, and phosphate by biochar/AlOOH nanocomposite. Chem Eng J 226:286–292

Zhang Z, Kong J (2011) Novel magnetic Fe_3O_4@C nanoparticles as adsorbents for removal of organic dyes from aqueous solution. J Hazard Mater 193:325–329

Zhang L, Liu P, Su Z (2006) Preparation of PANI-TiO_2 nanocomposites and their solid-phase photocatalytic degradation. Polym Degrad Stab 91:2213–2219

Zhang LJ, Peng H, Kilmartin PA, Soeller C, Travas-Sejdic J (2007) Polymeric acid doped polyaniline nanotubes for oligonucleotide sensors. Electroanalysis 19:870–875

Zhang H, Zong R, Zhao J, Zhu Y (2008) Dramatic visible photocatalytic degradation performance due to synergetic effect of TiO2 with PANI. Environ Sci Tech 42:3803–3807

Zhang HD, Tang CC, Long YZ, Zhang JC, Huang R, Li JJ, Gu CZ (2014) High-sensitivity gas sensors based on arranged polyaniline/PMMA composite fibers. Sens Actuators A 219:123–127

Zuo Y, Chen G, Zeng G, Li Z, Yan M, Chen A, Guo Z, Huang Z, Tan Q (2015) Transport, fate, and stimulating impact of silver nanoparticles on the removal of Cd(II) by Phanerochaete chrysosporium in aqueous solutions. J Hazard Mater 285:236–244

Textile Wastewater Treatment Options: A Critical Review

Khadija Siddique, Muhammad Rizwan, Munazzam Jawad Shahid, Shafaqat Ali, Rehan Ahmad, and Hina Rizvi

Abstract Textile industry is one of the largest water-consuming industries in the world, and its wastewater contains many pollutants such as dyes, degradable organics, detergents, stabilizing agents, desizers, inorganic salts, and heavy metals. In Pakistan, most of the textile industries discharge untreated wastewater into water bodies without any treatment, which percolates into the groundwater posing a threat to the health and socioeconomic life of the people. Pretreatment, dyeing, printing, and finishing are the main steps in dyeing and printing process of textile industries. A large amount of wastewater is being generated by all these processes, which contains many pollutants like reactive dyes, chemicals, high chemical oxygen demand (COD), biological oxygen demand (BOD), and organic compounds. Research has been conducted since long to treat textile wastewater in an economical and efficient way. There are many processes for removal of polluted compounds from water that include physicochemical, biological, combined treatment processes, and other technologies. All over the world, ecological standards are gaining importance in every step of textile unit. Due to the strict implementation of environmental standards, it is important to adopt an eco-friendly model of textile industry that overcomes all flaws from its start to end product. The main challenge is to develop a design that can be considered as cost-effective and to substitute chemicals that are less harmful or can be easily treated. On the basis of wastewater characteristics and literature review, appropriate scheme of treatment processes was proposed.

Keywords Textile wastewater • Treatment • Toxicity • Chemicals • Pollution

Textile Industry Wastewater: Challenges

The increasing population in Pakistan is requiring economic growth so the industrial progress has been stirred up to meet the demands of growing population. On the other hand, the regulatory measures are being neglected from the very

K. Siddique • M. Rizwan • M.J. Shahid • S. Ali (✉) • R. Ahmad • H. Rizvi
Department of Environmental Sciences and Engineering, Government College University, Allama Iqbal Road, Faisalabad 38000, Pakistan
e-mail: shafaqataligill@yahoo.com

N.A. Anjum et al. (eds.), *Enhancing Cleanup of Environmental Pollutants*,
DOI 10.1007/978-3-319-55423-5_6

first, and the situation is getting worse as the implementation policy for control measures is being neglected (Husain and Hussain 2012). The textile sector is playing an important role in Pakistan's economy as it is providing employment to 38% of people; along with, it is an important source of foreign exchange. Out of the total export, 65% of country export is provided by the textile sector alone (Bauer 2001). In all over the country, many industries are working and strengthening the economy by their production; out of this total production, textile industry accounts for 46%. Some of the industrial products are also exported to foreign countries; textile products are also exported and provide 9% of gross national product (GNP) (Sudipta et al. 2005). Keeping in view, all these facts, we can say that textile industry is the backbone of Pakistan economy. The textile sector is based on 670 industries that are working in all over the country. Out of this 670, 300 are situated in Karachi alone, and the remaining 370 are working in different areas of Punjab (Ara 1998).

It has been published in the yearbook of China that 390 million tons of sewage water is producing each year in China. Out of these 390 million tons, 51% is produced by industrial sector, and this rate is increased by 1% each year (Ho and McKay 2003). According to a rough estimate, the textile sector has a major contribution toward 51% of the sewage wastewater as 70 billion tons per year of wastewater is coming out of dyeing industries alone. This wastewater has heavy pollution load, and it is ridiculous to discharge this water without any prior treatment. As compared to agricultural use, the industrial use of water is very little. The heavy pollution load in wastewater makes water resources unfit for other uses. In water-scarce countries like Pakistan, the reuse of water is a constant demand because an extensive amount of water is needed for agricultural activities. Therefore, water management is a challenge for us as freshwater resources are decreasing rapidly and water is getting polluted with industrial activities (Anindya et al. 2005).

Textile industry is one of the biggest industries in the world, and a large amount of water is consumed in its processing. Different stages of textile industry are named as singeing, desizing, scouring, bleaching, mercerizing, dyeing, printing, and finishing. All textile industries use these processes according to their requirement (El-Gohary and Tawfik 2009). The environmental problems created by textile industry wastewater are due to increased oxygen demand, high color, and large amount of suspended solids. Wastewater of textile unit contains many pollutants, like inorganic compounds, dye waste, color residues, catalytic chemicals, and cleaning solvents (USEPA 1997). It has been studied that in all over the world, overall production of dyes is 700,000 tons each year (Riera-Torres et al. 2010). There are different combinations of dyes that are being used to color different stuffs. Some of these dyes are degraded naturally, but some need special treatment, as they can't be degraded naturally. There are different types of dyes that are chemically different from each other. These dyes include azo dyes, xanthene dyes, nitro dyes, phthalocyanine dyes, etc. (Gupta and Suhas 2009). Dyes can be further classified as acid dyes, basic dyes, and reactive dyes. The combination of different dyes used to achieve different shades makes the treatment process more difficult as each dye has different chemical natures (Andre et al. 2005). It is believed that all over the world, more than one million tons of dyes are

manufactured each year and out of this, 0.28 million tons are discharged into wastewater (Robert and Sanjeev 2005). Textile industry wastewater especially from dyeing and printing industries needs proper treatment before its discharge in water bodies as major contribution of the largest amount of textile wastewater is from the developing countries. In textile processing industry, wastewater contains many pollutants and needs to be treated as they can cause serious health impacts to aquatic life as well as human beings (Lau and Ismail 2009). Therefore, it is an utmost need to treat textile wastewater so that problems related to pollution caused by it can be avoided.

Pretreatment, dyeing, printing, and finishing are the main steps in dyeing and printing process of textile industries. A large amount of wastewater is being generated by all these processes, which contains many pollutants like reactive dyes, chemicals, high chemical oxygen demand (COD), biological oxygen demand (BOD), and organic compounds (El-Gohary and Tawfik 2009). Research has been conducted since long to treat textile wastewater in an economical and efficient way. There are many processes for removal of polluted compounds from water that include physicochemical, biological, and combined treatment processes and other technologies (Phan et al. 2000). There are many sulfide compounds used in textile industry that are environmental concerns because of their hazardous nature. So, a combination of biological and chemical methods is being reviewed for sulfur treatment (Nguyen and Juang 2013). All over the world, ecological standards are gaining importance in every step of textile unit. Due to the strict implementation of environmental standards, it is important to adopt an eco-friendly model of textile industry that overcomes all flaws from its start to end product (Robinson et al. 1997).

The main challenge is to develop a design that can be considered as cost-effective and to substitute chemicals that are less harmful or can be easily treated. Recycling can be a preferred option in this regard as it can solve two problems. First of all, recycling means less generation of waste. Secondly, it is economically beneficial to develop techniques to use recycled products. Control techniques can be divided into three types: (1) an efficient design using less polluting agents and minimizing waste generation; (2) after generation of waste, an effective treatment option for this wastewater; and (3) finding suitable steps where recycled products can be applied (Sule and Bardhan 1999). Dyeing and finishing processes in textile industry are major threats as they are using large quantities of chemicals and dyeing agents that cannot be treated easily (Mustafa and Delia 2006). Organic nature of these chemicals makes the problem serious as they have complex structure. Heavy metals are another concern.

Main Steps in Textile Processing Industry

The main processes of a textile industry include singeing, desizing, scouring bleaching, mercerizing, dyeing, printing, finishing, and marketing. Textile wastewater includes (a) suspended solids, (b) mineral oils, (c) nonrecyclable or low

recyclable surfactants, (d) wet-finishing process that produces phenols (e.g., dyeing), (e) halogenated organics produced in bleaching that is using solvents, and (f) textile effluents that are usually hot and highly colored and may have heavy metals (e.g., chromium, copper, zinc).

Treatment Options

Textile wastewater handling is a blend of different methods. The principal phase comprises typically of physical steps. Physicochemical methods have been extensively used in textile treatment plants, which give good removal efficiency of suspended materials, but it is not as much effective to remove COD. Various textile wastewater approaches are given below.

Physical Methods of Decoloration

Equalization and Homogenization

Textile dyeing wastewater usually needs pre-handling to ensure uniform flow of water for steady operation. Generally, the flexible container is fixed to handle the wastewater. Meanwhile, to avoid the cotton fur and the slurry settle in depth, air is used in the container for mixing. Eight hours of retention time is usually required.

Floatation

Floatation is a triple-phase combination of water, gas, and solid. In this process, air under pressure is introduced that combines with particles in the form of bubbles. This mixture settled down due to its lower density, and the heavy material separated out due to higher density. It can successfully eliminate the fibers from textile wastewater.

Adsorption

Some organic dyes are not easily biodegradable because of their structure. They have long chain of carbon, which causes a limitation, and they are resistant to degrade in normal biotic conditions. Treatment of such organic dyes is important, and it demands best knowledge of abiotic conditions to degrade such compounds. Adsorption is the greatest applied technique in wastewater management that can mix the wastewater and the spongy material powder or granules, such as carbon and clay, or allows the wastewater to pass through the sieve bed made up of granular

matter. Through this technique, contaminants in the wastewater are adsorbed on the surface of the spongy material or sieve.

Adsorption is said to be a feasible abiotic condition to treat such organic waste. It is important to have an idea about the conditions affecting adsorption capabilities of such compounds, which may depend on water hardness, time of treatment, and many other factors. Sludge of adsorption process is an important component so it is necessary to develop better understanding about the treatment process and sludge quality (Ozcan et al. 2004). It has been suggested that there should be 3 g per liter of sludge, and minimum time of reaction should be 24 h and 6 days for maximum. The maximum time limit is rarely needed because most of the dyes require 1-day treatment only. Hardness of water should be 80 mg per liter, which gives best removal. The removal efficiency of dyes from this process is considered to be 1 g per liter to 30 mg per liter. The concept of activated sludge treatment gives tremendous improvement in treatment process. There are various materials used as adsorbents in sludge treatment such as charcoals, activated carbons, clays, soils, and coagulants (Silva et al. 2004). Some information about molecule size and charge on dye, its pH, and salt complex is important because adsorption process is not that simple but it's a combination of adsorption and ion exchange process. Although there is a vast variety of adsorbent available in the market, not all are appropriate for commercial use. Price, ease to handle the adsorbent, and binding capacity are parameters which should be kept in mind while applying them in treatment processes for commercial use. Lignocellulose is one of the effective adsorbents, which is used on a large scale because it is not costly and effective against acid dyes (Pignon et al. 2000). Adsorption is a time-consuming process, and sludge produced by this process may not be easy to handle which is the main drawback of this process.

Low-Cost Adsorbents

The nonconventional low-cost adsorbent should have some specific properties in order to be used as dye adsorption. Those properties can be (a) efficient to remove an extensive variety of dyes, (b) high rate of adsorption and capacity, (c) high ability to tolerate extensive range of wastewater parameters, and (d) highly selective for different concentrations.

Natural Materials

Clays

Natural clay minerals have grabbed the attention of mankind since the civilization time. Clay materials are famous as adsorbents due to their low cost, ease of availability in most of the world continents, high potential for ion exchange, and

sorption properties. The clay materials have a layered structure and mostly favorable as host materials. The classification of clay materials is based on the differences in the layered structures such as mica (illite), smectites (saponite, montmorillonite), serpentine, pyrophyllite (talc), kaolinite, vermiculite, and sepiolite (Shichi and Takagi 2000). The natural clay shows adsorption capabilities due to a net negative charge on the mineral structure. The negative charge of clay minerals attracts the positive-charged species, and so adsorption takes place. The sorption properties depend on the high porosity and high surface area (Alkan et al. 2004). Montmorillonite clay possesses the largest surface area and highest capacity for cation exchange. The current market price of montmorillonite clay is about US$ 0.04–0.12/kg and is considered as 20 times cheaper than the activated carbon (Babel and Kurniawan 2003). The clay minerals such as kaolinite, bentonite, diatomite, and Fuller's earth are now becoming popular to be used in recent years due to their unique adsorption capacity for organic and inorganic molecules. Different scholars have extensively studied the interactions between the dyes and clay particles reported in articles (Alkan et al. 2005, 2004; Gu¨rses et al. 2004; Wang et al. 2004; Al-Bastaki and Banat 2004; Ozcan et al. 2004; Ozdemir et al. 2004; Al-Ghouti et al. 2003; Atun et al. 2003).

Siliceous Materials

Natural siliceous sorbents such as glasses, alunite, silica beads, perlite, and dolomite are becoming popular to be used for wastewater due to their abundance, low price, and availability. The most prominent in inorganic materials are the silica beads (Crini and Morcellet 2002; Woolard et al. 2002; Harris et al. 2001; Phan et al. 2000), having silanol groups on the hydrophilic surface responsible for the chemical reactivity. Their porous texture, mechanical stability, and high surface area are the key factors, which make them suitable as sorbents in decontamination applications. The presence of acidic silanol on the siliceous material surface causes an irreversible and strong nonspecific adsorption. So the negative features of sorbents should be eliminated. The interaction of siliceous materials with dyes can be promoted by modifying the silica surface using silane-coupling agents having amino functional group (Krysztafkiewicz et al. 2002). Another important sorbent from siliceous materials is alunite (Dill 2001). Alunite mineral comes from the jarosite group and consists of approximately 50% SiO_2. The characteristics of alunite are discussed in the review by Dill in 2001. The untreated alunite does not show good adsorbent properties (Ozacar and Sengil 2003). In order to use alunite as good adsorbent for removing colors, a suitable process is done to obtain alunite-type layered structure (Ozacar and Sengil 2002).

Zeolites

Zeolites are the highly porous aluminosilicates having different cavity structures. Zeolites are extensively used as substitute materials in particular areas such as sorptive applications. Zeolites are useful in removing the trace amounts of pollutants, e.g., phenols and heavy metal ions due to their cage-like structures appropriate for ion exchange. A lot of the literature is available on sorbent behavior of the neutral zeolites (Ozdemir et al. 2004; Armagan et al. 2004; Meshko et al. 2001). The zeolite efficiency to remove dyes may not be better than clay materials, but the easy access, availability and low cost make them suitable for many applications (Calzaferri et al. 2000).

Biosorbents

Chitin and Chitosan

The emerging biosorption method uses biopolymers such as chitin and chitosan for sorption of dyes. Chitin and chitosan are renewable, abundant, and biodegradable resources. Several studies on chitin and chitosan revealed that chitosan-based biosorbents are competent materials and have tremendously high attraction for many categories of dye years (Chiou and Li 2002, 2002; Chao et al. 2004; Chiou et al. 2004). They are versatile materials and can be used as sorbents in different forms, from flake types to bead types, gels, or fibers (Wu et al. 2000, 2001a, b). Wong et al. (2004) demonstrated the chitosan performance to remove acid dyes as an adsorbent in detail. According to his research, the adsorption capacities of chitosan for acid red 18, acid red 73, acid orange 10, and acid orange 12 were 693.2, 728.2, 922.9, and 973.3 mg/g, respectively.

Peat

Peat possesses porosity and is a complex soil material having organic matter in several stages of decomposition. The classification of peat is based on nature of parent materials. Peats are identified into four groups such as moss peat, woody peat, herbaceous peat, and sedimentary peat. The peat is plentiful, inexpensive, and available as biosorbent for a variety of pollutants. The polar property of peat makes them suitable for removal of dyes from solution (Allen et al. 2004; Ho and McKay 2003). The raw peat has some limitations such as low mechanic strength; poor chemical stability, to leach fulvic acid; a high affinity for water; and a tendency to shrink or/and swell (Sun and Yang 2003).

Biomass

Bioadsorption and/or decolorization of dye wastewater by white-rot fungi, (dead or living) biomass, and other microbial cultures was the subject of much research as reviewed in several recent papers (McMullan et al. 2001; Robinson et al. 2001; Stolz 2001; Pearce et al. 2003; Aksu 2005). In fungal decolorization, fungi can be categorized into two classes based on their life state: living cells to biosorb and biodegrade dyes and dead cells to adsorb dye (Fu and Viraraghavan 2001a). The recent studies have focused on the removal of dyes with strains of *Aspergillus niger* (Fu and Viraraghavan 2002a, b) and *Rhizopus arrhizus* (Aksu and Tezer 2000). Fu and Viraraghavan (2001b, 2002a, b) confirmed that *Aspergillus niger* as biosorbent shows remarkable properties for dye removal.

Miscellaneous Sorbents

Starch has been studied as low-cost sorbent (Delval et al. 2001, 2002, 2003) and cyclodextrins (Crini and Morcellet 2002; Crini et al. 2002a, b; Crini 2003). Starch belongs to carbohydrate class and is present as an energy storage material in living plants. It has also been demonstrated that cross-linked cyclodextrin gels can be used for efficient extraction of dyes. The sorption properties are enhanced due to existence of CD molecules in the polymer network (Crini and Morcellet 2002; Crini et al. 2002a, b; Crini 2003).

Chemical Methods

Oxidative Process

Oxidative procedures are characterized as an extensively applied chemical technique for the handling of textile discharge, where decolorization is the purpose. The key chemical is hydrogen peroxide (H_2O_2) that forms hydroxyl radicals, which are strong oxidizing agents and are capable to decolorize a variety of dyes (Entezari and Pe´trier 2004). Oxidation process is being used from so long, and it is found to be an easy to handle process that has been extensively used on commercial basis. Hydrogen peroxide is highly stable, and there are various methods of its activation, which are named accordingly.

Fenton Treatment

It is a very useful technique for wastewater treatment. It has its own specification which is found to be very effective to treat COD and gives the best removal against

many dyes. In the first technique, hydroxyl radical is produced from H_2O_2 during Fenton reaction, where hydrogen peroxide is added to an acidic mixture (pH = 2–3) having Fe^{2+} ions. The reaction is exothermic and must be performed at temperature greater than ambient (Hassan and Hawkyard 2002). Besides many advantages, this process also has a limitation. Sludge produced by this process contains many impurities, and it requires proper land disposal that is not easy to handle. Fenton sludge recycling is a proposed technique to get rid of harmful impacts that makes it easy to handle this sludge (Joseph et al. 2000). Mechanical handling of this sludge is a possible option. The sludge contains phosphate that can be removed, that makes this sludge less harmful, and it may be treated through biotic processes.

Ozonation

Ozone is being used for the wastewater treatment since 1970. It is highly instable which makes it a strong oxidizer. When compared to chlorine having oxidizing potential of 1.36, it was found to be a better oxidizing agent with an oxidizing potential of 2.07 (Koch et al. 2002). It was mainly used against drinking water, and the main purpose was to make it clean, but its other properties against toxic compounds of wastewater make it a favorable option in textile wastewater treatment. It was found to be effective against many aromatic hydrocarbons, phenols, pesticides, etc. It is a very active and rapid decolorization handling method. Ozonation can tackle with the double bonds in dyes, and COD can be lowered by this method. Many of the nonbiodegradable products can be easily decomposed. 18.5 and 9.1 mg/l concentrations of ozone are enough to remove 50 and 60% COD after 60 and 90 min, respectively (Selcuk 2005). In this process, the usual application is the use of sodium hypochlorite that has the ability to break azo bond. The shortcoming of this process is that it releases amine compounds and these can cause cancer. It also has a limitation that it is readily decomposed in water having a life span of just 20 min. This is the main drawback of this treatment, and the time may get shortened enough when the wastewater having dyes is projected toward this treatment (El-Din and Smith (2002)). Other factors may influence its stability in water such as pH, temperature, etc. Ozone stability is highly affected by the presence of alkaline salts. It may get reduced when alkaline water is treated against it, while natural salts have a positive impact and enhance its stability (Arslan 2001). Temperature has a negative impact on ozone solubility. With increasing temperature, it becomes less soluble in water (Ma and Graham 2000).

Several options are keeping concern regarding the reduction in the parameter like COD, BOD, and TOC. Ince and Tezcanli (2001) stated that ozone treatment doesn't reflect any changes in COD. Ikehata (1975) conveyed a decrease in COD and BOD standards, while Koch et al. (2002) found that the use of ozone treatment will increase in the value of two parameters. Practices with TOC decline are constant, viz., treatment with ozone does not effect it. Meanwhile, addition in oxygen in soluble composites with ozone is not successful at an initial stage.

Carriere et al. (1991) advocate ozone treatment as a tertiary treatment, succeeding as an activated sludge process. The ratio of other substances present in dye wastewater is lesser than the present in the pure solution (up to 20% of dye leftover in the water after ozone treatment). At the very first step, eradication of foaming and reducing agents increases color removal efficiency by ozone treatment (Andreozzi et al. 2001a).

H_2O_2 UV Radiation

All the above-stated complications (sludge evolution and renewal increase the intensity of polluted wastewater caused by ozonation) can be stated away by oxygen addition with hydrogen peroxide, initiated with UV light. The single element used in the treatment is H_2O_2, and due to its final breakdown into oxygen, it is not problematic. Peroxide is activated by UV light. Aspects persuading H_2O_2/UV processes are concentration of hydrogen peroxide, the strength of UV radiation, pH, dye composition, and dyebath structure. Overall, discoloration is utmost successful at pH = 7, at greater UV irradiant concentrations (1600 W rather than 800 W), with an ideal concentration of H_2O_2, which varies for diverse dye sessions, and through a dyebath that does not cover oxidizing agents having an oxidizing capacity advanced than that of peroxide (Andreozzi et al. 2001a). According to Andreozzi et al. (2001b), the easiest decomposable dyes are acid dyes, and with an accumulative number of azo groups, the discoloration efficiency declines. Arslan et al. (2000) reported prolonged decoloration required by the yellow and green dyes, while on the other hand, quick decoloration is showed by the direct, metal-complex, and disperse dyes. In the collection of blue dyes eliminated, only blue dyes were not vat decolorized, yet their composition alters with the procedure in such a way that they can be simply filtrated. The filtrate is colorless. For pigments, H_2O_2/UV method is not appropriate, since they form a filmlike covering which is tough to eliminate.

Hydrogen Peroxide

The efficiency of method relies on the peroxidase usage, its strength, pH, and the temperature of the medium. Fukushima and Tatsumi (2001) studied the discoloration of acid dye by three kinds of peroxidases [horseradish (HRP), soybean (SPO), and *Arthromyces ramosus* (ARP)] as peroxide activator. By calculating the absorbance capacity, they found that the persistency was the highest via ARP. The discoloration rate augmented with higher peroxidase accumulation and temperature of medium and was the highest at pH 9.5.

NaOCl

Cl compounds are useful in the chemical oxidation of colored wastewaters. Electrophilic breakdown occurs at the amino group by Cl+pledgees and speeds up the consequent azo bond cleavage. Namboodri et al. (1994) reported the adequate discoloration of acid and direct dyes. Treatment of reactive dyes prerequisite longer times, while solutions of metal-complex dyes persisted partially colored (Manu and Chaudhari 2003). Disband dyes do not decolorize with NaOCl. Decoloration rate rises with increase in chlorine intensity and declining pH of medium. According to Omura (1994), dyes encompassing amino or exchanged amino groups on the naphthalene ring, i.e., dyes derivative from aminonaphthol- and naphthylamine-sulfonic acids, are the greatest subject for chlorine decoloration. One feature which has come to the front in current years, and which is related to chlorine-centered decoloration practices, is that, for atmosphere causes, the upcoming use of chemicals comprising chlorine should be controlled. Since 5 and 60% of European chemical manufacture openly or ultimately rest on chlorine, the influence of such a prohibition could be huge, mainly for organic colorant production. However, it must be illustrated that even though about 40% of worldwide used pigments comprise chlorine, this corresponds to less than 0.02% of the total chlorine production (Clarke and Steinle 1995).

Ion Exchange

It's a treatment process that has been used to treat wastewater excluding dye-containing wastewater. The main reason of avoidance was a misconception, and it was thought that this method is not effective against dye-containing wastewater and its effectiveness slows down further when wastewater is loaded with other additives in consort with dyes. This flaw was removed with an excellent work of Baouab et al. (2001) who proved in his experiment that sulfur-containing dyes and those with acidic nature could better be treated with a combination of anion exchange column that is packed in series and a nonpolar resin. This was a great turning point in treatment of textile wastewater because it added another positive option against dye treatment and it could be further explored within time. The ion exchange resins needed to be regenerated after one-time removal, and this task was completed with the help of organic solvents. The organic solvents are not that much cheap, and their use increased the operational cost that was the major drawback of ion exchange method.

The research on the highlighted above method provided wise choices and the use of quaternized cellulose. The sulfonate group of dye makes an association with the amine group of resin through columbic forces, or other bonding forces may be developed between them such as van der Waals forces or hydrogen bonding (Glover 1993). The efficiency of a resin to remove dye from wastewater can be judged through these bonding. If there is a strong bonding present between dye and

resin, there will be effective removal of dye. There are many theories about the effectiveness of this method. According to Laszlo (1994), chloride concentration has a negative impact of dye removal efficiency. With the increased concentration of chlorine, there will be less bonding between dye and resin, while sulfate and carbonate have a null impact on this bonding so their concentration does not affect the dye removal efficiency. In the same way, with the addition of sodium hydroxide, the binding process completely gets stopped. This can be positively used in treatment process, and using sodium hydroxide can regenerate the resin. The main reason of this poor bonding is that, when pH is increased, the proton may be removed from quaternary amine and makes conjugate base which may increase the hydroxyl group that may result in a repulsion force between dye and resin.

Coagulation and Sedimentation

This technique is one of the most used techniques in the past. In this process, some of the chemicals are added in the water that assists the charged particles to make some compound that can be coagulated in water. Usually, the colloids carry negative charges so the coagulants are normally inorganic or organic cationic coagulants (with positive charge in water). Some of the organic polymers cause coagulation to an extent that these coagulants combine to give groups and form sediments that is easy to extract (Ciardelli and Ranieri 2001). The most commonly used chemicals are $FeCI_3$, $AI_2\ (SO_4)_3$, $FeSO_4$, and lime (Verma et al. 2012).

Electrocoagulation

In this technique, effluents are treated in a chamber in which metal electrodes are used to treat wastewater. Electrode plates are suspended in effluent solution, and it can remove metal oxide at a specific pH. Metal oxides are coagulated and can be easily removed from the solution. This method is effective and has been reviewed in many articles (Khandegar and Saroha 2013). This technique uses direct current source between metal electrodes immersed in the effluent, which causes the dissolution of electrode plates into the effluent. The metal ions, at an appropriate pH, can form wide range of coagulated species and metal hydroxides that destabilize and aggregate particles or precipitate and adsorb the dissolved contaminants. Therefore, the objective of the present manuscript is to review the potential of electrocoagulation for the treatment of industrial effluents, mainly removal of dyes from textile effluent.

Reverse Osmosis

Reverse osmosis membranes have a holding degree of 90% or greater for most kinds of ionic complexes. Decolorization and removal of chemical auxiliaries in dyehouse wastewater can be done in a single step by reverse osmosis. Reverse

osmosis causes the elimination of all mineral salts, hydrolyzed responsive dyes, and chemical auxiliaries. This process needs a very high energy since a very high pressure is required herein (Babu et al. 2007).

Nanofiltration

Nanofiltration has been used for the management of color discharges from the textile industry. Nanofiltration membranes hold low molecular weight organic complexes, divalent ions, big monovalent ions, hydrolyzed responsive dyes, and dyeing auxiliaries (Ellouze et al. 2012). In most available studies regarding dyehouse discharges, the amount of mineral salts does not surpass 20 g/L, and the amount of dyestuff does not surpass 1.5 g/L (Babu et al. 2007).

Biological Treatment

As compared to physiochemical and photochemical methods, biological methods can be categorized as cost-effective substitutes of textile wastewater treatment. All the other methods are costly and have major drawbacks when applied to textile industry. All the possibilities of biological methods have been studied, and they are being applied in textile industries using different microorganisms (Sarayu and Sandhya 2012). It has been studied that a single strain of bacteria or fungi is effective to remove a dye, but it cannot be applied to remove another dye. Therefore, this method can't be adopted at commercial scale (Mendez-Paz et al. 2005). Recently, a natural colonized algae and duckweed plants were found to be very effective to treat textile wastewater in a pond experiment (Sekomo et al. 2014). Biological methods can be categorized as aerobic and anaerobic processes, and they give the best results when applied to remove organic pollutants from textile wastewater (Frank et al. 2001). In field applications, aerobic methods did not give the best results in color removal. Many of the dyes, especially azo dyes, are found to be resistant in aerobic application (Mustafa and Delia 2006). Urban anaerobic sludge blanket reactor has been introduced in textile wastewater treatment, and it gives the best results in treatment of xenobiotic compounds. It has the ability to handle very resistant compounds also (Jantsch et al. 2002).

Aerobic Biodegradation

There is a natural process in the aquatic ecosystem named as aerobic biodegradation that is necessary to treat the wastewater of rivers and streams and makes them clean from pollution loads. The biodegradability of many compounds can be judged by many parameters such as chemical oxygen demand (COD), biological oxygen demand (BOD), dissolved oxygen (DO), and the evaluation of carbon dioxide

(Dos Santos et al. 2003). The main factor of the whole procedure is the assessment of the chemicals that can be easily biodegraded. There are OECD 301 guidelines available that must be adopted, and by using this method, there should be 70% DOC removal (OECD 1993).

If the compound is assessed as biodegradable and conditions are favorable, there is a possibility that the compound will be biodegraded in wastewater plant same like it can be degraded in natural environment (Cruz and Buitron 2000). Strotmann et al. (1995) made a research and developed COz/DOC scheme for effective removal of DOC. In this design, the compound was mineralized and DOC was eliminated. There were remarkable results of this procedure, and when it was compared with Zahn-Wellens test, it provided better information of biodegradability of compounds. On the basis of these results, the behavior of many compounds can be explored in natural environment and in wastewater treatment plants as well.

Anaerobic Biodegradation

Anaerobic degradation is degradation when there is an absence of oxygen or very low oxygen present in the medium. This kind of degradation usually occurs in lower sediments in natural aqueous environment because that is poor oxygen medium. Some kind of sewage waste is also degraded by this procedure. So it can be predicted that a compound having low solubility in water and can be adsorbed on solids can be subjected to anaerobic degradation. Anaerobic bacteria or microorganisms achieve this task. This is a complete sequence step process in which bacteria that act in acidic medium act on organics such as carbohydrates and fats. These organics may be converted in alcohols and other simple compounds with the action of acidic bacteria. These products then stimulate the acetogenic bacteria, which further convert them in carbon dioxide and molecular hydrogen. Then, after reduction of these products, methane is generated, and methanogen bacteria perform this task. Biogas is an important parameter in anaerobic treatment that gives an assessment about the rate of experiment. There are many researches available which can explore the aerobic and anaerobic treatment, but a comparative study of both procedures is missing. There was an effort to assess the volume of biogas, but there are no set standards to make predictions on the basis of this research (Cruz and Buitron 2000; Dos Santos et al. 2004).

Complexometric Methods (Refining with Cucurbituril)

It's a tough choice to use the effective method to treat wastewater because each process has its own merits and demerits. When we used activated carbon treatment, this can be effective against organic dye removal, but the other impurities can't be handled by using this process in the same way; each process has its own limitation. It was not until 1905, when there was a little noise about an organic compound

introduced with the name of cucurbituril. But a remarkable research was not conducted on this compound. Freeman et al. (1981) explored its chemical properties. Cucurbituril is a polymer that is made up of glycoluril and formaldehyde. Studies have revealed that the complex has fairly good sorption capability for various types of textile dyes. Cucurbituril is recognized to make a complex with aromatic dyes, and it is reflected that this method is effective for the absorbance of reactive dyes (Robinson et al. 2001). Cucurbituril was not found to be soluble in aqueous medium, and its macrocyclic property made it more appropriate against dye treatment. It makes insoluble complexes that can be easily removed from wastewater. Later, Buschmann et al. (1996) did an extensive research on this compound. This was an effective method and can be used in solid state as well. The removal efficiency of cucurbituril was checked against many dyes such as acid, base, reactive, and direct dyes, and it provided excellent results against all of them. The rate of removal depends on many factors such as there may be high solubility of the complex formed, or there may be poor bonding between dye and cucurbituril. One of the plus points of this method is that it can never be disturbed by the presence of organic compounds in wastewater.

Comparison of Different Treatment Methods

There are different methods and technologies that are being applied to treat the textile wastewater. Different methods provide different efficiencies to remove color and organic waste. For example, advanced oxidation process is found to be most effective and gives the best result in color removal. Fenton's reagents (H_2O_2 and Fe^{2+}) and ozonation are the termed as advanced oxidation technologies that can be applied to textile wastewater to achieve the best results, but they have some limitations as well. They are costly, and a large amount of waste in the form of sludge is produced by these methods. The sludge produced by this method is difficult to manage (Marco and Jose 2007). Some of the physical methods such as coagulation flocculation are also found to be effective, but lime, alum, and polyelectrolytes used in this process cause an enormous amount of sludge that is difficult to manage and treat, as it can't be disposed easily. Therefore, this method can't be applied alone in textile wastewater treatment. Adsorption process is an expensive process as it uses activated carbon that is very costly. Other adsorbents used in adsorption of dyes have high cost, and the textile industry can't adopt this method due to high operational cost. Reverse osmosis technique in textile wastewater treatment is found to be very useful, but its operational cost is also very high, as it requires very high pressure, and a large amount of energy is consumed in this process. The budget of textile industries adopting membrane filtration techniques can be disturbed as nanofiltration and ultrafiltration processes require high energy, and sludge produced by this process is not easy to handle (Allegre et al. 2006). Another method uses ultraviolet light, and oxidation compounds such as H_2O_2 are also being used to treat textile waste, but different catalysts used in

this process produce by-products that are very harmful (Muruganandham and Swaminathan 2004). There are some methods having high color removal efficiencies. Electrochemical oxidation is one of them as it has the ability to remove color, and by-products produced by this method are nontoxic and easy to handle. But it has its own limitation as its operational cost is also very high and it can disturb the budget of textile industry (Mohan et al. 2007).

Generally, a combination of two or more advanced oxidation processes such as UV/ozone, UV/H_2O_2, ultrasound/ozone, sonophotochemical/sonophotocatalytic oxidation, etc. leads to an enhanced generation of the hydroxyl radicals, which eventually results in higher oxidation rates. The efficacy of the process and the extent of synergism depend not only on the enhancement in the number of free radicals but also on the alteration of the reactor conditions or configuration leading to a better contact of the generated free radicals with the pollutant molecules and also better utilization of the oxidants and catalytic activity (Gogate and Pandit 2000a).

Combining ozone and hydrogen peroxide with ultrasound leads to a better utilization of both the oxidant, hence higher degradation rates due to the dissociation of ozone and hydrogen peroxide under the action of ultrasound. The mass transfer resistance, which is a major limiting factor for the application of ozone or hydrogen peroxide alone, is also eliminated due to the enhanced turbulence generated by ultrasound. The operating frequency is a crucial factor in deciding the synergism and should not be increased beyond 500 kHz (Gogate and Pandit 2000b). The problems of high-frequency operation and existence of optima beyond which the rates of degradation decrease have been discussed in detail in the earlier work (Gogate et al. 2002). Ozone/hydrogen peroxide hybrid technique gives better results as compared to the use of ozone or hydrogen peroxide especially for the treatment of pollutants, refractory toward ozone, e.g., organophosphoric acid tri-esters. As the synergism is strongly dependent on the efficient use of hydroxyl radicals, concentration of radical scavenging agents plays a crucial role in deciding the overall efficacy of the process (Gogate and Pandit 2004).

In the case of sonophotochemical/sonophotocatalytic reactors, it is important to have simultaneous irradiation of ultrasound and UV light rather than sequential operation. Addition of hydrogen peroxide or ozone to this hybrid system until an optimum value as an additional source of the free radicals also increases the extent of destruction (Fung et al. 2001) The major factor controlling the overall efficiency of destruction is, however, the stability of the photocatalyst under the effect of ultrasound, and efforts are required in terms of new designs, which will protect the catalyst but at the same time will give enhanced effects (Fung et al. 2001). Photo-Fenton processes offer additional advantages in terms of possibility in the use of sunlight instead of UV light with a minor decrease in the rate of degradation, which is a very important factor for the scale-up and commercial use as the costs of treatments will be substantially lower for the sunlight irradiation.

All the processes discussed above have their own merits and demerits. Indeed, the selection of the process that gives the best outcome with less polluting by-products and low cost is a difficult task (Rajkumar and Kim 2006) (Table 1).

Table 1 Representative studies on the applications of combined treatment systems on textile effluent

Treatment processes	First stage	Second stage	Outcome	References
Physical/ membrane treatment	Coagulation	Ultrafiltration	Achieved substantial colloidal particle removal (>97%) of turbidity removal) regardless of type and dosage of coagulants used, but degree of membrane fouling was highly dependent on type of coagulants used. Study has proven that inorganic coagulants were more efficient to reduce fouling compared to polymeric coagulants	Choo et al. (2007)
Membrane treatment	Ultrafiltration	Nanofiltration	Authors claimed that UF was an appropriate pretreatment of an NR/RO process for textile wastewater reuse. To deal with the wastewater with high variability values of COD and conductivity, they observed that flux decline was significant at the lowest cross flow velocity studied due to the solid deposition onto the membrane surface	Barredo-Damas et al. (2006)
Physical/ membrane treatment	Coagulation/ flocculation	Nanofiltration	Study reported that the quality of permeate after coagulation/ flocculation did not match the requirement of reuse on the site. However, this method could act as pretreatment of NF to limit membrane fouling. By using this integrated approach, high-quality permeate could be obtained	Suksaroj et al. (2005)

(continued)

Table 1 (continued)

Treatment processes	First stage	Second stage	Outcome	References
Chemical/ membrane treatment (2005)	Electrochemical oxidation	Membrane filtration	Study indicated the feasibility of combined processes for treatment of textile wastewater. Membrane prior to electro-chemical oxidation process showed promising results in terms of COD, turbidity, and color removal (RCOD = 89.2%, Rturbidity = 98.3%, Rcolor = 91.1%) compared to electrochemical oxidation prior to membrane process (RCOD = 86.2%, Rturbidity = 95.1%, Rcolor = 85.2%). This is due to lower color concentration remaining in wastewater after the electrochemical oxidation process	Chen et al. (2005)
Chemical/ biological treatment (2003)	Ozonation	Aerobic	The use of ozonation as pretreatment was able to increase the bioavailability of the dye before it was treated with the aerobic process. To achieve higher color (99.8%) and DOC (85%) removal, higher doses of ozone were required. This would make it less economically favorable	Libra and Sosath (2003)
Physical/ membrane treatment	Sand filtration and membrane filtration	Nanofiltration	Sand filtration and MF in a pilot plant were fundamental in reduction of suspended solids (100%) and turbidity (78%). To completely remove COD, conductivity, and color, NF was responsible for removal	Marcucci et al. (2002)

A combination of physical, chemical, and biological method can be cost-effective and efficient treatment option for textile wastewater treatment. In a recent study, a combination of Fenton and anaerobic oxidation (F + SBR) reactor was found to be very effective in removing *E. coli* and toxic organic compounds (Blanco et al. 2012). A best strategy toward the textile industry pollution reduction is adoption of cleaner production technologies.

There are three strategies that can be implemented in textile industry designs. These strategies are briefly summarized hereunder.

Less Polluting Raw Material

Selection of less polluting raw material is a prescreening process, and by adopting this strategy, textile companies can reduce waste generation from the very first step such as, instead of azo dyes, use vat dyes when possible, and reuse dye and wash wastewater for preceding process (Tsai and Chou 2004).

Substituted Products

The less polluting and easily degradable chemicals can substitute highly polluted chemicals that cannot be easily degraded. In the same way, textile companies can select the treatment designs that cause less pollution like substitution of chemical treatment with the mechanical one (Fitzpatrick et al. 2010).

Process Modification

Industries should adopt the process that is cost-effective, is energy efficient, and according to local conditions provides the best degradation. Usually a hybrid model can be used to achieve the best removal (Van der Bruggen et al. 2004). The objective of this study was to provide the best treatment options according to Pakistan situation. The combination of two processes enhances the ability to degrade the pollutants. The best design should have unique characteristics such as (a) the capacity to provide high biodegradation and maximum removal rate that cannot be achieved by the single process, (b) retention time which does not exceed the time of single process, and (c) its cost-effectiveness.

Conclusions and Perspectives

It must be said that the advanced oxidation processes or even the hybrid methods may not be useful in degrading large quantum of the effluent with economic efficiency and hence it is advisable to use these methods for reducing the toxicity of the pollutant stream to a certain level beyond which biological oxidation can take care of the complete mineralization of the biodegradable products. An optimized pretreatment stage (in terms of the oxidant dose and the reduction in the toxicity

level) will substantially decrease the total treatment time and hence the size of the reactor using the combination technique. It is recommended that the added oxidants, e.g., hydrogen peroxides, are completely utilized in the pretreatment stage alone, as its continued presence may hamper the activity of the microorganisms. It is also important to analyze the constituents of the effluent stream after the pretreatment stage as it may happen that some of the intermediates formed as a result of the oxidation are biorefractory or more toxic than the parent compound.

It is also important to develop realistic and generalized kinetic and yet mechanistic models for predicting the rates of the degradation process as a function of different operating parameters. The developed kinetic model should consider the effect of all the constituents of effluent stream even if the concentrations are in traces, e.g., radical scavengers and also the different reactions taking place in the chain of radical reactions. In Pakistan, most of the textile industries discharge untreated wastewater into water bodies without any treatment, which percolates into the groundwater posing a threat to the health and socioeconomic life of the people. Characterization of wastewater is necessary to determine the type and scheme of treatment required. This chapter proposes the treatment options to control textile wastewater pollution. It is clear that textile wastewater can be treated through different processes including Fenton treatment, ozonation, adsorption, nanofilteration, aerobic biological treatment, and anaerobic treatment such as upflow anaerobic sludge blanket reactor, etc. After comparing the advantages and disadvantages of these processes, the best strategy is to use aerobic and anaerobic biological treatment in combination for textile industry wastewater treatment (Manu and Sanjeev 2003). Moreover, instead of focusing on end-of-pipe treatment, the adoption of cleaner production technologies is necessary to reduce pollution at source. This can be done through selection of less polluting alternate raw materials, reuse of wash water, and conservation of water, chemicals, and energy by following cleaner production practices in textile industries.

References

Aksu Z (2005) Application of biosorption for the removal of organic pollutants: a review. Process Biochem 40:997–1026

Aksu Z, Tezer S (2000) Equilibrium and kinetic modeling of biosorption of Remazol black B by Rhizopus arrhizus in a batch system: effect of temperature. Process Biochem 36:431–439

Al-Bastaki N, Banat F (2004) Combining ultrafiltration and adsorption on bentonite in a one-step process for the treatment of colored waters. Resour Conserv Recycl 41:103–113

Al-Ghouti MA, Khraisheh MAM, Allen SJ, Ahmad MN (2003) The removal of dyes from textile wastewater: a study of the physical characteristics and adsorption mechanisms of diatomaceous earth. J Environ Manage 69:229–238

Alkan M, Demirbas O, Celikcapa S, Dogan M (2004) Sorption of acid red 57 from aqueous solutions onto sepiolite. J Hazard Mater 116:135–145

Alkan M, Celikcapa S, Demirbas O, Dogan M (2005) Removal of reactive blue 221 and acid blue 62 anionic dyes from aqueous solutions by sepiolite. Dyes Pigments 65:251–259

Allegre C, Moulin P, Maisseu M, Charbit F (2006) Treatment and reuse of reactive dyeing effluents. J Membr Sci 269:15–34
Allen SJ, McKay G, Porter JF (2004) Adsorption isotherm models for basic dye adsorption by peat in single and binary component systems. J Colloid Interface Sci 280:322–333
Andre BDS, Iemke AEB, Francisco JC, Jules BVL (2005) The transformation and toxicity of anthraquinone dyes during thermophilic (55_C) and mesophilic (30_C) anaerobic treatments. J Biotechnol 115:345–353
Andreozzi R, Caprio V, Marotta R, Tufano V (2001a) Kinetic modeling of pyruvic acid ozonation in aqueous solutions catalyzed by Mn(II) and Mn (IV) ions. Water Res 35:109–120
Andreozzi R, Caprio V, Marotta R (2001b) Oxidation of benzothiazole, 2-mercaptobenzothiazole and 2-hydroxybenzothiazole in aqueous solution by means of H_2O_2yUV or photoassisted Fenton systems. J Chem Technol Biotechnol 76:196–202
Anindya G, Ishtiaque SM, Rengasamy RS (2005) Tensile failure of yarns as a function of structure and testing parameters. Textile Res J 75:741–744
Ara S (1998) The textile sector, Environmental Report, Ministry of Environment, Government of Pakistan, Islamabad
Armagan B, Turan M, Celik MS (2004) Equilibrium studies on the adsorption of reactive azo dyes into zeolite. Desalination 170:33–39
Arslan I (2001) Treatability of a simulated disperse dye bath by ferrous iron coagulate, ozonation and ferrous iron catalyzed ozonation. J Hazard Mater 85:229–241
Arslan I, Balcioglu IA, Bahnemann DW (2000) Advanced chemical oxidation of reactive dyes in simulated dye house effluents by ferrioxalate-Fenton/UV-A and TiO_2/UV-A processes. Dyes Pigments 47:207–218
Atun G, Hisarli G, Sheldrick WS, Muhler M (2003) Adsorptive removal of methylene blue from colored effluents on Fuller's earth. J Colloid Interface Sci 261:32–39
Babel S, Kurniawan TA (2003) Low-cost adsorbents for heavy metals uptake from contaminated water: a review. J Hazard Mater B 97:219–243
Babu BR, Parande AK, Raghu S, Kumar TP (2007) Textile technology-cotton textile processing: waste generation and effluent treatment. J Cotton Sci 11:141–153
Baouab MHV, Gauthier R, Gauthier H, Rammah MEB (2001) Cationized sawdust as ion exchanger for anionic residual dyes. J Appl Polym Sci 82:31–37
Barredo-Damas S, Alcaina-Miranda MI, Iborra-Clar MI, Bes-Pia A, Mendoza-Roca JA, Iborra-Clar A (2006) Study of the UF process as pretreatment of NF membranes for textile wastewater reuse. Desalination 200:745–747
Bauer C, Jacques P, Kalt A (2001) Photooxidation of an azo dye induced by visible light incident on the surface of TiO_2. J Photochem Photobiol A Chem 140:87–92
Blanco J, Torrades F, Varga MD, Garcia-Montano J (2012) Fenton and biological-Fenton coupled processes for textile wastewater treatment and reuse. Desalination 286:394–399
Buschmann HJ, Jonas C, Schollmeyer E (1996) The selective removal of dyes from waste water. Eur Water Pollut Control 6:21–24
Calzaferri G, Bru¨hwiler D, Megelski S, Pfenniger M, Pauchard M, Hennessy B, Maas H, Devaux A, Graf A (2000) Playing with dye molecules at the inner and outer surface of zeolite L. Solid State Sci 2:421–447
Carriere J, Jones JP, Broadbent AD (1991) Book of papers. AATCC Int Conf Exhibi, Charlotte 1:231
Chao AC, Shyu SS, Lin YC, Mi FL (2004) Enzymatic grafting of carboxyl groups on to chitosan to confer on chitosan the property of a cationic dye adsorbent. Bioresour Technol 91:157–162
Chen X, Shen Z, Zhu X, Fan Y, Wang W (2005) Advanced treatment of textile wastewater for useusing electrochemical oxidation and membrane filtration. Water SA 31:127–132
Chiou MS, Li HY (2002) Equilibrium and kinetic modelling of adsorption of reactive dye on cross-linked chitosan beads. J Hazard Mater 93:233–248
Chiou MS, Ho PY, Li HY (2004) Adsorption of anionic dyes in acid solutions using chemically cross-linked chitosan beads. Dyes Pigments 60:69–84

Choo KH, Choia SJ, Hwang ED (2007) Effect of coagulant types on textile wastewater reclamation in a combined coagulation/ultrafiltration system. Desalination 202:262–270
Ciardelli G, Ranieri N (2001) The treatment and reuse of wastewater in the textile industry by means of ozonation and electroflocculation. Water Res 35:567–572
Clarke EA, Steinle D (1995) Health and environmental safety aspects of organic colorants. Rev Prog Coloration 25:1
Crini G (2003) Studies of adsorption of dyes on beta-cyclodextrin polymer. Bioresour Technol 90:193–198
Crini G, Morcellet M (2002) Synthesis and applications of adsorbents containing cyclodextrins. J Sep Sci 25:1–25
Crini G, Morin-Crini N, Badot PM (2002a) Adsorption of toxic aromatic derivatives on polysaccharide gels. Hydro Sci 133:58–61
Crini G, Morin N, Rouland JC, Janus L, Morcellet M, Bertini S (2002b) Adsorption de be'tanaphtol sur des gels de cyclodextrinecarboxyme ´thylcellulose re'ticule's. Eur Polym J 38:1095–1103
Cruz A, Buitron G (2000) Biotransformation of disperse blue 79 by an anaerobic sequencing batch biofilter. Water Sci Technol 42:317–320
Delval F, Crini G, Janus L, Vebrel J, Morcellet M (2001) Novel crosslinked gels with starch derivatives. Polymer-water interactions. Applications in waste water treatment. Macromol Symp 166:103–108
Delval F, Crini G, Morin N, Vebrel J, Bertini S, Torri G (2002) The sorption of several types of dye on crosslinked polysaccharides derivatives. Dyes Pigments 53:79–92
Delval F, Crini G, Vebrel J, Knorr M, Sauvin G, Conte E (2003) Starch-modified filters used for the removal of dyes from waste water. Macromol Symp 203:165–171
Dill HG (2001) The geology of aluminium phosphates and sulphates of the alunite group minerals: a review. Earth Sci Rev 53:35–93
Dos Santos AB, Cervantes FJ, Yaya-Beas RE, Van Lier JB (2003) Effect of redox mediator, AQDS, on the decolourisation of a reactive azo dye containing triazine group in a thermophilic anaerobic EGSB reactor. Enzyme Microb Technol 33:942–951
Dos Santos AB, Bisschops IAE, Cervantes FJ, Van Lier JB (2004) Effect of different redox mediators during thermophilic azo dye reduction by anaerobic granular sludge and comparative study between mesophilic (30 C) and thermophilic (55 C) treatments for decolourisation of textile wastewaters. Chemosphere 55:1149–1157
El-Din M, Smith DW (2002) Ozonation of Kraft pulp mill effluents process dynamics. J Environ Eng Sci 1:45–57
El-Gohary F, Tawfik A (2009) Decolorization and COD reduction of disperse and reactive dyes wastewater using chemical-coagulation followed by sequential batch reactor (SBR) process. Desalination 249:1159–1164
Ellouze E, Tahri N, Amar RB (2012) Enhancement of textile wastewater treatment process using nanofiltration. Desalinization 286:16–23
Entezari MH, Pe´trier C (2004) A combination of ultrasound and oxidative enzyme: sonobiodegradation of phenol. Appl Catal Environ 53:257–263
Fitzpatrick B, Johnson J, Kump D, Smith J, Voss S, Shaffer H (2010) Rapid spread of invasive genes into a threatened native species. Proc Natl Acad Sci U S A 107:3606–3610
Frank PVZ, Lettinga G, Field JA (2001) Azo dye decolourization by anaerobic granular sludge. Chemosphere 44:1169–1176
Freeman WA, Mock WL, Shih NY (1981) Cucurbituril. J American Chem Sot 103:7367–7368
Fu Y, Viraraghavan T (2001a) Fungal decolorization of dye wastewaters: a review. Bioresour Technol 79:251–262
Fu Y, Viraraghavan T (2001b) Removal of C.I. Acid blue 29 from an aqueous solution by *Aspergillus niger*. Am Assoc Text Chem Color Rev 1:36–40
Fu Y, Viraraghavan T (2002a) Removal of Congo red from an aqueous solution by fungus *Aspergillus niger*. Adv Environ Res 7:239–247

Fu Y, Viraraghavan T (2002b) Dye biosorption sites in *Aspergillus niger*. Bioresour Technol 82:139–145

Fukushima M, Tatsumi K (2001) Degradation pathways of pentachlorophenol by photo-Fenton systems in the presence of iron(III), humic acid and hydrogen peroxide. Environ Sci Technol 35:1771–1778

Fung PC, Poon CS, Chu CW, Tsui SM (2001) Degradation kinetics of reactive red by $UVyH_2O_2yUS$ process under continuous mode operation. Water Sci Technol 44:67–72

Glover B (1993) Dyes application and evaluation in encyclopedia of chemical technology, vol 8, 4th edn. Wiley, New York, p 72

Gogate PR, Pandit AB (2000a) Engineering design methods for cavitational reactors I: sonochemical reactors. AICHE J 46:372–379

Gogate PR, Pandit AB (2000b) Engineering design methods for cavitational reactors II: hydrodynamic cavitation. AICHE J 46:1641–1649

Gogate PR, Pandit AB (2004) A review of imperative technologies for wastewater treatment II: hybrid methods. Adv Environ Res 8:553–597

Gogate PR, Mujumdar S, Pandit AB (2002) A sonophotochemical reactor for the removal of formic acid from wastewater. Indus Eng Chem Res 41:3370–3378

Gogate PR, Mujumdar S, Pandit AB (2003) Sonochemical reactors for waste water treatment. Adv Environ Res 4:283–299

Gu¨rses A, Karaca S, Dogar C, Bayrak R, Acikyildiz M, Yalcin M (2004) Determination of adsorptive properties of clay/water system: methylene blue sorption. J Colloid Interface Sci 269:310–314

Gupta VK, Suhas (2009) Application of low-cost adsorbents for dye removal review. J Environ Manage 90:2313–2342

Harris RG, Wells JD, Johnson BB (2001) Selective adsorption of dyes and other organic molecules to kaolinite and oxide surfaces. Colloids Surf A Physicochem Eng Asp 180:131–140

Hassan MM, Hawkyard JC (2002) Decolorization of aqueous dyes by sequential oxidation treatment with ozone and Fenton's reagent. J Chem Technol Biotechnol 77:834–841

Ho YS, McKay G (2003) Sorption of dyes and copper ions onto biosorbents. Process Biochem 38:1047–1061

Husain I, Hussain J (2012) Groundwater pollution by discharge of dyeing and printing industrial wastewater in Bandi river, Rajasthan, India. Intl J Env Bioenergy 2:100–119

Ikehata A (1975) 1st international symposium an ozone for water and wastewater treatment. Rice R G and Browning M E, (Eds.), waterbury, conn. USA, p 688

Ince HN, Tezcanli G (2001) Reaction dyestuff degradation by combined sonolysis and ozonation. Dyes Pigments 49:145–153

Jantsch TG, Angelidaki I, Schmidt JE, Brana de Hvidsten BE, Ahring BK (2002) Anaerobic biodegradation of spent sulphite liquor in a UASB reactor. Bioresour Technol 84:15–20

Joseph JH, Destaillats H, Hung HM, Hoffmann MR (2000) The sonochemical degradation of azobenzene and related azo dyes: rate enhancement via Fenton's reaction. J Phys Chem A 104:301–307

Khandegar V, Saroha AK (2013) Electrocoagulation for the treatment of textile industry effluent – a review. J Environ Manage 128:949–963

Koch M, Yediler A, Lienert D, Insel G, Kettrup M (2002) A ozonation of hydrolyzed azo dye reactive yellow 84 (CI). Chemosphere 46:109–113

Krysztafkiewicz A, Binkowski S, Jesionowski T (2002) Adsorption of dyes on a silica surface. Appl Surf Sci 199:31–39

Laszlo JA (1994) Removing acid dyes from textile wastewater using biomass for decolorization. Am Dyestufl Reporter 83:17–21

Lau WJ, Ismail AF (2009) Polymeric nanofiltration membranes for textile dye wastewater treatment: preparation, performance evaluation, transport modelling, and fouling control- a review. Desalination 245:321–348

Libra JA, Sosath F (2003) Combination of biological and chemical processes for the treatment of textile wastewater containing reactive dyes. J Chem Technol Biotechnol 78:1149–1156
Ma J, Graham NJD (2000) Degradation of atrazine by manganese catalyzed ozonation-influence of radical scavengers. Water Res 34:3822–3828
Manu B, Chaudhari S (2003) Decolorization of indigo and azo dyes in semicontinuous reactors with long hydraulic retention time. Process Biochem 38(8):1213–1221
Marco SL, Jose AP (2007) Degradation of reactive black 5 by Fenton/ UV-C and ferrioxalate/ H2O2/solar light processes. Dyes Pigments 74:622–629
Marcucci M, Ciardelli G, Matteucci A, Ranieri L, Russo M (2002) Experimental campaigns on textilewastewater for reuse by means of different membrane processes. Desalination 149:137–143
McMullan G, Meehan C, Conneely A, Kirby N, Robinson T, Nigam P, Banat IM, Marchant R, Smyth WF (2001) Microbial decolourisation and degradation of textile dyes. Appl Microbiol Biotechnol 56:81–87
Mendez-Paz D, Omil F, Lema JM (2005) Anaerobic treatment of azo dye acid orange 7 under batch conditions. Enzyme Microb Technol 36:264–272
Meshko V, Markovska L, Mincheva M, Rodrigues AE (2001) Adsorption of basic dyes on granular activated carbon and natural zeolite. Water Res 35:3357–3366
Mohan N, Balasubramanian N, Ahmed B (2007) Electrochemical oxidation of textile wastewater and its reuse. J Hazard Mater 147:644–651
Mustafa I, Delia ST (2006) Biological treatment of acid dyeing wastewater using a sequential anaerobic/aerobic reactor system. Enzyme Microb Technol 38:887–892
Muruganandham M, Swaminathan M (2004) Photochemical oxidation of reactive azo dye with UV-H_2O_2 process. Dyes Pigments 62:269–275
Namboodri CG, Perkins W, Walsh WK (1994) Decolorizing dyes with chlorine and ozone-part II. Am Dyestufl Rep 83:17–26
Nguyen TA, Juang R (2013) Treatment of waters and wastewaters containing sulfur dyes: a review. Chem Eng J 219:109–117
Ozacar M, Sengil AI (2002) Adsorption of acid dyes from aqueous solutions by calcined alunite and granular activated carbon. Adsorption 8:301–308
Ozacar M, Sengil AI (2003) Adsorption of reactive dyes on calcined alunite from aqueous solutions. J Hazard Mater B 98:211–224
Ozcan AS, Erdem B, Ozcan A (2004a) Adsorption of acid blue193 from aqueous solutions onto Na-bentonite and DTMA-bentonite. J Colloid Interface Sci 280:44–54
OECD, OECD Guidelines for Testing of Chemicals (1993) 301 A: DOC Die- Away Test; 301 B: COz-Evolution Test (Modified Sturm test); 301 C: MIT1 Test (I); 301 D: Closed Bottle Test; 301 E: Modified OECD Screening Test; 301 F: Manometric Respirometry Test; 302 A: Modified SCAS Test; 302 B: Zahn- Wellens/EMPA Test; 302 C: Modified MIT1 Test (II)
Omura T (1994) Design of chlorine-fast reactive dyes-part 4: degradation of amino-containing azo dyes by sodium hypochlorite. Dyes Pigments 26:33–50
Ozcan AS, Erdem B, Ozcan A (2004b) Adsorption of acid blue 193 from aqueous solutions onto Na-bentonite and DTMA-bentonite. J Colloid Interface Sci 280:44–54
Ozdemir O, Armagan B, Turan M, Celik MS (2004) Comparison of the adsorption characteristics of azo-reactive dyes on mezoporous minerals. Dyes Pigments 62:49–60
Pearce CI, Lloyd JR, Guthrie JT (2003) The removal of colour from textile wastewater using whole bacterial cells: a review. Dyes Pigments 58:179–196
Phan TNT, Bacquet M, Morcellet M (2000) Synthesis and characterization of silica gels functionalized with monochlorotriazinyl beta-cyclodextrin and their sorption capacities towards organic compounds. J Incl Phenom Macrocycl Chem 38:345–359
Pignon H, Brasquet C, Le Cloirec P (2000) Coupling ultrafiltration and adsorption onto activated carbon cloth application to the treatment of highly coloured wastewater. Water Sci Technol 42:355–362
Rajkumar D, Kim JG (2006) Oxidation of various reactive dyes with in situ electro-generated active chlorine for textile dyeing industry wastewater treatment. J Hazard Mater 136:203–212

Riera-Torres M, Gutierrez-Bouzan C, Crespi M (2010) Combination of coagulation-flocculation and nanofiltration techniques for dye removal and water reuse in textile effluents. Desalination 252:53–59
Robert M, Sanjeev C (2005) Adsorption and biological decolourisation of azo dye reactive red 2 in semicontinuous anaerobic reactors. Process Biochem 40:699–705
Robinson T, McMullan G, Marchant R, Nigam P (1997) Remediation of dyes in textile effluent: a critical review on current treatment technologies with a proposed alternative. Colorage 44:247–255
Robinson T, McMullan G, Marchant R, Nigam P (2001) Remediation of dyes in textile effluent: a critical review on current treatment technologies with a proposed alternative. Bioresour Technol 77:247–255
Sarayu K, Sandhya S (2012) Current technologies for biological treatment of textile wastewater – a review. Appl Biochem Biotechnol 167:645–661
Sekomo CB, Rousseau DPL, Saleh AS, Lens PNL (2014) Heavy metal removal in duckweed and algae ponds as a polishing step for textile wastewater treatment. Ecol Eng 44:102–110
Selcuk H (2005) Decolorization and detoxification of textile wastewater by ozonation and coagulation processes. Dyes Pigments 64:217–222
Shichi T, Takagi K (2000) Clay minerals as photochemical reaction fields. J Photochem Photobiol C Photchem Rev 1:113–130
Silva JP, Sousa S, Rodrigues J, Antunes H, Porter JJ, Goncalves I, Dias SF (2004) Adsorption of acid orange 7 dye in aqueous solutions by spent brewery grains. Sep Purif Technol 40:309–315
Stolz A (2001) Basic and applied aspects in the microbial degradation of azo dyes. Appl Microbiol Biotechnol 56:69–80
Strotmann UJ, Schwartz H, Pagga U (1995) The combined CO_2/DOC test a new method to determine the biodegradability of organic compounds. Chemosphere 30:525–538
Sudipta C, Sandipan C, Bishnu PC, Akhil RD, Arun KG (2005) Adsorption of a model anionic dye, eosin Y, from aqueous solution by chitosan hydrobeads. J Colloid Interface Sci 288:30–35
Suksaroj C, Heran M, Allegre C, Persin F (2005) Treatment of textile plant effluent by nanofiltrationand/or reverse osmosis for water reuse. Desalination 178:333–341
Sule AD, Bardhan MK (1999) Objective evaluation of feel and handle, appearance and tailorability of fabrics. Part-II: the KES-FB system of Kawabata Colourage. Colourage 46:23–28
Sun Q, Yang L (2003) The adsorption of basic dyes from aqueous solution on modified peat-resin particle. Water Res 37:1535–1544
Tsai WT, Chou YH (2004) Government policies for encouraging industrial waste reuse and pollution prevention in Taiwan. J Clean Prod 12:725–736
USEPA (1997) EPA Office of compliance sector notebook project. Profile of the Textile Industry, Washington, DC
Van der Bruggen B, Koninckx A, Vandecasteele C (2004) Separation of monovalent and divalent ions from aqueous solution by electrodialysis and nanofiltration. Water Res 38:1347–1353
Verma AK, Dash RR, Bhunia P (2012) A review on chemical coagulation/flocculation technologies for removal of colour from textile wastewaters. J Environ Manage 93:154–168
Wang CC, Juang LC, Hsu TC, Lee CK, Lee JF, Huang FC (2004) Adsorption of basic dyes onto montmorillonite. J Colloid Interface Sci 273:80–86
Wong YC, Szeto YS, Cheung WH, McKay G (2004) Adsorption of acid dyes on chitosan-equilibrium isotherm analyses. Process Biochem 39:693–702
Woolard CD, Strong J, Erasmus CR (2002) Evaluation of the use of modified coal ash as a potential sorbent for organic waste streams. Appl Geochem 17:1159–1164
Wu FC, Tseng RL, Juang RS (2000) Comparative adsorption of metal and dye on flake- and bead-types of chitosan prepared from fishery wastes. J Hazard Mater B73:63–75
Wu FC, Tseng RL, Juang RS (2001a) Kinetic modelling of liquid-phase adsorption of reactive dyes and metal ions on chitosan. Water Res 35:613–618
Wu FC, Tseng RL, Juang RS (2001b) Enhanced abilities of highly swollen chitosan beads for color removal and tyrosinase immobilization. J Hazard Mater B 81:167–177

Decontamination of Hexavalent Chromium-Polluted Waters: Significance of Metallic Iron Technology

Marius Gheju

Abstract Chromium (Cr) is an important metal used in a variety of industrial applications, which significantly contribute to pollution of air, soil, and waters. In natural environments, chromium can exist mainly in two of its most stable oxidation states, (+III) and (+VI). Among them, Cr(VI) is the most hazardous due to its high mobility in the environment and severe harmful effects exerted on all living matters. Therefore, it should be removed from all contaminated waters. During the last 25 years, there has been great interest in using metallic iron (Fe^0) for the abatement of Cr(VI) pollution. The first mechanism, known as the reductive-precipitation mechanism, was proposed at the beginning of the nineties, and attributed the efficiency of Fe^0 in removing Cr(VI) mainly to the direct electron transfer from the Fe^0 surface to Cr(VI), followed by precipitation of the resulted cations as simple hydroxides and/or mixed Fe(III)-Cr(III) (oxi)hydroxides. Recently, new perspectives were added to this early mechanism. A new concept, known as the adsorption-coprecipitation mechanism, suggests that direct reduction with Fe^0, if applicable, is less important than had previously been assumed by the reductive-precipitation mechanism; accordingly, contaminants are quantitatively removed in Fe^0/H_2O systems principally by adsorption, coprecipitation, and size exclusion, while reduction, when possible, is mainly the result of indirect reducing agents produced by Fe^0 corrosion. In spite of the substantial research work that has proven the capability of metallic iron as a reactive material to remove Cr(VI), there is no consensus at this time in what regards the mechanism of this process. Therefore, after providing an overview of chromium occurrence, chemistry, and toxicity, this work will critically review the existing knowledge on this subject, clearly demonstrating that mechanism of Cr(VI) removal with Fe^0 is more complex than the simple reductive precipitation.

Keywords Hexavalent chromium • Metallic iron • Water treatment

M. Gheju (✉)
Faculty of Industrial Chemistry and Environmental Engineering, Politehnica University Timisoara, Bd. Vasile Parvan Nr.6, 300223 Timisoara, Romania
e-mail: marius.gheju@upt.ro

N.A. Anjum et al. (eds.), *Enhancing Cleanup of Environmental Pollutants*,
DOI 10.1007/978-3-319-55423-5_7

Introduction

Chromium is an element discovered by Nicolas Vauquelin, a professor of chemistry at the Paris École des Mines. In 1797 he was the first who produced chromium oxide (CrO_3) by dissolving crocoite ($PbCrO_4$) in hydrochloric acid; a year later, he was able to isolate metallic chromium by heating the oxide in a charcoal oven. The element was named after the Greek word "chroma," meaning color, because of the many different colored compounds displayed by chromium (Guertin et al. 2005). On the periodic table, chromium is the 24th element, member of group VI B along with molybdenum and tungsten, with an average atomic weight of 52 and an electron configuration of [Ar] $3d^5$ $4s^1$ (Shupack 1991; Barnhart 1997; Guertin et al. 2005). Chromium is found throughout the environment within the ranges of 10–150 mg/kg, 0.1–6 μg/L, and 0.015–0.03 μg/m^3, in soil, water, and air, respectively (Choppala et al. 2013). Chromium oxidation states range from (−IV) to (+VI) (Cotton et al. 1999; Guertin et al. 2005); however, from a thermodynamic standpoint, the most stable chromium compounds are in the +III and +VI states, characterized by different toxicities and chemical behaviors (Fendorf 1995; Kimbrough et al. 1999). The main equilibria of hexavalent chromium species in aqueous solution are (Cieslak-Golonka 1995; Fendorf 1995; Zink et al. 2010):

$$H_2CrO_4 + H_2O \Leftrightarrow HCrO_4^- + H_3O^+ \quad K = 10^{-0.7} \tag{1}$$

$$HCrO_4^- + H_2O \Leftrightarrow CrO_4^{2-} + H_3O^+ \quad K = 10^{-6.5} \tag{2}$$

$$HCrO_4^- + HCrO_4^- \Leftrightarrow Cr_2O_7^{2-} + H_2O \quad K = 33.3 \tag{3}$$

The dimerization of the $HCrO_4^-$ oxyanion occurs at pH 2–6 (Cotton et al. 1999); $Cr_2O_7^{2-}$ becomes significant when total Cr(VI) concentrations are greater than 52 mg/L or even dominates when total Cr(VI) concentrations are greater than 1.56 g/L (Palmer and Wittbrodt 1991; Palmer and Puls 1994). However, since such high Cr(VI) concentrations are not commonly found in natural waters (Rai et al. 1989), under environmentally relevant pH values, hexavalent chromium exists only as $HCrO_4^-$ (predominant at pH < 6.5) and CrO_4^{2-} (predominant at pH > 6.5) oxyanions (Fendorf 1995). Hexavalent chromium anions are species with high solubility in water; in the same time, being negatively charged, they are only weakly sorbed onto inorganic surfaces. Hence, Cr(VI) species have a significant mobility in water and soil (Fendorf 1995; Fendorf et al. 2000; Lin 2002). On the other hand, trivalent chromium is a weak Bronsted acid which readily hydrolyzes in solution and precipitates as $Cr(OH)_3$ (Rai et al. 1987, 1989; Palmer and Wittbrodt 1991; Kotas and Stasicka 2000):

$$[Cr(OH_2)_6]^{3+} + H_2O \Leftrightarrow [Cr(OH_2)_5(OH)]^{2+} + H_3O^+ \quad K_{a1} = 10^{-3.8} \tag{4}$$

$$[Cr(OH_2)_5(OH)]^{2+} + H_2O \Leftrightarrow [Cr(OH_2)_4(OH)_2]^{+} + H_3O^{+} \quad K_{a2} = 10^{-6.1} \quad (5)$$

$$[Cr(OH_2)_4(OH)_2]^{+} + H_2O \Leftrightarrow [Cr(OH_2)_3(OH)_3] + H_3O^{+} \quad K_{a3} = 10^{-6.3} \quad (6)$$

$$[Cr(OH_2)_3(OH)_3] + H_2O \Leftrightarrow [Cr(OH_2)_2(OH)_4]^{-} + H_3O^{+} \quad K_{a4} = 10^{-11.5} \quad (7)$$

Since the hydrolyzed forms of Cr(III) have a low solubility and binds strongly to both inorganic and organic particles, trivalent chromium has a much lower mobility in water and soil than hexavalent chromium. Hexavalent chromium compounds resemble important anions for diverse biochemical processes, such as sulfates and phosphates; thus, they readily penetrate cell membranes via anion transport mechanisms, which make them highly toxic to most living organisms (Costa 1997, 2003; Borthiry et al. 2007; Cheung and Gua 2007); in addition, Cr(VI) compounds are well-established human carcinogens by the inhalation route of exposure (Wise et al. 2002, 2006; Beaver et al. 2009; Zhang et al. 2011) and potential carcinogens by the ingestion route of exposure (Stout et al. 2009; Stern 2010; Linos et al. 2011; Yuan et al. 2011; Zhitkovich 2011). On the contrary, Cr(III) compounds have a low solubility at circumneutral pH and do not resemble any biological nutrient, which makes them having a low membrane permeability; as a result, toxicity of Cr(III) compounds to a living cell is up to 1000 times less than of Cr(VI) (Rai et al. 1987; Bagchi et al. 2002; Costa 2003; Zhang et al. 2011). Moreover, Cr(III) is recognized as an essential micronutrient for lipid, protein, and fat metabolism in animals and humans, which plays an important role as a regulator of insulin activity (Anderson 1997, 1998; Guertin et al. 2005; Pechova and Pavlata 2007).

Chromium is a major heavy metal pollutant of aquatic environments, released mainly from industrial processes such as ore mining and refining, preparation of chromium compounds, metallurgy, leather tanning and mordanting processes, textile dying, metal electroplating, wood preservation, production of colored glass and ceramics, corrosion control in cooling water, refractory industry, anodizing of aluminum and waste disposal (Guertin et al. 2005; Gheju 2011). As a result, chromium contamination has been often reported in many industrial sites due to unsuitable storage, accidental leakages or improper disposal practices (Blowes et al. 1999; Kotas and Stasicka 2000; Guertin et al. 2005; Flury et al. 2009). It is estimated that the annual chromate discharge worldwide as a result of all industrial activities is 239×10^3 t (Kim et al. 2002). Because of high toxicity of Cr (VI), the World Health Organization considers chromium as a priority pollutant and proposed a maximum allowable limit for total chromium of 50 μg/L for drinking water (WHO 2011). Several technologies have been proposed to remove hexavalent chromium from polluted waters (Mohan and Pittman 2006; Owlad et al. 2009; Gheju 2011; Hashim et al. 2011; Malaviya and Singh 2011; Barrera-Diaz et al. 2012; Choppala et al. 2013; Kalidhasan et al. 2016). These include reduction to Cr (III) followed by precipitation (Clifford et al. 1986; Chang 2003; Erdem and Tumen 2004; Gheju and Balcu 2011), sorption on various adsorbents (Jia et al. 2014; Di Natale et al. 2015; Perez et al. 2015; Zhao et al. 2015; Gore et al. 2016), ion

exchange (Gode and Pehlivan 2005; Xing et al. 2007; Shi et al. 2009), membrane separation processes (Aroua et al. 2007; Muthukrishnan and Guha 2008; Xu et al. 2014; Kumar et al. 2015), biological remediation (Zazo et al. 2008; Ahmad et al. 2010; Tang et al. 2014; Thacher et al. 2015; Mamais et al. 2016), electrochemical remediation (Cheballah et al. 2015; El-Taweel et al. 2015; Sun et al. 2015), and photocatalytic remediation (Dozzi et al. 2012; Liu et al. 2012a; Shi et al. 2015; Naimi-Joubani et al. 2015; Boruah et al. 2016). Because of the differences in solubility and toxicity between Cr(VI) and Cr(III), the conventional procedure generally used to treat Cr(VI) contaminated waters consist in chemical reduction of Cr(VI) followed by precipitation of the resulted Cr(III). Its reduction to trivalent chromium is beneficial because, this way, a more mobile and more toxic chromium species is converted to a less mobile and less toxic one. The chemical agents commonly investigated for Cr(VI) reduction are ferrous iron, sulfur dioxide, hydrogen sulfide, sulfides, polysulfides, sulfites, metabisulfites, and thiosulfates (Baldea and Nioc 1970; Bowers et al. 1986; Clifford et al. 1986; Beukes et al. 2000; Lan et al. 2006; Kim et al. 2007). Over the past 25 years, there has been great interest in using another reagent with reductive capability, metallic iron (Fe^0), for the removal of Cr(VI). Therefore, the objective of this chapter is to provide new insight on the use of Fe^0 for the treatment of Cr(VI)-polluted waters.

The Beginnings

The early 1990s studies of Gillham, O'Hannesin and their research team (Reynolds et al. 1990; Gillham and O'Hannesin 1991, 1994; O'Hannesin and Gillham 1993), focused on chlorinated aliphatics, are now recognized as the starting point of remediation with elemental metals (Noubactep and Care 2010b; Noubactep and Schoner 2010). However, the ability of metals to degrade chlorinated hydrocarbons was not a new discovery, being already patented in the early 1970s by Sweeney and Fischer (1972). The Fe^0-mediated removal of chlorinated organic compounds from contaminated waters was further studied in the course of the 1980s (Sweeney 1981a, b; Senzaki and Kumagai 1988, 1989). The scientific community, unfortunately, largely overlooked all this work, presumably because it appeared in the patent literature, in non-refereed journals, or in non-English journals (Gillham and O'Hannesin 1994; Gillham 2008). Moreover, the technology of using metallic iron for water potabilization was already established in Europe around year 1890 (Mwakabona et al. 2017). In spite of all these early evidences, studies of Gillham and O'Hannesin are the ones which truly marked the beginning of using metallic iron as reactive material in passive underground porous walls. This happens because they proved the effectiveness of this reagent in removal of chlorinated aliphatics at the right moment, in the middle of a growing concern regarding pollution of groundwater. In the early 1990s, this was a brand-new water treatment technology that received a great deal of attention after McMurty and Elton (1985) published their original idea of using an underground reactive media for in situ

treatment of polluted groundwater. A passive underground porous wall, or permeable reactive barrier (PRB), is a porous reactive or adsorptive medium that is placed in the path of a contaminated groundwater plume with the aim of either to capture the contaminants, or to transform them into less harmful substances, as the groundwater flows through the barrier (Blowes et al. 1997; Noubactep and Schoner 2010).

Just like for the organic chlorinated compounds, the effectiveness of treating hexavalent chromium-polluted waters with metallic iron was also demonstrated well before 1990. To the best of author knowledge, one of the first works in the field of Cr(VI) removal with metallic iron was published by Hoover and Masseli (1941) 76 years ago. The authors reported complete reduction of 250 ppm chromate with scrap sheet steel punchings within 4 h, at pH 2.2; in addition, the copresent copper was also removed from wastewater by deposition on scrap iron, process which further facilitates Cr(VI) reduction. Almost three decades later, Case and Jones (1969) investigated the simultaneous removal of Cu and Cr(VI) starting from the well-known cementation process; it was demonstrated that, under acidic conditions (pH 1.5–3), reduction of Cr(VI) with Fe^0 was both rapid and quantitative (Case and Jones 1969). Then, in a subsequent study, Case (1974) revealed that Cr (VI) reduction process was catalyzed in the copresence of Cu, as a result of copper cementation, in concordance with previous observations of Hoover and Masseli (1941). Several years later, Gould (1982) studied the kinetics of hexavalent chromium reduction with reagent-grade iron wires under acidic conditions, showing that reduction rate was dependent on the hydrogen ion concentration, hexavalent chromium concentration and iron surface area. The results of Gould were partially confirmed by Bowers et al. (1986) who evaluated the kinetics of Cr(VI) reduction with scrap iron fillings. In spite of all these pioneering works, the use of metallic iron for the abatement of Cr(VI) aquatic pollution has received a great deal of attention only after Gillham and O'Hannesin published their aforementioned studies in the early 1990s. As far as I know, Blowes and Ptacek (1992) were the first who assessed the ability of several reactive solid materials, including Fe^0 (fine-grained Fe^0, coarse-grained Fe^0, siderite and pyrite), to remove chromate from contaminated groundwater; the reported results suggested that, while all of these materials may be used to remove Cr(VI) at low groundwater velocities, only fine-grained Fe^0 would be suitable for locations with rapid groundwater flow. In a subsequent work carried out 5 years later, Blowes et al. (1997) further studied the ability of the same four Fe-bearing solids to remove dissolved Cr(VI) from synthetic groundwater; the new results confirmed the high reduction efficiency of metallic iron, while showing that Cr(III) solids formed inside the PRB will remain stable after the input of dissolved Cr(VI) ceases. The results of a kinetic study carried out by Cantrell et al. (1995) demonstrated the capacity of metallic iron to rapidly remove not only CrO_4^{2-} but also TcO_4^- and UO_2^{2+}, suggesting that a relatively inexpensive barrier of practical dimensions can be used for in situ remediation purposes. All these findings were confirmed in two subsequent studies which investigated the subsurface chromate remediation with Fe^0 in systems of natural aquifer materials (NAM), concluding that copresence of NAM has a beneficial effect on the efficiency of Cr(VI) removal with metallic iron

(Powell et al. 1995; Powel and Puls 1997). The favorable effect of pH and NAM copresence was attributed to the ability of NAM to undergo dissolution and provide protons and, hence, to the capacity of NAM to buffer pH (Powell et al. 1995; Powel and Puls 1997). A pilot-scale field PRB composed of a Fe^0/coarse sand/native aquifer solid mixture was initiated in September 1994 at Elizabeth City, USA, to evaluate the in situ remediation of a mixed plume of chromate, trichloroethylene, cis-dichloroethylene and vinyl chloride. Monitoring studies carried out at this site reported that dissolved chromate concentrations were reduced from 4.5 mg/L to less than 0.01 mg/L, while significant reductions in chlorinated organic compounds were also achieved (Bennett et al. 1997; Puls et al. 1999b). The success of this pilot-scale test eventually led to full-scale (46 m long, 0.6 m thick, 7.3 m deep) implementation of the PRB technology at the site in June 1996 (Blowes et al. 1999). Before the realization of the PRB, batch and column laboratory tests were conducted using native aquifer materials from the Elizabeth City site and three types of granular Fe^0, to determine the mixture which would be the best suited for simultaneously treating Cr(VI) and TCE contaminated groundwater; of the reactive mixtures tested, the ones containing 100% granular Fe^0 had the most rapid reaction rates for both Cr(VI) and TCE removal; therefore, the PRB was composed entirely of granular iron (Blowes et al. 1999). Most of the studies investigating the Elizabeth City PRB suggested that responsible for the removal of Cr(VI) was the reductive precipitation mechanism, which involves two steps: (1) direct (heterogeneous) reduction of Cr(VI) to Cr(III) with Fe^0 and (2) precipitation of Cr(III) as $Cr(OH)_3$ or as Fe(III)-Cr(III) (oxy)hydroxides (Blowes et al. 1998, 1999, 2000; Puls et al. 1999a). However, there are also scientists who suggested that indirect reduction with Fe(II) (dissolved or present in the structure of some solid secondary minerals) may also have an important contribution to removal of Cr(VI) from groundwater (Wilkin et al. 2003, 2005). Even though the hydraulic conductivity of the PRB continuously decreased in time due to buildup of mineral precipitates (Wilkin et al. 2003, 2005), consistent removal of Cr(VI) in any of the down-gradient compliance wells was still observed after 15 years of operation, from influent concentrations of up to 10 mg/L to less than detection limits (Wilkin et al. 2014).

Chemistry of Hexavalent Chromium Removal with Fe^0

Mechanism of Hexavalent Chromium Removal

Most of the early research dealing with the metallic iron remediation of hexavalent chromium pollution was mainly focused on the in situ treatment of polluted groundwater with Fe^0-based PRBs. Their main aim was to investigate the efficiency and practical applicability of this new technology, as well as the parameters affecting its long-term performance under natural field conditions. Only few works have attempted to elucidate the Cr(VI) removal mechanism and/or to

characterize the mineral species generated at the surface of Fe^0 during this process. For instance, XPS investigations carried out by McCafferty et al. (1988) on the surface composition of Fe^0 passivated in aqueous chromate solutions showed that chromium and iron were present in the passive film only as Cr(III) and Fe(III), with the outer portion of the passive film enriched in Cr^{3+}, while Fe^{3+} being prevalent in the inner portion; the concentration of Cr(III) in the passive layer decreased with increasing concentration of chromate, from 15% at 10^{-4} M CrO_4^{2-} to 9% at 10^{-1} M CrO_4^{2-} (McCafferty et al. 1988). Studying the chromate removal in the presence of Fe^0 filings and quartz grains, Pratt et al. (1997) identified the mineralogical and geochemical nature of the secondary reaction products formed during the process; it was reported that all detectable chromium in the near-surface Fe^0 coating (50 Å) occurred as Cr(III), which reside in a lattice environment similar to that in Cr_2O_3 (Pratt et al. 1997). Starting from the well-known fact that metallic iron is a powerful reductant and it can serve as electron donor, direct reductive dechlorination was initially considered as the most likely cause of chlorinated organics removal with metallic iron (Reynolds et al. 1990; Gillham and O'Hannesin 1991, 1994; O'Hannesin and Gillham 1993):

$$Fe^{2+} + 2e^- \Leftrightarrow Fe^0 \quad E^o = -0.44\ V \tag{8}$$

$$Fe^0 + R\text{-}Cl + H_2O \rightarrow Fe^{2+} + HO^- + R\text{-}H + Cl^- \tag{9}$$

Because Cr(VI) reduction by Fe^0 is also favorable from a thermodynamic standpoint, most of the early 1990s studies suggested that Cr(VI) removal in zerovalent iron PRBs occurs by a similar mechanism, which involves, in a first step known as direct (heterogeneous) reduction, the direct electron transfer from the surface of Fe^0 to Cr(VI) (Cantrell et al. 1995; Blowes et al. 1997, 2000; Pratt et al. 1997; Puls et al. 1999a, b; Scherer et al. 2000):

$$2HCrO_4^- + 3Fe^0 + 14H^+ \rightarrow 3Fe^{2+} + 2Cr^{3+} + 8H_2O \tag{10}$$

It was suggested that direct Cr(VI) reduction with Fe^0 may occur through the following steps: (1) Cr(VI) diffusion from the bulk solution to the Fe^0 surface, (2) adsorption of Cr(VI) onto the surface of Fe^0, (3) reduction of Cr(VI) at the surface of Fe^0, (4) desorption of some reduction products from the surface, and (5) transport of desorbed reduction products to the bulk solution (Scherer et al. 2000; Ai et al. 2008; Fiuza et al. 2010; Noubactep 2010a, b; Vega et al. 2010). However, this mechanism does not explain the electron transport through the air-formed passive oxide layers, which cover, usually, the commercial Fe^0 materials (Ritter et al. 2002; Odziemkowski and Simpraga 2004). Numerous studies have attempted to characterize oxides covering the unreacted Fe^0 materials, generated either due to the high temperature thermal production processes, or due to contact with air during their storage. These investigations have shown that "as received" Fe^0 materials were covered with mineral species such as magnetite (Fe_3O_4),

hematite (α-Fe_2O_3), maghemite (γ-Fe_2O_3), goethite (α-FeOOH), lepidocrocite (γ-FeOOH), fayalite (Fe_2SiO_4) and wustite (FeO) (Astrup et al. 2000; Ritter et al. 2002; Odziemkowski and Simpraga 2004; Kohn et al. 2005; Yang et al. 2007; Chen et al. 2008). Raman microspectroscopy analysis of commercial Fe^0 materials (Odziemkowski and Simpraga 2004) revealed that air-formed passive layer was comprised from an inner layer (magnetite), which is conducting with respect to electrons, and an outer layer (hematite, maghemite), which does not conduct electrons. When the oxide layer is fractured or presents a heterogeneous thickness, the reaction will occur either in the inner non-oxidized Fe^0 core or throughout the fractures. Additionally, it was also suggested that Cr(VI) direct reduction can still take place if Fe^0 particles are totally covered with oxidation layers, but, in this case, at a considerably slower rate (Vega et al. 2010). Instead, when the oxide layer becomes too thick, electron transport is totally inhibited and the reduction of chromate at Fe^0 surface can no longer occur (Qiu et al. 2000). Thus, the existence of corrosion layers should, at least theoretically, indicate that Fe^0 is not reactive toward contaminants, which is in contrast with the proven effectiveness of Fe^0 technology. One possible reason of the high efficiency of Cr(VI) removal with Fe^0 could be the fact that thermal electrons, such as those involved in chemical reactions, can travel much longer distances within a solid than photoelectrons can; since oxide layers are usually thin, they allow the electron transfer to occur (Qiu et al. 2000). Another explanation may be the breakdown of the passivating Fe_2O_3 layer by autoreduction in contact with water, under the reducing conditions that prevail inside a PRB; this process opens up the structure of the protective oxide and promotes localized corrosion, either by dissolving into solution or by forming additional magnetite, which has a porous structure and allows the electron transfer from Fe^0 to Cr(VI) (Eqs. 11 and 12) (Ritter et al. 2002; Odziemkowski and Simpraga 2004):

$$Fe_2O_3 + 6H^+ + 2e^- \rightarrow 2Fe^{2+} + 3H_2O \tag{11}$$

$$3Fe_2O_3 + 2H^+ + 2e^- \rightarrow 2Fe_3O_4 + H_2O \tag{12}$$

However, even electrically conductive layers, such as magnetite, may passivate the Fe^0 if they inhibit the movement of Fe^{2+} to solution (Farrell et al. 2000). Hence, the best explanation of the Fe^0 technology effectiveness could be the fact that direct reduction is not the sole mechanism involved in the removal of Cr(VI) with Fe^0 (Gheju 2011). In one of the pioneering works in this field, Gould (1982) reported that 1.33 mole of Fe^0 was dissolved for each mole of Cr(VI) reduced; based on this observation, he suggested that molecular hydrogen and/or atomic active hydrogen species generated during iron dissolution could be the reductants responsible for the high effectiveness of Cr(VI) reduction with Fe^0 under acidic conditions (Gould 1982). This possibility was later confirmed by Cantrell et al. (1995), who suggested that Fe^{2+} and H_2 may also be considered as possible reductants of Cr(VI). Gheju et al. (2008) and Gheju and Balcu (2010) reported a rapid decrease of Fe^{2+} in

column effluent, indicating that Fe^{2+} was an important reducing agent for Cr(VI), due to the high Fe^{2+} concentrations in column pore water (Gheju et al. 2008); actually, Fe^{2+} concentrations were much higher than should theoretically be according to the stoichiometry of Eq. 10, suggesting that, at least at low pH, the primary source of soluble Fe^{2+} was Fe^0 dissolution by H^+ ions (Gheju et al. 2008). All these results are in accord with findings reported in several other studies who also suggested that Fe^{2+} released from the oxidation of Fe^0 with Cr(VI), H^+, or H_2O may reduce Cr(VI) to Cr(III) (Qiu et al. 2000; Chen et al. 2007; Jeen et al. 2008; Flury et al. 2009). Therefore, a second Cr(VI) reduction pathway–the indirect (homogeneous) reduction–should be also taken under consideration, involving Cr (VI) reduction by dissolved ferrous iron and molecular/atomic hydrogen, generated as a result of Fe^0 corrosion (Gould 1982; Bowers et al. 1986; Ponder et al. 2000; Scherer et al. 2000; Marsh and McInerney 2001; El-Shazly et al. 2005; Reardon 2005; Noubactep 2009a):

$$2Fe^0 + O_2 + 2H_2O \rightarrow 2Fe^{2+} + 4HO^- \quad (13)$$

$$Fe^0 + 2H_2O \rightarrow Fe^{2+} + H_2 + 2HO^- \quad (14)$$

$$Fe^0 + 2H^+ \rightarrow Fe^{2+} + H_2 \quad (15)$$

$$1/2Fe^0 + H^+ \rightarrow 1/2Fe^{2+} + H^* \quad (16)$$

$$H^* + H^* \rightarrow H_2 \quad (17)$$

$$HCrO_4^- + 3Fe^{2+} + 7H^+ \rightarrow 3Fe^{3+} + Cr^{3+} + 4H_2O \quad (18)$$

$$1/3CrO_4^{2-} + 5/3H^+ + 1/2H_2 \rightarrow 1/3Cr^{3+} + 4/3H_2O \quad (19)$$

$$3H^* + Cr(VI) \rightarrow Cr^{3+} + 3H^+ \quad (20)$$

Under circumneutral pH conditions, both direct and indirect reduction pathways are followed by precipitation of the resulted cations, as simple hydroxides and/or mixed chromium(III)-iron(III) (oxy)hydroxides (Palmer and Puls 1994; Cantrell et al. 1995; Pratt et al. 1997; Puls et al. 1999a; Blowes et al. 2000; Fiuza et al. 2010):

$$Fe^{2+}{}_{(aq)} + 2HO^-{}_{(aq)} \rightarrow Fe(OH)_{2(s)} \quad (21)$$

$$Fe^{3+}{}_{(aq)} + 3HO^-{}_{(aq)} \rightarrow Fe(OH)_{3(s)} \quad (22)$$

$$Cr^{3+}{}_{(aq)} + 3HO^-{}_{(aq)} \rightarrow Cr(OH)_{3(s)} \quad (23)$$

$$(1-x)Fe^{3+}{}_{(aq)} + (x)Cr^{3+}{}_{(aq)} + 3H_2O_{(l)} \rightarrow Cr_xFe_{1-x}(OH)_{3(s)} + 3H^+{}_{(aq)} \quad (24)$$

$$(1-x)Fe^{3+}{}_{(aq)} + (x)Cr^{3+}{}_{(aq)} + 2H_2O_{(l)} \rightarrow Cr_xFe_{1-x}(OOH)_{(s)} + 3H^+{}_{(aq)} \quad (25)$$

where x varies from 0 to 1.

Then, chromium and iron hydroxides may be further converted to oxides (Gheju 2011):

$$2Cr(OH)_3 \rightarrow Cr_2O_3 + 3H_2O \quad (26)$$

$$3Fe(OH)_2 \rightarrow Fe_3O_4 + H_2 + 2H_2O \quad (27)$$

$$Fe(OH)_3 \rightarrow FeOOH + H_2O \quad (28)$$

$$3FeOOH + H^+ \rightarrow Fe_3O_4 + 2H_2O \quad (29)$$

The stability of chromium fixation was confirmed by Calderon and Fullana (2015) who studied the effect of aging of nano-Fe^0 on the release of retained heavy metals; they showed that while some of the adsorbed Zn, Cu, Ni, and Cd were released back to the water during the aging of Fe^0, no redissolution of Cr was observed, which might be ascribed to Cr(III) incorporation into the nano-Fe^0 core and not at the surface (Calderon and Fullana 2015).

Because the standard reduction potential of the $Fe^{3+}{}_{(aq)}/Fe^{2+}{}_{(aq)}$ and $Fe^{3+}{}_{(s)}/Fe^{2+}{}_{(s)}$ couples is $E^o = (-0.02) - (+0.77)$ V (Stumm 1990) and $E^o = (-0.35) - (-0.65)$ V (White and Paterson 1996), respectively, from thermodynamic perspective, it seems that solid Fe(II) is a stronger reducing agent than dissolved Fe(II) (Noubactep 2009a; He et al. 2016). Therefore, another indirect pathway may involve Cr(-VI) reduction by secondary mineral phases containing Fe(II), such as ferrous sulfides, magnetite, siderite, or green rust, commonly reported as corrosion products formed on the Fe^0 surface (Fendorf et al. 2000; Williams and Scherer 2001; Doyle et al. 2004; Noubactep 2007):

$$3Fe^{II}Fe^{III}{}_2O_4 + HCrO_4{}^- + 14H_2O + H^+ \rightarrow 4[Fe_{0.75}Cr_{0.25}](OH)_3 + 6Fe(OH)_3 \quad (30)$$

$$3\left[Fe^{II}{}_4Fe^{III}{}_2(OH)_{12}\right][SO_4{}^{\cdot}3H_2O] + 4HCrO_4{}^- + 5H_2O \rightarrow 16[Fe_{0.75}Cr_{0.25}](OH)_3 + 2H^+ + 3SO_4{}^{2-} + 6Fe(OH)_3 \quad (31)$$

$$3FeS_2 + CrO_4{}^{2-} + 8H^+ \rightarrow Cr^{3+} + 3Fe^{2+} + 3S_2{}^{2-} + 4H_2O \quad (32)$$

$$2FeS + 3CrO_4{}^{2-} + 9H_2O \rightarrow 4[Fe_{0.25}Cr_{0.75}](OH)_3 + Fe^{2+} + S_2O_3{}^{2-} + 6HO^- \quad (33)$$

$$3FeCO_3 + HCrO_4{}^- + 8H_2O \rightarrow 4[Fe_{0.75}Cr_{0.25}](OH)_3 + 2H^+ + 3HCO_3{}^- \quad (34)$$

It is well known that under circumneutral neutral conditions, metallic iron is usually covered by thin layers of iron oxides (Gheju 2011); since all these iron corrosion products are mostly positively charged, this makes them good adsorbents for negatively charged pollutants such as Cr(VI) (Noubactep 2015). Therefore, adsorption is another possible Cr(VI) removal mechanism or, at least, an important step of the Cr(VI) removal mechanism, which must be taken under consideration in Fe^0/H_2O systems. For instance, adsorption of Cr(VI) on goethite was described to occur as follows (Geen et al. 1994):

$$\text{Fe-OH} + \text{CrO}_4^{2-} + \text{H}^+ \Leftrightarrow \text{Fe-CrO}_4^- + \text{H}_2\text{O} \quad (35)$$

It was suggested that adsorption of Cr(VI) on goethite takes place via a two-step specific mechanism (Fendorf et al. 1997; Grossl et al. 1997). The first step involves an initial ligand exchange reaction of aqueous Cr(VI) oxyanions with OH ligands, forming an inner-sphere monodentate surface complex; the subsequent stage involves a second ligand exchange reaction, resulting in the formation of an inner-sphere bidentate surface complex (Fendorf et al. 1997; Grossl et al. 1997). In a very recent study, He et al. (2016) revealed that Fe(II)/Fe(III) hydroxides were highly effective in the removal of aqueous Cr(VI). The results indicated that the amount of Cr(VI) removed from solution was proportional to the absolute content of structural Fe(II) in Fe(II)/Fe(III) hydroxides. In addition, it was also reported that the process proceeds in two steps: a first rapid stage at the beginning (first 10 min), followed by a second one, less rapid. The initial rapid phase was supposed to be governed by a complicated mechanism comprised of simultaneous adsorption and reduction, with adsorption having an important role (He et al. 2016).

Since it was demonstrated that Cr(VI) is adsorbed effectively to iron oxides, it is obvious that it will be retained in a similar way also onto iron oxide layers existent at the surface of Fe^0. For example, Ai et al. (2008) showed that Cr(VI) is first adsorbed on the surface of Fe/Fe_2O_3 core-shell nanowires and only thereafter partially reduced to Cr(III). The adsorption-reduction mechanism was considered the dominant mechanism of Cr(VI) removal with nano-Fe^0 particles or wires; having a core-shell structure, Fe^0 nanomaterials exhibit characteristics of both adsorbent (due to the iron (oxy)hydroxides layers) and reductant (due to the metallic iron core) (Ai et al. 2008; Li et al. 2008). Similarly, Qiu et al. (2000) also suggested that chromate must first be adsorbed onto the Fe^0 surface, in order to be reduced to Cr(III). Fu et al. (2015a) proposed a two-step Cr(VI) removal mechanism, including both the physical adsorption of Cr(VI) on the surface or inner layers of the sepiolite-supported nano-Fe^0 particles and the subsequent reduction of Cr(VI) to Cr(III) by Fe^0. The significant enhancement of Cr(VI) removal with Fe^0 in the presence of natural aquifer materials (NAM) was ascribed to Cr(VI) adsorption on oxyhydroxide layers, favored by the pH buffering capacity of NAM (Powell et al. 1995).

Analysis of exhausted Fe^0 surface conducted by Lai and Lo (2008) after Cr(VI) reduction experiments revealed the presence of a mixed oxide: Cr_2O_3-Cr_2O_7; the Cr(III)-O-Cr(VI) bonds were presumably the result of $Cr_2O_7^{2-}$ electrostatic attraction by the positive charges of the polymeric Cr(III) hydroxides (Lai and Lo 2008). In a very recent study, Sheng et al. (2016) suggested that Cr(VI) was mainly adsorbed on nano-Fe^0 at the initial stage and then rapidly and almost completely reduced to Cr(III) with reaction time proceeding. Nevertheless, there are also studies which suggest that adsorption of Cr(VI) at the surface of secondary mineral passive layers may occur only at high concentrations of Cr(VI) or at low concentrations of Fe^0 (Li et al. 2008). A similar observation was made by

Isaacs et al. (2002), who indicated that chromate was only weakly adsorbed onto passive films, being incorporated into the secondary mineral layer only after Fe^0 exposure to a saturated chromate solution for extended periods. Moreover, under alkaline pH conditions, the possibility of CrO_4^{2-} removal by adsorption onto the metallic iron oxides was ruled out (Cantrell et al. 1995).

Not only Cr(VI) but also the resulted Cr(III) may be adsorbed at the surface of Fe^0; Blowes et al. (1997) were the first who suggested the possibility that Cr(III) could be removed also by adsorption onto the goethite formed at the surface of metallic iron. Astrup et al. (2000) reported that chromium was present at the surface of reacted Fe^0 only as Cr(III), adsorbed, and coprecipitated with Fe-(oxy) hydroxides. Qiu et al. (2000) also noticed that reduced Cr(III) was partially adsorbed on the Fe^0 surface.

Finally, another pathway that was suggested for the removal of Cr(VI) in Fe^0/H_2O systems is the sequestration within the matrix of mineral phases which precipitate out of solution. In other words, not only Cr(III) but also Cr(VI) may be entrapped in the structure of growing iron hydroxides, and, there should be no reasons why reduction should precede coprecipitation as a rule (Noubactep 2007):

$$\mathrm{Cr(VI)} + \mathrm{nFe(OH)_{x(s)}} \rightarrow \mathrm{Cr(VI)} - \left[\mathrm{Fe(OH)_x}\right]_{\mathrm{n(s)}} \tag{36}$$

$$\mathrm{Cr(III)} + \mathrm{nFe(OH)_{x(s)}} \rightarrow \mathrm{Cr(III)} - \left[\mathrm{Fe(OH)_x}\right]_{\mathrm{n(s)}} \tag{37}$$

This Cr(VI) removal pathway was confirmed by Gheju and Balcu (2011) who noticed that, even though Cr(VI) is highly soluble, it was partially removed from the clarifier influent by coprecipitation with Cr(III) and Fe(III). In a study carried out by Yoon et al. (2011) over the pH range of 5–7.5, it was reported that removal rates were faster under oxic conditions than under anoxic conditions; starting from this observation, it was suggested that Cr(VI) was reduced to Cr(III) either directly by Fe^0 or indirectly by dissolved Fe(II) (Yoon et al. 2011). However, under oxic and circumneutral conditions, Fe(II) is rapidly oxidized to Fe(III), which decreases the probability of Cr(VI) reduction by Fe(II). Therefore, in my opinion, the faster removal efficiencies observed under oxic conditions were actually the result of Cr(VI) sequestration within the matrix of the more voluminous Fe(III) precipitates formed in the presence of O_2.

Summarizing, it can be concluded that mechanism of Cr(VI) removal with Fe^0 is not just simple reductive precipitation; actually, it is the result of a complex interplay of processes such as adsorption, reduction, and (co)precipitation, and it is yet to be discussed which pathway is likely to be dominant. This is in accord with recent studies suggesting that, in Fe^0/H_2O systems, Fe^0 should be regarded as generator of indirect reducing agents (Fe(II) and H/H_2) and that contaminants are removed mainly by adsorption, coprecipitation, and size-exclusion processes, while contaminant reduction, when possible, mainly results from indirect reducing agents (Noubactep 2009a; Crane and Noubactep 2012; Gatcha-Bandjun et al. 2014).

Kinetics of Hexavalent Chromium Removal

In the first kinetic study on Cr(VI) reduction with Fe^0 it was noticed that Cr(VI) removal was dependent on Cr(VI) concentration, H^+ concentration and iron surface area (Gould 1982). Cr(VI) reduction with Fe^0 was found to be half-order with respect to both Cr(VI) and H^+, first order with respect to Fe^0 surface area, and the overall reaction kinetics was represented as follows (Gould 1982):

$$\frac{dC_{Cr(VI)}}{dt} = -k \cdot C_{Cr(VI)}^{0.5} \cdot C_{H^+}^{0.5} \cdot A \tag{38}$$

where k ($L \cdot cm^{-2} \cdot min^{-1}$) is the rate constant, A is the surface area of iron ($cm^2 \cdot L^{-1}$), and $C_{Cr(VI)}$ and C_{H+} are the concentrations of Cr(VI) and H^+, respectively ($mol \cdot L^{-1}$).

The work of Gould (1982) was followed by a plethora of studies investigating the kinetics of Cr(VI) reduction with Fe^0. Depending on the experimental conditions, the kinetics of Cr(VI) removal with metallic iron was reported to be zero order (Bowers et al. 1986; Gheju and Iovi 2006), first order (Cantrell et al. 1995; Ponder et al. 2000; Kaplan and Gilmore 2004; El-Shazly et al. 2005; Zhang et al. 2008), 2/3 order (Fiuza et al. 2010; Mitra et al. 2011), or second order (Ai et al. 2008). In all these works, the kinetics of Cr(VI) removal with Fe^0 was studied by applying the classical concepts of chemical reactions in a homogeneous media, while the prevailing mechanism of Cr(VI) removal was considered to be the direct reduction with Fe^0. However, since Cr(VI) removal in Fe^0/H_2O system is a heterogeneous process between a liquid phase (Cr(VI) aqueous solution) and a solid phase (metallic iron/iron oxides), some researchers suggested that a corresponding approach should be applied in order to describe more correctly the kinetics of Cr(VI) removal with Fe^0. For instance, Fiuza et al. (2010) suggested that a shrinking particle-type model is more suitable for the initial steps of the process; accordingly, the kinetics of heterogeneous Cr(VI) removal with Fe^0 was described by an equation of the following type (Fiuza et al. 2010):

$$-\frac{dC}{dt} = \beta \frac{k_1 A C^{\alpha}}{V} \tag{39}$$

where C is the concentration of Cr(VI) in the solution, β is the stoichiometric coefficient, k_1 is a rate constant, A is the surface area of the iron, α is the chemical reaction order, and V is the initial volume of solution.

Experiments carried out over the normal pH range agreed with the appropriateness of the chosen model, since the kinetic reaction order (0.6–0.8) agrees with the proposed theoretical value of 2/3, assumed on the likeness to the shrinking particle models with spherical symmetry. The average rate constant for the heterogeneous chemical reaction, as determined from different experiments, was $711.2\ mg^{1/3} \cdot min^{-1}$ (Fiuza et al. 2010). Even though this study considered that kinetic rates should be proportional to Fe^0 surface area, no attempt has been made to incorporate the passivation process in the rate equation. Starting from this observation, a new kinetic

model was proposed for the removal of Cr(VI) with Fe^0, which considered the combined processes of (1) Cr(VI) reduction via the direct route with Fe^0 and (2) passivation of the active Fe^0 surface, leading to the formation of a thin oxide layer, mostly magnetite (Mitra et al. 2011). By applying this new model, the kinetics of direct Cr(VI) reduction with Fe^0 iron was found to be 2/3 order with respect to Cr(VI) concentration; in addition, it was noticed that both the direct reduction and passivation rate constants depend linearly on the hydrogen ion concentration, both decreasing with increasing pH. Accordingly, the overall expression for the rate of uptake of Cr(VI) in the Fe^0/H_2O system was described as follows (Mitra et al. 2011):

$$-\frac{dC}{dt} = k_1 A(t) C(t)^{2/3} + k_2 A(t) C(t) \tag{40}$$

where $C(t)$ is the transient concentration of Cr(VI) in aqueous phase, $A(t)$ is the transient active area of Fe(0) left at time t, and k is the rate constant; the subscripts 1 and 2 refer to the processes of direct reduction and passivation, respectively.

Parameters Affecting Hexavalent Chromium Removal with Fe^0

pH

One of the most important factors affecting the removal of Cr(VI) with metallic iron is pH. According to the stoichiometry of Eq. 10, it requires 7 moles of hydrogen ion for the direct reduction of each mole of Cr(VI) with Fe^0; the same amount is necessary also for the indirect reduction of each mole of Cr(VI) with Fe (II) (Eq. 18). Thus, as the Le Chatelier's principle states, the Cr(VI) reduction process will be enhanced by the increase of the concentration of hydrogen ions in solution. This theoretical assumption was confirmed by the results of numerous studies, conducted under various experimental conditions, which showed that pH significantly affects the rate of Cr(VI) reduction by Fe^0: the amount of reduced Cr(VI) increases with decreasing pH (Gheju and Iovi 2006; Chen et al. 2007; Qian et al. 2008; Alidokht et al. 2011; Yoon et al. 2011; Chakrabarti et al. 2014). The favorable effect of decreasing pH can be also ascribed to sorption of negatively charged Cr(VI) oxyanions onto Fe^0 surface and to oxidative dissolution of Fe^0 and release of indirect reductants (Fe^{2+}, H/H_2), both processes being favored at low pH. Nevertheless, in a recent study it was shown that, under alkaline conditions (pH 7–12), the rate of Cr(VI) removal is independent of pH, which suggests that the reaction mechanism remains the same over this pH range (Fuller et al. 2013).

Cr(VI) Initial Concentration

Chromate reduction experiments with metallic iron in batch or column reactors, carried out over a wide range of Cr(VI) concentrations, revealed that, generally, observed reaction rates decreased with increasing Cr(VI) concentration, probably due to lower rates of Fe^0 corrosion and increasing surface passivation at higher Cr(VI) concentrations (Gheju and Iovi 2006; Yang 2006; Lai and Lo 2008; Li et al. 2008; Alidokht et al. 2011; Gheju and Balcu 2011; Wang et al. 2012); however, there are also studies which suggested that this rate dependence could be a consequence of the oxidation kinetics of Fe^0 and not a specific effect of the hexavalent chromium being reduced (Ponder et al. 2000).

Size of Fe^0 Particles

The size of Fe^0 particles is another factor which significantly influences the efficiency of Cr(VI) removal with metallic iron. Several experimental studies indicated a better removal of Cr(VI) from solution for the fine-grained Fe^0 than for coarse-grained Fe^0, suggesting that the reaction is surface area dependent: the smaller the particle size, the larger the specific surface area, and the greater the Fe^0 reactivity toward pollutants (Blowes et al. 1997; Li et al. 2008; Gheju and Balcu 2010; Noubactep and Care 2010a).

Copresence of Inorganic and/or Organic Species

Inorganic and organic substances are ubiquitously present in aquatic environments, and, therefore, the effect of their copresence was also a well-studied topic; however, there is still some controversy on how such species can affect Cr(VI) reduction, attributable to a lack of consistency of the experimental conditions. For instance, while some studies concluded that copresence of Mg^{2+} or Ca^{2+} caused a decrease in the Cr(VI) removal capacity of Fe^0 (Lai and Lo 2008; Liu and Lo 2011), other works showed that addition of Ca^{2+} or Mg^{2+} slightly enhanced Cr(VI) reduction at pH 9.5, whereas it had little effect at pH 6 (Liu et al. 2008b). According to Lo et al. (2006), $CaCO_3$ has no apparent effect on the reactivity of Fe^0; in contrast, Yang (2006) concluded that addition of dissolved $CaCO_3$ significantly enhanced reduction of Cr(VI). The removal of Cr(VI) was slightly impacted in the presence of Ni and slightly accelerated in the presence of Zn alone or in combination with Ni (Dries et al. 2005). Investigating the effect of sand on the reduction of Cr(VI) by Fe^0, Kjeldsen and Locht (2002) reported a slightly higher reduction capacity for the 100% Fe^0 content than for the mixture of sand (25–50%) with Fe^0. On the other hand, studies carried out by Song et al. (2005) and Oh et al. (2007b) revealed an enhancement of Cr(VI) reduction when sand was added to the Fe^0/H_2O system. Because of the volumetric expansion of the iron corrosion products, the porosity of

the Fe^0-based PRBs decreases in time, leading to a short service life of the system. Even though mixing Fe^0 and sand cannot improve Fe^0 efficiency in terms of reactivity, it could be a useful tool to delay porosity loss. It was suggested that 50% (vol) should be regarded as the highest proportion of metallic iron in the reactive mixture, in order to obtain a long-term efficiency of Fe^0 beds (Noubactep and Care 2010b). Therefore, mixing Fe^0 and inert additives is a prerequisite for PRB or household Fe^0 filters sustainability (Noubactep and Care 2010b). The effect induced by inorganic constituents may be also influenced by the nature of surface coating applied to nano-Fe^0 particles. For instance, it was reported that the presence of Ca^{2+} enhanced the removal of Cr(VI) with polyacrylate/nano-Fe^0, even though no obvious influence on the colloidal stability was observed; this effect was attributed to reduced electrostatic repulsion between Fe^0 and the negatively charged Cr(VI) ions (Dong et al. 2016d). In contrast, the presence of Ca^{2+} decreased the Cr(VI) removal by starch/nano-Fe^0, attributable to a higher degree of particle settling caused by the presence of Ca^{2+} (Dong et al. 2016d).

Similar contradictory results were reported also with regard to the influence of organic compounds. Several studies performed in the presence of humic acids (HA) concluded that such compounds exhibited an insignificant inhibitory effect on metallic iron reactivity (Liu et al. 2008b; Zhang et al. 2008); on the other hand, a marked enhancement of Cr(VI) removal with Fe^0 was observed by Liu and Lo (2011) when HA were introduced into the reaction system; this phenomenon was ascribed to HA capacity of suppressing the precipitation of iron corrosion products at the surface of Fe^0, by forming soluble and colloidal Fe-humate complexes (Liu and Lo 2011). Dong et al. (2016d) reported that removal of Cr(VI) with both polyacrylate- and starch-stabilized nano-Fe^0 decreased with increasing concentration of HA; this was associated with occupation of the reactive sites (which provided an electrosteric repulsion effect in the case of polyacrylate), and with increased settling of the nano-Fe^0 particles (in the case of starch) (Dong et al. 2016d). By studying the comparative effect of HA and fulvic acids (FA), it was observed a faster Cr(VI) removal in the presence of HA compared to FA (Mak and Lo 2011). The dual effect of HA on Cr(VI) removal with metallic iron was attributed by Wang et al. (2011) to their capacity to act both as an adsorbent, competing with chromate anions for reactive sites on the surface of Fe^0 (the inhibitory effect), and also as electron shuttles, due to quinone moieties which may promote the electron transfer. On the other hand, it was suggested that no redox reaction occurred in both FA and HA, and, therefore, removal of Cr(VI) is only the result of interactions with Fe^0 (Mak and Lo 2011). Recent studies carried out by Dong et al. (2016a) indicated that the presence of FA can either enhance or decrease the colloidal stability and reactivity of nano-Fe^0 particles toward Cr(VI), depending on the nanoparticle characteristics (e.g., pH_{pzc}), geochemical conditions (e.g., pH) and concentrations of FA. For instance, at low FA concentrations, adsorption of FA on the nano-Fe^0 surface enhanced the particle stabilization (i.e., a reduced particle aggregation), which resulted in more available surface sites and a facilitated Cr(VI) reduction; instead, when the FA concentrations were too high, the active surface sites of nano-Fe^0 were completely saturated, so that Cr(VI) removal decreased even

though the FA enhanced the dispersion of nano-Fe^0 particles (Dong et al. 2016a). Studies performed by Zhang et al. (2008) showed that reduction of Cr(VI) by Fe^0 was suppressed in the presence of citrate, while Liu et al. (2009) observed a faster Cr(VI) reduction by metallic iron in the presence of citrate. Instead, Liu et al. (2012a) reported that while the long-term performance of Fe^0 was not effectively improved in the presence of citric acid, introduction of photoirradiation dramatically increased the reduction rate of Cr(VI) in the presence of citric acid; this enhancement was attributed to photoreductive dissolution of the oxide layer existent on Fe^0 surface (Liu et al. 2012a).

Summarizing, there is a clear need for more rigorous quantification of the influence of both inorganic and organic substances on Cr(VI) reduction efficiency.

Biogeochemical Interactions

Even though important attention has been given in the last years to the biogeochemical interactions that could influence Fe^0 reactivity, the effect of microorganisms copresence is not yet well understood. It seems that indigenous microorganisms can exert either beneficially or detrimentally effects on Cr (VI) removal with metallic iron, depending on the local geochemistry conditions. Anaerobic Cr(VI) bioreduction may be stimulated in the presence of metallic iron, through the depletion of O_2 and production of H_2 during Fe^0 corrosion (Eqs. 13, 14 and 15). However, high Fe^0 concentrations should be avoided, since they could have an inhibitory effect by increasing the pH beyond the optimum range of the bacteria (Fernandez et al. 2004). In addition, microorganisms might also potentially enhance Cr(VI) removal efficiency by mediating mineral dissolution of passive layers, or by alleviating pore volume reduction caused by the formation and entrapment of H_2 gas (Gandhi et al. 2002; Vazquez et al. 2006; Singh et al. 2013). Furthermore, an enhanced microbial activity may also detrimentally affect the reactivity of metallic iron toward Cr(VI), as a result of reducing PRB permeability and reactivity by mediating formation of mineral precipitate or biomass and gas accumulation (Scherer et al. 2000; Gandhi et al. 2002).

Dissolved Oxygen

Under environmental relevant conditions, dissolved O_2 is considered to be the most corroding factor in Fe^0/H_2O systems, with a well-known role in acceleration of the kinetics of Fe^0 corrosion (Eq. 13) (Bilardi et al. 2013; Domga et al. 2015). For instance, it was reported that, in oxygenated waters, Fe^0 can be corroded up to 65 times faster compared to oxygen-free waters (Cohen 1959). Similarly, the degree of Fe^0 corrosion within the PRB clearly decreased in groundwater with lower oxygen concentrations (3.5–5 mg/L), located at greater depths, compared to groundwater with higher oxygen concentrations (5–6 mg/L), situated at lower depths (Flury et al. 2009). However, under oxic conditions, Fe^0 surface is generally

covered by external nonconductive oxide layers, which hinder both transfer of electron from Fe^0 surface to dissolved oxygen and diffusion of dissolved oxygen from solution to the Fe^0 surface. This will lead to a slow diffusion of dissolved oxygen through the oxide film coating the Fe^0 surface (Kaplan and Gilmore 2004). Therefore, although Fe^0 corrosion by dissolved oxygen is thermodynamically favored (Crane and Scott 2012), it seems that even under oxic conditions Fe^0 is mostly oxidized by water (Eq. 14); accordingly, the main process involving dissolved oxygen that contributes to corrosion of Fe^0 in aqueous solutions (Le Chatelier's principle) is oxidation of Fe(II) to Fe(III) (Stratmann and Muller 1994; Domga et al. 2015):

$$2Fe^{2+} + 1/2O_2 + H_2O \rightarrow 2Fe^{3+} + 2HO^- \tag{41}$$

All these suggest that Fe(II) species are the major corrosion products under anoxic conditions, whereas Fe(III) species are the more abundant corrosion products under oxic conditions (Flury et al. 2009; Domga et al. 2015). Even though both experimental and theoretical studies have indicated the possible deleterious effects of dissolved oxygen on PRB performance, it seems that, however, PRB longevity is not well correlated with concentration of O_2 in groundwater (Henderson and Demond 2007). In order to explain this apparent contradiction, it should be reminded that the first mechanism proposed in the early 1990s for the removal of Cr(VI) (the "reductive-precipitation" mechanism) attributed the efficiency of Fe^0 treatment systems to contaminant chemical transformations (e.g., direct reductive degradation and precipitation); thus, the only role that corrosion oxide layers formed at Fe^0 surface could have is to suppress Fe^0 reactivity. However, according to the more recent "adsorption-coprecipitation" concept, contaminants are quantitatively removed in Fe^0/H_2O systems mainly by adsorption, coprecipitation, and size exclusion, while reduction, when possible, is mainly the result of indirect reducing agents produced by Fe^0 (Noubactep 2007). This new concept may therefore explain the observed longevity of PRBs in groundwater with high levels of dissolved oxygen. Even though it is a very important parameter in Fe^0/H_2O systems, to the best of my knowledge, the influence of dissolved oxygen on the removal of Cr(VI) with Fe^0 was rigorously investigated only by the work of Yoon et al. (2011). Batch experiments carried out in this study indicated that removal rates were faster under oxic conditions than under anoxic conditions. Furthermore, this study also indicates that the presence of dissolved oxygen plays an important role not only on the kinetics of Cr(VI) removal but also in development of various Cr(VI) reduction products; for instance, chromite ($FeCr_2O_4$) was the reaction product obtained under oxic conditions, while Cr(III)/Fe(III) hydroxide/oxyhydroxides were produced under anoxic conditions (Yoon et al. 2011).

Progress in Cr(VI) Removal with Fe^0

Scrap Iron

Numerous types of Fe^0-based materials have been investigated in the last decades for the removal of Cr(VI) (Gheju 2011). Aware of the importance of metal reuse, numerous authors have been involved in researches concerning the removal of Cr(VI) from contaminated water by use of scrap iron. As aforementioned, in one of the first works in the field of Cr(VI) removal with Fe^0, Hoover and Masselli (1941) suggested that scrap steel can be successfully used for the remediation of aquatic Cr(VI) pollution. Bowers et al. (1986) evaluated the kinetics of Cr(VI) reduction with scrap iron fillings, estimating that large-size scrap iron particles are significantly more economical than conventional reducing reagents, while creating no special handling or health hazard in the work environment. The galvanic reduction of hexavalent chromium with scrap iron in a divided parallel plate cell was investigated by Abdo and Sedahmed (1998); the advantages of this technique over direct chemical reduction are that the reduced chromium salt is free of iron impurities, making possible to recover Cr(III) as pure $Cr_2(SO_4)_3$ after a preconcentration step, and that electrical energy is produced from the galvanic cell as by-product (Abdo and Sedahmed 1998). A fixed bed of scrap bearing iron spheres, through which the chromium solution passed in recirculating mode, was used by El-Shazly et al. (2005) to study the removal of Cr(VI) from industrial waste solutions under different experimental conditions. Junyapoon and Weerapong (2006) also suggested that, because of their low toxicity and cost, scrap iron filings seem to be a very good reactive material for the rapid removal of Cr(VI) from plating wastewater. Several studies were carried out using scrap iron with various shapes and sizes to investigate the kinetics of Cr(VI) reduction, and the effect of experimental parameters on Cr(VI) removal efficiency (Gheju and Iovi 2006, Gheju et al. 2008, Gheju and Balcu 2010, 2011). Oh et al. (2007a) successfully treated landfill leachate containing both organic contaminants (trichloroethylene, tetrachloroethylene) and heavy metals (Cr, Mn, Cu, Zn, As, Cd, and Pb) by using two industrial wastes: steel scrap and converter slag; the reported results suggested that PRBs comprising these wastes might be effective in treating landfill leachate containing mixed contaminants (Oh et al. 2007a). Chen et al. (2008) successfully removed chromate from electroplating wastewater by using cast iron waste in a plug flow reactor. Zhang et al. (2008) studied the effect of some organic and inorganic anions on Cr(VI) removal with waste Fe^0 chips. Batch and column experiments of Cr(VI) reduction to Cr(III) with metallic iron collected from a mechanical workshop were conducted by Prasad et al. (2011) to explore the effect of process conditions on removal efficiency. Wang et al. (2012) studied the effects of pH, empty bed contact time, and initial Cr(VI) concentration on Cr(VI) reduction with scrap iron in a fixed bed reactor.

Commercial Metallic Iron

During the 1990s, there has been an intense activity directed at the development and implementation of PRB remediation technology. Due to its important advantages (cost-effectiveness, low maintenance, ability to treat multiple contaminants, low impact on groundwater flow, availability of aboveground land for other activities, possible application in urban areas) over the conventional pump and treat systems, the PRB technology was considered, at that time, a very promising method in the field of groundwater remediation. The most frequently used reactive medium employed in laboratory studies, small-scale field PRB tests and full-scale PRBs was metallic iron, mainly under the form of commercially Fe^0-based alloy particles. Such iron particles, commonly referred to as "granular iron," "iron filings," "iron chips," or "iron shavings," were produced all over the world (Ada Iron & Metal, Master Builder, Peerless Metal, Powders & Abrasive, Connelly GPM, Gotthart Maier, Aesar, SHOWA Chemical, US Metal, Cercona, Sigma, Shinyo Pure Chemical etc.), with various dimensions (0.1–20 mm) and surface areas (0.05–2.8 m^2/g) (Gheju 2011). In addition, few studies reported also the use of commercial "steel wool" (Ozer et al. 1997; Gromboni et al. 2010; Chakrabarti et al. 2014).

Nano-sized Metallic Iron

In spite of the PRB technology advantages, its practical application has also several drawbacks, the most important being the decrease in time of Cr(VI) removal efficiency due to deposition of secondary mineral layers at the surface of Fe^0 (Scherer et al. 2000; Liu et al. 2012a). Therefore, substantial work on enhancing the reactivity of metallic iron particles has been reported in the last years. One of the most studied approaches to optimize Fe^0 reactivity toward a wide range of contaminants, including Cr(VI), consisted in increasing the surface area of metallic iron by working with nano-sized particles instead of milli- or micro-Fe^0 (Noubactep et al. 2012). Assuming Fe^0 particles as being spherical, there is an inverse relationship between the diameter and specific surface area (Sun et al. 2006):

$$\mathrm{SSA} = \frac{6}{\rho \cdot d} \tag{42}$$

where SSA (m^2/kg) is the specific surface area of Fe^0 particles, d (m) is the diameter of Fe^0 particles, and ρ (kg/m^3) is the density of Fe^0 particles.

From Eq. 42 it clearly results that the smaller the particle size, the higher the surface area to volume ratio, leading to a higher surface reactivity of the Fe^0 particle (Yirsaw et al. 2016; Sheng et al. 2016). However, it is very important to point out that, if quantum size effects (prevalent only for $Fe^0 < 10$ nm) are neglected, the reactivity of metallic iron remains unchanged with decreasing particle size; in fact, the higher removal efficiency of nano-Fe^0 (up to 1000 times greater compared with micro- or milli-Fe^0) is mainly the result of a greater density of reactive sites on the

particle surface (Karn et al. 2009; Noubactep et al. 2012; Yirsaw et al. 2016). The better reactivity is not the sole advantage of nano-Fe^0 technology. Due to their very small particle size (1–100 nm), they can be suspended in slurry and injected easily into soil pores toward shallow or deep aquifers, a property that is particularly beneficial when contamination lies underneath a building (Zhang 2003; Li et al. 2006; Karn et al. 2009). Therefore, because the nano-Fe^0 technology presents such new opportunities for the remediation of environmental pollution, it may serve as an alternative to the (already now) conventional Fe^0 PRB technology (Li et al. 2006). Nevertheless, even if it is well recognized that nano-Fe^0 particles are powerful reagents for a wide variety of environmental contaminants, there are some important drawbacks, which question the potential of using nanoscale iron particles for in situ remediation. First, they have a strong tendency to aggregate and adhere to the surfaces of suspended solids or sediments, which make them rapidly inert and immobile (Zhang 2003; Li et al. 2006; Karn et al. 2009; Chekli et al. 2016). Second, the high reactivity of nano-Fe^0 particles will make them react not only with the target pollutants but also with other nontarget substances, which will eventually lead to a limited lifetime of the nanoparticles in the environment and a lower efficiency of the nanotechnology (Comba et al. 2011; Chekli et al. 2016). Third, considering the subsurface injection procedure of iron nanoparticles, it has been suggested that the mobility of the particles is likely to be significantly retarded in aquifer by voluminous expansion due to particle corrosion, leading to pore clogging; moreover, the effect of pore clogging can make the contaminant plume to be inadvertently directed to a different location instead of being treated (Crane and Scott 2012; Noubactep et al. 2012). Due to practically unavoidable phenomena during the synthesis process, nano-Fe^0 particles develop a core-shell morphology, with a Fe^0 core surrounded by an outer layer of iron corrosion products (iron (oxy) hydroxides) of at least 3 nm. Once introduced into the environment, the nature of outer oxide layer changes relatively quickly (Chekli et al. 2016; Lefevre et al. 2016; Liu et al. 2016; Yirsaw et al. 2016). After immersion in anoxic water for 72 h, the corrosion layer turns into a complex mixture comprising wustite, goethite, and/or akaganeite; instead, in oxic water, the entire core-shell structure transforms first into circular spheres composed of magnetite/maghemite, when aging time is up to 24 h, and then subsequently evolves into a flaky and/or acicular-shaped structure of lepidocrocite, after 48 h (Liu et al. 2016). Therefore, it can be concluded that reactions at the nano-Fe^0/H_2O interface will influence not only the nature of the outer iron oxide layer but also the core-shell structure (Liu et al. 2016).

In the recent years, there has been important interest in investigating possibilities to prevent attraction and agglomeration of iron nanoparticles. The most studied possibility consisted in applying a coating to change the nanoparticle surface properties. It has been proved in several studies that both natural (carboxymethyl cellulose, chitosan, xanthan gum, starch, biochar, sepiolite) (Qian et al. 2008; Comba and Sethi 2009; Geng et al. 2009; Lin et al. 2010; Alidokht et al. 2011; Esfahani et al. 2015; Fu et al. 2015a; Su et al. 2016) and synthetic (polyacrylate, hexadecyltrimethylammonium, polystyrene sulfonate, polyaspartate, SiO_2) (Li et al. 2007, 2012; Phenrat et al. 2008; Lin et al. 2010) stabilizing agents can

be successfully employed to avoid sedimentation and aggregation of the iron nanoparticles, leading to higher Cr(VI) removal efficiencies and better transport through soils. The concentration of surface coating can influence both the colloidal stability and reactivity of nano-Fe^0 particles. Even though, generally, the colloidal stability increases with increasing concentration of surface coating, it seems that, however, there is an optimum concentration of surface coating for the best Cr (VI) removal (Dong et al. 2016d). Working with polyacrylate- and starch-stabilized nano-Fe^0, Dong et al. (2016d) noticed that, while below the optimum concentration of surface coating, increasing concentration of surface coating led to higher reactivity of nano-Fe^0 toward Cr(VI), above the optimum concentration, the efficiency of Cr(VI) removal decreased with increasing concentration of surface coating.

Studies of Cr(VI) removal carried out using stabilized nano-Fe^0 have shown that, due to its properties, the stabilizing layer has not only the advantage of diminishing the effect of nano-Fe^0 particles aggregation, but, as well, it can also suppress the formation of the insoluble (oxi)hydroxides (Xu and Zhao 2007). In addition, the surface coating may not only slow down the oxidation rate of the nano-Fe^0 particles but also the transformation of iron oxides. For instance, the structural evolution in static water showed that, for the bare nano-Fe^0, magnetite and/or maghemite is the dominant corrosion product after 90 days of aging, while for the carboxymethyl cellulose/nano-Fe^0, acicular-shaped structures of crystalline lepidocrocite were the primary corrosion end products after aging; moreover, the amount of lepidocrocite present in the corrosion products of CMC/nano-Fe^0 increased with increasing loading of CMC, which reveals that the coating influenced the transformation of iron oxides (Dong et al. 2016b).

A very recent new strategy for producing stable Fe^0 nanoparticles is the use of plant extracts as "green" reducing agents. These organic compounds may act both as reducing agents in the synthesis of nanoparticles and as stabilizing agents for the produced nanoparticles; in addition, the obtained nanoparticles are also free of contamination and have a well-defined size and morphology (Madhavi et al. 2013; Mystrioti et al. 2015, 2016; Poguberovici et al. 2016).

Even though Fe^0 nanomaterials hold great promise in a range of contaminant removal, the toxicity, biocompatibility, bioaccumulation, translocation potential, and persistence of the Fe^0 nanoparticles have to be carefully evaluated before this technology is extensively used (Karn et al. 2009; Yirsaw et al. 2015). Since most contaminated sites rely also on bioremediation as a concurrent or terminal process to meet remediation goals, a special attention should be given on understanding how iron nanoparticles will affect site geochemistry, microbial abundance/diversity, and their interrelationships (Kirschling et al. 2010). Even though in the last decade an increasing number of studies have investigated the environmental implications of iron-based nanomaterials, the conclusions are still inconsistent (Lefevre et al. 2016; Simeonidis et al. 2016). According to some authors, nano-Fe^0 exerts no toxic effects on aquatic bacterial community. For instance, the results of a 36-day study indicate that addition of 100 mg/L iron nanoparticles to aerobic river water

was not toxic to the indigenous river water bacterial community (Barnes et al. 2010). Similarly, Kirschling et al. (2010) also reported that nano-Fe^0 particles had no deleterious effect on total bacterial abundance in the aquifer microcosms; moreover, this study further suggested that biodegradable polymer (polyaspartate) coating on nanoparticles, used for successful injection, can stimulate microbial growth (Kirschling et al. 2010). In another study, Qiu et al. (2012) indicated that both nano-Fe^0 and its reaction products that remained in the water body are nontoxic to environmental medium. On the contrary, other researchers reported several toxic effects of iron nanoparticles. Lee et al. (2008) found a strong bactericidal effect of nano-Fe^0 particles in aquatic systems, which conducted to a rapid deactivation of *Escherichia coli*. Diao and Yao (2009) also observed a very fast and complete inactivation of *Bacillus subtilis* and *Pseudomonas fluorescens*. El-Temsah and Joner (2012) concluded that nano-Fe^0 particles are likely to give adverse toxicological effects not only on microorganism but also on invertebrate organisms, such as earthworm species like *Eisenia fetida* and *Lumbricus rubellus*. These authors noticed that earthworms exposed to nano-Fe^0 concentrations greater than 500 mg/kg soil were significantly affected in terms of weight changes and mortality, while reproduction was affected also at 100 mg nano-Fe^0/kg (El Temsah and Joner 2012). Not only microorganisms but also plants may be affected by the presence of nano-Fe^0 particles. Even though nano-Fe^0 particles had no obvious inhibitory effects on the germination of rice seeds, however, at higher concentrations (>500 mg/kg), they induced visible iron deficiency chlorosis and significant concentration-dependent inhibition of seedling growth (Wang et al. 2016b). However, it seems that adverse effects of nano-Fe^0 could be reduced after aging that can be involved in the formation of iron oxide layers (Li et al. 2010; El-Temsah and Joner 2012). In addition, very recent studies showed that surface coating (e.g., with CMC) may not only influence the particle stabilization, but also the nano-Fe^0 particle cytotoxicity; for instance, while the inactivation of *E. coli* by bare nano-Fe^0 was significant and concentration dependent, an increasing reduction in cytotoxicity of nano-Fe^0 with increasing CMC ratio was observed, even though the particles became more dispersed (Dong et al. 2016c). In addition to all these results, it is important to point out that the environmental conditions encountered in situ have a very important role in how nano-Fe^0 can affect natural ecosystem functions (Lefevre et al. 2016).

Bimetallic Iron-Based Materials

Another possibility to achieve higher reactivity of metallic iron toward hexavalent chromium is by coating another metal onto the surface of metallic iron particle. For example, bimetallic particles can be prepared by cementation, a process which involves the electrochemical precipitation of a more noble (more electropositive) metal ion from solution (e.g., Cu^{2+}) by a less noble metal (e.g., Fe^0), while the less noble metal is dissolved (Noubactep 2009b, 2010a; Hu et al. 2010):

$$Cu^{2+}{}_{(aq)} + Fe^{0}{}_{(s)} \rightarrow Cu^{0}{}_{(s)} + Fe^{2+}{}_{(aq)} \quad (43)$$

Bimetallic particles will act as galvanic couples during reaction, being electrically connected in the water, while the potential difference between the two metals has a catalytic effect on the reduction of the less noble metal (Bigg and Judd 2000). However, according to Noubactep (2009b), the assumption that bimetallic systems enhance reductive transformation of contaminants by Fe^0 is incompatible with the premise that Fe^0 is the reductant in Fe^0-H_2O system; based on thermodynamic considerations, this author further suggests that increased contaminant removal by bimetallic systems is rather an argument for indirect reduction by Fe(II) or H/H_2 within the oxide film on Fe^0 and a negation of the well-established concept of direct reductive transformations as major decontamination process in Fe^0/H_2O systems (Noubactep 2009b).

There are numerous studies reporting the removal of Cr(VI) with various types of bimetallic particles. Hu et al. (2010) observed higher Cr(VI) removal capacity per unit weight of metallic iron for Fe/Cu bimetallic particles prepared by cementation; however, it was also suggested that due to the greater oxidation potential of Cr(VI), the metallic copper could also be oxidized to Cu^{2+}:

$$3Cu + 2CrO_4{}^{2-} + 10H^+ \rightarrow 2Cr(OH)_3 + 3Cu^{2+} + 2H_2O \quad (44)$$

Therefore, in order to avoid rapid loss of bimetallic catalytic ability, the copper layer must be thick enough (Hu et al. 2010). Reduction of Cr(VI) by bimetallic Fe/Ag nanoparticles (synthesized by reductive deposition of Ag^+ on freshly prepared Fe^0 nanoparticles) was studied as a function of temperature, solution pH, initial concentration of Cr(VI), and dose of bimetallic reductant (Singh et al. 2011); the maximum Cr(VI) reduction capacity, predicted by a quadratic mathematical model under the optimum conditions of temperature (43 °C), Cr(VI) concentration (65.7 mg/L), initial pH (2), and Fe/Ag particles dose (0.4 g/L), was 55.96 mg/g, very close to the experimental value of 55.18 mg/g and higher than the experimentally determined un-optimized reduction capacity of 42.39 mg/g (Singh et al. 2011). Rivero-Huguet and Marshall (2009) prepared bimetallic (Fe/Ag, Fe/Al, Fe/Cu, Fe/Co, Fe/Mg, Fe/Ni, Fe/Pd, Fe/Zn) and trimetallic particles (Fe/Cu/Zn, Fe/Pd/Cu, Fe/Pd/Zn) by cementation of one or two noble metals on the surface of metallic iron; the as-obtained particles were up to 100 times more effective in what concerns the removal of Cr(VI) (Rivero-Huguet and Marshall 2009). In a recent study, Fe/Al bimetallic particles were synthesized by depositing the Fe^0 on the Al^0 surface through the reaction of Al^0 with Fe^{2+} and employed to treat Cr(VI)-polluted wastewater (Fu et al. 2015b); it was shown that Fe/Al bimetallic particles with 0.75 g Fe/g Al possess more advantages, including (1) high removal efficiency for Cr(VI) not only in acidic but also in neutral and alkaline conditions (pH 11), (2) no Fe^{2+}/Fe^{3+} release at pH 3–11 and low (< 0.2 mg/L) Al^{3+} release in acidic and neutral conditions, and (3) at pH 3 Fe/Al bimetallic particles can be used four times without losing activity (Fu et al. 2015b). Fe-Ni-montmorillonite nanocomposites

were prepared via two methods: (1) incorporation of preformed Fe-Ni nanoparticles in the clay matrix, and (2) in situ generation of Fe-Ni nanoparticles in the clay matrix (Kadu et al. 2011; Kadu and Chikate 2013); it was reported that the in situ-formed nanocomposites possess superior reduction capacity as compared to both loaded nanocomposites and Fe-Ni nanoparticles, due to increased number of available surface Fe^0 atoms that significantly contributes toward reduction of adsorbed Cr(VI) on the surface (Kadu et al. 2011; Kadu and Chikate 2013).

The galvanic noble metal-Fe system can be generated not only by plating the noble metal on the surface of metallic iron, but also by using mixtures of Fe^0 and noble metal particles. This technique was applied by Lugo-Lugo et al. (2010, 2014), who investigated the removal of Cr(VI) using a bimetallic mixture comprised of metallic copper and iron plates; batch experiments carried out at pH 2 revealed that single Fe and Cu systems showed lower efficiency compared with the Fe/Cu galvanic system (Lugo-Lugo et al. 2010, 2014). The use of a bimetallic system comprised of Fe^0 and a less noble metal, Al^0 (more electronegative), was also reported (Han et al. 2016). It was shown that a 80 g/40 g mixture of acid-washed Fe^0/Al^0 had a much better Cr(VI) removal efficiency than 120 g Fe^0 or Al^0 alone. Several explanations were given for the observed results, including (1) because the standard reduction potential of Al^{3+}/Al^0 (−1.67 V) is much lower than of Fe^{2+}/Fe^0 (−0.44 V), acid-washed Al^0 can be regarded as a stronger reductant for Cr(VI) than acid-washed Fe^0, (2) due to the same difference in standard reduction potentials, the generated Fe^{2+} ions can be reduced by Al^0, leading to formation of Fe^0 particles on the surface of Al^0, and (3) Al^0 acted as an electron source which prevented the formation of iron corrosion products on the Fe^0 surface, maintaining thus the surface activity of Fe^0 (Han et al. 2016).

Metallic Iron-Porous Support Composites

Another strategy that has been recently developed to enhance the Fe^0 capacity to remove Cr(VI) consist in supporting nano-Fe^0 particles on various adsorbent materials. Having a rich surface area and a porous structure, adsorbents can provide stable sites for nanoparticles and prevent their oxidation and agglomeration; in addition, since nanoparticles are well dispersed and more stable in the interlayer of porous matrix, they will exhibit an improved reactivity toward Cr(VI) (Lv et al. 2011; Wu et al. 2015). Because they are chemically stable and relatively inexpensive, various minerals were investigated as porous support for nano-Fe^0. Shi et al. (2011) used bentonite-supported nanoscale Fe^0 for the removal of Cr(VI) from aqueous solutions; the results indicated that Fe^0 acted as a reductant, while bentonite only played a role as a dispersant and stabilizer (Shi et al. 2011). Silica-based molecular sieves with uniform pore sizes used for supporting nano-Fe^0 demonstrated a rapid removal of Cr(VI), in comparison to that of unsupported nano-Fe^0 (Petala et al. 2013); furthermore, it was shown that impregnation of metallic iron within the mesoporous silica matrix also prevented agglomeration of the resulted

composites, increasing thus accessibility of Cr(VI) to the surface of Fe^0 (Petala et al. 2013). The enhancement of Fe^0 nanoparticles efficiency was investigated also via their intercalation within the structure of zeolites. Experiments carried out using montmorillonite and HDTMA-modified montmorillonite (Wu et al. 2012, 2015) showed that montmorillonite-Fe^0 composites are more stable, more reactive, and less pH dependent than bare nano-Fe^0. In addition, it was also observed that HDTMA-montmorillonite-Fe^0 composites reduced the greatest amount of Cr(VI), whereas the unsupported Fe^0 nanoparticles removed the least amount (Wu et al. 2012). Similar results were observed with clinoptilolite-supported nano-Fe^0 composites, which had better removal ability for Cr(VI) than the sum of pure zeolite and nano-Fe^0 (Kong et al. 2016). Enhanced removal of Cr(VI) from contaminated water was reported by Li et al. (2007) who used zeolite/Fe^0 pellets prepared by mixing Fe^0 and clinoptilolite-zeolite, untreated or treated with the cationic surfactant HDTMA; the improved removal efficiency was ascribed to both sorption and reduction of chromate during the remediation process (Li et al. 1999, 2007). Pumice, another commonly available rock with a stable structure and low cost, can also be used as a porous material to support nano-Fe^0. Experiments carried out by Liu et al. (2015) showed that pumice was effective in enhancing the dispersibility of nano-Fe^0 particles, while the resulted composite exerts a good capacity to remediate wastewater containing heavy metals, including Cr(VI) and Hg(II) (Liu et al. 2015). Layered double hydroxides (LDH) were also tested as a support of nano-Fe^0, to synthesize multifunctional composites for the removal of Cr(VI) (Sheng et al. 2016); treatability experiments revealed an improved efficiency of the LDH/nano-Fe^0 composites for Cr(VI) removal in comparison with bare nano-Fe^0, due to a decreased agglomeration of nano-Fe^0, good accessibility of Cr(VI) to iron particles, and a synergistic effect between reduction by nano-Fe^0 and adsorption by LDH (Sheng et al. 2016). Finally, porous Fe^0-supported composite obtained by immobilization of the nano-Fe^0 particles on the surface of sepiolite was also suggested as potential advantageous candidate material for the removal of Cr(VI), in terms of high efficiency, stability, and reactivity (Esfahani et al. 2015; Fu et al. 2015a).

Another way to prepare porous Fe^0 composites could be the supporting of the nano-Fe^0 particles on porous carbon-based materials, such as activated carbon, nanotubes, or graphene. For instance, nanoscale Fe^0-loaded activated carbons were proved to be highly reactive toward Cr(VI), which resulted in a more rapid and stable reaction with Cr(VI) compared to pure nanoscale Fe^0 (Wu et al. 2013). Nanoscale Fe^0 iron multiwalled carbon nanotube composites were used by Lv et al. (2011) to remove Cr(VI) from wastewater; the Fe^0-nanotube composites exhibited 36% higher efficiency on Cr(VI) removal, compared to bare Fe^0 or Fe^0-activated carbon composites (Lv et al. 2011). Magnetic Fe^0-graphene nanocomposites synthesized by a facile thermodecomposition demonstrate an extremely rapid and efficient Cr (VI) removal from the polluted water, especially in solutions with low pH (Zhu et al. 2012). Fe^0 nanoparticles decorated on graphene were synthesized via chemical route by Jabeen et al. (2011) and investigated for Cr(VI) removal; it was shown that Fe^0-decorated graphene sheets have enhanced magnetic property, surface area

and Cr(VI) adsorption capacity compared to bare nano-Fe particles (Jabeen et al. 2011). Porous carbon-encapsulated nano-Fe^0 composites prepared through carbothermal reduction of Fe(III) impregnated on a porous carbon carrier were also tested for their capacity to remove Cr(VI) (Hoch et al. 2008; Zhuang et al. 2014; Dai et al. 2016). The as-prepared C-Fe^0 composites are in a size range that can provide both rapid remediation of Cr(VI) and good transport through water-saturated porous media (Hoch et al. 2008). The high ability of the composites to completely remove Cr(VI) was ascribed to a synergistic effect of the high reactivity of nano-Fe^0 and high efficiency of the mass transfer of pollutant through the porous structure of the carbon carrier; in addition these composites also exhibited other advantages including (1) enhanced stability of the nano-Fe^0, (2) strong magnetic property, and (3) regeneration ability (Dai et al. 2016; Zhuang et al. 2014).

Supporting nano-Fe^0 particles on natural or synthetic polymers was also tested in several studies. Lopez-Tellez et al. (2011) used a cheap, biodegradable and readily available biosorbent, orange peel pith, as support for iron and iron oxide nanoparticles; the Cr(VI) removal capacity of the biocomposite was significantly higher than that of the untreated biomass, which was attributed to the coupled reducing capability of iron nanoparticles with the adsorption capacity of cellulose (Lopez-Tellez et al. 2011). Composites comprised of Fe^0 nanoparticles supported on polyaniline nanofibers were synthesized using a facile polymerization method and successfully applied for the removal of Cr(VI) from polluted solutions with a wide pH range (Gu et al. 2012; Bhaumik et al. 2014). The composites demonstrated a significantly higher performance for the removal of Cr(VI) than polyaniline nanofibers, due to an adsorption-coupled reduction mechanism (Bhaumik et al. 2014). Fe^0 nanoparticles immobilized on epichlorohydrin/chitosan beads with high mechanical and thermal stability were successfully used for reduction of Cr(VI) from wastewater (Liu et al. 2012b); since high removal efficiency (76.6%) was obtained also for the first cycle after regeneration, it was concluded that such composites are regenerable (Liu et al. 2012b). Chitosan-stabilized Fe^0 particles attached onto bamboo biochar exhibited enhanced removal of Cr(VI) (Zhou et al. 2014). Agarose-Fe^0 spherical hydrogels with an average diameter of 5 mm, synthesized via green immobilization of nano-Fe^0 particles inside hollow agarose capsules, successfully removed a mixture of contaminants comprised of Cr(VI) and trichloroethylene (Luo et al. 2016); since only a small amount of Fe (0.22%) was detected on the surface, while the major part was immobilized inside the hollow agarose capsules, oxidation of nano-Fe^0 particles due to exposure to air can be avoided. Furthermore, it was suggested that macroporosity of agarose capsules ensures better contact between encapsulated nano-Fe^0 particles and contaminants, due to superior diffusion (Luo et al. 2016). In another very recent study, a synthetic cationic resin, Dowex 50WX2, was used as porous support of the nano-Fe^0 particles (Toli et al. 2016); the polymeric composite was then applied for the treatment of Cr(VI) contaminated waters, with satisfactory reaction rate and high degree of iron utilization (0.8 mol Cr(VI)/mol Fe^0); additionally, it was estimated that the composite resin can be reused many times, since it maintained a good efficiency (87.3%) for Cr(VI) reduction even after three cycles of regeneration (Toli et al. 2016).

Heterogeneous Fenton-Like Systems

The Fenton reaction is an advanced oxidation processes with great potential for the treatment of organic pollutants, which requires H_2O_2 and Fe^{2+} as starting reactants for generation of the highly reactive hydroxyl radicals. However, there are several shortcomings (e.g., low working pH, formation of large amounts of iron sludge) which limit the practical applicability of the homogeneous Fenton process (Wang et al. 2016a). Since Fe^0 is a well-known precursor of Fe(II) in Fe^0-H_2O systems, replacing dissolved Fe(II) with solid Fe^0 was suggested in order to overcome some of these drawbacks (Rusevova et al. 2012). Another important advantage of such heterogeneous Fenton-like processes is the treatment of wastewaters containing both heavy metals and bio-refractory organic pollutants (Yin et al. 2014). For instance, the removal of coexisting Cr(VI) and 4-chlorophenol (4-CP) from aqueous solutions was recently studied in a system comprising two stages (Yin et al. 2014). The first stage was initiated by addition of Fe^0, resulting in complete removal of Cr(VI) and partial removal of 4-CP; this step occurred in the first 10 min of the process. The second stage was started by addition of H_2O_2 and occurred 20 min after Fe^0 addition; this step was primarily a Fenton degradation of 4-CP. The sequential addition of reagents was found to be preferable to the simultaneous addition system, which apparently had a slower reaction rate (Yin et al. 2014).

Increasing Metallic Iron Reactivity Prior to/During Its Use

During the manufacturing of the commercially metallic iron particles, they are usually covered with different kinds of passive oxide layers, due to the high temperatures involved in the manufacturing processes (Ritter et al. 2002). Since most studies considered the oxide layers as impeding the Cr(VI) reduction, removing the oxide layers, prior of the metallic particle use, was considered as a possible solution for the enhancement of metallic iron reactivity. Mechanical polishing, electropolishing, chemical polishing (acid, alkaline, organic), and sonication were among the most used treatment methods proposed to remove the passive layers; all these methods usually gave a more or less important increase of Fe^0 particles' reactivity (McCafferty et al. 1988; Fernandez-Sanchez et al. 2004; Junyapoon and Weerapong 2006; Qian et al. 2008; Zhang et al. 2008; Rivero-Huguet and Marshall 2009; Fiuza et al. 2010; Lugo-Lugo et al. 2010; Mitra et al. 2011; Lu et al. 2012; Fu et al. 2015c; Han et al. 2016). However, an opposite effect was also reported after acid washing and sonication of metallic iron, ascribed to a more severe mineral precipitation on the treated Fe^0 surface (Lai and Lo 2008). Unfortunately, all these treatment methods have important drawbacks, including technical inconveniences, cost increases, and, most importantly, the rapid regeneration of a new oxide layer on the surface of Fe^0 particles (Noubactep 2015); hence, application of such methods at large scale is questionable. According to Liu et al. (2008a),

precluding the formation of surface oxides during synthesis and storage of metallic iron particles could be a more advantageous option. This goal was achieved by electrodepositing a Fe^0 film on titanium substrate, followed by a rapid posttreatment of the as-synthesized particles to prevent the occurrence of surface oxides during storage or utilization (Liu et al. 2008a). In a subsequent study, the morphology of the electrodeposited film was adjusted by adding organic compounds into the electrolyte; this allowed the electrodeposited iron film to receive a nano-sized structure, which resulted in significantly higher efficiency of Cr (VI) reduction at neutral pH (Liu et al. 2009). Fe^0-magnetite mixtures prepared by light mechanochemical mixing of fine magnetites with 5% micro-sized Fe (0) exerted a considerably enhanced reductive reactivity toward Cr(VI) over the pH range of 4–8, as compared to either one of the two solids alone; the explanation seems to be a mechanism of Fe(II) replenishment, by which Fe^0 replenishes the Fe (II) on the magnetite surface that has been oxidized to Fe(III) as a result of Cr (VI) reduction to Cr(III) (Villacis-Garcia et al. 2015). Recent reports have indicated that efficiency of Cr(VI) removal with nanoscale Fe^0 was significantly enhanced as a result of applying high energy electron beam irradiation (HEEBI) to improve the dispersion of nanoscale particles (Zhang et al. 2013); in addition, the increased efficiency of HEEBI was found to be stable for at least 2 months and to increase with temperature while decreasing with pH. This phenomenon was attributed to an increase in number of active sites on Fe^0 with increasing the dispersion of nanoscale particles, induced by charge and thermal effects (Zhang et al. 2013). Similarly, weak magnetic field (WMF) applied during Cr(VI) removal with Fe^0 leads to an increase in removal rates by a factor of 1.12–5.89, due to acceleration of iron corrosion process (hence, more Fe(II)) and alleviation of the detrimental effect of the passive layer (Feng et al. 2015). Remarkably, this effect was significant also at higher pH and higher initial Cr(VI) concentration, when reduction of Cr(VI) by Fe^0 is normally hindered. In spite of its favorable effect, application of WMF had no influence on the mechanism of Cr(VI) removal by Fe^0, which consisted mainly in the indirect reduction of Cr(VI) to Cr(III) by Fe(II) (Feng et al. 2015). It is apparent that also visible light has the capability to significantly enhance Cr(VI) removal with Fe^0, in comparison with the dark process; this phenomenon is attributable to a heterogeneous photocatalytic mechanism that takes place in the visible range, promoted by the layer of iron oxides acting as semiconductors after excitation with light, overcoming thus the passivation process (Montesinos et al. 2014). Coupling of the nano-Fe^0 technology with ultrasound was recently reported to greatly enhance the rate and efficiency of Cr(VI) removal (Zhou et al. 2015); the positive effect was attributed to several causes including (1) enhancement of the dispersion of Fe^0, (2) increase of the Fe^0 available surface area, (3) activation of Fe^0 surface, resulting in new reactive sites, and (4) removal of the corrosion products from the surface of Fe^0, which created adequate reactive sites for Cr(VI) removal (Zhou et al. 2015). Granulation of the nano-Fe^0 particles was proposed as a solution to avoid iron passivation and rapid aggregation of the nano-sized particles, in an attempt to enhance the efficacy of Fe^0 on remediation of Cr(VI)-containing wastewater (Shih et al. 2015). While the primary grain size of Fe^0 particles was around

10 nm, they grow up after granulation with polymeric additive (polyvinyl alcohol-co-vinyl acetate-co-itaconic acid) to a spherical pellet of around 5 micrometers. The results of this study show that while the original nano-Fe^0 lost its ability to remove Cr(VI) at pH above 2, granulated-Fe^0 moderately reduced Cr(VI) over the pH range of 2–6; nevertheless, by evaluating the kinetics Cr(VI) reduction, it was noticed that reactivity of original nano-Fe^0 was much higher than of granulated-Fe^0, attributable to a greater number of active sites on the raw nano-Fe^0 particles, which could be corroded by the medium rapidly (Shih et al. 2015). Polyoxometalates (POM) are a large class of metal oxygen clusters, with high stability of their oxidation and reduction states, well known for their ability to catalyze redox reactions by serving as electron shuttle (Genovese and Lian 2015). Therefore, using POM can be another way to enhance the removal of Cr(VI) with Fe^0. It has been reported that POM does not catalyze the direct reduction of Cr(VI) with Fe^0; instead, the presence of POM will catalyze the oxidation of Fe^0 with O_2 and the generation of H_2O_2 (Eq. 45), by shuttling electrons between Fe^0 and O_2 (Eqs. 46 and 47) (Fu et al. 2015c):

$$Fe^0 + O_2 + 2H^+ \rightarrow Fe^{2+} + H_2O_2 \tag{45}$$

$$2POM + Fe^0 \rightarrow 2POM^- + Fe^{2+} \tag{46}$$

$$2POM^- + O_2 + 2H^+ \rightarrow 2POM + H_2O_2 \tag{47}$$

Because H_2O_2 can reduce Cr(VI) to Cr(III) under acidic conditions (pH 3), it has been concluded that the enhancement of Cr(VI) removal with Fe^0 in the copresence of POM is attributable to generation of increased amounts of H_2O_2, hence, to indirect reduction of Cr(VI) with H_2O_2 (Fu et al. 2015c).

Finally, another approach used to increase the reactivity of Fe^0 is the addition of chelating agents during the process of Cr(VI) removal, with the aim to avoid the formation of passivation layer on the surface of Fe^0 or to increase the rate of direct or indirect Cr(VI) reduction (Fu et al. 2013; Dong et al. 2016e). By studying the removal of Cr(VI) with nano-Fe^0 over the pH range of 5.6–7 and aerobic conditions, it was shown that removal efficiency increased with increasing concentration of copresent ethylenediamine disuccinic acid (EDDS), due to chelation of the generated Cr(III) and Fe(III) and inhibition of their precipitation (Dong et al. 2016e). This phenomenon was not observed anymore under alkaline conditions (pH 9), when Cr(VI) removal was slightly decreased in the copresence of EDDS; in this case, the chelating agent facilitates the oxidation of nano-Fe^0/Fe(II) by dissolved oxygen and thus the formation of passivation layer. Instead, in the absence of dissolved oxygen, EDDS had a similar positive effect on the removal of Cr(VI) with nano-Fe^0 also at pH 9, just like at pH 5.6–7 (Dong et al. 2016e). Similarly, Fu et al. (2013) noticed an important enhancement of simultaneous removal of Cr(VI) and Acid Red 73 azo-dye with Fe^0, at pH 3, in the copresence of 3 mM oxalate or EDTA, with better results for oxalate. In respect to the removal of Cr(VI), the higher removal efficiency noticed in the copresence of the organic chelating agents was ascribed to their ability to form $Fe(C_2O_4)$ or FeEDTA complexes with ferrous iron, which favors the generation of H_2O_2 and thus the

subsequent reduction of Cr(VI) by H_2O_2 (which is 3 orders of magnitude faster than the reaction of H_2O_2 and Fe^{2+}); in the same time the direct reduction of Cr(VI) with Fe^0 is also faster when the above complexes are involved (Fu et al. 2013).

Recovery of Exhausted Metallic Iron

In order to achieve an efficient removal of Cr(VI) for a longer period of time, the metallic iron particles should be reactivated for further reuse, when the removal efficiency falls below a certain threshold. Liu et al. (2008a) investigated the recovery of Fe^0 reactivity by cathodic reduction of passive films; the results indicated that galvanostatic reduction at pH 4.0 was more effective to remove the oxide layers than both acid immersion at pH 2.5 and cathodic reduction at pH 2.5 (Liu et al. 2008a). An innovative electrochemical depassivation system was proposed by Lu et al. (2012) to recover Fe^0 reactivity and promote the longevity of PRB. The results of this study have shown that the longer the electrolysis took, the higher the initial removal rate; however, the longevity of the reactivated Fe^0 was influenced not only by the length of electrochemical depassivation process, but also by the number of recovery cycles, which also affects Fe^0 characteristics and leads to a more rapid loss of reactivity (Lu et al. 2012). The recycling capability of nano-Fe^0, nano-Fe-Ni, and Fe-Ni-montmorillonite nanocomposites was assessed by treating the spent materials with 0.01 M NaOH and 5% H_2O_2, followed by washing with acetone; it was reported that, after this treatment, the reactivated materials have been successfully used for another 2–5 subsequent cycles before being deactivated (Kadu and Chikate 2013). The partially oxidized Fe^0-polyaniline composites resulted after removal of Cr(VI) were easily regenerated by washing with 1 M p-toluene sulfonic acid or 1 M hydrochloric acid, and efficiently reused for further Cr(VI) removal (Gu et al. 2012). Acid washing treatment with a 1 M H_2SO_4 solution restored almost entirely the reactivity of sponge iron pellets toward Cr(VI) (Zafarani et al. 2014); the slightly decrease of Cr (VI) removal efficiency after the acidic reactivation was attributed to Fe^0 surface decrease and/or to ineffectiveness of the acidic cleaning on removing the whole produced oxide layers (Zafarani et al. 2014). Exhausted carbon-encapsulated iron composites were regenerated by washing with a mixture of 0.5 M HCl and citric acid solution for 1 h (Zhuang et al. 2014); while HCl eluted the adsorbed Cr(III), citric acid had the role to remove the trace amounts of unreduced Cr(VI), via reduction to Cr(III). The regeneration was very effective, as resulted from three successive removal cycles which presented only a slightly decline of Cr(VI) removal efficiency (Zhuang et al. 2014). The successive combination of two geofixation methods, chemical reduction of Cr(VI) by nano-Fe^0 and application of whey as an organic substrate to promote biotic reduction of Cr(VI), was recently reported to be not only an efficient remediation approach, but also a method for partially recycling the spent nano-Fe^0 (Němeček et al. 2015a). Application of whey facilitated the development of anaerobic bacterial microflora, which directly contributed to reduction of Cr(VI); in the same time, the bacterial microflora contributed also indirectly to the reduction of

Cr(VI) by partially recycling the oxidized nano-Fe^0 from Fe(III) to the soluble Fe(II), which subsequently reduced the Cr(VI) (Němeček et al. 2015a, b). Sharma et al. (2015) suggested that the exhausted nano-Fe^0 immobilized on microcrystalline cellulose could be in situ regenerated as a result of the redox process which involves the simultaneous reduction of Fe(III) to Fe^0 and oxidation of cellulose to cellulose dialdehyde.

Conclusions

Chromium can exist in the environment in two main oxidation states, Cr(III) and Cr(VI), which are characterized by different chemical behaviors and toxicities. While Cr(III) is considered an essential nutrient for the human body, Cr(VI) is toxic to most living organisms, a known human carcinogen by the inhalation route of exposure, and a possible human carcinogen by the oral route of exposure. Because of Cr(VI) significant mobility in the subsurface environment, the potential risk of groundwater contamination is high. Starting with the early 1990s, metallic iron was successfully used as a reactive material in numerous laboratory and field tests, to minimize the subsurface migration of chlorinated-hydrocarbon compounds. This success has stimulated significant interest in the application of metallic iron technology to other pollutants that may be present in groundwater, such as hexavalent chromium. Reducing Cr(VI) to Cr(III) with metallic iron was considered a satisfactory solution in eliminating toxicity of Cr(VI), because a more mobile and more toxic chromium species is converted to a less mobile and less toxic form. Substantial research work has been reported in the last two decades regarding the mechanism, kinetics, and influence of major process variables on the efficiency of Cr(VI) removal with metallic iron. In addition, there has been great interest in searching new methods of enhancing the reactivity of metallic iron toward Cr(VI), such as using of nano-sized Fe^0 particles, using of bimetallic particles, using of porous composite particles, removing the oxide layers existent at Fe^0 surface, or precluding the formation of such layers during synthesis or storage of metallic iron particles. But, by far, the most promising method for achieving high Cr(VI) removal efficiencies seems to be the use of nano-sized Fe^0 particles. However, more research over the toxicity, persistence, and environmental fate of these particles is needed before their widespread application. There is no consensus at this time in what regards the mechanism of Cr(VI) removal with Fe^0. The first mechanism proposed at the beginning of the nineties attributed the efficiency of metallic iron technology mainly to the direct electron transfer from the Fe^0 surface to Cr(VI) (direct reduction), followed by precipitation as simple or/and mixed Fe(III)-Cr(III) (oxi)hydroxides. However, recent studies suggested that, in Fe^0/H_2O systems, contaminants are mainly removed via adsorption, coprecipitation/entrapment, and size-exclusion processes. According to this new concept, direct reduction, when possible, is less important than indirect reduction by Fe^0 corrosion products (Fe(II),

H/H_2). The present work undoubtedly showed that mechanism of Cr(VI) removal with Fe^0 generally involves multiple pathways including adsorption, reduction, and coprecipitation/entrapment.

Acknowledgments This work was supported by a grant of the Romanian National Authority for Scientific Research and Innovation, CNCS-UEFISCDI, project number PN-II-RU-TE-2014-4-0508.

References

Abdo MSE, Sedahmed GH (1998) A new technique for removing hexavalent chromium from waste water and energy generation via galvanic reduction with scrap iron. Energy Convers Manag 39:943–951

Ahmad WA, Zakaria ZA, Khasim AR, Alias MA, Ismail SMHS (2010) Pilot-scale removal of chromium from industrial wastewater using the ChromeBac™ system. Bioresour Technol 101:4371–4378

Ai Z, Cheng Y, Zhang L, Qiu J (2008) Efficient removal of Cr(VI) from aqueous solution with Fe and Fe_2O_3 core-shell nanowires. Environ Sci Technol 42:6955–6960

Alidokht L, Khataee AR, Reyhanitabar A, Oustan S (2011) Reductive removal of Cr(VI) by starch-stabilized Fe0 nanoparticles in aqueous solution. Desalination 270:105–110

Anderson RA (1997) Chromium as an essential nutrient for humans. Regul Toxicol Pharmacol 26: S35–S41

Anderson RA (1998) Chromium, glucose intolerance and diabetes. J Am Coll Nutr 17:548–555

Aroua MK, Zuki FM, Sulaiman NM (2007) Removal of chromium ions from aqueous solutions by polymer-enhanced ultrafiltration. J Hazard Mater 147:752–758

Astrup T, Stipp SLS, Christensen TH (2000) Immobilization of chromate from coal fly ash leachate using an attenuating barrier containing zerovalent iron. Environ Sci Technol 34:163–168

Bagchi D, Stohs SJ, Downs BW, Bagchi M, Preuss HG (2002) Cytotoxicity and oxidative mechanisms of different forms of chromium. Toxicology 180:5–22

Baldea I, Nioc G (1970) Reaction between chromate and thiosulfate. II. Kinetics of tetrathionate formation. Inorg Chem 9:110–114

Barnes RJ, Van der Gast CJ, Riba O, Lehtovirta LE, Prosser JI, Dobson PJ, Thompson IP (2010) The impact of zero-valent iron nanoparticles on a river water bacterial community. J Hazard Mater 184:73–80

Barnhart J (1997) Chromium chemistry and implications for environmental fate and transport. J Soil Contam 6:561–568

Barrera-Diaz CE, Lugo-Lugo V, Bilyeu B (2012) A review of chemical, electrochemical and biological methods for aqueous Cr(VI) reduction. J Hazard Mater 223–224:1–12

Beaver LM, Stemmy EJ, Constant SL, Schwartz A, Little LG, Gigley JP, Chun G, Sugden KD, Ceryak SM, Patierno SR (2009) Lung injury, inflammation and Akt signaling following inhalation of particulate hexavalent chromium. Toxicol Appl Pharmacol 235:47–56

Bennett TA, Blowes DW, Puls RW, Gillham RW, Hanton-Fong CJ, Ptacek CJ (1997) A porous reactive wall for treatment of Cr(VI) and trichloroethylene in groundwater. In: Proceedings of the 213th ACS national meeting, April, San Francisco, pp 243–245

Beukes JP, Pienaar JJ, Lachmann G (2000) The reduction of hexavalent chromium by sulphite in wastewater – an explanation of the observed reactivity pattern. Water SA 26:393–395

Bhaumik M, Choi HJ, McCrindle RI, Maity A (2014) Composite nanofibers prepared from metallic iron nanoparticles and polyaniline: high performance for water treatment applications. J Colloid Interface Sci 425:75–82

Bigg T, Judd SJ (2000) Zero-valent iron for water treatment. Environ Technol 21:661–670
Bilardi S, Calabro PS, Care S, Moraci N, Noubactep C (2013) Improving the sustainability of granular iron/pumice systems for water treatment. J Environ Manag 121:133–141
Blowes DW, Ptacek CJ (1992) Geochemical remediation of groundwater by permeable reactive walls: removal of chromate by reaction with iron-bearing solids. In: Proceeding of the subsurface restoration conference, third international conference on groundwater quality research, June 21–24, Dallas, pp 214–216
Blowes DW, Ptacek CJ, Jambor JL (1997) In-situ remediation of chromate contaminated groundwater using permeable reactive walls: laboratory studies. Environ Sci Technol 31:3348–3357
Blowes DW, Ptacek CJ, Bener SG, McRae CWT Puls RW (1998) Treatment of dissolved metals using permeable reactive barriers. In: Proceedings of the groundwater quality: remediation and protection conference, September, Tubingen, Germany, IAHS Publication 250, pp 483–490
Blowes DW, Gillham RW, Ptacek CJ, Puls RW, Bennett TA, O'Hannesin SF, Hanton-Fong CJ, Bain JG (1999) An in situ permeable reactive barrier for the treatment of hexavalent chromium and trichloroethylene in ground water, vol 1 Design and installation, EPA/600/R-99/095a. U.S. Environmental Protection Agency, Washington, DC
Blowes DW, Ptacek CJ, Benner SG, McRae CWT, Bennett TA, Puls RW (2000) Treatment of inorganic contaminants using permeable reactive barriers. J Contam Hydrol 45:123–137
Borthiry GR, Antholine WE, Kalyanaraman B, Myers JM, Myers CR (2007) Reduction of hexavalent chromium by human cytochrome b5: generation of hydroxyl radical and superoxide. Free Radic Biol Med 42:738–755
Boruah PK, Borthakur P, Darabdhara G, Kamaja CK, Karbhal I, Shelke MV, Phukan P, Saikiad D, Da MR (2016) Sunlight assisted degradation of dye molecules and reduction of toxic Cr(VI) in aqueous medium using magnetically recoverable Fe3O4/reduced graphene oxide nanocomposite. RSC Adv 6:11049–11063
Bowers AR, Ortiz CA, Cardozo RJ (1986) Iron process for treatment of Cr(VI) wastewaters. In: Proceedings of the 41st industrial waste conference, May 13–15, Purdue University, West Lafayette, pp 465–473
Calderon B, Fullana A (2015) Heavy metal release due to aging effect during zero valent iron nanoparticles remediation. Water Res 83:1–9
Cantrell KJ, Kaplan DI, Wietsma TW (1995) Zero-valent iron for the in situ remediation of selected metals in groundwater. J Hazard Mater 42:201–212
Case OP (1974) Metallic recovery from waste waters utilizing cementation. Edison Water Quality Research Laboratory, National Environmental Research Center, Edison, New Jersey, EPA-670/2-74-008
Case OP, Jones RBL (1969) Treatment of brass mill effluents. Connecticut Research Commission RSA-68-34
Chakrabarti S, Mitra P, Banerjee P, Sarkar D (2014) Reduction of hexavalent chromium present in wastewater by steel wool in a continuous flow system. APCBEE Procedia 10:59–63
Chang LY (2003) Alternative chromium reduction and heavy metal precipitation methods for industrial wastewater. Environ Prog 22:174–182
Cheballah K, Sahmoune A, Messaoudi K, Drouiche N, Lounici H (2015) Simultaneous removal of hexavalent chromium and COD from industrial wastewater by bipolar electrocoagulation. Chem Eng Process 96:94–99
Chekli L, Bayatsarmadi B, Sekine R, Sarkar B, Maoz Shen A, Scheckel KG, Skinner W, Naidu R, Shon HK, Lombi E, Donner E (2016) Analytical characterisation of nanoscale zero-valent iron: a methodological review. Anal Chim Acta 903:13–35
Chen SS, Cheng CY, Li CW, Chai PH, Chang YM (2007) Reduction of chromate from electroplating wastewater from pH 1 to 2 using fluidized zero valent iron process. J Hazard Mater 142:362–367
Chen SS, Hsu BC, Hung LW (2008) Chromate reduction by waste iron from electroplating wastewater using plug flow reactor. J Hazard Mater 152:1092–1097

Cheung KH, Gua JD (2007) Mechanism of hexavalent chromium detoxification by microorganisms and bioremediation application potential: a review. Int Biodeterior Biodegrad 59:8–15
Choppala G, Bolan N, Park JH (2013) Chromium contamination and its risk management in complex environmental settings. Adv Agron 120:129–172
Cieslak-Golonka M (1995) Toxic and mutagenic effects of chromium(VI). A review. Polyhedron 15:3667–3689
Clifford D, Subramanian S, Sorg TJ (1986) Water treatment processes. III. Removing dissolved inorganic contaminants from water. Environ Sci Technol 20:1072–1080
Cohen M (1959) The formation and properties of passive films on iron. Can J Chem 37:286–291
Comba S, Sethi R (2009) Stabilization of highly concentrated suspensions of iron nanoparticles using shear-thinning gels of xanthan gum. Water Res 43:3717–3726
Comba S, Di Molfetta A, Sethi R (2011) A comparison between field applications of nano-, micro-, and millimetric vero-valent vron for the remediation of contaminated aquifers. Water Air Soil Pollut 215:595–607
Costa M (1997) Toxicity and carcinogenity of Cr(VI) in animal models and humans. Crit Rev Toxicol 27:431–442
Costa M (2003) Potential hazards of hexavalent chromate in our drinking water. Toxicol Appl Pharmacol 188:1–5
Cotton FA, Wilkinson G, Murillo CA, Bochmann M (1999) Advanced inorganic chemistry. John Wiley & Sons, New York
Crane RA, Noubactep C (2012) Elemental metals for environmental remediation: lessons from hydrometallurgy. Fresenius Environ Bull 21:1192–1196
Crane RA, Scott TB (2012) Nanoscale zero-valent iron: future prospects for an emerging water treatment technology. J Hazard Mater 211–212:112–125
Dai Y, Hu Y, Jiang B, Zou J, Tian G, Fu H (2016) Carbothermal synthesis of ordered mesoporous carbon-supported nano zero-valent iron with enhanced stability and activity for hexavalent chromium reduction. J Hazard Mater 309:249–258
Di Natale F, Erto A, Lancia A, Musmarra D (2015) Equilibrium and dynamic study on hexavalent chromium adsorption onto activated carbon. J Hazard Mater 281:47–55
Diao M, Yao M (2009) Use of zero-valent iron nanoparticles in inactivating microbes. Water Res 43:5243–5251
Domga R, Togue-Kamga F, Noubactep C, Tchatchueng JB (2015) Discussing porosity loss of Fe^0 packed water filters at ground level. Chem Eng J 263:127–134
Dong H, Ahmad K, Zeng G, Li Z, Chen G, He Q, Xie Y, Wu Y, Zhao F, Zeng Y (2016a) Influence of fulvic acid on the colloidal stability and reactivity of nanoscale zero-valent iron. Environ Pollut 211:363–369
Dong H, Zhao F, Zeng G, Tang L, Fan C, Zhang L, Zeng Y, He Q, Xie Y, Wu Y (2016b) Aging study on carboxymethyl cellulose-coated zero-valent ironnanoparticles in water: chemical transformation and structural evolution. J Hazard Mater 312:234–242
Dong H, Xie Y, Zeng G, Tang L, Liang J, He Q, Zhao F, Zeng Y (2016c) The dual effects of carboxymethylcellulose on the colloidal stability and toxicity of nanoscale zero-valent iron. Chemosphere 144:1682–1689
Dong H, He Q, Zeng G, Tang L, Zhang C, Xie Y, Zeng Y, Zhao F, Wu Y (2016d) Chromate removal by surface-modified nanoscale zero-valent iron: effect of different surface coatings and water chemistry. J Colloid Interface Sci 471:7–13
Dong H, Zeng Y, Zeng G, Huang D, Liang J, Zhao F, He Q, Xie Y, Wu Y (2016e) EDDS-assisted reduction of Cr(VI) by nanoscale zero-valent iron. Sep Purif Technol 165:86–91
Doyle CS, Kendelewicz T, Bostiki BC, Brown GE Jr (2004) Soft x-ray spectroscopic studies of the reaction of fractured pyrite surfaces with Cr(VI)-containing aqueous solutions. Geochim Cosmochim Acta 68:4287–4299
Dozzi MV, Saccomanni A, Selli E (2012) Cr(VI) photocatalytic reduction: effects of simultaneous organics oxidation and of gold nanoparticles photodeposition on TiO_2. J Hazard Mater 211–212:188–195

Dries J, Bastiaens L, Springael D, Agathos SN, Diels L (2005) Combined removal of chlorinated ethenes and heavy metals by zerovalent iron in batch and continuous flow column systems. Environ Sci Technol 39:8460–8465

El-Shazly AH, Mubarak AA, Konsowa AH (2005) Hexavalent chromium reduction using a fixed bed of scrap bearing iron spheres. Desalination 185:307–316

El-Taweel YA, Nassef EM, Elkheriany I, Sayed D (2015) Removal of Cr(VI) ions from waste water by electrocoagulation using iron electrode. Egypt J Pet 24:183–192

El-Temsah YS, Joner EJ (2012) Ecotoxicological effects on earthworms of fresh and aged nano-sized zero-valent iron (nZVI) in soil. Chemosphere 89:76–82

Erdem M, Tumen F (2004) Cr(VI) removal from aqueous solution by the ferrite process. J Hazard Mater B109:71–77

Esfahani AR, Hojati S, Azimi A, Farzadian M, Khataee A (2015) Enhanced hexavalent chromium removal from aqueous solution using a sepiolite-stabilized zero-valent iron nanocomposite: impact of operational parameters and artificial neural network modeling. J Taiwan Inst Chem Eng 49:172–182

Farrell J, Kason M, Melitas N, Li T (2000) Investigation of the long-term performance of zero-valent iron for reductive dechlorination of trichloroethylene. Environ Sci Technol 34:514–521

Fendorf SE (1995) Surface reactions of chromium in soil and waters. Geoderma 67:55–71

Fendorf S, Eick MJ, Grossl P, Sparks DL (1997) Arsenate and chromate retention mechanisms on goethite. 1. Surface structure. Environ Sci Technol 31(2):315–320

Fendorf SE, Wielinga B, Hansel C (2000) Chromium transformations in natural environments: the role of biological and abiological processes in chromium(VI) reduction. Int Geol Rev 42:691–701

Feng P, Guan X, Sun Y, Choi W, Qin H, Wang J, Qiao J, Li L (2015) Weak magnetic field accelerates chromate removal by zero-valent iron. J Environ Sci 31:175–183

Fernandez-Sanchez JM, Sawvel EJ, Alvarez PJJ (2004) Effect of Fe^0 quantity on the efficiency of integrated microbial-Fe^0 treatment processes. Chemosphere 54:823–829

Fiuza A, Silva A, Carvalho G, Fuente AV, Delerue-Matos C (2010) Heterogeneous kinetics of the reduction of chromium (VI) by elemental iron. J Hazard Mater 175:1042–1047

Flury B, Frommer J, Eggenberger U, Mader U, Nachtegaal M, Kretzschmar R (2009) Assessment of long-term performance and chromate reduction mechanisms in a field scale permeable reactive barrier. Environ Sci Technol 43:6786–6792

Fu FL, Han WJ, Tang B, Hu M, Cheng ZH (2013) Insights into environmental remediation of heavy metal and organic pollutants: simultaneous removal of hexavalent chromium and dye from wastewater by zero-valent iron with ligand-enhanced reactivity. Chem Eng J 232:534–540

Fu R, Yang Y, Xu Z, Zhang X, Guo X, Bi D (2015a) The removal of chromium (VI) and lead (II) from groundwater using sepiolite-supported nanoscale zero-valent iron (S-NZVI). Chemosphere 138:726–734

Fu F, Cheng Z, Dionysiou DD, Tang B (2015b) Fe/Al bimetallic particles for the fast and highly efficient removal of Cr(VI) over a wide pH range: performance and mechanism. J Hazard Mater 298:261–269

Fu F, Hu M, Tang B, Han W, Cheng Z (2015c) Removal of Cr(VI) from wastewater using acid-washed zero-valent iron catalyzed by polyoxometalate under acid conditions: efficacy, reaction mechanism and influencing factors. J Taiwan Inst Chem Eng 47:177–181

Fuller SJ, Stewart DI, Burke IT (2013) Chromate reduction in highly alkaline groundwater by zerovalent iron: implications for its use in a permeable reactive barrier. Ind Eng Chem Res 52 (13):4704–4714

Gandhi S, Oh BT, Schnoor JL, Alvarez PJJ (2002) Degradation of TCE, Cr(VI), sulfate, and nitrate mixtures by granular iron in flow-through columns under different microbial conditions. Water Res 36:1973–1982

Gatcha-Bandjun N, Noubactep C, Loura Mbenguela B (2014) Water treatment with Fe^0/H_2O systems: learning from internal electrolysis. Fresenius Environ Bull 23:2663–2669

Geen A, Robertson AP, Leckie JO (1994) Complexation of carbonate species at the goethite surface: implications for adsorption of metal ions in natural waters. Geochim Cosmochim Acta 58(9):2073–2086

Geng B, Jin Z, Li T, Qi X (2009) Preparation of chitosan-stabilized Fe0 nanoparticles for removal of hexavalent chromium in water. Sci Total Environ 407:4994–5000

Genovese M, Lian K (2015) Polyoxometalate modified inorganic–organic nanocomposite materials for energy storage applications: a review. Curr Opin Solid State Mater Sci 19:126–137

Gheju M (2011) Hexavalent chromium reduction with zero-valent iron (ZVI) in aquatic systems. Water Air Soil Pollut 222(1–4):103–148

Gheju M, Balcu I (2010) Hexavalent chromium reduction with scrap iron in continuous-flow system. Part 2: effect of scrap iron shape and size. J Hazard Mater 182:484–493

Gheju M, Balcu I (2011) Removal of chromium from Cr(VI) polluted wastewaters by reduction with scrap iron and subsequent precipitation of resulted cations. J Hazard Mater 196:131–138

Gheju M, Iovi A (2006) Kinetics of hexavalent chromium reduction by scrap iron. J Hazard Mater B135:66–73

Gheju M, Iovi A, Balcu I (2008) Hexavalent chromium reduction with scrap iron in continuous-flow system. Part 1: Effect of feed solution pH. J Hazard Mater 153:655–662

Gillham RW (2008) Development of the granular iron permeable reactive barrier technology (good science or good fortune). In: Yeung AT, Lo IMC (eds) Advances in environmental geotechnology and global sustainable development. Advanced Technovation Limited, Hong-Kong, pp 5–15

Gillham RW, O'Hannesin SF (1991) Metal-catalysed abiotic degradation of halogenated organic compounds. Ground Water 29:752–761

Gillham RW, O'Hannesin SF (1994) Enhanced degradation of halogenated aliphatics by zero-valent iron. Ground Water 32:958–967

Gode F, Pehlivan E (2005) Removal of Cr(VI) from aqueous solution by two Lewatit-anion exchange resins. J Hazard Mater 119:175–182

Gore CT, Omwoma S, Chen W, Song YF (2016) Interweaved LDH/PAN nanocomposite films: application in the design of effective hexavalent chromium adsorption technology. Chem Eng J 284:794–801

Gould JP (1982) The kinetics of hexavalent chromium reduction by metallic iron. Water Res 16:871–877

Gromboni CF, Donati GL, Matos WO, Neves EFA, Nogueira ARA, Nobrega JA (2010) Evaluation of metabisulfite and a commercial steel wool for removing chromium(VI) from wastewater. Environ Chem Lett 8:73–77

Grossl PR, Eick M, Sparks DL, Goldberg S, Ainsworth CC (1997) Arsenate and chromate retention mechanisms on goethite. 2. Kinetic evaluation using a pressure-jump relaxation technique. Environ Sci Technol 31:321–326

Gu H, Rapole SB, Sharma J, Huang Y, Cao D, Colorado HA, Luo Z, Haldolaarachchige N, Young DP, Walters B, Wei S, Guo Z (2012) Magnetic polyaniline nanocomposites toward toxic hexavalent chromium removal. RSC Adv 2:11007–11018

Guertin J, Jacobs JA, Avakian CP (2005) Chromium(VI) handbook. CRC Press, Boca Raton

Han W, Fu F, Cheng Z, Tang B, Wua S (2016) Studies on the optimum conditions using acid-washed zero-valent iron/aluminum mixtures in permeable reactive barriers for the removal of different heavy metal ions from wastewater. J Hazard Mater 302:437–446

Hashim MA, Mukhopadhyay S, Sahu JN, Sengupta B (2011) Remediation technologies for heavy metal contaminated groundwater. J Environ Manag 92:2355–2388

He H, Wu D, Wang Q, Luo C, Duan N (2016) Sequestration of hexavalent chromium by Fe(II)/Fe(III) hydroxides: structural Fe(II) reactivity and PO_4^{3-} effect. Chem Eng J 283:948–955

Henderson AD, Demond AH (2007) Long-term performance of zero-valent iron permeable reactive barriers: a critical review. Environ Eng Sci 24:401–424

Hoch LB, Mack EJ, Hydutsky BW, Hershman JM, Skluzacek JM, Mallouk TE (2008) Carbothermal synthesis of carbon-supported nanoscale zero-valent iron particles for the remediation of hexavalent chromium. Environ Sci Technol 42:2600–2605

Hoover CR, Masselli JW (1941) Disposal of waste liquors from chromium plating. Ind Eng Chem 33:131–134

Hu CY, Lo SL, Liou YH, Hsu YW, Shih K, Lin CJ (2010) Hexavalent chromium removal from near natural water by copper-iron bimetallic particles. Water Res 44:3101–3108

Isaacs HS, Virtanen S, Ryan MP, Schmuki P, Oblonski LJ (2002) Incorporation of Cr in the passive film on Fe from chromate solutions. Electrochim Acta 47:3127–3130

Jabeen H, Chandra V, Jung S, Lee JW, Kim KS, Kim SB (2011) Enhanced Cr(VI) removal using iron nanoparticle decorated graphene. Nanoscale 3:3583–3585

Jeen SW, Blowes DW, Gillham RW (2008) Performance evaluation of granular iron for removing hexavalent chromium under different geochemical conditions. J Contam Hydrol 95:76–91

Jia CG, Zhang YP, Wang H, Ou GN, Liu QM, Lin JM (2014) Rapid biosorption and reduction removal of Cr(VI) from aqueous solution by dried seaweeds. J Cent South Univ 21 (7):2801–2809

Junyapoon S, Weerapong S (2006) Removal of hexavalent chromium from aqueous solutions by scrap iron fillings. KMITL Sci Technol J 6:1–12

Kadu BS, Chikate RC (2013) nZVI based nanocomposites: role of noble metal and clay support on chemisorptive removal of Cr(VI). J Environ Chem Eng 1:320–327

Kadu BS, Sathe YD, Ingle AB, Chikate RC, Patil KR, Rode CV (2011) Efficiency and recycling capability of montmorillonite supported Fe–Ni bimetallic nanocomposites towards hexavalent chromium remediation. Appl Catal B Environ 104:407–414

Kalidhasan S, Kumar ASK, Rajesh V, Rajesh N (2016) The journey traversed in the remediation of hexavalent chromium and the road ahead toward greener alternatives – a perspective. Coord Chem Rev 317:157–166

Kaplan DI, Gilmore TJ (2004) Zerovalent iron removal rates of aqueous Cr(VI) measured under flow conditions. Water Air Soil Pollut 155:21–33

Karn B, Kuiken T, Otto M (2009) Nanotechnology and in situ remediation: a review of the benefits and potential risks. Environ Health Perspect 117:1832–1831

Kim SD, Park KS, Gu MB (2002) Toxicity of hexavalent chromium to *Daphnia magna*: influence of reduction reaction by ferrous iron. J Hazard Mater A93:155–164

Kim C, Lan Y, Deng B (2007) Kinetic study of hexavalent Cr(VI) reduction by hydrogen sulfide through goethite surface catalytic reaction. Geochem J 41:397–405

Kimbrough DE, Cohen Y, Winer AM (1999) A critical assessment of chromium in the environment. Crit Rev Environ Sci Technol 29:1–46

Kirschling TL, Gregory KB, Minkley EG, Lowry GV, Tilton RD (2010) Impact of nanoscale zero valent iron on geochemistry and microbial populations in trichloroethylene contaminated aquifer materials. Environ Sci Technol 44:3474–3480

Kjeldsen P, Locht T (2002) Removal of chromate in a permeable reactive barrier using zero-valent iron. In: Proceedings of the groundwater quality conference: natural and enhanced restoration of groundwater pollution, June 2001, Sheffield, IAHS Publication 275, pp 409–414

Kohn T, Livi KJT, Roberts AL, Vikesland PJ (2005) Longevity of granular iron in groundwater treatment processes: corrosion product development. Environ Sci Technol 39:2867–2879

Kong X, Han Z, Zhang W, Song L, Li H (2016) Synthesis of zeolite-supported microscale zero-valent iron for the removal of Cr^{6+} and Cd^{2+} from aqueous solution. J Environ Manag 169:84–90

Kotas J, Stasicka Z (2000) Chromium occurrence in the environment and methods of its speciation. Environ Pollut 107:263–283

Kumar RV, Basumatary AK, Ghoshal AK, Pugazhenthi G (2015) Performance assessment of an analcime-C zeolite-ceramic composite membrane by removal of Cr(VI) from aqueous solution. RSC Adv 5(9):6246–6254

Lai KCK, Lo IM (2008) Removal of chromium(VI) by acid-washed zero-valent iron under various groundwater geochemistry conditions. Environ Sci Technol 42:1238–1244
Lan YQ, Yang JX, Deng B (2006) Catalysis of dissolved and adsorbed iron in soil suspension for chromium(VI) reduction by sulfide. Pedosphere 16:572–578
Lee C, Kim JY, Lee WI, Nelson KL, Yoon J, Sedlak DL (2008) Bactericidal effect of zero-valent iron nano-scale particles on *Escherichia coli*. Environ Sci Technol 42:4927–4933
Lefevre E, Bossa N, Wiesner MR, Gunsch CK (2016) A review of the environmental implications of in situ remediation by nanoscale zero valent iron (nZVI): behavior, transport and impacts on microbial communities. http://dx.doi.org/10.1016/j.scitotenv.2016.02.003
Li Z, Jones HK, Bowman RS, Helferich R (1999) Enhanced reduction of chromate and PCE by pelletized surfactant-modified zeolite/zero valent iron. Environ Sci Technol 33:4326–4330
Li XQ, Elliott DW, Zhang WX (2006) Zero-valent iron nanoparticles for abatement of environmental pollutants: materials and engineering aspects. Crit Rev Solid State Mat Sci 31:111–122
Li Z, Jones HK, Zhang P, Bowman RS (2007) Chromate transport through columns packed with surfactant-modified zeolite/zero valent iron pellets. Chemosphere 68:1861–1866
Li XQ, Cao J, Zhang WX (2008) Stoichiometry of Cr(VI) immobilization using nanoscale zerovalent iron (nZVI): a study with high-resolution X-Ray Photoelectron Spectroscopy (HR-XPS). Ind Eng Chem Res 47:2131–2139
Li Z, Greden K, Alvarez P, Gregory K, Lowry G (2010) Adsorbed polymer and NOM limits adhesion and toxicity of nano scale zero-valent iron (nZVI) to *E. coli*. Environ Sci Technol 44:3462–3467
Li Y, Jin Z, Li T (2012) A novel and simple method to synthesize SiO_2-coated Fe nanocomposites with enhanced Cr (VI) removal under various experimental conditions. Desalination 288:118–125
Lin CJ (2002) The chemical transformations of chromium in natural waters – a model study. Water Air Soil Pollut 139:137–158
Lin YH, Tseng HH, Wey MY, Lin MD (2010) Characteristics of two types of stabilized nano zero-valent iron and transport in porous media. Sci Total Environ 408:2260–2267
Linos A, Petralias A, Christophi CA, Christoforidou E, Kouroutou P, Stoltidis M, Veloudaki A, Tzala E, Makris KC, Karagas MR (2011) Oral ingestion of hexavalent chromium through drinking water and cancer mortality in an industrial area of Greece – an ecological study. Environ Health 10:50–57
Liu T, Lo IMC (2011) Influences of humic acid on Cr(VI) removal by zero-valent iron from groundwater with various constituents: implication for long-term PRB performance. Water Air Soil Pollut 216:473–483
Liu J, Liu H, Wang C, Li X, Tong Y, Xuan X, Cui G (2008a) Synthesis, characterization and re-activation of a Fe0/Ti system for the reduction of aqueous Cr(VI). J Hazard Mater 151:761–769
Liu T, Tsang DCW, Lo IMC (2008b) Chromium(VI) reduction kinetics by zero-valent iron in moderately hard water with humic acid: iron dissolution and humic acid adsorption. Environ Sci Technol 42:2092–2098
Liu J, Wang C, Shi J, Liu H, Tong Y (2009) Aqueous Cr(VI) reduction by electrodeposited zero-valent iron at neutral pH: acceleration by organic matters. J Hazard Mater 163:370–375
Liu L, Wei S, Liu Y, Shao Z (2012a) Influence of photoirradation on reduction of hexavalent chromium by zero-valent iron in the presence of organic acids. Desalination 285:271–276
Liu T, Wang ZL, Zhao L, Yang X (2012b) Enhanced chitosan/Fe0-nanoparticles beads for hexavalent chromium removal from wastewater. Chem Eng J 189–190:196–202
Liu T, Wang ZL, Sun Y (2015) Manipulating the morphology of nanoscale zero-valent iron on pumice for removal of heavy metals from wastewater. Chem Eng J 263:55–61
Liu A, Liu J, Han J, Zhang WX (2016) Evolution of nanoscale zero-valent iron (nZVI) in water: microscopic and spectroscopic evidence on the formation of nano- and micro-structured iron oxides. J Hazard Mater. doi:10.1016/j.jhazmat.2015.12.070

Lo IMC, Lam CSC, Lai KCK (2006) Hardness and carbonate effects on the reactivity of zero-valent iron for Cr(VI) removal. Water Res 40:595–605

Lopez-Tellez G, Barrera-Diaz CE, Balderas-Hernandez P, Roa-Morales G, Bilyeu B (2011) Removal of hexavalent chromium in aquatic solutions by iron nanoparticles embedded in orange peel pith. Chem Eng J 173:480–485

Lu X, Li M, Tang C, Feng C, Liu X (2012) Electrochemical depassivation for recovering Fe0 reactivity by Cr(VI) removal with a permeable reactive barrier system. J Hazard Mater 213–214:355–360

Lugo-Lugo V, Barrera-Diaz C, Bilyeu B, Balderas-Hernandez P, Urena-Nunez F, Sanchez-Mendieta V (2010) Cr(VI) reduction in wastewater using a bimetallic galvanic reactor. J Hazard Mater 176:418–425

Lugo-Lugo V, Bernal-Martinez LA, Urena-Nunez F, Linares-Hernandez I, Almazan-Sanchez PT, Vazquez-Santillan PJB (2014) Treatment of Cr(VI) present in plating wastewater using a Cu/Fe galvanic reactor. Fuel 158:203–214

Luo F, Chen Z, Megharaj M, Naidu R (2016) Simultaneous removal of trichloroethylene and hexavalent chromium by green synthesized agarose-Fe nanoparticles hydrogel. Chem Eng J 294:290–297

Lv X, Xu J, Jiang G, Xu X (2011) Removal of chromium(VI) from wastewater by nanoscale zero-valent iron particles supported on multiwalled carbon nanotubes. Chemosphere 85:1204–1209

Madhavi V, Prasad TNVKV, Reddy AVB, Reddy BR, Madhavi G (2013) Application of phytogenic zerovalent iron nanoparticles in the adsorption of hexavalent chromium. Spectrochim Acta A Mol Biomol Spectrosc 116:17–25

Mak MSH, Lo IMC (2011) Influences of redox transformation, metal complexation and aggregation of fulvic acid and humic acid on Cr(VI) and As(V) removal by zero-valent iron. Chemosphere 84:234–240

Malaviya P, Singh A (2011) Physicochemical technologies for remediation of chromium-containing waters and wastewaters. Crit Rev Environ Sci Technol 41:1111–1172

Mamais D, Noutsopoulos C, Kavallari I, Nyktari E, Kaldis A, Panousi E, Nikitopoulos G, Antoniou K, Nasioka M (2016) Biological groundwater treatment for chromium removal at low hexavalent chromium concentrations. Chemosphere 152:238–244

Marsh TL, McInerney MJ (2001) Relationship of hydrogen bioavailability to chromate reduction in aquifer sediments. Appl Environ Microbiol 67:1517–1521

McCafferty E, Bernett MK, Murday JS (1988) An XPS study of passive film formation on iron in chromate solutions. Corros Sci 28:559–576

McMurty DC, Elton RO (1985) New approach to in-situ treatment of contaminated groundwaters. Environ Prog 4(3):168–170

Mitra P, Sarkar D, Chakrabarti S, Dutta BK (2011) Reduction of hexa-valent chromium with zero-valent iron: batch kinetic studies and rate model. Chem Eng J 171:54–60

Mohan D, Pittman CU (2006) Activated carbons and low cost adsorbents for remediation of tri- and hexavalent chromium from water. J Hazard Mater 137:762–811

Montesinos VN, Quici N, Litter MI (2014) Visible light enhanced Cr(VI) removal from aqueous solution by nanoparticulated zerovalent iron. Catal Commun 46:57–60

Muthukrishnan M, Guha BK (2008) Effect of pH on rejection of hexavalent chromium by nanofiltration. Desalination 219:171–178

Mwakabona HT, Ndé-Tchoupé AI, Njau KN, Noubactep C, Wydra KD (2017) Metallic iron for safe drinking water provision: Considering a lost knowledge. Water Res http://dx.doi.org/10.1016/j.watres.2017.03.001

Mystrioti C, Sparis D, Papasiopi N, Xenidis A, Dermatas D, Chrysochoou M (2015) Assessment of polyphenol coated nano zero valent iron for hexavalent chromium removal from contaminated waters. Bull Environ Contam Toxicol 94:302–307

Mystrioti C, Xanthopoulou TD, Papassiopi N, Xenidis A (2016) Comparative evaluation of five plant extracts and juices for nanoiron synthesis and application for hexavalent chromium reduction. Sci Total Environ 539:105–113

Naimi-Joubani M, Shirzad-Siboni M, Yang JK, Gholami M, Farzadkia M (2015) Photocatalytic reduction of hexavalent chromium with illuminated ZnO/TiO_2 composite. J Ind Eng Chem 22:317–323

Němeček J, Pokorný P, Lacinová L, Černík M, Masopustová Z, Lhotský O, Filipová A (2015a) Cajthaml T, Combined abiotic and biotic in-situ reduction of hexavalent chromium in groundwater using nZVI and whey: A remedial pilot test. J Hazard Mater 300:670–679

Němeček J, Pokorný P, Lhotský O, Knytl V, Najmanová P, Steinová J, Černík M, Filipová A, Filip J, Cajthaml T (2015b) Combined nano-biotechnology for in-situ remediation of mixed contamination of groundwater by hexavalent chromium and chlorinated solvents. Sci Total Environ. doi:10.1016/j.scitotenv.2016.01.019

Noubactep C (2007) Processes of contaminant removal in "Fe^0-H_2O" systems revisited: the importance of co-precipitation. Open Environ J 1:9–13

Noubactep C (2009a) An analysis of the evolution of reactive species in Fe0/H_2O systems. J Hazard Mater 168:1626–1631

Noubactep C (2009b) On the operating mode of bimetallic systems for environmental remediation. J Hazard Mater 164:394–395

Noubactep C (2010a) Elemental metals for environmental remediation: learning from cementation process. J Hazard Mater 181:1170–1174

Noubactep C (2010b) Metallic iron for safe drinking water worldwide. Chem Eng J 165:740–749

Noubactep C (2015) Metallic iron for environmental remediation: a review of reviews. Water Res 85:114–123

Noubactep C, Care S (2010a) On nanoscale metallic iron for groundwater remediation. J Hazard Mater 182:923–927

Noubactep C, Care C (2010b) Dimensioning metallic iron beds for efficient contaminant removal. Chem Eng J 163:454–460

Noubactep C, Schoner A (2010) Metallic iron for environmental remediation: learning from electrocoagulation. J Hazard Mater 175:1075–1080

Noubactep C, Care S, Crane R (2012) Nanoscale metallic iron for environmental remediation: prospects and limitations. Water Air Soil Pollut 223:1363–1382

O'Hannesin SF, Gillham RW (1993) In situ degradation of halogenated organics by permeable reaction wall. Ground Water Currents, EPA/542/N-93/003

Odziemkowski MS, Simpraga RP (2004) Distribution of oxides on iron materials used for remediation of organic groundwater contaminants: implication for hydrogen evolution reactions. Can J Chem 82:1–12

Oh BT, Lee JY, Yoon J (2007a) Removal of contaminants in leachate from landfill by waste steel scrap and converter slag. Environ Geochem Health 29:331–336

Oh YJ, Song H, Shin WS, Choi SJ, Kim YH (2007b) Effect of amorphous silica and silica sand on removal of chromium(VI) by zero-valent iron. Chemosphere 66:858–865

Owlad M, Aroua MK, Daud WAW, Baroutian S (2009) Removal of hexavalent chromium-contaminated water and wastewater: a review. Water Air Soil Pollut 200:59–77

Ozer A, Altundogan HS, Erdem M, Tumen F (1997) A study on the Cr(VI) removal from aqueous soluţions by steel wool. Environ Pollut 97:107–112

Palmer CD, Puls RW (1994) Natural attenuation of hexavalent chromium in groundwater and soils, Office of Research and Development, EPA/540/5-94/505. Office of Research and Development, Washington, DC

Palmer CD, Wittbrodt PR (1991) Processes affecting the remediation of chromium-contaminated sites. Environ Health Perspect 92:25–40

Pechova A, Pavlata L (2007) Chromium as an essential nutrient: a review. Vet Med 52:1–18

Perez E, Ayele L, Getachew G, Fetter G, Bosch P, Mayoral A, Diaz I (2015) Removal of chromium(VI) using nano-hydrotalcite/SiO_2 composite. J Environ Chem Eng 3:1555–1561

Petala E, Dimos K, Douvalis A, Bakas T, Tucek J, Zboril R, Karakassides MA (2013) Nanoscale zero-valent iron supported on mesoporous silica: characterization and reactivity for Cr (VI) removal from aqueous solution. J Hazard Mater 261:295–306

Phenrat T, Saleh N, Sirk K, Kim HJ, Tilton RD, Lowry GV (2008) Stabilization of aqueous nanoscale zerovalent iron dispersions by anionic polyelectrolytes: adsorbed anionic polyelectrolyte layer properties and their effect on aggregation and sedimentation. J Nanopart Res 10:795–814

Poguberovic SS, Krcmara DM, Maletica SP, Konya Z, Tomasevic Pilipovic DD, Kerkez DV, Roncevic SD (2016) Removal of As(III) and Cr(VI) from aqueous solutions using "green"zerovalent iron nanoparticles produced by oak, mulberry and cherry leaf extracts. Ecol Eng 90:42–49

Ponder SM, Darab JG, Mallouk TE (2000) Remediation of Cr(VI) and Pb(II) aqueous solutions using supported, nanoscale zero-valent iron. Environ Sci Technol 34:2564–2569

Powell RM, Puls RW (1997) Proton generation by dissolution of intrinsic or augmented aluminosilicate minerals for in situ contaminant remediation by zero-valence-state iron. Environ Sci Technol 31:2244–2251

Powell RM, Puls RW, Hightower SK, Sabatini DA (1995) Coupled iron corrosion and chromate reduction: mechanisms for subsurface remediation. Environ Sci Technol 29:1913–1922

Prasad PVVV, Das C, Golder AK (2011) Reduction of Cr(VI) to Cr(III) and removal of total chromium from wastewater using scrap iron in the form of zerovalent iron(ZVI): batch and column studies. Can J Chem Eng 89(6):1575–1582

Pratt AR, Blowes DW, Ptacek CJ (1997) Products of chromate reduction on proposed subsurface remediation material. Environ Sci Technol 31:2492–2498

Puls RW, Blowes DW, Gillham RW (1999a) Long-term performance monitoring for a permeable reactive barrier at the U.S. Coast Guard Support Center, Elizabeth City, North Carolina. J Hazard Mater 68:109–124

Puls RW, Paul CJ, Powell RM (1999b) The application of in situ permeable reactive (zero-valent iron) barrier technology for the remediation of chromate-contaminated groundwater: a field test. Appl Geochem 14:989–1000

Qian H, Wu Y, Liu Y, Xu X (2008) Kinetics of hexavalent chromium reduction by iron metal. Front Environ Sci Eng China 2:51–56

Qiu SR, Lai HF, Roberson MJ, Hunt ML, Amrhein C, Giancarlo LC, Flynn GW, Yarmoff JA (2000) Removal of contaminants from aqueous solution by reaction with iron surfaces. Langmuir 16:2230–2236

Qiu X, Fang Z, Yan X, Gu F, Jiang F (2012) Emergency remediation of simulated chromium (VI)-polluted river by nanoscale zero-valent iron: laboratory study and numerical simulation. Chem Eng J 193–194:358–365

Rai D, Sass BM, Moore DA (1987) Chromium(III) hydrolysis constants and solubility of chromium(III) hydroxide. Inorg Chem 26:345–349

Rai D, Eary LE, Zacara LM (1989) Environmental chemistry of chromium. Sci Total Environ 86:15–23

Reardon EJ (2005) Zerovalent irons: styles of corrosion and inorganic control on hydrogen pressure buildup. Environ Sci Technol 39:7311–7317

Reynolds GW, Hoff JT, Gillham RW (1990) Sampling bias caused by materials used to monitor halocarbons in groundwater. Environ Sci Technol 24:135–142

Ritter K, Odziemkowski MS, Gillham RW (2002) An in situ study of the role of surface films on granular iron in the permeable iron wall technology. J Contam Hydrol 55:87–111

Rivero-Huguet M, Marshall WD (2009) Reduction of hexavalent chromium mediated by micro- and nano-sized mixed metallic particles. J Hazard Mater 169:1081–1087

Rusevova K, Kopinke FD, Georgi A (2012) Nano-sized magnetic iron oxides as catalysts for heterogeneous Fenton-like reactions – influence of Fe(II)/Fe(III) ratio on catalytic performance. J Hazard Mater 241–242:433–440

Scherer MMS, Richter S, Valentine RL, Alvarez PJJ (2000) Chemistry and microbiology of reactive barriers for in situ groundwater cleanup. Crit Rev Environ Sci Technol 30:363–411

Senzaki T, Kumagai Y (1988) Removal of chlorinated organic compounds from wastewater by reduction process: treatment of 1,1,2,2-tetrachloroethane with iron powder. Kogyo Yosui 357:2–7

Senzaki T, Kumagai Y (1989) Removal of chlorinated organic compounds from wastewater by reduction process: II. treatment of trichloroethylene with iron powder. Kogyo Yosui 369:19–25

Sharma AK, Kumar R, Mittal S, Hussain S, Arora M, Sharma RC, Babu JN (2015) In situ reductive regeneration of zerovalent iron nanoparticles immobilized on cellulose for atom efficient Cr (VI) adsorption. RSC Adv 5:89441–89446

Sheng G, Hu J, Li H, Li J, Huang Y (2016) Enhanced sequestration of Cr(VI) by nanoscale zero-valent iron supported on layered double hydroxide by batch and XAFS study. Chemosphere 148:227–232

Shi T, Wang Z, Liu Y, Jia S, Changming D (2009) Removal of hexavalent chromium from aqueous solutions by D301, D314 and D354 anion-exchange resins. J Hazard Mater 161:900–906

Shi L, Zhang X, Chen Z (2011) Removal of Chromium (VI) from wastewater using bentonite-supported nanoscale zero-valent iron. Water Res 45:886–892

Shi GM, Zhang B, Xu XX, Fu YH (2015) Graphene oxide coated coordination polymer nanobelt composite material: a new type of visible light active and highly efficient photocatalyst for Cr (VI) reduction. Dalton Trans 44:11155–11164

Shih YJ, Chen CW, Hsia KF, Dong CD (2015) Granulation for extended-release of nanoscale zero-valent iron exemplified by hexavalent chromium reduction in aqueous solution. Sep Purif Technol 156:1073–1081

Shupack SI (1991) The chemistry of chromium and some resulting analytical problems. Environ Health Perspect 92:7–11

Simeonidis K, Mourdikoudis S, Kaprara E, Mitrakasd M, Polavarapu L (2016) Inorganic engineered nanoparticles in drinking water treatment: a critical review. Environ Sci Water Res Technol 2:43–70

Singh KP, Singh AK, Gupta S, Sinha S (2011) Optimization of Cr(VI) reduction by zero-valent bimetallic nanoparticles using the response surface modeling approach. Desalination 270:275–284

Singh R, Bishnoi NR, Kirrolia A, Kumar R (2013) Synergism of Pseudomonas aeruginosa and Fe^0 for treatment of heavy metal contaminated effluents using small scale laboratory reactor. Bioresour Technol 127:49–58

Song DI, Kim YH, Shin WS (2005) A simple mathematical analysis on the effect of sand in Cr (VI) reduction using zero valent iron. Korean J Chem Eng 22:67–69

Stern AH (2010) A quantitative assessment of the carcinogenicity of hexavalent chromium by the oral route and its relevance to human exposure. Environ Res 110:798–807

Stout MD, Herbert RA, Kissling GE, Collins BJ, Travlos GS, Witt KL, Melnick RL, Abdo KM, Malarkey DE, Hooth MJ (2009) Hexavalent chromium is carcinogenic to F344/N rats and B6C3F1 mice after chronic oral exposure. Environ Health Perspect 117:716–722

Stratmann M, Müller J (1994) The mechanism of the oxygen reduction on rust covered metal substrates. Corros Sci 36:327–359

Stumm W (1990) Aquatic chemical kinetics. John Wiley and Sons, Chichester

Su H, Fang Z, Tsang PE, Fang J, Zhao D (2016) Stabilisation of nanoscale zero-valent iron with biochar for enhanced transport and in-situ remediation of hexavalent chromium in soil. Environ Pollut 214:94–100

Sun YP, Li XQ, Cao J, Zhang WX, Wang HP (2006) Characterization of zero-valent iron nanoparticles. Adv Colloid Interf Sci 120:47–56

Sun TR, Pamukcu S, Ottosen LM, Wang F (2015) Electrochemically enhanced reduction of hexavalent chromium in contaminated clay: kinetics, energy consumption, and application of pulse current. Chem Eng J 262:1099–1107

Sweeney KH (1981a) The reductive treatment of industrial wastewaters: I. Process description. American Institute of Chemical Engineers, Symposium Series, Water-1980 209(77):67–71

Sweeney KH (1981b) The reductive treatment of industrial wastewaters: II. Process applications. American Institute of Chemical Engineers, Symposium Series, Water-1980 209(77):72–78
Sweeney KH, Fischer JR (1972) Reductive degradation of halogenated pesticides. U.S.A. Patent, 3,640,821
Tang J, Hu Y, Baig SA, Sheng T, Xu X (2014) Hexavalent chromium reduction by *Escherichia coli* in the presence of ferric iron. Desalin Water Treat 52:22–24
Thacher R, Hsu L, Ravindran V, Nealson KH, Pirbazari M (2015) Modeling the transport and bioreduction of hexavalent chromium in aquifers: Influence of natural organic matter. Chem Eng Sci 138:552–565
Toli A, Chalastara K, Mystrioti C, Xenidis A, Papassiopi N (2016) Incorporation of zero valent iron nanoparticles in the matrix of cationic resin beads for the remediation of Cr (VI) contaminated waters. Environ Pollut 214:419–429
Vazquez-Morillas A, Vaca-Mier M, Alvarez PJ (2006) Biological activation of hydrous ferric oxide for reduction of hexavalent chromium in the presence of different anions. Eur J Soil Biol 42:99–106
Vega A, Fiuza A, Guimaraes F (2010) Insight into the phenomenology of the Cr(VI) reduction by metallic iron using an electron probe microanalyzer. Langmuir 26:11980–11986
Villacis-Garcia M, Villalobosa M, Gutierrez-Ruizca M (2015) Optimizing the use of natural and synthetic magnetites with very small amounts of coarse Fe(0) particles for reduction of aqueous Cr(VI). J Hazard Mater 281:77–86
Wang Q, Cissoko N, Zhou M, Xu X (2011) Effects and mechanism of humic acid on chromium (VI) removal by zero-valent iron (Fe0) nanoparticles. Phys Chem Earth 36:442–446
Wang Y, Wang X, Wang X, Liu M, Xia S, Yin D, Zhang Y, Zhao J (2012) Reduction of hexavalent chromium with scrap iron in a fixed bed reactor. Front Environ Sci Eng 6(6):761–769
Wang N, Zheng T, Zhang G, Wang P (2016a) A review on Fenton-like processes for organic wastewater treatment. J Environ Chem Eng 4:762–787
Wang J, Fang Z, Cheng W, Yan X, Tsang PE, Zhao D (2016b) Higher concentrations of nanoscale zero-valent iron (nZVI) in soil induced rice chlorosis due to inhibited active iron transportation. Environ Pollut 210:338–345
White AF, Paterson ML (1996) Reduction of aqueous transition metal species on the surface of Fe (II)-containing oxides. Geochim Cosmochim Acta 60:3799–3814
WHO (2011) Guidelines for drinking-water quality, 4th edn. World Health Organisation, Geneva
Wilkin RT, Puls RW, Sewell GW (2003) Long-term performance of permeable reactive barriers using zero-valent iron: geochemical and microbiological effects. Ground Water 41(4):493–503
Wilkin RT, Su C, Ford RG, Paul CJ (2005) Chromium-removal processes during groundwater remediation by a zerovalent iron permeable reactive barrier. Environ Sci Technol 39 (12):4599–4605
Wilkin RT, Acree SD, Ross RR, Puls RW, Lee TR, Woods LL (2014) Fifteen-year assessment of a permeable reactive barrier for treatment of chromate and trichloroethylene in groundwater. Sci Total Environ 468–469:186–194
Williams AGB, Scherer MM (2001) Kinetics of Cr(VI) reduction by carbonate green rust. Environ Sci Technol 35:3488–3494
Wise JP, Wise SS, Little JE (2002) The cytotoxicity and genotoxicity of particulate and soluble hexavalent chromium in human lung cells. Mutat Res 517:221–229
Wise SS, Holmes AL, Wise JP (2006) Particulate and soluble hexavalent chromium are cytotoxic and genotoxic to human lung epithelial cells. Mutat Res 610:2–7
Wu P, Li S, Ju L, Zhu N, Wu J, Li P, Dang Z (2012) Mechanism of the reduction of hexavalent chromium by organo-montmorillonite supported iron nanoparticles. J Hazard Mater 219–220:283–288
Wu L, Liao L, Lv G, Qin F, He Y, Wang X (2013) Micro-electrolysis of Cr (VI) in the nanoscale zero-valent iron loaded activated carbon. J Hazard Mater 254–255:277–283
Wu L, Liao L, Lv G, Qin F (2015) Stability and pH-independence of nano-zero-valent iron intercalated montmorillonite and its application on Cr(VI) removal. J Contam Hydrol 179:1–9

Xing Y, Chen X, Wang D (2007) Electrically regenerated ion exchange for removal and recovery of Cr(VI) from wastewater. Environ Sci Technol 41:1439–1443
Xu Y, Zhao D (2007) Reductive immobilization of chromate in water and soil using stabilized iron nanoparticles. Water Res 41:2101–2108
Xu HM, Wei JF, Wang XL (2014) Nanofiltration hollow fiber membranes with high charge density prepared by simultaneous electron beam radiation-induced graft polymerization for removal of Cr(VI). Desalination 346:122–130
Yang Y (2006) Reduction of TCE and chromate by granular iron in the presence of dissolved $CaCO_3$. Master of Science Thesis, University of Waterloo
Yang JE, Kim JS, Ok YS, Yoo KR (2007) Mechanistic evidence and efficiency of the Cr (VI) reduction in water by different sources of zerovalent irons. Water Sci Technol 55:197–202
Yin X, Liu W, Ni J (2014) Removal of coexisting Cr(VI) and 4-chlorophenol through reduction and Fenton reaction in a single system. Chem Eng J 248:89–97
Yirsaw BD, Megharaj M, Chen Z, Naidu R (2016) Environmental application and ecological significance of nano-zero valent iron. J Environ Sci 44:88–98
Yoon IH, Bang S, Chang JS, Kim MG, Kim KW (2011) Effects of pH and dissolved oxygen on Cr(VI) removal in Fe(0)/H_2O systems. J Hazard Mater 186:855–862
Yuan TH, Lian IB, Tsai KY, Chang TK, Chiang CT, Su CC, Hwang YH (2011) Possible association between nickel and chromium and oral cancer: a case-control study in central Taiwan. Sci Total Environ 406:1046–1052
Zafarani HR, Bahrololoom ME, Javidi M, Shariat MH, Tashkhourian J (2014) Removal of chromate ion from aqueous solutions by sponge iron. Desalin Water Treat 52:7154–7162
Zazo JA, Paull JS, Jaffe PR (2008) Influence of plants on the reduction of hexavalent chromium in wetland sediments. Environ Pollut 156:29–35
Zhang WX (2003) Nanoscale iron particles for environmental remediation: an overview. J Nanopart Res 5:323–332
Zhang R, Sun H, Yin J (2008) Arsenic and chromate removal from water by iron chips -effects of anions. Front Environ Sci Eng China 2:203–208
Zhang XH, Zhang X, Wang XC, Jin LF, Yang ZP, Jiang CX, Chen Q, Ren XB, Cao JX, Wang Q, Zhu YM (2011) Chronic occupational exposure to hexavalent chromium causes DNA damage in electroplating workers. Public Health 11:224–231
Zhang J, Zhang G, Wang M, Zheng K, Cai D, Wu Z (2013) Reduction of aqueous CrVI using nanoscale zero-valent iron dispersed by high energy electron beam irradiation. Nanoscale 5:9917–9923
Zhao Y, Qi W, Chen G, Ji M, Zhang Z (2015) Behavior of Cr(VI) removal from wastewater by adsorption onto HCl activated Akadama clay. J Taiwan Inst Chem Eng 50:190–197
Zhitkovich A (2011) Chromium in drinking water: sources, metabolism, and cancer risks. Chem Res Toxicol 24:1617–1629
Zhou Y, Gao B, Zimmerman AR, Chen H, Zhang M, Cao X (2014) Biochar-supported zerovalent iron for removal of various contaminants from aqueous solutions. Bioresour Technol 152:538–542
Zhou X, Lv B, Zhou Z, Li W, Jing G (2015) Evaluation of highly active nanoscale zero-valent iron coupled with ultrasound for chromium(VI) removal. Chem Eng J 281:155–163
Zhu J, Wei S, Gu H, Rapole SB, Wang Q, Luo Z, Haldolaarachchige N, Young DP, Guo Z (2012) One-pot synthesis of magnetic graphene nanocomposites decorated with core@double-shell nanoparticles for fast chromium removal. Environ Sci Technol 46:977–985
Zhuang L, Li Q, Chen J, Ma B, Chen S (2014) Carbothermal preparation of porous carbon-encapsulated iron composite for the removal of trace hexavalent chromium. Chem Eng J 253:24–33
Zink S, Schoenberg R, Staubwasser M (2010) Isotopic fractionation and reaction kinetics between Cr(III) and Cr(VI) in aqueous media. Geochim Cosmochim Acta 74:5729–5745

Dual Functional Styrene-Maleic Acid Copolymer Beads: Toxic Metals Adsorbent and Hydrogen Storage

R.B. Amal Raj, Renuka R. Gonte, and K. Balasubramanian

Abstract When the concentration of heavy toxic metals exceeds the constraint, adverse health effects in human as well as in other living organisms materialize. Even though the entire evading of exposure to such metals is not possible, abstraction of such metals is effected by either physical or chemical processes such as adsorption, electrochemical methods, chemical precipitation, ultrafiltration and coagulation floatation. Precipitation or oxidation-reduction methods which convert the metal ions to insoluble compounds or extortionate sludges during the metal ion isolation may lead to a secondary pollution. Of these methods, adsorption is accepted as one of the most adequate and fiscal methods for the abstraction of metal ions at low ion concentrations. This chapter spotlights on the cross-linked styrene-maleic acid copolymeric beads for the adsorption of toxic heftily ponderous metal ions from aqueous systems and a material for hydrogen storage at room temperature. The suspension polymerized adsorbents were highly cross-linked to achieve better mechanical properties, and the porosity is introduced in the copolymer matrix. Discrete metal ions such as Cu(II), Co(II), Ni(II), Zn(II) and Au(III) and dyes such as Congo red (CR) were magnificently adsorbed by the highly cross-linked styrene-maleic acid copolymeric beads. XRD and SAXS results verified that these copolymer beads are additionally highly efficacious in in situ reduction of Au (III) ions from dihydrogen monoxide to Au (0) nanogold formation. The obtained experimental data were interpreted utilizing distinct adsorption isotherms and kinetic models such as Freundlich isotherm, Langmuir isotherm, Temkin isotherm, pseudo-first-order kinetic model, pseudo-second-order kinetic model and intraparticle diffusion models. Langmuir and Freundlich isotherm models were fitting for the adsorption of metal ions and are followed by pseudo-first-order kinetics in the initial stages and pseudo-second-order kinetics in the later stage of adsorption. Adsorption of metal ions was governed by intraparticle diffusion, and the desorption of metal ions was carried out utilizing dilute HCl. To assess the

R.B. Amal Raj
Centre for Biopolymer Science and Technology, A Unit of CIPET, Cochin 683501, India

R.R. Gonte • K. Balasubramanian (✉)
Department of Materials Engineering, Defence Institute of Advanced Technology (DU), Ministry of Defence, Pune 411 025, India
e-mail: meetkbs@gmail.com

N.A. Anjum et al. (eds.), *Enhancing Cleanup of Environmental Pollutants*,
DOI 10.1007/978-3-319-55423-5_8

adsorption of Congo red dye molecules, composites of SMA with sugarcane molasses and sawdust were additionally synthesized, and the composite exhibits exceptional adsorption of Congo red dye which was validated utilizing distinct isotherm and kinetic models. The adsorption of hydrogen by the cross-linked SMA copolymer beads at room temperature withal was evaluated. The augmented rate of hydrogen adsorption was prosperously accomplished by the prelude of highly cross-linked interpenetrating networks inside the microspheres and porosity prelude into the copolymer network. The rate of hydrogen adsorption is virtually commensurable for the various cross-linked polymers and is independent of their divinylbenzene content. Even with perpetuated exposure of upto 65 hours, saturation cannot be accomplished; thus the slow micropore opening mechanism being involved that is more immensely colossal pores are filled first is envisaged. Enhanced cross-linked SMA beads modified with metal-organic frameworks (MOF) were synthesized by the slow diffusion of TEA. Maleic acid, which is a dicarboxylic acid, will influence the morphology of the MOFs composed in the polymer matrix and thus the hydrogen storage capacity. SMA functionalized with MOF samples exhibit hydrogen storage capacities where Zn-SMA complexes exhibit hydrogen storage capacity of 0.57 wt% at 300 K and 0.61bars. The ethanol adsorption and retention of the modified beads can be scrutinized for a cache of liquid hydrogen in fuel cells. Advantages in the utilization of these polymer beads in fuel cell encompass embedded catalyst activity, low cost, efficacious solvent and simultaneous hydrogen storage and operation at higher temperatures, thus providing a solution for current fuel cells.

Keywords Metal pollution • Styrene-maleic acid copolymer beads • Adsorbent • Hydrogen torage

Introduction

Recent years have experienced incrementing cognizance for water pollution, and its far-reaching effects have prompted concerted efforts towards pollution abatement (Donmez et al. 1999). Rapid industrialization has solemnly contributed to the relinquishment of toxic heftily ponderous metals in the water streams. Many industrial wastewaters contain substances that are difficult to abstract via conventional secondary treatment; are toxic or hazardous; are volatile and cannot be transferred to the atmosphere; have the potential for engendering noxious vapours or odours, or for imparting colour to the wastewater; and are present in diminutively minuscule concentrations that make their abstraction via other methods difficult. Mining, electroplating, metal processing, textile and battery manufacturing industries are the main sources of heavy metal contamination (Babel and Opiso 2007; Nwuche and Ugoji 2008). These activities pollute dihydrogen monoxide streams, especially rivers, and make them lose their potential value and benign use (Celik and Demirbas 2005; Kadirvelu et al. 2001). Contamination of aqueous

environments by heftily ponderous metals and dyes is a worldwide environmental concern due to their toxic effects and accumulation through aliment chain (Kapoor et al. 1999; Sternberg and Dorn 2002). Amongst these heavy metal ions, the ions of Cd, Zn, Hg, Pb, Cr, Cu, As, etc., have gained consequentiality due to their highly toxic nature even at low concentrations. The high concentration of these heavy metals in the environment can be detrimental to a variety of living species. Extortionate ingestion of these metal ions by humans can cause accumulative poisoning, cancer, nervous system damage and ultimately death (Corapcioglu and Huang 1987; Issabayeva et al. 2007). Abstraction of trace amounts of heavy metal ions from wastewater and imbibing dihydrogen monoxide is of great paramountcy on account of their high toxicity (Gundogan et al. 2004; Abdel-Ghani et al. 2009; Resmi et al. 2010).

Adsorption finds applications in tertiary waste water treatment as a polishing step before final discharge into nearby. Adsorption is commonly used in the treatment of industrial wastewaters containing organic compounds not easily biodegraded during secondary (biological) treatment or toxic (Al-Rekabi et al. 2007). Adsorption using ion-exchange resins is one of the most popular methods for the removal of heavy metals from the water and wastewater (Omer et al. 2003; Rengaraj et al. 2004). Ion-exchange resins have been developed as a major option for treating wastewaters over the past few decades (Rawat et al.1990; Rengaraj et al. 2007). Porous materials such as clay (Jaber et al. 2005), activated carbon (Zhu et al. 2009), zeolites (Wingenfelder et al. 2009) and biomass (Deng and Ting 2005) are usually used as toxic metal ion adsorbents because of their high surface area, large pore volume and the presence of exchangeable ions presenting themselves as good candidates for adsorbents. For better adsorption performance, the pore size of a porous adsorbent should match the adsorbates atomic/molecular size (Yang 2003).

Hydrogen is considered as a potential alternative for fossil fuel due to its attractive properties such as nontoxicity, clean combustion and high energy density (Schlapbach and Zuttel 2001). The chemical energy of hydrogen is approximately three times larger than the energy density of liquid hydrocarbon (Schlapbach 2002). Hydrogen storage will be required particularly for vehicular applications, stationary power generation, hydrogen delivery and refueling infrastructure. However, a number of significant technological hurdles need to be overcome for realizing these applications including safe, compact and high-capacity hydrogen storage systems. Physisorptive hydrogen storage on porous materials is considered to be potential method for vehicular application with a view of storage of large amounts of hydrogen at near-ambient temperatures and safe pressures. Porous polymers, such as hypercross-linked polymers, integrate incipient merits to the adsorbent family because of their low cost, facile processing and high thermal and chemical stability (Davankov and Tsyurupa 1990; Lee et al. 2006).

Sorbents may be synthetic or natural which include activated carbons (Rivera-Utrilla et al. 2003); zeolites (Inglezakis et al. 2003); clays(Yavuz et al. 2003; Al-Asheh et al. 2003); silica beads (Krysztafkiewicz et al. 2002); low-cost adsorbents such as industrial by-products (Netpradit et al. 2004; Gupta and Suhas 2009), agricultural wastes (Robinson and Chandran 2002) and biomass (Vasudevan et al.

2003); and polymeric materials like organic polymeric resins (Zhang et al. 2003; Atia et al. 2003) and macroporous hypercross-linked polymers (Azanova and Hradil 1999; Pan et al. 2003) to name as few as significant examples. Polymeric adsorbents possess rigid microporous structure with large surface area (greater than 1000 m^2/g) (Goltz et al. 1994). Commercially available resins in bead form (typically 0.5 mm diameter) are usually composed of copolymers of styrene-divinylbenzene (DVB) and acrylic acid ester-divinylbenzene which possess a wide range of surface porosities, polarities and macropore sizes. The porosities can be built through emulsion polymerization, and this creates a polymer matrix with surface areas ranging up to 1100 m^2/g (Thomas and Crittenden 1998; Yang 2003). Another advantage possessed is the inclusion of functional groups in the polymer matrix enhancing it adsorptive capacity. Styrene-divinylbenzene, polymethacrylate, divinylbenzene-ethylvinylbenzene, vinylpyridine, sulphonated or chloromethylated ion-exchange resins are a few examples of widely used adsorbents (Har et al. 2001; Toro et al. 2009). Polymeric adsorbents are possible by controlling/tailoring their pore structure and on-site regenerability (Leng 2009). In fact, the polymeric sorbents used for cyclic adsorption processes should satisfy the following requirements: large selectivity derived from equilibrium, kinetic or steric effect, large adsorption capacity, fast adsorption kinetics, easy regenerability, improved mechanical strength and low cost (Den 2006). Tailoring the adsorbent properties to meet the above requisites can result in adsorbents with immensely colossal internal pore volume, internal surface area, controlled surface properties through culled functional groups, controlled pore size distribution and impuissant interactions between adsorbate and adsorbent.

In this chapter we have successfully developed well-organized styrene-maleic acid copolymer beads and composites for adsorption of toxic chemicals and hydrogen as a highly innovative and eco-friendly method that can be employed for large-scale cleanups of water and as a storage material for hydrogen. Chemical modification of the SMA beads was also carried out by a simple transformation technique characterized by different techniques. The synthesis of polymeric adsorbents in the form of spherical beads is carried out using three different types of heterogeneous polymerization technique, viz., suspension polymerization, precipitation polymerization and emulsion polymerization (Odian 2004). Special techniques such as FTIR spectroscopy, UV-visible spectroscopy, scanning electron microscopy (SEM), X-ray diffraction technique (XRD), small-angle X-ray scattering (SAXS) and thermogravimetric analysis (TGA) have been developed in order to characterize and study the properties associated with the materials.

In fact, adsorption isotherms are important to describe the adsorption mechanism for the interaction of metal ions/dyes on the adsorbent surface, for the design of an adsorption process, and to determine the efficiency of adsorption. Several adsorption isotherms pristinely utilized for gas phase adsorption are available and rarely adopted to correlate adsorption equilibria in heavy metal/dye adsorption. Some well-known ones are Freundlich, Langmuir, Temkin and Dubinin-Radushkevich (D-R) (Febrianto et al. 2009). To investigate the mechanism of adsorption and its potential rate-controlling steps that include mass convey and chemical reaction processes, kinetic models have been exploited to analyze the experimental data.

Several kinetic models such as pseudo-first-order, pseudo-second-order, Elovich and intraparticle diffusion have been applied to examine the rate-controlling mechanism of the adsorption process. Thermodynamic considerations are paramount to conclude whether the adsorption process is spontaneous or not. The adsorption of metal ions/dye onto adsorbents is studied at fine-tuned temperature.

Experiment and Characterization

Cross-Linked SMA Beads

Synthesis of Cross-Linked SMA Beads

Styrene (S) and divinylbenzene (DVB) were purified by extracting with 10% sodium hydroxide to remove the monomethyl hydroquinone (MEHQ) inhibitor and washed repeatedly with distilled water till pH of the elute was 7 (Fig. 1a) and finally dried over anhydrous calcium hydride. Maleic anhydride (MAn) and azobisisobutyronitrile (AIBN) were recrystallized from 80:20 chloroform/methanol mixture prior to use (Deb and Mathew 1996). Homogeneous solution of the purified monomers (styrene, maleic anhydride), cross-linker (DVB) and initiator (AIBN) was obtained in methyl isobutylketone (MIBK) under nitrogen atmosphere (Fig. 1b). A four-neck reaction vessel equipped with an overhead stirrer, purging tube, thermometer vial and water condenser was placed in oil bath. The organic

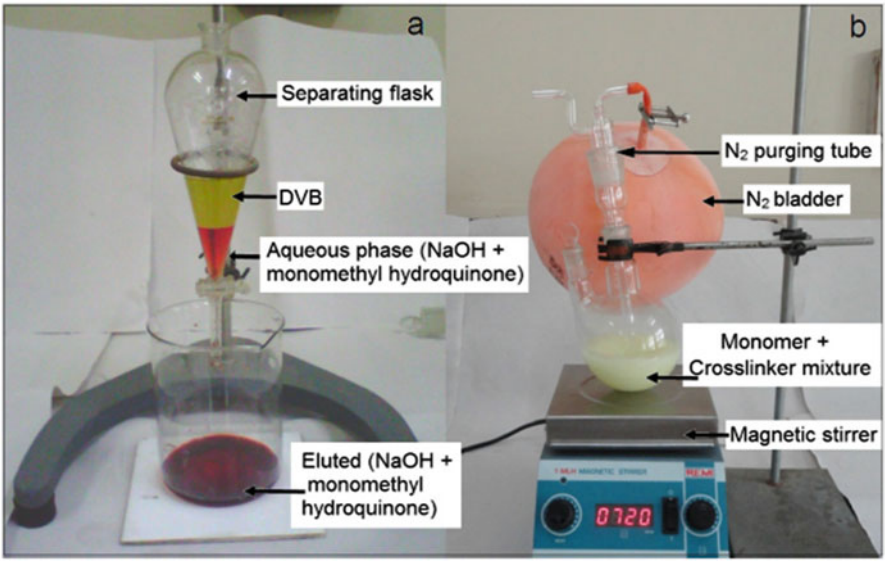

Fig. 1 (**a**) Purification of DVB; (**b**) monomer-cross-linker mixture (Gonte 2013)

monomer solution was added to this reaction vessel containing aqueous solution saturated with sodium chloride and in situ formed magnesium hydroxide from the reaction between magnesium chloride and sodium hydroxide, under continuous agitation at 60 °C (Deb and Mathew 1996). The water-to-monomer ratio was kept to 4:1 during polymerization. The monomer droplets converting to polymer particles were prevented from coalescing by continuous agitation and optimized $Mg(OH)_2$ formation (suspension stabilizers).

Characterization

The density and cross-linking density of the synthesized cross-linked SMA beads were determined. The conversion of maleic anhydride to maleic acid and the functional group analysis of the copolymer were carried out using FTIR (Shimadzu Model FTIR-8400). JEOL ASM 6360A scanning electron microscope (SEM) was used to study the structural morphology. Thermogravimetric analysis was carried out using a thermal analyzer (Shimadzu Model TGA-50) to determine the thermal stability of the copolymer beads. Swelling capacity of the SMA beads was determined in ethanol.

Cross-Linked SMA as Adsorbent

Preparation of Metal Ion and Dye Solution

Single metal ion stock solutions (2000 mgL^{-1}) were prepared dissolving the copper sulphate pentahydrate ($CuSO_4 \cdot 5H_2O$), cobalt chloride ($CoCl_2 \cdot 6H_2O$), nickel sulphate ($NiSO_4 \cdot 6H_2O$), zinc sulphate ($ZnSO_4 \cdot 7H_2O$) and chloroauric acid ($HAuCl_4 \cdot 3H_2O$) salts in 1000 mL water. Stock solution of Congo red dye and direct red dye was prepared with concentration of 100 mgL^{-1} in water. The various experimental concentrations were then obtained by diluting the stock solution.

Batch Adsorption Experiments

The adsorption of Zn(II) ions was carried out by using 0.5 g beads soaked in 30 mL $ZnSO_4$ solution of various concentrations (200 mgL^{-1}, 250 mgL^{-1} and 500 mgL^{-1}) for 2 h, and at the end of the desired set time duration, 1.0 mL of supernatant solution was used to detect the concentration of the metal ions remaining in the solution. The effect of solution pH on adsorption was observed for a batch of 0.5 g SMA in 30 mL solution of concentration 100 mgL^{-1}. The amount of SMA beads was also varied from 0.2 to 1.0 g for fixed metal ion concentration (250 mgL^{-1}) for 2 h to obtain another set of data. The concentration of the metal ions was evaluated

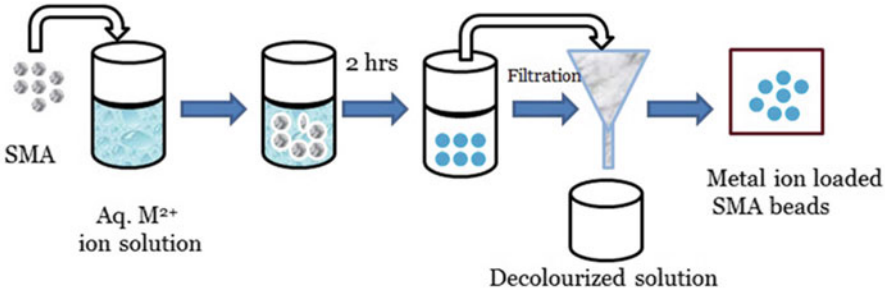

Fig. 2 Schematic presentation of batch adsorption process (Gonte 2013)

by titrating fixed volume of Zn(II) solution at specific time interval against standard EDTA solution (Gonte et al. 2011a, b). For Cu(II), Co(II), Ni(II), Au(III) ions, Congo red and direct red dye, adsorption was determined spectrophotometrically at 720 nm, 510 nm, 660 nm, 310 nm, 500 nm and 500 nm, respectively. The schematic presentation of the batch adsorption study is as shown in Fig. 2.

SMA Biocomposites

Synthesis of SMA-Sawdust (SMA-SD) Composites

The composite of styrene-maleic acid sawdust (SMA-SD) was synthesized by suspension polymerization as described in copolymer synthesis. Sawdust was washed in distilled dihydrogen monoxide to abstract any adhering impurities, dried and sieved. The homogeneous coalescence of organic monomers, i.e. styrene, MAn, DVB and free radical initiator AIBN (0.8 wt% predicated on monomers), was yare in MIBK solvent. The aqueous phase consisting of saturated salt solution (NaCl, $Mg(OH)_2$) was yare in reaction vessel. The two phases were commixed together under inert conditions. When the gel point of the polymerization was achieved at about 70 °C, fine sawdust (by wt%) was integrated to the polymerization cumulation and stirred at 800 rpm to obtain the composite beads of 300–600 μm. These SMA-SD composite beads were then isolated from the aqueous phase and washed perpetually with dihydrogen monoxide, followed by toluene, to abstract unreacted monomers and with dilute hydrochloric acid for abstraction of magnesium hydroxide and determinately dihydrogen monoxide washed to abstract the acid and salts adhering to the surface of the polymer beads (Shelar et al. 2011).

Synthesis of SMA-Sugarcane (SMA-SM) Composites

Sugarcane molasses were obtained and washed repeatedly with distilled water, dried and sieved. The composites of styrene-maleic acid-sugarcane molasses (SMA-SM) were synthesized by the above mentioned process.

Batch Adsorption of Metal Ions and Dyes

Spectroscopic detection and quantification method as described in batch adsorption experiments was used for batch adsorption process for removal of dye (Congo red dye) and inorganic pollutants (Cu(II), Ni(II) and Co(II) ions) from aqueous solution. 100 mgL^{-1} concentrations of the dye were prepared as the stock solution, while the stock metal ion solution was of concentration 1000 mgL^{-1}. Cu(II), Co(II), Ni(II) and Congo red dye were determined spectrophotometrically at 720 nm, 510 nm, 660 nm and 500 nm, respectively.

Chemically Modified SMA Beads

Synthesis of SMA Metal-Organic Frameworks

SMA-metal-organic frameworks were synthesized by a slight modification of the literature method of slow diffusion of TEA (Li et al. 1998). Briefly, dimethylformamide (DMF) solution containing $Zn(NO_3)_2.6H2O$ and dicarboxylic acid in a ratio of 1:2 mole % was diluted using toluene. The requisite amount of SMA beads was allowed to swell in this solution. The mixture was placed under reduced pressure for 5 h to ensure complete filling up of pores of SMA beads. After 5 h, the supernatant liquid was decanted, and slow vapour diffusion of triethylamine (TEA) in toluene was allowed. The system was sealed and kept undisturbed for 2 days at room temperature 300 K. SMA beads were then washed with DMF and dried under vacuum at 50 °C to constant weight. Three different dicarboxylic acid linkers, namely, 1,4-benzenedicarboxylic acid (BDC), 1,6-naphthalenedicarboxylic acid (NDC) and 1,8-biphenyldicarboxylic acid (BPDC), were used in the formation of MOFs with Zn(II) as the central metal ion. The schematic formation of Zn-SMA-DCA frameworks is shown in Fig. 3.

In another method of formation of SMA-MOFs, no additional dicarboxylic acid was used. Instead the Zn(II) ions were allowed to react with the carboxylic acid groups of SMA to form Zn(II) SMA complexes or Zn-SMA metal-organic frameworks (Deb et al. 2005; Gonte et al. 2011a, b). The schematic presentation is shown in Fig. 4.

Synthesis of SMA Polyaniline Semi-interpenetrating Networks

The synthesis of SMA-PANI semi-interpenetrating networks was based on a literature report by P C Deb (Deb et al. 2005). Benzoyl peroxide was recrystallized from 1:1 chloroform/methanol solution. Aniline was vacuum distilled prior to use. The semi-IPNs were synthesized by oxidative polymerization of aniline with benzoyl peroxide. The oxidative polymerization of aniline to polyaniline (PANI)

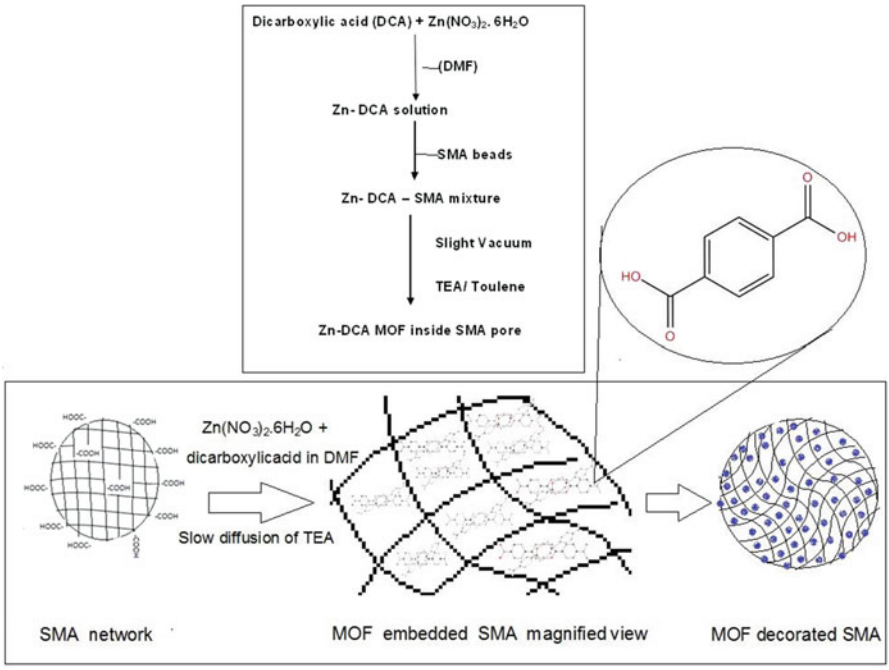

Fig. 3 Schematic representation of formation of Zn-SMA-DCA MOFs (Gonte 2013)

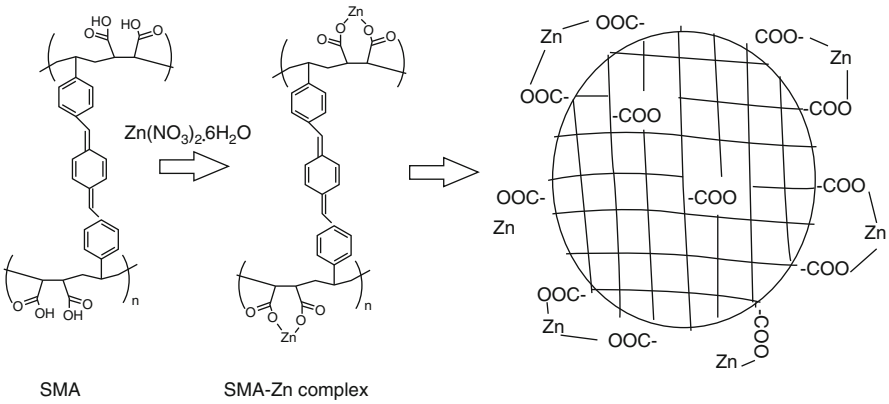

Fig. 4 Schematic representation of formation of Zn-SMA-MOFs (Gonte 2013)

is known to form emaraldine type of polyaniline. The schematic representation of which is shown in Fig. 5.

Known weight of SMA microspheres was suspended in acetone solution containing 0.6 M benzoyl peroxide and evacuated to remove entrapped air as well as to allow easy entry of BP solution inside the pores of SMA beads.

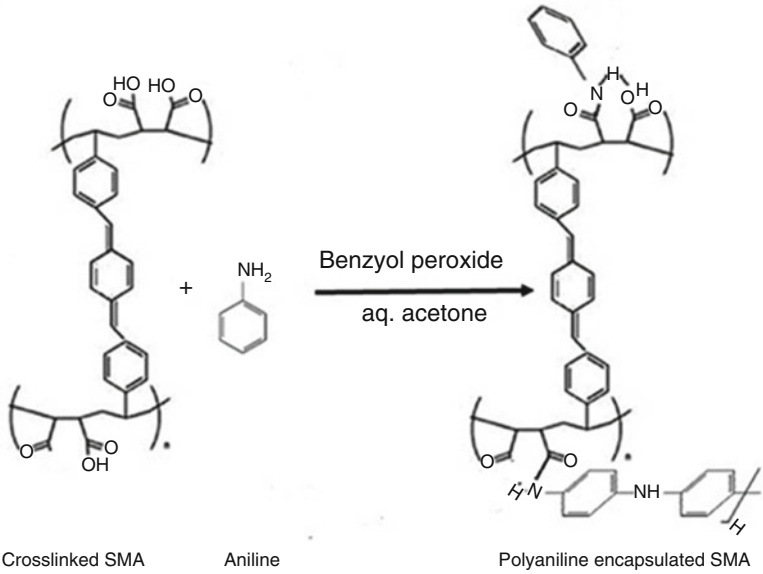

Fig. 5 Schematic representation of formation of SMA-PANI semi-IPNs (Gonte 2013)

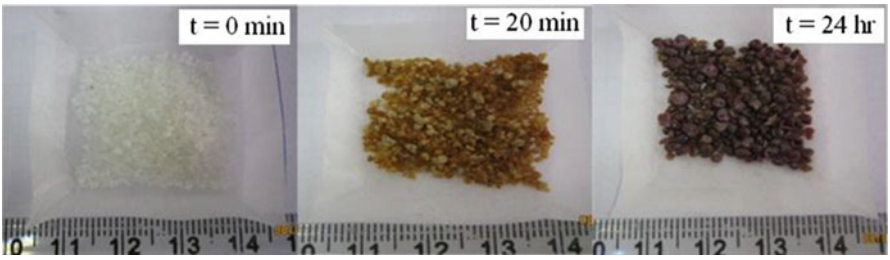

Fig. 6 Colour displayed by SMA beads during formation of SMA-PANI semi-IPNs (Gonte 2013)

The copolymer beads were then repeatedly washed with acetone to remove excess of BP. These microspheres were then added to aqueous acetone solution of freshly distilled aniline, and the mixture was stirred slowly but continuously for 24 h. The colour of the SMA beads changed from pale yellow to brown black in 15 min on stirring indicating the start of polymerization of aniline. The colour of the beads was further changed to purple black indicating polyaniline formation after 24 h as shown in Fig. 6. The solution containing fine black particles was decanted off, and the copolymer was purified by continuous soxhlation using acetone and then dried at 50 °C under reduced pressure to constant weight (Gonte et al. 2011a, b).

Characterization of Chemically Modified SMA Copolymer Beads

The modified SMA beads were characterized using Fourier transform infrared (FTIR) spectroscopy, scanning electron microscopy (SEM), thermogravimetric analysis (TGA) and swelling capacity in ethanol.

Hydrogen Adsorption

Hydrogen gas adsorption studies were carried out using SORPTOMATIC 1990 instrument (Thermo Finnigan, Italy), which records the fall of pressure and automatically converts the same into amount of gas adsorbed as per ASTM standards. The instrument was standardized with hydrogen and nitrogen to determine the dead volume. About 0.7 g of beads was evacuated (10–6 torr) at 343 K for 2 h in a previously evacuated glass sample holder to ensure cleanliness of surface and availability of clean pores for adsorption. A typical measurement for sample was continued for about 24 h at room temperature 300 K.

Result and Discussion

Cross-Linked SMA Beads

Effect of Experimental Parameters

Under the optimized reaction conditions, five different compositions of the cross-linked SMA beads were synthesized by varying the cross-linker content in the reaction mixture which is summarized in Table 1. The yield for all the compositions was found to be almost constant (≈70%). The size of the cross-linked copolymer beads was found to be highly influenced by the stirring speed of the overhead stirrer. The effect of rpm on the bead diameter was investigated by carrying out the speed of the overhead stirrer to 400 rpm, 600 rpm and 800 rpm. The organic phases, when stirred with the aqueous phase under varying agitation speed, dispersed the monomers in the form of minute droplets along with the aqueous phase. The size of the droplet formed thus controls the bead diameter. During polymerization process, the viscosity of the medium also increases, and at the gel point, beads start to gain

Table 1 Synthesis data for SMA copolymer beads

Polymer designation	A1	A2	A3	A4	A5
S:MA (mole ratio)	1:1.6	1:1.6	1:1.6	1:1.6	1:1.6
S:DVA (mole ratio)	1:0.26	1:0.41	1:0.53	1:0.66	1:0.80

Table 2 Effect of agitation speed on the bead size

rpm	400	600	800
Bead dia (μ)	800–1000	300–500	200–400

Table 3 Calculated parameters of the SMA copolymer beads

Copolymer	Density (ρ) (g/mL)	Pore volume (V_p) (mL)	Porosity (Φ)	Crosslink density ($\times 10^{-3}$)
A1	0.892	1.878	1.565	8.980
A2	0.909	2.176	1.813	9.543
A3	0.919	1.918	1.598	11.546
A4	0.933	1.715	1.429	11.748
A5	0.951	1.645	1.370	11.344

shape. The control of rpm at and after this stage of polymerization is particularly important. It was observed that, with stirring speed of 200 rpm, there was a tendency of the beads to adhere post-polymerization, resulting in formation of a hard mass. The bead diameter as a function of controlled rpm control is presented in Table 2.

True Density, Pore Volume, Porosity and Cross-Link Density

True Density

Cross-linked SMA copolymer beads (1.0 g) were dried to constant weight (W_o) and placed in a 10 mL specific gravity bottle of known weight at 27 °C. Ethanol (7.0 mL) was added to this bottle, and the mixture was maintained under identical conditions for 24 h at 27 °C. The specific gravity bottle was then filled with ethanol and weighed carefully (Wan et al. 2004). The true density of the cross-linked SMA beads was calculated and is summarized in Table 3.

$$\rho = \frac{W_o}{10 - \frac{W_1 - W_0}{ds}}$$

where W_1 is the total weight of beads and solvent and ds is the density of solvent (ds = 0.789 g/mL).

Pore Volume and Porosity

Known amount of SMA beads were placed in a sintered glass tube, and the entire assembly was placed in ethanol at 27 °C for 24 h. The excess solvent was removed and volume of ethanol absorbed by the beads was estimated V_p was estimation; porosity (Φ) of the beads was calculated following methods of Rosenberg et al. (1983), Greig and Sherrington (2003) and Wan et al. (2004) as follows:

$$V_p = \frac{W_o}{\rho}$$

$$\varnothing = \frac{V_p}{V_o}$$

where V_p is the pore volume in the beads, V_o is the true volume of the beads, W_o is the weight of dry beads and ρ is the true density of the polymer.

Cross-Link Density

The cross-linking density ρ_c of the cross-linked SMA beads was calculated from the Flory-Rehner equation (Wan et al. 2004):

$$\rho_c = \frac{1}{(2M_C)^{-1}}$$

where M_c is the average molecular weight per cross-linking unit calculated as

$$M_C = \frac{\left[\rho \times V_S \times \left(V_r^{\frac{1}{2}} \frac{V_R}{2}\right)\right]}{-\left[\ln(1 - V_r) + V_r + \chi V_r^2\right]}$$

where V_r is the volume of polymer in the swollen state equilibrium, χ is the polymer solvent interaction parameter taken as 0.5, V_s is the molar volume of solvent and ρ is the true density of the polymer.

CHNS-Elemental Analysis

The CHN analysis of the cross-linked beads was performed in CHNS analyzer, Elementar Vario 111. The elemental analysis of total carbon and hydrogen provides the composition of the polymeric matter. It could be clearly seen from the obtained data (Table 4) that the carbon content of the copolymer beads increases with increase in the cross-linker (DVB) concentration of copolymer compositions. The carboxyl content of the polymer is reduced due to introduction of high density of

Table 4 Elemental composition of the copolymer beads

Copolymer	%C	%H	%O
A1	80.26	7.709	12.031
A2	83.11	8.033	8.857
A3	83.56	8.102	8.857
A4	81.35	7.531	11.119
A5	85.56	8.042	6.398

cross-linking. The elemental analysis data indicates the presence of 1.879, 1.383, 1.302, 1.737 and 0.999 millimoles of maleic acid per gram of polymer A1, A2, A3, A4 and A5, respectively. However, sudden increase in carboxyl content was observed with A4 beads. This may be due to pronounced association of cross-linker and maleic anhydride leading to higher content of acid in the copolymer. Increasing the DVB content increases the cross-linking intensity and porosity of the networks (Gonte et al. 2012).

FTIR Spectroscopic Analysis

The FTIR spectra of the cross-linked SMA beads were recorded on Shimadzu spectrophotometer to confirm the presence of carboxylic acid and styrene functional groups in the synthesized polymer (Fig. 7).

The FTIR spectra show the presence of peaks around 2930 and 2840 cm^{-1} corresponding to the asymmetric and symmetric stretch of C-H_2, while the peak positioned at 2930 cm^{-1} corresponds to the OH stretch of carboxylic acid. The presence of 3500 cm^{-1} and 1710 cm^{-1} (shoulder peak) confirmed the free acid formed after hydrolysis of anhydride groups of cross-linked copolymer, and the broad band peak around 3000 cm^{-1} indicates the presence of high concentration of COOH groups. Bands at 3000 cm^{-1}, 2920 cm^{-1} and 2850 cm^{-1} correspond to the asymmetric and symmetric C-H stretch, and the peaks around 1943–1728 cm^{-1}

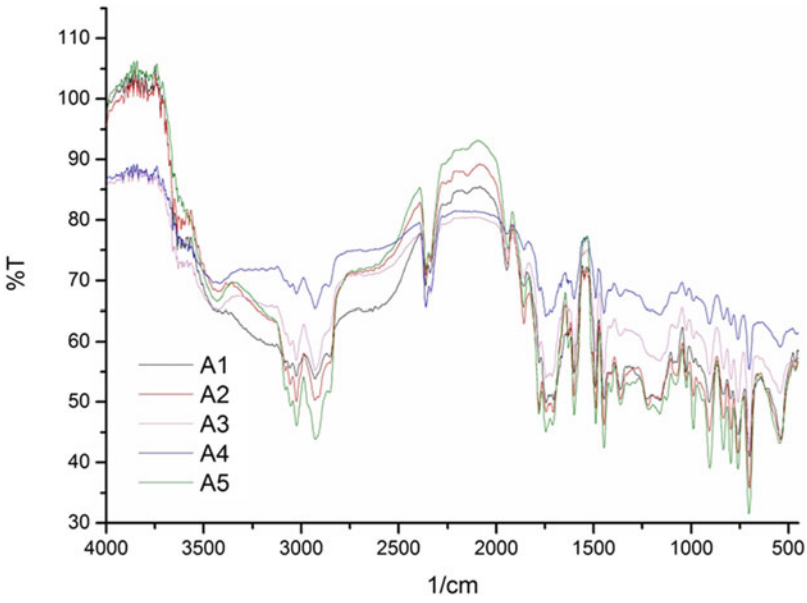

Fig. 7 IR spectra of cross-linked copolymer beads (Gonte 2013)

correspond to the aromatic ring substitution of styrene groups. The peaks within range 3100–3000 cm^{-1} correspond to aromatic stretching vibrations. Peaks at 1461 cm^{-1} and 1561 cm^{-1} represent C = C (stretch) of the aromatic ring and carboxylate ion peak, respectively. Absorption peak at 3020 cm^{-1} characterizes =C-H stretching for aromatic fragments. Thus the presence of both maleic acid and styrene groups in the copolymer beads was confirmed from the IR specta for all the 05 compositions of cross-linked SMA beads.

SEM Analysis

The SEM analysis of the copolymer beads was performed to analyze the variation occurred by increasing the cross-linker content in the beads. The SEM images of the copolymer beads were obtained by coating the beads with an ultrathin coating of electrically conducting material (platinum) either by low-vacuum sputter coating or by high-vacuum evaporation. These coated samples were then mounted on the SEM moulds and scanned. The low-magnification SEM images confirmed the spherical shape of the beads, while the magnified micrographs revealed the presence of fissures, flow lines, micropores and voids. Increase in the microporosity and development of well-defined flow lines were observed with increase in the DVB content in the polymer beads as can be seen from Fig. 8.

The SEM images also indicate the increased compact packing observed in the beads with increasing divinylbenzene content suggesting the establishment of rigid interpenetrating network formation and increased cross-linking. Homogeneity in the pore size is also observed with increase in cross-linking, and thereby distinct fineness is introduced in the internal structure (Gonte et al. 2012). The SEM micrographs were then analyzed using the Biovis Material Plus software to estimate the pore size and pore density. The micrographs show uniform distribution of pores in size up to 75 μm.

Thermogravimetric Analysis

The thermogravimetric analysis showed that the cross-linked copolymer is thermally stable up to 400 °C (Gonte et al. 2011a, b), and complete decomposition occurs after 450 °C as can be observed from Fig. 9. The initial slight notch observed at around 220 °C is due to the decomposition of maleic acid to maleic anhydride which remains as the residue after even complete combustion of the copolymer and is reflected as residual weight. The shape decrease in the temperature around 400 °C corresponds to the decomposition of styrene groups of the copolymer. The nature of curve with the various compositions of the SMA beads follows a similar pattern indicating that the increased DVB content shows no significant effect on the thermal stability of the copolymer.

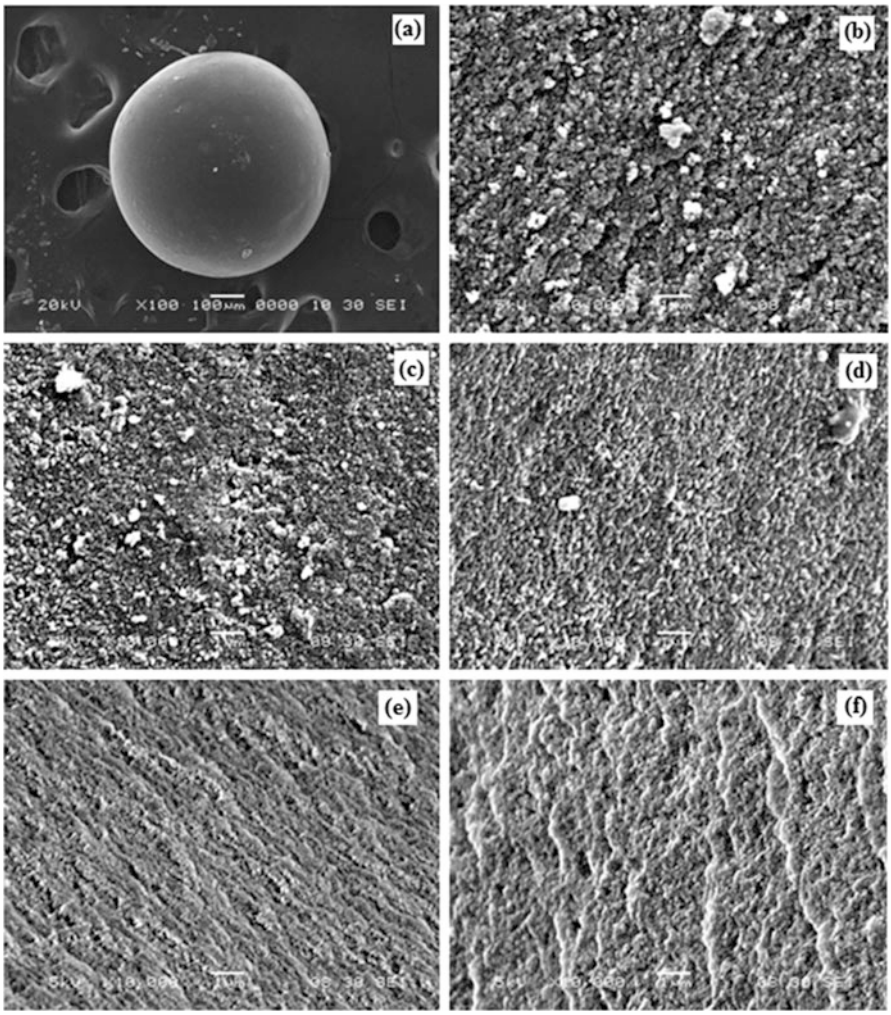

Fig. 8 SEM micrograph of the samples; (**a**) low-magnification SEM image of SMA; high magnification micrographs of (**b**) A1, (**c**), A2 (**d**), A3 (**e**), A4 and (**f**) A5 (Gonte 2013)

Cross-Linked SMA as Adsorbent

Characterization of the Metal Ion-Loaded SMA Copolymer Beads

The SEM images of the metal ion-adsorbed SMA beads showed no significant change in the morphology of the beads. The presence of the metal ion in the adsorbents was observed around the fissures and voids on the external surface of the beads. The presence of the metal ions in the beads was confirmed from the EDX analysis. The FTIR spectra indicated the slight decrease in the intensity of the

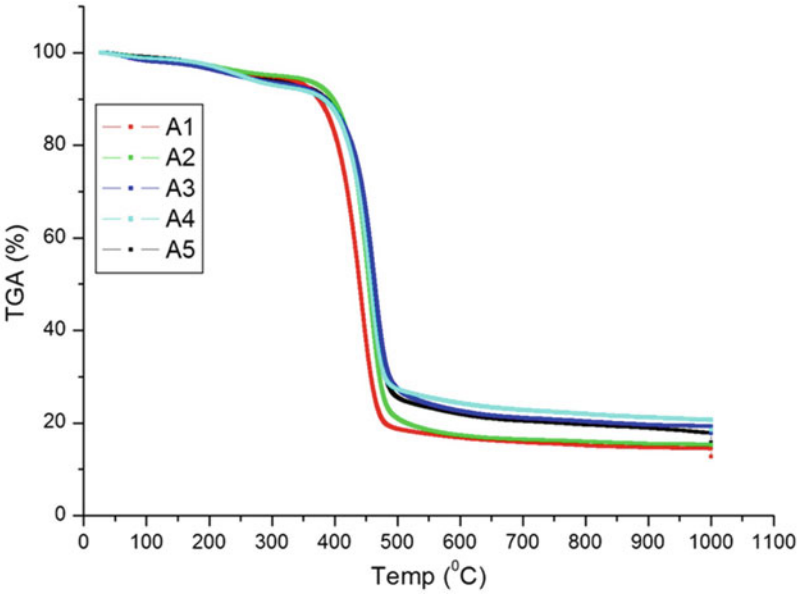

Fig. 9 Thermogravimetric curves of SMA beads (Gonte 2013)

carboxylate ion 1710 cm^{-1} peak noted after adsorption and complex formation between the metal ions and carboxyl group of the beads. The formation of varying colours of the beads on adsorption of Au(III) ions indicated the formation of nanogold within the polymer matrix which was confirmed from the XRD analysis. The XRD pattern for the Au(III) ion-embedded polymer matrix revealed the peaks with d spacing of 2.3427, 1.4388 and 1.2612. The appearance of these diffraction peaks in the gold ion-adsorbed SMA bead, indicates the presence of pure gold in nano form embedded into the polymer matrix (Gonte et al. 2011a, b). This reduction of Au(III) to Au(0) was observed due to the presence of trace amount of sodium ions entrapped in the polymer matrix during synthesis as an impurity. The XRD analysis of the metal ion-adsorbed beads is shown in Fig. 10. The XRD analysis of the metal ion-adsorbed beads shows the peak corresponding to d spacing of 4.04, 2.66, 2.47 and 1.96 for Cu(II) complexes; d spacing of 8.57, 5.57, 5.03 and 3.36 for Co(II) complexes and d spacing of 2.64, 2.188 and 1.16 for Ni(II) complexes with SMA beads (Sicilia-Zafrac et al. 1999; Deshdmukh and Deshpande 2011). Additionally, the core sizes of the embedded nanogold were deduced from the SAXS data. The small-angle X-ray scattering confirmed the presence of spherical agglomerates with typical radius of 48 nm and presence of larger aggregates of size in the range of 200 nm.

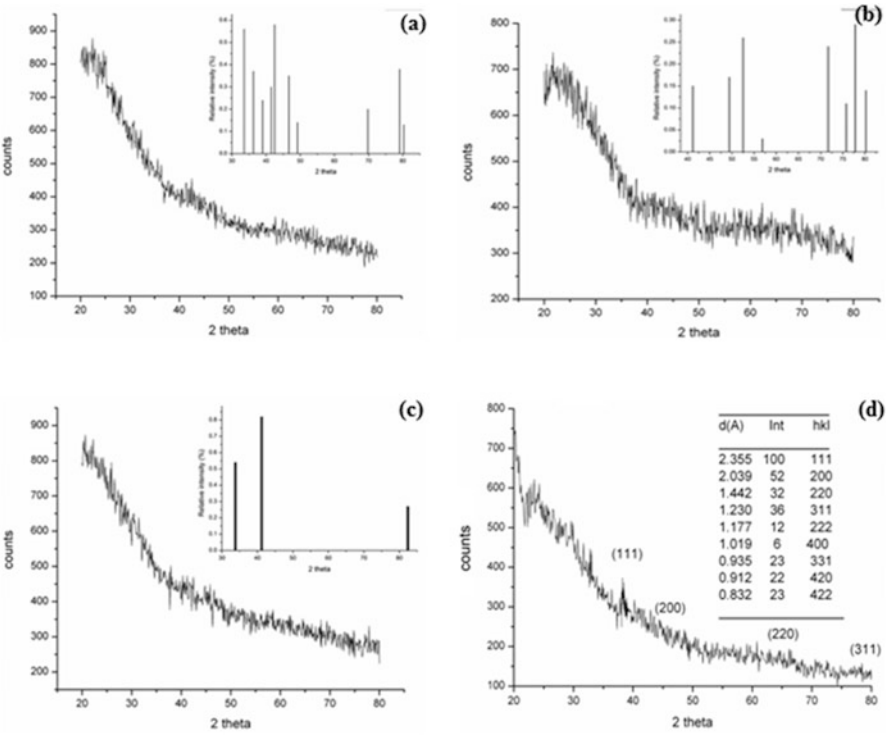

Fig. 10 XRD spectrum of SMA complexes with (**a**) Cu(II), (**b**) Co(II), (**c**) Ni(II) and (**d**) Au(III) (Gonte 2013)

Effect of pH

The removal of metal ions from aqueous solutions by adsorption was found to be highly dependent on the pH of the solution. Adsorption of Cu(II), Co(II), Zn(II) and Ni(II) ions was observed for increases with an increase in the pH from 4.0 to 8.0 as shown in Fig. 11. The decrease in the adsorption below pH 6 can be explained by the fact that at pH below 6.0, the H_3O+ ions present in the aqueous solutions compete with the free metal ions for the active sites with carboxylic groups. The carboxyl groups get protonated which block the site for adsorption, and further the steric hindrance created by the protonation of acid decreases the metal ion uptake. The increase in the adsorption efficiency of the SMA with increase in pH from 4.0 to 7.0 was observed in case of all four metal ions, which suggests that the mechanism of uptake is same in all cases. In the case of Congo red and direct red dye, adsorption was attempted at its neutral pH 7.0 since both these dyes were found to be chemically and structurally stable at this pH. Drastic colour change was noticed even with slight change in pH.

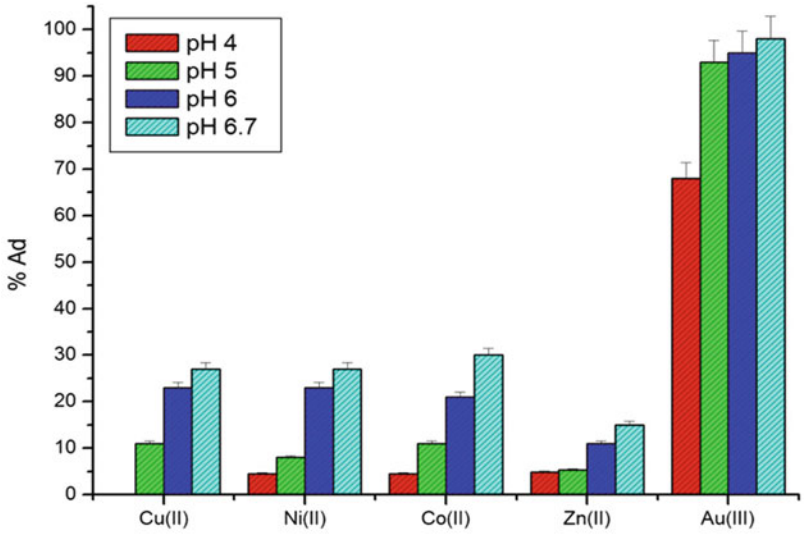

Fig. 11 pH-dependent adsorption for SMA beads (Gonte 2013)

Effect of SMA Copolymer Dose

An increase in the amount of adsorbents leads to a significant increase in the active sites which shows an enhanced adsorption of various metal ions and dyes. Thus, it was observed that adsorption increases with increase in SMA dose of 0.1 g–1.0 g (Fig. 12). However, further increase in sorbent dose showed no significant increase in adsorption. This can be attributed to the presence of very low concentration of metal ions/dyes in the solution such that the equilibrium is achieved, and no further adsorption occurs. Removal of metal ions increases with increased adsorbent dosage due to increase in active sites.

Equilibrium Adsorption Isotherms

The distribution of adsorbed chemical species between the liquid phase and the solid phase at equilibrium state was studied by fitting the obtained experimental equilibrium data to the various adsorption isotherm models, namely, Langmuir model, Freundlich model, Temkin model and Dubinin-Radushkevich (D-R) model. Adsorption isotherm graphs, i.e. equilibrium adsorption capacity (q_e) versus equilibrium concentration of the residual metal ions/dye in the solution (C_e), were plotted. The equilibrium adsorption capacity was calculated using the equation:

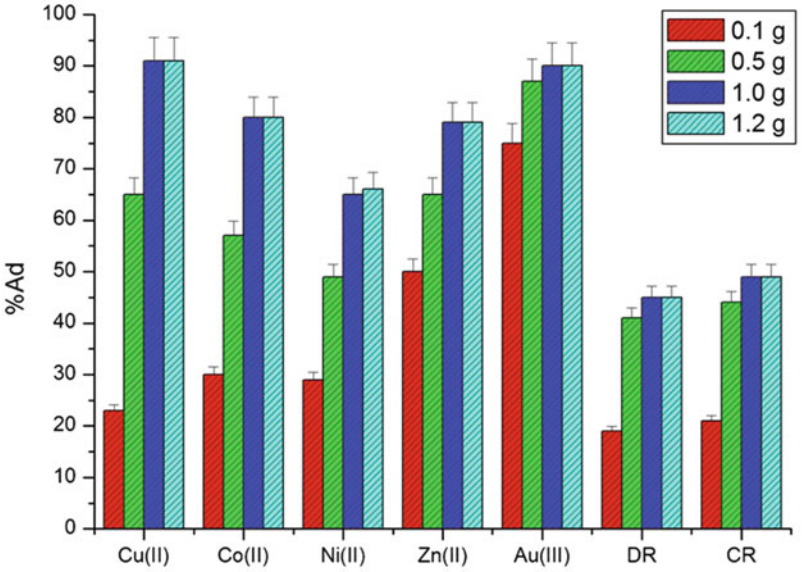

Fig. 12 Effect of SMA dose on adsorption of metal ions/dyes (Gonte 2013)

$$q_e = \frac{(C_0 - C_e)}{V} \times M$$

where q_e (mgg^{-1}) is the equilibrium adsorption capacity, C_o and C_e are the initial and equilibrium concentration (mgL^{-1}) of metal ions/dye in solution, V (L) is the volume of solution and M (g) is the weight of the adsorbent used.

Langmuir Isotherm Model

Langmuir model postulates monomolecular layer adsorption without any interaction between the adsorbed molecules, and linearized form of this equation is represented as (Hostetler et al. 1998):

$$\frac{C_e}{q_e} = \frac{1}{q_{max} \times K_L} + \frac{C_e}{q_{max}}$$

where C_e is the equilibrium concentration (mgL^{-1}), q_e is the amount of metal ion sorbed (mgg^{-1}), q_{max} is q_e for a consummate monolayer (mgg^{-1}) and K_L is a constant cognate to the affinity of the binding sites (Lmg^{-1}).

The plot of C_e/q_e versus C_e as shown in Fig. 13 yields the Langmuir constants q_{max} and K_L. R_L is calculated from the initial conc. of metal ion/ dye as:

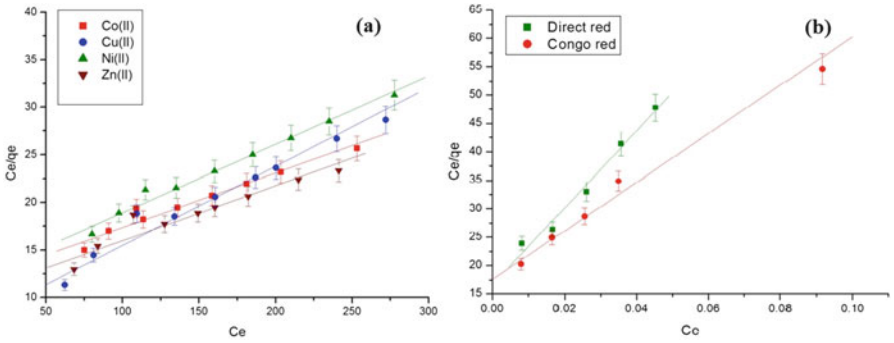

Fig. 13 Langmuir plots for adsorption of (**a**) metal ion (**b**) dyes (Gonte 2013)

$$R_{\mathrm{L}} = \frac{1}{1 + (K_{\mathrm{L}} \times C_0)}$$

The R_{L} value obtained for all the metal ions and dyes are greater than zero and less than unity indicating that the adsorption occurs as monolayer adsorption onto the heterogeneous/microporous surface of the SMA beads. The regression coefficient values of Cu (II), Co (II), Ni(II), Zn(II), Au(III), direct red and Congo red are 0.9755, 0.9798, 0.9896, 0.9548, 0.9813, 0.9905 and 0.9911, respectively. The high regression coefficient values of 0.97–0.99 indicate a high correlation between the experimental and theoretical data.

Freundlich Isotherm Model

The Freundlich isotherm model postulates adsorption occurs on heterogeneous surfaces and adsorption capacity is cognate to the concentration of metal ions at equilibrium. The linearized form of Freundlich equation is:

$$\ln q_{\mathrm{e}} = \frac{1}{n} \times \ln C_{\mathrm{e}} + \ln K_{\mathrm{F}}$$

where q_{e} and C_{e} are the equilibrium concentrations of metal ions in adsorbed (mg/g) and liquid phases (mg/L), respectively. K_{F} and n are the Freundlich constants related to adsorption capacity and intensity, respectively.

The plot of ln q_{e} versus ln C_{e} is shown in Fig. 14 and yields the value of Freundlich constant n and K_{F}. A favourable adsorption is indicated from the values of the order Cu(II) > Au(III) > Ni (II) > Zn (II) > Co (II) > Congo red > direct red. The regression coefficient values of Cu (II), Co (II), Ni(II), Zn(II), Au(III), direct red and Congo red are 0.9939, 0.9792, 0.9972, 0.9994, 0.9988, 0.9919 and 0.9948, respectively. The regression coefficients ($\approx$ 0:99) also indicate a high correlation of the experimental data with the theoretical calculations.

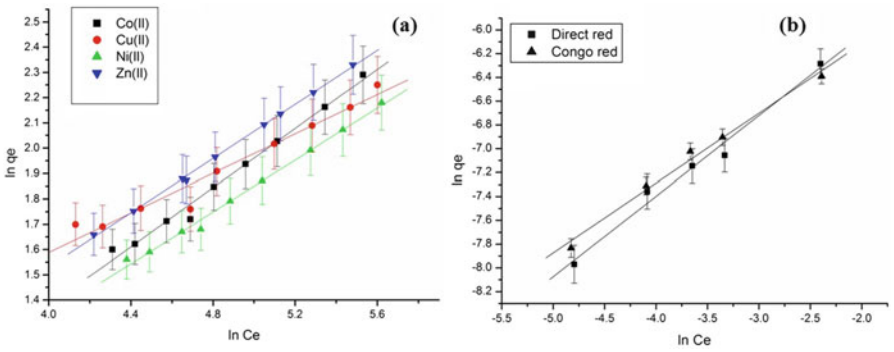

Fig. 14 Freundlich plots for adsorption of (**a**) metal ions and (**b**) dyes (Gonte 2013)

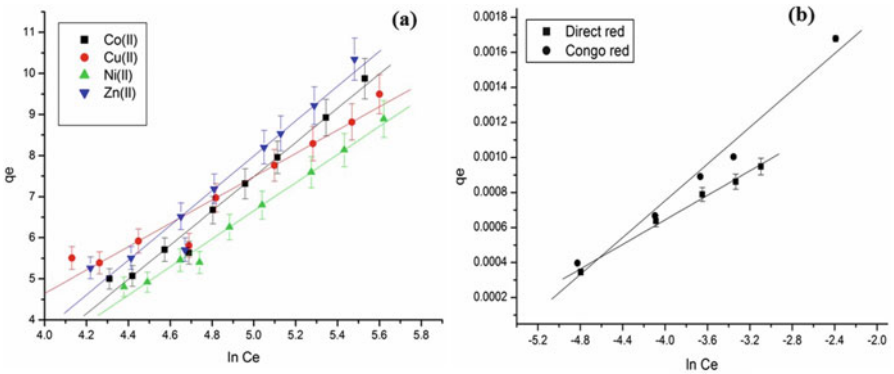

Fig. 15 Temkin plots for adsorption of (**a**) metal ions, (**b**) Au(III) ions and (**c**) dyes (Gonte 2013)

Temkin Isotherm Model

The effects of heat of adsorption that decrements linearly with coverage of the adsorbate and adsorbent interactions are postulated by the Temkin's model which is represented as:

$$q_e = \frac{RT}{bT} \times (\ln \alpha T) + \frac{RT}{bT} \times \ln C_e$$

where R is the gas constant 8.314×10^{-3} kJ mol^{-1} K^{-1}, T is the absolute temperature K, bT is the Temkin constant related to the heat of adsorption (kJmol^{-1}) and αT is the equilibrium binding constant corresponding to the maximum binding energy (l/g).

The linear plots of q_e versus log C_e determines the constants αT and bT (Fig. 15). The regression coefficient values of Cu (II), Co (II), Ni(II), Zn(II), Au(III), direct red and Congo red are 0.9743, 0.9896, 0.9936, 0.9760, 0.9810, 0.9959 and 0.9875, respectively. The satisfactory linear fit obtained for all metal ions and dyes is indicated from the regression coefficient values.

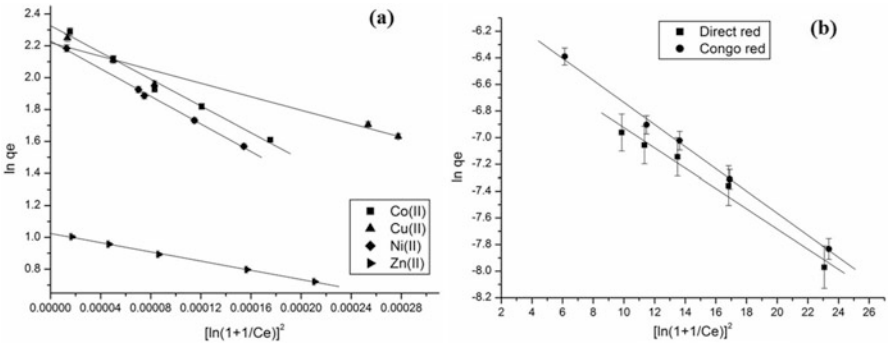

Fig. 16 Dubinin-Radushkevich plots for adsorption of (**a**) metal ions and (**b**) dyes (Gonte 2013)

Dubinin-Radushkevich (D-R) Isotherm Model

Dubinin-Radushkevich models estimate the mean free energy of adsorption. The linearized form of the D-R equation is represented as:

$$\ln q_e = \ln q_{max} - K\epsilon^2$$

where K (mo l^2 kJ^{-2}) is a constant related to the mean adsorption energy and ϵ is the Polanyi potential, calculated from equation:

$$\epsilon = RT \ln\left(1 + \frac{1}{C_e}\right)$$

The plot of ln q_e versus ϵ^2 (Fig. 16) yields the constant K, which presages the mean free energy E of adsorption per molecule of the adsorbate when it is transferred to the surface of the solid from illimitability in the solution. The regression coefficient values of Cu (II), Co (II), Ni(II), Zn(II), Au(III), direct red and Congo red are 0.9743, 0.9896, 0.9936, 0.9760, 0.9810, 0.9959 and 0.9875, respectively. The adsorption is assumed to be physisorption in the early stages followed by chemisorption of the chemical species involved.

Kinetic Studies

Kinetic experiments were conducted to determine the adsorption mechanism and the potential rate-controlling steps. These kinetic results also enable to select the optimum condition for full-scale batch adsorption process. The rate constants were calculated by using the conventional rate expression. The amount of metal ion/dye sorbed, q_t, was calculated as:

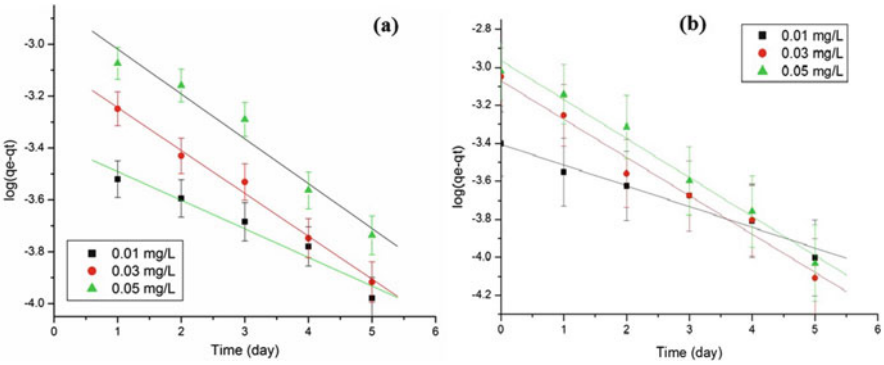

Fig. 17 Pseudo-first-order plots for adsorption of (**a**) direct red and (**b**) Congo red dye (Gonte 2013)

$$q_t = \frac{(C_o - C_t)}{M} \times V$$

where q_t (mg/g) is the equilibrium adsorption capacity.

Pseudo-First-Order Kinetic Model

This kinetic model assumes that rate of adsorption of solute on the adsorbent is based on the adsorption capacity. The pseudo-first-order rate equation is given as:

$$\log(q_e - q_t) = \log q_e - \frac{k_1}{2.303} \times t$$

where k_1 is the first-order adsorption rate constant (min^{-1}). The graph of log ($q_e - q_t$) versus t gives a straight line plot (Fig. 17) with negative slopes from which the pseudo-first-order rate constant is calculated. The correlation coefficient values of dyes (0.99) obtained by this method show good quality of linearization.

Pseudo-Second-Order Kinetic Model

The pseudo-second-order kinetic models correlate between the amount of metal ions/dye on the adsorbent surface and its amount adsorbed at equilibrium. The rate is directly proportional to the number of active surface sites, which is calculated as:

$$\frac{t}{q_t} = \frac{1}{k_2 \times {q_e}^2} + \frac{1}{q_e} \times t$$

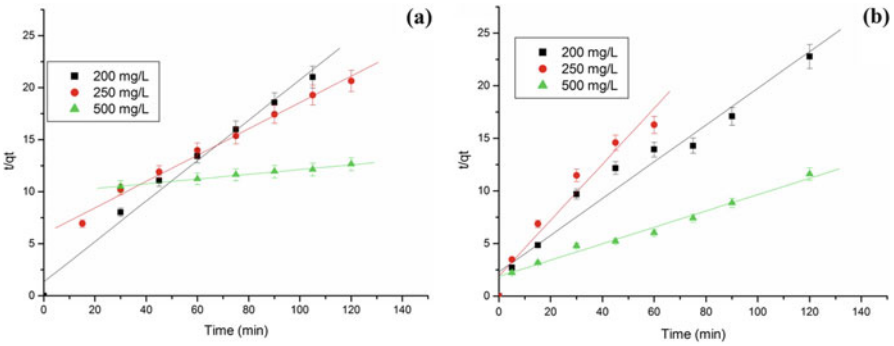

Fig. 18 Pseudo-second-order plots for adsorption of (**a**) Cu(II) and (**b**) Zn(II) ions (Gonte 2013)

where k_2 is the second-order adsorption rate constant ($gmg^{-1}\ min^{-1}$). The constant k_2 is used to calculate the initial sorption rate h (mg/ (g min)), at $t \rightarrow 0$ as follows:

$$h = k_2 \times {q_e}^2$$

The application of the pseudo-second-order kinetics by plotting t/q_t versus t (Fig. 18) yielded the second-order rate constant k_2. The calculated q_e values for Cu(II) and Zn(II) agree very well with the experimental values as compared to other metal ions and dyes; however, the correlation coefficient obtained for all the adsorbates gives best fit linearized plots.

Adsorption Mechanism

The mechanism involved in the adsorption of metal ions and dyes onto the SMA beads was identified by fitting the experimental data to the intraparticle diffusion plot, a graph of q_t versus $t^{1/2}$ (Fig. 19) from the equation:

$$q_t = K_{int} \times t^{1/2}$$

where K_{int} is the intraparticle diffusion rate constant ($mgg^{-1}\ min^{-0.5}$).

The first sharper portion is the external surface adsorption, the second portion is the gradual adsorption stage and the third step is the final equilibrium stage. The three-step adsorption process was observed only for the metal ions, whereas for dyes only two-step adsorption was indicated without achieving the final equilibrium stage.

Desorption Studies

The reusability of the SMA beads was tested by observing the desorption of the various metal ions and dyes from the cross-linked SMA bead surface using hydrochloric acid solutions. Desorption ratio was calculated from the equation:

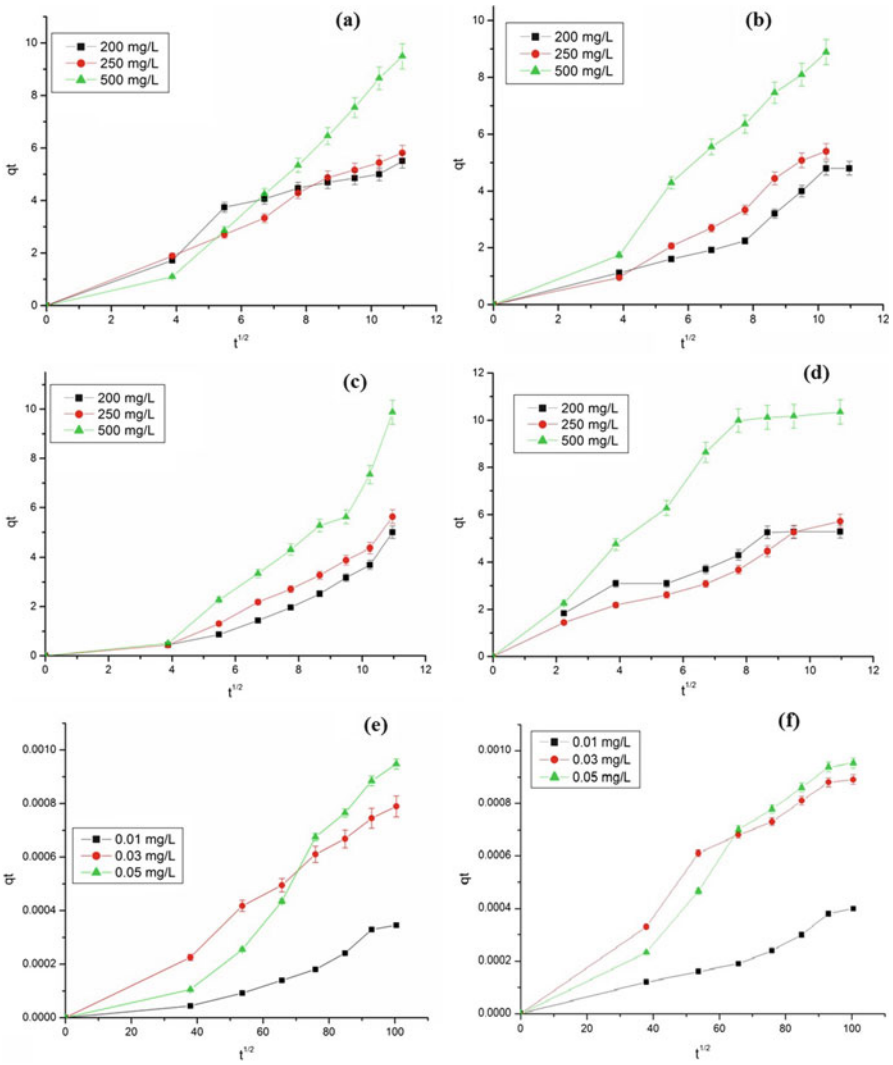

Fig. 19 Intraparticle diffusion graphs of (**a**) Cu(II), (**b**) Ni(II), (**c**) Co(II), (**d**) Zn(II), (**e**) direct red and (**f**) Congo red dye (Gonte 2013)

$$\text{Desorption ratio} = \frac{\text{amt.of adsorbate desorbed}}{\text{amt.of adsorbate adsorbed}} \times 100$$

Rapid desorption (≈ 80%) of metal ions was noted within the first 10 min as can be observed from Fig. 20. It can be clearly noted that desorption of Cu (II) ions occurs to its maximum 97% within 15 min after which no further desorption occurred. Desorption of Ni(II) and Co(II) reached its maximum within 30 min. In case of dyes, ≈85% complete desorption occurred using 0.5 M HCl solution in

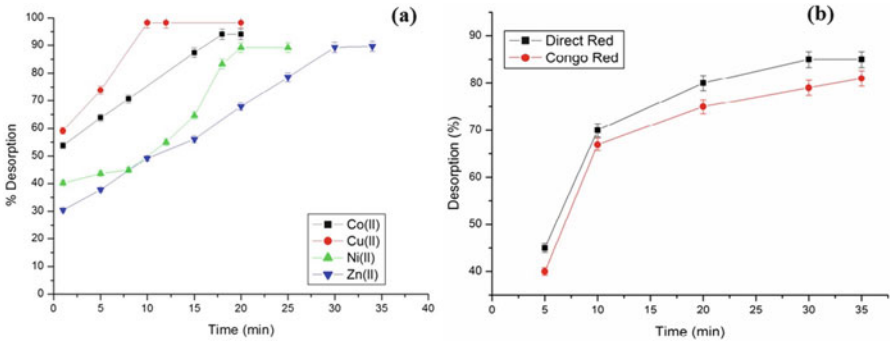

Fig. 20 Desorption curves of (**a**) metal ions and (**b**) dye (Gonte 2013)

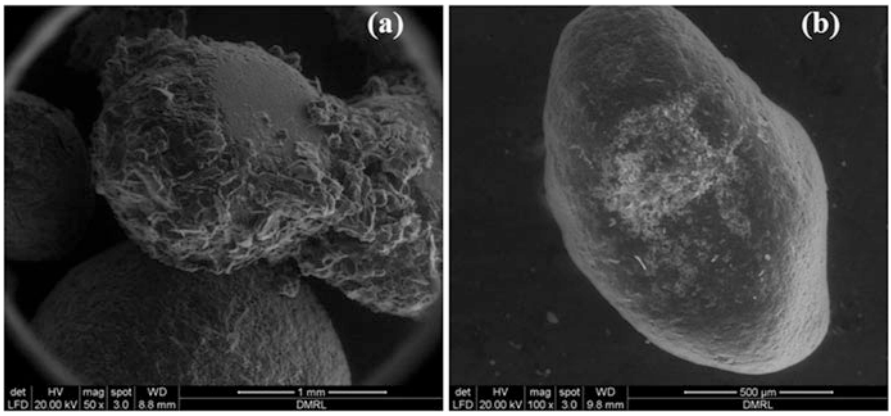

Fig. 21 SEM images of (**a**) SD-SMA and (**b**) SM-SMA (Gonte 2013)

30 min. Thus the results show that the cross-linked SMA copolymer beads can be successfully regenerated and can be used for re-adsorption of metal ions/dyes from aqueous solution.

SMA Biocomposites

The SD-SMA and SM-SMA composite beads with varying wt% of biomaterials (5 wt %, 10 wt% and 20 wt%) were synthesized. It was observed that uniform-sized spherical beads were developed with addition of sawdust up to 20 wt%, and with sugarcane molasses, elliptical beads of uniform size were obtained up to 10 wt% addition. Additionally, the SEM images of the composite beads (SD-SMA and SM-SMA) formed were in the size range 300–600 µm as can be seen from the SEM micrographs. The micrographs also confirmed the spherical shape of SD-SMA composite beads (Fig. 21a) and elliptical shape of SM-SMA composite beads (Fig. 21b).

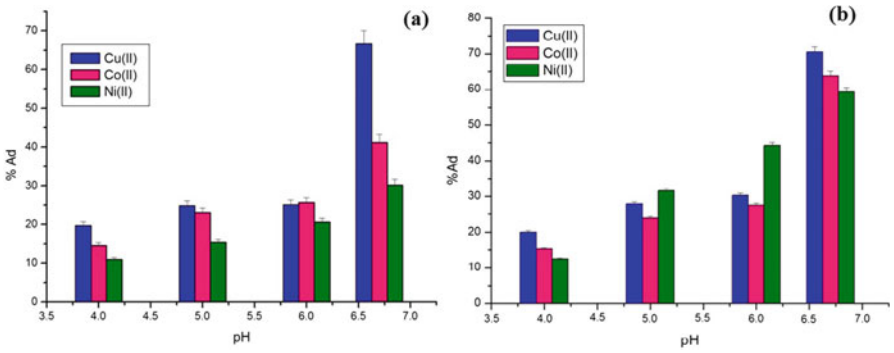

Fig. 22 Effect of pH on adsorption using (**a**) SD-SMA and (**b**) SM-SMA composite (Gonte 2013)

Effect of Solution pH

The adsorption of Congo red dye was studied at pH 7. The Congo red dye was found to be chemically and structurally stable at pH 7. Drastic colour change was descried with remote transmutation in pH. The adsorption of metal ions (Cu(II), Co(II) and Ni(II)) was studied by varying the pH of the solution from pH 4.0 to pH 8. It was observed adsorption increases with increase in the pH of the solution, exhibiting maximum adsorption at pH 6.7 (Fig. 22). The SM-SMA composite beads demonstrated enhanced adsorption as compared to SD-SMA composite groups which can be attributed to the astronomically immense number of lignin and cellulosic groups of SM.

Effect of Composite Dose

Increasing the amount of composite beads from 0.1 to 0.5 g for a fixed volume of solution at pH 6.7 and 200 mgL^{-1} metal ion conc., adsorption was observed to increase which is due to significant increase in the active adsorption sites. The enhanced adsorption was again noted with SM-SMA composite beads (Fig. 23). However, further increase in sorbent dose showed no significant increase in adsorption.

Equilibrium Adsorption Isotherms

Langmuir Model

Langmuir model was found to be applicable in the interpretation of adsorption of CR dye and metal ions (Fig. 24) onto SD-SMA and SM-SMA composite beads. The equilibrium data when validated with the theoretical equation (Sousa et al. 2009)

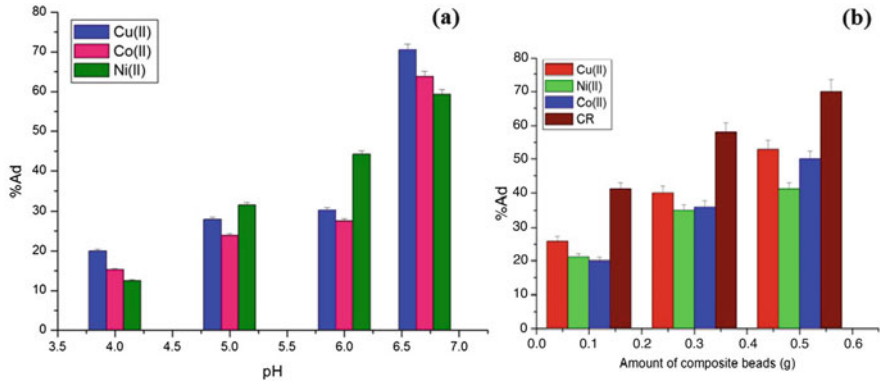

Fig. 23 Effect of composite dose on adsorption of metal ions and dye using (**a**) SD-SMA and (**b**) SM-SMA (Gonte 2013)

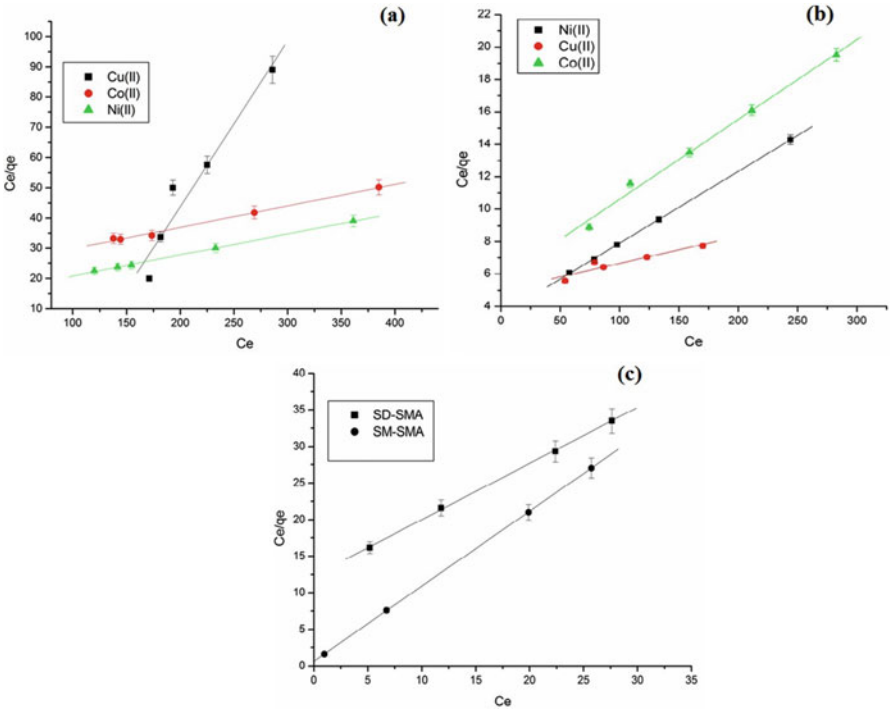

Fig. 24 Langmuir adsorption isotherm for adsorption of metal ions onto (**a**) SD-SMA and (**b**) SM-SMA and adsorption isotherm for (**c**) CR (Gonte 2013)

gave rise to the linear plots, indicating that the Langmuir model could be well applied to the system:

$$\frac{C_e}{q_e} = \frac{1}{q_{max} \times K_L} + \frac{C_e}{q_{max}}$$

Freundlich Model

The Freundlich constants were calculated by plotting graph of ln q_e versus ln C_e using the linearized isotherm equation (Zuorro et al. 2010; Zhang et al. 2010) for adsorption of dyes and metal ions (Fig. 25) onto the biocomposite beads:

$$\ln q_e = \frac{1}{n} \times \ln C_e + \ln K_F$$

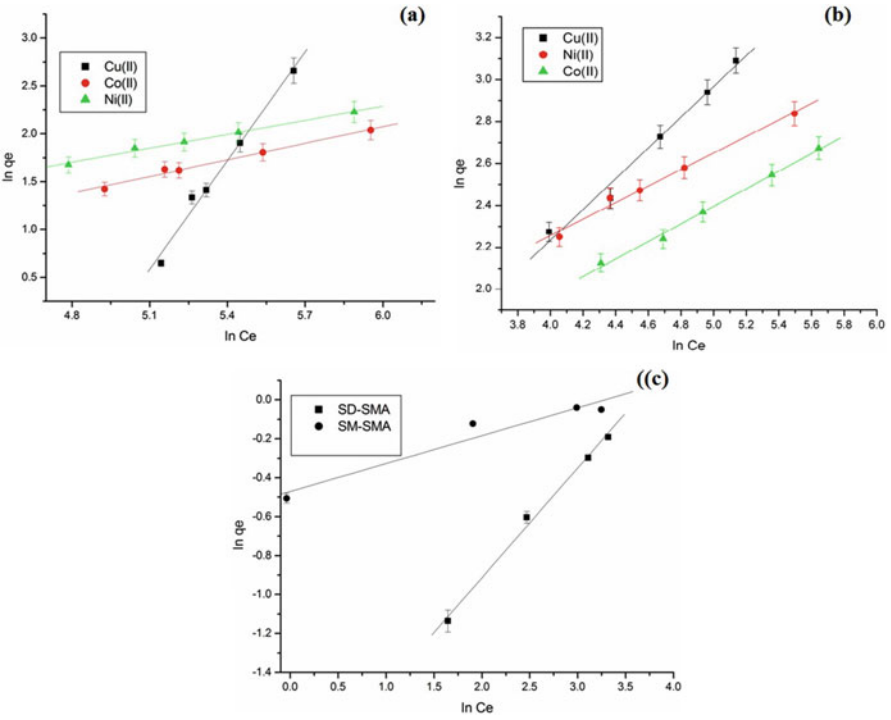

Fig. 25 Freundlich adsorption isotherm for adsorption of metal ions onto (**a**) SD-SMA and (**b**) SM-SMA and adsorption isotherm for (**c**) CR (Gonte 2013)

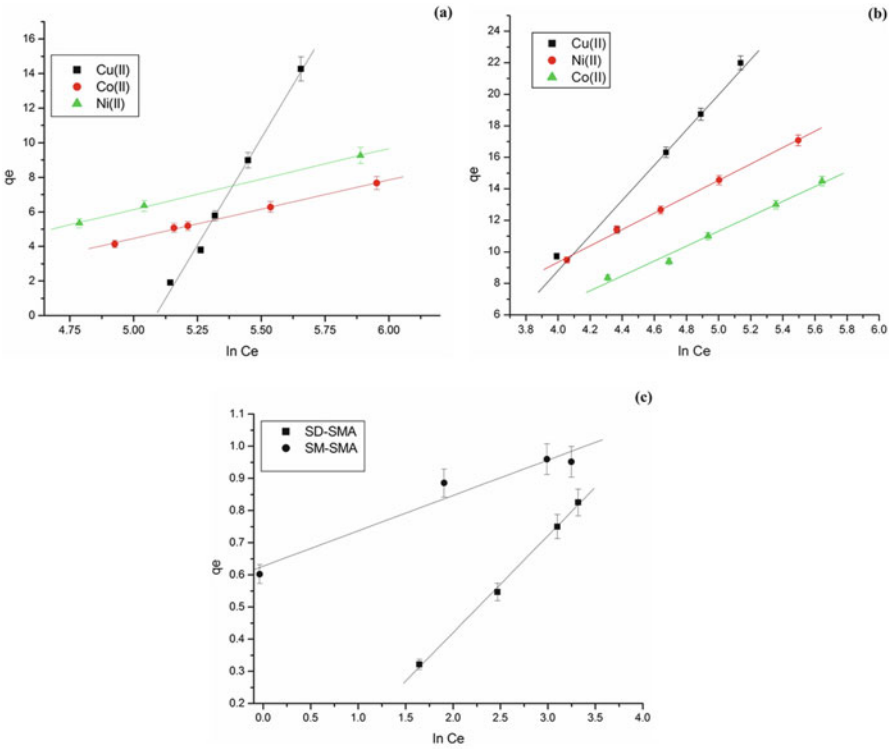

Fig. 26 Temkin adsorption isotherm for adsorption of metal ions onto (**a**) SD-SMA and (**b**) SM-SMA and adsorption isotherm for (**c**) CR (Gonte 2013)

Temkin Model

Temkin isotherm model was used to calculate the maximum binding energy using the linearized equation (Zuorro and Lavecchia 2010) as:

$$q_e = \frac{RT}{bT} \times (\ln \alpha T) + \frac{RT}{bT} \times \ln C_e$$

The graph of q_e versus ln C_e for adsorption of dyes and metal ions (Fig. 26) yields the value of αT corresponding to the maximum binding energy. The values indicate a good potential for adsorption of metal ions and dyes onto the composite beads with high correlation coefficient values.

Kinetic Models

Pseudo-First-Order

Lagergren pseudo-frst-order linearized equation was used to determine the adsorption mechanism (Demirbas et al. 2002):

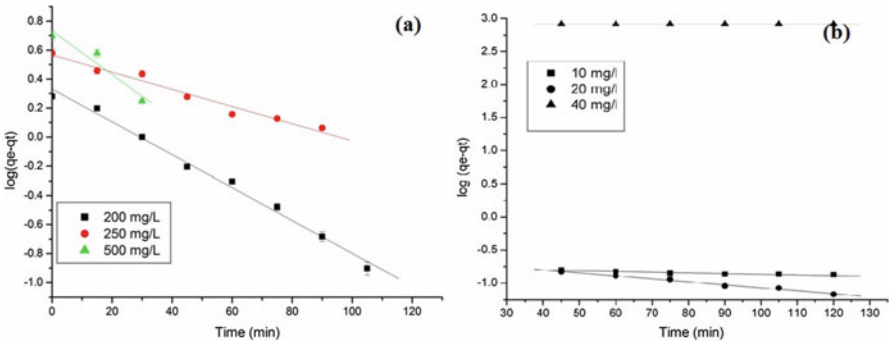

Fig. 27 Pseudo-first-order plots using SD-SMA for adsorption of (**a**) Cu(II) and (**b**) CR (Gonte 2013)

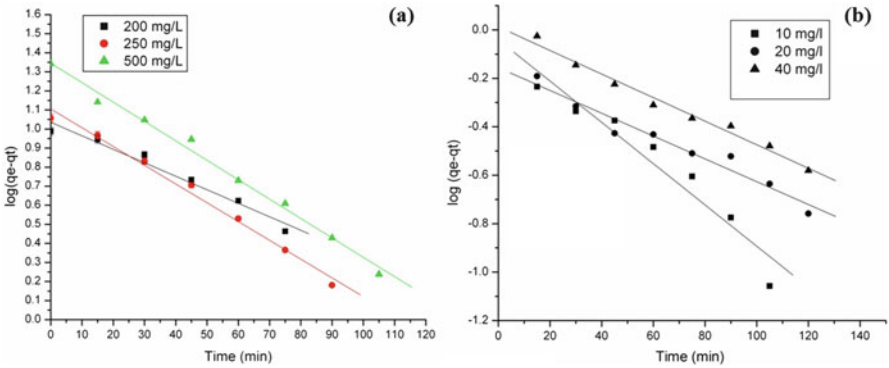

Fig. 28 Pseudo-first-order plots using SM-SMA for adsorption of (**a**) Cu(II) and (**b**) CR (Gonte 2013)

$$\log(q_e - q_t) = \log\ q_e - \frac{k_1}{2.303} \times t$$

The linearized graphs of the pseudo-first-order kinetics of Cu(II) and CR are presented in Figs. 27 and 28 for SD-SMA and SM-SMA composite beads, respectively. The rate constants obtained for all the different conc. of metal ions are also comparable indicating the same adsorption mechanism applies and that adsorption occurs by monolayer formation onto the composite beads, thus suggesting that a pseudo-first-order rate governs the adsorption process.

Pseudo-Second Order

The linearized pseudo-second-order rate equation (Demirbas et al. 2002) was used to calculate the rate constant in predicting the rate control kinetics:

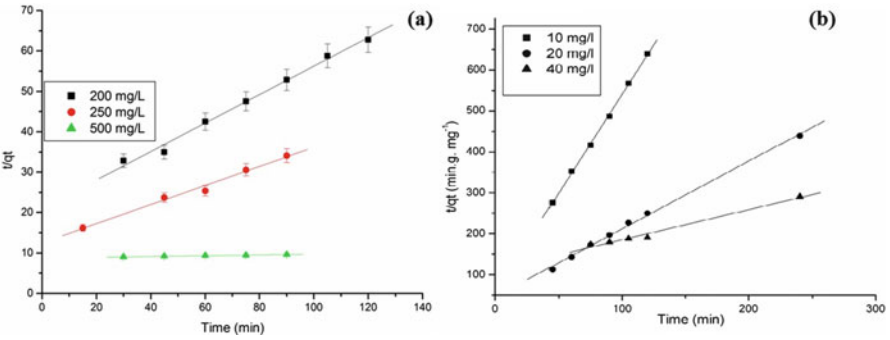

Fig. 29 Pseudo-second-order plots using SD-SMA for adsorption of (**a**) Cu(II) and (**b**) CR (Gonte 2013)

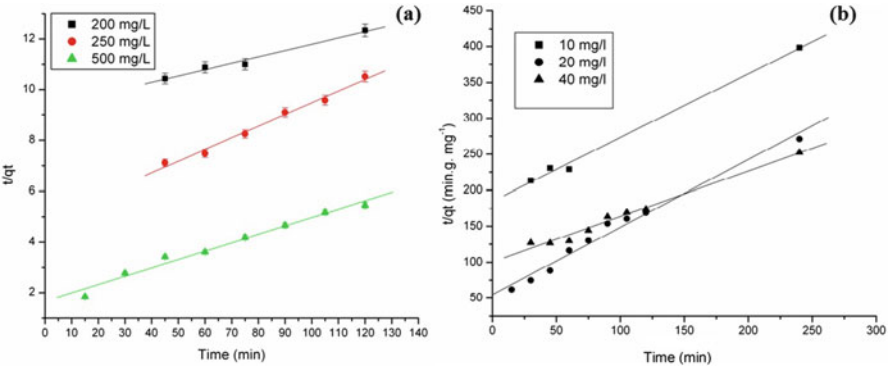

Fig. 30 Pseudo-second-order plots using SM-SMA for adsorption of (**a**) Cu(II) and (**b**) CR (Gonte 2013)

$$\frac{t}{q_t} = \frac{1}{k_2 \times {q_e}^2} + \frac{1}{q_e} \times t$$

The linearized form of the pseudo-second-order model for SD-SMA and SM-SMA composite beads for Cu(II) and CR is shown in Figs. 29 and 30, respectively. The high correlation coefficient values obtained for metal ions and dyes support the assumption that adsorption of metal ions is through chemisorption involving valence forces through the sharing or exchange of electrons between adsorbent and metal ions.

Intraparticle Diffusion Model

Intraparticle diffusion model was used to describe the adsorption mechanism onto SD-SMA and SM-SMA composite beads. Figures 31 and 32 show the plot

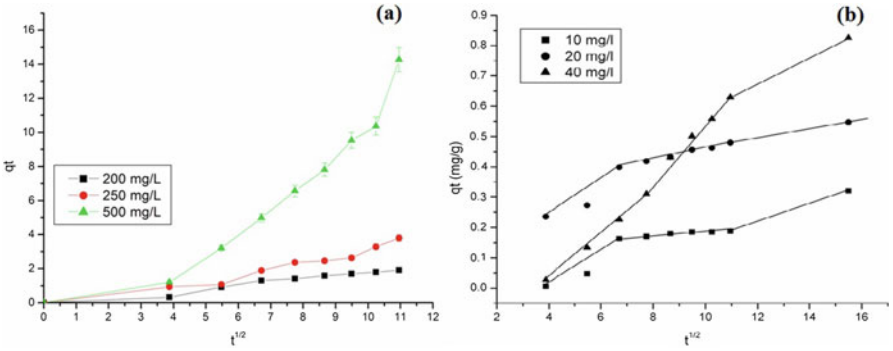

Fig. 31 Intraparticle diffusion plots using SD-SMA for adsorption of (**a**) Cu(II) and (**b**) CR (Gonte 2013)

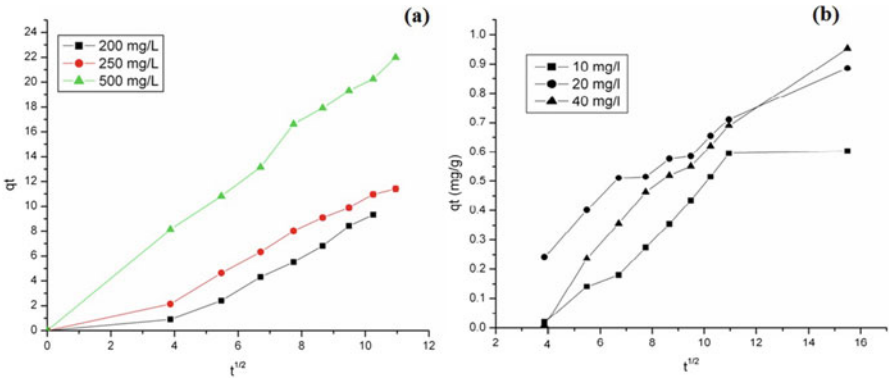

Fig. 32 Intraparticle diffusion plots using SM-SMA for adsorption of (**a**) Cu(II) and (**b**) CR (Gonte 2013)

of q_t vs $t^{1/2}$ for Cu(II) and CR on SD-SMA and SM-SMA composite beads. Adsorption occurs in two-step adsorption. The first is the instantaneous diffusion, where the rate of diffusion is fast, and the second step is a rate-controlled step. These observations are in good agreement with the literature (Parab et al. 2010).

Chemically Modified SMA Beads

Characterization

The FTIR spectra of SMA-MOFs beads showed a drastic decrease carboxylate ion 1725 cm^{-1} peak indicating the formation of metal carboxylates into the polymer matrix as can be clearly seen from Fig. 33a. The presence of 1311 cm^{-1} peak

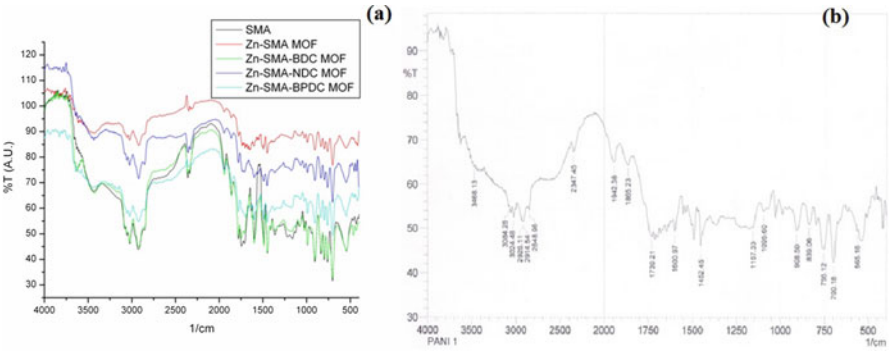

Fig. 33 Hydrogen adsorption onto SMA beads (Gonte 2013)

corresponding to aromatic C-N stretch, the asymmetric stretching frequency of N-H at 3335 cm^{-1}, C-N stretch at 1172 cm^{-1} and a low-intensity 1620 cm^{-1} (sharp peak) corresponding to N-H bends were observed in FTIR spectrum of SMA-PANI IPNs (Fig. 33b). Thus the presence of C-N and N-H peaks in the IR spectrum indicates the formation of polyaniline in the semi-IPN. Moreover, the CHNS-elemental analysis of PANI-encapsulated SMA polymer showed the presence of 0.395% N corresponding to ≈ 2:8 mole% of polyaniline in the semi-IPNs. The SEM analysis of the cut surface of the modified SMA beads revealed well-defined structure formation in the interiors/pores of the SMA beads. The thermal stability of the various modified polymer matrixes were confirmed from the thermogravimetric analysis (TGA), which revealed no change in the shape of the decomposition curve on formation of metal complexes or semi-IPNs as compared to the SMA copolymer. The chemical modifications showed no effect on the thermal stability of the polymer matrix, exhibiting the usable temperature range from RT to 400 °C. The residual mass, however, decreased by 7–10%, which is expected due to the formation of metal-carboxylate complexes with the carboxylic acid groups which decrease the concentration of maleic anhydride content of the polymer.

Hydrogen Adsorption

The hydrogen adsorption studies were conducted by allowing the beads to be in contact with the gas in discreet pressure ranges within 0–900 torr. For this study, a Sorptomatic 1900, which allows accurate measurements up to 900 torr, has been used (Gonte et al. 2012). All the measurements were carried out at room temperature 300 K.

It was observed that the rate of hydrogen adsorption is almost comparable for the various cross-linked polymers, independent of their DVB content (Fig. 34).

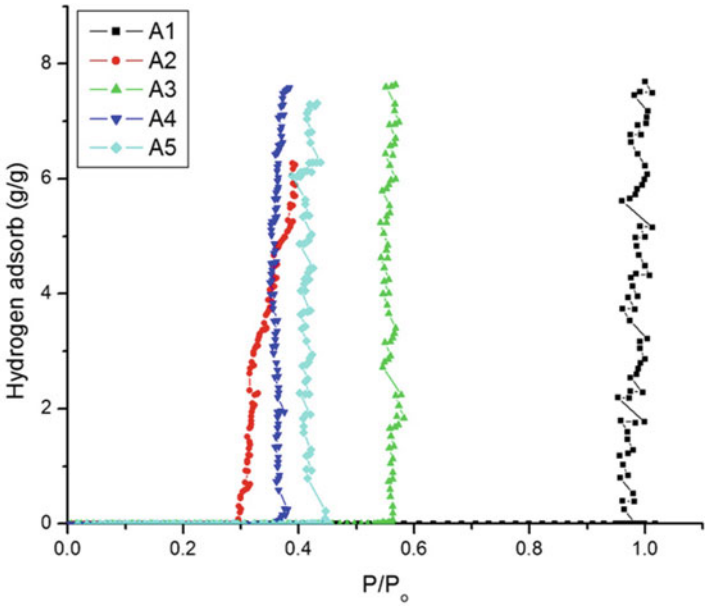

Fig. 34 Hydrogen adsorption onto modified SMA beads (Gonte 2013)

Hydrogen adsorption analysis on SMA beads under the same desired acquisition parameters as observed by (Deb et al. 2005) showed the rate of adsorption to be 3 wt% per hr., as compared to the highly cross-linked beads where the rate is about 30 wt% per h. In the case of A1, A3 and A5, positive adsorption was observed. These results are in good agreement with the previously reported results on hydrogen adsorption in the SMA copolymer matrix (Deb et al. 2005).

Hydrogen adsorption in the Zn-SMA-MOF beads and Zn-SMA-DCA MOFs beads were also studied under the same parameters at room temperatures (300 K) (Fig. 35). Instantaneous hydrogen adsorption on these beads for 25 h revealed that hydrogen storage capacity of the hypercross-linked polymer beads (0.67 wt %) decreases slightly due to the formation of metal complex and entrapment of MOFs in the pores. These findings can be attributed to the blockage of pores by the complex formation and MOF decoration. This effect was found to diminish with long exposure time of 3 days where similar hydrogen adsorption capacity ($\approx$ 0.8 wt%) was noted for all types of beads (Gonte et al. 2011a, b).

With PANI-encapsulated polymer, the adsorption was observed to take place at around 500 torr pressure and showed continuous uptake without reaching the limiting saturation pressure. The decrease in the rate of hydrogen adsorption by PANI-encapsulated polymers indicates towards the decrease in the pore size due encapsulation, which occurs even in the pores of the SMA polymer microspheres. The size of the pore and overall microsphere diameter has found to have a profound influence on the hydrogen adsorption capacity of the polymer. However, the pore surface of the SMA polymer that is coated with polyaniline will tend to reduce the

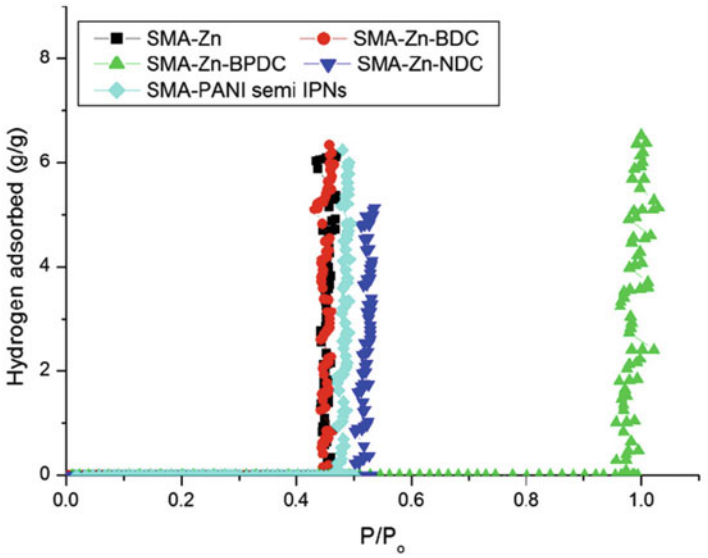

Fig. 35 Hydrogen adsorption onto modified SMA beads (Gonte 2013)

porosity of the polymer as confirmed from SEM findings (Gonte et al. 2011a, b) which results in decrease in hydrogen adsorption capacity.

Conclusions

The present chapter describes about the styrene-maleic acid copolymer beads as adsorbent for removal of heavy metal ions and dyes from aqueous solutions and also as adsorbent material for hydrogen storage. Thus the copolymer matrix was synthesized by suspension polymerization method which yields the spherical bead-shaped copolymer. Effect of agitation speed on bead dimension was studied. Five different compositions were made varying the cross-linker divinylbenzene content, and the mechanical, morphological and thermal properties were analyzed and one final composition was selected as adsorbent. Characterization of SMA beads was carried out using various techniques such as FTIR, SEM, TGA, XRD and SAXS, and the effect of experimental parameters on adsorption were studied. Adsorption studies on cross-linked SMA beads were carried out using various adsorption isotherms and kinetic models. The results thus indicate that cross-linked SMA copolymer bead can prove to be a potential candidate for treatment of industrial wastewater containing various metal ions and dyes. These copolymer beads were also capable of in situ reduction of Au (III) to Au(0) without the use of any additional reducing or capping agents.

SMA-biocomposite beads were synthesized for the increment in the effectiveness of the adsorption process, and characterization studies were carried out. Biocomposites of SMA prove to be highly effective for the removal of dye stuffs supported by the obtained data. Langmuir, Freundlich and Temkin isotherm adsorption models were utilized for the mathematical analysis of the adsorption equilibrium for both SD-/SM-SMA composite beads. The results obtained by the adsorption isotherms gave best fit for experimental data, and the equilibrium could be well described by Langmuir and Freundlich isotherm models indicating monolayer adsorption in the first step followed by heterogeneous surface binding, suggesting chemisorptive uptake of metal ions and dye from aqueous solution. Hydrogen adsorption studies were carried out for both cross-linked SMA beads and chemically modified SMA beads. Enhanced rate of hydrogen adsorption at room temperature was successfully achieved by the introduction of highly cross-linked interpenetrating networks inside the microspheres. No drastic change in the rate of adsorption was noticed after complexation with Zn(II) suggesting the involvement of metal complexes in adsorption.

In summary, it is concluded that the cross-linked styrene-maleic acid copolymer beads can be considered as suitable adsorbent for removal of heavy metal ions and dyes having a wide concentration range in aqueous systems. Such copolymer matrix is highly effective for batch as well as for continuous flow process. These adsorbents can be effectively recycled for further use. Biocomposites of SMA prove to be highly effective for the removal of dye stuffs. Such cost-effective adsorbent using inexpensive removal technique can find wide industrial applications. Hydrogen adsorption can be achieved under optimized conditions.

References

Abdel-Ghani N, Hegazy AK, El-Chaghaby G (2009) *Typha domingensis* Leaf powder for decontamination of aluminium, iron, zinc and lead: biosorption kinetics and equilibrium modelling. Intl J Environ Sci Technol 6:243–248

Al-Asheh S, Banat FA, Abu-Aitah L (2003) Adsorption of phenol using different types of activated bentonites. Sep Purif Technol 33:1–10

Al-Rekabi WS, Qiang H, Qiang WW (2007) Improvements in wastewater treatment technology. Pak J Nutr 6:104–110

Atia A, Donia AM, Abou-El-Enein SA (2003) Studies on uptake behavior of copper(II) and lead (II) by amine chelating resins with different textural properties. Separat Purif Technol 33:295–301

Azanova VV, Hradil J (1999) Sorption properties of macroporous and hyper-crosslinked copolymers. React Func Polym 41:163–175

Babel S, Opiso EM (2007) Removal of Cr from synthetic wastewater by sorption into volcanic ash soil. Intl J Environ Sci Technol 4:99–108

Celik A, Demirbas A (2005) Removal of heavy metal ions from aqueous solutions via adsorption onto modified lignin from pulping wastes. Energy Sources 27:1167–1177

Corapcioglu M, Huang C (1987) The adsorption of heavy metals onto hydrous activated carbon. Water Res 21:1031–1044

Davankov V, Tsyurupa M (1990) Structure and properties of hyper crosslinked polystyrene – the first representative of a new class of polymer networks. React Polym 13:27–42
Deb PC, Mathew A (1996) Synthesis of spherical copolymer beads of styrene-maleic ahydride by aqueous suspension polymerization. J Polym Sci Part A Polym Chem 34:1605–1607
Deb PC, Rajput LD, Agrawal AK, Singh PK, Hande V, Sasane S (2005) Crosslinked styrene-maleic acid copolymer complexes of some transition metals and their adsorption behaviour. Polym Adv Technol 16:681–687
Demirbas O, Alkan M, Sousa MW, Sousa M, Oliveira IR, Oliveira A, Cavalcante R, Fechine P et al (2002) The removal of Victoria blue from aqueous solution by adsorption on a low-cost material. Adsorption 8:341–349
Den S (2006) Sorbent technology – encyclopedia of chemical processing; CRC Press, Taylor & Francis Group
Deng S, Ting YP (2005) Polyethylenimine-modified fungal biomass as a high capacity adsorbent for chromium anion removal. Environ Sci Technol 39:8490–8496
Deshdmukh JH, Deshpande MN (2011) X-ray diffraction studies of Cu (II), Co (II), Fe (II) complexes with (RS)-4-(7-chloro-4-quinolyl amino) pentyldiethylamine diphosphate. J Chem Pharmaceut Res 3:706–712
Donmez C, Aksu Z, Ozturk A, Kutsal T (1999) A comparative study on heavy metal biosorption characteristics of some algae. Process Biochem 34:885–892
Farajzadeh MA, Fallahi MR (2005) Study of phenolic compounds removal from aqueous solution by polymeric sorbent. J Chinese Che Soc 521:295–301
Febrianto J, Kosasih A, Sunarso J, Ju Y, Indraswati N, Ismadji S (2009) Equilibrium and kinetic studies in adsorption of heavy metals using biosorbent: a summary of recent studies. J Hazard Mater 162:616–645
Goltz HR, Jones KC, Tegen MH (1994) High surface area polymeric adsorbents for VOC capture and on-site regeneration. Air and Waste Management Association, 87th Annual Meeting and Exhibition, Cincinnati
Gonte RR (2013) Styrene-maleic acid co-Polymer beads and composites for adsorption of toxic chemicals and hydrogen Dept Appl Chem Defence Inst Adv Technol (DU) – PhD Thesis.
Gonte RR, Balasubramanian K, Deb P (2011a) Synthesis and characterization of metal organic frameworks. Proc Intl Conf Nano Eng Adv Comput (ICNEAC-2011) 1:529–531
Gonte RR, Balasubramanian K, Deb P (2011b) Adsorption properties of crosslinked mesoporous (styrene – maleic acid) – Zn (II) complexes. Intl J Indus Engg Technol 3:279–288
Gonte RR, Balasubramanian K, Deb PC, Singh P (2012) Synthesis and characterization of mesoporous hypercrosslinked poly (styrene Co-maleic anhydride) microspheres. Intl J Polymeric Mater 61:919–930
Greig JA, Sherrington DC (2003) Molecular sieve behaviour in polymeric reagents. Polymer 19:163–172
Gundogan R, Acemioglu B, Alma M (2004) Copper (II) adsorption from aqueous solution by herbaceous peat. J Colloidal Interface Sci 269:303–320
Gupta V, Suhas (2009) Application of low-cost adsorbents for dye removal: a review. J Environ Manag 90:2313–2342
Har MP, Fuller G, Brow AR, Dale JA, Plant S (2001) Sulphonated poly(styrene-co-divinylbenzene) ion exchange resins: acidities and catalytic activities in aqueous reactions. J Mol Catalysis A Chem 182-183:439–445
Hostetler MJ, Wingate JE, Zhong CJ, Harris JE, Vachet RW, Clark MR et al (1998) Alkanethiolate gold cluster molecules with core diameter from 1.5 to 5.2 nm: Core and monolayerproperties as a function of core size. Langmuir 14:17–30
Inglezakis VJ, Loizidou MD, Grigoropoulou HP (2003) Ion exchange of Pb_2C, Cu_2C, and Cr_3C on natural clinoptilolite: selectivity determination and influence of acidity on metal uptake. J Colloid Interface Sci 261:49–54
Issabayeva G, Aroua M, Sulaiman N (2007) Continuous adsorption of lead ions in a column packed with palm shell activated carbon. J Hazard Mater 155:109–113

Jaber M, Miehé-Brendlé J, Michelin L, Delmotte L (2005) Heavy metal retention by organoclays: synthesis, applications, and retention mechanism. Chem Mater 17:5275–5281

Kadirvelu K, Thamaraiselvi K, Namasivayam C (2001) Removal of heavy metals from industrial wastewaters by adsorption onto activated carbon prepared from an agricultural solid waste. Bioresource Technol 76:63–65

Kapoor A, Viraraghavan T, Cullimore DR (1999) Removal of heavy metals using the fungus *Aspergillus niger*. Bioresource Technol 1:95–104

Krysztafkiewicz A, Binkowski S, Jesionowski T (2002) Adsorption of dyes on a silica surface. Appl Surf Sci 199:3–39

Lee JY, Wood CD, Bradshaw D, Rosseinsky M, Cooper A (2006) Hydrogen adsorption in microporous hypercrosslinked polymers. Chem Commun 25:2670–2672

Leng Y (2009) Materials characterization: introduction to microscopic and spectroscopic methods. J. Wiley, Weinheim. ISBN: 978-3-527-33463-6

Li H, Eddaoudi M, Groy TL, Yaghi OM (1998) Establishing microporosity in open metal-organic frameworks: gas sorption isotherms for Zn(BDC) (BDC=1,4- benzenedicarboxylate). J Am Chem Soc 120:8571–8572

Markovska L, Meshko V, Marinkovski M (2006) Modeling of adsorption kinetics of zinc onto granular activated carbon and natural zeolite. J Serbian Chem Soc 71:957–967

Netpradit S, Thiravetyan P, Towprayoon S (2004) Application of waste metal hydroxide sludge for adsorption of azo reactive dyes. Water Res 38:71–78

Nwuche CO, Ugoji E (2008) Effects of heavy metal pollution on the soil microbial activity. Intl J Environ Sci Technol 5:409–414

Odian G (2004) Principles of polymerization, 4th edn. J. Wiley, New Delhi. ISBN: 0-471-27400-3

Omer Y, Yalcin A, Fuat G (2003) Removal of copper, nickel, cobalt and manganese from aqueous solution by kaolinite. Water Res 37:948–952

Pan BC, Xiong Y, Su Q, Li AM, Chen JL (2003) Role of amination of a polymeric adsorbent on phenol adsorption from aqueous solution. Chemosphere 51:953–962

Parab H, Joshi S, Sudersanan M, Shenoy N, Lali A, Sarma U (2010) Removal and recovery of cobalt from aqueous solutions by adsorption using low cost lingo cellulosic biomasscoir pith. J Environ Sci Health Part A 45:603–611

Rawat J, Ahmad A, Agrawal A (1990) Equilibrium studies for the sorption of Cu^{2+} on lanthanum diethanolaminea chelating material. Colloid Surf 46:239–253

Rengaraj S, Kim Y, Joo C, Choi K, Yi J (2004) Batch adsorptive removal of copper ions in aqueous solutions by ion exchange resins: 1200H and IRN97H. Korean Jo Chem Engg 21:187–194

Rengaraj S, Yeon J, Kimb Y, Jung Y, Ha Y, Kima W (2007) Adsorption characteristics of Cu (II) onto ion exchange resins 252H and 1500H: kinetics, isotherms and error analysis. J Hazard Mater 143:469–477

Resmi G, Thampi S, Chandrakaran S (2010) Brevundimonas vesicularis : a novel bio-sorbent for removal of lead from wastewater. Intl J Environ Res 4:281–288

Rivera-Utrilla J, Bautista-Toledo I, Ferro-Garcia MA, Moreno-Castilla C (2003) Bioadsorption of Pb(II) Cd(II), and Cr(VI) on activated carbon from aqueous solutions. Carbon 41:323–330

Robinson T, Chandran B (2002) Studies on desorption of individual textile dyes and a synthetic dye effluent from dye adsorbed agricultural residues using solvents. Bioresourse Technol 84:299–301

Rosenberg G, Shabaeva A, Moryakov V, Musin T, Tsyurupa M, Davankov V (1983) Sorption properties of hypercrosslinked polystyrene sorbents. React Polym Ion Exch Sorbents 1:175–182

Schlapbach L (2002) Hydrogen as a fuel and its storage for mobility and transport. MRS Bull 27:675–676

Schlapbach L, Zuttel A (2001) Hydrogen storage materials for mobile application. Nature 414:353–358

Shelar G, Gonte R, Ayalew AKB (2011) Porous biocomposite beads of sawdust for effluent treatment. Proc Intl Conf Nano Eng Adv Comput (ICNEAC-2011) 1:451–454

Sicilia-Zafrac A, Gonzalez-Perezc J, Niclos-Gutierrezc J (1999) Synthesis, XRD structures and properties of Diaqua(iminodiacetato)copper(II), [Cu(IDA)(H O)], and 2 2 aqua(benzimidazole)(iminodiacetato)copper(II), [Cu(IDA)(hbzim)(H O)]. Polyhedron 18:3341–3351

Sousa FW, Sousa M, Oliveira IR, Oliveira AG, Cavalcante RM, Fechine P et al (2009) Evaluation of a low-cost adsorbent for removal of toxic metal ions from wastewater of an electroplating factory. J Environ Manag 90:3340–3344

Sternberg SPK, Dorn R (2002) Cadmium removal using cladophora in batch, semi-batch and flow reactors. Bioresource Technol 81:249–255

Thomas WJ, Crittenden BD (1998) Adsorption technology and design. Butterworth-Heinemann, London

Toro CA, Rodrigo R, Cuellar J (2009) Kinetics of the sulphonation of macroporous poly(styrene-co-divinylbenzene) microparticles. Chem Engg Transct 17:49–54

Vasudevan P, Padmavathy V, Dhingra SC (2003) Kinetics of biosorption of cadmium on bakers yeast. Bioresourse Technol 89:81–87

Wan Y, Huang W, Wang Z, Zhu XX (2004) Preparation and characterization of high loading porous crosslinked poly(vinyl alcohol) resins. Polymer 45:71–77

Wingenfelder U, Hansen C, Furrer G, Schulin R (2009) Removal of heavy metals from mine waters by natural zeolites. Environ Sci Technol 39:4606–4613

Yang R (2003) Adsorbents: fundamentals and applications. Wiley, Hoboken

Yavuz O, Altunkaynak Y, Guzel F (2003) Removal of copper, nickel, cobalt and manganese from aqueous solution by kaolinite. Water Res 37:948–952

Zhang A, Asakura T, Uchiyama G (2003) The adsorption mechanism of uranium(VI) from seawater on a macroporous fibrous polymeric adsorbent containing amidoxime chelating functional group. React Func Polym 57:67–76

Zhang Y, Li Y, Li X, Yang L, Bai X, Ye Z, Zhou L, Wang L (2010) Selective removal for Pb^{2+} in aqueous environment by using novel macroreticular PVA beads. J Hazard Mater 181:898–907

Zhu J, Deng B, Yang J, Gang D (2009) Modifying activated carbon with hybrid ligands for enhancing aqueous mercury removal. Carbon 47:2014–2025

Zuorro A, Lavecchia R (2010) Adsorption of Pb(II) on spent leaves of green and black tea. Am J Appl Sci 7:153–159

Synthesis and Characterization of Composite Cation-Exchange Material and Its Application in Removing Toxic Pollutants

Mohammad Kashif Uddin and Rani Bushra

Abstract Polyaniline (PANI)-based composite cation-exchange material was synthesized under different experimental conditions by the incorporation of polyaniline into the matrices of inorganic precipitate. The experimental parameters such as concentration, mixing volume ratio, and pH were established for the synthesis of the material. The composite material exhibits improved ion-exchange capacity along with chemical and thermal stability. The distribution coefficient studies (K_d) of metal ions on the material were performed in diverse solvent systems. On the basis of K_d values, it is easy to determine the selectivity of the material. Some analytically important separations of heavy metal ions in synthetic and real mixtures were achieved on the columns of the composite cation-exchange material. Batch adsorption studies were carried out to study the effect of various parameters like effect of pH, initial concentration, and contact time.

Keywords Composite adsorbent • Synthesis • Characterization • Analytical applications • Adsorption

Introduction

Presently, environmental pollution is the burning issue of the world. The toxic metal ions, rapidly discharged from the industrial sources particularly in the natural water resources are causing damage to the environment and ecosystem. Some heavy metals are nutritionally essential for health, in its small amounts, but become toxic if present in more than permissible limit, as they are not metabolized by the body and accumulated in the soft tissues. The natural and anthropogenic sources of these metal ions include natural weathering of the earth's crust, mining, soil erosion, industrial discharge, urban runoff, sewage effluents and pest or disease

M.K. Uddin
Basic Engineering Sciences, College of Engineering, Majmaah University, Al-Majmaah 11952, Kingdom of Saudi Arabia

R. Bushra (✉)
Department of Applied Physics, Aligarh Muslim University, Aligarh 202002, UP, India
e-mail: bushrachem07@gmail.com

N.A. Anjum et al. (eds.), *Enhancing Cleanup of Environmental Pollutants*,
DOI 10.1007/978-3-319-55423-5_9

control agents applied to plants, air pollution fallout, etc. (Ming 2005). Therefore, there is need to pay more attention toward the treatment of heavy metal ions by synthesize novel materials. Among the list, metals like iron, cobalt, copper, chromium (III), molybdenum, selenium, manganese, and zinc are nutritionally essential, but they have adverse health effects below or beyond the level required for optimum nutrition; while metals such as mercury, plutonium, arsenic, cadmium, silver, strontium, thallium, beryllium, barium, antimony, and lead are toxic in nature as they have no beneficial effects on human health, and their long time accumulation can cause serious issues. Among these, arsenic has been found to be a human carcinogen at extremely low levels of exposure, which should be the major priority in consideration of regulatory control of human exposure (NAS/NRC 1999). Metals like silicon, nickel, boron, and vanadium are toxic at higher levels and not known to be essential to human health but may be suspected that these have some beneficial effects at low levels of exposure.

Metal(loids) and Their Biotoxicity

Mercury

In general, mercury is a neurotoxicant which can cause damage to the nervous system, brain cells, chronic fatigue, depression, and poor memory and is therefore toxic for human health (Wojcik et al. 2006; Vas and Monestier 2008). High levels of mercury exposure may also cause birth defects and permanent brain or kidney damage. Mercury, in its transformed form named methylmercury, becomes more noxious. It can easily enter into blood and organs, especially the brain, in this form. Children have more exposure to the different forms of mercury because intake of air, water, and food for children per kilogram of body weight is greater than for adults. Because of these severe health effects of mercury intake, the permissible limit in drinking water set by EPA and WHO is at very low level, 0.002 mg/L and 0.001 mg/L, respectively (WHO 2004).

Lead and Nickel

As per the Occupational Safety and Health Administration (OSHA) of the United States Department of Labor, lead exposure causes severe damage to the nervous, urinary and reproductive systems, which resulted into many forms of health effects, i.e., loss of appetite, nausea, vomiting, stomach cramps, constipation, difficulty in sleeping, fatigue, moodiness, headache, joint or muscle aches, anemia, and decreased sexual drive (ATSDR 2007; Castro-González and Méndez-Armenta 2008). The Joint FAO/World Health Organization Expert Committee on Food

Additives (JECFA) established a provisional tolerable weekly intake (PTWI) for lead as 0.025 mg/kg body weight (JECFA 2004). The WHO provisional guideline of 0.01 mg/L is set as the standard for drinking water (WHO 2004). Nickel also if exceeds from its critical level may bring some serious lung and kidney problems aside from gastrointestinal distress, pulmonary fibrosis, and skin dermatitis (Borba et al. 2006).

Cadmium

Cadmium, like zinc, occurs naturally in sulfide ores. Long-term exposure to cadmium targeted the kidney the most with other several organs like the liver, lungs, bones, placenta, brain, and central nervous system (Castro-González and Méndez-Armenta 2008). It is released in the environment from both natural and human activities, which includes volcanic activity, weathering and erosion, river transport, tobacco smoking, mining, smelting and refining of nonferrous metals (IPCS 1992; WHO 2000), fossil fuel combustion, incineration of municipal waste, etc., while food constitutes the main environmental source of cadmium. Highest cadmium levels are found in the kidney and liver of mammals and in certain species of oysters, scallops, mussels, and crustaceans. Too much intake of cadmium causes disturbances in calcium metabolism, which leads to the softening of the bones and osteoporosis. The International Agency for Research on Cancer (IARC) has classified cadmium as carcinogenic to humans (Group 1), after receiving sufficient evidence for its carcinogenicity in humans (IARC 1993; Straif et al. 2009). The Joint FAO/WHO has recommended the provisional tolerable weekly intake (PTWI) as 0.007 mg/kg body weight for cadmium (JECFA 2004). The EPA maximum contaminant level for cadmium in drinking water is 0.005 mg/L, whereas the WHO adopted the provisional guideline of 0.003 mg/L (WHO 2004a).

Arsenic

Arsenic is present in environment in different oxidation states (As (V), As (III), As (0), and As (−III)) (Cutter 1992). The two predominant oxidation states of inorganic arsenic, arsenite and arsenate, are very harmful to mankind and plants. Natural sources of arsenic include volcanism, forest fires, and groundwater. The mining, smelting, pulp and paper production, glass manufacturing, cement manufacturing, and the burning of fossil fuels and waste products are also responsible for their production in the environment.

Acute and chronic arsenic exposure from drinking contaminated groundwater with a high concentration of arsenic of 100 to over 2000 mg/L (ppb) (Tchounwou et al. 1999) has been reported in Argentina, Bangladesh, India, Mexico, Mongolia, Thailand, and Taiwan. Long-term exposure to arsenic results in arsenic poisoning,

especially to those people who live in the areas of high arsenic-concentrated drinking water (Hopenhayn-Rich et al. 2000; Pi et al. 2000; Berg et al. 2001, Liu et al. 2002). According to a study by the National Academy of Sciences, arsenic in drinking water causes lung, skin, kidney, and liver cancer. It also has a negative impact on the central and peripheral nervous system. To maximize health risk reduction, the USEPA in 2001 decided to reduce the drinking water maximum contaminant limit (MCL) to 0.010 mg/L, which is now the same as the WHO guidelines (USEPA 2005). JECFA established a PTWI for inorganic arsenic as 0.015 mg/kg body weight (FAO/WHO 2005; JECFA 2004). Organoarsenic intakes of about 0.05 mg/kg body weight/day seemed not to be associated to hazardous effects (Uneyama et al. 2007).

Copper

Copper is a metallic element that occurs naturally as a free metal, or associated with other elements in compounds that comprise various minerals. Annually 75,000 tons of copper is released into the atmosphere, out of which 25% came from natural sources while the rest from anthropogenic origin. Dissolved copper in water and food are the most common sources of human exposure. About 40% of dietary copper comes from yeast breads, white potatoes, tomatoes, cereals, beef, and dried beans (IOM 2001; Subar et al. 1998). The maximum limit of copper in drinking water is 0.05 mg/dm^3 (Fewtrell et al. 1996), because its excessive intake reported adverse health effects like gastrointestinal distress, nausea, vomiting, and abdominal pain.

Composite Cation-Exchange Materials in Remediation of Heavy Metal Ions

Composite Ion-Exchange Materials

The conventional heavy metal removal processes have some inherent shortcomings. But in recent years, some new processes such as biosorption, neutralization, precipitation, ion exchange, adsorption, etc. have been developed and extensively used for the removal of heavy metal from wastewater. Among them ion exchange is proved to be the most helpful method in adsorption of metal ions because ion exchangers have high capacity and specificity for the metal ions, even if found in low concentrations. The increasing current literatures on ion exchangers show its great importance as these are providing new opportunities for both chemists and analysts.

Many hybrid ion exchangers with conjugated properties of polymer and intrinsic properties of inorganic exchanger have been introduced. The incorporation of inorganic matrix into conducting polymers enhances the performance of both the "host" and the "guest," thereby leads to interesting concept of physical and chemical properties. These conjugated polymers have attracted attention in both science and technology and its applications in batteries, molecular electronic devices, light-emitting diodes (LED), etc. (Salaneck et al. 1993; Skotheim 1986). It can be used as a sorbent, ion exchanger, photocatalyst, ion-selective membrane electrode, and antimicrobial agent and also finds a large number of applications in pollution control and water treatment process (Bushra et al. 2014a, b, c, d; Khan et al. 2014a, b; Shahadat et al. 2014).

Synthesis Strategy

The composite cation-exchange material was synthesized by incorporating the conducting polymer gel (polyaniline, poly-o-toluidine, etc.) into the inorganic moiety that followed the method exactly like our previous work (Nabi et al. 2012a, b). As an example, following is one of the synthesis schemes of one of the composite cation-exchange material (Fig. 1). Moreover, in order for complete description of composite cation-exchange material, a number of physicochemical properties and characterizations have to be performed like ion-exchange capacity, pH titration, chemical and thermal stability, elution behavior, distribution coefficients (Kd values), structural studies, FTIR, Raman, TGA-DTA, X-ray, SEM, TEM, and AFM.

Ion-Exchange Capacity

Ion-exchange capacity is determined by using the column method. It is defined as total number of chemical equivalents available for exchange per some unit weight and under the specific conditions. It is expressed in terms of milliequivalents/gm of the exchanger.

pH Titrations

Topp and Pepper method (Topp and Pepper 1949) was used for conducting the pH titrations of the composite material using alkali or alkaline earth metal chlorides and their hydroxides in different volume ratios. In general, it is used to determine the nature of the ionogenic group and the number of replaceable H^+ ions per molecule of the composite material.

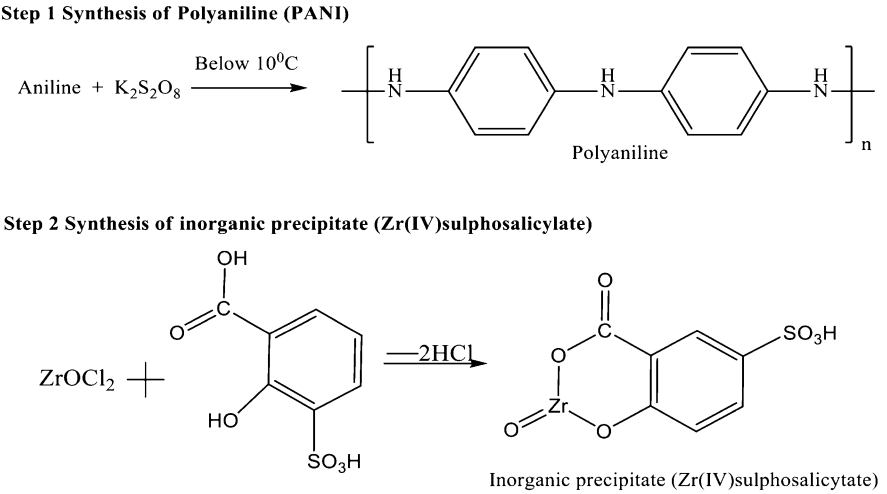

Fig. 1 Schematic representation of the synthesis scheme of one of the composite cation-exchange materials

Chemical and Thermal Stability

Chemical stability of the composite material is examined by treating the material with different inorganic and organic acids. It establishes whether the material can sustain in a solvent or not. Thermal gravimetric (TG) analysis was useful to measure the thermal stability.

Elution Behavior

Elution behavior was performed for the maximum elution of H^+ ions from the composite material with optimum concentration of eluent. The concentration of eluent depends on the nature of ionogenic group present in the material, which in turn depends upon the pKa values of the acids used in its preparation.

Distribution Coefficients

Distribution coefficients (K_d values) of the metal ions in different solvents can be determined by batch method. Composite material in H^+ form mixed with different metal nitrate solutions in different Erlenmeyer flasks was shaken for 6 h in a temperature-controlled shaker at 25 ± 2 °C to attain equilibrium. The concentration of metal ion before and after equilibrium was determined by EDTA titrations, and the values of distribution coefficient were calculated by using the equation:

$$K_d = \frac{\text{milli equivalent of metal ions/g of ion-exchanger}}{\text{milli equivalent of metal ions/mL of solution}} \text{ mL g}^{-1}$$

$$K_d = \frac{I - F}{F} \times \frac{V}{M} \text{ mL g}^{-1}$$

where I is the volume of EDTA used before treatment of metal ion exchanger and F is the volume of EDTA consumed by metal ion left in solution phase.

When the metal ions (M^{2+} and M^{3+}) were treated with composite cation-exchange material (H^+ form), the following reactions took place:

$$2\,RH^+ + M^{2+} \rightarrow R_2M^{2+} + 2\,H^+$$

$$3RH^+ + M^{3+} \rightarrow R_3M^{3+} + 3H^+$$

where RH^+ is cation-exchange material, M^{2+} and M^{3+} are bivalent and trivalent metal ions, respectively.

Characterizations

Fourier Transform Infrared Spectroscopy (FTIR)

It is a molecular characterization technique, which is used to identify the chemical bond of molecule by producing an infrared absorption spectrum. This technique provides a rapid detection of the functional groups present in the material.

Raman Spectroscopy

This spectroscopy provides information about molecular vibrations, used to study the changes during chemical bonding and vibrational, rotational, and other low-frequency modes in the composite materials.

X-ray Diffraction

It is a very important structural analytical technique, which is helpful in determining the arrangement of atoms within a crystal. The peaks in the XRD spectra provide many information regarding the phase composition, unit cell lattice parameters, crystal system, crystallite size, and microstrain.

Thermogravimetric Analysis or Thermal Gravimetric Analysis (TGA)

It is an important technique that finds out any change in the chemical composition of the material. Simultaneous TGA-DTA/DSC techniques used to measure both heat flow and weight changes (TGA) in a material with respect to temperature or time.

Microscopy

Scanning electron microscopy (SEM) is a type of electron microscope in which high-energy electrons scanned the surface of the material. The technique is used to find any change in morphology of the material's sample.

Transmission electron microscopy (TEM) is an analysis method to track particle size and distribution of the material. It is capable of imaging at a significantly higher resolution than light microscopes.

Atomic force microscopy (AFM) or scanning force microscopy (SFM) is a technique used to view three dimensions of the sample surface. It can produce the surface images of the sample with extremely high magnifications, up to 1000,000X.

Applications

Separations

Separation of Heavy Metal Ions in Synthetic Mixtures

Quantitative separations of some important metal ions can be achieved, by using column method. In this process, the composite cation-exchange material (1.0 g)

packed in a glass column should be washed with demineralized water, and then the targeted metal ions can be passed through it at a maintained flow rate. The process should be repeated two or three times to ensure the complete adsorption of metal ions. After that effluent can be collected and titrated against the standard solution of the disodium salt of EDTA for the complete separation of metal ions.

Separation of Heavy Metal Ions in Real Samples by FAAS

Real water samples from river, canal, sewage water, and tap water and industrial wastewater samples from lead storage battery and electroplating industries were collected and filtered through Millipore cellulose membrane filter. To achieve preconcentration method, the solution of pH 6.0 can be passed through the exchanger column at a flow rate of 5.0 mL min^{-1}. The adsorbed ions then can be eluted with 5.0 mL of 2.0 M nitric acid in acetone with a flow rate of 1.0 mL min^{-1}.

Analysis of Heavy Metal Ions Using Membrane Selective Electrodes

Membrane electrodes of composite material with excellent reproducibility and wide working pH range are also used for the detection and determination of toxic metal ions, by choosing the method of (Coetzee and Benson 1971). Different membranes can be prepared by mixing the material with PVC, followed by dissolving it into various solvents including tetrahydrofuran (THF), which further followed the pouring into Pyrex glass circles, and then their selectivity was checked by using mixed solution method (Moody and Thomas 1971) in standard solution. From the calibration data, the concentration of unknown solution (toxic metals) can be determined. Potentiometric titrations and instrumental analysis (UV-Vis, HPLC, etc.) should also be carried out, to ascertain the concentration of chosen pollutant. The potential of the membrane electrode can be measured at room temperature (25 + 2 °C) using the digital potentiometer. Following cell assembly can be set up for the conduction of emf (electromotive force) measurements:

Ag, AgCl | KCl (satd): Sample solution | membrane | 0.1 M M^{2+} | Ag, AgCl

Several studies have been reported the same, which describes in detail the preparation, characterization, and applications of composite cation-exchange material. Some newly composite cation-exchange materials; polyaniline Zr(IV) molybdophosphate in the analysis of Pb^{2+}, Hg^{2+}, Cd^{2+}, Cr^{2+}, and Fe^{3+} from synthetic and real samples (Khan et al. 2014a, b); poly-o-toluidine Zr(IV)iodate analyze Zr^{4+} and Cd^{2+} (Nabi et al. 2012a, b); polyaniline Ti(IV)As for the photochemical degradation of industrial dyes (Shahadat et al. 2012); polyaniline Zr(IV)sulfosalicylate as antimicrobial agent (Nabi et al. 2011a, b); acetonitrile stannic(IV)selenite in the quantitative binary separations of Pb^{2+}–Th^{4+}, Ni^{2+}–Th^{4+}, Ni^{2+}–Zn^{2+}, Cu^{2+}–Ce^{4+}, Al^{3+}–Bi^{3+}, and Al^{3+}–Zn^{2+} (Nabi et al. 2011a); and acrylonitrile stannic(IV) tungstate for heavy toxic metal ions released from wastewater

stream (Nabi et al. 2009) are synthesized recently and utilized in the treatment of environmental pollutants. Polyaniline Ti(IV) arsenophosphate and poly-o-toluidine Zr(IV) tungstate (Bushra et al. 2012; Bushra 2012) are also recently synthesized by Bushra et al. These composite cation-exchange materials showed selective behavior toward heavy metal ions from tap water, electroplating wastewater samples, and organic pollutants. Besides its use as ion exchanger, they also exhibited the characteristics of conducting material, antimicrobial agent, as well as a photocatalyst for the degradation of textile industry dye. Inamuddin et al. synthesized poly-o-methoxyaniline Zr(1 V) molybdate (Inamuddin 2010) for cadmium determination and also determined the ion-exchange kinetic parameters for the poly-o-methoxyaniline Zr(IV) molybdate and polyaniline Ce(IV) molybdate composite cation exchanger (Al-Othman and Inamuddin 2011a, b). Polystyrene based strongly on basic anion-exchange resin De-acidity FF-IP and utilized in the elimination of malathion from aqueous solution (Naushad et al. 2013). The practical applicability of cellulose acetate Zr (IV) molybdophosphate synthesized by Naushad et al. was demonstrated in the quantitative determination and separation of Ca^{2+} and Pb^{2+} from commercially available vitamin and mineral formulation (Nabi and Naushad 2008; Al-Othman et al. 2011c). Khan et al. reported the use of some composite cation-exchange material for the selective separation of Pb^{2+}, Cd^{2+}, Hg^{2+}, and pesticides (Khan et al. 1980, 1999, 2002).

Hybrid material styrene-supported Zr(IV) phosphate, polymethylmethacrylate, polyacrylonitrile, styrene- and pectin-based Ce(IV) phosphate, Th(IV) phosphate, and Zr(IV) phosphate have showed numerous analytical applications (Varshney et al. 2003; Varshney and Pandith 1996).

Adsorption Studies

Adsorption of Organic Pollutants Using Composite Cation-Exchange Material

In this chapter, a compact research work was also done to explore the adsorption properties of composite material toward phenol. The ability of composite material to remove phenol was tested using batch assays. All the experiments were conducted in a series of 250 ml flasks by mixing ion exchanger with aqueous phenol solutions. The parameters studied were pH (2–10), contact time (10–240 min), and various initial phenol concentrations (10–100 mg/L) at laboratory ambient temperature (approximately 35 $\pm$ 3 °C) in 50 ml pH-adjusted solutions. The amount of final residual concentration of phenol was determined at 270 nm, by means of a UV-vis spectrophotometer.

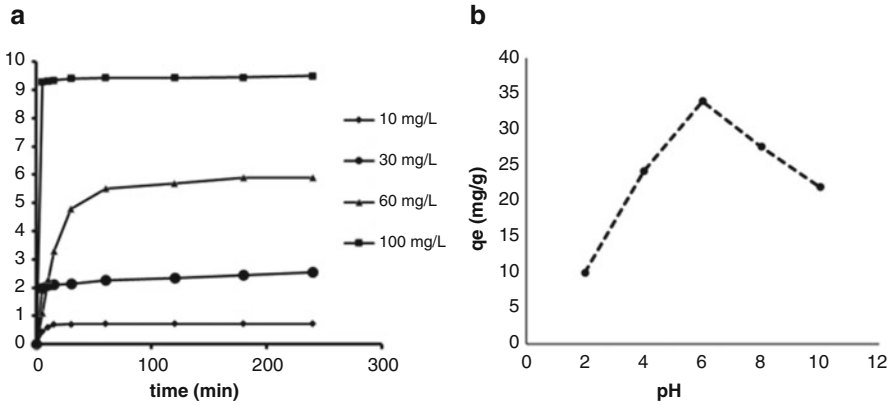

Fig. 2 Effect of time and initial concentration (**a**) and effect of pH (**b**)

Effect of Contact Time and Initial Concentration

The effect of contact time and concentration on the adsorption of phenol are shown in Fig. 2a. The adsorption rate of organic pollutants by the adsorbents was relatively rapid, and the adsorption equilibrium could reach in less than 24 h (Lin et al. 2009). Figure 2a shows the effect of contact time and initial concentration on the adsorption of the phenol on composite material. The adsorption equilibrium of phenol was achieved maximum after 2 h, and no remarkable changes were observed for longer contact time, which indicated that the equilibrium time and adsorption rate of phenol on composite material was rapid than that of some other adsorbents (Lin et al. 2009).

The mechanism of the phenol uptake generally depends on the initial concentration as it provides an important driving force to overcome all mass transfer limitations of phenol between the aqueous and solid phases. It was clear from Fig. 2a that the q_e values increased with the increase in the initial phenol concentrations. At low concentration, the specific sites might be responsible for the adsorption, while in case of increasing concentrations, these specific sites are saturated (Khan et al. 2014a, b). It has been found that the adsorption was concentration dependent and increased with increase in initial phenol concentrations. The equilibrium adsorption capacity at 10, 30, 60, and 100 mg/L initial phenol concentrations were found to be 0.70, 2.95, 3.85, and 9.40 mg/g, respectively.

Effect of pH

The solution pH is the useful parameter, which usually imposes a great influence on the adsorption process of the composite material, so the effect of pH was studied in different initial pH ranging from 2.0–10. Figure 2b displays the adsorption capacity of the composite material for phenol, with different pH values. It can be observed

from Fig. 2b that the adsorption capacity of phenol increased from pH 2.0 to pH 6.0 and decreased from pH 6.0 to pH 10.0. The largest difference in the adsorption capacity between phenols was obtained at pH 6.0, as at this pH, the adsorption capacity was highest. A slight decrease in adsorption capacity was observed from pH 6.0 and may be attributed to formation of phenolate anions. At pH 2.0, the surface of the adsorbent would be protonated and led to donor-acceptor interactions between the aromatic rings of the phenol (Khan et al. 2014a, b), while at high pH values (pH 10 to 12) of alkalinity, the phenol would be ionized in solution, and this led to increase the ionic strength (Khan et al. 2014a, b). It is expected that the selective adsorption and separation of phenol can be achieved at pH 6.0 to 7.0 if they are in a competitive environment.

Composite ion-exchange materials can be applied in a number of disciplines including conducting adhesives, gas sensors, optoelectronics, electrostatic materials, electromagnetic shielding, printed circuit boards, artificial nerves, aircraft structures, electromechanical actuators, drug release systems, catalyst, light-emitting diodes and solar cells, corrosion inhibitors, charge dissipaters, metallization, electrically conductive textiles, chemical and biological sensors, separation and preconcentration of metal ions, photovoltaics, electroplating, photocatalysis, adhesive, fillers, Schottky diodes, solid lubricants, and rechargeable batteries.

Conclusions

This chapter discussed about the synthesis, characterization, and applications of PANI-based composite cation-exchange material. The composite material has been synthesized via sol-gel route and characterized based on FTIR, TGA, XRD, and SEM analysis. The material can be explored further for the removal and recovery of important toxic ions from industrial effluents. Their adsorption properties toward phenol have also been explored using batch process.

References

Agency for Toxic Substance and Disease Registry (ATSDR) (2007) Toxicological profile for lead., U.S. Department of Health and Humans Services, Public Health Humans Services, Centers for Diseases Control. Atlanta

Al-Othman ZA, Inamuddin NM (2011a) Determination of ion-exchange kinetic parameters for the poly-o-methoxyaniline Zr(1V) molybdate composite cation-exchanger. Chem Eng J 166:639–645

Al-Othman ZA, Inamuddin NM (2011b) Forward (M2+−H+) and reverse (H+−M2+) ion exchange kinetics of the heavy metals on polyaniline Ce(IV) molybdate: A simple practical approach for the determination of regeneration and separation capability of ion exchanger. Chem Eng J 171:456–463

Al-Othman ZA, Naushad M, Nilchi A (2011c) Development, characterization and ion exchange thermodynamics for a new crystalline composite cation exchange material: application for the

removal of Pb^{2+} ion from a standard sample (Rompin Hematite). J Inorg Organometal Polymer Mater 21(3):547–559

Berg M, Tran HC, Nguyen TC, Pham HV, Schertenleib R, Giger W (2001) Arsenic contamination of groundwater and drinking water in Vietnam: a human health threat. Environ Sci Technol 35:2621–2626

Borba CE, Guirardello R, Silva EA, Veit MT, Tavares CRG (2006) Removal of nickel (II) ions from aqueous solution by biosorption in a fixed bed column: experimental and theoretical breakthrough curves. Biochem Eng J 30:184–191

Bushra R, Shahadat M, Raeissi AS, Nabi SA (2012) Development of nano-composite adsorbent for removal of heavy metals from industrial effluent and synthetic mixtures; its conducting behavior. Desalination 289:1–11

Bushra R, Naushad M, Adnan R, ZA ALO, Rafatullah M (2014a) Polyaniline supported nanocomposite cation exchanger: Synthesis, characterization and applications for the efficient removal of Pb^{2+} ion from aqueous medium. J Indust Engg Chem 21:1112–1118

Bushra R, Shahadat M, Ahmad A, Nabi SA, Umar K, Oves M, Raeissi AS, Muneer M (2014b) Synthesis, characterization, antimicrobial activity and applications of polyanilineTi (IV) arsenophosphate adsorbent for the analysis of organic and inorganic pollutants. J Hazard Mater 264:481–489

Bushra R, Shahadat M, Khan MA, Adnan R, Arshad M (2014c) Preperation of polyaniline based nanocomposite material and their environmental applications. Intl J Environ Sci Technol. doi:10.1007/s13762-014-0726-5

Bushra R, Shahadat M, Khan MA, Inamuddin AR, Rafatullah M (2014d) Optimization of polyaniline supported Ti(IV) arsenophosphate composite cation exchanger based ion-selective membrane electrode for the determination of lead. Indus Engg Chem Res 53:19387–19391

Castro-González MI, Méndez-Armenta M (2008) Heavy metals: implications associated to fish consumption. Environ Toxicol Phar 26:263–271

Coetzee CJ, Benson AJ (1971) A cesium-sensitive electrode. Anal Chim Acta 57:478–480

Cutter GA (1992) Kinetic controls on metalloid speciation in sea water. Mar Chem 40:65–80

FAO/WHO (2005) Expert committee on food additives, Arsenic

Fewtrell L, Kay D, Jones F, Baker A, Mowat A (1996) Copper in drinking water. An investigation into possible health effects. Public Health 110:175–178

Hopenhayn-Rich C, Browning SR, Hertz-Picciotto I, Ferreccio C, Peralta C, Gibb H (2000) Chronic arsenic exposure and risk of infant mortality in two areas of Chile. Environ Health Perspect 108:667–673

IARC (1993) Summaries and evaluations: Cadmium and cadmium compounds (Group 1). Lyon, International Agency for Research on Cancer, 119

Inamuddin IYA (2010) Synthesis and characterization of poly-o- methoxyaniline Zr (1V) molybdate Cd(II) selective composite cation-exchanger. Desalination 250:523–529

IOM (2001) Dietary reference intakes for vitamin A, vitamin K, arsenic, boron, chromium, copper, iodine, iron, manganese, molybdenum, nickel, silicon, vanadium and zinc. A report of the Panel on micronutrients, subcommittees on upper reference levels of nutrients and of interpretation and use of dietary reference intakes, and the standing committee on the scientific evaluation of dietary reference intakes. Food and Nutrition Board, Institute of Medicine. Washington, National Academy Press

IPCS (1992) Cadmium—environmental aspects. World Health Organization, International Programme on Chemical Safety, Geneva

Joint FAO/WHO Expert Committee on Food Additives (JECFA) (2004) Safety evaluation of certain food additives and contaminants. WHO Food Additives Series No. 52

Khan AA, Niwas R, Vershney KG (1980) Preparation and properties of styrene supported zirconium(IV) tungstophosphate: a Hg(II) selective inorganic-organic ion exchangers. Indian J Chem 37:464–472

Khan AA, Niwas R, Vershney KG (1999) Synthesis and ion exchange behavior of polyaniline Sn (IV) arsenophosphate: a polymeric inorganic ion exchanger. Colloid Surf A Phys Engg Asp 150:7–14

Khan AA, Niwas R, Alam MM (2002) Ion exchange kinetics on styrene supported Zirconium (IV) tungstophosphate: an organic-inorganic type of cation exchanger. Indus J Chem Technol 9:256–260

Khan MA, Bushra R, Ahmad A, Nabi SA, Khan DA, Akhtar A (2014a) Ion exchangers as adsorbents for removing metals from aquatic media. Arch Environ Contam Toxicol 66:259–269

Khan MA, Uddin MK, Bushra R, Ahmad A, Nabi SA (2014b) Synthesis and characterization of polyaniline Zr (IV) molybdophosphate for the adsorption of phenol from aqueous solution. React Kinet Mech Catal 112:1–19

Lin K, Pan J, Chen Y, Cheng R, Xu X (2009) Study the adsorption of phenol from aqueous solution on hydroxyapatite nanopowders. J Hazard Mater 161:231–240

Liu J, Zheng BS, Aposhian HV, Zhou YS, Chen ML, Zhang AH, Waalkes MP (2002) Chronic arsenic poisoning from burning high-arsenic-containing coal in Guizhou, China. Environ Health Perspect 110:119–122

Ming Ho Y (2005) Environmental toxicology: biological and health effects of pollutants, Chap. 12, 2nd edn. CRC Press LLC, BocaRaton. ISBN 1-56670-670-2

Moody GJ, Thomas JRD (1971) Selective ion sensitive electrode. Marrow, Watford

Nabi SA, Naushad M (2008) Synthesis, characterization and analytical applications of a new Composite cation exchanger cellulose acetate-Zr(IV) molybdophosphate. Colloid Surf A Phys Engg Asp 316:217–225

Nabi SA, Naushad M, Bushra R (2009) Synthesis and characterization of a new organic–inorganic Pb^{2+} selective composite cation exchanger acrylonitrile stannic (IV) tungstate and its analytical applications. Chem Eng J 152:80–87

Nabi SA, Bushra R, Naushad M, Al-Othman ZA (2011a) Synthesis, characterization, and analytical applications of a new composite cation exchange material acetonitrile stannic(IV) selenite: adsorption behavior of toxic metal ions in nonionic surfactant medium. Sep Sci Technol 46:847–857

Nabi SA, Shahadat M, Bushra R, Oves M, Ahmed F (2011b) Synthesis and characterization of polyanilineZr(IV)sulphosalicylate composite and its applications (1) electrical conductivity, and (2) antimicrobial activity studies. Chem Eng J 73:706–714

Nabi SA, Bushra R, Shahadat M (2012a) Removal of toxic metal ions by using composite cation-exchange material. J Appl Polym Sci 125:3438–3446

Nabi SA, Raeissi AS, Shahadat M, Bushra R, Khan AM (2012b) Synthesis and characterization of novel cation exchange adsorbent for the treatment of real samples for metal ions. Chem Eng J 200-202:426–432

NAS/NRC (1999) Arsenic in drinking water. National Academy of Sciences/National Research Council, Washington, DC, pp 251–257

Naushad M, Al-Othman ZA, Khan MR (2013) Removal of malathion from aqueous solution using De-Acidite FF-IP resin and determination by UPLC-MS/MS: equilibrium, kinetics and thermodynamics studies. Talanta 115:15–23

Pi JB, Kumagai Y, Sun GF, Yamauchi H, Yoshida T, Iso H, Endo A, Yu LY, Yuki KC, Miyauchi T, Shimojo N (2000) Decreased serum concentrations of nitric oxide metabolites among Chinese in an endemic area of chronic arsenic poisoning in Inner Mongolia. Free Radic Biol Med 28:1137–1142

Salaneck WR, Lundstrom I, Ranby B (1993) Conjugated polymers and related materials. University Press, Oxford, pp 65–169

Shahadat M, Nabi SA, Bushra R, Raeissi AS, Umar K, Ansari MO (2012) Synthesis, characterization, photolytic degradation, electrical conductivityand applications of a nanocomposite adsorbent for the treatment of pollutants. RSC Adv 2:7207–7220

Shahadat M, Bushra R, Rafatullah M, Tow TT (2014) A comparative study for the synthesis and characterization of polyaniline based nanocomposite materials. RSC Adv 4:20686

Skotheim TA (1986) Handbook of conducting polymers, vol 1. Dekker, New York, p 2

Straif K, Benbrahim-Tallaa L, Baan R, Grosse Y, Secretan B, El Ghissassi F, Bouvard V, Guha N, Freeman C, Galichet L, Cogliano V (2009) WHO international agency for research on cancer monograph working group. Lancet Oncol 10:453–454

Subar AF, Krebs-Smith SM, Cook A, Kahle LL (1998) Dietary sources of nutrients among US adults, 1989 to 1991. J Am Diet Assoc 98:537–547

Tchounwou PB, Wilson B, Ishaque A (1999) Important considerations in the development of public health advisories for arsenic and arsenic-containing compounds in drinking water. Rev Environ Health 14:211–229

Topp NE, Pepper KW (1949) Properties of ion-exchange resins in relation to their structure. Part I Titration curves J Chem Soc:3299–3310

Uneyama C, Toda M, Yamamoto M, Morikawa K (2007) Arsenic in various foods: cumulative data. Food Addit Contam 24:447–534

United States Environmental Protection Agency (USEPA) (2005) Arsenic in drinking water fact sheet. 10.07.2011

Varshney KG, Gupta P, Agrwal A (2003) 22nd National conference in chemistry 03, Indian Council of Chemists, I.I.T. Roorkee

Vas J, Monestier M (2008) Immunology of mercury. Ann N Y Acad Sci 1143:240–267

Vershney KG, Pandith AHJ (1996) Synthesis and characterization of Styrene supported Zirconium phosphate; a new hybrid ion- exchange material. Chem Environ Res 5(1–4):141–154

WHO (2000) Cadmium. In: Air quality guidelines for Europe, 2nd edn. World Health Organization Regional Office for Europe, Copenhagen

WHO (2004) Guidelines for drinking-water quality. Sixty-first meeting, Rome, 10–19 June 2003. Joint FAO/WHO Expert Committee on Food Additives

Wojcik DP, Godfrey ME, Christie D, Haley BE (2006) Mercury toxicity presenting as chronic fatigue, memory impairment and depression: diagnosis, treatment, susceptibility, and outcomes in a New Zealand general practice setting (1994-2006). Neuroendocrinol Lett 27:415–423

Remediation of Soils Polluted with Inorganic Contaminants: Role of Organic Amendments

R. Forján, V. Asensio, R.S. Guedes, A. Rodríguez-Vila, E.F. Covelo, and P. Marcet

Abstract The use of amendments made with organic wastes for remediating degraded and polluted soils has shown to be an effective and low-cost treatment to increase soil quality. This improvement in soil quality is reflected in fertility levels, physical and biological quality of the soil, allowing and supporting vegetal covering of previously degraded areas. The addition of organic amendments in polluted soils is considered one of the most promising recovery techniques at present. This is because organic amendment makes use of waste which would in most cases be unutilized for any activities and cause other damage to the environment. Organic amendments, such as biochar, Technosols, sewage sludge and compost, seek to convert waste into environmental benefits at low cost. The use of these techniques accelerates processes such as sorption, precipitation and the formation of complexes that are produced naturally in the soils and which reduce the mobility and bioavailability of pollutants; additionally, its application may stimulate the microorganism development that acts in degradation of both organic and inorganic pollutants. Despite these benefits, the use of wastes as soil amendments has been questioned, as some of them contain high metal concentrations that aggravate the contamination of the degraded soils. Nevertheless, some studies have shown that most of the metals added to soils with the use of waste amendments are in the unavailable form for plants and that when managed properly, applied in appropriate concentrations or mixed treatments, can result in even greater benefits than previously analysed.

R. Forján • A. Rodríguez-Vila • E.F. Covelo • P. Marcet (✉)
Department of Plant Biology and Soil Science, Faculty of Biology, University of Vigo, As Lagoas-Marcosende, 36310 Vigo, Pontevedra, Spain
e-mail: marcet@uvigo.es

V. Asensio
Department of Plant Biology and Soil Science, Faculty of Biology, University of Vigo, As Lagoas-Marcosende, 36310 Vigo, Pontevedra, Spain

Department of Plant Nutrition, University of São Paulo – Center of Nuclear Energy in Agriculture (USP-CENA), Av. Centenário 303, 13400-970 Piracicaba, SP, Brazil

R.S. Guedes
Institute of Agricultural Sciences, Federal Rural University of Amazonia, 66077-530 Belém, Brazil

N.A. Anjum et al. (eds.), *Enhancing Cleanup of Environmental Pollutants*,
DOI 10.1007/978-3-319-55423-5_10

Keywords Soil pollution • Inorganic contaminants • Remediation • Organic amendments

Introduction

Soil Definition

Soil (Soil Taxonomy 1999) can be defined as (i) the unconsolidated mineral or organic material on the immediate surface of the earth that serves as a natural medium for the growth of land plants and (ii) the unconsolidated mineral or organic matter on the surface of the earth that has been subjected to and shows effects of genetic and environmental factors of climate (including water and temperature effects) and macro- and microorganisms, conditioned by relief, acting on parent material over a period of time. A product-soil differs from the material from which it is derived in many physical, chemical, biological and morphological properties and characteristics. In fact, soil is a natural body comprised of solids (minerals and organic matter), liquid and gases that occurs on the land surface, occupies space and is characterized by one or both of the following: horizons, or layers, that are distinguishable from the initial material as a result of additions, losses, transfers and transformations of energy and matter or the ability to support rooted plants in a natural environment. Soils continue to modify over time as a product of weathering and other biotic and anthropogenic activities.

Soil Pollution

Pollution refers to the state of existence of undesirable substances (pollutants) in the environment beyond a permissible limit, which can harmfully affect every sphere of life. Notably, the sources of pollution can be both natural and anthropogenic. Natural sources include geothermal activities, comets, space dust and volcanic activities. Whereas, anthropogenic sources have arisen mainly on account of rapid industrialization and extensive use of chemical substances such as hydrocarbons, pesticides, chlorinated hydrocarbons and heavy metals (Marcano et al. 2003). The latter mentioned source is the major contributor to pollution in contrast to the former (Dubus et al. 2000). Out of a large number of aforementioned anthropogenic sources, toxicological manifestations caused by heavy metals are well known and are considered as highly detrimental (Gaur et al. 2014). The steadily growing population is increasing the production of municipal waste, which contains both organic and inorganic pollutants including potentially toxic elements. Trace elements are accumulated in soil through pedogenic and anthropogenic activities (Moaref et al. 2014; Ahmad et al. 2015).

Trace Elements

There are several sources for trace elements in the environment. Trace elements are released into the environment by many human activities. They are also used in a large variety of industrial products, which in the long term have to be deposited as waste. Parent rocks and metallic minerals dominate the natural sources, while the main anthropogenic sources are agricultural and metallurgical activities between others (Bradl 2005). Trace elements are negligible chemical constituents of soils but are essential as micronutrients for plants. Although trace elements are mainly inherited from parent rocks, their distribution within the soil profiles and their partitioning between the soil components reflect various pedogenic processes as well as the impact of external factors (Kabata-Pendias 2001). The problem of trace elements is associated with the proliferation of industry. Most of the waste generated by industries ultimately ends its journey in soil and water.

Organic Waste Production and Degraded Soils

Worldwide, soil is being seriously degraded as a result of increasing industrial, agricultural and civil activities. Soil contamination, both diffuse and localized, can lead to damage to several soil functions and contamination of surface and groundwater (Vamelari et al. 2010). Trace element contamination of soil is a major concern in most parts of the world due to anthropogenic activities, particularly with the rapid expansion of the industrial activities. A parallel concern is the massive generation of organic waste by human activities, which has led to the proposal of several alternatives to avoid landfilling and promote recycling. Organic amendments are known to improve soil structure and fertility by adding essential nutrients and enhance microbial community of soil (Oldare et al. 2008, 2011). The addition of these organic amendments to soil is a way of enhancing natural mechanisms such as precipitation, complexation, adsorption and absorption, which reduces the bioavailability of the pollutants (Pérez-de-Mora et al. 2007). Moreover, these organic amendments provide a facility to establish plants on polluted soil by binding pollutants, increasing nutrients and stimulating native microbial community (Pérez-de-Mora et al. 2006, 2007; Zaniewicz-Bajkowska et al. 2007; Oldare et al. 2011).

Soil Organic Matter and Trace Element Behaviour

Soil organic matter (SOM) is a mixture of plant and animal residues in different stages of decomposition, substances synthesized microbiologically and/or chemically from the breakdown products and the bodies of live and dead microorganisms and their decomposing remain (Schnitzer and Khan 1972). Humus includes humic

substances plus resynthesized products of microorganisms, which are stable and a part of the soil. Humic substances are a series of relatively high-molecular-weight, brown- to black-coloured substances formed by secondary synthesis reactions. The term is used as a generic name to describe the coloured material or its fractions obtained on the basis of solubility characteristics (Stevenson 1982). Soil organic matter plays a critical role in trace element behaviour. It can decrease the mobility and bioavailability of elements by sorption, chelation and sequestration. Different forms of soil organic matter can also decrease trace element attenuation by soils, enhancing transport of elements onto the solution phase or, by keeping them bound in solution, preventing sorption of elements onto the solid phase.

Various physical, chemical and biological vectors can mobilize trace elements. The most important biogeochemical processes, which influence trace element mobility, include sorption processes, redox reactions as well as weathering processes and speciation (Bradl 2004).

The list of main soil parameters governing processes of sorption and desorption of trace elements (Kabata-Pendias 2001) includes:

- pH and Eh values
- Fine granulometric fraction (<0.02 mm)
- Organic matter
- Oxides and hydroxides, mainly Fe, Mn and Al
- Microorganisms

Adsorption can be defined as the accumulation of a substance or material at an interface between the solid surface and the bathing solution. Adsorption can include the removal of solute molecules from the solution and of solvent solid surface and the attachment of the solute molecule to the surface (Stumm 1992; Sparks 2003). Adsorption does not include surface precipitation or polymerization processes. Adsorption, surface precipitation and polymerization are all examples of sorption. Sorption involves the loss of a metal ion from an aqueous to a contiguous solid phase and consists of three important processes: adsorption, surface precipitation and fixation (Apak 2002; Bradl 2004).

Wastes as Amendments

Different organic and inorganic wastes have been evaluated as amendments to improve some physical, chemical and biological properties of degraded soils (Forsberg et al. 2008; Rodríguez-Jordá et al. 2012; Asensio et al. 2013a; Santos et al. 2014). Some amendments, such as waste compost and sewage sludge, can contain high concentrations of hazardous trace elements that can increase the environmental risk of their application. Therefore, their use should be carefully monitored (Santos et al. 2014). The addition of organic amendments to a polluted soil can dilute the contamination and alter chemical forms so that toxicity is reduced via a range of exposure pathways, for example, the soil solution and the condition for living organisms. Organic matter is an important component for

adsorption of trace elements in many soils. Metals can adsorb on negatively charged phenolic and carboxylic sites of the humics. The addition of organic matter would therefore increase the binding capacity of the soil.

The surface areas and cation exchange capacity (CEC) of SOM are higher than those of clay minerals (Sparks 2003). The role that SOM plays in the retention of ions is indeed significant, even in soils where the SOM content is very low. Metals sequestered in the structure of organic molecules may not readily desorb, suggesting that this may be a mechanism for attenuation. An ideal organic amendment will rapidly decrease the mobility and bioavailability of the contaminant, preventing leaching, plant uptake, etc. The traditional practice of waste disposal is to apply it to the soil, due to its capacities to retain, filter, decompose, recycle or immobilize the waste products. The soil can absorb and degrade many types of potential pollutants, but its capacities are not unlimited. When this buffer property is exceeded, the soil itself may become a contaminant. A key question for remediation by chemical immobilization is how to select an appropriate amendment. An ideal amendment will rapidly decrease the mobility and bioavailability of the pollutant, preventing the introduction of the contaminant into the food chain. It is generally assumed that a decrease in metal concentration in the soil solution reduces metal leaching and metal uptake by and toxicity to plants and soil organisms.

In this chapter, different organic amendments and their effect on soil quality and its trace element sorption capacity were presented. Soils can help us to construct a better world, and organic amendments must return to soil helping to solve pollution and climatic problems as we mentioned above. Four of the most used amendments in soil recovery during the last decades are described in this chapter. We start with sewage sludge and compost, and we also described modern soil amendments such as biochar and tailor-made Technosols, which are developed based on the model of terra preta and other anthropogenic soils.

Organic Amendments

Sewage Sludge

Sewage sludge is the mud produced in wastewater treatment plants. Due to their high concentration in organic matter and nitrogen, and also to its low price, it has been used as a soil amendment several decades ago. However, when sewage sludges started to be used for that purpose, some problems were detected. High concentration of metals, pathogens, parasites and sodium in some of the sludges caused serious problems to the soils amended with that waste, especially in the croplands (Singh and Agrawal 2008). The concentration and presence of those chemical and biological compounds depend on the wastewater treatment plant and are widely variable among sites. Due to those problems, some countries limited or even prohibited the use of sewage sludges as soil amendment (European

Commission 1991; United States Environmental Protection Agency 1993; CONAMA 2006). Nevertheless, some solutions were created, being the most effective composting the sludge and maintaining it at a high temperature during the process. The composting process eradicates most pathogens and, at the same time, stabilizes the organic matter to more humified forms and avoids undesirable odours in the final product (Yu and Huang 2009). Avoiding the use of sewage sludges with high concentration of those elements can mainly solve the problem of metals, but, nonetheless, recent studies carried out in different countries observed two facts demonstrating that the use of sewage sludges as amendments for polluted soils not only decreases the problem of high metal concentration but also even increases soil sorption capacity. The first fact is that most metals are in non-available form in the sewage sludges. Consequently, plants cannot take up those metals, and they would not be leached to the groundwater, as they are strongly complexed with some soil components such as organic matter and clay fraction (Álvarez et al. 2002; Wang et al. 2008a; Asensio et al. 2013b; Bowszys et al. 2015). The second fact is that the high concentration of organic matter in the sludge and, in some cases, also of clay fraction increases the sorption capacity of the soil (Paradelo et al. 2011; Garrido et al. 2012; Navarro 2012; Asensio et al. 2014). That means that the soil will have the capacity of retaining a higher amount of metals than before being amended, which would be very helpful in case it is polluted with inorganic contaminants. In fact, because sewage sludges can increase soil sorption capacity is the main factor why they can be used for the remediation of soils polluted with inorganic contaminants. However, there is still controversy about their use as soil amendments also within the scientific community due to the high concentration of metals and pathogens in some of the sludges. Because of that, it is still important that the sewage sludge used as soil amendment is subjected to an adequate chemical analysis in order to verify that the concentrations of pollutants in available form are not over the threshold limit, and it is complicated for the authorities to control all of the sludges used for that.

There are a few field studies where the efficiency of sewage sludges for remediation of soils polluted with inorganic contaminants was proven. Hattab et al. (2015) evaluated a case of composted sewage sludge (CSS), which was successfully applied to a metallurgical landfill located behind a steel and iron factory, currently active. The landfill soil was polluted with Mo, Zn, Cu, Cr, As and Co. The application of CSS significantly decreased the mobility of Mo, Cr and Co. Asensio et al. (2013b) studied the case of a mine tailing soil polluted with chromium and copper where, after the application of sewage sludge, the concentration of both metals significantly decreased. Pogrzeba et al. (2015) evaluated the use of a mixture of sewage sludge and coal fly ashes (called “slush”) for being applied to a soil located near a former lead and zinc plant. The soil was polluted by Cd, Pb and Zn, and, after the application of just 3% of slush (slush/soil ratio), the concentration of the three metals was significantly reduced and even had a positive impact on the total number of soil bacteria and fungi. Notably, most research studies have been done under laboratory or greenhouse conditions, and, therefore, more field experiment is necessary to confirm the effect of sewage sludges after being added to the soil.

Compost

Despite the sewage sludge efficiency in the remediation of contaminated soils, its use presents limitations due to its composition, which can have a high concentration of phosphorus and nitrogen (causing eutrophication of waterbodies), as well as significant amounts of metals (Peyton et al. 2016). Prior to land application, the stabilization of sludge can be an appropriate technique to reduce the risk of hazardous substances present in the waste. The most preferred method of neutralization of sewage sludge is composting. Sewage sludge can be composted by mixing sludge with other organic bulking agents such as straw, bark or green waste, etc.

Composting is the process in which organic matter is transformed into compost by aerobic microorganisms; it comprises three major phases: mesophilic, thermophilic and cooling phase (the compost stabilization phase). It is a complicated process aimed at destruction of pathogenic organisms by the metabolic heat generated by the thermophilic phase, which degrades a big number of hazardous organic pollutants; stabilization of organic matter, drying of the sludge; and production of material which can be environmentally used as a soil improvement or fertilizer. The use of composting for remediation of contaminated soil has been well documented (Barker and Bryson 2002; Taiwo 2011; Taiwo et al. 2016). Siebielec and Chaney (2012) applied compost to remediate contaminated soil from a military site in Maryland, USA. The study of Mangkoedihardjo et al. (2008) was able to remove 50% of hexavalent chromium in chromium eluted soil using the combined compost and plant technology.

During the composting process, the metal content can be reduced by the addition of some chemicals, microbial inoculants and earthworm. The principal advantage claimed for biological process over the use of chemicals during composting is the low capital cost. Additionally, the compost quality may decrease due to trace element content. Its quality can be improved by adding some chemical compounds. Many studies have been carried out by using some sorbents like natural zeolite (Zorpas et al. 2008; Villasenor et al. 2011), lime (Fang and Wong 1999) and lime and sodium sulphide (Wang et al. 2008b). These chemical compounds used as amendments can improve compost quality by removing or changing mobile and available form of metals to less mobile or residual or less available form.

Reduction of Heavy Metals During Composting Using Microorganisms

The inoculation of microorganisms could be very useful to improve the composting process by enhancing enzymatic activity, and quality level of the compost is acceptable. Biosorption is the process in which some microorganisms, such as bacteria, fungi or algae, are used to remove environmental contaminants. These biological materials have received increasing attention for heavy metal removal and recovery due to their good performance, low cost and large available quantities

(Wang and Chen 2009). The biosorption process includes the following mechanisms: transport across cell membrane, complexation, ion exchange, precipitation and physical adsorption (Javanbakht et al. 2014). Liu et al. (2009) proved that the composting methods without inoculants and with inoculants of *Phanerochaete chrysosporium* could effectively transform Pb fractions, reduce active Pb and alleviate the potential harm of Pb-contaminated waste. The biosorption efficiency of filamentous fungus, *Aspergillus fumigatus*, towards remediation of heavy metals has also been evaluated (Shazia et al. 2013). Potent metal biosorbents of bacteria include the genera *Bacillus* (Tunali et al. 2006) and *Pseudomonas* (Chang et al. 1997; Uslu and Tanyol 2006).

Vermicompost

A step forward in composting is the vermicompost. The vermicomposting is the process of waste biodegradation, involving the joint action of earthworms and beneficial microbial communities (Suthar et al. 2012). In this process, the sludge is stabilized effectively because of many beneficial impacts of inoculated worms upon aerobic degradation mechanism in waste stabilization system. Although microbes are responsible for biochemical degradation of organic matter, earthworms are the important drivers of the process, conditioning the substrate and altering the biological activity (Aira et al. 2009; Gomez-Brandon et al. 2011). Earthworms promote appropriate conditions in decomposing waste subsystems, ingest organic solids, convert a portion of the organics to worm biomass and respiration products and expel worm cast as partially stabilized matter with low contents of hazardous substances (Dominguez and Edwards 2011).

Vermicomposting can be an appropriate technique to reduce the level of hazardous substances from wastewater sludge solids (Negi and Suthar 2013). Vermicomposting is the usual method that is managed by earthworms, and in addition to decomposing of organic waste, the availability of trace elements like Pb and Cd decreases due to bioaccumulation of these metals and organo-complex formation during this process (Ghyasvand et al. 2008). Li et al. (2010) showed that *Eisenia fetida* can accumulate Cu, Zn, Pb and Cd. The adult earthworm was speculated to have such an ability to store high concentrations of heavy metals in the non-toxic forms. Azizi et al. (2015) examined the effect of vermiconversion activity on heavy metal concentration in the vermicompost produced as well as *L. rubellus* multiplication and growth during the process. Hartenstein et al. (1980) studied that earthworms can bioaccumulate high concentrations of heavy metals like cadmium (Cd), mercury (Hg), lead (Pb) copper (Cu), manganese (Mn), calcium (Ca), iron (Fe) and zinc (Zn) in their tissues. They can particularly ingest and accumulate extremely high amounts of zinc (Zn), lead (Pb) and cadmium (Cd). Cadmium levels up to 100 mg per kg of dry weight have been found in tissues. Ireland (1983) reported that the earthworm species *Lumbricus terrestris* can bioaccumulate in their tissues 90–180 mg lead (Pb)/g of dry weight, while in *Lumbricus rubellus* and *Dendrobaena rubida*, it was 2600 mg/gm and 7600 mg/gm of dry weight, respectively. Singh and

Kalamdhad (2012), in their review, concluded that during the vermicomposting, earthworms can accumulate a high concentration of trace elements in the non-toxic forms and are capable to reduce possible toxic effects of unessential trace elements by utilizing them for physiological metabolism. Singh and Kalamdhad (2013) have also reported the reduction in the exchangeable and carbonate fractions of Cu, Ni and Cr in all trials of water hyacinth vermicomposting.

Green Compost

Bioremediation actively enhances the effects of naturally occurring biological processes that degrade contaminants in soil. A method of green remediation is the green waste compost application or a combined composting and vermicomposting system.

The application of green compost for the remediation of inorganic contaminants is one of the most inexpensive and simple techniques in operational terms. This is the reuse of plant materials, which undergo a process known as composting, in which organic matter is partially decomposed by aerobic heterotrophic organisms, in order to obtain, as soon as possible, a stable material, rich in substances like humic and mineral nutrients. Initially, the use of green composts was limited to agriculture, where great benefits were observed mainly to soil fertility; however, currently these composts are commonly added to other soil-forming materials for use on landfill caps and the revegetation of sites where contaminated soil has been removed (Bending et al. 1999). The green composts increase the soil organic matter content, raise fertility and improve the soil structure prior to the establishment of vegetation (Alvarenga et al. 2008). It can also be used to restore remediated areas as a plant-supporting soil (Sellers et al. 2004) and can directly help in the remediation process of contaminated soils (Bardos and van Veen 1996). Remediation of soils with compost can also improve biodegradation of organic contaminants by microorganisms from the compost as well as immobilization of heavy metals by the compost itself.

The use of composted vegetal materials has been strongly encouraged and gradually better explored for the remediation of contaminated soils. Rapid mobilization and vertical transport of trace metals and As were also a consequence of adding this material to soil (Beesley and Dickinson 2010). However, Mikutta and Kretzschmar (2011) claim that partial stabilization of As via outer-sphere complexation with protonated amino groups and/or Fe-bridged ternary inner-sphere complexation with carboxylate/phenolate groups on the surface can also occur. Both processes are important in soil remediation.

In areas contaminated by metals, Beesley et al. (2010a) reported high potential of composts in reducing the bioavailability of Zn and Cd, drastically reducing the phytotoxicity effect of such element. Green waste compost proved to be more effective than lignite, probably because of the difference in chemical composition and extent of dissolution (Tsang et al. 2014). One of the beneficial effects of compost is related to the organic matter's ability to retain metal cations and to evaluate it. Kumpiene et al. (2007) tested in lysimeter the metals leaching under

field conditions and reported high adsorption capacity for organic matter with respect to Pb. It is believed that the greatest contribution of organic matter in green composts is due to the high fulvic and humic acid concentrations of compost, which give them high metal-binding capacities (Perminova and Hatfield 2005; O'Dell et al. 2007). According to Tsang et al. (2014), green waste composts contain carboxylate groups 8.8% and 46.1% inorganic ash (surface hydroxyl groups), which in the treatment of soils contaminated by metals such as Cu results in higher immobilization rate compared to other treatments like lignite. According to Karami et al. (2011), the simultaneous use of biochar may be a way to maximize the use of green compost remediation of soils contaminated with lead and copper. These authors affirm that combination of compost and biochar had a synergistic effect with a greater efficacy for reducing Pb concentrations in pore water and uptake to plants. The potential of green composts in combination with biochar was also reported by Beesley et al. (2010c) who observed a significant reduction of water-soluble Cu and As concentrations; however, the mechanisms that promote these effects in the soil are still poorly understood and require further investigation. There are promising prospects about the green composts used in the remediation of contaminated soils. According to Dutta and Das (2010), this technique increases every year and the level of interest in research and development. However, Pitt et al. (1999) emphasize the importance of the source of material used in preparing compounds due to the possibility of introducing other contaminants in the soil.

Biochar

Origin: Terra Preta de Indio

The terra preta of the Brazilian Amazon are anthropogenic dark earths, characterized by enhanced levels of soil fertility and popular locally for growing cash crops such as papaya and mango. These crops are said to grow three times faster than on surrounding land, a landscape characterized by soils of generally low fertility. Although the terra preta occur in small patches averaging 20 ha, sites as large as 350 ha have been reported (Smith 1999). The origin of biochar is connected to the ancient Amerindian populations in the Amazon region, locally known as terra preta de índio, where dark earth was created through the use of slash-and-char technique (Ahmad et al. 2014). Similar soils have not only been identified elsewhere within the region, namely, Ecuador and Peru, but also beyond, in West Africa (Benin, Liberia) and the savanna of South Africa (Lehmann et al. 2003; Sohi et al. 2009a). In countries like England or Japan, the use of charcoal was the topic of research related to agriculture in the late nineteenth century and throughout the twentieth century. The use of biochar in soil is common in Japan; there are old texts of 1697 where the use of biochar in agriculture is detailed (Lehmann and Joseph 2009a, b). In terra preta soils, the presence of ceramic artefacts and pyrolysed organic matter (Fig. 1b), called biochar, as well as non-pyrolysed (Fig. 1a) is common.

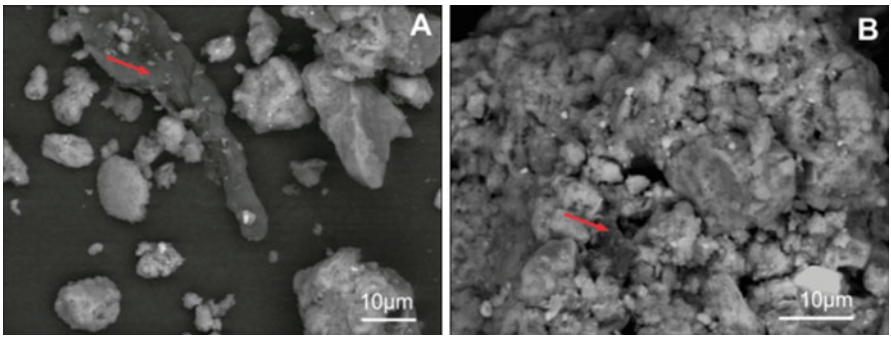

Fig. 1 Electronic microscope images of "terra preta de índio", where we can observe fragment of organic matter non-pyrolysed (**a**) and pyrolysed (**b**)

Biochar: Definition

Although the International Biochar Initiative (IBI) standardized its definition as "a solid material obtained from the thermochemical conversion of biomass in an oxygen-limited environment" (IBI 2012), different ways can elaborate the biochar, for example, prunings, biomass from different crops, different waste ranching and sewage sludge which may be the material to be pyrolysed. Biomass should be chosen depending on the desired ratio of products and pyrolysis technique used. To produce biochar, the starting material determines some of its features and content of macro- and micronutrients, physical structure, the water holding capacity, etc.; this is very important for the effects of biochar which may have to be applied as a soil amendment (Sohi et al. 2009b).

Biochar is a carbon-rich, fine-grained, porous substance, which is produced by thermal decomposition of biomass under oxygen-limited conditions and at relatively low temperatures (<700 °C) (Lehmann and Joseph 2009a,b; Sohi et al. 2009a). The definition adopted by the International Biochar Initiative (IBI) furthermore specifies the need for purposeful application of this material to soil for both agricultural and environmental gains (Sohi et al. 2009a). This fact distinguishes biochar from charcoal, which is used as a fuel for heat, as an adsorbent material or as a reducing agent in metallurgical processes (Lehmann and Joseph 2009a,b). Figure 2 presents images in scanning electron microscope and respective spectrums. Additionally, Fig. 2a, b presents images in scanning electron microscope in which high porosity in carbon structures is observed. These structures are often described as tubular forms that can be found along the material and are considered one of its main characteristics (Sohi et al. 2009a; Wang et al. 2015). The formation of this porous structure basically depends on the material and the pyrolysis temperature used in the preparation of biochar. Thus, biochar, for example, produced from wheat between 500 and 700 °C produced a material with a surface area > 300 m^2/g, while the same material is produced between 300 and 400 °C, with a surface area < 200 m^2/g (Tang et al. 2013). According to Sparks (2003), these porous structures are of great importance

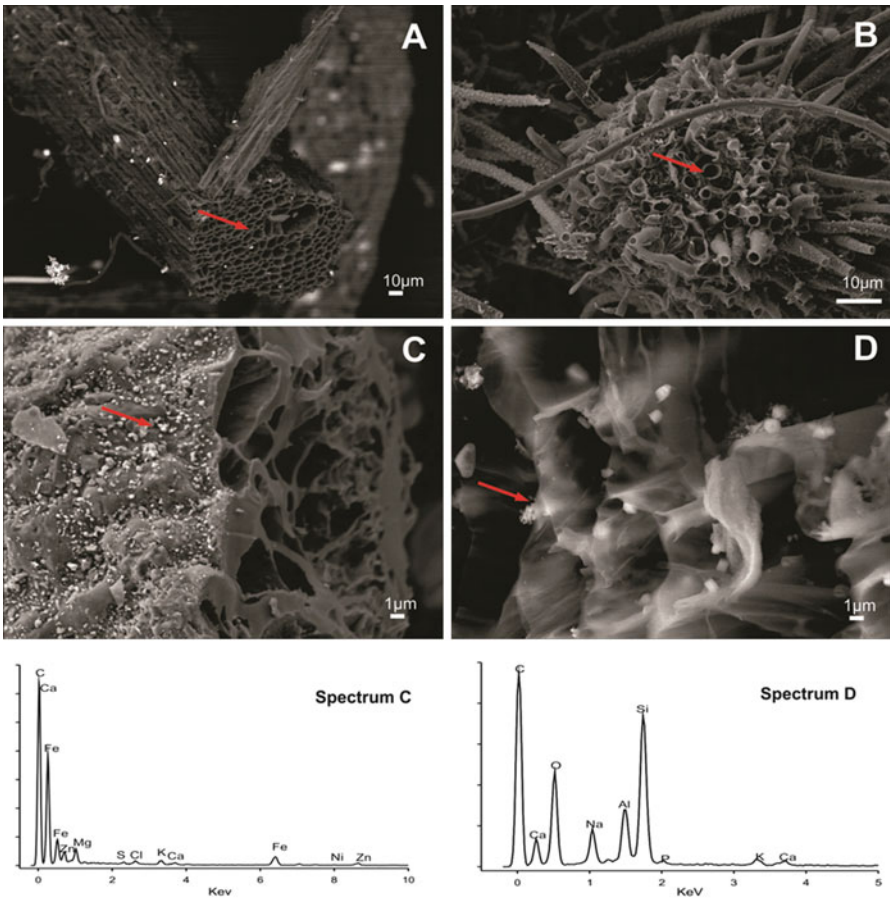

Fig. 2 Images in scanning electron microscopy with energy dispersive spectrometer (SEM-EDS) for maize biochar, with tubular microstructures (**a**, **b**) and surface interactions (**c**, **d**)

in the soil metal adsorption process since it is a process dependent on contact between molecules and the structure surface and, moreover, favours the retention by intraparticle diffusion.

Figure 2c, d shows spectrums of the chemical composition on points of interest of the biochar surface, where we can observe the interaction of carbon with salt crystallized after the pyrolysis process that may occur due to a pyrolysis process at lower temperatures such as 300 °C (Wang et al. 2015). Various macronutrients composing biochar such as Ca, P, S, Mg and K and micronutrients such as Si, Fe, Zn, In and Ni can also be viewed. The chemical composition of biochar increases the soil fertility, and the inputs of metals in the soil are insignificant in a slow decomposition process (Nguyen et al. 2009; Sohi et al. 2009a, b).

Biochar can be produced at temperatures of 200–900 °C in the presence of little or no oxygen, which is commonly known as pyrolysis (Ahmad et al. 2014). The importance of temperature in this context has been argued as a most important feature when developing the biochar (Schmidt et al. 2011). Certain types of biochar can degrade relatively rapidly in some soils, which suggests that pyrolysis could be optimized to generate a more stable biochar. Other physical and chemical properties of biochars are influenced by the properties of the feedstock and by pyrolysis conditions such as furnace residence time (Kloss et al. 2012). For example, surface area increases with an increase in pyrolysis temperature. However, a reduction in surface area at $\geq$700 °C has also been reported (Uchimiya et al. 2011).

Biochar Use

Four major areas where biochar is being used (Lehmann and Joseph 2009a, b) include (i) environmental management which includes soil improvement, (ii) waste management, (iii) climate change mitigation and (iv) energy production. This section discusses the biochar use in soil improvement.

Biochar has high values of pH, cation exchange capacity and key macro-elements and can enhance soil productivity (Beesley et al. 2010a; Zhang et al. 2013). But one of the most interesting properties of biochar in comparison to other soil amendments is reduction of heavy metal accumulation in soils. Biochar has a large surface area and complex metal ions on their surface and therefore reduces bioavailability. Traditional amendments (sludge or compost) can contain trace elements and incorporate them into the soil. The waste material used to make biochar usually has a low or negligible content of trace elements (Beesley et al. 2010a, b; Fellet et al. 2011; Park et al. 2011). For this, and for the characteristics listed above, biochar is currently gaining strength as an amendment to restore degraded or contaminated soils. Biochar can be used as single amendment or mixed with other amendments to enhance the positive influences of these amendments (Forján et al. 2015, 2016).

Biochar and Trace Element Pollution

Several experiments have demonstrated the capacity of biochar to reduce the soil metal content or its availability. For example, hardwood-derived biochar can diminish water-soluble concentrations of some metals, for example, Cd, Zn and Cu, and consequently their phytotoxic effect (Beesley et al. 2010a). Cao et al. (2009) demonstrated the capacity of biochar derivative of dairy manure to sorb Pb and indicated that dairy manure can be converted into biochar as sorbent for metals, implying that manure can potentially serve as a remediation amendment. Another example of the capacity to reduce leaching of metals was demonstrated by Choppala et al. (2012) who showed that the application of biochar derived from chicken manure to chromate (CrVI)-contaminated soils enhanced the reduction of

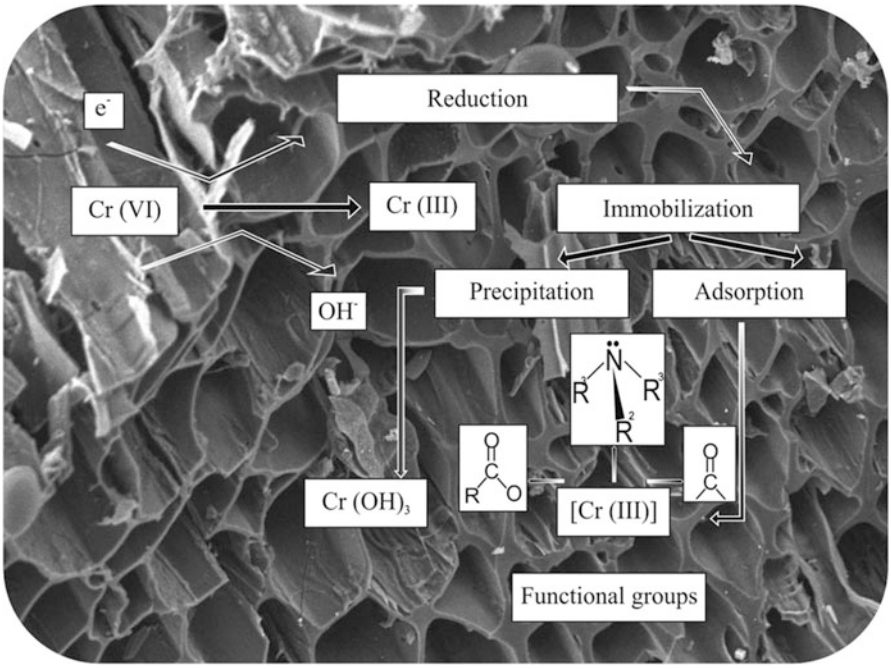

Fig. 3 Concomitant reduction and immobilization of chromium in *black* carbon-amended soils (Bolan et al. 2013)

mobile Cr(VI) to less mobile Cr(III), thereby decreasing the leaching of Cr. After that, Bolan et al. (2013) proposed a model in reduction and immobilization of chromium in biochar carbon-amended soils (Fig. 3).

Park et al. (2011) concluded that biochar reduces the bioavailability and phytotoxicity of trace elements. The immobilization and phytoavailability of Cd, Cu and Pb were examined using naturally contaminated shooting range and spiked soils. Biochar samples prepared from chicken manure and green waste were used as soil amendments. The results obtained showed that biochar application to metal-contaminated soil has the potential of in situ remediation by immobilizing metals, thereby reducing metal availability to the plants. In addition, biochar improves agronomic properties by increasing nutrient availability and microbial activity. Chicken manure-derived biochar was more effective in both the immobilization of metals and increasing plant growth than green waste-derived biochar. Therefore, chicken manure-derived biochar can be used to enhance phytostabilization of metal-contaminated soils.

Biochar can also be utilized by its sorptive capacity to remove contamination in the water treatment process. The precedent for a centralized approach is the current use of activated carbon for the removal of trace elements (Sohi et al. 2009a, b).

Uchimiya et al. (2010) demonstrated that the biochar not only can reduce the concentration of metals in soil, but it can also do it in the water. Experiments were conducted to test for the ability of biochar to immobilize a mixture of heavy metals (Cd, Cu, Pb, Ni, Pb) in water, and the results confirmed the premise. A more recent experiment realized by Frišták et al. (2015) investigated the utilization of two different woody-derived biochars for Cd^{2+}, Zn^{2+} and Cu^{2+} ion separation from aqueous solutions. The experiment confirmed that garden wood rests with leaf mass-derived biochar could be utilized as an effective sorbent for bivalent ions. These last experiments are important because heavy metals enter ecosystems not only from primary industrial sources such as metal plating or mining but also from secondary pollution via wastewater and sewage sludge. Heavy metals in wastewater or industrial effluents may pose unforeseen ecotoxicological risks if they escape from the wastewater treatment facilities into the receiving waters. Even if they are withheld and removed from wastewater successfully, they may damage the biology of the treatment plant and require expensive adsorption and cleaning technologies Frišták et al. (2015). A more recent experiment realized by Frišták et al. (2015) investigated the use of two different woody-derived biochars for Cd^{2+}, Zn^{2+} and Cu^{2+} ion separation from aqueous solutions. Physicochemical characterization confirmed the main differences in sorbent surface area and cation exchange capacity. The garden wood rests with leaf mass-derived biochar can be utilized as an effective sorbent for bivalent ions.

An example of a large-scale experiment was made by Aspen Center for Environmental Studies in the Hope Mine (ACES 2011). ACES' Hope Mine Biochar project was the first and largest whole-mine reclamation project using biochar that has ever been done in the USA. This was an experimental project to test the effects of biochar in mine reclamation and to restore a devastated landscape. The Hope Mine is located approximately six miles from Aspen, CO. It was an active silver mine in the early nineteenth century that changed hands through a number of owners until the USFS took ownership of it in 2003. Mine waste formed large piles of toxic grey rock, containing no vegetation that ran directly into Castle Creek, Aspen's water supply. While the Aspen Water Department found no evidence of heavy metals leeching into Castle Creek, there was a concern for potential catastrophic erosion. If a heavy rain event were to cause the mine waste piles to slide into Castle Creek, it could shut off Aspen's water supply for an extended period. Some of the preliminary year-one results showed biochar performed better for revegetation than compost alone; the plots with biochar held much greater soil moisture than the plots without; an excellent root zone was being developed in areas with both compost and biochar treatments; and slope stability and erosion control were achieved in just 1 year with biochar. Biochar improves the characteristics of the degraded soil and stopped erosion, and thus, heavy metals were fixed. With this experiment, to prevent possible contamination with heavy metals was achieved.

Tailor-Made Technosols

Anthropogenic Soils

Ancient cultures attributed maintenance of the fertility of cultivated soils to the periodic addition of organic and inorganic amendments (anthropogenic materials). In fact, anthropogenic soils have been formed throughout human history and, in certain cases, have produced soils that are more fertile, with a higher productive capacity and of better quality than natural soils present under the same pedoclimatic conditions (Sombroek et al. 1993). This is true for many soils defined as "plaggen soils" in coastal areas of central and northern Europe and for the soils known as "terra preta de índio", in Brazil (Macías and Camps 2010).

Technosols have emerged as a new reference soil group, and it was included by the International Union of Soil Sciences (IUSS) in the World Reference Base for Soil Resources in the IUSS (2006). This term makes reference to soils whose properties and pedogenesis are dominated by their technical origin. This fact is reflected by the presence of artefacts (materials created or substantially modified by humans, e.g. bricks, pottery, glass, industrial waste, garbage and mine spoil) (unconsolidated residues derived from anthropogenic activities, with similar characteristics) to the geologic and biogenic components of the soils, which may act as fresh parent material and which, under the influence of soil-forming factors, may originate new soils (Dudal et al. 2002) or because they are sealed by technic hard rock (material created by humans, e.g. pavement). In summary, it is a soil dominated or strongly influenced by human-made materials and more frequently found in urban and industrial areas (Macía et al. 2014).

These concepts are new opportunities for soil science in integrating food production, waste management, conservation and development of soil as needed for environmental sustainability, using soil as adsorbents and as reactors that eliminate pollutants, reducing their mobility and bioavailability. Concepts like "tailor-made Technosols" go in this direction, which may be an example development triangle of waste management-carbon sink-pollution control, which has been used as a foundation for land reclamation processes with Technosols. However, Technosols can be designed, formulated and developed with components, properties, edaphic structure and unwanted organisms, which solved specific problems or environmental degradation or contamination of soil, water and ecosystems. An adequate technosol selection, based on its nature and intrinsic properties, can constitute a valuable and cost-effective solution for soil remediation and waste management and may be an adequate resource for mining restoration (Almendro-Candel et al. 2014).

A good example of the use of Technosols to recover degraded soils was the case of the experiment of a copper mine (Touro, Spain) conducted by Macías et al. (2009). Touro mine is an old abandoned copper mine. Mine tailings and other mine areas without vegetation or soil which supports oxidation of metal sulphides generated acid drainage and polluted the waters of nearby rivers. With different

Fig. 4 Copper mine landscape in untreated and treated Technosols at 1, 5 and 10 years

Fig. 5 Soil profiles in copper mine areas untreated and treated with Technosol at 1, 5 and 10 years

residues by suitable formulations based on the imitation of the components and properties of some natural soils, Technosols to solve or mitigate the problems with metals or environmental limitations were developed. After the application of the different Technosols was achieved assessing liming elements and nutrients in the waste, this allowed the correction of the problems of toxicity and acidification of soil and water (Macías et al. 2009; Macías and Camps 2010). Currently, the Technosols are combined with other amendments, such as biochar. This mixture is made to maximize binding of metals. Forján et al. (2015) used a mixture of Technosols and biochar on a degraded soil of a copper mine. In this case, the biochar was made of biomass (*A. dealbata*). The application of this amendment (technosol-biochar) on a degraded mine soil increased the capacity of the soil to sorb Cu and Zn. To this end, Fig. 4 shows the application of tailor-made Technosols in the recovery of old copper mine areas over 10 years. The application areas show significant changes in the landscape like low and medium vegetation formation, as a result of improving soil fertility and reducing the phytotoxicity elements in the area. According to Carvalho et al. (2013), the high nutrient content in Technosols is what allows the germination and growth of vegetation. However, Fig. 5 shows mine soil profiles treated (and not) with Technosols at different evolution times in soil

recovery process, where we can observe a stabilization process of organic matter, soil browning and progressive profile development. Improving the physical, chemical and biological qualities in Technosols has been frequently reported (Séré et al. 2010; Macía et al. 2014), and in this context, Scalenghe and Ferraris (2009) analysed the first 40 years of the technosol development, which reported higher levels of organic matter, hydraulic conductivity and the development of a wide range of plant species.

Recent experiments, in addition to mixing biochar and technosol, have included phytoremediation plants. Rodríguez-Vila et al. (2015, 2016) applied an amendment consistent in a mix of technosol-biochar and with *Brassica juncea* in mine soils. The application of amendments made of wastes and biochar to a copper-polluted settling pond soil improved the soil conditions for the establishment of mustards by reducing the extreme soil acidity, increasing the C and N concentrations and generally reducing the $CaCl_2$-extractable concentration of metals. However, the used technosol increased the Pb and Zn pseudototal concentrations in the amended soils. It was not possible to grow up mustards in the untreated mine soil due to the extremely degraded conditions of that soil. The incorporation of technosol and biochar as a soil amendment reduced the mobility factor for Cu, Ni and Pb and generally reduced the sum of metal concentrations in the mobile fractions. The application of amendments reduced the total Cu concentration in *B. juncea* but generally increased both the Pb and Zn concentration in plant tissues. We suggest caution when adding organic wastes to the soil, as they can lead to increase concentrations of Zn in phytoavailable form. In this case, we can see positive influence of technosol in some parameters such as pH, C and N, generally reducing the $CaCl_2$-extractable concentration of metals. However, negative influence in this case is the increased of $CaCl_2$-extractable concentration of Pb and Zn. The total balance of the application of Technosols in a degraded soil is positive.

One problem attributed to the Technosols is that the components with which it is made may contain metals. Some authors have demonstrated that Technosols can contribute to retain these toxic elements, which are retained due to the characteristics of Technosols. Because of this, metals are not available. This is important due to the positive influences of the Technosols are not affected and these continue to be beneficial to retain metals from contaminated or degraded soil. Nowadays, the Technosols are designed with a very low content of metals and can be used in several types of soils, not only in degraded soils. Urban soils are an option of the application of this kind of "artificial" soils. The soil recovery potential of this mixture of residues is very interesting, despite the potential contribution to the pollutant input. Tailor-made Technosols must fulfil the environmental and productive functions of natural soils. Environmental problems associated with the use of Technosols may be prevented if (1) the characteristics of the materials used, as well as how the constituent z mixtures evolve over time, are well known and suitable for such purposes and (2) the characteristics of the final products obtained are suited to the pedoclimatic conditions and to uses of the area to be restored (Xunta de Galicia 2008). By producing such soils, we aim to (1) simultaneously solve problems associated with waste management and with the restoration of degraded or

contaminated soils, in an affordable and environmentally sound manner, (2) eliminate or greatly reduce the impacts of waste products in the most sensitive systems (water, air and biota) and (3) stabilize organic C forms in soils and biomass.

Asensio et al. (2013a) evaluated soil quality of different mine soils treated with different Technosols at different time and with or without vegetation. In order to assess the quality of these soils, a soil quality index (SQI) was created by totaling the scores of the minimum data set (MDS) selected through a principal component analysis (PCA) proved to be a valid and useful tool (Asensio et al. 2013a). The selected mine (old copper mine) is located in Touro (Galicia, Northwest Spain). Two different zones at the mine were sampled: the settling pond (B) and the mine tailing (M). Most selected characteristics for the SQI of reclaimed settling ponds or mine tailings, such as pH, total N concentration or clay percentage, are usually selected for other type of soils. Variables related to carbon fractions (humin C, humic acids C and fulvic acids C) were also selected as soil quality indicators for both mine zones. However, other variables are characteristic of soils at metal mines and amended with sewage sludges, such as the concentration of several metals. Although authors initially expected that some variable related to Cu, such as pseudototal Cu, had been selected for the SQI of copper mine soils, they were not. This could be due to, given the high Cu concentration in all analysed soils (in the reclaimed ones as well) even with remarkably different values among them, Cu variations that appear to be not sufficiently relevant in the PCA to modify significantly their quality assessments. However, that does not mean that copper is not considered at all, since it is strongly correlated with several soil variables included in the SQI and, therefore, represented by them. In the case of the SQI for settling pond soils, copper concentrations are represented by soil pH, CECe (effective cation exchange capacity), SOC (soil organic carbon), humin C and clay. In the SQI for mine tailings, copper is represented by soil pH. This fact additionally offers an evidence of the robustness of the method used for calculating the SQI of highly polluted soils.

The treatment that most increased the quality was amending with wastes because it increased soil pH, CECe, MWD (mean weight diameter), concentrations of all chemical forms of soil organic C, total N concentration, clay percentage and phytoavailable K concentration. In applying the proposed SQIs, authors observed that the untreated mine sites had a very low quality and that the treated sites had a significantly higher index. The reclamation treatment that most increased the SQI of the mine soils was the recent addition of wastes. It demonstrated that the addition of trace elements in the amendments to an original polluted soil has not been a problem. Organic amendments increase the soil quality, although trace elements are included in them.

Conclusions

Amendments made from waste such as sludge, technosol, biochar or compost can enhance natural attenuation of trace elements and lead to a decrease in the availability of trace elements. The amendments have evolved over the years from the most basic as sludge to the most developed as the biochar, because many authors have investigated to improve its characteristics. It is also concluded that not all amendments may be used in any type of soil due to the characteristics of these. For example, Technosols should be used in highly degraded soils or soils for industrial purposes, because the tailor-made Technosols can bring metals to the soil. On the other hand, compost and biochar are clean amendments and can be used in all soil types. These amendments can help with the immobilization of the trace elements and do not provide additional metals. Finally, the application of sludge alone is obsolete. Sludge should not be used alone because it is rapidly lost through leaching, and if it contains metals, this can be a problem.

References

ACES (Aspen Center for Environmental Studies) (2011) Hope Mine Biochar project. July 2010–August 2011, Aspen, Colorado

Ahmad M, Upamali Rajapaksha A, Eun Lim J, Zhang M, Bolan N, Mohan D, Vithanage M, Soo Lee D, Sik Ok Y (2014) Biochar as a sorbent for contaminant management in soil and water: a review. Chemosphere 99:19–33

Ahmad I, Akhtar MJ, Zahir ZA, Mitter B (2015) Organic amendments: effects on cereals growth and cadmium remediation. Int J Environ Sci Technol 12:2919–2928

Aira M, Monroy F, Dominguez J (2009) Changes in bacterial numbers and microbial activity of pig slurry during gut transit of epigeic and anecic earthworms. J Hazard Mater 162:1404–1407

Almendro-Candel MB, Navarro-Pedreño J, Jordán MM, Gómez I, Meléndez-Pastor I (2014) Use of municipal solid waste compost to reclaim limestone quarries mine spoils as soil amendments: effects on Cd and Ni. J Geochem Explor 144:363–366

Alvarenga P, Goncalves AP, Fernandes RM, De Varennes A, Vallini G, Duarte E, Cunha-Queda AC (2008) Evaluation of composts and liming materials in the phytostabilization of a mine soil using perennial ryegrass. Sci Total Environ 406:43–56

Álvarez EA, Mochón MC, Sánchez JCJ, Rodríguez MT (2002) Heavy metal extractable forms in sludge from wastewater treatment plants. Chemosphere 47:765–775

Apak R (2002) In "Encyclopedia of surface and colloid science" Hubbard A (ed). Dekker, New York, p 385

Asensio V, Guala SD, Vega FA, Covelo EF (2013a) A soil quality index for reclaimed mine soils. Environ Toxicol Chem 32:2240–2248

Asensio V, Vega FA, Singh BR, Covelo EF (2013b) Effects of tree vegetation and waste amendments on the fractionation of Cr, Cu, Ni, Pb and Zn in polluted mine soils. Sci Total Environ 443:446–4453

Asensio V, Forján R, Vega FA, Covelo EF (2014) Planting trees and amending with waste increases the capacity of mine tailings soils to retain Ni, Pb and Zn. Spanish J Soil Sci 4:225–238

Azizi AB, Choi M, Noor ZM, Noorlidah A (2015) Effect on heavy metals concentration from vermiconversion of agro-waste mixed with landfill leachate. Waste Manag 38:431–435

Bardos RP, van Veen HJ (1996) Review of longer term or extensive treatment technologies. Land Contam Reclam 4:19–36
Barker A, Bryson G (2002) Bioremediation of heavy metals and organic toxicants by composting. Sci World J 2:407–420
Beesley L, Dickinson NM (2010) Carbon and trace element mobility in an urban soil amended with green waste compost. J Soils Sediments 10:215–222
Beesley L, Moreno-Jiménez E, Gomez-Eyles J (2010a) Effects of biochar and greenwaste compost amendments on mobility, bioavailability and toxicity of inorganic and organic contaminants in a multi-element polluted soil. Environ Pollut 158:2282–2287
Beesley L, Moreno-Jiménez E, Gomez-Eyles JC, Harris E, Robinson B, Sizmur T (2010b) A review of biochars' potential role in the remediation, revegetation and restoration of contaminated soils. Environ Pollut 159:3269–3282
Beesley L, Moreno-Jimenez E, Clemente R, Lepp N, Dickinson N (2010c) Mobility of arsenic, cadmium and zinc in a multi-element contaminated soil profile assessed by in-situ soil pore water sampling, column leaching and sequential extraction. Environ Pollut 158:155–160
Bending NAD, McRae SG, Moffat AJ (1999) Soil-forming materials: their use in land reclamation. The Stationery Office, London
Bolan NS, Choppala G, Kunhikrishnan A, Park J, Naidu R (2013) Biotransformation of trace elements in soils in relation to bioavailability and remediation. Rev Environ Contam Toxicol 225:1–56
Bowszys T, Wierzbowska J, Sternik P, Busse MK (2015) Effect of the application of sewage sludge compost on the content and leaching of zinc and copper from soils under agricultural use. J Ecol Eng 16:1–7
Bradl HB (2004) Adsorption of heavy metal ions on soils and soils constituents. J Colloid Interface Sci 277:1–18
Bradl HB (2005) Heavy metals in the environment: origin, interaction and remediation. Elsevier, Burlington
Cao XD, Ma LN, Gao B, Harris W (2009) Dairy-manure derived biochar effectively sorbs lead and atrazine. Environ Sci Technol 43:3285–3291
Carvalho A, Nabais C, Roiloa SR, Rodríguez Echeverría S (2013) Revegetation of abandoned copper mines: the role of seed banks and soil amendments. Web Ecol 13:69–77
Chang JS, Law R, Chang C (1997) Biosorption of lead, copper and cadmium by biomass of *Pseudomonas aeruginosa* PU21. Water Res 31:1651–1658
Choppala GK, Bolan NS, Mallavarapu M, Chen Z, Naidu R (2012) The influence of biochar and black carbon on reduction and bioavailability of chromate in soils. J Environ Qual 41:1–10
CONAMA (2006) Resolution 375/2006, date 29/8/2006, Brazil
Dominguez J, Edwards CA (2011) Relationship between composting and vermicomposting. In: Edwards CA, Arancon NQ, Sherman R (eds) Vermiculture technology—earthworms, organic wastes, and environmental management. CRC Press, Boca Raton, pp 11–26
Dubus IG, Hollis JM, Brown CD (2000) Pesticides in rainfall in Europe. Environ Pollut 110:331–344
Dudal R, Nachtergaele F, Purnell M (2002) The human factor of soil formation. Symposium 18, vol. II, paper 93. Transactions 17th World Congress of Soil Science, Bangkok
Dutta S, Das AK (2010) Analytical perspective on waste management for environmental remediation. TrAC-Trends Anal Chem 29:636–644
European Commission (1991) Council directive 91/692/EEC of 23 December 1991, European Union
Fang M, Wong J (1999) Effects of lime amendment on availability of heavy metals and maturation in sewage sludge composting. Environ Pollut 106:83–89
Fellet G, Marchiol L, Delle Vedove G, Peressotti A (2011) Application of biochar on mine tailings: effects and perspectives for land reclamation. Chemosphere 83:1262–1267
Forján R, Asensio V, Rodríguez-Vila A, Covelo EF (2015) Contribution of waste and biochar amendment to the sorption of metals in a copper mine tailing. Catena 137:120–125

Forján R, Asensio V, Rodríguez-Vila A, Covelo EF (2016) Contributions of a compost-biochar mixture to the metal sorption capacity of a mine tailing. Environ Sci Pollut Res 23 (3):2595–2602

Forsberg S, Gustafsson J, Kleja DB, Ledin S (2008) Leaching of metals from oxidizing sulphide mine tailings with and without sewage sludge application. Water Air Soil Pollut 194:331–341

Frišták V, Pipíška M, Lesný J, Soja G, Friesl-Hanl W, Packová A (2015) Utilization of biochar sorbents for Cd^{2+}, Zn^{2+}, and Cu^{2+} ions separation from aqueous solutions: comparative study. Environ Monit Assess 187:4093. doi:10.1007/s10661-014-4093-y

Garrido T, Mendoza J, Arriagada F (2012) Changes in the sorption, desorption, distribution, and availability of copper, induced by application of sewage sludge on Chilean soils contaminated by mine tailings. J Environ Sci 24:912–918

Gaur N, Flora G, Yadav M, Tiwari A (2014) A review with recent advancements on bioremediation-based abolition of heavy metals. Evnviron Sci Process Impacts 16:180–193

Ghyasvand S, Alikhani H, Ardalan M, Savaghebi G, Hatami H (2008) Effect of pre-thermocomposting on decrease of cadmium and lead pollution in vermicomposting of municipal solid waste by *Eisenia fétida*. Am Eurasian J Agric Environ Sci 4:537–540

Gomez-Brandon M, Lazcano C, Lores M, Dominguez J (2011) Short-term stabilization of grape marc through earthworms. J Hazard Mater 187:291–295

Hartenstein R, Neuhauser EF, Collier J (1980) Accumulation of heavy metals in the earthworm *E. foetida*. J Environ Qual 9:23–26

Hattab N, Motelica-Heino M, Faure O, Bouchardon J-L (2015) Effect of fresh and mature organic amendments on the phytoremediation of Technosols contaminated with high concentrations of trace elements. J Environ Manag 159:37–47

IBI (2012) Standardized product definition and product testing guidelines for biochar that is used in soil. International Biochar Initiative, April 2012

Ireland MP (1983) Heavy metals uptake in earthworms; earthworm ecology. Chapman and Hall, London

IUSS (2006) Working Group WRB. World reference base for soil resources 2006. World soil resources reports 103, FAO, Rome

Javanbakht V, Alavi SA, Zilouei H (2014) Mechanisms of heavy metal removal using microorganisms as biosorbent. Water Sci Technol 69:1775–1787

Kabata-Pendias A (2001) Trace elements in soils and plants, 3rd edn. CRC Press, Boca Raton

Karami N, Clemente R, Moreno-Jiménez E, Lepp NW, Beesley L (2011) Efficiency of green waste compost and biochar soil amendments for reducing lead and copper mobility and uptake to ryegrass. J Hazard Mater 191:41–48

Kloss S, Zehetner F, Dellantonio A, Hamid R, Ottner F, Liedtke V, Schwanninger M, Gerzabek MH, Soja G (2012) Characterization of slow pyrolysis biochars: effects of feedstocks and pyrolysis temperature on biochar properties. J Environ Qual 41:990–1000

Kumpiene J, Lagerkvist A, Maurice C (2007) Stabilization of Pb and Cu contaminated soil using coal fly ash and peat. Environ Pollut 145:365–373

Lehmann J, Joseph S (2009a) Biochar for environmental management: an introduction. In: Lehmann J, Joseph S (eds) Biochar for environmental management science and technology. Earthscans, London, pp 1–12

Lehmann J, Joseph S (2009b) Biochar for environmental management: science and technology. Earthscan, London, p 404

Lehmann J, Kern DC, Glaser B, Woods WI (2003) Amazonian dark earths: origin, properties, management. Kluwer Academic Publishers, Dordrecht, p 523

Li L, Xu Z, Wu J, Tian G (2010) Bioaccumulation of heavy metals in the earthworm *Eisenia fetida* in relation to bioavailable metal concentrations in pig manure. Bioresource Technol 101:3430–3436

Liu J, Xu X, Huang D, Zeng G (2009) Transformation behavior of lead fractions during composting of lead-contaminated waste. Trans Nonferrous Metals Soc China 19:1377–1382

Macía P, Fernández-Costas C, Rodríguez E, Sieiro P, Pazos M, Sanromán MA (2014) Technosols as a novel valorization strategy for an ecological management of dredged marine sediments. Ecol Eng 67:182–189

Macías F, Camps Arbestain C (2010) Soil carbon sequestration in a changing global environment. Mitigat Adapt Strateg 15:511–529

Macías-García F, Camps Arbestain, M, Macías F (2009) Utilización de Tecnosoles derivados de residuos en procesos de restauración de suelos de la mina Touro. En: Minería Sostenible. Cámara Oficial Mineira de Galicia. A Coruña, pp 651–661

Mangkoedihardjo L, Ratnawati R, Alfianti N (2008) Phytoremediation of hexavalent chromium polluted soil using *Pterocarpus indicus* and *Jatropha curcas*. World Appl Sci J 4:338–342

Marcano V, Benitez P, Palacios-Prü E (2003) A review with recent advancements on bioremediation-based abolition of heavy metals. Planet Space Sci 1:159–166

Mikutta C, Kretzschmar R (2011) Spectroscopic evidence for ternary complex formation between arsenate and ferric iron complexes of humic substances. Environ Sci Technol 45:9550–9557

Moaref S, Sekhavatjou MS, Hosseini Alhashemi A (2014) Determination of trace elements concentration in wet and dry atmospheric deposition and surface soil in the largest industrial city, southwest of Iran. Int J Environ Res 8:335–346

Navarro A (2012) Effect of sludge amendment on remediation of metal contaminated soils. Minerals 2:473–492

Negi R, Suthar S (2013) Vermistabilization of paper mill wastewater sludge using *Eisenia fetida*. Bioresour Technol 128:193–198

Nguyen BT, Lehmann J, Kinyangi J, Smernik R, Riha SJ, Engelhard MH (2009) Long-term black carbon dynamics in cultivated soil. Biogeochemistry 92:163–176

O'Dell R, Silk W, Green P, Claassen V (2007) Compost amendment of Cu-Zn minespoil reduces toxic bioavailable heavy metal concentrations and promotes establishment and biomass production of *Bromus carinatus* (Hook and Arn.) Environ Pollut 148:115–124

Oldare M, Pell M, Svensson K (2008) Changes in soil chemical and microbiological properties during 4 years of application of various organic residues. Waste Manag 28:1246–1253

Oldare M, Arthurson V, Pell M, Svensson K, Nehrenheim E, Abubakar J (2011) Land application of organic waste-effects on the soil ecosystem. Appl Energy 88:2210–2218

Paradelo R, Villada A, Barral MT (2011) Reduction of the short-term availability of copper, lead and zinc in a contaminated soil amended with municipal solid waste compost. J Hazard Mater 188:98–104

Park JH, Choppala GK, Bolan NS, Chung JW, Cuasavathi T (2011) Biochar reduces the bioavailability and phytotoxicity of heavy metals. Plant Soil 348:439–451

Pérez-de-Mora A, Madejón E, Burgos P, Cabrera F (2006) Trace element availability and plant growth in a mine-spill contaminated soil Ander assisted natural remediation I. Soils. Sci Total Environ 363:28–37

Pérez-de-Mora A, Madrid F, Cabrera F, Madejón E (2007) Amendments and plant cover influence on trace element pools in a contaminated soil. Geoderma 139:1–10

Perminova IV, Hatfield K (2005) Remediation chemistry of humic substances: theory and implications for technology. In: Perminova IV, Hatfield K, Hertkorn N (eds) Use of humic substances to remediate polluted environments: from theory to practice, NATO science series. IV: earth and environmental series. Springer, Dordrecht, pp 3–36

Peyton DP, Healy MG, Fleming GTA, Grant J, Wall D, Morrison L, Cormican M, Fenton O (2016) Nutrient, metal and microbial loss in surface runoff following treated sludge and dairy cattle slurry application to an Irish grassland soil. Sci Total Environ 541:218–229

Pitt R, Lantrip J, Harrison R, Henry C, Xue D (1999) Infiltration through disturbed urban soils and compost-amended soil effects on runoff quality and quantity. EPA/600/R-00/016. U.S. Environmental Protection Agency, Office of Research and Development, Washington, DC

Pogrzeba M, Galimska-Stypa R, Krzyżak J, Sas-Nowosielska A (2015) Sewage sludge and fly ash mixture as an alternative for decontaminating lead and zinc ore regions. Environ Monit Assess 187:4120. doi:10.1007/s10661-014-4120-z

Rodríguez-Jordá MP, Garrido F, García-González MT (2012) Effect of the addition of industrial by-products on Cu, Zn, Pb and As leachability in a mine sediment. J Hazard Mater 213–214:46–54
Rodríguez-Vila A, Asensio V, Forján R, Covelo EF (2015) Chemical fractionation of Cu, Ni, Pb and Zn in a mine soil amended with compost and biochar and vegetated with Brassica juncea L. J Geochem Explor 158:74–81
Rodríguez-Vila A, Asensio V, Forján R, Covelo EF (2016) Assessing the influence of technosol and biochar amendments combined with Brassica juncea L. on the fractionation of Cu, Ni, Pb and Zn in a polluted mine soil. J Soils Sediments 16:339–348
Santos ES, Magalhães MCF, Abreu MM, Macías F (2014) Effects of organic/inorganic amendments on trace elements dispersion by leachates from sulfide-containing tailings of the São Domingos mine, Portugal. Time evaluation. Geoderma 226–227:188–203
Scalenghe R, Ferraris S (2009) The first forty years of a technosol. Pedosphere 19:40–52
Schmidt M, Torn MS, Abiven S, Dittmar T, Guggenberger G, Janssens IA, Kleber M, Kogel-Knabner I, Lehmann J, DAC M, Nannipieri P, Rasse DP, Weiner S, Trumbore SE (2011) Persistence of soil organic matter as an ecosystem property. Nature. doi:10.1038/nature10386
Schnitzer M, Khan SU (1972) Humic substances in the environment. Marcel Dekker, New York
Sellers G, Hutchings TR, Moffat AJ (2004) Remediated materials – their potential use in urban greening. SEESOIL 16:47–59
Séré G, Schwartz C, Ouvrard S, Renat J, Watteau F, Villemin G, Morel JL (2010) Early pedogenic evolution of constructed Technosols. J Soils Sediments 10:1246–1254
Shazia A, Mahmood-ul-Hassan M, Rizwan A, Vishandas S, Muhammad Y (2013) Metal tolerance potential of filamentous fungi isolated from soils irrigated with untreated municipal effluent. Soil Environ 32:55–62
Siebielec G, Chaney R (2012) Testing amendments for remediation of military range contaminated soil. J Environ Manag 108:8–13
Singh RP, Agrawal M (2008) Potential benefits and risks of land application of sewage sludge. Waste Manag 28:347–358
Singh J, Kalamdhad A (2012) Reduction of heavy metals during composting – a review. Int J Environ Protection 2:36–43
Singh J, Kalamdhad A (2013) Assessment of bioavailability and leachability of heavy metals during rotary drum composting of green waste (water hyacinth). Ecol Eng 52:59–69
Smith NJH (1999) The Amazon River forest: a natural history of plants, animals, and people. Oxford University Press, New York
Sohi S, Lopez-Capel E, Krull E, Bol R (2009a) Biochar, climate change and soil: a review to guide future research. Land and Water Science Report 05/09, CSIRO, pp 1–56
Sohi S, Lopez-Capel E, Krull E, Bol R (2009b) Biochar's roles in soil and climate change: a review of research needs. Land and Water Science Report 05/09, CSIRO, p 64
Soil Survey Staff (1999) Soil taxonomy: a basic system of soil classification for making and interpreting soil surveys, 2nd edn. Natural Resources Conservation Service. U.S. Department of Agriculture Handbook, p 436
Sombroek WG, Nachtergaele FO, Hebel A (1993) Amounts, dynamics and sequestration carbon in tropical and subtropical soils. A J Human Environ 22:417–426
Sparks DL (2003) Environmental soil chemistry: second edition. Elsevier, Burlington
Stevenson FJ (1982) Humus chemistry, genesis, composition, reactions. Wiley, New York
Stumm W (1992) Chemistry of the solid-water Interface. Wiley Interscience, New York
Suthar S, Mutiyar PK, Singh S (2012) Vermicomposting of milk processing industry sludge spiked with plant wastes. Bioresour Technol 116:214–219
Taiwo AM (2011) Composting as a sustainable waste management technique in developing countries. J Environ Sci Technol 4:93–102
Taiwo AM, Gbadebo M, Oyedepo J, Ojekunle Z, Alo O, Oyeniran Z, Onalaja O, Ogunjimi OT, Taiwo D (2016) Bioremediation of industrially contaminated soil using compost and plant technology. J Hazard Mater 304:166–172

Tang T, Zhu W, Kookana R, Katayama A (2013) Characteristics of biochar and its application in remediation of contaminated soil. J Biosci Bioeng 116:653–659

Tsang DCW, Yip ACK, Olds WE, Weber PA (2014) Arsenic and copper stabilization in a contaminated soil by coal fly ash and green waste compost. Environ Sci Pollut Res 21:10194–10204

Tunali S, Cabuk A, Akar T (2006) Removal of lead and copper ions from aqueous solutions by bacterial strain isolated from soil. Chem Eng J 115:203–211

Uchimiya M, Lima IS, Klasson KT, Chang S, Wartelle LY, Rodgers JM (2010) Immobilization of heavy metal ions (CuII, CdII, NiII, and PbII) by broiler litter-derived biochars in water and soil. J Agric Food Chem 58:5538–5544

Uchimiya M, Chang S, Klasson KT (2011) Screening biochars for heavy metal retention in soil: role of oxygen functional groups. J Hazard Mater 190:432–441

United States Environmental Protection Agency (1993) A plain English guide to the EPA part 503 biosolids rule. United States Environmental Protection Agency, Washington, DC

Uslu G, Tanyol M (2006) Equilibrium and thermodynamic parameters of single and binary mixture biosorption of lead (II) and copper (II) ions onto pseudomonas putida: effect of temperature. J Hazard Mater 135:87–93

Vamelari T, Bandiera M, Mosga G (2010) Field crops for phytoremediation of metal-contaminated land – a review. Environ Chem Lett 8:1–17

Villasenor J, Rodriguez L, Fernandez F (2011) Composting domestic sewage sludge with natural zeolites in a rotary drum reactor. Bioresour Technol 102:1447–1454

Wang X, Chen L (2009) Biosorbents for heavy metals removal and their future. Biotechnol Adv 27:195–226

Wang P, Zhang S, Wang C, Hou J, Guo P, Lin Z (2008a) Study of heavy metal in sewage sludge and in Chinese cabbage grown in soil amended with sewage sludge. Afr J Biotechnol 7:1329–1334

Wang X, Chen L, Xia S, Zhao J (2008b) Changes of Cu, Zn, and Ni chemical speciation in sewage sludge co-composted with sodium sulfide and lime. J Environ Sci 20:156–160

Wang X, Zhou W, Liang G, Song D, Zhang X (2015) Characteristics of maize biochar with different pyrolysis temperatures and its effects on organic carbon, nitrogen and enzymatic activities after addition to fluvo-aquic soil. Sci Total Environ 538:137–144

Xunta de Galicia (2008) Instrucción Técnica de Residuos. ITR 01/08. Elaboración de suelos (tecnosoles) derivados de residuos

Yu H, Huang GH (2009) Effects of sodium acetate as a pH control amendment on the composting of food waste. Bioresour Technol 100:2005–2011

Zaniewicz-Bajkowska A, Rosa R, Franczuk J, Kosterna E (2007) Direct and secondary effect of liming and organic fertilization on cadmium content in soil and in vegetables. Plant Soil Environ 53:473–481

Zhang X, Wang H, He L, Lu K, Sarmah A, Li J, Bolan NS, Pei J, Huang H (2013) Using biochar for remediation of soils contaminated with heavy metals and organic pollutants. Environ Sci Pollut Res 20:8472–8483

Zorpas A, Vassilis I, Loizidou M (2008) Heavy metals fractionation before, during and after composting of sewage sludge with natural zeolite. Waste Manag 28:2054–2060

Enhancing Decontamination of PAHs-Polluted Soils: Role of Organic and Mineral Amendments

Fabián Fernández-Luqueño, Fernando López-Valdez, Carolina Pérez-Morales, Selvia García-Mayagoitia, Cesar R. Sarabia-Castillo, and Sergio R. Pérez-Ríos

Abstract The organic and mineral amendments are an important tool for remediation and bioremediation of contaminated soils. The addition of these amendments in the polluted soils is a strategy that requires scientific and technological bases for reaching high degradation rates because after the amendment addition, many biological, chemical, and physical processes are started. The organic soil amendments as the wastewater sludge (biosolids), compost, vermicompost, manures, digestates, or any stabilized organic by-product or organic waste could be used to dissipate pollutants. Additionally, foundry sand, gypsum, coal combustion products, and volcanic ashes, among others, are mineral amendments also useful for the degradation of pollutants. This chapter provides the cutting-edge knowledge for enhancing the remediation or bioremediation processes through the addition of organic and/or mineral materials in order to improve the performance of the polluted system and enhance the biological, chemical, and physical interactions. The objectives of this chapter are (i) to analyze the relevant state of the art, (ii) to discuss the main advantages and disadvantages linked with the use of organic and mineral amendments for remediation, and (iii) to provide some experiences on remediation and bioremediation of PAHs-polluted soils.

Keywords Agricultural soil • Bioremediation • Chemical fertilizer • Environmental pollution • Remediation • Sustainable development

F. Fernández-Luqueño (✉) • S. García-Mayagoitia • C.R. Sarabia-Castillo
Sustainability of Natural Resources and Energy Program, Cinvestav-Saltillo, Ramos Arizpe, Coahuila, CP 25900, Mexico
e-mail: cinves.cp.cha.luqueno@gmail.com

F. López-Valdez • C. Pérez-Morales
Instituto Politécnico Nacional-CIBA, Tepetitla de Lardizábal, Tlaxcala, CP 90700, Mexico

S.R. Pérez-Ríos
ICAP—Instituto de Ciencias Agropecuarias, Universidad Autónoma del Estado de Hidalgo, Tulancingo, Hgo, CP 43600, Mexico

N.A. Anjum et al. (eds.), *Enhancing Cleanup of Environmental Pollutants*,
DOI 10.1007/978-3-319-55423-5_11

Introduction

Environmental contamination of (polycyclic aromatic hydrocarbon) PAHs occurs daily because large amounts of them are extracted, produced, refined, transported, and delivered to the environment during industrial activities, pollution events, or atmospheric deposition. This raises concern about the negative effect of PAHs on the human and environmental health and on the agricultural soils as a route of contaminants entering the food chain (Marchal et al. 2014). Organic or inorganic amendments are added to the soils to improve their structure, to increase their organic content, to preserve the moisture, or to increase the availability of nutrients. However, in a PAHs-polluted soil, organic or inorganic amendments also are used as cosubstrate or as source of microbial communities (Fernández-Luqueño et al. 2011). Several environmental factors such as organic matter, clay minerals, temperature, water content, pH, salinity, supply of oxygen, and bioavailability of nutrients, among others, affect the removal of pollutants in soils. On the one hand, it is well known that a number of materials might be considered organic amendments or organic fertilizers such as manure, sludge, compost, yard debris, cover crops, straw, sawdust, bark, etc. However, there are other organic materials used worldwide instead of mineral fertilizers, for example, guano (from bats), biochar, blood meal, bone meal, coffee grounds, eggshell, and fish scrap, among others (López-Valdez et al. 2015); on the other hand, synthetic or mineral fertilizers are extensively used in modern agriculture to increase or maintain crop yields. However, these chemical compounds have implications on soil fertility, crop yields, water quality, and gas emissions, which are well documented. Additionally, the organic or inorganic amendments described above are also well known as materials with potential of improving/increasing the PAHs dissipation in soils (Table 1).

The objectives of this chapter are (i) to analyze the relevant state of the art, (ii) to discuss the main advantages and disadvantages linked with the use of organic and mineral amendments for remediation, and (iii) to provide some experiences on remediation and bioremediation of PAHs-polluted soils. It also provides information about several research projects linked with bioremediation, biostimulation, bioaugmentation, or phytoremediation of PAHs-polluted soils, which were carried out by our research group during the last 3 years. All our experiments were carried out with agricultural soil from Mexico and/or with alkaline-saline soils from the former Lake Texcoco (Mexico).

General Considerations

Recently, different papers and/or book chapters have reviewed the biodegradation and bioremediation of PAHs-polluted soils (Alagic et al. 2015; Bisht et al. 2015; Sungthong et al. 2015). Environmental remediation deals with the treatment and

Table 1 Representative studies on organic and inorganic amendments commonly used as cosubstrate to decontamination of PAHs-polluted soils

Substrate/ Cosubstrate	Degraded Pollutant	Rate of degradation/ dissipation	Degradation mechanisms which are improved	References
AC (activated carbon)	Phenanthrene	54.1% in 20 days	Amended soils generally had the highest extends of C-phenanthrene mineralization.	Oyelami et al. (2015)
	3-Ring PAHs	57% in 21 days	AC showed the greatest decrease in pore water concentrations, yet had similar PAH uptake to roots and shoots.	Brennan et al. (2014)
	PAHs	59% in 12 months	Pore water concentrations decreased, reducing the freely available concentrations compared to an unamended soil.	Hale et al. (2012)
	PAHs	53% in 2 months	Is effective in reducing, leaching, and bioaccumulation of PAHs.	Jakob et al. (2012)
	PAHs	46% in 2 months	Increases the soil fertility.	
	PAHs	63% in 6 weeks	The PAHs has a higher attenuation for the creosote soil, probably could be attributed to the AC pore blockage by oil/lipids.	Brândli et al. (2008)
	PAHs	98% in 3 months	In the case of MAC (magnetic activated carbon), there is no positive effect, because the recovery of the amendment is not complete and could have ecotoxicity in soil.	Han et al. (2015)
APG (alkyl polyglucoside)	PAHs	30 mg L^{-1}	It helps solubilizing of contaminants and better plant growth, providing a carbon source and energy for the growth of rhizosphere microorganisms and enhanced soil enzyme activities.	Liu et al. (2013)

(continued)

Table 1 (continued)

Substrate/ Cosubstrate	Degraded Pollutant	Rate of degradation/ dissipation	Degradation mechanisms which are improved	References
ABP (arquad-bentonite-palmitic acid)	Phenanthrene	55% in 21 days	ABP-amended soils show a PAH mineralization process favorably occurring in soil.	Biswas et al. (2015)
Bacterial consortium	Phenanthrene	90% in 125 days	The inoculation of the PAH-degrading consortium support high microbial activity and larger population sizes of the PAH degrading bacteria than treatments without inoculums, leading to more rapid and complete biodegradation with the half-lives of the target PAHs being shortened significantly.	Li et al. (2015a, 2015b)
	Phenanthrene	95% in 10 days	The consortiums also can degrade pyrene but in low concentrations.	Bacosa and Inoue (2015)
	TPH (total petroleum hydrocarbons)	82% in 94 days	The combination of microbial consortia inoculation and mature compost as biostimulant is an appropriate bioremediation approach for soil matrix.	Gómez and Sartaj (2013)
Bacterial strain	PAHs	62.9% in 4 months	The bacterial community diversity is positively correlated with specific petroleum degraders and biosurfactant producers.	Hou et al. (2015)
	TPH (total petroleum hydrocarbons)	65.8% in 90 days 78% in 168 h	The bioaugmentation also resulted in complete removal of higher weight PAH and dibenzo-anthracene. Using bacteria enhance the mineralization in the degradation mechanism.	Nanekar et al. (2013) Liu et al. (2015)

(continued)

Table 1 (continued)

Substrate/ Cosubstrate	Degraded Pollutant	Rate of degradation/ dissipation	Degradation mechanisms which are improved	References
	PHC (petroleum hydrocarbon)	70% in 3 years	The microbes can stimulate plant growth.	Gurska et al. (2015)
	Pyrene	44.8% in 4 weeks	The consortiums can degrade pyrene and also fluoranthene in contaminated soils.	Radzi et al. (2015)
Bamboo leaves	Pyrene	62% in 90 to 180 days	Plant residues are potential additive for increase soil PAHs removal by improving soil texture, oxygen transfer, and providing rich carbon source for microbial growth.	Chen and Yuan (2012)
Biobarrier (biofilm)	Diesel hydrocarbons	39% in 2 weeks	The biobarriers enhance the electrokinetic treatment in soil.	Mena et al. (2015)
Biochar	PAHs	>50% in 60 days	Biochar has greater potential to beneficially reduce bioavailability of organic and inorganic contaminants.	Beesley et al. (2010)
		>40% in 56 days	Biochar effectively reduces the organic contaminants.	Gomez-Eyles et al. (2011)
	PAHs	56–67% in 8 weeks	SSBC (sewage sludge biochar) and SS (sewage sludge) applications were effective at significantly reducing the bioaccumulation of PAHs from contaminated soils.	Khan et al. (2013)
	PAHs	71.8–98.6% in 48 h (washing soil remediation)	Biochars can remove PAHs and also recover the surfactant used in soil washing effluents.	Li et al. (2014)

(continued)

Table 1 (continued)

Substrate/ Cosubstrate	Degraded Pollutant	Rate of degradation/ dissipation	Degradation mechanisms which are improved	References
Biosolid	PAHs	83% in 180 days	Using biosolid as an amendment could enhance the degradation of heavy hydrocarbon fraction.	Silvana et al. (2014)
	PAHs	42.3% in 60 days	Organic waste amendments helped to significantly decrease soil PAHs in a plant-microbe bioremediation system.	Zhang et al. (2012)
Compost	PAHs	90% in 30 days	Compost application could be a source of organic pollutants in agricultural soils, can also promote degradation of PAHS.	Bellino et al. (2015)
	PAHs	90% in 3 months	Compost addition was beneficial overall for enhancing PAH removal, at the initial stage.	Wu et al. (2013)
	Diesel	82.44–88.86% in 30 days	The bulking agent has increased the diesel degradation about 6%.	Khamforoush and Bijan-Manesh (2013)
	TPH (total petroleum hydrocarbons)	60% in 2 years	There is a positive effect of organic matter application in supporting the growth and metabolic activities of microorganisms capable of degrading organic contaminants.	Doni et al. (2015)
Composted biosolids	Anthracene	49.1% in 378 days	The effect on PAHs was more prominent for two to three ring PAHs than for four to six ring PAHs.	Attanayake et al. (2015)

(continued)

Table 1 (continued)

Substrate/ Cosubstrate	Degraded Pollutant	Rate of degradation/ dissipation	Degradation mechanisms which are improved	References
Earthworm (*Hyperodrilus africanus*)	TPH (total petroleum hydrocarbons)	84.99% in 90 days	Earthworm significantly enhanced the physicochemical parameters of soil resulting in a decrease of the total organic carbon, sulfate, nitrate, phosphate, sodium, potassium, calcium, and magnesium.	Ekperusi and Aigbodion (2015)
Fungal inoculum	PAHs	95–96% in 5 weeks	An improvement in the soil quality occurred during the field scale treatment, demonstrating that the soil was suitable for earthworms.	Winquist et al. (2014)
Graphene/biochar	Phenanthrene	94.9% in 5 days	The graphene/biochar has a higher removal efficiency of phenanthrene and mercury.	Tang et al. (2015)
Lignocellulosic mixture	AH (aliphatic hydrocarbons)	79.7% in 60 days	The lignocellulosic mixture might be regarded as a slow release fertilizer which can be used in alternative to rapid-release inorganic fertilizers.	Covino et al. (2015)
Mycoremediation + biochar	PAHs	92% in 42 days	The sequential application of biochar and mycoremediation increases fungal activity and PAH degradation capacity.	García-Delgado et al. (2015)
Mineral salt medium	TPH (total petroleum hydrocarbons)	90% in 70 days	The use of nutrients and tilling activities was proven to increase the TPH biodegradation process, notably in the diesel range.	Suja et al. (2014)
Mucor circinelloides (MC) enzymes	Diesel oil	34.5% in 15 days	The addition of *M. circinelloides* enzyme preparation to the culture medium caused an increase in degradation of aromatic hydrocarbons.	Marchut-Mikolajczyk et al. (2015)

(continued)

Table 1 (continued)

Substrate/ Cosubstrate	Degraded Pollutant	Rate of degradation/ dissipation	Degradation mechanisms which are improved	References
Mushroom and bacteria	Phenanthrene	95.07% in 3 months	The application of *P. cornucopiae* planting and bacterial inoculation is a promising and optimal method for bioremediation of soil co-contaminated with Cd and phenanthrene.	Jiang et al. (2015)
Nutrients (C, N, P, Ca)	Diesel	90% in 12 weeks	The addition of nutrients to stimulate the indigenous soil microorganism improved the remediation process.	Khudur et al. (2015)
	TPH (total petroleum hydrocarbons)	47–58% in 187 days	Biodegradation of DOC as a preferential substrate to TPH occurs regardless of nutrient amendment and results in a delay in diesel bioremediation; it helps to predict better the efficiency of a subsequent bioremediation phase.	Sutton et al. (2014)
	PAHs	70% in 60 days	With the biostimulation can shorten the timespan of soil resilience from about 270 to 60 days and improve nutrient balance in burned soils.	Andreolli et al. (2015)
	Petroleum hydrocarbons	47% in 60 days	Significant biodegradation was achieved as a result of aeration and moisture amendment but in low nutrient doses.	Akbari and Ghoshal (2014)
	Oil	95% in 6 months	The growth of hydrocarbonoclastic bacterial communities is enhanced with the addition of Ca alone or in combination with dipicolinic acid;	Al-Mailem et al. (2015)

(continued)

Table 1 (continued)

Substrate/ Cosubstrate	Degraded Pollutant	Rate of degradation/ dissipation	Degradation mechanisms which are improved	References
			this information is useful for constructing biotechnologies for hydrocarbon bioremediation at high temperature.	
Poultry droppings	TPH (total petroleum hydrocarbons)	25% per day	The poultry droppings can be used as manure material for remediation of crude-oil contaminated soils.	Ezenne et al. (2014)
RC (residual carbon)	PAHs	98% in 5 months	The RC appears to capture a more relevant part of the condensed carbonaceous organic matter.	Poot et al. (2014)
Sand	TPH (total petroleum hydrocarbons)	268% in 135 days	Sand amendment increases soil porosity.	Li et al. (2015a, b)
Surfactant	Phenanthrene	80% In 15 days	Enhance the initial reduction of PHE and PYR.	Liao et al. (2015)
	Petroleum hydrocarbons	90% in 115 weeks	The flushing with surfactant enhances dispersion and biodegradation of diesel.	Guerin (2015)
	PAHs	92.6% in 30 days	Using the surfactant facilitate the microbial degradation in soil.	Gong et al. (2015)
	PAHs	48.57% in 72 h	Using mixed-surfactant-enhanced remediation of PAH-contaminated soil during soil washing technique.	Shi et al. (2015)
	Diesel	49.65% in 3 weeks	The biosurfactant increase diesel solubility and increase diesel biodegradation along with coinoculation of two biosurfactant-producing strains.	Mnif et al. (2015)
	Crude oil	90% in 35 days	The use of biosurfactant is an improved cost-effective biodegradation of crude oil.	Sajna et al. (2015)

(continued)

Table 1 (continued)

Substrate/ Cosubstrate	Degraded Pollutant	Rate of degradation/ dissipation	Degradation mechanisms which are improved	References
	Pyrene	69.4% in 182 days	Biosurfactants have the ability to increase apparent aqueous solubility and bioavailability of PAHs, and they can be used to stimulate the biodegradation of these persistent contaminants contained in sewage sludge.	Vecino et al. (2015)

removal of pollutants from the environment such as soil, air, groundwater, surface water, and sediments, among other media. The US-EPA encourages adoption of green remediation as the practice of considering all environmental effects of cleanup actions and incorporating options to minimize the environmental footprints of cleanup actions, because the process of cleaning up a PAHs-polluted soil uses energy, water, and other natural or material resources and consequently creates an environmental footprint of its own (US-EPA 2011).

On one hand, biodegradation is a natural way of recycling wastes or pollutants, which is usually used in relation to ecology, waste management, and mostly associated with bioremediation, a technology for environmental remediation. On the other hand, bioremediation is defined as the treatment of pollutants or waste by the use of living organisms in order to eliminate, attenuate, degrade, transform, or break down (through metabolic or enzymatic action) the undesirable substances to inorganic components, such as CO_2, H_2O, and NO_3^- (Fernández-Luqueño et al. 2011).

According to de Lorenzo (2008) and Steliga (2008), biostimulation is the addition of nutrients to increase the autochthonous biomass of substrates to promote co-metabolism. This technique increases the PAHs dissipation by autochthonous microorganisms, which have the capacity to remove PAHs, when the environment is nutrient or substrate deficient (Fernández-Luqueño et al. 2011). In a biostimulation process, there is an addition of substrates, nutrients, oxygen, water, or surfactants to increase the removal of PAHs. Bioaugmentation is the application to a system of microorganisms that have the capacity to degrade target contaminants (Teng et al. 2010). However, bioaugmentation has been also recognized as the addition of microorganisms to enhance a specific biological activity in a number of areas, including agriculture, remediation, and forestry. The microorganisms used to bioaugmentation may be indigenous, exogenous, or genetically engineered. On the other side, phytoremediation is a strategy that employs plants to

degrade, stabilize, and/or remove PAHs, which can be an alternative green technology method for remediation of PAHs-polluted soils, water, and air. Phytoremediation, as a green technology option, is defined as the use of plants to remove pollutants from the environment or to render them harmless. Phytoremediation includes seven main strategies such as (i) phytoextraction, also referred to as phytosequestration, phytoaccumulation, or phytoabsorption; (ii) phytodegradation, also referred to as phytotransformation; (iii) phytofiltration, also referred to as rhizofiltration; (iv) phytohydraulics; (v) phytostabilization, also referred to as phytoimmobilization; (vi) phytostimulation, also referred to as rhizodegradation; and (vii) phytovolatilization.

The use and exploitation of organic or inorganic amendments in remediation aims at enhancing the efficiency of the cleanup process. According to Wiszniewska et al. (2016) and Straszko et al. (2015), depending on the needs, both inorganic and organic amendments may be used either to immobilize pollutants or to increase their uptake and translocation to harvestable plant biomass. The above-cited authors stated that the mode of the action and effectiveness of numerous amendments in soil remediation is quite well recognized. However, the use of synthetic chelators, nanoparticles, biochar, agro- and industrial wastes, and other advanced devices/materials may cause some negative effects on the environment, while there is not available information concerning long-term influence of soil amendments on the ecosystems. It has to be remembered that a bunch of processes just after the addition of organic or inorganic amendments are onset, changed, or halted in the soil, plant, rhizosphere, and air surrounding the plant. Rooming-in of all these processes has the ability to increase or decrease the global remediation rate in the polluted system (Fig. 1).

First Experiment: Wastewater Sludge-Mediated Removal of PAHs from Soils

In earlier studies, Fernández-Luqueño et al. (2008, 2009) found that after 112 days, polyacrylamide accelerated the removal of anthracene from an alkaline-saline soil and an agricultural soil and phenanthrene in an agricultural soil of Acolman. However, it was not possible to determine which wastewater sludge characteristic increased the dissipation of PAHs nor know how large the wastewater sludge intrinsic capacity for PAHs dissipation is. The objectives of the present research were (i) to determinate why wastewater sludge stimulates and accelerates the removal of PAHs from polluted soils and (ii) to evaluate how large the wastewater sludge intrinsic capacity for PAHs dissipation is.

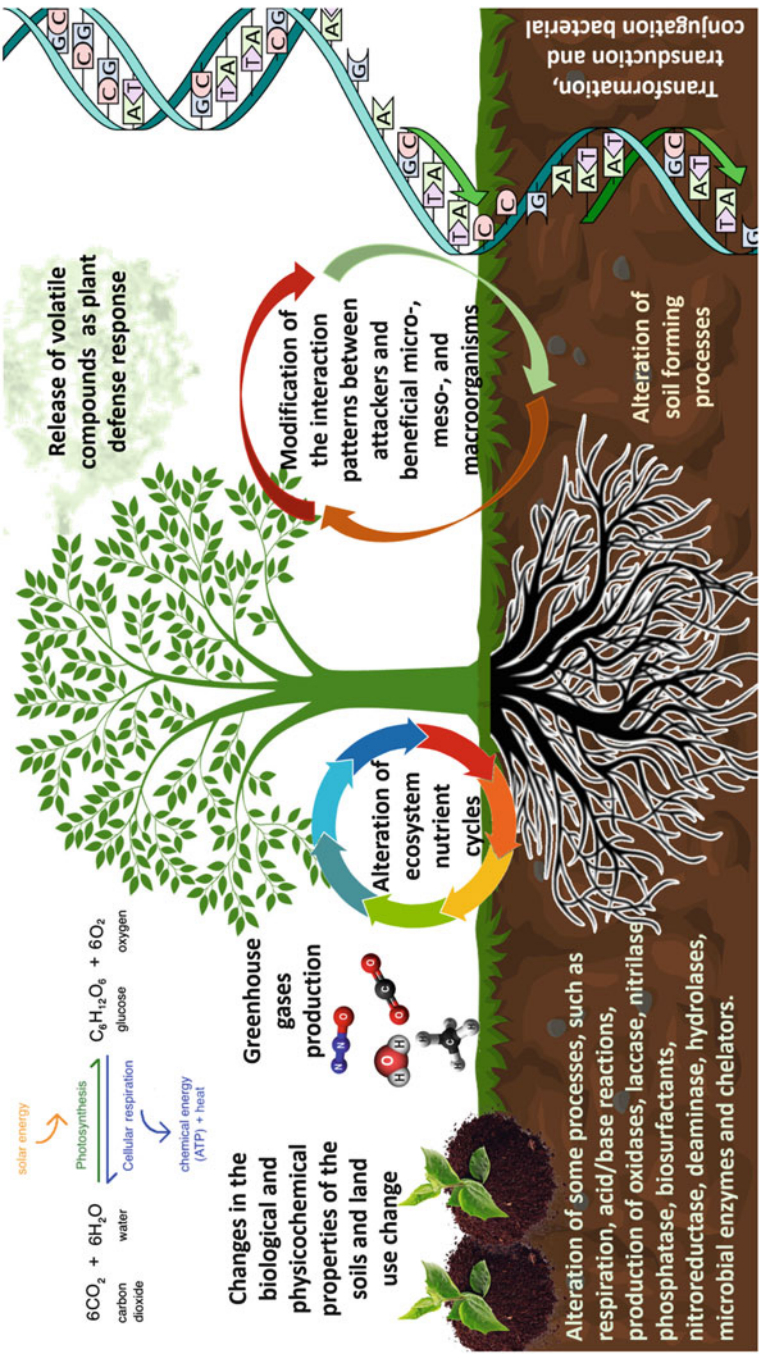

Fig. 1 Schematic representation of some alterations in the plant-soil ecosystem and in some enzymatic and microbiological activities during the onset, change, or halt of physiological processes in soils, plants, and microorganisms just after the addition of organic or inorganic amendments in order to increase the PAHs dissipation

Table 2 Summary of major characteristics of the Texcoco and Acolman soil and the wastewater sludge

	Acolman soil	Texcoco soil	Sludge
pH_{H_2O}	6.0	9.3	6.4
Organic carbon (g kg^{-1})	8.1	58.2	509
Inorganic carbon (g kg^{-1})	0.2	0.8	ND[a]
Total Kjeldahl nitrogen (g kg^{-1})	0.7	1.2	27.7
$N\text{-}NH_4^+$ (mg kg^{-1})	3.4	3.7	500
$N\text{-}NO_3^-$ (mg kg^{-1})	53	30	86
$N\text{-}NO_2^-$ (mg kg^{-1})	0.6	0.3	7.9
Textural classification	Sandy loam	Loamy sand	ND

[a]Not determined

Area Description and Soil Sampling

The first sampling site was located in the former lake of Texcoco in the valley of México City (México) (N.L. 19° 30′, W.L. 98° 53′) at 2250 m above sea level with a mean annual temperature of 16 °C and mean annual precipitation of 600 mm (mainly from June through September). Soil physicochemical properties can be found in Table 2. Soil was sampled at random by augering the 0–15 cm top layer of three plots of approximately 0.5 ha. The soil from each plot was pooled so that three soil samples were obtained. The second sampling site, which served as a control, is located near the ex-convent of Acolman in the State of México (N.L. 19°38′, W.L. 98°55′) and the former Lake Texcoco at 2250 m above sea level and with a mean annual temperature of 14.9 °C and an average annual precipitation of 624 mm (mainly from June through August). Soil physicochemical properties can be found in Table 2. Soil was sampled at random by augering the 0–15 cm top layer of three plots of approximately 0.5 ha. The soil from each plot was pooled so that three soil samples were obtained. As such, a total of six soil samples were obtained, three from Acolman and three from the former Lake Texcoco.

Soil Preparation

The soil was characterized and treated as follows. The soil from each plot at both sites was passed separately through a 5 mm sieve, adjusted to 40% water holding capacity (WHC) by adding distilled water (H_2O), and conditioned at 22 ± 2 °C for 10 days in drums containing a beaker with 100 mL 1 M sodium hydroxide (NaOH) to trap CO_2 evolved and a beaker with 100 mL distilled H_2O to avoid desiccation of the soil.

PAHs and Sludge Characteristics

Hydrocarbons were obtained from Sigma (USA) with purity >98% for phenanthrene and >97% for anthracene. Acetone was purchased from J.T. Baker (USA) with purity 99.7%. Wastewater sludge was obtained from Reciclagua Ambiental (Sistema Ecológico de Regeneración de Aguas Residuales Ind., S. A. de C. V.) in Lerma, State of México (México). Reciclagua treats wastewater from different companies such as alimentary industries. Ninety percent of the wastewater is of alimentary industries origin, mainly from textile industries, and the rest from household. The sludge obtained after the addition of a flocculant is passed through a belt filter to reduce water content. Wastewater sludge was sampled aseptically in plastic bags. Sludge physicochemical properties can be found in Table 2.

Treatments and Experimental Setup

Subsamples (189) of 20 g soil of each of the six soil samples (three plots × two soils) were added to 120 mL glass flasks. Twenty-one flasks were used for each of the nine treatments (Table 3). The wastewater sludge used in the sterile treatment was sterilized three times with pressurized steam at 121 °C supplied by an autoclave for 30 min with an interval of a day. Three flasks were chosen at random from each treatment of the six soil samples, i.e., 189 subsamples. One and half g soil was extracted for PAHs with acetone and analyzed on a GC. The remaining 18.5 g soil was frozen. These provided zero-time samples. The remaining flasks were placed in 945 mL glass jars containing a vessel with 10 mL distilled H_2O and a vessel with 20 mL 1 M NaOH to trap CO_2 evolved. The jars were sealed and stored in the dark

Table 3 Treatments applied to the Texcoco (TEX) and Acolman (ACOL) soil

Treatment	Characteristics
TEX-SLUDGE-POLY	Soil[a] + phenanthrene[b] + anthracene[c] + sludge-with poly[d]
TEX-SLUDGE	Soil + phenanthrene + anthracene + sludge[e]
TEX-STERILE-SLUDGE	Soil + phenanthrene + anthracene + sterilized dry sludge[f]
TEX-PAH	Soil + phenanthrene + anthracene
ACOL-SLUDGE-POLY	Soil[a] + phenanthrene[b] + anthracene[c] + sludge-with poly[d]
ACOL-SLUDGE	Soil + phenanthrene + anthracene + sludge[e]
ACOL-STERILE-SLUDGE	Soil + phenanthrene + anthracene + sterilized dry sludge[f]
ACOL-PAH	Soil + phenanthrene + anthracene
SLUDGE-PAH	Sludge + phenanthrene + anthracene

[a]20 g dry soil
[b]1200 mg phenanthrene kg^{-1} dry soil
[c]520 mg anthracene kg^{-1} dry soil
[d]108 g dry sludge flocculated with polyacrylamide kg^{-1} dry soil
[e]108 g dry sludge without polyacrylamide kg^{-1} dry soil
[f]108 g sterilized dry sludge flocculated with polyacrylamide kg^{-1} dry soil

for 112 days at 22 ± 2 °C. After 3, 7, 14, 28, 56, and 112 days, three jars were selected at random from each treatment, and the soil was analyzed for PAHs as mentioned before. Every third day, the remaining flasks were opened and aired for 10 min to avoid anaerobic conditions, sealed, and further incubated.

Chemical and PAHs Analysis

Details about chemical procedures to characterize soils and sludge can be found in Fernández-Luqueño et al. (2008, 2009), while some technical details to the PAHs analysis can be found in Fernández-Luqueño et al. (2013).

Statistical Analyses

Concentration of phenanthrene and anthracene was subjected to one-way analysis of variance using PROC GLM (SAS Institute 1989) to test for significant differences between treatments, and the least significant difference (LSD) was then calculated. The relationships between the different treatments were analyzed by principal component analysis (PCA) using the orthogonal/varimax rotation. Details about statistical analyses can be found in Fernández-Luqueño et al. (2008, 2009, 2013). All data presented were the mean of three replicates in soil from three different flasks, i.e., $n = 27$, and that were sampled at 3, 7, 14, 28, 56, and 112 days.

Results and Discussion

After 112 days, the largest dissipation of anthracene and phenanthrene was found in the Acolman soil amended or not with wastewater sludge with or without polyacrylamide. Acolman and Texcoco-unamended soils dissipated PAHs at lower rate than soils added with wastewater sludge. Texcoco soil amended with sterilized wastewater sludge dissipated only 12% of anthracene and 74% of phenanthrene, while Acolman soil amended with sterilized sludge dissipated 70% of anthracene and 98% of phenanthrene at 112 days. Unamended wastewater sludge polluted with PAHs dissipated only 8% of anthracene and 51% of phenanthrene. We found that polyacrylamide accelerated the removal of PAHs from the Acolman and Texcoco soil and it may be as an effect of the N release upon polyacrylamide decomposition. Sojka et al. (2007) stated that polyacrylamide affects the adsorption of PAHs on the soil matrix thereby augmenting their bioavailability and degradation. Moreover, Wen et al. (2010) found microorganisms able to degrade polyacrylamide from activated sludge and oil-contaminated soil. Additionally, it is known that polyacrylamide restores the soil structure and greatly increased soil aggregate

stabilization (Hu et al. 2012), which the polyacrylamide and/or its decomposition could increase the supply of oxygen, regulate the water content, and improve the nutrient bioavailability to remove PAHs.

It was found that unamended wastewater sludge spiked with PAHs dissipated only 51% of phenanthrene and 8% of anthracene. It is well known that wastewater sludge contains nutrients, organic matter, polyacrylamide, and microorganisms to improve the PAHs dissipation when it is mixed with soil, but these data suggest that the interrelationship between wastewater sludge and soil is very important to increase the remediation of PAHs-polluted soil. In addition, we found that the dissipation of PAHs decreased significantly in sterilized wastewater sludge treatments. It implies that wastewater sludge contains microorganisms able to dissipate PAHs and/or that some physical or chemical properties from wastewater sludge are affected during the sterilizing. However, Fernández-Luqueño et al. (2008) did not find changes in CO_2 emission nor in NO_3^-, NO_2^-, or NH_4^+ concentrations from sterilized wastewater sludge compared to unsterilized wastewater sludge. Additionally, it has been demonstrated that changes in pH as effect of wastewater sludge addition or nutrients from the wastewater sludge had no significant effect on the PAHs dissipation in soil spiked with phenanthrene and anthracene (Fernández-Luqueño et al. 2008).

Wastewater sludge stimulates and accelerates the dissipation of anthracene and phenanthrene from PAHs-polluted soil as effect of the polyacrylamide content and its microbial community but not by pH change nor by its nutrient concentrations. In addition, it is also well known that polyacrylamide could also increase the nanoparticle concentration in wastewater sludge and that may have improved the PAHs dissipation (Fernández-Luqueño et al. 2014). On the scatter plot, the treatments are clearly separated from each other (Fig. 2). Acolman PAHs-polluted soil treated with wastewater sludge can be found in the upper right quadrant, while unamended PAHs-polluted wastewater sludge lies in the lower left quadrant (Fig. 2a). Texcoco PAHs-polluted soil amended with wastewater sludge can be found in the upper right quadrant, while unamended PAHs-polluted wastewater sludge lies in the lower left quadrant (Fig. 2b). The PAHs dissipation improved in the following order: SLUDGE-PAH < TEX-SLUDGE = TEX-STERILE-SLUDGE < TEX-PAH < TEX-SLUDGE-POLY < ACOL-SLUDGE = ACOL-STERILE-SLUDGE = ACOL-PAH < ACOL-SLUDGE-POLY treatment.

Polyacrylamide accelerated removal of PAHs from soils, while wastewater sludge increased the removal of PAHs from soils, but the physical, chemical, and microbial soil properties, the contaminant, and microorganisms in both soil and wastewater sludge are the experimental variables that control the effect. Wastewater sludge does not have the capacity to dissipate PAHs by itself, i.e., it must be treated with remediation technologies before its final disposal; otherwise the PAHs contamination will be persistent.

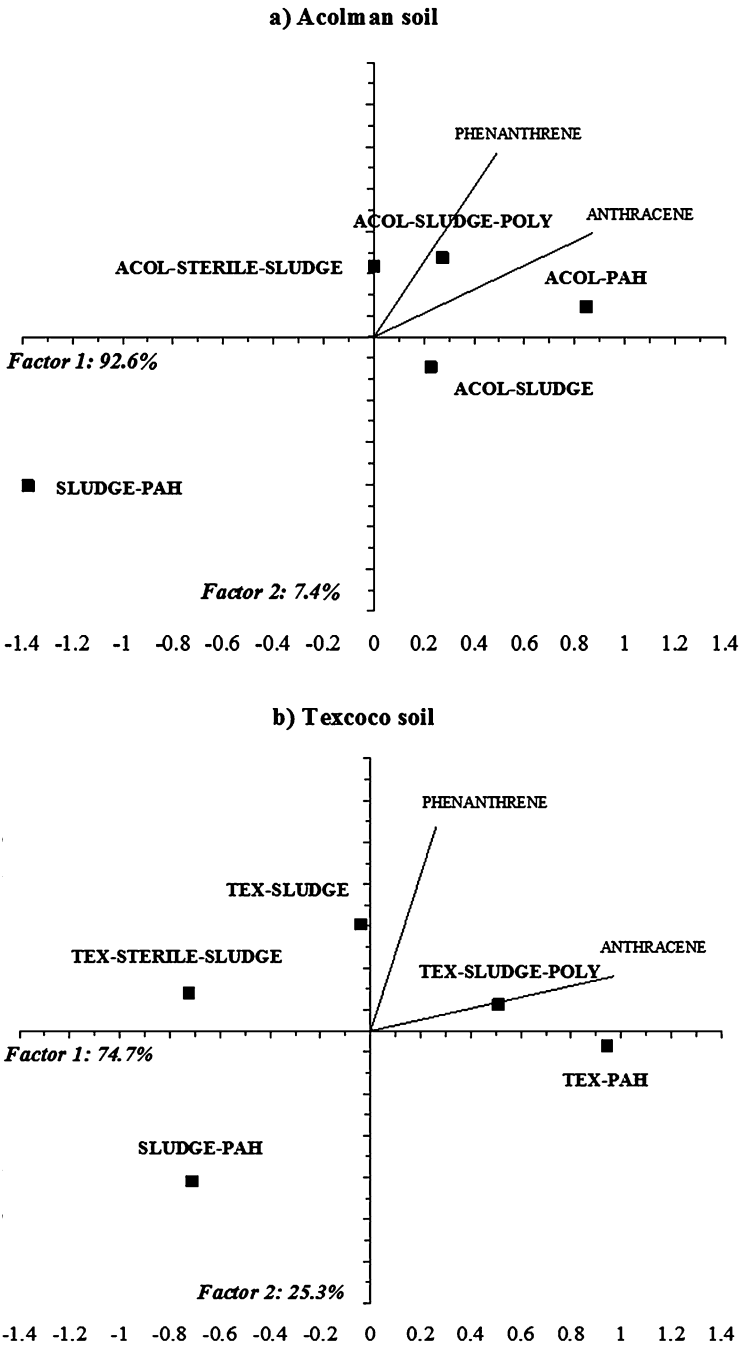

Fig. 2 Principal component analysis of PAHs dissipation in an agricultural soil (**a**) or in a saline-alkaline soil (**b**), amended or not with wastewater sludge. Treatment description can be found in Table 2

Second Experiment: PAHs Dissipation in Polluted Soils at Increasing Salt Content

In a previous experiment, which soil from Texcoco was used (pH 10.0 and electrolytic conductivity (EC) 12 dS m^{-1}), the application of wastewater sludge to soil increased the removal of phenanthrene and anthracene and nearly halved their final concentration after 112 days (Betancur-Galvis et al. 2006). However, soils with pH 9.3 and EC 7.3 dS m^{-1}, the application of wastewater sludge had no significant effect on the removal of anthracene after 112 days (Fernández-Luqueño et al. 2008). It can be speculated that soil characteristics like salt content or the differences in the wastewater sludge affected the dissipation of PAHs-polluted soils. Therefore, soil samples from the former lake of Texcoco at EC 6 dS m^{-1}, 30 dS m^{-1}, 80 dS m^{-1}, or 146 dS m^{-1} were contaminated with phenanthrene and anthracene and amended with the same wastewater sludge. The dissipation of phenanthrene and anthracene was monitored in an aerobic incubation at 22 ± 2 °C for 56 days. The objective of this study was to investigate how salinity might affect removal of PAHs when wastewater sludge was added to soil.

Area Description and Soil Sampling

The soil samples were taken from soils of the former lake of Texcoco, Texcoco, Mexico, located in N 19° 30′, W 98° 53′ at an altitude of 2250 m above sea level, annual mean temperature of 16 °C, and annual mean precipitation of 600 mm. The soil was characterized as alkaline-saline. The pH ranges were between 9.0 and 10.6; electrolytic conductivity (EC) by saturation extracts was between 6 and 150 dS m^{-1} and a large exchangeable sodium percentage (60–80%). Four different sites were selected with different EC at 6, 30, 80, and 146 dS m^{-1}. At each of the four sites, three 400 m^2 plots were defined, and the soil was sampled at random by augering the 0–15 cm top layer 30 times. The soil from each plot was pooled separately so that 12 soil samples were obtained (four soils at different EC by triplicate).

PAHs, Sludge Characteristics, Soil Preparation, Treatments, and Experimental Setup

Information regarding PAHs and sludge characteristics can be found in Fernández-Luqueño et al. (2008, 2009, 2013). The soils from the four sites and each plot were sieved using a 5 mm sieve and were adjusted to 40% of water holding capacity (WHC) by adding distilled water (H_2O). After that, the soil was kept at 22 ± 2 °C for 10 days in drums containing a beaker with 100 mL 1 M sodium hydroxide (NaOH) that was used in order to capture the CO_2 produced and a beaker with

100 mL distilled H_2O to avoid desiccation of the soil. Forty-eight subsamples of 5.0 g soil of each of the 12 soil samples (three plots × four soils) were added to 120 mL glass flasks. Eighteen flasks were contaminated with 2.0 mL acetone in which phenanthrene and anthracene were dissolved and amended with 1162 mg fresh wastewater sludge kg^{-1} (soil + PAHs + sludge), 18 were contaminated with 2.0 mL acetone where phenanthrene and anthracene were dissolved (soil + PAHs), and 18 were left unamended (soil). The flasks were placed in a desiccator under vacuum for 20 min and removed, and 15 g soil was added to each flask. The soil was then mixed thoroughly. The amount of PAHs added to the 20 g soil was equivalent to 1200 mg phenanthrene kg^{-1} and 520 mg anthracene kg^{-1}. The amount of wastewater sludge was added approximately 150 mg inorganic N kg^{-1}. Three flasks were chosen at random from each treatment of the three plots and four soils, while 1.5 g soil was extracted for PAHs with acetone and analyzed on a gas chromatograph (GC). These provided zero-time samples. The jars were sealed and stored in the dark at 22 ± 2 °C for 56 days. Additionally, 15 jars containing a vessel with 10 mL distilled H_2O and a vessel with 20 mL 1 M NaOH were sealed and served as controls to quantify the CO_2 captured from the air. After 3, 7, 14, 28, and 56 days, three jars were selected at random from each treatment, and the soil was analyzed for PAHs as mentioned before. The remaining flasks were opened and aired each 3 days for 10 min to avoid anaerobic conditions, were sealed, and were incubated over again.

Chemical Analysis

Details about chemical procedures to characterize soils and sludge can be found in Fernández-Luqueño et al. (2008, 2009), while some technical details to the PAHs analysis can be found in Fernández-Luqueño et al. (2013).

Statistical Analyses

Concentration of phenanthrene and anthracene was subjected to one-way analysis of variance using PROC GLM (SAS Institute 1989). Data shown are the mean of nine values ($n = 9$), i.e., three measurements of three plots. Details about statistical analyses can be found in Fernández-Luqueño et al. (2008, 2009, 2013).

Results and Discussion

The concentration of phenanthrene decreased sharply in soil with EC 6 dS m^{-1} in the first 14 days but did not change significantly thereafter. Applying sludge to soil with 6 dS m^{-1} accelerated the removal of phenanthrene from soil and decreased the

concentration after 56 days ($p < 0.05$). The concentration of phenanthrene decreased significantly in soil with EC 30 and 80 dS m^{-1}, i.e., 3.1 mg kg^{-1} day^{-1} (standard error of the estimate (SEE) 0.7) and −4.6 mg kg^{-1} day^{-1} (SEE 1.4), respectively. Application of sewage sludge decreased the concentration of phenanthrene and anthracene in soil with EC 30 and 80 dS m^{-1} after 56 days. The concentration of phenanthrene decreased sharply in soil with EC 146 dS m^{-1} in the first 14 days but did not change significantly thereafter. Applying sludge to soil with 146 dS m^{-1} had no significant effect on the concentration of phenanthrene after 56 days. The mean concentration of phenanthrene was significantly lower in soil with EC 6 dS m^{-1} than in soil with EC 30 and 80 dS m^{-1} but higher than in soil with EC 146 dS m^{-1}, independent of the application of wastewater sludge ($p < 0.05$).

The concentration of anthracene decreased in soil with EC 6 dS m^{-1} between day 7 and 14 but did not change significantly thereafter. Applying sludge to soil with 6 dS m^{-1} accelerated the removal and decreased the amount of anthracene after 56 days. The concentration of anthracene in soil with EC 30 and 80 dS m^{-1} was lower after 56 days than at the onset of the incubation although decreases were small, i.e., only 5% anthracene was removed in soil with EC 30 dS m^{-1} and 12% in soil with 80 dS m^{-1} after 56 days. Applying sludge to these two soils decreased the amount of anthracene significantly compared to the unamended soil after 56 days ($p < 0.05$). The concentration of anthracene decreased sharply in soil with EC 146 dS m^{-1} at 14 days after the onset of the experiment but did not change significantly thereafter. Applying sludge to the PAHs-contaminated soil with 146 dS m^{-1} had no significant effect on the concentration of anthracene. The mean concentration of anthracene was significantly lower in soil with EC 6 dS m^{-1} than in soil with EC 30 and 80 dS m^{-1} but significantly higher than in soil with EC 146 dS m^{-1} ($p < 0.05$). In the sludge-amended soil, the concentration of anthracene was significantly higher in soil with EC 30 and 80 dS m^{-1} than in soil with EC 6 and 146 dS m^{-1} ($p < 0.05$).

The concentration of phenanthrene and anthracene decreased in soil with EC 6 dS m^{-1} until day 14 and remained constant thereafter. Approximately 49% of the phenanthrene and 26% of anthracene added to soil were removed from within 56 days. It is well known that autochthonous microorganisms can remove PAHs from soil (Mansur et al. 2014; Sun et al. 2012) even in the presence of salt (Li et al. 2013; Wen et al. 2011). In a previous experiment, 99% phenanthrene and 85% anthracene were removed from an agricultural soil (Fernández-Luqueño et al. 2009). The removal of phenanthrene and anthracene was much lower from soil with EC 30 dS m^{-1}, i.e., 11% and 5%, respectively, or with EC 60 dS m^{-1}, i.e., 15% and 12%, respectively. It was hypothesized that the high pH and EC in soil of Texcoco inhibited the removal of PAHs (Aichberger et al. 2006; Betancur-Galvis et al. 2006). However, nearly all the ANTHR and PHEN were removed from soil with EC 146 dS m^{-1} after 56 days, i.e., >95%. This made it clear that other factors affected the removal of PAHs from soil and salt content and pH were not determinant factors (Aichberger et al. 2006).

A PCA analysis of the soil factors indicated that none of the soil characteristics measured, i.e., EC, WHC, particle size distribution, organic and inorganic C, or pH,

determined the removal of phenanthrene or anthracene from soil. The four soils studied were clearly separated from each other, but there was no clear relationship between soil characteristics and the amount of PAHs removed from the soils. For instance, the soils with EC 80 dS m^{-1} had a positive PC1, i.e., high WHC and silt content, while the soil with EC 30 dS m^{-1} had a negative PC1, i.e., high sand and organic C content, but similar amounts of PAHs were removed. Additionally, the removal of PAHs was larger in soil with EC 146 dS m^{-1} than in soil with EC of 6 dS m^{-1}, so that salt content was not the determinant factor. Even the microbial activity as evidenced by the emission of CO_2 was not related to removal of PAHs from soil. The production of CO_2 was similar in soil with EC 80 dS m^{-1} and 146 dS m^{-1}, but the removal of PHEN and ANTHR was much larger in the latter than in the first. As such, the EC and the other measured soil characteristics did not determine removal of PAHs from soil and another not measured factor or factors intervened. These factors, such as specific surface area of the clays and/or the nature of the clay mineral (Clark et al. 2007; Matus et al. 2008; Rasmussen et al. 2007), might have affected availability and thus removal of PAHs from soil. It can be speculated that the "availability" or "bio-accessibility" of the studied PAHs (Reichenberg and Mayer 2006) might have been another factor that determined removal of anthracene and phenanthrene from soil. In a previous experiment, it was found that removal of anthracene was faster from the top 0–2 cm layer than from the 2–8 or 8–15 cm layers (Betancur-Galvis et al. 2006). Further investigation revealed that fluctuating water contents increased anthracene availability contributing to an increased removal (Vázquez-Núñez et al. 2009). It can be speculated that the large salt content in soil with EC 146 dS m^{-1} dispersed the soil particles in such a way that the PAHs were not physically protected and became available for degradation (Nelson et al. 1996). Consequently, salts in soil with EC 146 dS m^{-1} did not inhibit the removal of PAHs.

It is worthwhile to notice that the percentage of anthracene and phenanthrene removed from soil with EC 30 and 80 dS m^{-1} was similar after 56 days, but in soil with EC 6 and 146 dS m^{-1}, the dissipation of anthracene was lower than that of phenanthrene. The removal of anthracene is normally slower from soil than that of phenanthrene. This can be attributed to the low solubility of anthracene in aqueous systems (0.07 mg L^{-1}) compared to that of phenanthrene (1.29 mg L^{-1}), which renders it only slowly available for microbial degradation (Adelaja et al. 2015). This would indicate that in soil with EC 30 and 80 dS m^{-1}, the availability or "bio-accessibility" of phenanthrene and anthracene was low, so that their removal was low and similar. It is well known that application of organic material accelerates the removal of PAHs from soil (Tian et al. 2015). Adding sludge to soil can affect the removal of PAHs in different ways. First, the sludge contains larger amounts of C substrate that will stimulate microbial activity thereby accelerating removal of PAHs from soil. Second, the sludge contains nutrients that will further stimulate microbial activity. Third, sludge contains large amounts of microorganisms that can contribute to the removal of PAHs from soil. Fourth, sludge can change soil conditions, such as pH and EC, thereby stimulating or inhibiting removal of PAHs. Fifth, organic matter might conduce absorption and/or adsorption processes on the dissipation of PAHs concentration. Wastewater sludge reduced the

concentrations of phenanthrene and anthracene in soil after 56 days compared to the amount extracted at the beginning of the experiment, although the effect was much smaller in soils with EC 30 and 80 dS m^{-1} than in soil with EC 6 dS m^{-1}. In soil with EC 146 dS m^{-1}, the removal rate of phenanthrene and anthracene was so high that sludge had no effect on their dissipation rate. This would indicate that a positive effect of wastewater sludge on removal of phenanthrene and anthracene would only be observed when the PAHs are available and not shielded from microbial degradation. The removal of PAHs was high in soil with 6 or 146 dS m^{-1} but low in soils with EC 30 or 80 dS m^{-1}. It appears that "bio-accessibility" of anthracene and phenanthrene in soil was a more important determinant in their removal than soil characteristics, such as EC, pH, particle size distribution, organic matter content, or microbial activity. Wastewater sludge had a positive effect on removal of phenanthrene and anthracene from soil, but the degree of its effect appeared to be related to availability of the contaminant.

Third Experiment: Testing the Effect of Application Rates of Wastewater Sewage Sludge on the Decontamination of PAHs-Polluted Soils

Sludge might change soil conditions, such as pH and EC, thereby stimulating or inhibiting removal of PAHs. The question remains if the amount of wastewater sludge applied to a soil will affect the removal of PAHs. As part of a study into the removal of PAHs from an alkaline-saline soil using organic wastes, soil of the former Lake Texcoco with EC 7.6 dS m^{-1} and pH 9.7 was spiked with phenanthrene and anthracene and amended with different concentrations of wastewater sludge, i.e., 1.5, 4.5, 9, or 18 g dry sludge kg^{-1}, which was equivalent to approximately 0, 50, 150, 300, and 600 kg N ha^{-1} added to the 0–15 cm soil layer with density 1.3 kg dm^3 considering that 40% of the organic N mineralized. Phenanthrene and anthracene were monitored in an aerobic incubation at 22 ± 2 °C for 56 days. The objective of this study was to investigate if the amount of wastewater sludge added to an alkaline-saline soil accelerated the removal of phenanthrene and anthracene.

Area Description and Soil Sampling

The sampling site is located in the former lake of Texcoco in the Valley of México City (México) (N.L. 19° 30′, W. L. 98° 53′). Soil was sampled at random by augering the 0–15 cm top layer of three plots of approximately 0.5 ha. The soil from each plot was pooled so that three soil samples were obtained and 5.0 mm sieved and characterized. Characteristics of the soil are given in Table 2.

PAHs, Sludge Characteristics, Treatments, and Experimental Setup

PAHs and sludge properties are described in the above of this chapter. Some characteristics of the sludge can be found in Table 2. Subsamples (90) of 5.0 g dry soil of each plot ($n = 3$) were added to 120 ml glass flasks and contaminated with 2 ml acetone in which PAHs were dissolved. An additional 18 subsamples were not contaminated and served as control. All the flasks were placed under vacuum in a desiccator for 20 min and removed, and 15 g soil was added to each flask. The soil was then mixed thoroughly. The amount of PAHs added to the 20 g soil was such that 1200 mg phenanthrene kg^{-1} and 520 mg anthracene kg^{-1} were applied. Eighteen of the contaminated soil samples were amended with 1.5 g dry sludge kg^{-1}, 18 with 4.5 mg dry sludge kg^{-1}, 18 with 9 g dry sludge kg^{-1}, 18 with 18 g dry sludge kg^{-1}, while 18 were left unamended. Sludge water was removed by air-drying. The amount of wastewater added was such that approximately 0, 50, 150, 300, and 600 kg N ha^{-1} was added considering a soil density of 1.3 kg dm^3 for a 15 cm soil layer, and 40% of the organic N was mineralized during the experiment. Proportional amounts of distilled water were then added to all treatments so that the same water content, approximately 40% WHC, was obtained in each treatment. Further, three flasks were chosen at random from each treatment of the three plots. Ten g soils were extracted for inorganic N with 100 ml 0.5 M K_2SO_4 solution, shaken for 30 min, filtered through Whatman no. 42 filter paper®, and analyzed, while 1.5 g soil was extracted for PAHs with acetone and analyzed on a gas chromatograph (GC). These provided zero-time samples. Additional details about the experimental setup can be found in the second paragraph of the section "Treatments and Experimental Setup" of this chapter.

Chemical Analysis and Determination of PAHs

Details about chemical procedures to characterize soils and sludge can be found in Fernández-Luqueño et al. (2008, 2009), while some technical details to the PAHs analysis can be found in Fernández-Luqueño et al. (2013).

Statistical Analyses

Concentration of phenanthrene and anthracene was subjected to one-way analysis of variance using PROC GLM (SAS Institute 1989) to test for significant differences between treatments, and the least significance difference (MSD) was then calculated (SAS Institute 1989).

Results and Discussion

The concentration of phenanthrene decreased in all treatments at 14 days after the onset of the experiment. In the unamended soil, 57% of the phenanthrene was removed from soil after 56 days. Application of wastewater sludge increased the removal rate of phenanthrene from soil significantly compared to the unamended soil after 56 days ($p < 0.05$). However, the amount of wastewater sludge applied had no significant effect on the amount of phenanthrene removed after 56 days. The concentration of anthracene decreased in all treatments after 14 days. In the unamended soil, 56% of the anthracene was removed from soil after 56 days. Application of wastewater sludge increased the removal rate of anthracene from soil significantly compared to the unamended soil after 56 days ($P < 0.05$). However, the amount of wastewater sludge applied had no significant effect on the amount of anthracene removed after 56 days. Autochthonous microorganisms can remove PAHs from soil (Nikolopoulou et al. 2013) even in the presence of salt (Castillo-Carvajal et al. 2014) and at pH > 10 (Wang et al. 2015). This was confirmed in this experiment as approximately 55% of the phenanthrene and anthracene was removed from soil after 56 days. Both the physicochemical characteristics of contaminants as well as the physical, chemical, and biological properties of soils affect the degradation of PAHs. However, some of the results indicated that the removal of the PAHs in this experiment was low. First, the removal of PAHs is normally most accentuated in the first days after spiking the soil, and further decreases are normally small. Betancur-Galvis et al. (2006) found that 33% of added phenanthrene was removed from an agricultural soil in 7 days and an additional 15% in the next 105 days. The effect was even more outspoken in Texcoco soil with EC 12 dS m^{-1} and pH 10 as 25% of phenanthrene was removed within 7 days and only 4% in the next 105 days. In the experiment reported here, a significant decrease in the concentration of phenanthrene was only observed after 14 days. Second, the percentage of removal of anthracene and phenanthrene was similar in this experiment, although the removal of phenanthrene is normally higher than that of anthracene. Betancur-Galvis et al. (2006) found that only 16% of added anthracene was removed from an agricultural soil, while 33% phenanthrene in 7 days. The slower degradation of anthracene can be attributed to its low solubility in aqueous systems (0.07 mg l^{-1}) compared to that of phenanthrene (1.29 mg l^{-1}), which renders it only slowly available for microbial degradation. It appears that in our experiment, the bio-accessibility of both PAHs was similar so that the difference in solubility did not affect their degradation.

Application of wastewater to soil of Texcoco sometimes accelerates removal of phenanthrene from soil, but not always. Fernández-Luqueño et al. (2009) reported that in soil of Texcoco with EC 30 dS m^{-1} or 80 dS m^{-1}, removal of anthracene was not affected by the application of wastewater sludge. Betancur-Galvis et al. (2006), however, found that the removal of phenanthrene in wastewater sludge-amended soil with EC 12 dS m^{-1} and pH 10 was 54% compared to only 25% in the unamended soil after 7 days and 71% and 29%, respectively, after 112 days.

In the experiment reported here, the wastewater sludge had less effect on the removal of phenanthrene and anthracene than as reported by Betancur-Galvis et al. (2006) but more than found by Fernández-Luqueño et al. (2009). This would indicate that the application of the wastewater sludge from the same treatment plant had not always the same effect on the removal of anthracene and phenanthrene from soil. It can be speculated that the combination of soil and sludge characteristics will determine the removal of contaminants from soil. We found that the removal of PAHs in this soil was low at the onset of the experiment as the amount of phenanthrene and anthracene decreased after only 14 days, but after 56 days the removal $> 55\%$. Normally, the removal of PAHs is most accentuated in the first days, with subsequent decreases being very low. The removal of PAHs was similar in our study although the dissipation of the anthracene is normally much lower than that of phenanthrene. Addition of wastewater sludge increased the removal of the PAHs, but the effect was independent of application rate.

Conclusions and Perspectives

Biostimulation, bioaugmentation, and phytoremediation are techniques with outstanding efficiency to decontaminate PAHs-polluted soils. Polyacrylamide accelerated removal of PAHs from soils, while wastewater sludge increased the removal of PAHs from soils, but wastewater sludge does not have the capacity to dissipate PAHs by itself, i.e., it must be treated with remediation technologies before its final disposal; otherwise the PAHs contamination will be persistent. The bio-accessibility of anthracene and phenanthrene in soil was a more important determinant in their removal than soil characteristics, such as EC, pH, particle size distribution, organic matter content, or microbial activity. Wastewater sludge had a positive effect on removal of phenanthrene and anthracene from soil, but the degree of its effect appeared to be related to availability of the contaminant. The addition of wastewater sludge increased the PAHs dissipation, but the effect was independent of application rate. This research was carried out with phenanthrene and anthracene, but it has to be remembered that in a common oil spill, hundreds of PAHs are released to the environment, i.e., additional research is necessary to determinate the real potential of wastewater sludge to decontaminate an oil-polluted soil.

Acknowledgments The research was funded by the Sustainability of Natural Resources and Energy Program (Cinvestav-Saltillo). CR S-C and S G-M received grant-aided support from "Becas de Posgrado-CONACyT." F F-L and F L-V received grant-aided support from "Sistema Nacional de Investigadores-CONACyT."

References

Adelaja O, Keshavarz T, Kyazze G (2015) The effect of salinity, redox mediators and temperature on anaerobic biodegradation of petroleum hydrocarbons in microbial fuel cells. J Hazard Mater 283:211–217

Aichberger H, Andreas PL, Celis R, Braun R, Ottner F, Rost H (2006) Assessment of factors governing biodegradability of PAHs in three soils aged under field conditions. Soil Sediment Contam 15(1):73–85

Akbari A, Ghoshal S (2014) Pilot-scale bioremediation of a petroleum hyddrocarbon-contaminated clayey soil from a sub-Arctic site. J Hazard Mater 280:595–602

Alagic SC, Maluckov BS, Radojicic VB (2015) How can plants manage polycyclic aromatic hydrocarbons? May these effects represent a useful tool for an effective soil remediation? A review. Clean Techn Environ 17(3):597–614

Al-Mailem DM, Kansour MK, Radwan SS (2015) Moderately thermophilic, hydrocarbonoclastic bacterial communities in Kuwaiti desert soil: enhanced activity via Ca_2^+ and dipicolinic acid amendment. Extremophiles 19:573–583

Andreolli M, Lampis S, Brignoli P, Vallini G (2015) Bioaugmentation and biostimulation as strategies for the bioremediation of a burned woodland soil contaminated by toxic hydrocarbons: a comparative study. J Environ Manage 153:121–131

Attanayake CP, Hettiarachchi GM, Martin S, Pierzynsky GM (2015) Potential bioavailability of lead, arsenic, and polycylic aromatic hydrocarbons in compost-amended urban soils. J Environ Qual 44:930–944

Bacosa HP, Inoue C (2015) Polycyclic aromatic hydrocarbons (PAHs) biodegradation potential and diversity of microbial consortia enriched from Tsunami sediments in Miyagi, Japan. J Hazard Mater 283:689–697

Beesley L, Moreno-Jimenez E, Gómez-Eyles JL (2010) Effects of biochar and greenwaste compost amendments on mobility, bioavailability and toxicity of inorganic and organic contaminants in a multi-element polluted soil. Environ Pollut 158:2282–2287

Bellino A, Baldantoni D, De Nicola F, Iovieno P, Zaccardelli M, Alfani A (2015) Compost amendments in agricultural ecosystems: confirmatory path analysis to clarify the effects on soil chemical and biological properties. J Agric Sci (Camb.) 153:282–295

Betancur-Galvis LA, Alvarez-Bernal D, Ramos-Valdivia AC, Dendooven L (2006) Bioremediation of polycyclic aromatic hydrocarbon-contaminated saline–alkaline soils of the former Lake Texcoco. Chemosphere 62(11):1749–1760

Bisht S, Pandey P, Bhargava B, Sharma S, Kumar V, Sharma KD (2015) Bioremediation of polyaromatic hydrocarbons (PAHs) using rhizosphere technology. Braz J Microbiol 46 (1):7–21

Biswas B, Sarkar B, Mandal A, Naidu R (2015) Heavy metal-immobilizing organoclay facilities polycyclic aromatic hydrocarbon biodegradation in mixed-contaminated soil. J Hazard Mater 298:129–137

Brändli RC, Hartnik T, Henriksen T, Cornelissen G (2008) Sorption of native polyaromatic hydrocarbons (PAH) to black carbon and amended activated carbon in soil. Chemosphere 73:1805–1810

Brennan A, Moreno E, Alburquerque JA, Knapp CW, Switzer C (2014) Effects of biochar and activated carbon amendment on maize growth and the uptake and measured availability of polycyclic aromatic hydrocarbons (PAHs) and potentially toxic elements (PTEs). Environ Pollut 193:79–87

Castillo-Carvajal LC, Sanz-Martin JL, Barragan-Huerta BE (2014) Biodegradation of organic pollutants in saline wastewater by halophilic microorganisms: a review. Environ Sci Pollut Res 21:9578–9588

Chen B, Yuan M (2012) Enhanced dissipation of polycyclic aromatic hydrocarbons in the presence of fresh plant residues and their extracts. Environ Pollut 161:199–205

Clark GJ, Dogshun N, Sale PWG, Tang C (2007) Changes in chemical and biological properties of a sodic clay subsoil with addition of organic amendments. Soil Boil Biochem 39 (11):2806–2817

Covino S, D'Annibale A, Stazi SR, Cajthaml T, Cvancarová M, Stella T, Petruccioli M (2015) Assessment of degradation potential of aliphatic hydrocarbons by autochthonous filamentous fungi from a historically polluted clay soil. Sci Total Environ 505:545–554

De Lorenzo V (2008) Systems biology approaches to bioremediation. Curr Opin Biotechnol 19:579–589

Doni S, Macci C, Peruzzi E, Iannelli R, Masciandaro G (2015) Heavy metal distribution in a sediment phytoremediation system at pilot scale. Ecol Eng 81:146–157

Ekperusi OA, Aigbodion FI (2015) Bioremediation of petroleum hydrocarbons from crude oil-contaminated soil with the earthworm: *Hyperiodrilus africanus*. Biotech 5:957–965

Ezenne GI, Nwoke OA, Obalum SE, Ugwuishiwu BO (2014) Use of poultry droppings for remediation of crude-oil-polluted soils: effects of application rate on total and poly-aromatic hydrocarbon concentrations. Int Biodeter Biodegr 92:57–65

Fernández-Luqueño F, Marsch R, Espinosa-Victoria D, Thalasso F, Hidalgo-Lara ME, Munive A, Luna-Guido ML, Dendooven L (2008) Remediation of PAHs in a saline-alkaline soil amended with wastewater sludge and the effect on dynamics of C and N. Sci Total Environ 402:18–28

Fernández-Luqueño F, Thalasso F, Luna-Guido ML, Ceballos-Ramírez JM, Ordóñez-Ruíz IM, Dendooven L (2009) Flocculant in wastewater affects dynamics of inorganic N and accelerates removal of phenanthrene and anthracene in soil. J Environ Manage 90:2813–2818

Fernández-Luqueño F, Valenzuela-Encinas C, Marsch R, Martinez-Suarez C, Vázquez-Nunez E, Dendooven L (2011) Microbial communities to mitigate contamination of PAHs in soil-possibilities and challenges: a review. Environ Sci Pollut Res 18(1):12–30

Fernández-Luqueño F, Vázquez-Núñez E, Zavala-Días de la Serna FJ, Martínez-Suárez C, Salomón-Hernández G, Valenzuela-Encinas C, Franco-Hernández O, Ceballos-Ramírez JM, Dendooven L (2013) Bacterial community composition of a saline-alkaline soil amended or not with wastewater sludge and contaminated with polycyclic aromatic hydrocarbons (PAHs). Afr J Microbiol Res 7(28):3605–3614

Fernández-Luqueño F, López-Valdez F, Valerio-Rodríguez MF, Pariona N, Hernández-López JL, García-Ortíz I, López-Baltazar J, Vega-Sánchez MC, Espinosa-Zapata R, Acosta-Gallegos JA (2014) Effects of nanofertilizers on plant growth and development, and their interrelationship with the environmental. In: Fernández-Luqueño F, López-Valdez F (eds) Fertilizers: components, uses in agriculture and environmental impact. NOVA Science, New York, pp 211–224

García-Delgado C, Alfaro-Barta I, Eymar E (2015) Combination of biochar amendment and mycoremediation for polycyclic aromatic hydrocarbons immobilization and biodegradation in creosote-contaminated soil. J Hazard Mater 285:259–266

Gómez F, Sartaj M (2013) Field scale ex-situ bioremediation of petroleum contaminated soil under cold climate conditions. Intl J Biodeteriorat Biodegrad 85:375–382

Gómez-Eyles JL, Sizmur T, Collins CD, Hodson ME (2011) Effects of biochar and the earthworm Eisenia fetida on the bioavailability of polycyclic aromatic hydrocarbons and potentially toxic elements. Environ Pollut 159:616–622

Gong X, Xu X, Gong Z, Li X, Jia C, Guo M, Li H (2015) Remediation of PAH-contaminated soil at a gas manufacturing plant by a combined two-phase partition system washing and microbial degradation process. Environ Sci Pollut Res 22:12001–12010

Guerin TF (2015) Bioremediation of diesel from a rocky shoreline in an arid tropical climate. Mar Pollut Bull 99:85–93

Gurska J, Glick BR, Greenberg BM (2015) Gene expression of *Secale cereale* (Fall Rye) grown in petroleum hydrocarbon (PHC) impacted soil with and without plant growth-promoting rhizobacteria (PGPR), *Pseudomonas putida*. Water Air Soil Pollut 226:308

Hale SE, Elmquist M, Brändli R, Hartnik T, Jakob L, Henriksen T, Werner D, Cornelissen G (2012) Activated carbon amendment to sequester PAHs in contaminated soil: a lysimeter field trial. Chemosphere 87:177–184

Han Z, Sani B, Akkanen J, Abel S, Nybom I, Karapanagioti H, Werner D (2015) A critical evaluation of magnetic activated carbon's potential for the remediation of sediment impacted by polycyclic aromatic hydrocarbons. J Hazard Mater 286:41–47

Hou J, Liu W, Wang B, Wang Q, Luo Y, Franks AE (2015) PGPR enhanced phytoremediation of petroleum contaminated soil and rhizosphere microbial community response. Chemosphere 138:592–598

Hu X, Liu LY, Li SJ, Cai QG, Lu YL, Guo JR (2012) Development of soil crust under simulated rainfall and crust formation on a loess soil as influenced by polyacrylamide. Pedosphere 22:415–424

Jakob L, Hartnik T, Henriksen T, Elmquist M, Brändli RC, Hale SE, Cornelissen G (2012) PAH-sequestration capacity of granular and powder activated carbon amendments in soil, and their effects on earthworms and plants. Chemosphere 88:699–705

Jiang J, Liu H, Li Q, Gao N, Yao Y, Xu H (2015) Combined remediation of Cd-phenanthrene co-contaminated soil by *Pleurotus cornucopiae* and *Bacillus thuringiensis* FQ1 and the antioxidant responses in *Pleurotus cornucopiae*. Ecotoxicol Environ Saf 120:386–393

Khamforoush M, Bijan-Manesh MJ (2013) Application of the Haug model for process design of petroleum hydrocarbon-contaminated soil bioremediation by composting process. Int J Environ Sci Technol 10:533–544

Khan S, Wang N, Reid BJ, Freddo A, Cai C (2013) Reduced bioaccumulation of PAHs by *Lactuca sativa L.* grown in contaminated soil amended with sewage sludge and sewage sludge derived biochar. Environ Pollut 175:64–68

Khudur LS, Shahsavari E, Miranda A, Morrison PD, Nugegoda D, Ball AS (2015) Evaluating the efficacy of bioremediating a diesel-contaminated soil using ecotoxicological and bacterial community indices. Environ Sci Pollut Res 22:14809–14819

Li Y, Wang HQ, Hua F, Su MY, Zhao YC (2013) Effects of temperature and pH on fluoranthene biodegradation kinetics by the new strain *Rhodococcus baikonurensis* BAP-1. J Pure Appl Microbiol 7(4):3059–3069

Li H, Qu R, Li C, Guo W, Han X, He F, Ma Y, Xing B (2014) Selective removal of polycyclic aromatic hydrocarbons (PAHs) from soil washing effluents using biochars produced at different pyrolytic temperatures. Bioresour Technol 163:193–198

Li X, Wang X, Ren ZJ, Zhang Y, Li N, Zhou Q (2015a) Sand amendment enhances bioelectrochemical remediation of petroleum hydrocarbon contaminated soil. Chemosphere 141:62–70

Li CH, Wong YS, Wang HY, Tam NFY (2015b) Anaerobic biodegradation of PAHs in mangrove sediment with amendment of $NaHCO_3$. J Environ Sci (China) 30:148–156

Liao C, Liang X, Lu G, Thai T, Xu W, Dang Z (2015) Effect of surfactant amendment to PAHs-contaminated soil for phytoremediation by maize (*Zea mays* L.) Ecotox Eviron Safe 112:1–6

Liu F, Zhang X, Liu X, Chen X, Liang X, He C, Wei J, Xu G (2013) Alkyl polyglucoside (APG) amendment for improving the phytoremediation of Pb-PAH contaminated soil by the aquatic plant *Scirpus triqueter*. Soil Sediment Contam Int J 22:1013–1027

Liu PWG, Liou JW, Li YT, Su WL, Chen CH (2015) The optimal combination of entrapped bacteria for diesel remediation in seawater. Int J Biodeter Biodegr 102:383–391

López-Valdez F, Fernández-Luqueño F, Valerio-Rodríguez María F (2015) Mineral fertilizers, bio-fertilizers and PGPRs: advantages and disadvantages of its implementation. In: Sinha S, Pant KK, Bajpai S (eds) Fertilizer Technology II, Biofertilizers. Studium Press, New Delhi, pp 277–294

Mansur AA, Adetutu EM, Kadali KK, Morrison PD, Nurulita Y, Ball AS (2014) Assessing the hydrocarbon degrading potential of indigenous bacteria isolated from crude oil tank bottom sludge and hydrocarbon-contaminated soil of Azzawiya oil refinery, Libya. Environ Sci Pollut Res 21(18):10725–10735

Marchal G, Smith KEC, Mayer P, de Jonge LW, Karlson UG (2014) Impact of soil amendments and the plant rhizosphere on PAH behaviour in soil. Environ Pollut 188:124–131

Marchut-Mikolajzyk O, Kwapisz E, Wieczorek D, Antczak T (2015) Biodegradation of diesel oil hydrocarbons enhanced with *Mucor circinelloides* enzyme preparation. Int J Biodeter Biodegr 104:142–148

Matus FJ, Lusk CH, Maire CR (2008) Effect of soil texture, carbon input rates, and litter quality on free organic matter and nitrogen mineralization in Chilean rain forest and agricultural soils. Commun Soil Sci Plant Anal 39(1–2):187–201

Mena E, Saez C, Villaseñor J, Rodrigo MA, Cañizares P (2015) Feasibility of coupling permeable bio-barriers and electrokinetics the treatment of diesel hydrocarbons polluted soils. Electrochim Acta 181:192–199

Mnif I, Mnif S, Sahnoun R, Maktouf S, Ayedi Y, Elbouze-Chaabouni S, Ghribi D (2015) Biodegradation of diesel oil by a novel microbial consortium: comparison between co-inoculation with biosurfactant-producing strain and exogenously added biosurfactants. Environ Sci Pollut Res 22:4852–14861

Nanekar S, Dhote M, Kashyap S, Singh SK, Juwarkar AA (2013) Microbe assisted phytoremediation of oil sludge and role of amendments: a mesocosm study. Int J Environ Sci Technol 12:193–202

Nelson PN, Ladd JN, Oades JM (1996) Decomposition of ^{14}C-labelled plant material in a salt-affected soil. Soil Biol Biochem 28(4–5):433–441

Nikolopoulou M, Eickenbusch P, Pasadakis N, Venieri D, Kalogerakis N (2013) Microcosm evaluation of autochthonous bioaugmentation to combat marine oil spills. N Biotechnol 30:734–742

Oyelami AO, Ogbonnaya U, Muotoh C, Semple KT (2015) Impact of activated carbon on the catabolism of ^{14}C-phenanthrene in soil. Evnviron Sci Process Impacts 17:1173–1181

Poot A, Jonker MTO, Gillissen F, Koelmns AA (2014) Explaining PAH desorption from sediments using rock eval analysis. Environ Pollut 193:247–253

Radzi NASM, Tay KS, Abu Bakar NK, Emenike CU, Krishnan S, Hamid FS, Abas MR (2015) Degradation of polycyclic aromatic hydrocarbons (pyrene and fluoranthene) by bacterial consortium isolated from contaminated road side soil and soil termite fungal comb. Environ Earth Sci 74:5383–5391

Rasmussen C, Southard RJ, Horwath WR (2007) Soil mineralogy affects conifer forest soil carbon source utilization and microbial priming. Soil Sci Soc Am J 71(4):1141–1150

Reichenberg F, Mayer P (2006) Two complementary sides of bioavailability: accessibility and chemical activity of organic contaminants in sediments and soils. Environ Toxicol Chem 25 (5):1239–1245

Sajna KV, Sukumaran RK, Gottumukkala LD, Pandey A (2015) Crude oil biodegradation aided by biosurfactants from *Pseudozyma sp* NII 08165 or its culture broth. Bioresour Technol 191:133–139

SAS Institute (1989) Statistic guide for personal computers. Version 6.04, Edn. SAS Institute, Cary

Shi Z, Chen J, Liu J, Wang N, Sun Z, Wang X (2015) Anionic-nonionic mixed-surfactant-enhanced remediation of PAH-contaminated soil. Environ Sci Pollut Res 22:12769–12774

Silvana CE, Martinez MA, Arocena LA (2014) Estudio comparativo del agregado de enmiendas orgánicas e inorgánicas en procesos de biorremediaciòn de suelos norpatagónicos contaminados con petróleo. Rev Soc Quim Peru 80:251–261

Sojka RE, Bjorneberg DL, Entry JA, Lentz RD, Orts WJ (2007) Polyacrylamide in agriculture and environmental land management. Adv Agron 92:75–162

Steliga T (2008) Optimization research on biodegradation of hydrocarbon pollution in weathering soil samples from manufactures gas plant (MGP). Arch Environ Prot 34:51–70

Straszko J, Parus W, Paterkowski W (2015) Kinetics of catalytic combustion processes of air admixtures. Arch Environ Prot 41:86–97

Suja F, Rahim F, Taha MR, Hambali N, Razali MR, Khalid A, Hamzah A (2014) Effects of local microbial bioaugmentation and biostimulation on the bioremediation of total petroleum

hydrocarbons (TPH) in crude oil contaminated soil based on laboratory and field observations. Int J Biodeter Biodegr 90:115–122

Sun GD, Xu Y, Jin JH, Zhong ZP, Liu Y, Luo M, Liu ZP (2012) Pilot scale ex-situ bioremediation of heavily PAHs-contaminated soil by indigenous microorganisms and bioaugmentation by a PAHs-degrading and bioemulsifier-producing strain. J Hazard Mater 233:72–78

Sungthong R, van West P, Cantos M, Ortega-Calvo JJ (2015) Development of eukaryotic zoospores within polycyclic aromatic hydrocarbons (PAH)-polluted environments: a set of behaviors that are relevant for bioremediation. Sci Total Environ 511:767–776

Sutton NB, Grotenhuis T, Rijnaarts HHM (2014) Impact of organic carbon and nutrients mobilized during chemical oxidation on subsequent bioremediation of a diesel-contaminated soil. Chemosphere 97:64–70

Tang J, Lv H, Gong Y, Huang Y (2015) Preparation and characterization of a novel graphene/biochar composite for aqueous phenanthrene and mercury removal. Bioresour Technol 196:355–363

Teng Y, Lou Y, Sun M, Liu Z, Li Z, Christie P (2010) Effect of bioaugmentation by *Paracoccus* sp. strain HPD-2 on the soil microbial community and removal of polycyclic aromatic hydrocarbons from an aged contaminated soil. Bioresour Technol 101:3437–3443

Tian WJ, Wang LJ, Li D, Li FS (2015) Leachability of phenanthrene from soil under acid rain and its relationship with dissolved organic matter. Environ Earth Sci 73(7):3675–3681

US-EPA (2011) Introduction to green remediation. 2p. Retrieved from: http://www.epa.gov/remedytech/introduction-green-remediation (Verified January 1, 2016)

Vázquez-Núñez E, Rodriguez V, García-Gaytán A, Luna-Guido M, Betancur-Galvis LA, Marsch R, Dendooven L (2009) Using acetone as solvent to study removal of anthracene in soil inhibits microbial activity and alters nitrogen dynamics. Arch Environ Contam Toxicol 57 (2):239–246

Vecino X, Rodríguez-López L, Cruz JM, Moldes AB (2015) Sewage sludge polycyclic aromatic hydrocarbon (PAH) decontamination technique based on the utilization of a lipopeptide biosurfactant extracted from corn steep liquor. J Agric Food Chem 63:7143–7150

Wang JB, Wang C, Huang QY, Ding F, He XW (2015) Adsorption of PAHs on the sediments from the yellow river delta as a function of particle size and salinity. Soil Sediment Contam 24:103–115

Wen QX, Chen ZQ, Zhao Y, Zhang HC, Feng YJ (2010) Biodegradation of polyacrylamide by bacteria isolated from activated sludge and oil-contaminated soil. J Hazard Mater 175:955–959

Wen JW, Gao DW, Zhang B, Liang H (2011) Co-metabolic degradation of pyrene by indigenous white-rot fungus *Pseudotrametes gibbosa* from the northeast China. Int J Biodeter Biodegr 65 (4):600–604

Winquist E, Björklöf K, Schultz E, Räsänen M, Salonen K, Anasonye F, Cajthaml T, Steffen KT, Jorgensen KS, Tuomela M (2014) Bioremediation of PAH-contaminated soil with fungi—from laboratory to field scale. Int J Biodeter Biodegr 86:238–247

Wiszniewska A, Hanus-Fajerska E, Muszynska E, Ciarkowska K (2016) Natural organic amendments for improved phytoremediation of polluted soils: a review of recent progress. Pedosphere 26(1):1–12

Wu G, Kechavarzi C, Li X, Sui H, Pollard SJT, Coulon F (2013) Influence of mature compost amendment on total and bioavailable polycyclic aromatic hydrocarbons in contaminated soils. Chemosphere 90:2240–2246

Zhang J, Lin X, Liu W, Wang Y, Zeng J, Chen H (2012) Effect of organic wastes on the plant-microbe remediation for removal of aged PAHs in soils. J Environ Sci (China) 24:1476–1482

Index

N.A. Anjum et al. (eds.), *Enhancing Cleanup of Environmental Pollutants*,
DOI 10.1007/978-3-319-55423-5